ORGANOHALIDE RESPIRATION: NEW FINDINGS IN METABOLIC MECHANISMS AND BIOREMEDIATION APPLICATIONS

EDITED BY: Shanquan Wang, Jianzhong He, Chaofeng Shen and Michael J. Manefield

PUBLISHED IN: Frontiers in Microbiology

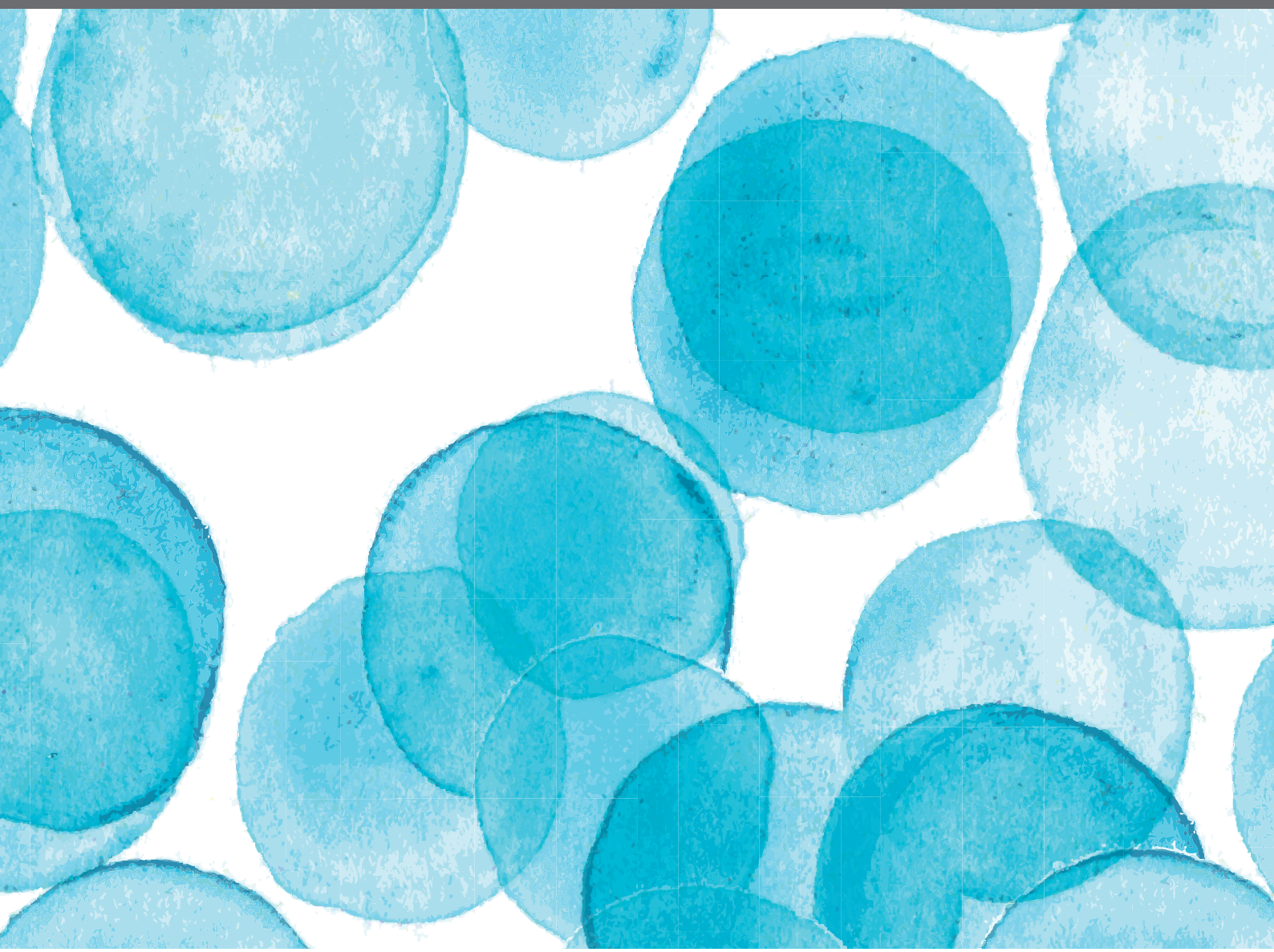

frontiers Research Topics

ISSN 1664-8714
ISBN 978-2-88945-848-6
DOI 10.3389/978-2-88945-848-6

About Frontiers

Frontiers is more than just an open-access publisher of scholarly articles: it is a pioneering approach to the world of academia, radically improving the way scholarly research is managed. The grand vision of Frontiers is a world where all people have an equal opportunity to seek, share and generate knowledge. Frontiers provides immediate and permanent online open access to all its publications, but this alone is not enough to realize our grand goals.

Frontiers Journal Series

The Frontiers Journal Series is a multi-tier and interdisciplinary set of open-access, online journals, promising a paradigm shift from the current review, selection and dissemination processes in academic publishing. All Frontiers journals are driven by researchers for researchers; therefore, they constitute a service to the scholarly community. At the same time, the Frontiers Journal Series operates on a revolutionary invention, the tiered publishing system, initially addressing specific communities of scholars, and gradually climbing up to broader public understanding, thus serving the interests of the lay society, too.

Dedication to Quality

Each Frontiers article is a landmark of the highest quality, thanks to genuinely collaborative interactions between authors and review editors, who include some of the world's best academicians. Research must be certified by peers before entering a stream of knowledge that may eventually reach the public - and shape society; therefore, Frontiers only applies the most rigorous and unbiased reviews.
Frontiers revolutionizes research publishing by freely delivering the most outstanding research, evaluated with no bias from both the academic and social point of view. By applying the most advanced information technologies, Frontiers is catapulting scholarly publishing into a new generation.

What are Frontiers Research Topics?

Frontiers Research Topics are very popular trademarks of the Frontiers Journals Series: they are collections of at least ten articles, all centered on a particular subject. With their unique mix of varied contributions from Original Research to Review Articles, Frontiers Research Topics unify the most influential researchers, the latest key findings and historical advances in a hot research area! Find out more on how to host your own Frontiers Research Topic or contribute to one as an author by contacting the Frontiers Editorial Office: researchtopics@frontiersin.org

ORGANOHALIDE RESPIRATION: NEW FINDINGS IN METABOLIC MECHANISMS AND BIOREMEDIATION APPLICATIONS

Topic Editors:
Shanquan Wang, Sun Yat-Sen University, China
Jianzhong He, National University of Singapore, Singapore
Chaofeng Shen, Zhejiang University, China
Michael J. Manefield, University of New South Wales, Australia

Microbial reductive dehalogenation mediated by organohalide-respiring bacteria plays a critical role in the natural halogen cycle, representing a promising solution for removal of organohalide pollutants. This Research Topic presents many of the more recent advances that have been made in this area. Authors from leading research groups contributed to this eBook, and provided mechanistic insights into organohalide respiration, as well as their bioremediation implications, at molecular, cellular, community and system levels.

Citation: Wang, S., He, J., Shen, C., Manefield, M. J., eds. (2019). Organohalide Respiration: New Findings in Metabolic Mechanisms and Bioremediation Applications. Lausanne: Frontiers Media. doi: 10.3389/978-2-88945-848-6

Table of Contents

05 ***Editorial: Organohalide Respiration: New Findings in Metabolic Mechanisms and Bioremediation Applications***
Shanquan Wang, Jianzhong He, Chaofeng Shen and Michael J. Manefield

SECTION 1
ORGANOHALIDE-RESPIRING BACTERIA

08 ***Debromination of Hexabromocyclododecane by Anaerobic Consortium and Characterization of Functional Bacteria***
Xingxing Peng, Dongyang Wei, Qiyuan Huang and Xiaoshan Jia

19 ***Diastereoisomer-Specific Biotransformation of Hexabromocyclododecanes by a Mixed Culture Containing* Dehalococcoides mccartyi *Strain 195***
Yin Zhong, Heli Wang, Zhiqiang Yu, Xinhua Geng, Chengyu Chen, Dan Li, Xifen Zhu, Huajun Zhen, Weilin Huang, Donna E. Fennell, Lily Y. Young and Ping'an Peng

29 ***Reductive Debromination of Polybrominated Diphenyl Ethers - Microbes, Processes and Dehalogenases***
Siyan Zhao, Matthew J. Rogers, Chang Ding and Jianzhong He

SECTION 2
RDASES AND ASSOCIATED ELECTRON TRANSPORT CHAINS

41 ***Functional Expression and Characterization of Tetrachloroethene Dehalogenase From* Geobacter *sp.***
Ryuki Nakamura, Tomohiro Obata, Ryota Nojima, Yohey Hashimoto, Keiichi Noguchi, Takahiro Ogawa and Masafumi Yohda

48 ***The Complexome of* Dehalococcoides mccartyi *Reveals its Organohalide Respiration-Complex is Modular***
Katja Seidel, Joana Kühnert and Lorenz Adrian

62 ***The Membrane-Bound C Subunit of Reductive Dehalogenases: Topology Analysis and Reconstitution of the FMN-Binding Domain of PceC***
Géraldine F. Buttet, Mathilde S. Willemin, Romain Hamelin, Aamani Rupakula and Julien Maillard

SECTION 3
DEHALOGENATING MICROBIAL COMMUNITY COMPOSITION AND FUNCTION

77 ***Syntrophic Partners Enhance Growth and Respiratory Dehalogenation of Hexachlorobenzene by* Dehalococcoides mccartyi *Strain CBDB1***
Anh T. T. Chau, Matthew Lee, Lorenz Adrian and Michael J. Manefield

90 ***Chlorinated Electron Acceptor Abundance Drives Selection of* Dehalococcoides mccartyi *(D. mccartyi) Strains in Dechlorinating Enrichment Cultures and Groundwater Environments***
Alfredo Pérez-de-Mora, Anna Lacourt, Michaye L. McMaster, Xiaoming Liang, Sandra M. Dworatzek and Elizabeth A. Edwards

104 ***Diversity and Dynamics of Microbial Community Structure in Different Mangrove, Marine and Freshwater Sediments During Anaerobic Debromination of PBDEs***
Ya Fen Wang, Hao Wen Zhu, Ying Wang, Xiang Ling Zhang and Nora Fung Yee Tam

119 ***Inhibitory Effects of Sulfate and Nitrate Reduction on Reductive Dechlorination of PCP in a Flooded Paddy Soil***
Yan Xu, Lili Xue, Qi Ye, Ashley E. Franks, Min Zhu, Xi Feng, Jianming Xu and Yan He

SECTION 4
ORGANOHALIDE BIOREMEDIATION

132 ***Microbial Community Changes in a Chlorinated Solvents Polluted Aquifer Over the Field Scale Treatment With Poly-3-Hydroxybutyrate as Amendment***
Bruna Matturro, Lucia Pierro, Emanuela Frascadore, Marco Petrangeli Papini and Simona Rossetti

143 ***Typical Soil Redox Processes in Pentachlorophenol Polluted Soil Following Biochar Addition***
Min Zhu, Lujun Zhang, Liwei Zheng, Ying Zhuo, Jianming Xu and Yan He

155 ***Effects of 1,1,1-Trichloroethane and Triclocarban on Reductive Dechlorination of Trichloroethene in a TCE-Reducing Culture***
Li-Lian Wen, Jia-Xian Chen, Jia-Yi Fang, Ang Li and He-Ping Zhao

165 ***Effects of Ferric Oxyhydroxide on Anaerobic Microbial Dechlorination of Polychlorinated Biphenyls in Hudson and Grasse River Sediment Microcosms: Dechlorination Extent, Preferences,* Ortho *Removal, and its Enhancement***
Yan Xu, Kelvin B. Gregory and Jeanne M. VanBriesen

181 **Dehalococcoides** ***as a Potential Biomarker Evidence for Uncharacterized Organohalides in Environmental Samples***
Qihong Lu, Ling Yu, Zhiwei Liang, Qingyun Yan, Zhili He, Tiangang Luan, Dawei Liang and Shanquan Wang

frontiers in Microbiology

EDITORIAL
published: 21 March 2019
doi: 10.3389/fmicb.2019.00526

Editorial: Organohalide Respiration: New Findings in Metabolic Mechanisms and Bioremediation Applications

Shanquan Wang[1]*, *Jianzhong He*[2], *Chaofeng Shen*[3] and *Michael J. Manefield*[4]

[1] School of Environmental Science and Engineering, Sun Yat-sen University, Guangzhou, China, [2] Department of Civil and Environmental Engineering, National University of Singapore, Singapore, Singapore, [3] Department of Environmental Engineering, College of Environmental and Resource Sciences, Zhejiang University, Hangzhou, China, [4] School of Civil and Environmental Engineering, University of New South Wales, Sydney, NSW, Australia

Keywords: Organohalide respiration, *Dehalococcoides*, electron transport chain, reductive dehalogenase, community composition and function, bioremediation

OPEN ACCESS

Edited by:
Elisabet Aranda, University of Granada, Spain

Reviewed by:
Ernest Marco-Urrea, Autonomous University of Barcelona, Spain
Siavash Atashgahi, Radboud University Nijmegen, Netherlands

***Correspondence:**
Shanquan Wang
wangshanquan@mail.sysu.edu.cn

Specialty section:
This article was submitted to Microbiotechnology, Ecotoxicology and Bioremediation, a section of the journal Frontiers in Microbiology

Received: *14 January 2019*
Accepted: *28 February 2019*
Published: *21 March 2019*

Citation:
Wang S, He J, Shen C and Manefield MJ (2019) Editorial: Organohalide Respiration: New Findings in Metabolic Mechanisms and Bioremediation Applications. Front. Microbiol. 10:526. doi: 10.3389/fmicb.2019.00526

Editorial on the Research Topic

Organohalide Respiration: New Findings in Metabolic Mechanisms and Bioremediation Applications

Organohalide-respiring bacteria can utilize several sets of functional enzymes to couple halogen removal with electron transfer from H_2 or organic matter (e.g., formate and lactate) to organohalides for cell growth (Fincker and Spormann, 2017; Atashgahi et al., 2018). Consequently, microbial reductive dehalogenation basing on the organohalide respiration represents a promising solution for cleanup of persistent organohalide pollutants and plays a pivotal role in the natural halogen cycle (Wang et al., 2018). The key enzymes catalyzing the above-described process are reductive dehalogenases (RDases). Although microbial reductive dehalogenation has been discovered many years ago, advances in characterizing major organohalide-respiring bacteria and in analyzing crystal structures of reductive dehalogenases were made recently (Löffler et al., 2013; Bommer et al., 2014; Payne et al., 2015). These progresses provides unprecedented insights into microbial reductive dehalogenation and brings us to a new stage to realize that there are many puzzles to solve in the mechanistic understanding and in the application of organohalide respiration in bioremediation. Therefore, this research topic was formulated to provide a platform for the publication of updated information and high-quality research papers on *organhalide-respiring bacteria*, *RDases and associated electron transport chains*, *dehalogenating microbial community composition and function*, and *organohalide bioremediation*. We received a total of 19 manuscripts, of which 15 were accepted for publication after a rigorous peer review process.

ORGANOHALIDE-RESPIRING BACTERIA

In an anaerobic microbial consortium, Peng et al. reported that a novel organohalide-respiring bacterium could be involved in debromination of hexabromocyclododecane (HBCD), and no known dehalogenating bacteria were detected in the consortium with PCR-based analysis. Moreover, with *Dehalococcoides mccartyi* type strain−195, Zhong et al. found the

diastereoisomer-specific biotransformation of HBCD with a debromination rate order of α-HBCD > β-HBCD > γ-HBCD. In addition to HBCD, Zhao et al. comprehensively reviewed bacterial lineages and pathways for the metabolic debromination of polybrominated diphenyl ethers (PBDEs). These studies provided interesting information on the organohalide-respiring bacteria of new lineages and novel dehalogenation specificities of known players in microbial reductive dehalogenation.

RDASES AND ASSOCIATED ELECTRON TRANSPORT CHAINS

Many reductive dehalogenase homologous (*rdh*) genes have been identified from a variety of dehalogenating bacteria. Nonetheless, most of *rdh* gene-encoding RDases have not been functionally characterized, which is mainly due to the difficulty in heterogeneous expression of the *rdh* genes. Nakamura et al. reported the successful expression, purification and characterization of PceA encoded by *pceA* from a *Geobacter* strain. Notably, PceA was purified and denatured under aerobic condition, which could be refolded in the presence of $FeCl_3$, Na_2S, and cobalamin under anaerobic condition to recover its PCE dechlorination activity. In view of organohalide respiration, the respiratory electron transfer chain in *D. mccartyi* was elucidated for the first time in Lorenz Adrian's lab, which is surprisingly a protein-dependent chain obviating quinone involvement (Kublik et al., 2016). From the same lab, Seidel et al. further provided insightful information on the participating protein subunits and their interactions of the multi-protein RDase complex mediating the electron transfer from H_2 to organohalides in *D. mccartyi* CBDB1. By contrast, in the quinone-dependent electron transport chains of organohalide-respiring *Dehalobacter*, Buttet et al. employed multiple strategies to show that PceC, originally proposed to be a transcriptional regulator, might be involved in electron transfer from the quinol pool to RDases. These studies provided very important information fulfilling the knowledge gaps in understanding the organohalide respiration process and the major participating enzymes.

DEHALOGENATING MICROBIAL COMMUNITY COMPOSITION AND FUNCTION

Dehalococcoides and other obligate organohalide-respiring bacteria generally need to work closely with other microorganisms for efficient dehalogenation in dehalogenating microbial communities. Chau et al. showed that dechlorination rates in co-cultures were enhanced two- to three-fold compared to *Dehalococcoides* pure cultures, in which the syntrophic partners consumed carbon monoxide (CO) generated by *Dehalococcoides* and consequently relieving CO autotoxicity. Moreover, multiple dehalogenating populations may co-exist in dehalogenating communities and at sites undergoing bioremediation, and many factors can drive their population changes. Pérez-de-Mora et al. showed that chloroethenes as electron acceptors was a major driving force behind *D. mccartyi* population selection and succession in KB-1 cultures and remediation sites. Also, Wang et al. showed the significant relationship between microbial community structure and PBDEs in different mangrove, marine and freshwater sediments. In addition to organohalides as electron acceptors, Xu et al. showed that the presence of other alternative electron acceptors (i.e., sulfate and nitrate) had inhibitory effects on the organohalide respiration. Therefore, these experimental evidences may provide very useful information to guide the optimization of dehalogenating microbial communities for successful bioremediation of organohalide pollutants.

ORGANOHALIDE BIOREMEDIATION

To enhance the efficiency of remediation, a variety of strategies have been tested, including adding organic polymers and electron shuttling materials. Matturro et al. showed very interesting information on the coupling of organohalide-respiring bacteria with bioreactor operation to tackle problems in organohalide bioremediation. For example, amendment of poly-3-hydroxybutyrate (PHB) in a pilot-scale PHB reactor was shown to effectively stimulate the growth of *Dehalococcoides* and consequently enhance the complete dechlorination of chlorinated solvents at contaminated sites. But amendments may not always work as expected. Zhu et al. demonstrated that the addition of biochar as an electron shuttle enhanced iron and sulfate reduction but decreased dechlorination of pentachlorophenol (PCP). Co-existing organohalides generally have inhibitory effects on organohalide respiration. Wen et al. provided experimental evidence showing inhibitory effects of trichloroethane and triclocarbon on trichloroethene dechlorination. Moreover, the presence of alternative electron acceptors may inhibit bioremediation of sites contaminated with organohalides. Xu et al. investigated the influence of a common competing electron acceptor, ferric oxyhydroxide (FeOOH), on reductive dechlorination of polychlorinated biphenyls (PCBs) in two river sediments (i.e., Hudson River and Grasse River sediments), and showed the inhibitory effects of FeOOH on PCB dechlorination, but in different manners. For example, complete and moderate inhibition of PCB dechlorination were observed upon the addition of 40 mmole/kg FeOOH in the Hudson River sediment and the Grasse sediment, respectively. Beside these biostimulation and bioaugmentation strategies, molecular tools may help improve the management of sites undergoing bioremediation. Lu et al. proposed the obligate organohalide-respiring bacterium, *D. mccartyi*, as a potential biomarker for identifying the possible contamination of uncharacterized organohalides in environmental samples, which could complement current chromatography-based tools in testing and analyzing organohalide contamination.

We want to thank all the authors and reviewers for their valuable contributions to this research topic, and we hope that this collection of reviews and original research articles will be helpful for researchers, engineers and students seeking

information about microbial reductive dehalogenation and remediation applications.

AUTHOR CONTRIBUTIONS

All authors listed have made a substantial, direct and intellectual contribution to the work, and approved it for publication.

ACKNOWLEDGMENTS

Topic editors acknowledge support of NSFC grants 41671310 and 41877111 to SW, Ng Teng Fong Charitable Foundation (NTFCF) fund R-302-000-198-720 to JH, and NSFC grants 21477110 and 2187876149 to CS.

REFERENCES

Atashgahi, S., Häggblom, M. M., and Smidt, H. (2018). Organohalide respiration in pristine environments: implications for the natural halogen cycle. *Environ. Microbiol.* 20, 934–948. doi: 10.1111/1462-2920.14016

Bommer, M., Kunze, C., Fesseler, J., Schubert, T., Diekert, G., and Dobbek, H. (2014). Structural basis for organohalide respiration. *Science* 346, 455–458. doi: 10.1126/science.1258118

Fincker, M., and Spormann, A. M. (2017). Biochemistry of catabolic reductive dehalogenation. *Annu. Rev. Biochem.* 86, 357–386. doi: 10.1146/annurev-biochem-061516-044829

Kublik, A., Deobald, D., Hartwig, S., Schiffmann, C. L., Andrades, A., von Bergen, M., et al. (2016). Identification of a multi-protein reductive dehalogenase complex in *Dehalococcoides mccartyi* strain CBDB1 suggests a protein-dependent respiratory electron transport chain obviating quinone involvement. *Environ. Microbiol.* 18, 3044–3056. doi: 10.1111/1462-2920.13200

Löffler, F. E., Yan, J., Ritalahti, K. M., Adrian, L., Edwards, E. A., Konstantinidis, K. T., et al. (2013). *Dehalococcoides mccartyi* gen. nov., sp nov., obligately organohaliderespiring anaerobic bacteria relevant to halogen cycling and bioremediation, belong to a novel bacterial class, *Dehalococcoidia classis.* nov., order *Dehalococcoidales* ord. nov and family *Dehalococcoidaceae.* fam. nov., within the phylum Chloroflexi. *Int. J. Syst. Evol. Microbiol.* 63:625–635. doi: 10.1099/ijs.0.034926-0

Payne, K. A., Quezada, C. P., Fisher, K., Dunstan, M. S., Collins, F. A., Sjuts, H., et al. (2015). Reductive dehalogenase structure suggests a mechanism for B12-dependent dehalogenation. *Nature* 517, 513–516. doi: 10.1038/nature13901

Wang, S., Qiu, L., Liu, X., Xu, G., Siegert, M., Lu, Q., et al. (2018). Electron transport chains in organohalide-respiring bacteria and bioremediation implications. *Biotechnol. Adv.* 36, 1194–1206. doi: 10.1016/j.biotechadv.2018.03.018

Conflict of Interest Statement: The authors declare that the research was conducted in the absence of any commercial or financial relationships that could be construed as a potential conflict of interest.

frontiers in Microbiology

ORIGINAL RESEARCH
published: 10 July 2018
doi: 10.3389/fmicb.2018.01515

Debromination of Hexabromocyclododecane by Anaerobic Consortium and Characterization of Functional Bacteria

Xingxing Peng[1], Dongyang Wei[2], Qiyuan Huang[1] and Xiaoshan Jia[1]**

[1] School of Environmental Science and Engineering, Sun Yat-sen University, Guangzhou, China, [2] South China Institute of Environmental Sciences, Guangzhou, China

A microbial consortium which can efficiently remove hexabromocyclododecane (HBCD) under anaerobic condition have been successfully enriched over 300 days. Under the optimal conditions, the degradation efficiency was 92.4% removal after treatment of 12 days with original addition of 500 μg/L HBCD, yielding 321.7 μg/L bromide in total as well. A typical debromination product, dibromocyclododecadiene (DBCD), was detected during the degradation process. The debromination profiles of three main HBCD diastereomers fitted well with first-order model (R^2: 0.96–0.99), with the rate constants ranging from 1.3×10^{-1} to 1.9×10^{-1}. The microbial community analysis by high throughput sequencing showed that the composition of the microbial communities varied dynamically with time and the population of functional bacteria increase sharply after enrichment. The population of *Bacteroidetes* increased from 5 to 47%. And some bacteria which are relatively minority in population at the beginning, such as *Azospira oryzae* (OTU2), *Microbacterium* (OTU13), and *Achromobacter insolitus* (OTU39) increased more than 22 times after enrichment (from 0.5 to 13%, 12%, and 11%, respectively). However, no reported dehalogenating bacteria were found after enrichment. And the contribution for debromination may come from new dehalogenating bacteria. All in all, the present study provided in-depth information on anaerobic microbial communities for HBCD removal by debromination.

Keywords: hexabromocyclododecane, anaerobic reactor, debromination, bacterial variation, functional bacteria

OPEN ACCESS

Edited by:
Chaofeng Shen,
Zhejiang University, China

Reviewed by:
Robert Heyer,
Universitätsklinikum Magdeburg, Germany
Chen Chen,
National University of Singapore, Singapore

****Correspondence:***
Xingxing Peng
pengxx6@mail.sysu.edu.cn
Xiaoshan Jia
eesjxs@mail.sysu.edu.cn

Specialty section:
This article was submitted to Microbiotechnology, Ecotoxicology and Bioremediation, a section of the journal Frontiers in Microbiology

Received: *14 November 2017*
Accepted: *18 June 2018*
Published: *10 July 2018*

Citation:
Peng X, Wei D, Huang Q and Jia X (2018) Debromination of Hexabromocyclododecane by Anaerobic Consortium and Characterization of Functional Bacteria. Front. Microbiol. 9:1515. doi: 10.3389/fmicb.2018.01515

INTRODUCTION

Hexabromocyclododecane (HBCD) is one type of additive brominated flame retardants (BFRs) applied in various polystyrene resins and textiles to improve the flammability resistance or chemically bound to synthetic matrices such as plastics, textiles, electronic circuitry and other materials to prevent fires. Recently, it was also found in high tech devices, such as wind turbines and defense systems (www.bsef.com, 2016). Usually, it can be released during the industrial process or washed from waste products, then discharged into municipal wastewater treatment plants (WWTPs) or was washed from waste products and infiltrated various ecosystems. Up to now,

the wide-spread existence of HBCD in the environment has drawn great attentions from many researchers due to the toxicity and persistence all over the world. It was reported in water (Morris et al., 2004), soil (Li et al., 2011), sediment (Kohler et al., 2008), plants (Li et al., 2011), animals (Law et al., 2006), humans (Eljarrat et al., 2009), and even indoor dust (Stapleton et al., 2008). Usually, the concentration of HBCD from μg/kg to mg/kg. Although HBCD is not acutely toxic, some research showed that its accumulation in the environment could cause adverse effects in human health, such as disruption of liver and thyroid hormone (Palace et al., 2008) and disorder of reproductions (Ema et al., 2008). Worse still, HBCD can accumulate along the food chain from the bottom to top, which is why the detection of HBCD serum concentrations in Norwegians is associated with the consumption of highly contaminated fish (Thomsen et al., 2008). Therefore, more studies for HBCD degradation are essential to eliminate its contamination in environment.

Conceptually, microbial degradation is to use living microorganisms to detoxify and degrade hazardous materials (Wang et al., 2014, 2015). It is generally considered to be an effective and safe way to remove contaminants from the environment, which has been widely applied in degrading pollutants such as pesticides (Chanika et al., 2011), plastic (Nakajima et al., 1999), additive (Wang and He, 2013), petroleum (Zhang et al., 2010), and surface-active agents (Fuchedzhieva et al., 2008). In our previous studies, biodegradation of TBBPA (another widely used BRF) has been successfully illuminated via analysis of bacterial consortium, isolation of pure culture, and deduction of co-metabolism pathway (Peng et al., 2012, 2013, 2014; Peng and Jia, 2013). To date, microorganisms have been reported to degrade HBCD both in aerobic and anaerobic conditions, such as *Pseudomonas* sp. Strain HB01, isolated from soil, can remove 81% of 1 mM γ-HBCD within 5 days of culture (Yamada et al., 2009). Under the anaerobic condition, a broken-down of technical HBCD mixture has been reported, (±)-a-HBCD exhibited an almost doubled half-life compared to (±)-β-HBCD and (±)-γ-HBCD (Davis et al., 2004; Gerecke et al., 2006). Usually, halogenated compounds can serve as electron acceptors in respiratory or co-metabolic processes, such as reduction of polychlorinated and polybrominated biphenyls (PCBs and PBBs) in anaerobic sediment enrichment cultures (Abraham et al., 2002). In addition, a small quantity of HBCD can be degraded in sediments, soils, and sewage sludge, while reductive dehalogenation (e.g., substitution of Br by a hydrogen atom) has been reported to be an important mechanism during biodegradation process under anaerobic condition. However, in most of the previous HBCD studies, the toxicology and the distribution of HBCD were emphasized, as well as the phenomenon of anaerobic degradation and degradation characteristics. Not enough attention has been paid to the acclimation and composition analysis of the microbial consortium. Hence, a more complete study including degradation characteristics, kinetics of HBCD stereoisomers, degrading pathway, and metabolites variation is in need.

Overall, the aim of this study is to obtain and characterize the microorganisms that effectively biodegrade HBCD by enrichment. Considering the wastewater treatment facilities have processed wastewaters containing HBCD for several years, it is probable to possess microorganisms able to metabolize HBCD. In this study, laboratory reactor systems based on the conventional sewage sludge process were set up and operated for more than 300 days to develop a biological process for the debromination of HBCD (**Figure 1**). The optimal debrominated condition was analyzed by batch experiment. Subsequently, the degradation data was used to conduct fitted kinetic model. Moreover, the microbial composition was analyzed at different time points during the enrichment period (0–300 days at the interval of 60 days). Finally, the comparison of these samples at the phylum level and operational taxonomic unit (OTU) description were conducted. To our knowledge, a more comprehensive analysis of the bacterial community in the enriched bacterial consortium of HBCD was firstly unraveled in the present study, and a shifting pattern was discovered during the enriched time.

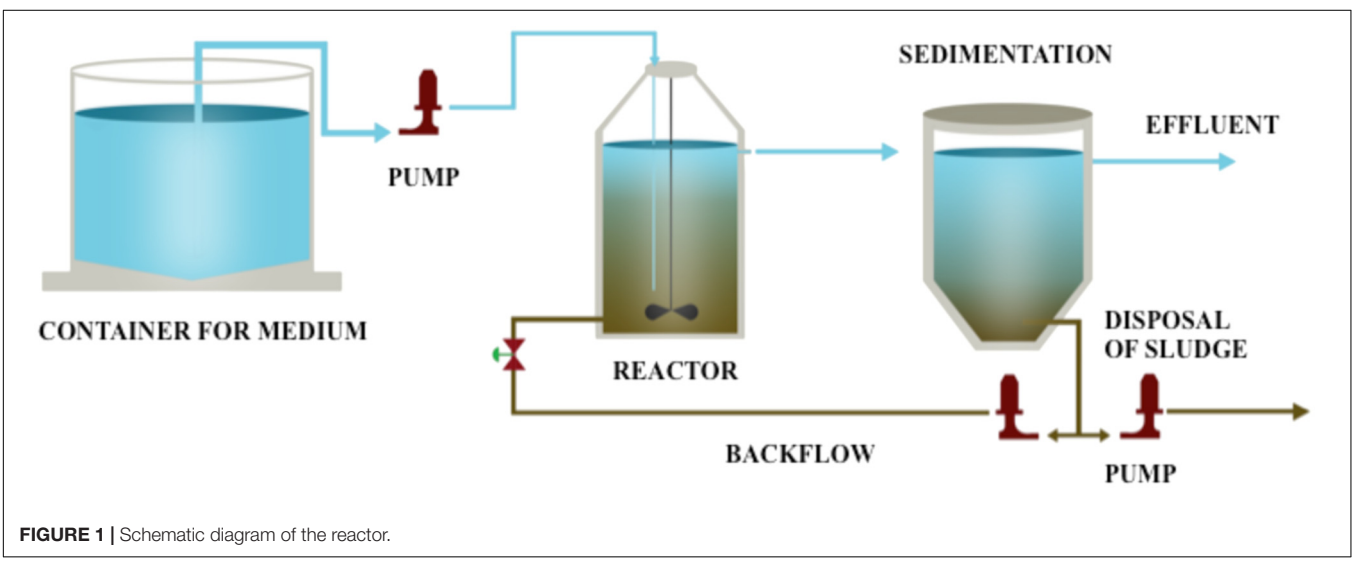

FIGURE 1 | Schematic diagram of the reactor.

MATERIALS AND METHODS

Chemicals

Hexabromocyclododecane (HBCD, 99% purity) was purchased from Sigma Chemical Co. (St. Louis, MO, United States), which was dissolved in acetone as stock solution (100,000 $mg \cdot L^{-1}$) before used. After filtration, it was rationed into the medium to obtain desired concentrations. All solvents (including acetone and methanol) used in this study were HPLC grade, which were purchased from Merck Company (Darmstadt, Germany). Other chemicals used for medium preparation were analytical grade and purchased from Sigma Chemical Co. (St. Louis, MO, United States). High quality water was obtained by using a Nanopure UV deionization system, Barnstead/Thermolyne Co. (Dubuque, IA, United States).

Characterization of Sewage Sludge

The sewerage sludge was obtained from the anaerobic tank of wastewater treatment plant (WWTP) in Zhongkai industrial park of Huizhou, Guangdong province, China, which has been used to treat wastewater containing various BFR for a long time. Total solid (TS), volatile solid (VS), suspended solid (SS), and volatile suspended solid (VSS) analyses were based on the Standard Analytical Methods promulgated by the American Public Health Association (APHA, 1995). The crude fiber and crude protein were measured according to ISO 6865:2000 and ISO 1871: 2009, respectively. Crude fat content was determined using Soxhlet extraction method according to ISO 6492:1999. Carbon (C), hydrogen (H), and Nitrogen (N) were analyzed by an elemental analyser (PE2400). The general physical and chemical properties of the sewage sludge are showed in **Table 1**.

Cultivation

The composition of the medium for the anaerobic reactor are as follows: NH_4Cl 2,600 mg/L, $MgCl_2 \cdot 7H_2O$ 1054 mg/L, K_2HPO_4 752 mg/L, $CaCl_2$ 520 mg/L, and trace solution 1 mL/L. The carbon sources used in this experiment were as follows: $NaHCO_3$ 800 mg/L, $Na_3C_6H_5O_7 \cdot 2H_2O$ 680 mg/L, and $C_6H_{12}O_6$ 1,000 mg/L. While the composition of the trace elements were listed as follows: $NiCl_2 \cdot 7H_2O$ 800 mg/L, $FeCl_3 \cdot 6H_2O$ 1,250 mg/L, $ZnCl_2$ 130 mg/L, $CoCl_3 \cdot 6H_2O$ 110 mg/L, $MnCl_2 \cdot 4H_2O$ 220 mg/L, $Na_2BO_3 \cdot 10H_2O$ 44 mg/L, $(NH_4)_6Mo_7O_{24} \cdot 4H_2O$ 80 mg/L, and $CuCl_2 \cdot 2H_2O$ 65 mg/L. The reactor was seeded with the anaerobic sludge incubated in the medium containing HBCD.

Initially, HBCD was added to the medium at concentration of 100 μg/L, and then the concentration was gradually increased from concentration of 200–500 μg/L. The pH of the mixture was adjusted to 7.0 before seeding. The anaerobic HBCD-utilizing sludge was enriched in a 3.0 L water-jacketed chemostat reactor at 30°C. The schematic overview used for the acclimation was shown in **Figure 1**. The reactor was running in continuous mode. Hydraulic retention time (HRT) was kept constant for 9 days, and the pH was maintained at 6.8–7.2 throughout the study.

TABLE 1 | General properties of the sewage sludge used in experiments.

Water content (%)	79.08 ± 1
TS (g/kg)	148.56 ± 0.5
VS (g/kg)	108.25 ± 0.2
SS (g/kg)	136.68 ± 0.6
VSS (g/kg)	102.86 ± 0.4
VSS/VS (%)	95.0 ± 2
Crude fiber (g/kg)	9.26 ± 0.02
Crude protein (g/kg)	62.74 ± 0.2
Crude fat (g/kg)	24.25 ± 0.1
C (%)	40.96 ± 0.2
H (%)	7.28 ± 0.02
N (%)	13.64 ± 0.5
C/N	3.0 ± 0.01

Batch Experiment Design

Several series of batch experiments were conducted with the successfully acclimated microbial consortia collected from the anaerobic reactor. In the batch experiments, 200 mL glass serum vials containing culture mixture were prepared for degradation study with three replicates. Samples were collected in the volume of 10 mL from batch reactor using glass syringe at each time point (0–12 days at the interval of 2 days) and filtered via 0.24 μm cellulose nitrate membrane. Among the 10 mL collections, 4 mL of which was used for TOC detection; the left was equally divided into three parts (2 mL/each), which were used for protein measurement, HBCD detection and bromide detection, respectively. Another series batch experiments were performed to select optimal culture conditions by comparison of different treatments. Different temperatures (20, 25, 30, 35, and 40°C), pH values (5, 6, 7, 8, and 9), HBCD concentrations (100, 500, 1,000, 5,000, and 10,000 μg/L), and carbon sources (sodium formate, sodium acetate, sodium propionate, sodium butyrate, and glucose) were test.

Chemical Analysis

Total organic carbon (TOC) was determined using a Total Organic Carbon Analyser (Shimadzu TOC-VCPH, Kyoto, Japan). Because of low microbial content in 2 mL samples, the biomass content in the solution could not be measured directly by the VSS content. In this study, protein content was converted to VSS, which was analyzed according to the reported method (Zubkov et al., 1999). HBCD was analyzed by gas chromatography-mass spectrometry (GC-MS) with a fused silica column DB5-MS (30 m × 0.25 mm id, 0.25 μm dj) using He as the mobile phase. Three diastereomers of HBCD were determined by liquid chromatography-tandem mass spectrometry (LC-MS/MS) with the model of Agilent 6120. The analytical conditions were 10 mM ammonium acetate in water as phase A and 2% mobile phase B (methanol) at flow rate of 0.3 mL/min. The debrominated products were analyzed by ultra-performance liquid chromatography quadrupole time-of-flight mass spectrometry (UHPLC/Q-TOF-MS, Agilent 1290, Palo Alto, CA, United States; Bruker, Germany) using electrospray ionization (ESI) positive mode.

Biodegradation Kinetics

Concentrations of individual diastereomers and ΣHBCD were normalized to the initial concentration vs. time. The biodegradation data were fitted to three decay models, i.e., zero-order (Eq. 1), first-order (Eq. 2) and second-order (Eq. 3).
Zero-order:

$$\frac{dc}{dt} = -k_0 \Leftrightarrow C_t = C_0 - k_0 \cdot t \quad (1)$$

First-order:

$$\frac{dc}{dt} = -k_1 \cdot C \Leftrightarrow C_t = C_0 \times e^{-kt} \quad (2)$$

Second-order:

$$\frac{dc}{dt} = -k_2 \cdot C^2 \Leftrightarrow C_t/(1 + C_0 \cdot k_2 \cdot t) \quad (3)$$

Where, C_0 is the initial concentration of substrate;
t is the degradation period in days;
C_t is the concentration of substrate at time t;
k_0 is the degradation rate constant of zero-order;
k_1 is the degradation rate constant of first-order;
k_2 is the degradation rate constant of second-order.

The degradation half-lives (T1/2) were determined using the algorithm (Eq. 4) .

$$T_{1/2} = ln\,2/k \quad (4)$$

DNA Extraction, PCR Amplification, and High Throughput Sequencing

DNA samples were extracted from mixed culture at different time points (including 0, 60, 120, 180, 240, and 300 days) by using FastDNA-Spin Kit for Soil (MP Biomedicals, California, CA, United States) according to a modified protocol described previously (Urakawa et al., 2010). For high throughput sequencing, 16S rRNA gene of V4 region was amplified using specific primer of 515F and 806R with the barcode. All PCR reactions were carried out with Phusion® High-Fidelity PCR Master Mix. Sequencing libraries were generated using TruSeq® DNA PCR-Free Sample Preparation Kit (Illumina, United States) following manufacturer's recommendations and index codes were added. The qualities of libraries were assessed on the Qubit@ 2.0 Fluorometer (Thermo Fisher Scientific) and Agilent Bioanalyzer 2100 system. At last, the libraries were sequenced on an Illumina HiSeq 2500 platform and 250 bp paired-end reads were generated. Paired-end reads were assigned to samples based on their unique barcode and truncated by cutting off the barcode and primer sequence. Paired-end reads were merged using FLASH. Quality filtering on the raw tags was performed to obtain the high-quality clean tags according to the QIIME (Bokulich et al., 2013). The tags were compared with the reference database using UCHIME algorithm to detect chimera sequences, and then the chimera sequences were removed (Edgar et al., 2011).

Construction of 16S rRNA Gene Clone Libraries

For better parallel the bacterial shift of baseline (no enrichment, 0 day) and final enrichment (300 days), 16S clone libraries based on 200 clones were constructed. 16S rRNA genes sequences were amplified with the forward primer 27f: 5′-AGRGTTTGATCMTGGCTCAG-3′ and the reverse primer 1492r: 5′-GGYTACCTTGTTACGACTT-3′. The reactions were run on a Stratagene RoboCycler (Stratagene, La Jolla, CA, United States) under the following conditions: 5 min initial denaturing step at 95°C followed by 25 cycles of 30 s at 95°C, 30 s at 55°C for annealing and 2 min at 72°C for extension. A negative control (reagent only) was conducted during DNA extraction, as well as positive and negative controls were conducted during PCR process. All PCR products were purified using Qiaquick PCR purification kit (Qiagen, Valencia, CA, United States) and cloned into the PCR 4-TOPO Vector using the TOPO TA Cloning kit according to the manufacturer's instructions (Version M, Invitrogen, Carlsbad, CA, United States). Two hundred positive clones of each sample were randomly selected by blue/white screening, then incubated in 100 μl LB broth overnight in 37°C. One microliter of cloned inserts was re-amplified using vector-specific primers (M13f-20 and M13r) to avoid co-amplification of *E. coli* host-cell DNA, as well as the PCR conditions were conducted as described above. The products suffered amplified rDNA restriction analysis by restriction enzymes (HhaI and HaeIII) separately under condition described by manufacturer (Invitrogen, Carlsbad, CA, United States), as well as the fragment pattern was determined by electrophoresis. Digestion pattern was analyzed using Gel-Pro Analyser Software version 6.0 (Media Cybernetics, Inc.) with 85 and 32 clones sequenced in the absence of repeated clones. Sequences that were less than 3% divergent were grouped into OTUs. Chimera sequences were removed using Ribosomal Database Project II (Maidak et al., 2001). Bellerophon (version 3) and excluded for further analysis. The sequences were compared to Gen-Bank entries using BLAST-n to obtain preliminary phylogenetic affiliations of the clones by the percentage of similarity.

Statistical Analysis

Cluster analysis (CA) and UniFrac principal coordinate analysis (PCoA) are statistical techniques that sort observations into similar groups or sets, which were conducted using PAST software (Version 3.0). CA was based on taxonomy results and OTUs, whereas PCoA was based on RDP Classifier results, OTUs and UniFrac. It is a phylogeny-dependent method using phylogenetic information to compare the six samples.

RESULTS AND DISCUSSION

Debromination of ΣHBCD and Determination of Optimal Conditions

To elucidate the biotic or abiotic nature of ΣHBCD removal, sterile control was conducted (**Figure 2A**). The results of the treatment demonstrated that no significant removal of

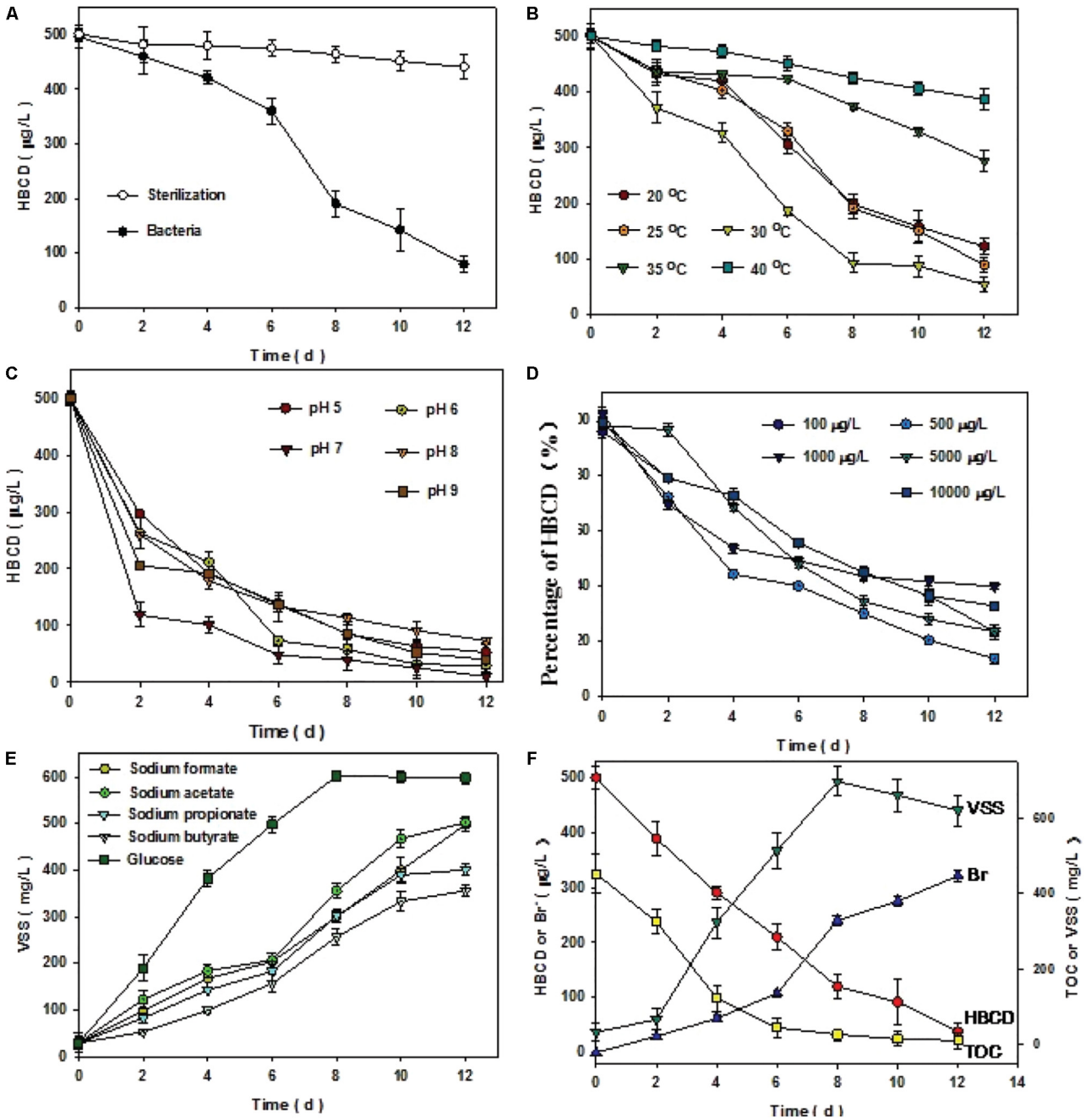

FIGURE 2 | Comparison of sterilization and bacterial treatment **(A)**. Optimal conditions of microbial consortium degrading HBCD after enrichment of 300 days **(B–E)**. Variation of VSS, TOC, HBCD, and bromide ions under the optimal condition **(F)**. The left vertical coordinate represented that the concentration of HBCD or bromide ions (Br^-), and the right coordinate represented the concentration of TOC or VSS. The initial concentration of HBCD and TOC were 500 $\mu g \cdot L^{-1}$ and 452 $mg \cdot L^{-1}$, respectively. The average of each gram of protein content in the mixed liquor is equal to 1.29 g biomass, i.e., VSS. Error bars represent the deviation of three replicates.

ΣHBCD was detected in the biomass-sterilizing microcosms. After 300 days, the results of experiments showed that compared with the sterilization batch, the microbe collected from anaerobic reactor degraded HBCD more effectively, with the HBCD concentration decreasing from 496 to 79 μg/L. Other parameters, including VSS, Br^-, HBCD, and TOC were also measured to strengthen our understanding of the process. About 30°C, pH7, 500 μg/L initial concentration of HBCD, and using glucose as carbon resource were the best condition with degradation rate of 92.4% (**Figures 2B–E**).

Under the optimal condition, GC-MS analyses for ΣHBCD showed that the initial ΣHBCD masses added to the microcosms

A

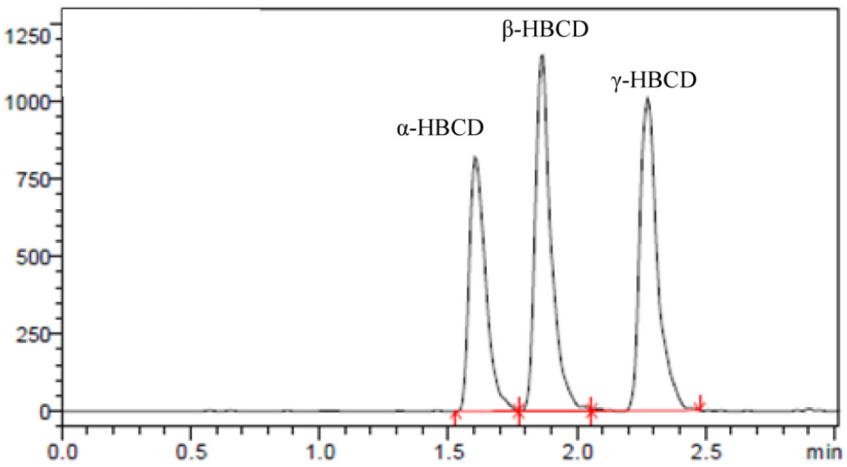

B

HBCD diameters	Zero-order kinetics: $C_t=C_0-k_0t$				Second-order kinetics: $C_t=(1+C_0k_2t)$			
	C_0 (μg/L)	k_0 (μg/L•d)	$t_{1/2}$ (d)	R^2	C^0 (μg/L)	$k_2(\times10^{-3})$ (μg/L•d)	$t_{1/2}$ (d)	R^2
α-HBCD	157.2	11.77	6.7	0.9193	183.1	1.38	4.0	0.9205
β-HBCD	135.9	10.74	6.3	0.9434	171.8	1.87	3.1	0.9179
γ-HBCD	162.0	11.18	7.2	0.9612	188.0	1.15	4.6	0.9382

C

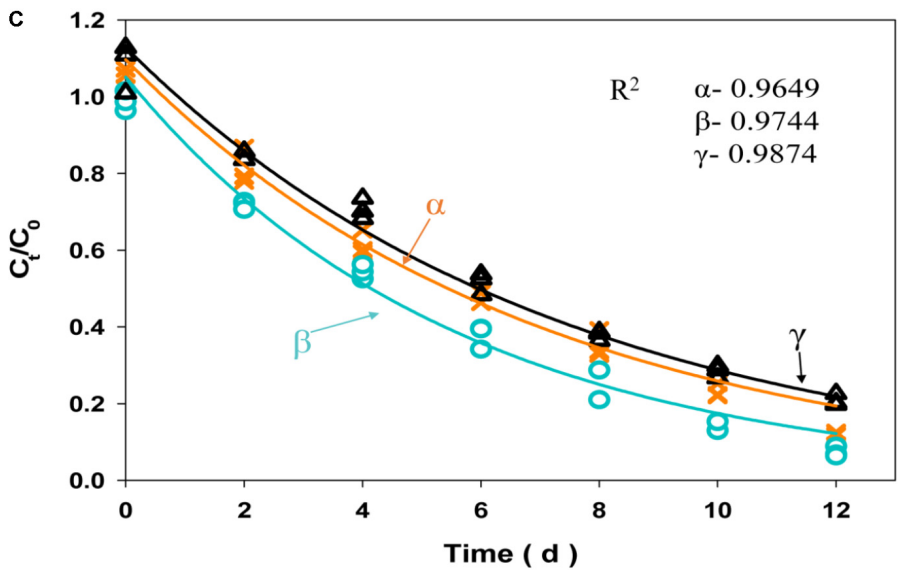

FIGURE 3 | LC/MS/MS chromatograms of three HBCD diastereomers, including α-HBCD, β-HBCD, and γ-HBCD **(A)**. Degradation of individual HBCD diastereomers fitted the zero- and second-order model **(B)**. Degradation of individual HBCD diastereomers was fitted the first-order model **(C)**. The solid lines represent the predicted first-order decay curve deduced from the experimental data. The R^2-value represents the coefficient for each HBCD diastereomers degradation model prediction

were 497 μg/L. Only relatively less biodegradation of ΣHBCD was observed in a lag phase of 6 h (from 497 to 421 μg/L). Thereafter, masses of ΣHBCD in test microcosms decreased sharply with the concentration from 421 to 69 μg/L, i.e., 86% of ΣHBCD had been degraded. Meanwhile, bromides were detected by using IC in the medium and its concentration increased to 321.7 μg/L after 12 days cultivation. The debromination rate is about 86% by mass balance. The dibromocyclododecadiene (DBCD, 322 m/z), a typical debromination product, was detected using UHPLC/Q-TOF-MS during reactive process (Supplementary Figure S1). Comparison of HBCD biodegradation and bromide generation, it could be deducted that bromide released from HBCD reduction by debromination process, which was consistent to the previous reports (Yamada et al., 2009). Transformation and correlation of VSS and TOC indicated that on the one hand, during 12 days cultivation, microbial growth experienced lag phase, log phase, and stationary phase, sequentially (**Figure 2F**; Fang and Jia, 1999); on the other hand, the biodegradation process with the generation of bromide was significantly negative correlated with the TOC analysis.

Debromination of HBCD Diastereomers and Kinetics

It was widely accepted that α-HBCD was the most dominant member among the three diastereomers accumulated in environment, part of which generated from selective biotransformation of β-, and γ-HBCD (Janák et al., 2005). In this study, three diastereomers, including α-HBCD, β-HBCD, and γ-HBCD, were successfully biodegraded by the acclimated microbial consortium in batch experiments (**Figure 3A**). In order to separately illustrate the biodegradation characteristics of the three diastereomers more accurately, three biodegradation kinetic models, including zero-order, first-order, and second-order, were applied to fit the debromination data of three diastereomers, (i.e., α-, β-, and γ-HBCD), respectively (**Figures 3B,C**). Determining from the HBCD biodegrading efficiency (C_t/C_0), it can be concluded that the biodegradation capability of the microbial consortium for the three diastereomers (α-, β-, and γ-HBCD), with the degradation efficiencies of 88.9, 92.6, and 79.1% after 12 days cultivations, respectively, were much higher than the previous reports that was only no more than 21% removal over 56-days incubation with active sludge (Davis et al., 2009; Harrad et al., 2009). No lag phase can be found in the biodegradation process. Biodegradation difference among the three diastereomers were found in the predicted C_t/C_0 curves, which followed the order of β-> γ-> α-, with consistence to the previous results discovered in the freshwater sediment mixtures (Morris et al., 2004), but was different to digester sludge with the order of β-> α-> γ- (Davis et al., 2009) and γ-> β-> α- (Gerecke et al., 2006), respectively. Compared to zero-order (R^2: 0.92–0.96) and second-order model (R^2: 0.92–0.94) (**Figure 3B**), the first-order model fitted biodegradation data of HBCD most with the R^2-values ranging from 0.96 to 0.99. The half-lives for the three diastereomers were 4.3 days (α-HBCD), 3.6 days (β-HBCD), and 5.2 days (γ-HBCD), respectively, which were much shorter than that in the digester sludge described previously with only 50% removal of HBCD in treatment of approximately 15 days (Davis et al., 2009). The results were also not consistent with the previous observation that α-HBCD was debrominated slightly slower than β-HBCD and γ-HBCD (Gerecke et al., 2006).

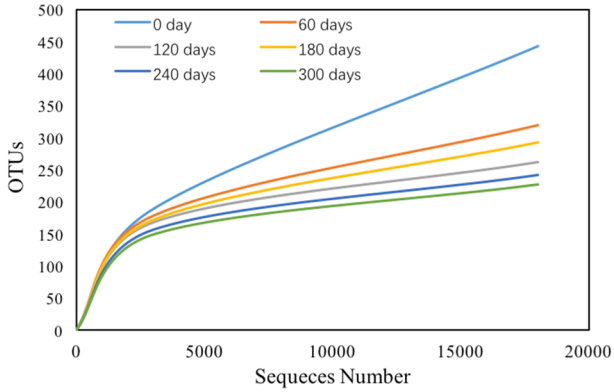

FIGURE 4 | Rarefaction curves of six samples.

Bacterial Community and Diversity Analysis

There were total 138,793 effective sequences obtained, and 2237 OTUs were observed at 97% similarity cutoff. The refraction curve of 97% cutoff similarity was shown in **Figure 4**, and the linearity of the rarefaction curve seemed to be smooth, suggesting that the sequencing depth was sufficient to describe patterns. The bacterial Goods coverage ranged from 0.992 to 0.995 (**Table 2**). All of these results demonstrated that the constructed library for each sample was fully satisfactory to characterize the bacterial communities. Considering Shannon-Wiener index (SWI) ranged from 1.213 to 3.542, the bacterial diversity declined with the enriched time increased. The trends of such index were almost in accordance with Ace and Chao's index. The Simpson index also showed similar trend to the SWI.

Unifrac Clustering of Six Samples at Different Enriched Time

A clustering algorithm (based on Bray–Curtis distance) was applied to measure consistencies among various bacterial communities of the six enriched samples and to group similar samples at the genus level. As shown in **Figure 5A**, the bacterial communities in the six samples could be clustered into three groups: (1) Group 1 contains sample 1 (0 day) and sample 2 (60 days); (2) Group 2 contains sample 3 (120 days) and sample 4 (180 days); (3) Group 3 contains sample 5 (240 days), and sample 6 (300 days). It is obvious that the bacterial community changed with the enriched time.

In order to provide additional support for this analysis, a PCoA analysis was conducted on these validation data based on relative abundances at the genus level. The sample 1 (0 day),

TABLE 2 | The α diversity of each sample.

Sample name	Time	OTUs	97% cutoff				
			Shannon	Chao1	Simpson	ACE	Goods_coverage
1	0	443	3.078	621.4	0.813	671.2	0.994
2	60	319	3.234	522.3	0.779	519.8	0.993
3	120	262	3.542	349.2	0.823	391.7	0.994
4	180	293	2.542	480.5	0.531	423.3	0.992
5	240	241	3.072	342.1	0.704	346.9	0.995
6	300	227	1.213	372.5	0.276	384.1	0.994

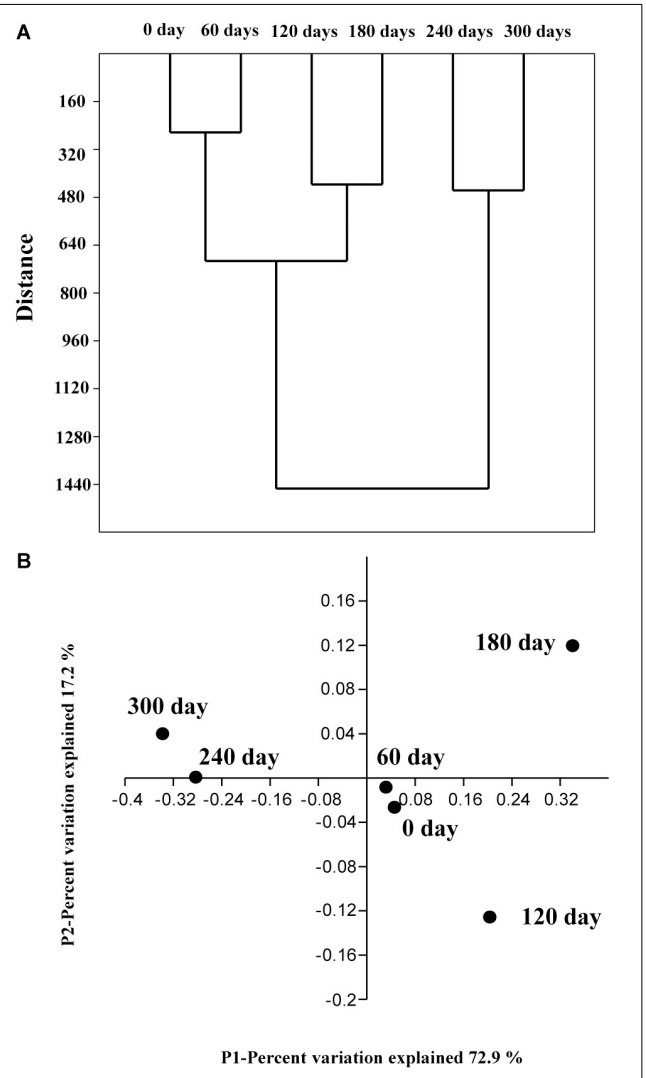

FIGURE 5 | Cluster analysis based on the Bray–Curtis distance **(A)** at the genus level with a 3% cutoff. The genera were divided into three groups. The four-dimensional principal coordinate plot obtained using the genus results of samples collected from 6 enriched times in **(B).**

sample 2 (60 days), sample 3 (120 days), and sample 4 (180 days) were cluster together (samples 1 and 2 are much closer), whereas the other samples fall into another group. A hypothesis can be proposed that the bacterial shift with the enriched time is primarily because of the increase of HBCD concentration during the enrichment process, which was consistent with the previous CA analysis.

Characterization of Bacterial Community

With the gradual increase of HBCD concentration in the process, i.e., from 10, 20–50 mg/L, microbial amount increased sharply (VSS: from 8.7 to 32 mg/L). The relative abundances of different phyla were analyzed, and in these six samples, *Proteobacteria* were the most abundant phylum, accounting for 30.5–59.3% of the total effective bacterial sequences (**Figure 6A**). The other dominant phyla were *Bacteroidetes* (8.6–44.9%, average 22.1%), *Actinobacteria* (14.8–23.6%, average 17.6%), *Firmicutes* (3.5–5.9%, average 4.8%), *Chloroflexi* (0.4–13.4%, average 3.7%), *Nitrospira* (0.07–1.8%, average 0.5%), *Verrucomicrobia* (0–1.2%, average 0.4%), *TM7* (0–0.7%, average 0.3%), and others (0.1–0.5%, average 0.2%). The results presented similar compositions at phylum level with another bacterial consortium degrading BFRs (Peng et al., 2012).

For clone library analysis, 128 clones from the library of baseline control culture and 56 clones from the library of HBCD microcosm were sequenced. Overall, as showed in the **Figure 6B**, the sequenced bacterial clones from baseline control culture refer to *Proteobacteria* (including α-, β-, and γ-*Proteobacteria* with the relative abundance of 2, 39, and 1%, respectively), *Firmicutes* (3%), *Actinobacteria* (4%), *Bacteroidetes* (5%), *Verrucomicrobia* (12%), *Chloroflexi* (17%), TM7 (7%), and unclassified group (11%), which presented similar compositions at phylum level with other sewerage sludge (Zhang et al., 2011). However, as showed in the **Figure 5B**, sequences from HBCD microcosm refer to α-*Proteobacteria* (2%), β-*Proteobacteria* (28%), γ-*Proteobacteria* (3%), *Firmicutes* (4%), *Actinobacteria* (12%), and *Bacteroidetes* (47%). It is worth mentioning that the pressure of HBCD greatly facilitated the growth of *Bacteroidetes* with the abundance from 5 to 47% in the process of acclimation, which may contain some functional microorganism degrading HBCD effectively. Moreover, *Actinobacteria* increased from the initial abundance of 4–12%. By comparison, *Firmicutes*, α-*proteobacteria,* and β-*proteobacteria* increased by a smaller extent, i.e., 1% more after HBCD treatment. However, the abundance of *TM7*, *Chloroflexi*, *Verrucomicrobia*, β-*proteobacteria*, and Unclassified group reduced in varying degrees. The previous

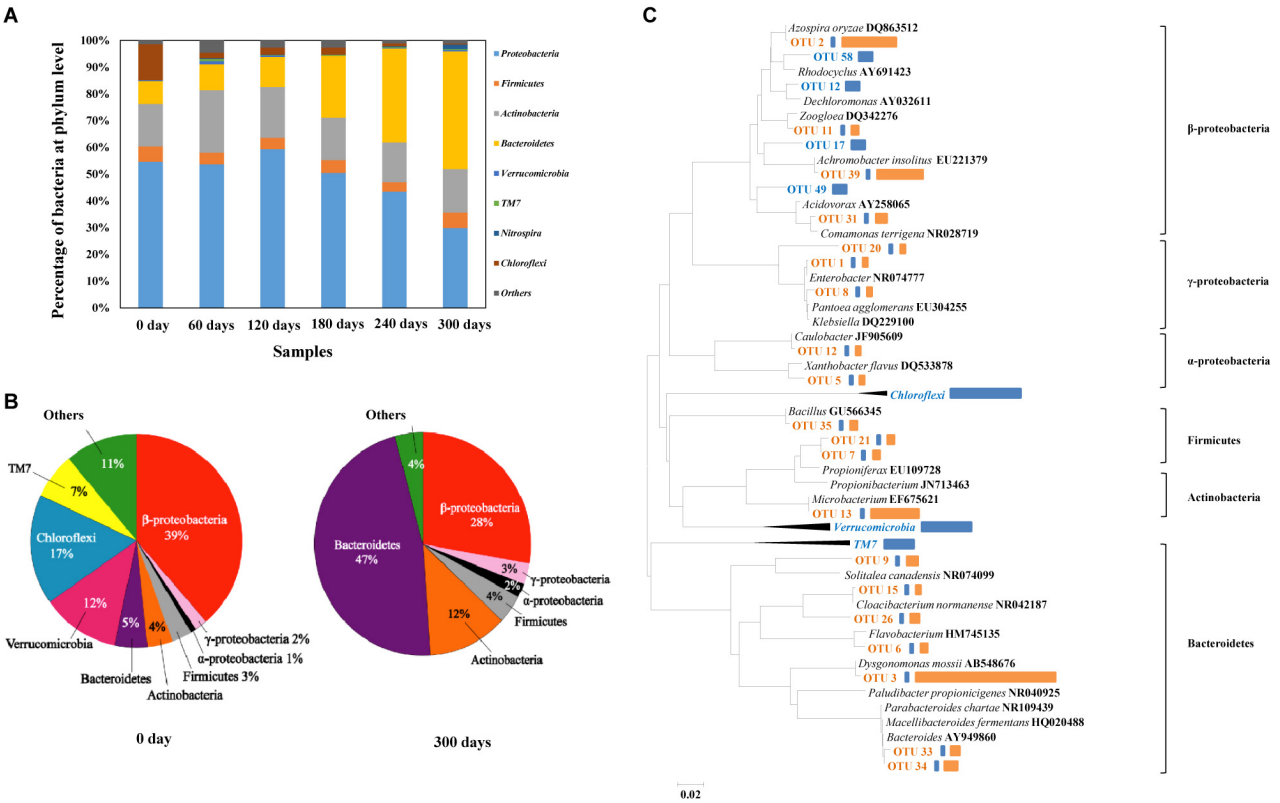

FIGURE 6 | Abundances of phylums in the six enrichment bacterial consortium samples based on high throughput sequencing **(A)**. Distribution of clones in baseline control (i.e., 0 day) and final enrichment (i.e., 300 days) **(B)**. Phylogenetic tree showing the shift of the top 25 most abundant OTUs on which 16S rRNA gene sequences were identified, sequences of baseline control in blue, sequences of baseline and HBCD enrichment in orange **(C)**. Representatives of phylum *Chloroflexi*, *Verrucomicrobia*, and TM7 were used as outgroups for the analysis. Bars to the right of the dendrogram indicated the relative abundance of OTUs based on number of sequences. The blue represented the relative abundance in baseline control, while the orange represented the relative abundance in HBCD enrichment.

report about the acclimation of microbial communities to mineralize the organic compounds indicated that some of enriched microorganism may be utilized to degrade the treated hazardous materials (Xiao and Roberts, 2013). Based on this, it can be speculated that the microbial enriched during the HBCD acclimated process may have a potential capability of degrading HBCD, just like *Pseudomonas,* which has been described previously (Yamada et al., 2009).

Variation of the Bacterial Composition

Among the sequenced clones, 85 and 32 OTUs were identified from the baseline control culture and the HBCD microcosm based on the standard of OTUs (>97% identity), respectively (Kunin et al., 2010). Meanwhile, parts of typical OTUs with high relative abundance or radical change were selected for further research. Compositional and functional shifts in bacterial communities due to environmental factors, such as temperature (Gregory et al., 1997; Hao et al., 2010), have been widely observed in many natural and artificial ecosystems, such as soil, oceans (Gretchen et al., 2010), and reactor etc. In the present study, the HBCD treatment time-series variations in microbial diversity between baseline control culture and HBCD microcosm were analyzed and relative abundance of sequence, especially the top 25 OTUs with high abundance or radical shift were compared (**Figure 6C**). Overall, the abundances of *Bacteroidetes* (OTU3), *Actinobacteria* (OTU13), β-*proteobacteria* (OTU2 and OTU39) increased sharply. However, some microbe with abundant sequences in baseline control, such as *TM7*, *Chloroflexi*, *Verrucomicrobia* nearly decreased to zero after treatment with HBCD for different period. Especially OTU3, with 98% identity to *Dysgonomonas mossii* (AB548676), possessed the largest increase in relative abundance (from 0.5 to 34%) after 300-days incubation with gradually increased HBCD concentrations. Like the increase in abundance of OTU3, OTU2 (*Azospira oryzae*), OTU39 (*Achromobacter insolitus*), and OTU13 (*Microbacterium*) increased from 0.5 to 13%, 11%, and 12%, respectively, which also showed a potential preference to HBCD. Considering the tremendously increased abundance of particular clones in HBCD culture vs. the baseline control culture, it could be presumed that the taxa with radical increase in relative abundance may be important for anaerobic biodegradation of HBCD. Therein, the dominance of *Microbacterium* sp. in the HBCD microcosm supported the proposed role in the HBCD biodegradation process to debromination and further

ring opening reaction (Håstein et al., 2006). In addition, a pure culture, identified as *Achromobacter* sp. by 16S rRNA gene sequence, has been isolated from the HBCD microcosm (unpublished data), which degraded HBCD effectively. Because HBCD degrading efficiency of the mixed culture is better than the pure culture of *Achromobacter* sp., other species obviously increased during the acclimated process, such as *Dysgonomonas* sp., *Azospira* sp., may also play important roles in HBCD degradation. It is worth mentioning that known bacteria for dehalogenation were not found after enrichment (Supplementary Table S1). New functional bacteria in reactive consortia may degrade HBCD by debromination.

CONCLUSION

In the present study, bacterial consortium, effectively removing HBCD by debromination, were enriched by increased the contaminant concentration for over 300 days. Under the optimal conditions, bacterial consortium effectively degraded HBCD, and its three main HBCD diastereomers (α-, β-, and γ-HBCD) fitted first-order model well. The overall microbial community of samples collected from different enriched time had distinct patterns. New functional bacteria may degrade HBCD because no reported dehalogenating bacteria were found. Finally, compared to the sample collected from 0 day, bacterial community obviously varied with the acclimatization time, which was characterized by the special accumulation of *Bacteroidetes*. Over all, these results provided in-depth the anaerobic microbial communities exposed to HBCD.

AUTHOR CONTRIBUTIONS

XP and XJ conceived and designed the experiments. XP and DW did the bulk of data analysis. XP and QH performed the experiments. XP, DW, QH, and XJ wrote the paper. All authors have read and approved the final manuscript.

ACKNOWLEDGMENTS

XP was supported in part by National Natural Science Foundation of China (41703086), Guangdong Province Scientific and Technological Project (2016A050503029), and Fundamental Research Funds for the Universities (161gpy27). XP wish to thank Prof. Tong Zhang (The University of Hong Kong) for the guidance of high throughput sequencing. We thank the seventh Sewage Treatment Plant in Huizhou for the samples provided.

SUPPLEMENTARY MATERIAL

The Supplementary Material for this article can be found online at: https://www.frontiersin.org/articles/10.3389/fmicb.2018.01515/full#supplementary-material

REFERENCES

Abraham, W. R., Nogales, B., Golyshin, P. N., Pieper, D. H., and Timmis, K. N. (2002). Polychlorinated biphenyl-degrading microbial communities in soils and sediments. *Curr. Opin. Microbiol.* 5, 246–253. doi: 10.1016/S1369-5274(02)00323-5

APHA (1995). *Standard Methods for the Examination of Water and Wastewater*. 19th Edn. Washington, DC: American Public Health Association.

Bokulich, N. A., Subramanian, S., Faith, J. J., Gevers, D., Gordon, J. I., Knight, R., et al. (2013). Quality-filtering vastly improves diversity estimates from Illuminaamplicon sequencing. *Nat. Methods* 10, 57–59. doi: 10.1038/nmeth.2276

Chanika, E., Georgiadou, D., Soueref, E., Karas, P., Karanasios, E., Tsiropoulos, N. G., et al. (2011). Isolation of soil bacteria able to hydrolyze both organophosphate and carbamate pesticides. *Bioresour. Technol.* 102, 3184–3192. doi: 10.1016/j.biortech.2010.10.145

Davis, J. W., Gonisor, S. J., Marty, G., Friederich, U., Ariano, J. M. (2004). "Investigation of the biodegradation of [14C] hexabromocyclododecane in sludge, sediment, and soil," in *Proceedings of the Third International Workshop on Brominated Flame Retardants*, Toronto, ON, 239.

Davis, J. W., Gonsior, S. J., Markham, D. A., Friederich, U., Hunziker, R. W., and Ariano, J. M. (2009). Current-use brominated flame retardants in water, sediment, and fish from English lakes. *Environ. Sci. Technol.* 43, 9077–9083. doi: 10.1021/es902185u

Edgar, R. C., Haas, B. J., Clemente, J. C., Quince, Q., and Knight, R. (2011). UCHIME improves sensitivity and speed of chimera detection. *Bioinformatics* 27, 2194–2200. doi: 10.1093/bioinformatics/btr381

Eljarrat, E., Guerra, P., Martínez, E., Farré, M., Alvarez, J. G., López-Teijón, M., et al. (2009). Hexabromocyclododecane in human breast milk: levels and enantiomeric patterns. *Environ. Sci. Technol.* 43, 1940–1946. doi: 10.1021/es802919e

Ema, M., Fujii, S., Hirata-Koizumi, M., and Matsumoto, M. (2008). Two-generation reproductive toxicity study of the flame retar-dant hexabromocyclododecane in rats. *Reprod. Toxicol.* 25, 335–351. doi: 10.1016/j.reprotox.2007.12.004

Fang, H. H. P., and Jia, X. J. (1999). Formation of interim by-products in methanogenic degradation of butyrate. *Water Res.* 33, 1791–1798. doi: 10.1016/S0043-1354(98)00409-6

Fuchedzhieva, N., Karakashev, D., and Angelidaki, I. (2008). Anaerobic biodegradation of fluoranthene under methanogenic conditions in presence of surface-active compounds. *J. Hazard. Mater.* 153, 123–127. doi: 10.1016/j.jhazmat.2007.08.027

Gerecke, A. C., Giger, W., Hartmann, P. C., Heeb, N. V., Kohler, H. P., Schmid, P., et al. (2006). Anaerobic degradation of brominated flame retardants in sewage sludge. *Chemosphere* 64, 311–317. doi: 10.1016/j.chemosphere.2005.12.016

Gretchen, E., Hofmann, J. P., Barry, P. J., Edmunds, R. D., Gates, D. A. T., and Hutchins, D. A., et al. (2010). The effect of ocean acidification on calcifying organisms in marine ecosystems: an organism-to-ecosystem perspective. *Annu. Rev. Ecol. Evol. Syst.* 41, 127–147. doi: 10.1146/annurev.ecolsys.110308.120227

Gregory, P., Zogg, D. R., David, B., Ringelberg, N. W., Macdonald, K. S., and Pregitzer, D. C. W. (1997). Compositional and functional shifts in microbial communities due to soil warming. *Soil Sci. Soc. Am. J.* 61, 475–481. doi: 10.2136/sssaj1997.03615995006100020015x

Hao, L. P., Lü, F., He, P. J., Li, L., and Shao, L. M. (2010). Predominant contribution of syntrophic acetate oxidation to thermophilic methane formation at high acetate concentrations. *Environ. Sci. Technol.* 45, 508–513. doi: 10.1021/es102228v

Harrad, S., Abdallah, M. A., Rose, N. L., Turner, S. D., and Davidson, T. A. (2009). Current-use brominated flame retardants in water, sediment, and fish from English lakes. *Environ. Sci. Technol.* 43, 9077–9083. doi: 10.1021/es902185u

Håstein, T., Hjeltnes, B., Lillehaug, A., Utne, S. J., Berntssen, M., and Lundebye, A. K. (2006). Food safety hazards that occur during the production stage:

challenges for fish farming and the fishing industry. *Rev. Sci. Tech.* 25, 607–625.

Janák, K., Covaci, A., Voorspoels, S., and Becher, G. (2005). Hexabromocyclododecane in marine species from the Western Scheldt Estuary: diastereoisomer-and enantiomer-specific accumulation. *Environ. Sci. Technol.* 39, 1987–1994. doi: 10.1021/es0484909

Kohler, M., Zennegg, M., Bogdal, C., Gerecke, A. C., Schmid, P., Heeb, N. V., et al. (2008). Temporal trends, congener patterns, and sources of octa-, nona-, and decabromodiphenyl ethers (PBDE) and hexabromocyclododecanes (HBCD) in Swiss lake sediments. *Environ. Sci. Technol.* 42, 6378–6384. doi: 10.1021/es702586r

Kunin, V., Engelbrektson, A., Ochman, H., and Hugenholtz, P. (2010). Wrinkles in the rare biosphere: pyrosequencing errors can lead to artificial inflation of diversity estimates. *Environ. Microbiol.* 12, 118–123. doi: 10.1111/j.1462-2920.2009.02051.x

Law, R. J., Bersuder, P., Allchin, C. R., and Barry, J. (2006). Levels of the flame retardants hexabromocyclododecane and tetra-bromobisphenol a in the blubber of harbor porpoises (*Phocoena phocoena*) stranded or bycaught in the UK, with evidence for an increase in HBCD concentrations in recent years. *Environ. Sci. Technol.* 40, 2177–2183. doi: 10.1021/es052416o

Li, Y. N., Zhou, Q. X., Wang, Y. Y., and Xie, X. J. (2011). Fate of tetrabromobisphenol A and hexabromocyclododecane brominated flame retardants in soil and uptake by plants. *Chemosphere* 82, 204–209. doi: 10.1016/j.chemosphere.2010.10.021

Maidak, B. L., Cole, J. R., Lilburn, T. G., Parker, J. C. T., Saxman, P. R., Farris, R. J., et al. (2001). The RDP-II (Ribosomal Database Project). *Nucleic Acids Res.* 29, 173–174. doi: 10.1093/nar/29.1.173

Morris, S., Allchin, C. R., Zegers, B. N., Haftka, J. J. H., Boon, J. P., Belpaire, C., et al. (2004). Distribution and fate of HBCD and TBBP-A flame retardants in North Sea estuaries and aquatic food webs. *Environ. Sci. Technol.* 38, 5497–5504. doi: 10.1021/es049640i

Nakajima, K. T., Shigeno, A. Y., Nomura, N., Onuma, F., and Nakahara, T. (1999). Microbial degradation of polyurethane, polyester polyurethanes and polyether polyurethanes. *Appl. Microbiol. Biotechnol.* 51, 134–140. doi: 10.1007/s002530051373

Palace, V. P., Pleskach, K., Halldorson, T., Danell, R., Wautier, K., Evans, B., et al. (2008). Biotransformation enzymes and thyroid axis disruption in juvenile rainbow trout (*Oncorhynchus mykiss*) exposed to hexabromocyclododecane diastereoisomers. *Environ. Sci. Technol.* 42, 1967–1972. doi: 10.1021/es702565h

Peng, X. X., and Jia, X. S. (2013). Optimization of parameters for anaerobic co-metabolic degradation of TBBPA. *Bioresour. Technol.* 148, 386–393. doi: 10.1016/j.biortech.2013.08.137

Peng, X. X., Qu, X. D., Luo, W. S., and Jia, X. S. (2014). Co-metabolic degradation of tetrabromobisphenol A by novel strains of *Pseudomonas* sp. and *Streptococcus* sp. *Bioresour. Technol.* 169, 271–276. doi: 10.1016/j.biortech.2014.07.002

Peng, X. X., Zhang, Z. L., Luo, W. S., and Jia, X. S. (2013). Biodegradation of tetrabromobisphenol A by a novel *Comamonas* sp. strain, JXS-2-02, isolated from anaerobic sludge. *Bioresour. Technol.* 128, 173–179. doi: 10.1016/j.biortech.2012.10.051

Peng, X. X., Zhang, Z. L., Zhao, Z. L., and Jia, X. S. (2012). 16S ribosomal DNA clone libraries to reveal bacterial diversity in anaerobic reactor-degraded tetrabromobisphenol A. *Bioresour. Technol.* 112, 75–82. doi: 10.1016/j.biortech.2012.02.060

Stapleton, H. M., Allen, J. G., Kelly, S. M., Konstantinov, A., Klosterhaus, S., Watkins, D., et al. (2008). Alternate and new brominated flame retardants detected in U.S. house dust. *Environ. Sci. Technol.* 42, 6910–6916. doi: 10.1021/es801070p

Thomsen, C., Knutsen, H. K., Liane, V. H., Frøshaug, M., Kvalem, H. E., Haugen, M., et al. (2008). Consumption of fish from a contam-inated lake strongly affects the concentrations of polybro-minated diphenyl ethers and hexabromocyclododecane in serum. *Mol. Nutr. Food Res.* 52, 228–237. doi: 10.1002/mnfr.200700123

Urakawa, H., Habbena, W. M., and Stahl, D. A. (2010). High abundance of ammonia-oxidizing *Archaea* in coastal waters, determined using a modified DNA extraction method. *Appl. Environ. Microbiol.* 76, 2129–2135. doi: 10.1128/AEM.02692-09

Wang, S. Q., and He, J. Z. (2013). Dechlorination of commercial PCBs and multiple other halogenated compounds by a sediment-free culture containing *Dehalococcoides* and *Dehalobacter*. *Environ. Sci. Technol.* 47, 10526–10534.

Wang, S. Q., Chng, K. R., Wilm, A., Zhao, S. Y., Nagarajan, N., and He, J. Z. (2014). Genomic characterization of three unique *Dehalococcoides* that respire on persistent polychlorinated biphenyls. *Proc. Natl. Acad. Sci. U.S.A.* 111, 12103–12108. doi: 10.1073/pnas.1404845111

Wang, S. Q., Chng, K. R., Wu, C., Bedard, D. L., and He, J. Z. (2015). Genomic characterization of *Dehalococcoides mccartyi* strain JNA that reductively dechlorinate perchloroethene and polychlorinated biphenyls. *Environ. Sci. Technol.* 49, 14319–14325. doi: 10.1021/acs.est.5b01979

Xiao, Y., and Roberts, D. J. (2013). Kinetics analysis of a salt-tolerant perchlorate-reducing bacterium: effects of sodium, magnesium, and nitrate. *Environ. Sci. Technol.* 47, 8666–8673. doi: 10.1021/es400835t

Yamada, T., Takahama, Y., and Yamada, Y. (2009). Isolation of pseudomonas sp strain hb01 which degrades the persistent brominated flame retardant gamma-hexabromocyclododecane. *Biosci. Biotechnol. Biochem.* 73, 1674–1678. doi: 10.1271/bbb.90104

Zhang, Z. Z., Gai, L. X., Hou, Z. W., Yang, C. Y., Ma, C. Q., Wang, Z. G., et al. (2010). Characterization and biotechnological potential of petroleum-degrading bacteria isolated from oil-contaminated soils. *Bioresour. Technol.* 101, 8452–8456. doi: 10.1016/j.biortech.2010.05.060

Zhang, T., Shao, M. F., and Ye, L. (2011). 454 Pyrosequencing reveals bacterial diversity of activated sludge from 14 sewage treatment plants. *ISME J.* 6, 1137–1147. doi: 10.1038/ismej.2011.188

Zubkov, M. V., Fuchs, B. M., Eilers, H., Burkill, P. H., and Amann, R. (1999). Determination of total protein content of bacterial cells by SYPRO staining and flow cytometry. *Appl. Environ. Microbiol.* 65, 3251–3257.

Conflict of Interest Statement: The authors declare that the research was conducted in the absence of any commercial or financial relationships that could be construed as a potential conflict of interest.

frontiers in Microbiology

ORIGINAL RESEARCH
published: 30 July 2018
doi: 10.3389/fmicb.2018.01713

Diastereoisomer-Specific Biotransformation of Hexabromocyclododecanes by a Mixed Culture Containing *Dehalococcoides mccartyi* Strain 195

*Yin Zhong[1], Heli Wang[1,2], Zhiqiang Yu[1], Xinhua Geng[3], Chengyu Chen[4], Dan Li[1,2], Xifen Zhu[1,2], Huajun Zhen[5], Weilin Huang[5], Donna E. Fennell[5], Lily Y. Young[5] and Ping'an Peng[1,2]**

[1] State Key Laboratory of Organic Geochemistry, Guangzhou Institute of Geochemistry, Chinese Academy of Sciences, Guangzhou, China, [2] University of Chinese Academy of Sciences, Beijing, China, [3] School of Chemistry and Chemical Engineering, Guangzhou University, Guangzhou, China, [4] College of Natural Resources and Environment, South China Agricultural University, Guangzhou, China, [5] Department of Environmental Sciences, Rutgers, The State University of New Jersey, New Brunswick, NJ, United States

OPEN ACCESS

Edited by:
Shanquan Wang,
Sun Yat-sen University, China

Reviewed by:
Ronald Oremland,
United States Geological Survey, United States
Safdar Bashir,
University of Agriculture Faisalabad, Pakistan

***Correspondence:**
Ping'an Peng
pinganp@gig.ac.cn

Specialty section:
This article was submitted to Microbiotechnology, Ecotoxicology and Bioremediation, a section of the journal Frontiers in Microbiology

Received: 22 March 2018
Accepted: 09 July 2018
Published: 30 July 2018

Citation:
Zhong Y, Wang H, Yu Z, Geng X, Chen C, Li D, Zhu X, Zhen H, Huang W, Fennell DE, Young LY and Peng P (2018) Diastereoisomer-Specific Biotransformation of Hexabromocyclododecanes by a Mixed Culture Containing Dehalococcoides mccartyi Strain 195. Front. Microbiol. 9:1713. doi: 10.3389/fmicb.2018.01713

Hexabromocyclododecane (HBCD) stereoisomers may exhibit substantial differences in physicochemical, biological, and toxicological properties. However, there remains a lack of knowledge about stereoisomer-specific toxicity, metabolism, and environmental fate of HBCD. In this study, the biotransformation of (±)α-, (±)β-, and (±)γ-HBCD contained in technical HBCD by a mixed culture containing the organohalide-respiring bacterium *Dehalococcoides mccartyi* strain 195 was investigated. Results showed that the mixed culture was able to efficiently biotransform the technical HBCD mixture, with 75% of the initial HBCD (~12 μM) in the growth medium being removed within 42 days. Based on the metabolites analysis, HBCD might be sequentially debrominated via dibromo elimination reaction to form tetrabromocyclododecene, dibromocyclododecadiene, and 1,5,9-cyclododecatriene. The biotransformation of the technical HBCD was likely diastereoisomer-specific. The transformation rates of α-, β-, and γ-HBCD were in the following order: α-HBCD > β-HBCD > γ-HBCD. The enantiomer fractions of (±)α-, (±)β-, and (±)γ-HBCD were maintained at about 0.5 during the 28 days of incubation, indicating a lack of enantioselective biotransformation of these diastereoisomers. Additionally, the amendment of another halogenated substrate tetrachloroethene (PCE), which supports the growth of strain 195, had a negligible impact on the transformation patterns of HBCD diastereoisomers and enantiomers. This study provided new insights into the stereoisomer-specific transformation patterns of HBCD by anaerobic microbes and has important implications for microbial remediation of anoxic environments contaminated by HBCD using the mixed culture containing *Dehalococcoides*.

Keywords: anaerobic degradation, debromination, stereoisomer, enantiomers, HBCD

INTRODUCTION

Hexabromocyclododecane (HBCD) is a widely used cyclic aliphatic brominated flame retardant found in polymers, textiles, electronic, and electric products. Due to its persistence in the environment and the associated environmental and human health risks (Marvin et al., 2011; Koch et al., 2015), HBCD has been included in the Annex A as a persistent organic pollutant (POP) by the Stockholm Convention (United Nations Environment Programme [UNEP], 2013). Currently, the production and use of HBCD have been banned in many countries (United Nations Environment Programme [UNEP], 2013). It is necessary to better understand the fate of HBCD released to the environment and to develop effective methods to remediate sites contaminated by HBCD.

Technical-grade HBCD is synthesized by bromination of 1,5,9-cyclododecatriene (Heeb et al., 2005), which theoretically leads to a mixture of three major diastereomeric pairs of enantiomers, i.e., (±)α-, (±)β-, and (±)γ-HBCD. The structures of (±)α-, (±)β-, and (±)γ-HBCD are shown in **Figure 1**. Different physiochemical properties (e.g., polarity, water solubility, and dipole moment) of these HBCD stereoisomers may lead to substantial differences in their toxicity, metabolism, and environmental fate (Hakk et al., 2012). Indeed, there is increasing evidence for the diastereoisomer- and/or enantiomer-specific distribution and accumulation in various environmental media (Yu et al., 2008; Haukås et al., 2009; Gao et al., 2011; Zhang et al., 2011; Wu et al., 2014), biota (Janák et al., 2005; Zheng et al., 2017), and even in human body (Shi et al., 2009).

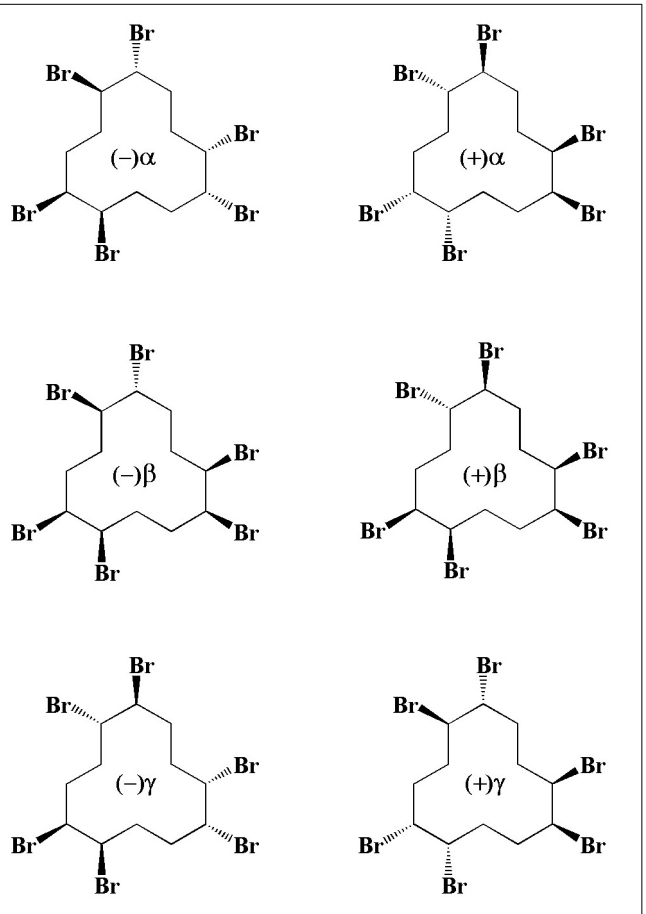

FIGURE 1 | Structure of (±)α-, (±)β-, and (±)γ-HBCD.

Due to its highly hydrophobic nature (log K_{ow} = 5.6), HBCD released to aquatic environments tends to partition to and be accumulated in anoxic sediments (Davis et al., 2005; Law et al., 2014). Anaerobic transformation and degradation is considered as a key pathway of natural attenuation of HBCD under anoxic conditions (Davis et al., 2005, 2006; Gerecke et al., 2006; Stiborova et al., 2015). Experiments with river sediments have shown faster rates of HBCD transformation in anaerobic conditions than in aerobic conditions, with β-HBCD transformation being faster than α- and γ-HBCD (Davis et al., 2005, 2006). However, very little is known about the transformability of HBCD by pure or mixed cultures of anaerobic microbes. Until now, only two HBCD-degrading bacteria have been isolated (Peng et al., 2015) and no mixed cultures containing anaerobic microbes have been demonstrated to be able to debrominate HBCD.

Organohalide-respiring bacteria (OHRB) are key players in natural attenuation of halogenated organic compounds in anoxic environments (Löffler et al., 2013; Wang et al., 2014; Adrian and Löffler, 2016). *Dehalococcoides* is the best-studied OHRB that can degrade halogenated POPs (Adrian and Löffler, 2016). *Dehalococcoides mccartyi* strain 195 (formerly *Dehalococcoides ethenogenes* strain 195) is the first bacterium known to completely dechlorinate tetrachloroethene (PCE) to ethene as the sole electron acceptor for growth (Maymó-Gatell et al., 1997; Löffler et al., 2013). It can cometabolize a broad variety of recalcitrant POPs in mixed cultures or in the presence of other electron acceptors, such as polychlorinated biphenyls (PCBs), polychlorinated dibenzo-*p*-dioxins (PCDD/Fs) and polybrominated diphenyl ethers (PBDEs) (Fennell et al., 2004; He et al., 2006; Liu and Fennell, 2008; Zhen et al., 2014). *D. mccartyi* strain CBDB1 is capable of debrominating many brominated compounds, such as tetra- and penta-brominated diphenyl ether, tetrabromobisphenol A, bromophenol blue, and hexabromobenzene (Lee et al., 2011; Yang et al., 2015). Our previous study showed that mixed cultures containing *D. mccartyi* strain 195 dehalogented halogenated compounds more efficiently than the pure culture (Fennell et al., 2004). Further, the organisms have been utilized successfully in the engineered remediation of natural environments contaminated by halogenated compounds (Schaefer and Steffan, 2016).

Therefore, this study was designed to examine the mixed culture containing *D. mccartyi* strain 195 for their ability to biotransform HBCD as the sole halogenated substrate or in the presence of PCE. Special attention was given to the change in the shift pattern transformation characteristics of diastereoisomers and enantiomers of HBCD. The results obtained here will give new insight into the biotransformation patterns of HBCD stereoisomers by OHRB under anaerobic conditions and facilitate

the practical application of OHRB during bioremediation of HBCD-contaminated anoxic environments.

MATERIALS AND METHODS

Chemicals and Culture Preparation

The technical HBCD mixture was purchased from Tokyo Chemical Industry (Tokyo, Japan). Hexabromobenzene (97%) was purchased from Alfa Aesar (Haverhill, MA, United States). Hexane (Merck, Darmstadt, Germany), isooctane (Alfa Aesar, Haverhill, MA, United States), and toluene (JT Baker, Phillipsburg, NJ, United States) were used as received.

The mixed culture containing *D. mccartyi* strain 195 was cultured in the presence of butyric acid and tetrachloroethene (PCE) as the electron donor and acceptor under anaerobic condition, respectively (Zhen et al., 2014). The quantitative polymerase chain reaction (qPCR) analysis and high throughput sequencing analysis showed that *D. mccartyi* strain 195 still was the only dehalogenating bacteria detected in the mixed culture, which was consistent with the result of our previous study (Fennell et al., 2004; Krumins et al., 2009; Zhen et al., 2014).

The composition of growth medium of this mixed culture was described previously by Fennell (1998). Briefly, the medium consisted of NH_4Cl (0.2 g L^{-1}), K_2HPO_4 (0.1 g L^{-1}), KH_2PO_4 (0.055 g L^{-1}), $MgCl_2{\cdot}6H_2O$ (0.2 g L^{-1}), $FeCl_2{\cdot}4H_2O$ (0.1 g L^{-1}), $Na_2S{\cdot}9H_2O$ (0.5 g L^{-1}), $NaHCO_3$ (6 g L^{-1}), resazurin (0.001 g L^{-1}), vitamin stock solutions and trace metal solution.

Biotransformation Experiment

A batch experiment was conducted for quantifying the transformability of HBCD by the mixed culture. Serum bottles (60 ml) sealed with a Teflon-coated gray butyl rubber stopper and crimped with an aluminum crimp cap were used as the batch reactor. Firstly, HBCD stock solution (1 mL) was added to each bottle containing 1 g of dry and sterile silica powder via a sterile glass syringe. After the solvent was evaporated under sterile and anaerobic conditions, the bottles were purged for 15 min with anoxic and sterile gas mixture (70% N_2/30% CO_2). The mixed culture (50 mL), with the density of *D. mccartyi* strain 195 at approximately 2×10^8 cells mL^{-1}, was transferred into each bottle under sterile and anaerobic conditions. The initial concentration of HBCD in the medium was ∼12 μM. Four sets of triplicate bottles were set up at 30°C. One set of bottles was amended with active cells and HBCD as the sole halogenated compound. The second set of bottles was amended with active cells, HBCD and PCE for testing the effects of PCE as an alternative electron acceptor (also a growth substrate) on the biotransformation of HBCD. The third set of bottles was amended with active cells and PCE as the sole halogenated compound. The fourth set of bottles were control reactors containing HBCD and cells killed by autoclaving for 30 min on each of three consecutive days. All treatments were conducted in triplicate. In addition, 100 μL of neat butyric acid and 50 μL of fermented yeast extract solution (50 g L^{-1}) were added into all bottles as carbon source and nutrient source every 2 weeks, respectively (Zhen et al., 2014). All bottles were shaken at 250 rpm on a shaker placed in the darkroom at 30°C. At predetermined time intervals, an aliquot of 1 mL of the cultures were sampled from each bottle via sterile and anoxic syringe and was freeze-dried for the analysis of residual concentration of HBCD, HBCD diastereoisomers, and enantiomers.

In order to identify the degradation products of HBCD, a separate experiment was performed using higher initial concentration of HBCD (∼38 μM) so that sufficient mass of the products was obtained. The other experimental conditions were kept the same as those of above batch experiments. At predetermined time, an aliquot of 1 mL of the cultures were sampled from each bottle via sterile and anoxic syringe and was freeze-dried for the analysis of HBCD products.

Analytical Methods

An Agilent 6890N network GC system equipped with Agilent 5973N network mass selective detector was employed for the determination of residual HBCD and potential low debrominated products. An Agilent 1100 series HPLC system with a API 4000 triple quadrupole mass spectrometer (LC-MS/MS) with a TurboIonSpray ionization interface was employed for the determination of HBCD diastereoisomers and enantiomers.

For quantifying concentrations of residual HBCD, the freeze-dried samples were spiked with 20 μL of 450 μM hexabromobenzene as the recovery surrogate and ultrasonically extracted twice with 1 mL of isooctane/hexane mixtures (9:1, v/v) for 15 min. Then, the supernatants were combined, concentrated and analyzed by GC-MS equipped with an on-column injector and a DB-5 capillary GC column (15 m length, 0.25 mm id and 0.1 μm film thickness) operating in negative chemical ionization (NCI) mode. The ions with m/z 79, 81, 561, and 563 were selectively monitored. A cold on-column injector was operated in track-oven mode. The oven operation temperature was set from 60°C for 1 min, increased to 260°C at 10°C min^{-1}, and held at 260°C for 5 min, and then increased to 320°C at 20°C min^{-1}. The ion source and quadrupole temperatures were set at 150 and 200°C, respectively. Helium was used as the carrier gas at a flow rate of 1.2 mL min^{-1}, and methane was used as the moderating gas. Quality assurance was performed by the analyses of spiked blanks. The recoveries of HBCD and hexabromobenzene in spiked blanks ranged from 96 to 108% and 98 to 113%, respectively. Limits of detection (LOD) and limits of quantification (LOQ) were defined a signal-to-noise ratio of 3 and 10, respectively. LOD and LOQ of HBCD were 0.03 and 0.11 ng, respectively.

For identifying potential debrominated products, triplicate samples were combined, concentrated, and analyzed by GC-MS equipped with a Rtx-5 ms fused silica capillary column (30 m length, 0.25 mm id, and 0.25 μm film thickness) operating in electron ionization (EI) mode. The GC column temperature was programmed to maintain at 80°C for 1 min, ramped at 10°C min^{-1}, to 300°C, and held at 300°C for 10 min. The temperature of injector was set to 250°C. The carrier gas was helium at a flow rate of 1 mL min^{-1}. Both ion source and GC-MS-EI interface temperature were held isothermally at 250°C. The mass spectrometer was run in electron

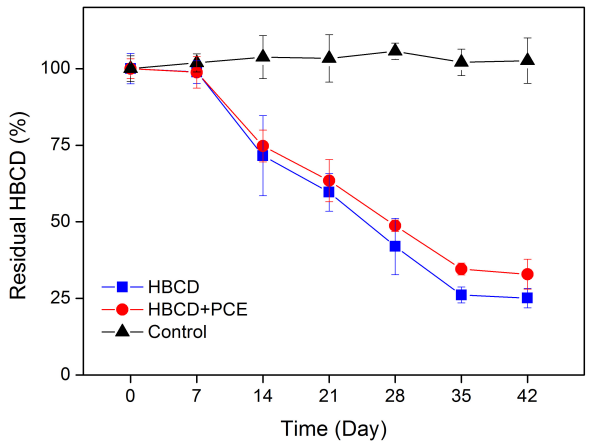

FIGURE 2 | Anaerobic transformation of the technical HBCD by the mixed culture in the presence or absence of PCE. The initial concentration of HBCD coating on the silicate in the growth medium was 12 μM.

impact ionization mode (70 eV) and was scanned from 45 to 700 amu.

Three major HBCD diastereoisomers (α-, β-, and γ-HBCD) and their enantiomers were analyzed using a LC-MS/MS according to the method described by Yu et al. (2008). The enantiomeric composition was expressed as enantiomeric fraction (EF). In order to avoid the matrix effect, ^{13}C-labeled α-, β-, and γ-HBCD were added as internal standards for both quantification and correction of EF values. The corrected EFs were calculated by the following equation:

$$EF = \frac{A_+/A_{+c13}}{A_+/A_{+c13} + A_-/A_{-c13}}$$

where A_+ and A_- represent the peak areas of (+)-enantiomer and (−)-enantiomer, respectively, while A_{+C13} and A_{-C13} represent the peak areas of (+)-enantiomer and (−)-enantiomer labeled by ^{13}C, respectively.

RESULTS AND DISCUSSION

The mixed culture containing *D. mccartyi* strain 195 have demonstrated the ability of dehalogenating recalcitrant POPs like PCBs and PCDD/Fs (Liu and Fennell, 2008; Zhen et al., 2014), which might also have the potential to transform HBCD. As shown in **Figure 2**, when technical HBCD was added as the sole halogenated amendment to the mixed culture, loss of the compounds was observed, supporting our hypothesis. After a lag period of approximately 7 days, the mixed culture exhibited high activity for the biotransformation of the technical HBCD. After 42 days of incubation, 75% of the initial HBCD (12 μM, equal to 7704 μg L^{-1}) in the growth medium of the live mixed culture disappeared. There was no significant degradation between 35 and 42 days. It was likely because the residual concentration of HBCD as the electron acceptor was too low to sustain the growth of dehalogenating bacteria, therefore, the degradation rate did not increase. Indeed, a similar phenomenon was reported in a previous study (Cupples et al., 2004). No apparent HBCD removal was observed in the killed control throughout the experiment period.

As shown in **Figure 3**, there were three metabolites produced during anaerobic degradation of HBCD, i.e., Peaks I, II, and III. As shown in **Figure 4**, Peaks I and II were tentatively identified as tetrabromocyclododecene and dibromocyclododecadiene, respectively, by comparison with mass spectral of debromination products of HBCD

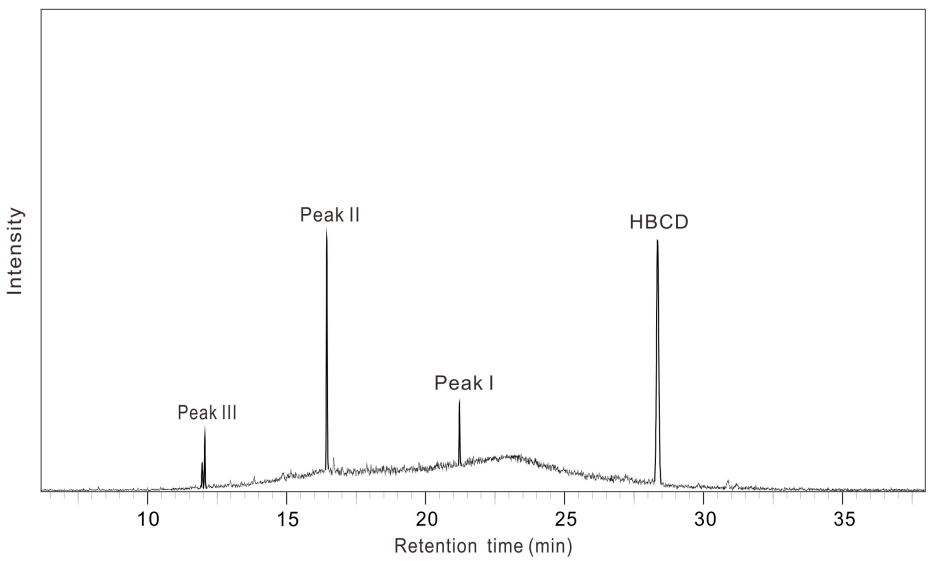

FIGURE 3 | Formation of degradation products of HBCD by the mixed culture.

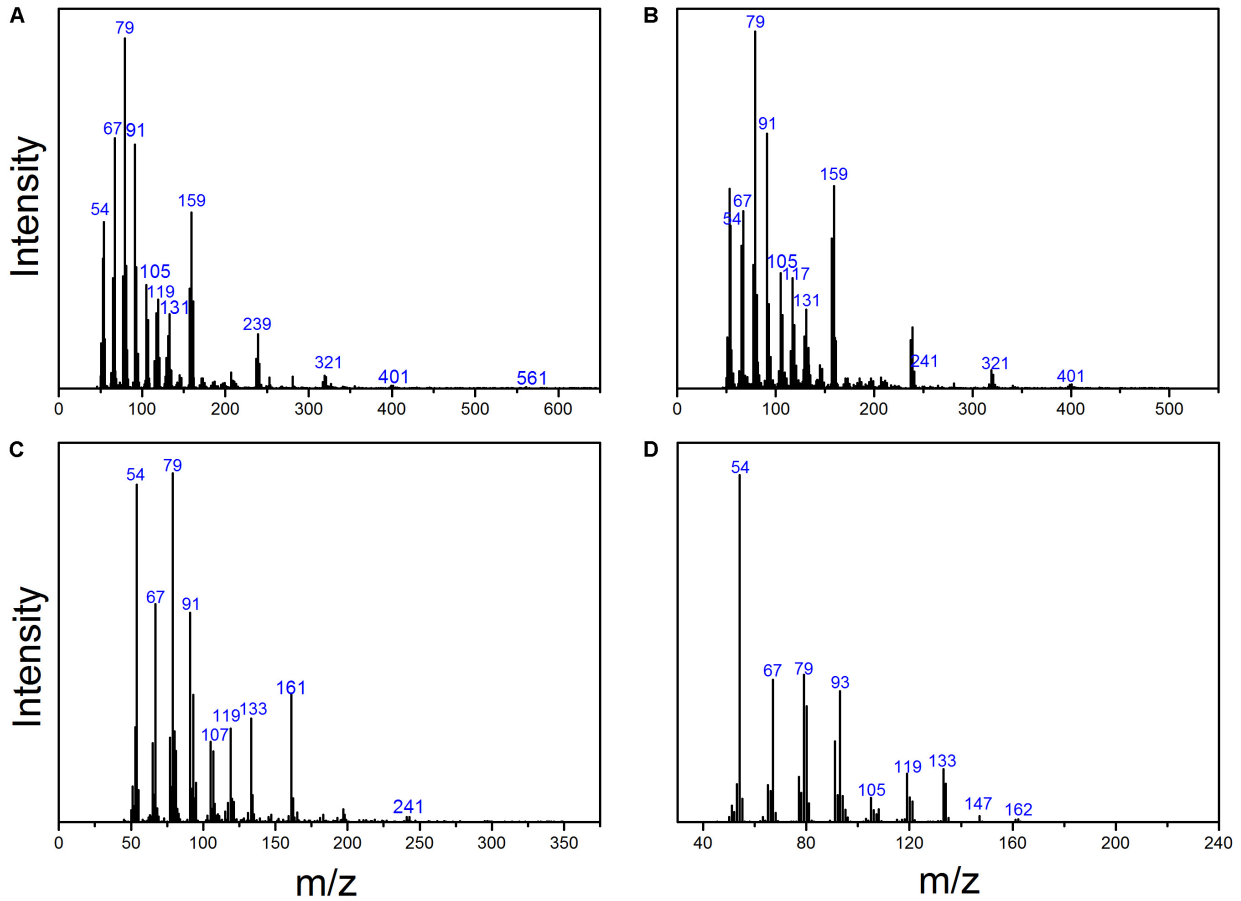

FIGURE 4 | Mass spectrum of HBCD and its debromination products. **(A)** HBCD; **(B)** Peak I, tetrabromocyclododecene; **(C)** Peak II, dibromocyclododecadiene; and **(D)** Peak III, 1,5,9-cyclododecatriene.

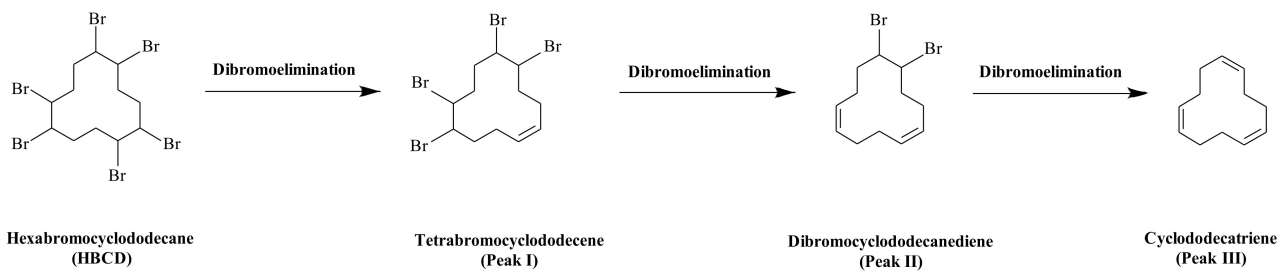

FIGURE 5 | The proposed debromination pathway of HBCD by the mixed culture.

reported in previous studies (Li et al., 2016, 2017). Peak III was identified by 1,5,9-cyclododecatriene by comparison with the respective retention time and mass spectrum of external standards. As shown in the proposed debromination pathway (**Figure 5**), HBCD was sequentially debrominated by anaerobic bacteria via dibromo elimination reaction to form tetrabromocyclododecene, dibromocyclododecadiene, and 1,5,9-cyclododecatriene. Similar debromination products and pathway have been reported in anaerobic degradation of HBCD by pure culture of *Achromobacter* sp. as well as in digester sludge and freshwater aquatic sediments (Davis et al., 2006; Peng et al., 2015).

Our observations are consistent with a prior report which showed *Achromobacter* sp. HBCD-1 could anaerobically transform 35.1% of 5000 $\mu g\ L^{-1}$ HBCD in its growth medium within 8 days (Peng et al., 2015). However, it is difficult to make a detailed comparison of our observations with other studies of transformation of HBCD by OHRB due to limited published data. Indeed, it is interesting to show that *Dehalococcoides* organisms utilized HBCD relatively rapidly compared to PBDEs

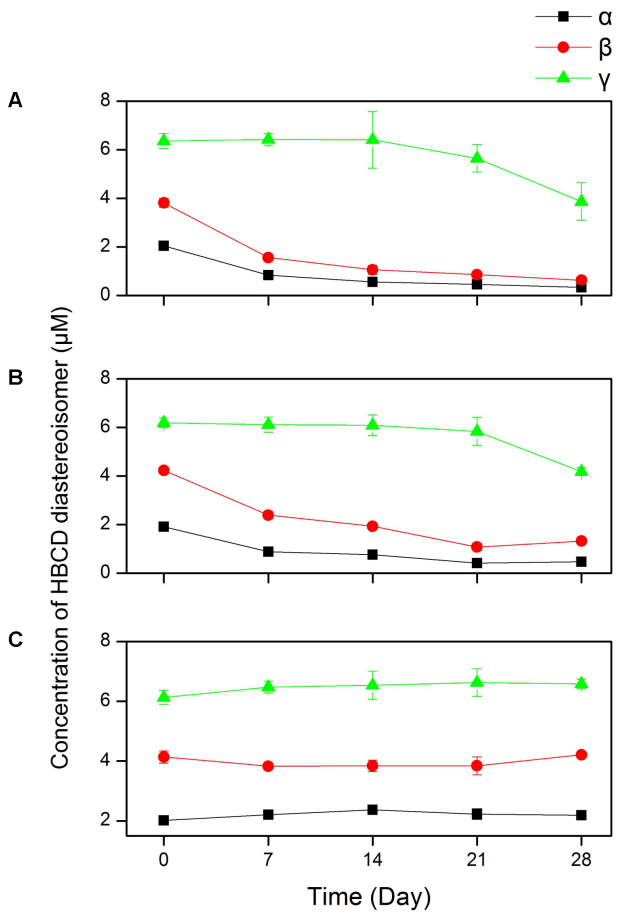

FIGURE 6 | The residual concentration of three HBCD diastereoisomers during the degradation of HBCD by the mixed culture when HBCD was amended as the sole halogenated substrate **(A)**, HBCD co-existed with PCE **(B)**, and in control with killed cells **(C)** in the growth medium.

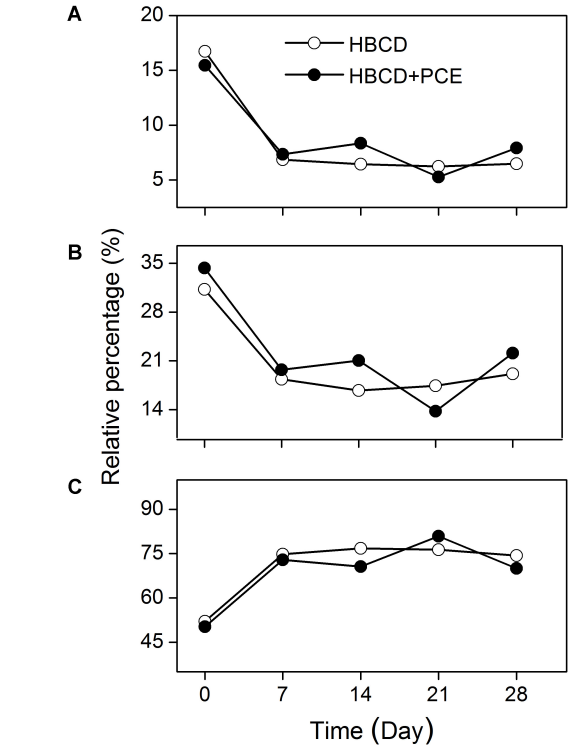

FIGURE 7 | The dynamics of the proportions of α-HBCD **(A)**, β-HBCD **(B)**, and γ-HBCD **(C)** to the total HBCD throughout the transformation experiment, where HBCD was degraded as the sole halogenated substrate or in the presence of PCE by the mixed culture.

(He et al., 2006). As shown by He et al. (2006), pure and enriched culture containing *D. mccartyi* strain 195 exhibited detectable debromination activity of octa-BDEs within 6 and 3 months, respectively. In previous studies, when more hydrophobic POPs were added as the sole electron acceptors (Fennell et al., 2004; He et al., 2006; Liu and Fennell, 2008; Zhen et al., 2014), the rates of dechlorination were slower. For instance, it was shown that less than 20% of the initial 1,2,3,4,7,8-hexachlorodibenzofuran in growth medium was dechlorinated to less chlorinated daughter products by a mixed culture containing *D. mccartyi* strain 195 after 195 days of incubation (Liu and Fennell, 2008). Nonetheless, our results mentioned above, in combination with the fact that *D. mccartyi* strain 195 has 17 putative reductive dehalogenase genes (Seshadri et al., 2005), warrant further study on the potential activities of *Dehalococcoides* organisms for the degradation of other POPs and/or halogenated contaminants.

Note that the biotransformation of the technical HBCD by the mixed culture containing *D. mccartyi* strain 195 was likely diastereoisomer-specific (**Figure 6**). After 28 days of incubation, the remaining percentages of α-HBCD, β-HBCD, and γ-HBCD were 16, 26, and 60%, respectively (**Figure 6A**). It suggested that the transformation rate of three HBCD diastereoisomers followed the order of α-HBCD > β-HBCD > γ-HBCD. The pattern of transformation rates of α-, β-, and γ-HBCD by the

TABLE 1 | Enantiomer fractions (EFs) of α-, β-, and γ-HBCD during the transformation of the technical HBCD mixture by the mixed culture containing *D. mccartyi* strain 195.

Treatment	Time (Day)	EF_α	EF_β	EF_γ
Control	0	0.51	0.49	0.51
	7	0.52	0.51	0.51
	14	0.52	0.51	0.51
	21	0.51	0.51	0.50
	28	0.53	0.50	0.50
HBCD	0	0.52	0.50	0.50
	7	0.49	0.50	0.50
	14	0.52	0.50	0.51
	21	0.52	0.50	0.51
	28	0.52	0.51	0.51
PCE+HBCD	0	0.52	0.50	0.50
	7	0.51	0.50	0.50
	14	0.52	0.51	0.50
	21	0.52	0.50	0.51
	28	0.49	0.51	0.50

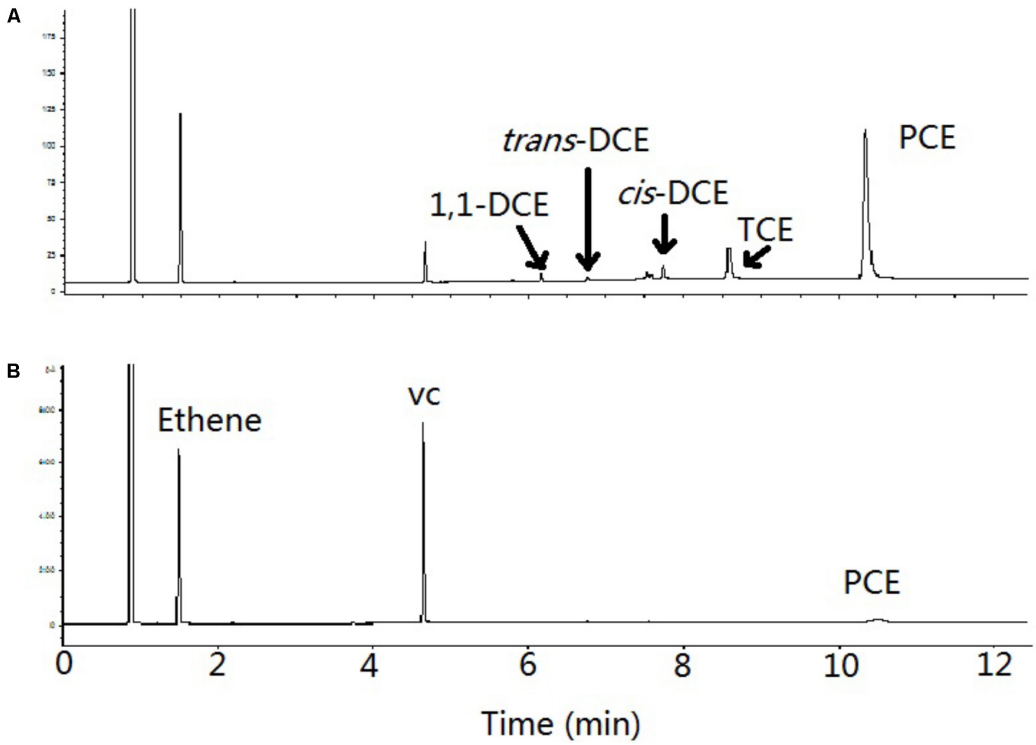

FIGURE 8 | Degradation of PCE and its intermediates by the mixed culture in presence of HBCD at day 7 **(A)** and day 28 **(B)**.

mixed culture used in this study (**Figure 6A**) was consistent with that of the three diastereoisomers by the anaerobic bacterium *Achromobacter* sp. HBCD-1 (Peng et al., 2015). In contrast, it was reported that the anaerobic biotransformation of α-HBCD in sewage sludge (Gerecke et al., 2006) and river sediments (Davis et al., 2006) was slower than that of β-HBCD and γ-HBCD. These different outcomes could be caused by a number of environmental factors. It is highly likely that other microbes, rather than *Dehalococcoides* or *Achromobacter* organisms, may be able to debrominate HBCD via different mechanisms in the sewage sludge and river sediments. It is also apparent that the initial concentrations of HBCD diastereoisomers in the technical HBCD mixtures used are likely very different from those present in the environments, causing varied rates of biotransformation of different diastereoisomers (Davis et al., 2006). Interestingly, α-HBCD with higher hydrophobicity was adsorbed more strongly on sediment particles in the environments (Marvin et al., 2011), rendering lower bioavailability of α-HBCD and hence retarded degradation rate in the environments. The diastereoisomer-specific degradation of HBCD in the presence of PCE by the mixed culture is shown in **Figure 6B** and discussed below in detail. No diastereoisomer-specific transformation was observed in control (**Figure 6C**).

For better understanding the effect of diastereoisomer-specific biotransformation on the change in stereoisomeric composition of HBCD, the dynamics of the proportions of individual diastereoisomers to the total HBCD throughout the debromination experiment should be considered. The proportion of γ-HBCD was the largest among the diastereoisomers and increased with time (**Figure 7C**), whilst those of all the other diastereoisomers tended to decrease with time (**Figures 7A,B**). In general, these results presented a plausible explanation for the observation that γ-HBCD was the most dominant diastereoisomer in many anoxic sediments (Harrad et al., 2009; Gao et al., 2011; Meng et al., 2011; Zhang et al., 2011; Klosterhaus et al., 2012; Wu et al., 2014). However, the increased proportion of γ-HBCD observed in this study was inconsistent with the phenomenon that the proportion of γ-HBCD in some river sediments was much lower than those of technical HBCD mixtures (Wu et al., 2014). This discrepancy could be explained by a scenario that abiotic transformation played an important role in the distribution and accumulation of HBCD diastereoisomers in the sediments, further reflecting the complexity of factors influencing the environmental fates of HBCD diastereoisomers.

Enantiomeric selectivity of HBCD played key role in the toxicity and fate of HBCD stereoisomers in the environment. There is strong evidence that the environmental fates of HBCD are enantioselective (Zhang et al., 2011; Zheng et al., 2017), while enantiomeric analysis has received relatively little attention in the literature on anaerobic degradation of HBCD. In this study, the occurrences of three pairs of enantiomers in the technical HBCD mixture, i.e., (±)α-, (±)β-, and (±)γ-HBCD, were confirmed. Further, EFs of the three HBCD diastereoisomers were calculated to determine whether enantiomeric selectivity was involved in the HBCD transformation by the mixed culture.

As shown in **Table 1**, the ranges of EFs of α-, β-, and γ-HBCD throughout the transformation experiment were 0.49–0.52, 0.50–0.51, and 0.50–0.51, respectively. That is, the EFs of the three diastereoisomers were close to 0.5, suggesting that the anaerobic transformation of HBCD was not an enantioselective process. Similarly, no enantioselective pattern was observed in the anaerobic degradation of HBCD in sewage sludge (Gerecke et al., 2006). However, the racemic α-, β-, and γ-HBCD could undergo enantioselective degradation under aerobic conditions (Heeb et al., 2014, 2017). For instance, an aerobic HBCD-degrading bacterium (*Sphingobium chinhatense* IP26) could transform (+)α-, (−)β-, and (−)γ-HBCD at a faster rate than those of their enantiomers (Heeb et al., 2017). Dehalogenase LinB from *Sphingobium indicum* B90A transformed (−)α-, (+)β-, and (+)γ-HBCD at faster rates than those of their enantiomers (Heeb et al., 2012), whilst dehalogenase LinA could transform only (−)β-HBCD substantially (Heeb et al., 2014). In addition, enantioselective transformation and enrichment of HBCD were even observed in animals (Janák et al., 2005; Du et al., 2012). These findings indicate that mechanisms of anaerobic biotransformation of HBCD enantiomers are considerably different from those of aerobic biodegradation.

Co-amendment of halogenated growth substrate (haloprimer) has been shown to stimulate the dehalogenating activity of *D. mccartyi* strain 195 for the debromination of recalcitrant halogenated compounds such as 1,2,3,4,7,8-hexachlorodibenzofuran (Ahn et al., 2008; Liu and Fennell, 2008). However, in this study, the biotransformation rate of the technical HBCD by the mixed culture was not enhanced when PCE was amended as an additional halogenated substrate (**Figure 2**). In addition, the presence of PCE had negligible effects on the transformation patterns of individual diastereoisomers and enantiomers (**Figures 6**, **7**, and **Table 1**). On the other hand, the degradation of PCE by the mixed culture and dechlorinated products (e.g., TCE, DCE, and vinyl chloride) was hardly influenced by the presence of HBCD after 28-day of incubation (**Figure 8**). These results indicate that the dehalogenases responsible for the debromination of HBCD by the mixed culture might be different from those of PCE. Another important implication of these results is that the addition of co-substrate PCE to stimulate the transformation of HBCD might not be useful when the mixed culture containing *D. mccartyi* strain 195 is applied into the remediation of anoxic environments contaminated by HBCD.

CONCLUSION

This study demonstrated that the mixed culture containing *D. mccartyi* strain 195 can relatively rapidly transform the technical HBCD mixture when added as the sole halogenated substrate and that the loss/transformation is stereoisomer-specific. It suggested that the transformation rate of three HBCD diastereoisomers followed the order of α-HBCD > β-HBCD > γ-HBCD. The pathway of HBCD degradation has been proposed. The results also showed that addition of PCE as a co-substrate had negligible effect on the removal of both PCE and HBCD by the mixed culture. This may indicate that *D. mccartyi* strain 195 utilizes different enzymes for the biotransformation of HBCD and PCE. The results not only provide insight to the environmental fate of HBCD stereoisomers and mechanistic understanding of biotransformation of HBCD, but also facilitate the practical guidance for design of bioremediation schemes by using halogen-respirators to treat environments contaminated with HBCD.

AUTHOR CONTRIBUTIONS

PP, LY, and WH designed the project. YZ, ZY, HW, XG, CC, DL, XZ, and HZ performed the experiments and data analyses. DF provided the culture. YZ wrote the manuscript. PP, LY, DF, ZY, and WH reviewed the manuscript. All authors have read and approved the manuscript.

FUNDING

This study was supported financially by the National Natural Science Foundation of China (Nos. 41473107 and 41773132) and GIGCAS (Nos. IS-2561, SKLOGA2016-A04, and SKLOGA201618).

ACKNOWLEDGMENTS

We thank Dr. Lisa A. Rodenburg for her assistance in the analysis of technical HBCD by on-column GC-MS. We also thank Ms. Maria Rivera for helping conduct the anaerobic experiment.

REFERENCES

Adrian, L., and Löffler, F. E. (2016). *Organohalide-Respiring Bacteria*. Heidelberg: Springer. doi: 10.1007/978-3-662-49875-0

Ahn, Y. B., Liu, F., Fennell, D. E., and Häggblom, M. M. (2008). Biostimulation and bioaugmentation to enhance dechlorination of polychlorinated dibenzo-p-dioxins in contaminated sediments. *FEMS Microbiol. Ecol.* 66, 271–281. doi: 10.1111/j.1574-6941.2008.00557.x

Cupples, A. M., Spormann, A. M., and McCarty, P. L. (2004). Vinyl chloride and *cis*-dichloroethene dechlorination kinetics and microorganism growth under substrate limiting conditions. *Environ. Sci. Technol.* 38, 1102–1107. doi: 10.1021/es0348647

Davis, J. W., Gonsior, S., Marty, G., and Ariano, J. (2005). The transformation of hexabromocyclododecane in aerobic and anaerobic soils and aquatic sediments. *Water Res.* 39, 1075–1084. doi: 10.1016/j.watres.2004.11.024

Davis, J. W., Gonsior, S. J., Markham, D. A., Friederich, U., Hunziker, R. W., and Ariano, J. M. (2006). Biodegradation and product identification of [14C] hexabromocyclododecane in wastewater sludge and freshwater aquatic sediment. *Environ. Sci. Technol.* 40, 5395–5401. doi: 10.1021/es060009m

Du, M., Lin, L., Yan, C., and Zhang, X. (2012). Diastereoisomer-and enantiomer-specific accumulation, depuration, and bioisomerization of hexabromocyclododecanes in zebrafish (*Danio rerio*). *Environ. Sci. Technol.* 46, 11040–11046. doi: 10.1021/es302166p

Fennell, D. E. (1998). *Comparison of Alternative Hydrogen Donors for Anaerobic Reductive Dechlorination of Tetrachloroethene*. Ithaca, NY: Cornell University.

Fennell, D. E., Nijenhuis, I., Wilson, S. F., Zinder, S. H., and Häggblom, M. M. (2004). *Dehalococcoides ethenogenes* strain 195 reductively dechlorinates diverse chlorinated aromatic pollutants. *Environ. Sci. Technol.* 38, 2075–2081. doi: 10.1021/es034989b

Gao, S., Wang, J., Yu, Z., Guo, Q., Sheng, G., and Fu, J. (2011). Hexabromocyclododecanes in surface soils from e-waste recycling areas and industrial areas in South China: concentrations, diastereomer-and enantiomer-specific profiles, and inventory. *Environ. Sci. Technol.* 45, 2093–2099. doi: 10.1021/es1033712

Gerecke, A. C., Giger, W., Hartmann, P. C., Heeb, N. V., Kohler, H. P. E., Schmid, P., et al. (2006). Anaerobic degradation of brominated flame retardants in sewage sludge. *Chemosphere* 64, 311–317. doi: 10.1016/j.chemosphere.2005.12.016

Hakk, H., Szabo, D. T., Huwe, J., Diliberto, J., and Birnbaum, L. S. (2012). Novel and distinct metabolites identified following a single oral dose of α- or γ-hexabromocyclododecane in mice. *Environ. Sci. Technol.* 46, 13494–13503. doi: 10.1021/es303209g

Harrad, S., Abdallah, M. A. E., Rose, N. L., Turner, S. D., and Davidson, T. A. (2009). Current-use brominated flame retardants in water, sediment, and fish from English lakes. *Environ. Sci. Technol.* 43, 9077–9083. doi: 10.1021/es902185u

Haukås, M., Hylland, K., Berge, J. A., Nygård, T., and Mariussen, E. (2009). Spatial diastereomer patterns of hexabromocyclododecane (HBCD) in a Norwegian fjord. *Sci. Total Environ.* 407, 5907–5913. doi: 10.1016/j.scitotenv.2009.08.024

He, J., Robrock, K. R., and Alvarez-Cohen, L. (2006). Microbial reductive debromination of polybrominated diphenyl ethers (PBDEs). *Environ. Sci. Technol.* 40, 4429–4434. doi: 10.1021/es052508d

Heeb, N. V., Grubelnik, A., Geueke, B., Kohler, H. P. E., and Lienemann, P. (2017). Biotransformation of hexabromocyclododecanes with hexachlorocyclohexane-transforming *Sphingobium chinhatense* strain IP26. *Chemosphere* 182, 491–500. doi: 10.1016/j.chemosphere.2017.05.047

Heeb, N. V., Schweizer, W. B., Kohler, M., and Gerecke, A. C. (2005). Structure elucidation of hexabromocyclododecanes-a class of compounds with a complex stereochemistry. *Chemosphere* 61, 65–73. doi: 10.1016/j.chemosphere.2005.03.015

Heeb, N. V., Wyss, S. A., Geueke, B., Fleischmann, T., Kohler, H. P. E., and Lienemann, P. (2014). LinA2, a HCH-converting bacterial enzyme that dehydrohalogenates HBCDs. *Chemosphere* 107, 194–202. doi: 10.1016/j.chemosphere.2013.12.035

Heeb, N. V., Zindel, D., Geueke, B., Kohler, H. P. E., and Lienemann, P. (2012). Biotransformation of hexabromocyclododecanes (HBCDs) with LinB-An HCH-converting bacterial Enzyme. *Environ. Sci. Technol.* 46, 6566–6574. doi: 10.1021/es2046487

Janák, K., Covaci, A., Voorspoels, S., and Becher, G. (2005). Hexabromocyclododecane in marine species from the Western Scheldt Estuary: diastereomer-and enantiomer-specific accumulation. *Environ. Sci. Technol.* 39, 1987–1994. doi: 10.1021/es0484909

Klosterhaus, S. L., Stapleton, H. M., La Guardia, M. J., and Greig, D. J. (2012). Brominated and chlorinated flame retardants in San Francisco Bay sediments and wildlife. *Environ. Int.* 47, 56–65. doi: 10.1016/j.envint.2012.06.005

Koch, C., Schmidt-Kötters, T., Rupp, R., and Sures, B. (2015). Review of hexabromocyclododecane (HBCD) with a focus on legislation and recent publications concerning toxicokinetics and-dynamics. *Environ. Pollut.* 199, 26–34. doi: 10.1016/j.envpol.2015.01.011

Krumins, V., Park, J. W., Son, E. K., Rodenburg, L. A., Kerkhof, L. J., Häggblom, M. M., et al. (2009). PCB dechlorination enhancement in Anacostia River sediment microcosms. *Water Res.* 43, 4549–4558. doi: 10.1016/j.watres.2009.08.003

Law, R. J., Covaci, A., Harrad, S., Herzke, D., Abdallah, M. A. E., Fernie, K., et al. (2014). Levels and trends of PBDEs and HBCDs in the global environment: status at the end of 2012. *Environ. Int.* 65, 147–158. doi: 10.1016/j.envint.2014.01.006

Lee, L. K., Ding, C., Yang, K. L., and He, J. Z. (2011). Complete debromination of tetra-and penta-brominated diphenyl ethers by a coculture consisting of *Dehalococcoides* and *Desulfovibrio* species. *Environ. Sci. Technol.* 45, 8475–8482. doi: 10.1021/es201559g

Li, D., Peng, P. A., Yu, Z., Huang, W., and Zhong, Y. (2016). Reductive transformation of hexabromocyclododecane (HBCD) by FeS. *Water Res.* 101, 195–202. doi: 10.1016/j.watres.2016.05.066

Li, D., Zhu, X., Zhong, Y., Huang, W., and Peng, P. A. (2017). Abiotic transformation of hexabromocyclododecane by sulfidated nanoscale zerovalent iron: kinetics, mechanism and influencing factors. *Water Res.* 121, 140–149. doi: 10.1016/j.watres.2017.05.019

Liu, F., and Fennell, D. E. (2008). Dechlorination and detoxification of 1, 2, 3, 4, 7, 8-hexachlorodibenzofuran by a mixed culture containing *Dehalococcoides ethenogenes* strain 195. *Environ. Sci. Technol.* 42, 602–607. doi: 10.1021/es071380s

Löffler, F. E., Yan, J., Ritalahti, K. M., Adrian, L., Edwards, E. A., Konstantinidis, K. T., et al. (2013). *Dehalococcoides mccartyi* gen. nov., sp. nov., obligately organohalide-respiring anaerobic bacteria relevant to halogen cycling and bioremediation, belong to a novel bacterial class, *Dehalococcoidia* classis nov., order *Dehalococcoidales* ord. nov. and family *Dehalococcoidaceae* fam. nov., within the phylum *Chloroflexi*. *Int. J Syst. Evol. Microbiol.* 63, 625–635. doi: 10.1099/ijs.0.034926-0

Marvin, C. H., Tomy, G. T., Armitage, J. M., Aront, J. A., McCarty, L., Covaci, A., et al. (2011). Hexabromocyclododecane: current understanding of chemistry, environmental fate and toxicology and implications for global management. *Environ. Sci. Technol.* 45, 8613–8623. doi: 10.1021/es201548c

Maymó-Gatell, X., Chien, Y. T., Gossett, J. M., and Zinder, S. H. (1997). Isolation of a bacterium that reductively dechlorinates tetrachloroethene to ethene. *Science* 276, 1568–1571. doi: 10.1126/science.276.5318.1568

Meng, X. Z., Duan, Y. P., Yang, C., Pan, Z. Y., Wen, Z. H., and Chen, L. (2011). Occurrence, sources, and inventory of hexabromocyclododecanes (HBCDs) in soils from Chongming Island, the Yangtze River Delta (YRD). *Chemosphere* 82, 725–731. doi: 10.1016/j.chemosphere.2010.10.091

Peng, X., Huang, X., Jing, F., Zhang, Z., Wei, D., and Jia, X. (2015). Study of novel pure culture HBCD-1, effectively degrading Hexabromocyclododecane, isolated from an anaerobic reactor. *Bioresour. Technol.* 185, 218–224. doi: 10.1016/j.biortech.2015.02.093

Schaefer, C. E., and Steffan, R. S. (2016). "Current and future bioremediation applications: bioremediation from a practical and regulatory perspective, Chapter 22," in *Organohalide-Respiring Bacteria*, eds L. Adrian and F. E. Loeffler (Heidelberg: Springer).

Seshadri, R., Adrian, L., Fouts, D. E., Eisen, J. A., Phillippy, A. M., Methe, B. A., et al. (2005). Genome sequence of the PCE-dechlorinating bacterium *Dehalococcoides ethenogenes*. *Science* 307, 105–108. doi: 10.1126/science.1102226

Shi, Z. X., Wu, Y. N., Li, J. G., Zhao, Y. F., and Feng, J. F. (2009). Dietary exposure assessment of Chinese adults and nursing infants to tetrabromobisphenol-A and hexabromocyclododecanes: occurrence measurements in foods and human milk. *Environ. Sci. Technol.* 43, 4314–4319. doi: 10.1021/es8035626

Stiborova, H., Vrkoslavova, J., Pulkrabova, J., Poustka, J., Hajslova, J., and Demnerova, K. (2015). Dynamics of brominated flame retardants removal in contaminated wastewater sewage sludge under anaerobic conditions. *Sci. Total Environ.* 533, 439–445. doi: 10.1016/j.scitotenv.2015.06.131

United Nations Environment Programme [UNEP] (2013). *The New POPs Under the Stockholm Convention*. Available at: http://chm.pops.int/TheConvention/ThePOPs/TheNewPOPs/tabid/2511/Default.aspx [accessed April 15, 2017]

Wang, S., Chng, K. R., Wilm, A., Zhao, S., Yang, K. L., Nagarajan, N., et al. (2014). Genomic characterization of three unique *Dehalococcoides* that respire on persistent polychlorinated biphenyls. *Proc. Natl. Acad. Sci. U.S.A.* 111, 12103–12108. doi: 10.1073/pnas.1404845111

Wu, M. H., Zhu, J. Y., Tang, L., Liu, N., Peng, B. Q., Sun, R., et al. (2014). Hexabromocyclododecanes in surface sediments from Shanghai, China: spatial distribution, seasonal variation and diastereoisomer-specific profiles. *Chemosphere* 111, 304–311. doi: 10.1016/j.chemosphere.2014.04.031

Yang, C., Kublik, A., Weidauer, C., Seiwert, B., and Adrian, L. (2015). Reductive dehalogenation of oligocyclic phenolic bromoaromatics by *Dehalococcoides mccartyi* strain CBDB1. *Environ. Sci. Technol.* 49, 8497–8505. doi: 10.1021/acs.est.5b01401

Yu, Z., Chen, L., Mai, B., Wu, M., Sheng, G., Fu, J., et al. (2008). Diastereomer-and enantiomer-specific profiles of hexabromocyclododecane in the atmosphere of an urban city in South China. *Environ. Sci. Technol.* 42, 3996–4001. doi: 10.1021/es7027857

Zhang, X., Zhang, D., Luo, Z., Lin, L., and Yan, C. (2011). Diastereoisomer- and enantiomer-specific profiles of hexabromocyclododecane in the sediment of Dongjiang River, South China. *Environ. Chem.* 8, 561–568. doi: 10.1071/EN10136

Zhen, H., Du, S., Rodenburg, L. A., Mainelis, G., and Fennell, D. E. (2014). Reductive dechlorination of 1, 2, 3, 7, 8-pentachlorodibenzo-p-dioxin and Aroclor 1260, 1254 and 1242 by a mixed culture containing *Dehalococcoides mccartyi* strain 195. *Water Res.* 52, 51–62. doi: 10.1016/j.watres.2013.12.038

Zheng, X., Qiao, L., Sun, R., Luo, X., Zheng, J., Xie, Q., et al. (2017). Alteration of diastereoisomeric and enantiomeric profiles of hexabromocyclododecanes (HBCDs) in adult chicken tissues, eggs, and hatchling chickens. *Environ. Sci. Technol.* 51, 5492–5499. doi: 10.1021/acs.est.6b06557

Conflict of Interest Statement: The authors declare that the research was conducted in the absence of any commercial or financial relationships that could be construed as a potential conflict of interest.

frontiers in Microbiology

REVIEW
published: 19 June 2018
doi: 10.3389/fmicb.2018.01292

Reductive Debromination of Polybrominated Diphenyl Ethers - Microbes, Processes and Dehalogenases

Siyan Zhao[1], *Matthew J. Rogers*[1], *Chang Ding*[2] *and Jianzhong He*[1]*

[1] *Department of Civil and Environmental Engineering, National University of Singapore, Singapore, Singapore,* [2] *Isotope Biogeochemistry, Helmholtz Centre for Environmental Research – UFZ, Leipzig, Germany*

Extensive utilization of polybrominated diphenyl ethers (PBDEs) as flame retardants since the 1960s in a variety of commercial products has resulted in ubiquitous environmental distribution of commercial PBDE mixtures. Dangers posed to biological populations became apparent after the discovery of elevated levels of PBDEs in biota, most notably in human breast milk and tissues. Environmental persistence of PBDEs results in significant transboundary displacement, threatening fragile ecosystems globally. Despite efforts to curtail usage of PBDEs, public concern remains about the effects of legacy PBDEs contamination and continued discharge of PBDEs in regions lacking restrictions on usage and manufacture. Among available technologies for remediation of PBDEs such as *ex-situ* soil washing, electrokinetic degradation, and biodegradation, this review focuses on bioremediation by microbes under anaerobic conditions. Bioremediation is generally preferred as it is less disruptive to contaminated ecosystems, is cost-effective, and can be implemented at sites that may be inaccessible to more traditional *ex-situ* methods. The aims of this review are to (1) summarize current knowledge of anaerobic microbes that debrominate PBDEs and their associated synergistic partnerships with non-dehalogenating microbes; (2) explore current understandings of the metabolic reductive debromination of PBDE congeners; (3) discuss recent discoveries on dehalogenase genes involved in debromination of PBDEs.

Keywords: flame retardants, organohalides, polybrominated diphenyl ethers (PBDEs), reductive debromination, debromination pathways, reductive dehalogenase genes

OPEN ACCESS

Edited by:
Qiang Wang,
Institute of Hydrobiology (CAS), China

Reviewed by:
M. Oves,
King Abdulaziz University, Saudi Arabia
Young-Mo Kim,
Pacific Northwest National Laboratory (DOE), United States

***Correspondence:**
Jianzhong He
jianzhong.he@nus.edu.sg

Specialty section:
This article was submitted to Microbiotechnology, Ecotoxicology and Bioremediation, a section of the journal Frontiers in Microbiology

Received: *30 January 2018*
Accepted: *28 May 2018*
Published: *19 June 2018*

Citation:
Zhao S, Rogers MJ, Ding C and He J (2018) Reductive Debromination of Polybrominated Diphenyl Ethers - Microbes, Processes and Dehalogenases. Front. Microbiol. 9:1292. doi: 10.3389/fmicb.2018.01292

INTRODUCTION

Polybrominated diphenyl ethers (PBDEs) have been widely used as flame retardant additives in a variety of manufactured products, from paints and plastics to textiles and televisions since 1960s. Deposition of anthropogenic PBDEs has subsequently been identified in air, soils, and water across the world (McGrath et al., 2017), even in remote areas including isolated mountaintop sediments, the Faroe Islands, and the Antarctic (Lindström, 1999; Gallego et al., 2007; Wild et al., 2015). In recent years, PBDEs concentrations as high as 10,000 ng/g soil have been detected at manufacturing and e-recycling sites (Alabi et al., 2012; Labunska et al., 2013; Li et al., 2015; Deng et al., 2016). Notably, PBDEs have the tendency to accumulate in biota (de Boer et al., 1998; Boon et al., 2002; Norstrom et al., 2002; Zhu and Hites, 2004) and have diverse toxicological effects including

endocrine disruption, metabolic disorders in biological populations, as well as neurological and developmental disorders in human (Siddiqi et al., 2003; Windham et al., 2015; ATSDR, 2017). Growing concerns over risks to human and environmental health have resulted in hepta- through tetra-BDEs being listed as persistent organic pollutants (POPs) on the United Nations Stockholm Convention in 2009 (United Nations Environment Programme, 2009).

Though restrictions and bans on manufacture and usage of PBDEs have been in place for several years, these legislations have no effect on the release of PBDEs from existing products or from recycled materials containing PBDEs. Environmental deposition of PBDEs can occur via release during manufacture and use of consumer products, improper disposal, and recycling of PBDEs containing products, volatilization during incineration, and discharge from wastewater treatment facilities. PBDEs are highly lipophilic, have low water solubility and low vapor pressures. These physical characteristics are largely dictated by the number and arrangement of bromine atoms on the molecule, with highly brominated PBDEs being more lipophilic, less soluble and less volatile (**Table 1**). Hence, highly brominated PBDEs adsorb readily to soils and sediments, where they persist and act as reservoirs leaching into other compartments over time (O'Driscoll et al., 2016). PBDEs also tend to bind to the organic fraction of particulate matter, soils, vegetation, and sediments following environmental deposition. Thus, PBDEs have a tendency to be exchanged between the atmosphere and surface, allowing passive transport over long distances.

PBDE formulations have been primarily manufactured as three different technical mixtures (**Figure 1**): penta-BDEs, octa-BDEs, and deca-BDEs. Although BDE-209 has historically been the most widely used PBDE congener, BDE −47, −99, −100, and −153 are the most commonly observed PBDEs in the environment (Darnerud et al., 2001), indicating that environmental transformation of highly brominated BDEs is an important pathway contributing to the dispersal and environmental impact of PBDEs. The partial debromination of deca- and octa-BDEs is particularly worrisome because the less brominated metabolites like tetra- and penta-BDEs are of higher toxicity (Palm et al., 2002). Both abiotic and biotic processes are responsible for the breakdown of PBDEs in the environment. Photolysis, which can occur in the atmosphere and at soil surfaces, of lesser brominated BDEs (BDE-28, BDE-47, BDE-99, BDE-100, BDE-153, and BDE-183) (Rayne et al., 2006; Fang et al., 2008) and of BDE-209 (Stapleton and Dodder, 2008) has been demonstrated under laboratory conditions, although there is only weak evidence that atmospheric photodegradation is a major contributor to environmental attenuation of PBDEs (Schenker et al., 2008). Anaerobic and anoxic sediments and soils are major sinks and environmental reservoirs for PBDEs, making anoxic debromination by microorganisms an important route for eliminating PBDEs in the environment.

Debromination of a variety of PBDEs, including the three primary technical mixtures, has been observed in soil, sewage sludge, and estuarine and marine sediments under different environmental conditions (redox, pH, available electron donors, etc.), although the process is typically slow and often results in incomplete debromination of PBDEs. Despite these apparent limitations of anaerobic microbial degradation of PBDEs, bioremediation is considered the most environmentally friendly technology to remediate PBDEs. Although bioremediation requires extensive site characterization to be successful and is often much slower than traditional *ex-situ* treatment strategies, it is less expensive, less disruptive to sites, and can be more complete in degrading hazardous compounds. Considering the fragility and inaccessibility of many of the environments and ecosystems plagued by PBDEs contamination, bioremediation via anaerobic microbes is the best available option for eliminating PBDEs from contaminated areas.

This review aims to summarize current knowledge of microbial reductive debromination of PBDEs under anaerobic conditions, the debromination pathways involved, and dehalogenase genes identified so far. Investigation of PBDEs debrominating microbes and exploration of the underlying mechanisms of debromination will enable more effective tracking the fate of PBDEs in the environment.

MICROORGANISMS INVOLVED IN REDUCTIVE DEBROMINATION OF PBDEs

The hydrophobicity of PBDEs impedes bioavailability, which results in low biomass of debrominating microorganisms. This low abundance is a critical challenge to enrichment, isolation, and characterization of PBDE debrominating bacteria. After pioneering efforts identified debromination of PBDEs in previously isolated organochlorine dehalogenating members of the genera *Sulfurospirillum* and *Dehalococcoides* (He et al., 2006) as well as *Desulfitobacterium* and *Dehalobacter* (Robrock et al., 2008), later studies successfully enriched and isolated PBDEs debrominating bacteria from multiple environmental sources (Lee et al., 2011; Ding et al., 2013, 2017) and confirmed the role of members of the genera *Dehalococcoides* and *Acetobacterium* in environmental debromination of PBDEs (**Figure 2**, **Table 2**).

Studies evaluating debromination potential with either technical PBDE mixtures or environmentally relevant BDE congeners in microcosms established from soils and sediments collected from various locations and environments have reported differences in both the rate and extent of PBDE debromination after long-term incubation (**Table 2**). When the primary goal is identification of functional bacteria, rather than developing enrichment cultures for fundamental studies, high-throughput sequencing and quantitative real-time PCR have been used to detect changes in microbial composition and identify specific populations whose increase correlates with debromination. Chen et al used this strategy to identify organohalide respiring *Dehalobacter, Dehalococcoides, Dehalogenimonas,* and *Desulfitobacterium* populations in a microcosm during reductive debromination of tetra-BDE 47 (Chen et al., 2018). Though some studies have purported to identify debrominating populations in microbial communities using less-sensitive molecular techniques [e.g., denaturing gradient gel electrophoresis (DGGE) and terminal restriction fragment length polymorphism (T-RFLP), Qiu et al., 2012;

TABLE 1 | Physical properties of PBDE mixtures.

Property	Penta-BDE	Octa-BDE	Deca-BDE
Molecular weight	Mixture	Mixture	959.22
Color	Clear, amber to pale yellow	Off-white	Off-white
Physical state	Highly viscous liquid	Powder	Powder
Melting point	−7 to −3°C (commercial)	85–89°C (commercial); 200°C (range, 167–257); 79–87°C; 170–220°C	290–306°C
Boiling point	>300°C (decomposition starts above 200°C)	Decomposes at >330°C (commercial)	Decomposes at >320, >400, and 425°C
Density (g/mL)	2.28 at 25°C; 2.25–2.28	2.76; 2.8 (commercial)	3.0; 3.25
Solubility:			
– Water	13.3 μg/L (commercial); 2.4 μg/L (pentabromodiphenyl ether component); 10.9 μg/L (tetrabromodiphenyl ether component)	<1 ppb at 25°C (commercial); 1.98 μg/L (heptabromodiphenyl ether component)	<0.1 μg/L
– Organic solvent(s)	10 g/kg methanol; miscible in toluene	Acetone (20 g/L); benzene (200 g/L); methanol (2 g/L)—all at 25°C	d-limonene (0.1823 g/100 g solvent); n-propanol (0.1823 g/100 g solvent)—all at 20°C *
Partition coefficients:			
– Log K_{OW}	6.64–6.97; 6.57 (commercial)	6.29 (commercial)	6.265
– Log K_{OC}	4.89–5.10	5.92–6.22	6.8
Vapor pressure	2.2×10^{-7}–5.5×10^{-7} mm Hg at 25°C; 3.5×10^{-7} mm Hg (commercial)	9.0×10^{-10}–1.7×10^{-9} mm Hg at 25°C; 4.9×10^{-8} mm Hg at 21°C (commercial)	3.2×10^{-8} mm Hg
Henry's Law constant (atm-m^3/mole)	1.2×10^{-5}; 1.2×10^{-6}; 3.5×10^{-6}	7.5×10^{-8}; 2.6×10^{-7}	1.62×10^{-6}; 1.93×10^{-8}; 1.2×10^{-8}; 4.4×10^{-8}

*Adapted from ATSDR (2017); * From Chen et al. (2016).*

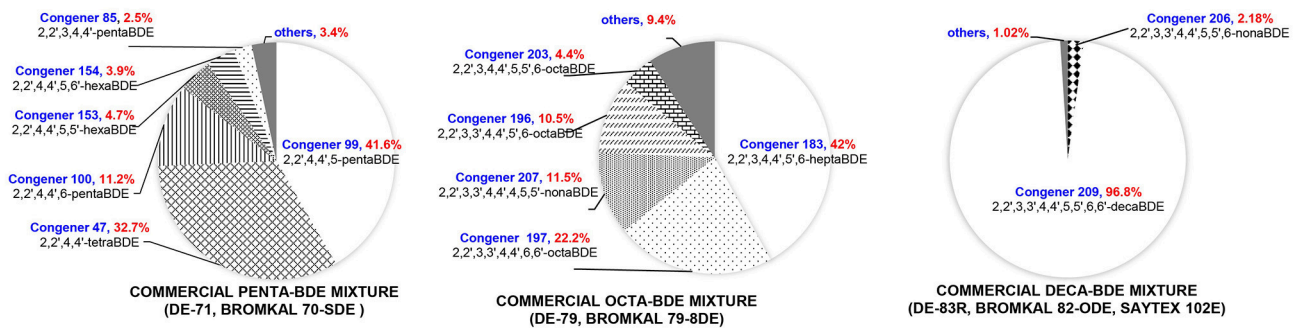

FIGURE 1 | Compositions of representative penta-, octa-, and deca-BDE mixtures. Congeners below 2% (w/w) are considered as others. As a result of the chemical process used to generate PBDE mixtures, the exact congener composition remains undefined and may vary significantly between different manufacturers and production batches (La Guardia et al., 2006).

Huang et al., 2014], these results must be viewed skeptically. Organohalide respiring bacteria are typically minor populations, even within enrichment cultures, whose presence can be masked by more dominant non-debrominating populations, thus large changes in detected abundance that appear to be related to debromination often only represent small relative changes in abundance of the population—which is difficult to discern by DGGE or T-RFLP. In such cases, researchers may make erroneous conclusions about the identity of debrominating populations in the microbial community.

PBDEs debromination has been reported by bacteria of at least six different genera, and can be broadly divided as either metabolic process—energy from debromination to support cell

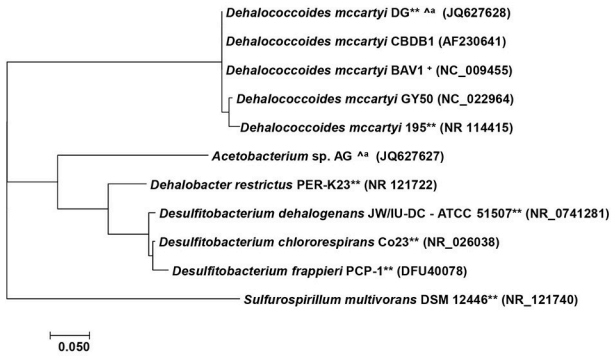

FIGURE 2 | Phylogenetic analysis of PBDE debrominating bacteria. The tree was constructed with MEGA 7 (Kumar et al., 2016) using Neighbor-joining method in Kimura 2-parameter mode (Kimura, 1980). $^{\wedge a}$, derived from same culture, **require auxiliary substrate, $^{+}$only in mixed culture.

growth, or co-metabolic process—not supporting cell growth (Tiehm and Schmidt, 2011). Co-metabolic dehalogenation typically requires supplementation with auxiliary substrates, e.g., other types of organohalides. Several studies of PBDEs debrominating microbial consortia and isolates have reported debromination only in the presence of additional halogenated electron acceptors (He et al., 2006; Robrock et al., 2008; Lee and He, 2010). Carbon sources may also act as auxiliary substrates, as in the case of the lactate, pyruvate or H_2-CO_2 dependent co-metabolic degradation of PBDEs identified in *Acetobacterium* sp. strain AG (Ding et al., 2013). The use of benign, non-halogenated auxiliary substrates in co-metabolic debromination makes strain AG a particularly interesting candidate for *in-situ* bioremediation. Co-metabolic reductive debromination of PBDEs is currently more frequently reported than metabolic debromination. However, metabolic reductive debromination is generally favored for site remediation because it does not require auxiliary substrates and has higher energy-utilization efficiency. Thus far, only *Dehalococcoides mccartyi* strains GY50 and GY52, both isolated from co-culture GY2 (Lee et al., 2011), have been shown to metabolically debrominate PBDEs (Ding et al., 2017). Strain GY50 is of particular interest as it completely debrominates penta-BDE mixtures to diphenyl ether, rather than producing partially debrominated end-products.

SYNERGISTIC INTERACTIONS IN MICROBIAL REDUCTIVE DEBROMINATION OF PBDEs

Synergistic metabolic interactions between organohalide respiring bacteria and other bacterial populations can increase the robustness of dehalogenation in microbial consortia by providing certain growth factors (He et al., 2007; Men et al., 2011). Although the exact nature of most of these synergisms is unknown, faster and extensive debromination in mixed microbial communities has been observed. Co-metabolic debromination in co-culture G consisting of *D. mccartyi* strain DG and *Acetobacterium* sp. strain AG, with presence of auxiliary substrate, TCE, is an example of this synergistic metabolic interactions (Ding et al., 2013). Culture G, a co-culture originating from a river bank, was found to reductively debrominate octa- and penta-BDE mixtures to less brominated congeners ranging from penta- to di-BDEs. Debromination of the BDE mixtures by strain DG was slower and also less extensive than that in the parent culture, by producing only trace amounts of penta- and tetra-BDEs after 6 weeks' incubation. Strain AG had the same penta-BDEs debromination capacity as culture G, albeit more slowly and less extensively than its parent culture, and had an octa-BDE debrominating profile similar to that of strain DG. Debromination of octa-BDE could be rescued in co-cultures of strain AG and strain DG, indicating a synergistic relationship between these two populations. The authors speculated that the *Acetobacterium* provides certain growth factors, such as vitamin B_{12} in the form of cobalamin, which are essential for PBDEs debromination by strain DG.

Besides supplying essential nutrients during synergistic interactions, another benefit of synergetic microbial interactions can be seen in the more extensive debromination of PBDEs by culture EC195 plus strain BAV1 compared to culture EC195 alone, as direct participants in debromination processes (He et al., 2006). The highly enriched autotrophic culture EC195 produced hepta- through di-BDEs from an octa-BDE mixture and *D. mccartyi* strain BAV1 did not debrominate octa-BDEs in pure culture. However, addition of strain BAV1 to EC195 resulted in further debromination, with generation of only tetra- through di-BDEs from the octa-BDE mixture. The hexa- and penta-BDE debromination by EC195 plus strain BAV1 suggests a role for BAV1 in synergistic debromination of lesser brominated PBDEs.

However, interactions among populations in mixed microbial communities do not necessarily improve debromination activity. For example, inhibition of methanogenic bacteria in culture GY-T-2 by the addition of BES increased the rate and extent of the debromination of PBDEs (Lee and He, 2010). It is possible that methanogens in GY-T-2 compete with the PBDE debrominating populations in the community for limiting factors, such as hydrogen, thereby inhibiting debromination.

REDUCTIVE DEBROMINATION OF PBDEs AND FUNCTIONAL GENES

Anaerobic reductive debromination of PBDEs was first observed in a bioreactor where di-BDE 15 was converted to mono-BDE 3 and diphenyl ether (Rayne et al., 2003). Later investigations of biological transformation of PBDE mixtures and some individual congeners (e.g., tetra-BDE 47, penta-BDE 99) identified and characterized anaerobic microbial reductive debromination of PBDEs in sewage sludge treatments as well as in terrestrial, marine, and estuarial soils and sediments, and in microbial consortia and isolates derived from these sources (Gerecke et al., 2005; He et al., 2006; Robrock et al., 2008; Tokarz et al., 2008; Lee and He, 2010; Lee et al., 2011; Xu et al., 2014; Zhu et al., 2014; Stiborova et al., 2015).

TABLE 2 | PBDE debrominating cultures.

	Sample ID	Source	Auxiliary substrate	deca-BDEs	octa-BDEs	penta-BDEs	Remarks	Duration	Citation
Pure cultures	*Dehalococcoides mccartyi* 195	Anaerobic sewage digestor sludge	TCE	No	hepta- through tetra-	N.A.		6 months	He et al., 2006
	Dehalococcoides mccartyi DG	Isolate from G	TCE	N.A.	penta- tetra-	tetra-	Minimal conversion; Lost octa-BDE debromination activity of parent culture, G, which can only be resumed by co-cultivating AG and DG;	Octa-BDEs 5 months; penta-BDEs 1 month	Ding et al., 2013
	Acetobacterium sp. AG	Isolate from G	Lactate	N.A.	penta- tetra-	penta- through di-			
	Dehalococcoides mccartyi CBDB1/n-ZVI	Saale river sediment	n-ZVI	20% conversion to diphenyl ether	N.A.	N.A.	No debromination of deca-BDE by CBDB1 without addition of n-ZVI; the role of CBDB1 in this study is uncertain due to pH and unbalanced hydrogen consumption.	1 month	Xu et al., 2014 Yang, 2017
	Dehalococcoides mccartyi GY50	Isolate from co-culture, GY2, sand, and silt near Lianjiang River	No	N.A.	N.A.	Diphenyl ether	GY2 share the same debromination activity with its isolate GY50; Complete debromination; *Ortho*-removal preferred; identified PBDE RDases, PbrA1, PbrA2, PbrA3	2 weeks	Lee et al., 2011; Ding et al., 2017
	Dehalococcoides mccartyi GY52	Variant of GY50 after consecutive transfer in TCE	No	N.A.	N.A.	Di-	A genome island where *pbrA1* and *pbrA2* locate was deleted from GY50	2 weeks	
	Desulfitobacterium chlororespirans Co23	2,3-CP dehalogenating compost soil	3-chloro-4-hyxdroxybenzoate	Similar debromination profile as ANAS195 (data not shown)				N.A.	Robrock et al., 2008
	Desulfitobacterium halogenans JW/IU-DC	Freshwater sediments-pond	3-chloro-4-hydroxphenylacetate	Similar debromination profile as ANAS195 (data not shown)				N.A.	Robrock et al., 2008
	Desulfitobacteriun frappieri PCP-1	A mixture of pentachlorophenol contaminated soil and anaerobic sewage sludge	pentachlorophenol	N.A.	hepta- hexa- penta-	penta 99 to tetra, tri, di; tetra 47 to tri and di	Debromination pathways were identified by spiking individual congeners; para- and meta-removal is preferred; debromination for higher brominated BDEs are slower;	3 months	Robrock et al., 2008
	Dehalobacter restrictus PER-K23	Anaerobic Rhine river sediment and ground anaerobic granular sludge	PCE	N.A.	hepta- hexa- penta-	penta 99 to tetra-; tetra47 to tri and di		3 months	Robrock et al., 2008

(Continued)

TABLE 2 | Continued

	Sample ID	Source	Auxiliary substrate	deca-BDEs	octa-BDEs	penta-BDEs	Remarks	Duration	Citation
	Sulfurospirillum multivorans DSM12446	Activated sludge	TCE	Octa- Hepta-	No	N.A.		2 months	He et al., 2006
Mixed Cultures	Culture G	Soil samples from a river bank in Wisconsin	TCE	N.A.	hexa-, penta-, tetra- (dominant), tri-,	penta- through di-	*Para*- and *meta*-removal preferred in octa-BDEs debromination; Penta-BDEs debromination similar as AG, strictly *para*-removal	octa-BDEs 5 months; penta-BDEs 1 month	Ding et al., 2013
	EC195	Highly enriched 195 containing autotrophic culture	TCE	No	hepta- hexa- penta- tetra- di-	N.A.	Additional one hexa and two penta, as well as tetra and di congeners produced compared with strain 195	3 months	He et al., 2006
	ANAS195	An enrichment culture with strain 195	TCE	No	hepta- through di-	N.A.	Faster and more extensive debromination compared with strain195	3 months	He et al., 2006
	EC195+BAV1	EC195 with strain BAV1	TCE	No	tetra- tri- di-	N.A.	BAV1 shows no debromination on deca- or octa-BDEs. More extensive debromination compared with EC195 suggests BAV1 can debrominate lesser brominated PBDEs	3 months	He et al., 2006
Microcosms	Plug-flow bioreactor with colonization water from wetland near munition dump		No	N.A.	N.A.	N.A.	Di-BDE 15 to mono-BDE 3 and diphenyl ether	12% and 61% conversion with HRT 3.4 h and 6.8 h, respectively	Rayne et al., 2003
	Sewage sludge from mesophilic digester in Dubendorf, Switzerland		4-bromobenzoic acid, 2,6-dibromobiphenyl, tetrabromobisphenyl A, hexabromocyclododecan, and decabromobiphenyl	Nona- Octa-	N.A.	N.A.	*Para*- and *meta*-removal preferred	238 days	Gerecke et al., 2005
	Loam sediment from Celey Bog Park, West Lafayette, IN, USA		Methanol and dextrose	Nona- through Hexa-	N.A.	Tetra- Tri-	*Para*-removal preferred	8 months for penta- and tetra-BDEs, 3.5 years for deca-BDE	Tokarz et al., 2008

(Continued)

TABLE 2 | Continued

Sample ID	Source	Auxiliary substrate	deca-BDEs	octa-BDEs	penta-BDEs	Remarks	Duration	Citation
A few soils and sediments from multiple locations in China, Singapore, and US		No	N.A.	Hexa- Penta- Tetra-	N.A.	*Dehalococcoides* exist in 11 out of 14 active microcosms; more extensive debromination was observed with TCE as auxiliary substrate	2 months	Lee and He, 2010
		TCE	N.A.	Hexa-through di-	N.A.			
Sediments at the riverside of Lianjiang Rriver, Guiyu, E-recycling town in China		No	Nona- through tri-BDE	N.A.	N.A.	Too ambitious to correlate *Pseudomonas* with PBDE debromination simply by DGGE study in original microcosm	3 months	Qiu et al., 2012
A few sediment slurries from mangrove, fresh water ponds, and marine subsurface sediments, Hongkong SAR		No	No	N.A.	Hexa 153 to hexa-, penta-, tetra-, tri-, and di-; tetra 47 to tri-	*Para*- removal preferred, followed by *meta*- and *ortho*-removal	90 days for tetra 47; 7.6 to 165 days for hexa 153	Zhu et al., 2014
River sediment from Erren River, Taiwan (heavily contaminated rivers)		No	Nono-through mono-BDE	N.A.	N.A.		6 months	Huang et al., 2014
Wastewater sludge samples, Hrade Kralove and Brno		No	A relative distribution of individual congeners changed with a significance increase of tetra 49			A mixture of mono-through hepta BDEs was spiked.	15 months	Stiborova et al., 2015
E-waste contaminated soils		Lactate	Deca-209 and tetra 47 decrease while penta-99, hexa-154, 153, and hepta 183 increase at significant levels			PBDEs contamination already exist in soils samples; iron-reducing conditions		
Mangrove sediment from Guandu and Bali, Taiwan		No	Nona-through di-	N.A.	N.A.	*Para*- removal preferred, followed by *meta*- and *ortho*-removal; Debrominating populations were tried to be identified through analysis of microbial communities; ZVI can enhance debromination	75 days	Yang et al., 2017
Subsurface sediment from mature mangrove forest in Maipo, Hongkong SAR		No	N.A.	N.A.	Tetra- 47 to tri, di-	Biochar accelerates PBDEs' reductive debromination in electron transfer among microbial populations. Abundance of dehalogenating populations were enriched	20 weeks	Chen et al., 2018

Debromination of PBDEs is partial in almost all observed systems, yielding lesser brominated metabolites, and typically occurs slowly and at nanomolar concentrations. Gerecke et al. reported microbial debromination of 5% of 11.2 nM deca-BDE 209 to nona- and octa-BDEs after 238 days in a microcosm established from sewage sludge (Gerecke et al., 2005). A separate study utilizing a *D. mccartyi*-containing microbial consortia, ANAS195, observed production of 500 nM hepta- to di-BDEs from 1.3 μM of an octa-BDE mixture with the presence of TCE after 6 months' incubation (He et al., 2006). Similarly, partial debromination of deca-BDE 209 and tetra-BDE 47 was reported after 90 days incubation by the autochthonous microbial community in e-waste contaminated soil containing a range of deca- to tri-BDEs (Song et al., 2015). Though uncommon, complete debromination of tetra- and penta-BDEs to diphenyl ether was demonstrated by Lee et al in a co-culture, GY2 (Lee et al., 2011), from which a novel *D. mccartyi* strain, GY50, that debrominated ∼1,180 nM tetra-BDE 47, penta-BDEs 99 and 100 to diphenyl ether in 2 weeks was isolated (Ding et al., 2017).

There is a marked variation in observed debromination rates, pathways, and relative abundance of daughter products among different studies of anaerobic microbial debromination. This is most likely due to regional differences in nutrient availability and bioavailability of PBDEs as well as site-specific variations in microbial community composition. However, it is generally true that more highly substituted PBDEs (deca- and octa-BDEs) are debrominated by fewer organisms and more slowly than lesser substituted congeners (penta- and tetra-BDEs), which is a common trend in microbial dehalogenation of aromatic organohalides [i.e., PBDEs, polychlorinated biphenyl ethers (PCBs), polychlorinated dibenzo-p-dioxins and polychlorinated dibenzofurans (PCDD/Fs), etc.]. This is thought to be a result of the increased hydrophobicity of more highly halogenated aromatics and of the reduced reactivity of more highly substituted aromatic rings resulting from changes in electron density (Fagervold et al., 2007; Cooper et al., 2015; Zhang et al., 2017, 2018). Instances of this phenomenon can be seen in several studies in which prevalence of octa-BDEs debromination was observed in pure cultures and defined mixed cultures than debromination of deca-BDEs (He et al., 2006; Robrock et al., 2008; Xu et al., 2014). Similarly, studies of the debromination potential of municipal sewage sludge (Shin et al., 2010) and various sediment slurries (Zhu et al., 2014) have noted debromination of hexa- to tetra-BDEs but no debromination of deca- or hepta-BDEs.

Attempts to identify the products of anaerobic microbial debromination have also revealed preferential removal of *para* and *meta* bromine substituents (**Figure 3**), a trend which is also present in microbial dehalogenation of aromatic organohalides, such as PCBs (Wang and He, 2013; Wang et al., 2014). This preference appears to exist regardless of the degree of bromine saturation, and has been observed in debromination of deca-BDE 209 (Gerecke et al., 2005) as well as in debromination of octa-BDEs (BDE 196, 203, and 197), hepta-BDE 183, hexa-BDE 153, penta-BDE 99, and tetra-BDE 47 (Robrock et al., 2008). The 2008 study by Robrock et al. also suggests preferential removal of double-flanked bromine moieties. Strict *para* and *para*-dominant debromination patterns in penta- and octa-BDE mixtures are also found in culture G with the presence of TCE, although *meta*- and *ortho*-bromine substitution were suggested as minor pathways in octa-BDE debromination (Ding et al., 2013). The only exception thus far identified not following preferential *para* and *meta* substitution is the predominance of *ortho*-bromine removal in co-culture GY2, as well as in *D. mccartyi* strain GY50 (derived from culture GY2), in stepwise conversion of penta-BDE 100 to di-BDE 15 via tetra-BDE 47 and tri-BDE 28 (Lee et al., 2011).

The preference on *para-*, *meta-*, or *ortho*-bromine substitution could be determined by the reductive dehalogenases present in the debrominating bacteria. Identification and characterization of reductive dehalogenases responsible for dehalogenation of specific compounds allow researchers to investigate the mechanisms of organohalide respiration and provide targets that can be used to monitor populations of organohalide respiring bacteria in laboratory and field-scale bioremediation studies. Reductive dehalogenases responsible for dehalogenation of a wide variety of halogenated compounds have been reviewed in Hug et al. (2013). Identification of PBDEs reductive dehalogenases is impeded by the co-metabolic nature of PBDEs debromination in most mixed cultures and isolates, as the presence of auxiliary substrates makes it more challenging to determine single gene products responsible for observed activities, and by marginal cell yield of PBDEs debrominating populations in mixed cultures.

The only PBDE reductive dehalogenases characterized to date, PbrA1, PbrA2, and PbrA3, were identified in *D. mccartyi* strain GY50 using a combination of transcriptomics and proteomics (Lee et al., 2011; Ding et al., 2017). The fortuitous emergence of two variant strains that exhibited distinct dehalogenation profiles to strain GY50 allowed for functional characterization of the three PBDE dehalogenases. The deletion of a genomic island containing both PbrA1 and PbrA2 in the genome of strain GY52 and the lack of di-BDE debromination in this strain provided strong evidence for the role of PbrA3 in debromination of penta- and tetra-BDEs to di-BDE (BDE 15), while simultaneously implicating PbrA1 and PbrA2 in removal of unflanked para-bromines from BDE 15 to mono-BDE (BDE 4) and diphenyl ether. Several hundred putative reductive dehalogenase homologous genes have been identified in the genomes of different *Dehalococcoides* strains and have been categorized into more than 50 orthologous groups based on amino acid similarity (Hug et al., 2013). The three PBDE reductive dehalogenases, PbrA1, PbrA2, and PbrA3, which catalyze different debromination pathways and attack bromine moieties at different positions, are phylogenetically distinct—sharing <40% amino acid sequence similarity with each other (**Figure 4**). It is not uncommon for reductive dehalogenase genes with similar functionality to exhibit significant disparities in nucleotide sequence, but the phylogenetic similarity of the PBDE reductive dehalogenases to enzymes which catalyze dehalogenation of other poly-halogenated aromatic compounds

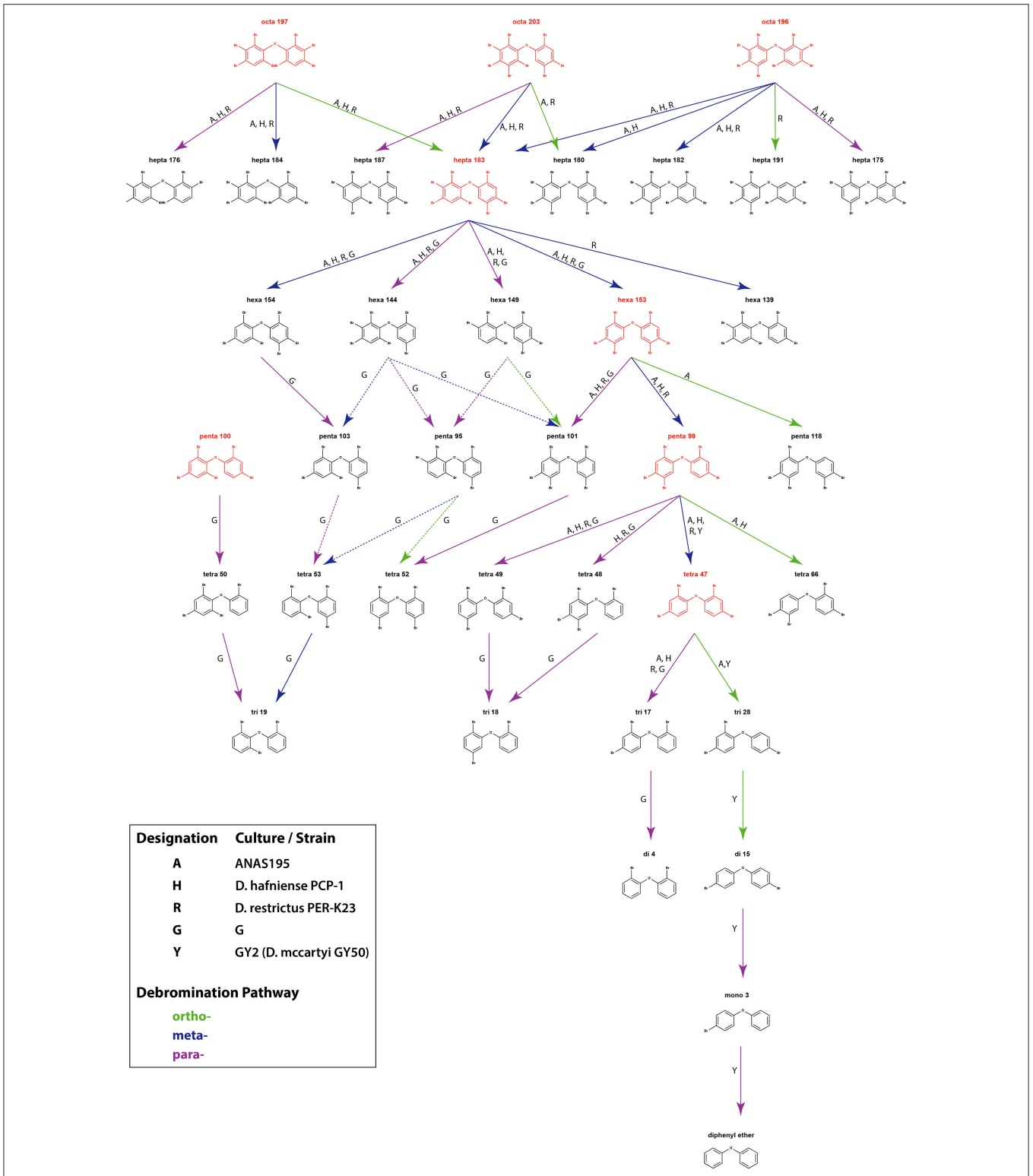

FIGURE 3 | Debromination pathways of PBDEs in mixed and pure microbial cultures.

may reveal some structural aspect that is common among enzymes mediating catalysis of these types of organohalides. While neither nucleotide nor amino acid sequence similarity among reductive dehalogenases is predictive of substrate range (Hug, 2016), the clustering of known reductive dehalogenase into orthologous groups at least provides a starting point

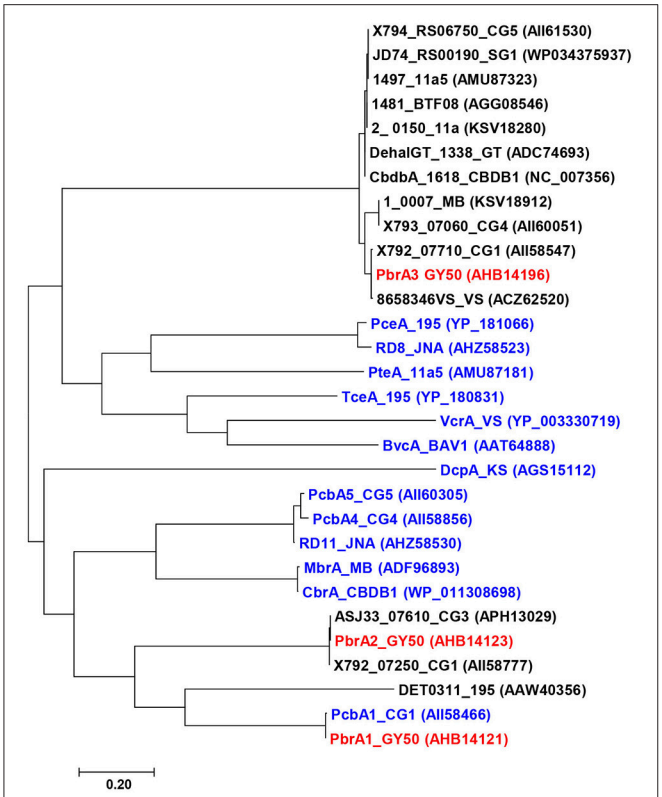

FIGURE 4 | Phylogenetic analysis of functionally characterized RDases (blue color) in *Dehalococcoides mccartyi* including orthologs (black color) of PBDE reductive dehalogenases (red color). The tree was constructed with MEGA 7 (Kumar et al., 2016) using maximum likelihood method in JTT matrix-based model (Jones et al., 1992).

for putatively identifying other PBDE reductive dehalogenases. For example, debromination of PBDEs and other brominated benzenes (Wagner et al., 2012) and phenols (Yang et al., 2015) by strain CBDB1 contains one reductive dehalogenase gene that clusters within the same ortholog group as PbrA3, though no functional genes were implicated in the original study. More information about the functions of uncharacterized dehalogenases is necessary before meaningful comparative analyses of these orthologs can be performed. The emergence and characterization of the GY52 variant facilitated description of the regiospecificity of these three dehalogenases and demonstrated a strategy by which other PBDE dehalogenases can be investigated.

OUTLOOK

Though production and usage of PBDE mixtures have declined after implementation of bans and voluntarily cessation of manufacture, the environmental persistence and potential for transboundary disbursement make PBDEs a continuing threat to biological populations around the globe. The degree of the debromination of PBDEs not only affects physical and chemical properties, but also toxicity and potential for bioaccumulation. Highly substituted deca-, nona-, and octa-BDEs are thermally labile and are partially degraded to lesser brominated congeners in the environment resulting in an increase in the risk presented by the original contamination. Because PBDEs preferentially sorb to organic matter, they tend to accumulate in anaerobic and anoxic soils and sediments. Harnessing the metabolic potential of anaerobic microbes that can detoxify PBDEs by removing bromine substituents has the potential to be a cost effective and efficient approach to remediate PBDEs in the environment.

Microbial debromination of PBDEs must overcome several obstacles before it can be considered a viable technology for bioremediation. Most of the bacteria that are currently known to debrominate PBDEs do so co-metabolically and partially. This incomplete debromination may often cause additional problems *in-situ* and the requirement for auxiliary substrates can severely limit the rate and extent of debromination. The only anaerobic microbe that can completely detoxify PBDEs and couple cell growth is *D. mccartyi* GY50 which can metabolize penta- and tetra-BDEs to produce diphenyl ether as an end-product. However, since deca- and octa-BDE mixtures also represent the majority of PBDEs production and pollution globally, further study is necessary to find other bacterial isolates and mixed cultures that can metabolize these highly brominated congeners. In general, co-cultures could likely be a promising solution to completely debrominate higher brominated BDEs to diphenyl ether via intermediates such as penta- and tetra-BDEs.

The slow growth rate and low cell yields associated with debrominating bacteria have impeded efforts to elucidate the mechanisms of microbial PBDE degradation. The isolation of *D. mccartyi* GY50 has revealed functional PBDE reductive dehalogenases for the first time, which may facilitate identification of additional PBDE dehalogenases in other *Dehalococcoides*. Discovery of enzymes responsible for the observed debromination of higher brominated deca- and octa-BDEs would be particularly valuable to the advancement of PBDEs bioremediation efforts. Recent advances in heterologous expression and purification of functional reductive dehalogenases will facilitate investigations into the dehalogenation potential of uncharacterized dehalogenases and may make it possible to establish a platform for *in-vitro* production of specific dehalogenases for bioremediation.

In summary, the innate capacity of some anaerobic microbes to detoxify different PBDEs can potentially be exploited as a tool to remediate contaminated soils and sediments. Application of these microbes *in-situ* has been hindered by the slow rate of cell growth and associated debromination of target compounds. Combining organohalide respiring bacteria with other physical and chemical processes to increase the rate and extent of anaerobic debromination of PBDEs has been investigated with varying degrees of success. Recent descriptions of PBDE debrominating isolates and defined microbial consortia have shed light on genes responsible for some, but not all, of the natural attenuation of PBDEs that has been observed. Future investigations to elucidate and characterize additional

PBDEs dehalogenases in anaerobic systems may provide a clearer picture of the mechanisms responsible for the partial degradation of highly substituted PBDEs in the environment and pave the way for development of new strategies to address the persistent threat that PBDEs pose to biological populations.

ETHICS STATEMENT

This article does not contain any studies with human participants or animals performed by any of the authors.

AUTHOR CONTRIBUTIONS

SZ, MR, and JH developed the structure of the article. SZ and MR drafted the article. SZ, MR, CD, and JH revised the article. JH did the final approval of the version to be published.

ACKNOWLEDGMENTS

The authors are grateful for financial support by the Ng Teng Fong Charitable Foundation fund under project No.: R-302-000-198-720.

REFERENCES

Alabi, O. A., Bakare, A. A., Xu, X., Li, B., Zhang, Y., and Huo, X. (2012). Comparative evaluation of environmental contamination and DNA damage induced by electronic-waste in Nigeria and China. *Sci. Total Environ.* 423, 62–72. doi: 10.1016/j.scitotenv.2012.01.056

ATSDR (2017). *Toxicological Profile for Polybrominated Diphenyl Ethers (PBDEs), Public Health Service, Department of Health and Human Services*. Atlanta, GA: Agency for Toxic Substances and Disease Registry.

Boon, J. P., Lewis, W. E., Tjoen-A-Choy, M. R., Allchin, C. R., Law, R. J., De Boer, J., et al. (2002). Levels of polybrominated diphenyl ether (PBDE) flame retardants in animals representing different trophic levels of the North Sea food Web. *Environ. Sci. Technol.* 36, 4025–4032. doi: 10.1021/es0158298

Chen, J., Wang, C., Pan, Y., Farzana, S. S., and Tam, N. F. (2018). Biochar accelerates microbial reductive debromination of 2,2',4,4'-tetrabromodiphenyl ether (BDE-47) in anaerobic mangrove sediments. *J. Hazard. Mater.* 341, 177–186. doi: 10.1016/j.jhazmat.2017.07.063

Chen, Y., Jiang, L., Zhao, X., Linag, S., Yu, M., Liu, W., et al. (2016). The research on the solubility of decabromodiphenyl ether based on recycling of waste electronic plastic by solvent process. *Proc. Environ. Sci.* 31, 827–831. doi: 10.1016/j.proenv.2016.02.083

Cooper, M., Wagner, A., Wondrousch, D., Sonntag, F., Sonnabend, A., Brehm, M., et al. (2015). Anaerobic microbial transformation of halogenated aromatics and fate prediction using electron density modeling. *Environ. Sci. Technol.* 49, 6018–6028. doi: 10.1021/acs.est.5b00303

Darnerud, P. O., Eriksen, G. S., Jóhannesson, T., Larsen, P. B., and Viluksela, M. (2001). Polybrominated diphenyl ethers: occurrence, dietary exposure, and toxicology. *Environ. Health Perspect.* 109, 49–68. doi: 10.1289/ehp.01109s149

de Boer, J., Wester, P. G., Klamer, H. J., Lewis, W. E., and Boon, J. P. (1998). Do flame retardants threaten ocean life? *Nature* 394, 28–29.

Deng, C., Chen, Y., Li, J., Li, Y., and Li, H. (2016). Environmental pollution of polybrominated diphenyl ethers from industrial plants in China: a preliminary investigation. *Environ. Sci. Pollut. Res.* 23, 7012–7021. doi: 10.1007/s11356-015-5902-8

Ding, C., Chow, W. L., and He, J. (2013). Isolation of *Acetobacterium* sp. strain AG, which reductively debrominates octa- and pentabrominated diphenyl ether technical mixtures. *Appl. Environ. Microbiol.* 79, 1110–1117. doi: 10.1128/AEM.02919-12

Ding, C., Rogers, M. J., Yang, K. L., and He, J. (2017). Loss of the ssrA genome island led to partial debromination in the PBDE respiring *Dehalococcoides mccartyi* strain GY50. *Environ. Microbiol.* 19, 2906–2915. doi: 10.1111/1462-2920.13817

Fagervold, S. K., May, H. D., and Sowers, K. R. (2007). Microbial reductive dechlorination of aroclor 1260 in baltimore harbor sediment microcosms is catalyzed by three phylotypes within the phylum *Chloroflexi*. *Appl. Environ. Microbiol.* 73, 3009–3018. doi: 10.1128/AEM.02958-06

Fang, L., Huang, J., Yu, G., and Wang, L. (2008). Photochemical degradation of six polybrominated diphenyl ether congeners under ultraviolet irradiation in hexane. *Chemosphere* 71, 258–267. doi: 10.1016/j.chemosphere.2007.09.041

Gallego, E., Grimalt, J. O., Bartrons, M., Lopez, J. F., Camarero, L., Catalan, J., et al. (2007). Altitudinal gradients of PBDEs and PCBs in fish from European high mountain lakes. *Environ. Sci. Technol.* 41, 2196–2202. doi: 10.1021/es062197m

Gerecke, A. C., Hartmann, P. C., Heeb, N. V., Kohler, H. P., Giger, W., Schmid, P., et al. (2005). Anaerobic degradation of decabromodiphenyl ether. *Environ. Sci. Technol.* 39, 1078–1083. doi: 10.1021/es048634j

He, J., Holmes, V. F., Lee, P. K., and Alvarez-Cohen, L. (2007). Influence of vitamin B_{12} and cocultures on the growth of *Dehalococcoides* isolates in defined medium. *Appl. Environ. Microbiol.* 73, 2847–2853. doi: 10.1128/AEM.02574-06

He, J., Robrock, K. R., and Alvarez-Cohen, L. (2006). Microbial reductive debromination of polybrominated diphenyl ethers (PBDEs). *Environ. Sci. Technol.* 40, 4429–4434. doi: 10.1021/es052508d

Huang, H.-W., Chang, B.-V., and Lee, C.-C. (2014). Reductive debromination of decabromodiphenyl ether by anaerobic microbes from river sediment. *Int. Biodeterior. Biodegrad.* 87, 60–65. doi: 10.1016/j.ibiod.2013.10.011

Hug, L. A. (2016). "Diversity, evolution, and environmental distribution of reductive dehalogenase genes," in *Organohalide-Respiring Bacteria,* eds L. Adrian and F. E. Löffler (Berlin; Heidelberg: Springer Berlin Heidelberg), 377–393.

Hug, L. A., Maphosa, F., Leys, D., Loffler, F. E., Smidt, H., Edwards, E. A., et al. (2013). Overview of organohalide-respiring bacteria and a proposal for a classification system for reductive dehalogenases. *Philos. Trans. R. Soc. B Biol. Sci.* 368:20120322. doi: 10.1098/rstb.2012.0322

Jones, D. T., Taylor, W. R., and Thornton, J. M. (1992). The rapid generation of mutation data matrices from protein sequences. *Comput. Appl. Biosci.* 8, 275–282. doi: 10.1093/bioinformatics/8.3.275

Kimura, M. (1980). A simple method for estimating evolutionary rates of base substitutions through comparative studies of nucleotide sequences. *J. Mol. Evol.* 16, 111–120. doi: 10.1007/BF01731581

Kumar, S., Stecher, G., and Tamura, K. (2016). MEGA7: Molecular evolutionary genetics analysis version 7.0 for bigger datasets. *Mol. Biol. Evol.* 33, 1870–1874. doi: 10.1093/molbev/msw054

Labunska, I., Harrad, S., Santillo, D., Johnston, P., and Brigden, K. (2013). Levels and distribution of polybrominated diphenyl ethers in soil, sediment and dust samples collected from various electronic waste recycling sites within Guiyu town, southern China. *Environ. Sci. Process Impacts* 15, 503–511. doi: 10.1039/c2em30785e

La Guardia, M. J., Hale, R. C., and Harvey, E. (2006). Detailed polybrominated diphenyl ether (PBDE) congener composition of the widely used penta-, octa-, and deca-PBDE technical flame-retardant mixtures. *Environ. Sci. Technol.* 40, 6247–6254. doi: 10.1021/es060630m

Lee, L. K., Ding, C., Yang, K.-L., and He, J. (2011). Complete debromination of tetra- and penta-brominated diphenyl ethers by a coculture consisting of *Dehalococcoides* and *Desulfovibrio* species. *Environ. Sci. Technol.* 45, 8475–8482. doi: 10.1021/es201559g

Lee, L. K., and He, J. (2010). Reductive debromination of polybrominated diphenyl ethers by anaerobic bacteria from soils and sediments. *Appl. Environ. Microbiol.* 76, 794–802. doi: 10.1128/AEM.01872-09

Li, Y., Niu, S., Hai, R., and Li, M. (2015). Concentrations and distribution of polybrominated diphenyl ethers (PBDEs) in soils and plants from a deca-BDE manufacturing factory in China. *Environ. Sci. Pollut. Res. Int.* 22, 1133–1143. doi: 10.1007/s11356-014-3214-z

Lindström, G., Wingfors, H., Dam, M., and Bavel, B. V, (1999). Identification of 19 polybrominated diphenyl ethers (PBDEs) in long-finned pilot whale (Globicephala melas) from the Atlantic. *Arch. Environ. Contam. Toxicol.* 36, 355–363. doi: 10.1007/s002449900482

McGrath, T. J., Ball, A. S., and Clarke, B. O. (2017). Critical review of soil contamination by polybrominated diphenyl ethers (PBDEs) and novel brominated flame retardants (NBFRs); concentrations, sources and congener profiles. *Environ. Pollut.* 230, 741–757. doi: 10.1016/j.envpol.2017.07.009

Men, Y., Feil, H., VerBerkmoes, N. C., Shah, M. B., Johnson, D. R., Lee, P. K. H., et al. (2011). Sustainable syntrophic growth of *Dehalococcoides ethenogenes* strain 195 with *Desulfovibrio vulgaris* Hildenborough and *Methanobacterium congolense*: global transcriptomic and proteomic analyses. *ISME J.* 6, 410–421. doi: 10.1038/ismej.2011.111

Norstrom, R. J., Simon, M., Moisey, J., Wakeford, B., and Weseloh, D. V. (2002). Geographical distribution (2000) and temporal trends (1981-2000) of brominated diphenyl ethers in Great Lakes hewing gull eggs. *Environ. Sci. Technol.* 36, 4783–4789. doi: 10.1021/es025831e

O'Driscoll, K., Robinson, J., Chiang, W.-S., Chen, Y.-Y., Kao, R.-C., and Doherty, R. (2016). The environmental fate of polybrominated diphenyl ethers (PBDEs) in western Taiwan and coastal waters: evaluation with a fugacity-based model. *Environ. Sci. Pollut. Res.* 23, 13222–13234. doi: 10.1007/s11356-016-6428-4

Palm, A., Cousins, I. T., Mackay, D., Tysklind, M., Metcalfe, C., and Alaee, M. (2002). Assessing the environmental fate of chemicals of emerging concern: a case study of the polybrominated diphenyl ethers. *Environ. Pollut.* 117, 195–213. doi: 10.1016/S0269-7491(01)00276-7

Qiu, M., Chen, X., Deng, D., Guo, J., Sun, G., Mai, B., et al. (2012). Effects of electron donors on anaerobic microbial debromination of polybrominated diphenyl ethers (PBDEs). *Biodegradation* 23, 351–361. doi: 10.1007/s10532-011-9514-9

Rayne, S., Ikonomou, M. G., and Whale, M. D. (2003). Anaerobic microbial and photochemical degradation of 4,4'-dibromodiphenyl ether. *Water Res.* 37, 551–560. doi: 10.1016/S0043-1354(02)00311-1

Rayne, S., Wan, P., and Ikonomou, M. (2006). Photochemistry of a major commercial polybrominated diphenyl ether flame retardant congener: 2,2′, 4,4′, 5,5′-hexabromodiphenyl ether (BDE153). *Environ. Int.* 32, 575–585. doi: 10.1016/j.envint.2006.01.009

Robrock, K. R., Korytar, P., and Alvarez-Cohen, L. (2008). Pathways for the anaerobic microbial debromination of polybrominated diphenyl ethers. *Environ. Sci. Technol.* 42, 2845–2852. doi: 10.1021/es0720917

Schenker, U., Soltermann, F., Scheringer, M., and Hungerbühler, K. (2008). Modeling the environmental fate of polybrominated diphenyl ethers (PBDEs): the importance of photolysis for the formation of lighter PBDEs. *Environ. Sci. Technol.* 42, 9244–9249. doi: 10.1021/es801042n

Shin, M., Duncan, B., Seto, P., Falletta, P., and Lee, D.-Y. (2010). Dynamics of selected pre-existing polybrominated diphenylethers (PBDEs) in municipal wastewater sludge under anaerobic conditions. *Chemosphere* 78, 1220–1224. doi: 10.1016/j.chemosphere.2009.12.057

Siddiqi, M. A., Laessig, R. H., and Reed, K. D. (2003). Polybrominated diphenyl ethers (PBDEs): new pollutants–old diseases. *Clin. Med. Res.* 1, 281–290. doi: 10.3121/cmr.1.4.281

Song, M. K., Luo, C. L., Li, F. B., Jiang, L. F., Wang, Y., Zhang, D. Y., et al. (2015). Anaerobic degradation of polychlorinated biphenyls (PCBs) and polybrominated diphenyl ethers (PBDEs), and microbial community dynamics of electronic waste-contaminated soil. *Sci. Total Environ.* 502, 426–433. doi: 10.1016/j.scitotenv.2014.09.045

Stapleton, H. M., and Dodder, N. G. (2008). Photodegradation of decabromodiphenyl ether in house dust by natural sunlight. *Environ. Toxicol. Chem.* 27, 306–312. doi: 10.1897/07-301R.1

Stiborova, H., Vrkoslavova, J., Pulkrabova, J., Poustka, J., Hajslova, J., and Demnerova, K. (2015). Dynamics of brominated flame retardants removal in contaminated wastewater sewage sludge under anaerobic conditions. *Sci. Total Environ.* 533, 439–445. doi: 10.1016/j.scitotenv.2015.06.131

Tiehm, A., and Schmidt, K. R. (2011). Sequential anaerobic/aerobic biodegradation of chloroethenes—aspects of field application. *Curr. Opin. Biotechnol.* 22, 415–421. doi: 10.1016/j.copbio.2011.02.003

Tokarz, J. A., Ahn, M. Y., Leng, J., Filley, T. R., and Nies, L. (2008). Reductive debromination of polybrominated diphenyl ethers in anaerobic sediment and a biomimetic system. *Environ. Sci. Technol.* 42, 1157–1164. doi: 10.1021/es071989t

United Nations Environment Programme (2009). *Stockholm Convention on Persistent Organic Pollutans (POPs)*. Geneva, Switzerland.

Wagner, A., Cooper, M., Ferdi, S., Seifert, J., and Adrian, L. (2012). Growth of *Dehalococcoides mccartyi* strain CBDB1 by reductive dehalogenation of brominated benzenes to benzene. *Environ. Sci. Technol.* 46, 8960–8968. doi: 10.1021/es3003519

Wang, S., Chng, K. R., Wilm, A., Zhao, S., Yang, K.-L., Nagarajan, N., et al. (2014). Genomic characterization of three unique *Dehalococcoides* that respire on persistent polychlorinated biphenyls. *Proc. Natl. Acad. Sci. U.S.A.* 111, 12103–12108. doi: 10.1073/pnas.1404845111

Wang, S., and He, J. (2013). Phylogenetically distinct bacteria involve extensive dechlorination of Aroclor 1260 in sediment-free cultures. *PLoS ONE* 8:e59178. doi: 10.1371/journal.pone.0059178

Wild, S., McLagan, D., Schlabach, M., Bossi, R., Hawker, D., Cropp, R., et al. (2015). An Antarctic research station as a source of brominated and perfluorinated persistent organic pollutants to the local environment. *Environ. Sci. Technol.* 49, 103–112. doi: 10.1021/es5048232

Windham, G. C., Pinney, S. M., Voss, R. W., Sjödin, A., Biro, F. M., Greenspan, L. C., et al. (2015). Brominated flame retardants and other persistent organohalogenated compounds in relation to timing of puberty in a longitudinal study of girls. *Environ. Health Perspect.* 123, 1046–1052. doi: 10.1289/ehp.1408778

Xu, G., Wang, J., and Lu, M. (2014). Complete debromination of decabromodiphenyl ether using the integration of *Dehalococcoides* sp. strain CBDB1 and zero-valent iron. *Chemosphere* 117, 455–461. doi: 10.1016/j.chemosphere.2014.07.077

Yang, C. (2017). *Anaerobic Transformation of Brominated Aromatic Compounds by Dehalococcoides mccartyi Strain CBDB1*. Doctoral Thesis.

Yang, C., Kublik, A., Weidauer, C., Seiwert, B., and Adrian, L. (2015). Reductive dehalogenation of oligocyclic phenolic bromoaromatics by *Dehalococcoides mccartyi* strain CBDB1. *Environ. Sci. Technol.* 49, 8497–8505. doi: 10.1021/acs.est.5b01401

Yang, C. W., Huang, H. W., and Chang, B. V. (2017). Microbial communities associated with anaerobic degradation of polybrominated diphenyl ethers in river sediment. *J. Microbiol. Immunol. Infect.* 50, 32–39. doi: 10.1016/j.jmii.2014.12.009

Zhang, S., Adrian, L., and Schuurmann, G. (2018). Interaction mode and regioselectivity in vitamin B_{12}-dependent dehalogenation of aryl halides by *Dehalococcoides mccartyi* strain CBDB1. *Environ. Sci. Technol.* 52, 1834–1843. doi: 10.1021/acs.est.7b04278

Zhang, S., Wondrousch, D., Cooper, M., Zinder, S. H., Schuurmann, G., and Adrian, L. (2017). Anaerobic dehalogenation of chloroanilines by *Dehalococcoides mccartyi* strain CBDB1 and *Dehalobacter* Strain 14DCB1 via different pathways as related to molecular electronic structure. *Environ. Sci. Technol.* 51, 3714–3724. doi: 10.1021/acs.est.6b05730

Zhu, H. W., Wang, Y., Wang, X. W., Luan, T. G., and Tam, N. F. Y. (2014). Intrinsic debromination potential of polybrominated diphenyl ethers in different sediment slurries. *Environ. Sci. Technol.* 48, 4724–4731. doi: 10.1021/es4053818

Zhu, L. Y., and Hites, R. A. (2004). Temporal trends and spatial distributions of brominated flame retardants in archived fishes from the Great Lakes. *Environ. Sci. Technol.* 38, 2779–2784. doi: 10.1021/es035288h

Conflict of Interest Statement: The authors declare that the research was conducted in the absence of any commercial or financial relationships that could be construed as a potential conflict of interest.

frontiers in Microbiology

ORIGINAL RESEARCH
published: 10 August 2018
doi: 10.3389/fmicb.2018.01774

Functional Expression and Characterization of Tetrachloroethene Dehalogenase From *Geobacter* sp.

*Ryuki Nakamura[1], Tomohiro Obata[1], Ryota Nojima[1], Yohey Hashimoto[2], Keiichi Noguchi[3], Takahiro Ogawa[4] and Masafumi Yohda[1,4]**

[1] Department of Biotechnology and Life Science, Tokyo University of Agriculture and Technology, Tokyo, Japan, [2] Department of Bioapplications and Systems Engineering, Tokyo University of Agriculture and Technology, Tokyo, Japan, [3] Instrumentation Analysis Center, Tokyo University of Agriculture and Technology, Tokyo, Japan, [4] Institute of Global Innovation Research, Tokyo University of Agriculture and Technology, Tokyo, Japan

Reductive dehalogenase (RDase) consists of two parts, RdhA and RdhB. RdhA is the catalytic subunit, harboring a cobalamin cofactor and two Fe–S clusters. RdhA is anchored to the cytoplasmic membrane via the membrane anchoring subunit, RdhB. There are many genes encoding RDases in the genome of organohalide-respiring bacteria, including *Dehalococcoides* spp. However, most genes have not been functionally characterized. Biochemical studies on RDases have been hampered by difficulties encountered in their expression and purification. In this study, we have expressed, purified and characterized RdhA of RDase for tetrachloroethene (PceA) from *Geobacter* sp. PceA was expressed as a fusion protein with a trigger factor tag in *Escherichia coli*. PceA was purified and denatured in aerobic condition. Subsequently, this protein was refolded in the presence of $FeCl_3$, Na_2S and cobalamin in anaerobic condition. The reconstituted PceA exhibited dechlorination ability for tetrachloroethene. UV-Vis spectroscopy has shown that it contains cobalamin and Fe-S clusters. Since this method requires anaerobic manipulation only in the reconstituting process and has a relatively high yield, it will enable further biochemical studies of RDases.

Keywords: reductive dehalogenase, tetrachloroethene, *Geobacter*, reconstitution, cobalamin

OPEN ACCESS

Edited by:
Jianzhong He,
National University of Singapore, Singapore

Reviewed by:
Jiandong Jiang,
Nanjing Agricultural University, China
Paul Race,
University of Bristol, United Kingdom

***Correspondence:**
Masafumi Yohda
yohda@cc.tuat.ac.jp

Specialty section:
This article was submitted to Microbiotechnology, Ecotoxicology and Bioremediation, a section of the journal Frontiers in Microbiology

Received: *24 December 2017*
Accepted: *16 July 2018*
Published: *10 August 2018*

Citation:
Nakamura R, Obata T, Nojima R, Hashimoto Y, Noguchi K, Ogawa T and Yohda M (2018) Functional Expression and Characterization of Tetrachloroethene Dehalogenase From Geobacter sp. Front. Microbiol. 9:1774. doi: 10.3389/fmicb.2018.01774

INTRODUCTION

Organohalides are recalcitrant pollutants that have caused contamination of soils and groundwater in many sites around the world. Various bacteria derive their metabolic energy from dehalorespiration, which uses organohalides as terminal electron acceptors in anaerobic respiration (Holliger et al., 1998). Organohalide-respiring bacteria include *Dehalococcoides, Dehalogenimonas, Dehalobacter, Desulfitobacterium, and Sulfurospirillum*, as well as the organohalide-respiring members of the Deltaproteobacteria. Organohalide-respiring bacteria play critical roles in anaerobic bioremediation of sites contaminated by organohalides (Jugder et al., 2016). Organohalide-respiring bacteria are equipped with the conserved membrane-associated proteins, reductive dehalogenases (RDases), which catalyze reductive dehalogenation reactions resulting in the generation of lesser-halogenated compounds (Jugder et al., 2015). RDase is composed of two components, RdhA and RdhB. The catalytically active subunit RdhA contains

one cobalamin and two Fe–S clusters (either two 4Fe–4S clusters or one 4Fe–4S and one 3Fe–4S cluster). There is one twin-arginine (TAT) signal sequence (RRXFXK) at the N-terminus, which mediates the transport of pre-folded RdhA into the periplasm. RdhA is associated with the outer side of the cytoplasmic membrane via the integral membrane protein RdhB.

Recent genome analyses of organohalide-respiring bacteria showed the existence of various RDase genes. Among these genes, there exist many RDase genes in genomes of *Dehalococcoides* spp. For example, 38 RdhA genes were identified in the genome of *D. mccartyi* strain MB (Low et al., 2015). However, the current understanding of RDase is limited to the results of studies on only several RDases, PceA (Schmitz et al., 2007; Sjuts et al., 2012), CprA (van de Pas et al., 1999, 2001), TceA (Magnuson et al., 2000), and vinyl chloride RDase (VcrA) (Muller et al., 2004; Parthasarathy et al., 2015). Existence of various RDases in *Dehalococcoides* spp. hampered the characterization of each RDase. It is difficult to culture organohalide-respiring bacteria for purification of RDases. Moreover, the heterologous expression of RDases is generally difficult because most RDases are oxygen-labile membrane-associated proteins. The heterologous expression of a few RDases was reported. Catabolic RDase BhbA from *Comamonas* is not oxygen sensitive and could be functionally expressed (Chen et al., 2013). PceA of *D. hafniense* strainY51 was overexpressed in a cobamide-producing bacterium *Shimwellia blattae* (Mac Nelly et al., 2014) and RdhA from *Nitratireductor pacificus* pht-3B (NpRdhA) in *Bacillus megaterium* (Payne et al., 2015). Recently, it was reported that heterologously expressed *Dehalococcoides* VcrA in *Escherichia coli*, was purified and reconstituted to its active form by the addition of hydroxocobalamin/adenosylcobalamin, Fe^{3+}, and sulfide in the presence of mercaptoethanol (Parthasarathy et al., 2015). VcrA was obtained as a fusion protein with a maltose binding protein as an insoluble protein. In this method, all purification and reconstitution processes were performed in anaerobic conditions. However, the method was laborious, and the yield was insufficient.

In the present study, we tried functional expression and characterization of PceA from *Geobacter* sp. We expressed PceA with a fusion protein with the trigger factor tag and also the Strep-tag (TF-PceA-Strep). After purification and denaturation in 8 M urea in aerobic conditions, PceA was reconstituted with Fe and cobalamin in anaerobic condition. Thus, the reconstituted TF-PceA-Strep exhibited RDase activity on PCE.

MATERIALS AND METHODS

Cloning and Expression of *PceA*

The *pceA* gene was obtained by PCR from the metagenome DNA of PCE dechlorinating bacterial consortium using the primers (5′-ATG GAT CGT AGA GAT TTT TTT AAA AAG GCA GC-3′ and 5′-CTA TGC CTT GTT CCA GAA GTC CG-3′). The amplified DNA was cloned into the T-vector pMD20 (TaKaRa Bio, Inc., Shiga, Japan) and subjected to DNA sequencing.

The full-length *pceA* was amplified using the primers (5′-CCC AAG CTT ATG GAT CGT AGA GAT TTT TTT AAA AAG G-3′ and 5′-CCC TCG AGC TAT GCC TTG TTC C-3′) and cloned into the HindIII/XhoI site of pET23b (Merck Millipore, Co., Billerica, MA, United States) (pET23b_PceA).

To express PceA as a fusion protein with TF, the gene was amplified with the primers (5′-CGA GCT CAT GGA TCG TAG AGA TTT TTT TAA AAA GG-3′ and 5′-CCC TCG AGC TAT GCC TTG TTC C-3′), and subcloned into the SacI/XhoI site of pCold TF vector (TaKaRa Bio, Inc.) (pCold TF-PceA). Then, the Strep-tag sequence was inserted at the C-terminus by the QuikChange method using the primers (5′-CGG ACT TCT GGA ACA AGG CAT GGA GCC ATC CGC AGT TTG AAA AGT AAG TCG ACC TGC AGT CTA GAT AG-3′ and 5′-CTA TCT AGA CTG CAG GTC GAC TTA CTT TTC AAA CTG CGG ATG GCT CCA TGC CTT GTT CCA GAA GTC CG-3′) (pCold TF-PceA-Strep).

Thus, the prepared plasmids (pET23b_PceA, pCold TF-PceA, and pCold TF-PceA-Strep) were used for the transformation of *E. coli* BL21 star (DE3). The transformed cells were grown in Luria-Bertani medium containing 100 μg/ml ampicillin at the specified temperatures. The cells were harvested by centrifugation at 5000 rpm for 15 min at 4°C.

Purification of TF-PceA-Strep and Cofactor Reconstitution

Approximately 3 g wet weight of TF-PceA-Strep was re-suspended in 30 ml of suspension buffer (50 mM potassium phosphate pH 8.0 containing 0.5 M NaCl, 20% glycerol, 1mM PMSF). After cell disruption using an ultrasonic disruptor (UD-201, TOMY, Co., Tokyo, Japan), the suspension was centrifuged for 15 min at 14,000 rpm. The supernatant was discarded, and the pellet was resuspended in 15 ml of the denaturation buffer (suspension buffer + 8 M urea). Following another round of sonication, the suspension was stirred on ice for 1 h to solubilize the pellet. Centrifugation for 15 min at 4°C at 14,000 rpm was performed to remove remaining insoluble material.

The supernatant containing denatured TF-PceA-Strep was loaded onto the Ni-affinity column (His-Trap FF, GE Healthcare, Buckinghamshire, United Kingdom), which had been washed with five column volumes of the denaturation buffer and eluted with four column volumes of 250 mM imidazole in the denaturation buffer.

Next, the reconstitution of TF-PceA-Strep was performed under anaerobic conditions. All buffers were purged with 99.99% Ar and placed in the anoxic glove box before use. Denatured TF-PceA-Strep was mixed with the reduction buffer (100 mM Tris-HCl pH 7.5, 200 mM DTT) to 5 mM of DTT, and incubated for 30 min with stirring. Then, Fe buffer (100 mM Tris-HCl pH 7.5, 100 mM $FeCl_3$) and S buffer (100 mM Tris-HCl pH 7.5, 30 mM Na_2S) were added up to 50 mol excess of Fe and S to TF-PceA-Strep. After 90 min incubation with stirring, cyanocobalamin was added to a final concentration of 10 mg/ml. Next, TF-PceA-Strep solution was applied to a PD-10 column (GE Healthcare) equilibrated with the refolding buffer (50 mM Tris-HCl pH 8.0, 0.5 M NaCl, 20% glycerol, 0.2% CHAPS, 1 mM

PMSF, and 10 mM DTT). The fractions containing reconstituted TF-PceA-Strep were collected.

PceA Dechlorination Activity Assay

Enzyme activity experiments were performed in the anoxic sealed serum vials of 10 ml volume with butyl rubber stopper. In an anoxic vial, 3 ml of 50 mM Tris-HCl pH 8.5 containing 0.2 mg/ml of the reconstituted TF-PceA-Strep, 1 mM Ti(III) citrate as the electron donor and 0.4 mM methyl viologen as the electron mediator was added. The reaction was started by injecting PCE to approximately 100 μM PCE. Headspace samples (100 μl) were injected into the gas chromatograph (Shimadzu GC 2014 gas chromatograph, Shimadzu, Co., Kyoto, Japan) equipped with a DB-624 column (60 m length, 0.32 mm diameter, and 1.80 μm film thickness, Agilent Technology, Santa Clara, CA, United States) and a flame ionization detector.

Mass Spectrometry

The band for TF-PceA-Strep in SDS-PAGE was excised and applied for the treatment by In-Gel Tryptic Digestion Kit (ThermoFisher Scientific, Co., Waltham, MA, United States). LC–MS/MS analysis of the digested peptides was performed using reversed-phase LC interfaced with a Q-TOF mass spectrometer (Bruker Daltonics, Co., Billerica, MA, United States). The digest peptides were separated using a PEGASIL ODS SP300-3 column (φ1 mm × 100 mm, 3 μm; Senshu Scientific, Co., Tokyo, Japan) eluted with a linear gradient of 0–100% buffer B (100% acetonitrile and 0.1% trifluoroacetic acid) in buffer A (0.1% trifluoroacetic acid in water) at a flow rate of 0.04 ml/min. MS and MS/MS data were acquired using the data-dependent top five method. The resulting MS/MS data were searched against the sequences of TF-PceA-Strep, using BioTools (Bruker Daltonics, Co.).

UV-Vis Spectroscopy

UV-Vis absorbance spectra were recorded with a Varian CARY 50 UV-VIS Spectrophotometer (Agilent Technologies) in aerobic condition.

Metal Analysis

Co and Fe content was analyzed by graphite furnace atomic absorption spectrometry (GFAAS). We used the Polarized Zeeman Atomic Absorption Spectrophotometer ZA3000 (Hitachi High-Technologies, Co., Tokyo, Japan) for GFAAS. At first, we made the calibration curves using the standard solutions of Fe and Co at the concentration of 0, 2.5, 5.0, 10, or 15 ppb in the Refolding Buffer (50 mM Tris-HCl pH 8.0, 0.5 M NaCl, 20% glycerol, and 0.2% CHAPS). Next, the reconstituted TF-PceA-Strep was diluted with 2% nitric acid. The diluted samples were applied for GFAAS analysis. The average values of triplicate measurements were used.

Circular Dichroism (CD) Measurement

The secondary structure of the refolded TF-PceA was analyzed by CD. Protein samples were prepared in 2 mM Tris-HCl, pH 8.0 at 8.9 μM and then filtrated with cellulose acetate filter (0.2 μm). CD spectrum with a wavelength range of 205–260 nm was measured at 20°C by CD spectrometer (J-820, JASCO, Tokyo, Japan) using a 2 mm optical path length cuvette.

RESULTS

Previously, we had constructed a PCE dechlorinating bacterial consortium. The consortium could dechlorinate tetrachloroethene (PCE) to *cis*-1,2-dichloroethene (*cis*-DCE) (**Supplementary Figure S1**). The 16S rRNA gene analysis of the metagenome showed the presence of *Dehalobacter* sp., *Geobacter* sp., *Sulfurospirillum* sp., *Clostridium* sp. and *Bacteroides* sp. Among these species, we speculated that *Dehalobacter* sp. or *Geobacter* sp. is responsible for dechlorination of PCE. Next, we attempted to amplify *pceA* genes from the metagenome using various primers designed from *pceA* genes of *Dehalobacter* sp. and *Geobacter* sp. We could obtain the full-length *pceA* gene, which exhibits significantly high sequence identity with that of *G. lovleyi* SZ (**Figure 1**). The Nucleotide sequence is available in the DDBJ/EMBL/GenBank databases under the accession number, LC342077. *G. lovleyi* SZ was obtained from the non-contaminated creek sediment microcosms based on their ability to derive energy from acetate oxidation coupled to PCE-to-*cis*-DCE dechlorination (Sung et al., 2006). The putative RDase from *Anaeromicrobium sediminis* also showed significant sequence identity. The sequence alignment of the three RDases is shown in **Figure 1**. In the N-terminal region, there exists the consensus motif of twin-arginine signal sequence, RRXFXK. Two iron–sulfur cluster binding (ISB) sites are also conserved. The first ISB, CKNCKKCADACP, corresponds to the conserved consensus sequence CXXCXXCXXXCP, found in bacterial ferredoxins (Bruschi and Guerlesquin, 1988). The second ISB is partly different from the consensus one. The latter motif, CXXCXXXCP, is conserved, but the first Cys residue is separated from the second Cys residue by 10 amino acid residues. The consensus sequence for cobalamin binding, DXHXXG...SXL...GG is partially conserved in PceA (Ludwig and Matthews, 1997). However, there are sequence variations in the corresponding sequences in the homologous putative PceAs.

To express the *Geobacter* PceA in *E. coli*, the *Geobacter pceA* was cloned into the pET23b vector (pET23b-pceA) and used to transform *E. coli* BL21 star (DE3). PceA was obtained as an aggregate in the insoluble fraction (**Figure 2A**). Next, we tried to express PceA as a fusion protein with the trigger factor tag (TF-PceA). TF-PceA was obtained as a soluble protein at the induction of protein expression at 18°C (**Figure 2B**). *E. coli* cells expressing TF-PceA were collected and disrupted by the lysozyme treatment at the anaerobic conditions in a glove box. The total cell lysate was applied for dechlorination assay for PCE. Unexpectedly, no PCE dechlorination activity was observed. We further tried to purify TF-PceA in aerobic conditions using the histidine tag attached to TF tag. However, TF-PceA was subjected to protease digestion during purification by Ni affinity chromatography. Next, we added Strep-tag at the C-terminus (TF-PceA-Strep). TF-PceA-Strep was purified by affinity chromatography using Strep-tactin column and size

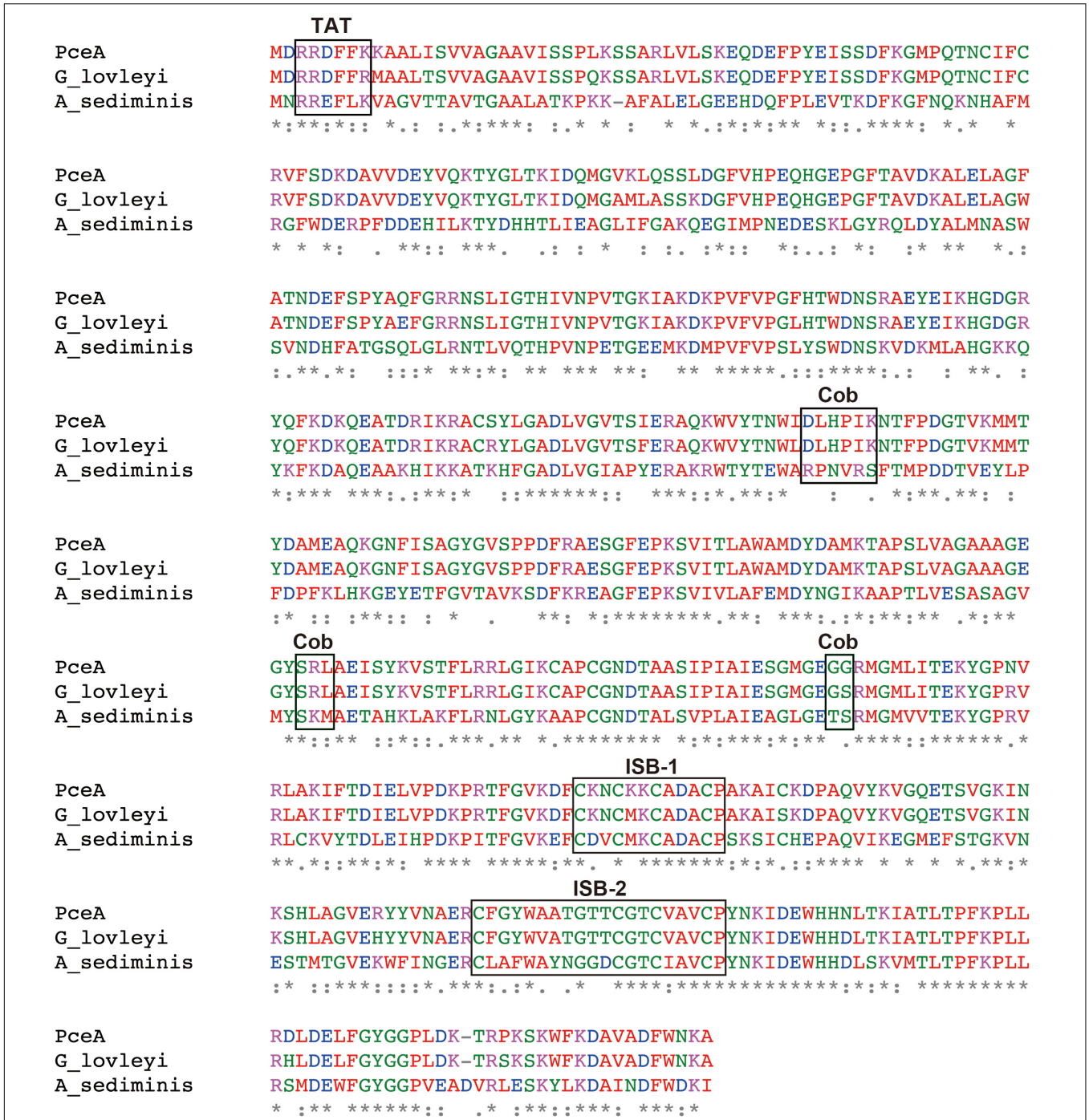

FIGURE 1 | Amino acid sequence alignment for the PceA of this study and other homologous PceAs. Sequence alignment was performed by Clustal Omega. The identical amino acids are marked by asterisk. Double dot and dot designate similar amino acid residues. PceA (this study), G_lovleyi SZ (PceA from *Geobacter lovleyi* SZ, AFN20668.1), and A_sediminis (PceA from *Anaeromicrobium sediminis*, WP_095136311.1). TAT, Twin-arginine motif; ISB-1 and ISB-2, iron–sulfur cluster binding motif; Cob, Cobalamin binding motif.

exclusion chromatography. In this case, no protease digestion was observed. In the mass spectroscopic analysis, the proteolytic peptide fragments covered approximately 40% of TF-PceA-Strep (**Supplementary Figure S2**). Since UV-Vis spectrum of the purified TF-PceA-Strep lacked the peak for cobalamin, we concluded that the active center was not correctly formed in TF-PceA-Strep.

We speculated that although active PceA was obtained in *E. coli*, it is difficult to purify, because all procedures must be performed in anaerobic conditions. Thus, we decided to

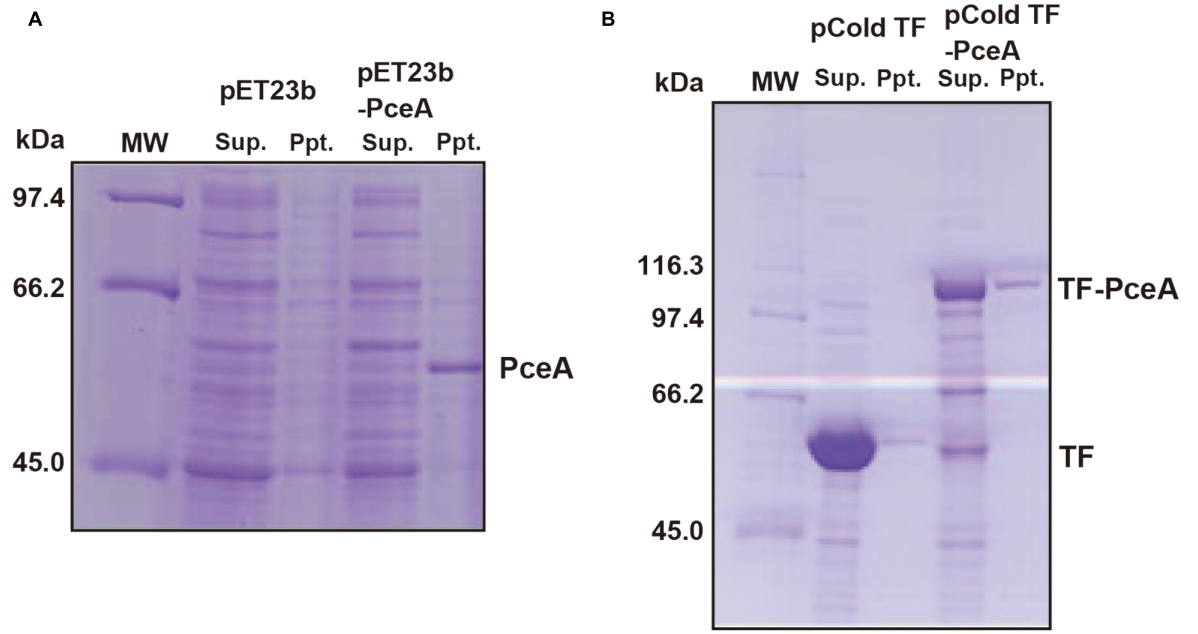

FIGURE 2 | Expression of PceA and TF-PceA in *Escherichia coli*. The supernatant and precipitate of the crude extracts of *E. coli* cells harboring designated plasmids are analyzed by SDS-PAGE. **(A)** pET23b and pET23b-PceA **(B)** pCold TF and pCold TF-PceA.

TABLE 1 | Fe and Co content in the reconstituted TF-PceA-Strep.

	TF-PceA-Strep	Co	Fe
Quantity (nmol)	2.645	3.77	28.2
Ratio	-	1.42	10.7

reconstitute active PceA *in vitro*. Since it was difficult to reconstitute PceA *in vitro*, we used TF-PceA-Strep. We expressed TF-PceA-Strep as an insoluble protein by culturing recombinant *E. coli* at 37°C. Then, the precipitated proteins were solubilized by buffer containing 8 M Urea. TF-PceA-Strep was purified by nickel affinity chromatography in the presence of 8 M urea. The denatured TF-PceA-Strep was applied for reconstitution in the anaerobic glove box. Denatured TF-PceA-Strep was mixed with DTT, $FeCl_3$, Na_2S and cobalamin in denaturation buffer, and the mixture was loaded onto a PD-10 desalting column equilibrated with the refolding buffer. TF-PceA-Strep was expected to reconstitute by removing urea, and unincorporated excess cofactors were also removed. CD spectrum shows that the reconstituted TF-PceA-Strep takes the folded conformation (**Supplementary Figure S3**).

Thus, prepared reconstituted TF-PceA-Strep was used for the dechlorination assay for PCE. The reconstituted TF-PceA-Strep was mixed with PCE in the presence of Ti(III) citrate as the electron donor and methyl viologen as the electron mediator. As shown in **Figure 3**, in the presence of TF-PceA-Strep, PCE decreased with the increase of TCE and *cis*-DCE. However, a decrease in PCE and the appearance of TCE and *cis*-DCE were not observed in the control experiments using a protein unrelated to reductive dehalogenation, Hsp104 from a thermophilic fungus.

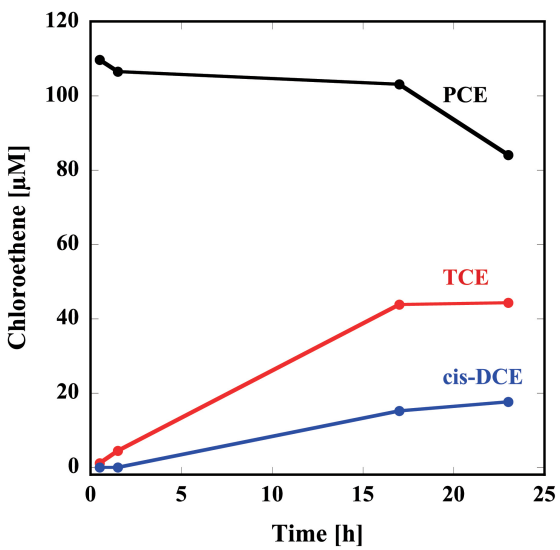

FIGURE 3 | Reduction of PCE to TCE and *cis*-DCE by the reconstituted TF-PceA-Strep. Time-course concentration changes of PCE (black), TCE (red), and *cis*-DCE (blue) are plotted.

Finally, we examined the reconstitution of the catalytic centers by UV-Vis spectrophotometry and metal analysis. Because of the apparatus limitation, we performed UV-Vis spectrophotometry in aerobic conditions. Before reconstitution, no peaks derived from the cofactor were detected. Alternatively, peaks attributed to each cofactor were detected from the sample after reconstruction; [4Fe–4S] at 420 nm, Co(I) at 360 and 550 nm, and Co(II) at

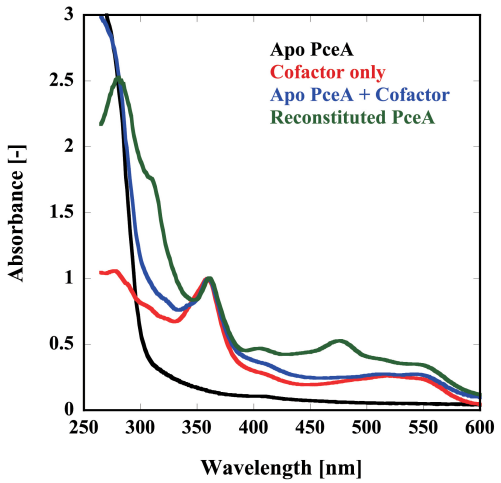

FIGURE 4 | Reconstitution of the catalytic center in TF-PceA-Strep observed by UV-Vis spectrum. UV-Vis spectra of apo-TF-PceA-Strep (refolded without cofactor) (black), cofactors only (red), apo-TF-PceA-Strep + cofactor (blue), and the reconstituted TF-PceA-Strep (green) are shown. The spectra were normalized by the absorbance of 360 nm.

310 nm (**Figure 4**). To obtain the quantitative data, the metal content of the reconstituted TF-PceA-Strep was analyzed by GFAAS (**Table 1**). The molar ratio of TF-PceA-Strep:Co:Fe was 1:1.4:10. This ratio was close to the theoretical value of 1:1:8, suggesting that TF-PceA-Strep and cofactor coexist with values close to the theoretical values.

DISCUSSION

There are many genes encoding RDases in the genome of organohalide-respiring bacteria, including *Dehalococcoides* spp. However, most of them have not been functionally characterized. Existence of multi RDases in a bacterium makes it also difficult to examine the substrate specificities of them. Since most RDases are membrane proteins labile for aerobic condition, it is generally difficult to obtain recombinant ones. The catalytic subunit, RdhA, is not embedded in the membrane. Therefore, it is possible to obtain RdhA as a soluble protein. However, generally, RdhA does not fold correctly in *E. coli* probably due to its partially hydrophobic nature to interact with the membrane bound RdhB.

PceA from *D. restrictus* was expressed as a fusion protein with the trigger factor (TF) tag, and purified under anaerobic conditions (Sjuts et al., 2012). Recently, heterologous production of RdhA of VcrA from *D. mccartyi* strain VS was reported (Parthasarathy et al., 2015). In both cases, UV-Vis and electron paramagnetic resonance spectroscopy revealed that catalytic centers are correctly constituted. In their methods, all purification procedures were conducted in anaerobic conditions. Therefore, it is difficult to perform in laboratories with ordinary instruments. Moreover, the yield is relatively small for detailed studies. Our idea was to obtain denatured RdhA in aerobic conditions and refold it with their cofactors.

In this study, we tried to express and characterize the PceA. The *pceA* gene is significantly homologous to that of *G. lovleyi*. This gene also showed high homology to the putative RDase from *A. sediminis*. The sequence identity was estimated to be 51%. The sequence identity with the other putative PceA is relatively modest. The identity with the PceA from *Dehalobacter* sp. E1 (EQB20894.1) is approximately 37%. The two ISB motifs are conserved with that of PceA from *Dehalobacter* sp. E1. However, cobalamin binding motif is not well-conserved. Because *Geobacter* sp. and *Dehalobacter* sp. seemed to be responsible for dechlorination of PCE in the original bacterial consortium, we concluded that the gene was originated from a *Geobacter* sp.

We expressed PceA as a fusion protein with the trigger factor tag and also the Strep-tag (TF-PceA-Strep). TF-PceA-Strep was denatured by buffer containing 8 M urea and purified by affinity chromatography using the histidine tag in trigger factor tag. Although TF-PceA-Strep was only partially purified in this study, it is possible to perform further purification using different types of chromatography. The reconstitution of TF-PceA-Strep was performed by size exclusion chromatography using a buffer containing cofactors in anaerobic conditions. Since TF-PceA-Strep can refold easily, this process requires only a small column. The reconstituted TF-PceA-Strep could convert PCE to *cis*-DCE via TCE. UV-Vis and GFAAS suggested binding of TF-PceA-Strep and a cofactor. The measured metal content of the reconstituted sample was partially larger than the theoretical value. This result is probably observed because the separation of free Fe and cobalamin by PD-10 is not sufficient.

We have established a heterologous platform to produce the TF-PceA-Strep enzyme, which can be reconstituted in its active form. It was expected that the function and structure of RDase would be clarified by the crystallization of RDase under anaerobic conditions. Further study is needed to understand all of the components related to the synthesis and activity of RdhA, with continued future research efforts investigating the accessory genes and their products, such as transcriptional regulators (PceC, MarR), anchoring proteins (RdhB or PceB), and maturation proteins (e.g., PceT). This platform may be employed for obtaining recombinant proteins with the same characteristics as RDase.

AUTHOR CONTRIBUTIONS

RNA performed all data collections. TOB, YH, TOG, and KN assisted the data collection. RNO constructed PCE dechlorinating bacterial consortium and assisted data collection. MY designed the study and wrote the manuscript.

FUNDING

This research was partially supported by the Okinawa Life Science Network Program, Okinawa Intellectual Cluster Program, and Okinawa Cutting-Edge Genome Project and the grants-in-aid for scientific research (JP18H04690) from the Ministry of Education, Science, Sports, and Culture of Japan.

ACKNOWLEDGMENTS

We sincerely appreciate Drs. Manjiri Ravindra Kulkarni and Yutaka Kuroda of Tokyo University of Agriculture and Technology for kind assistance in CD measurement.

SUPPLEMENTARY MATERIAL

The Supplementary Material for this article can be found online at: https://www.frontiersin.org/articles/10.3389/fmicb.2018.01774/full#supplementary-material

REFERENCES

Bruschi, M., and Guerlesquin, F. (1988). Structure, function and evolution of bacterial ferredoxins. *FEMS Microbiol. Rev.* 4, 155–175. doi: 10.1111/j.1574-6968.1988.tb02741.x

Chen, K., Huang, L., Xu, C., Liu, X., He, J., Zinder, S. H., et al. (2013). Molecular characterization of the enzymes involved in the degradation of a brominated aromatic herbicide. *Mol. Microbiol.* 89, 1121–1139. doi: 10.1111/mmi.12332

Holliger, C., Wohlfarth, G., and Diekert, G. (1998). Reductive dechlorination in the energy metabolism of anaerobic bacteria. *FEMS Microbiol. Rev.* 22, 383–398. doi: 10.1111/j.1574-6976.1998.tb00377.x

Jugder, B. E., Ertan, H., Bohl, S., Lee, M., Marquis, C. P., and Manefield, M. (2016). Organohalide respiring bacteria and reductive dehalogenases: key tools in organohalide bioremediation. *Front. Microbiol.* 7:249. doi: 10.3389/fmicb.2016.00249

Jugder, B. E., Ertan, H., Lee, M., Manefield, M., and Marquis, C. P. (2015). Reductive dehalogenases come of age in biological destruction of organohalides. *Trends Biotechnol.* 33, 595–610. doi: 10.1016/j.tibtech.2015.07.004

Low, A., Shen, Z., Cheng, D., Rogers, M. J., Lee, P. K., and He, J. (2015). A comparative genomics and reductive dehalogenase gene transcription study of two chloroethene-respiring bacteria, *Dehalococcoides mccartyi* strains MB and 11a. *Sci. Rep.* 5:15204. doi: 10.1038/srep15204

Ludwig, M. L., and Matthews, R. G. (1997). Structure-based perspectives on B12-dependent enzymes. *Annu. Rev. Biochem.* 66, 269–313. doi: 10.1146/annurev.biochem.66.1.269

Mac Nelly, A., Kai, M., Svatos, A., Diekert, G., and Schubert, T. (2014). Functional heterologous production of reductive dehalogenases from *Desulfitobacterium hafniense* strains. *Appl. Environ. Microbiol.* 80, 4313–4322. doi: 10.1128/AEM.00881-14

Magnuson, J. K., Romine, M. F., Burris, D. R., and Kingsley, M. T. (2000). Trichloroethene reductive dehalogenase from *Dehalococcoides ethenogenes*: sequence of tceA and substrate range characterization. *Appl. Environ. Microbiol.* 66, 5141–5147. doi: 10.1128/AEM.66.12.5141-5147.2000

Muller, J. A., Rosner, B. M., Von Abendroth, G., Meshulam-Simon, G., Mccarty, P. L., and Spormann, A. M. (2004). Molecular identification of the catabolic vinyl chloride reductase from *Dehalococcoides* sp. strain VS and its environmental distribution. *Appl. Environ. Microbiol.* 70, 4880–4888. doi: 10.1128/AEM.70.8.4880-4888.2004

Parthasarathy, A., Stich, T. A., Lohner, S. T., Lesnefsky, A., Britt, R. D., and Spormann, A. M. (2015). Biochemical and EPR-spectroscopic investigation into heterologously expressed vinyl chloride reductive dehalogenase (VcrA) from *Dehalococcoides mccartyi* strain VS. *J. Am. Chem. Soc.* 137, 3525–3532. doi: 10.1021/ja511653d

Payne, K. A., Quezada, C. P., Fisher, K., Dunstan, M. S., Collins, F. A., Sjuts, H., et al. (2015). Reductive dehalogenase structure suggests a mechanism for B12-dependent dehalogenation. *Nature* 517, 513–516. doi: 10.1038/nature13901

Schmitz, R. P., Wolf, J., Habel, A., Neumann, A., Ploss, K., Svatos, A., et al. (2007). Evidence for a radical mechanism of the dechlorination of chlorinated propenes mediated by the tetrachloroethene reductive dehalogenase of *Sulfurospirillum muftivorans*. *Environ. Sci. Technol.* 41, 7370–7375. doi: 10.1021/es071026u

Sjuts, H., Fisher, K., Dunstan, M. S., Rigby, S. E., and Leys, D. (2012). Heterologous expression, purification and cofactor reconstitution of the reductive dehalogenase PceA from *Dehalobacter restrictus*. *Protein Expr. Purif.* 85, 224–229. doi: 10.1016/j.pep.2012.08.007

Sung, Y., Fletcher, K. E., Ritalahti, K. M., Apkarian, R. P., Ramos-Hernandez, N., Sanford, R. A., et al. (2006). Geobacter lovleyi sp. nov. strain SZ, a novel metal-reducing and tetrachloroethene-dechlorinating bacterium. *Appl. Environ. Microbiol.* 72, 2775–2782. doi: 10.1128/AEM.72.4.2775-2782.2006

van de Pas, B. A., Gerritse, J., De Vos, W. M., Schraa, G., and Stams, A. J. (2001). Two distinct enzyme systems are responsible for tetrachloroethene and chlorophenol reductive dehalogenation in *Desulfitobacterium* strain PCE1. *Arch. Microbiol.* 176, 165–169. doi: 10.1007/s002030100316

van de Pas, B. A., Smidt, H., Hagen, W. R., Van Der Oost, J., Schraa, G., Stams, A. J., et al. (1999). Purification and molecular characterization of ortho-chlorophenol reductive dehalogenase, a key enzyme of halorespiration in *Desulfitobacterium dehalogenans*. *J. Biol. Chem.* 274, 20287–20292. doi: 10.1074/jbc.274.29.20287

Conflict of Interest Statement: The authors declare that the research was conducted in the absence of any commercial or financial relationships that could be construed as a potential conflict of interest.

frontiers in Microbiology

ORIGINAL RESEARCH
published: 12 June 2018
doi: 10.3389/fmicb.2018.01130

The Complexome of *Dehalococcoides mccartyi* Reveals Its Organohalide Respiration-Complex Is Modular

Katja Seidel[1], *Joana Kühnert*[1] *and Lorenz Adrian*[1,2]*

[1] Department Isotope Biogeochemistry, Helmholtz Centre for Environmental Research–UFZ, Leipzig, Germany, [2] Chair of Geobiotechnology, Technische Universität Berlin, Berlin, Germany

Dehalococcoides mccartyi strain CBDB1 is a slow growing strictly anaerobic microorganism dependent on halogenated compounds as terminal electron acceptor for anaerobic respiration. Indications have been described that the membrane-bound proteinaceous organohalide respiration complex of strain CBDB1 is functional without quinone-mediated electron transfer. We here study this multi-subunit protein complex in depth in regard to participating protein subunits and interactions between the subunits using blue native gel electrophoresis coupled to mass spectrometric label-free protein quantification. Applying three different solubilization modes to detach the respiration complex from the membrane we describe different solubilization snapshots of the organohalide respiration complex. The results demonstrate the existence of a two-subunit hydrogenase module loosely binding to the rest of the complex, tight binding of the subunit HupX to OmeA and OmeB, predicted to be the two subunits of a molybdopterin-binding redox subcomplex, to form a second module, and the presence of two distinct reductive dehalogenase module variants with different sizes. In our data we obtained biochemical evidence for the specificity between a reductive dehalogenase RdhA (CbdbA80) and its membrane anchor protein RdhB (CbdbB3). We also observed weak interactions between the reductive dehalogenase and the hydrogenase module suggesting a not yet recognized contact surface between these two modules. Especially an interaction between the two integral membrane subunits OmeB and RdhB seems to promote the integrity of the complex. With the different solubilization strengths we observe successive disintegration of the complex into its subunits. The observed architecture would allow the association of different reductive dehalogenase modules RdhA/RdhB with the other two protein complex modules when the strain is growing on different electron acceptors. In the search for other respiratory complexes in strain CBDB1 the remarkable result is not the detection of a standard ATPase but the absence of any other abundant membrane complex although an 11-subunit version of complex I (Nuo) is encoded in the genome.

Keywords: ***Dehalococcoides*, organohalide respiration, anaerobic respiration, reductive dehalogenase, protein complex, complexome analysis, blue native gel electrophoresis**

OPEN ACCESS

Edited by:
Shanquan Wang,
Sun Yat-sen University, China

Reviewed by:
Jiandong Jiang,
Nanjing Agricultural University, China
Elizabeth Anne Edwards,
University of Toronto, Canada

***Correspondence:**
Lorenz Adrian
lorenz.adrian@ufz.de

Specialty section:
This article was submitted to Microbiotechnology, Ecotoxicology and Bioremediation, a section of the journal Frontiers in Microbiology

Received: *27 March 2018*
Accepted: *14 May 2018*
Published: *12 June 2018*

Citation:
Seidel K, Kühnert J and Adrian L (2018) The Complexome of Dehalococcoides mccartyi Reveals Its Organohalide Respiration-Complex Is Modular. Front. Microbiol. 9:1130. doi: 10.3389/fmicb.2018.01130

INTRODUCTION

Organohalides are used in many different products such as pesticides, biocides, pharmaceuticals, plasticizers, personal care articles and flame retardants but are also produced by natural processes. Released into the environment they often represent persistent, toxic and bioaccumulating legacy contaminants (Jones and de Voogt, 1999). One particular process favored for bioremediation of organohalides in sediments, soils or groundwater is organohalide respiration catalyzed by organohalide-respiring bacteria (Steffan and Schaefer, 2016). Organohalide-respiring bacteria use the halogenated compounds as a terminal electron acceptor in an anaerobic respiration and gain energy for growth from this process. Several organohalide-respiring bacteria are strictly anaerobic and obligate organohalide respiring including strains of the genera *Dehalococcoides, Dehalogenimonas* and *Dehalobacter* separating them from many other described organohalide-respiring bacteria (Jugder et al., 2016; Fincker and Spormann, 2017). *Dehalococcoides mccartyi* strain CBDB1 is physiologically well characterized and its genome is sequenced (Kube et al., 2005). The strain can grow with hydrogen as sole electron donor and various halogenated electron acceptors, including chlorinated and brominated benzenes, polychlorinated dioxins, polychlorinated biphenyls, chlorophenols, oligocyclic phenolic bromoaromatics, and perchloroethene (Bunge et al., 2003; Adrian et al., 2009; Yang et al., 2015). The key enzyme in reductive dehalogenation is the reductive dehalogenase (RdhA), a 50–60 kDa protein with a cobalamin and two iron-sulfur clusters as co-factors. A Tat-leader peptide indicates its export to the outer side of the monoderm cell envelop of *Dehalococcoides* (Schubert et al., 2018). Earlier, we have obtained evidence that the RdhA protein is coordinated in a multi-protein reductive dehalogenase complex, referred to as organohalide respiration complex (OHR complex) in the text. The current hypothesis is that the OHR complex represents a fully functional stand-alone respiratory chain, obviating quinone or cytochrome involvement (Kublik et al., 2016; Hartwig et al., 2017). The other proposed subunits in the OHR complex are RdhB, which is the putative membrane integral RdhA anchoring protein, the *o*rganohalide respiration involved *m*olybdo*e*nzyme (OmeA), its putative membrane-integrated anchor OmeB, HupX, a protein with four predicted iron-sulfur clusters and a hydrogen uptake hydrogenase with its [NiFe] large subunit (HupL) and iron-sulfur containing small subunit (HupS) (**Figure 1**). RdhB and OmeB are predicted to be membrane integrated, while HupX and HupS are predicted to be membrane attached via one transmembrane domain each. The current mechanistic model hypothesizes that electrons are fed into the complex via HupL, and then transferred via iron-sulfur clusters in HupS, HupX and OmeA to the RdhA which reduces organohalides. The electric current through this electron chain might induce conformational changes in the complex that drive proton translocation across the membrane, but nothing of this is yet tested. The reaction would in some way resemble the reaction in the Rnf complex, where a redox reaction drives the translocation of cations across the membrane in an autonomous protein complex. The Rnf complex uses the redox reaction between reduced ferredoxin and NAD^+, both located in the cytoplasm, to shuttle Na^+ ions (Imkamp et al., 2007; Hess et al., 2013). In contrast the OHR complex is believed to take both redox substrates from outside the cell. The role of the molybdopterin dinucleotide binding motif in OmeA is not understood and the formation of such a molybdenum-containing cluster is not confirmed. The genes for the seven different OHR complex proteins are distributed into different operons on the genome. The genes *hupL*, *hupS*, and *hupX* are co-localized while *omeA* and *omeB* are located together on a separate locus. The reductive dehalogenases constitute a large paralog group in *D. mccartyi* strain CBDB1 with 32 different loci on the genome each containing one *rdhA* and one *rdhB* gene plus regulatory genes (Schubert et al., 2018).

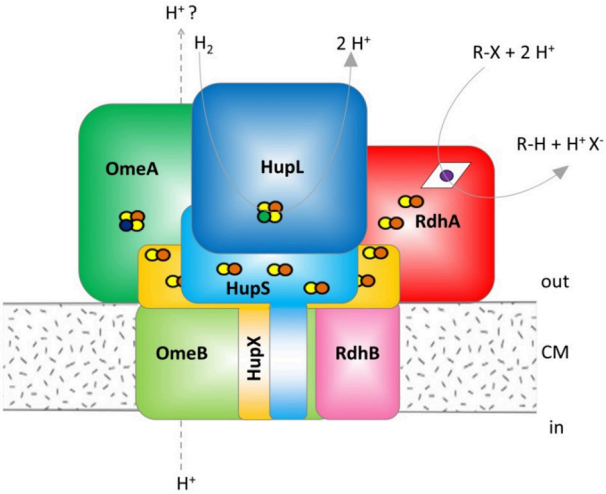

FIGURE 1 | Hypothetical model of the organohalide complex, modified from Kublik et al. (2016) representing multiple interactions between subunits. HupL, hydrogenase large subunit 48 kDa; HupS, hydrogenase small subunit 37.1 kDa, HupX, iron/sulfur protein 30.4 kDa, OmeA, organohalide respiration involved molybdoenzyme A 106 kDa; OmeB, organohalide respiration involved molybdoenzyme B 44.8 kDa; RdhA, reductive dehalogenase homologous protein active subunit ~55 kDa; RdhB, reductive dehalogenase homologous anchoring protein B 11.2 kDa. The colors were defined (**Supplemental Table 2**) and used throughout the manuscript for all graphs and tables. The yellow/red dots indicate Fe/S clusters, the blue dot indicates a molybdenum ion, the green dot a nickel ion and the violet dot a cobalt ion bound to a corrinoid.

Evidence for the formation of a dehalogenating multiprotein complex came from experiments with blue native gels where biochemical activity was detected in gel slices corresponding to a molecular weight of 150–250 kDa, but not in gel areas corresponding to the molecular weight of a single RdhA subunit (Kublik et al., 2016). In addition activity was detected at high molecular weight fractions in gel filtration experiments and could also not be found in the eluate after ultrafiltration at 100 kDa exclusion pore size. Subsequently, the mass spectrometric analysis of bands in blue native gels gave evidence for the

Abbreviations: DDM, N-dodecyl-ß-D-maltoside; BN-PAGE, blue native polyacrylamide gel electrophoresis; OHR, Organohalide respiration.

composition of the OHR complex. No experimental evidence however, is available yet for the interaction of single proteins within the complex and it is not clear which proteins mediate the cohesion of the complex. In addition no experimental evidence is yet available showing a specific interaction of an RdhA with its genome co-localized RdhB. The two most abundant RdhA proteins in cultures of strain CBDB1 growing with chlorobenzenes as electron acceptor are the RdhA proteins with the locus tags CbdbA80 and CbdbA84. CbdbA84 was isolated from a native gel and showed dechlorination activity with chlorinated benzenes. Accordingly it was annotated as chlorobenzene reductase (CbrA) (Adrian et al., 2007b). The experimental work with *Dehalococcoides* strains is strongly affected by the extremely low amounts of cell mass obtained from cultivation. The dependence of growth on toxic, low-soluble electron acceptors as well as the slow growth rate of the organisms of about 3 days per division results in maximum cell numbers of about 1–5 $\times$ 10^8 cells per mL in a fully grown culture. This, however, represents only about 1–5 mg protein per liter in cultures because the cells are very small (0.5 $\times$ 0.5 $\times$ 0.2 μM) and contain low amounts of protein compared to other microorganisms usually cultivated in the laboratory. The lack of cell walls and the small size also reduces harvesting efficiency. Therefore, all biochemical experiments with *Dehalococcoides* strains are performed with protein amounts below 50 μg total protein and all biochemical experimental approaches are restricted to highly sensitive methods such as activity tests, gel electrophoresis and mass spectrometry. Whereas, a cloning system is not available for *Dehalococcoides* species due to low growth rates, first progress was recently achieved with heterologous expression of *Dehalococcoides* redox proteins in *E. coli* (Hartwig et al., 2015).

Complexome analysis (also called complexome profiling) is an approach in which protein complexes are mildly extracted from cells and applied to non-destructive methods to separate protein complexes from each other. Density gradient centrifugation, gel filtration and native gel electrophoresis have been applied for protein separation but only native gel electrophoresis allows very sensitive detection when a low amount of material is available (Heide et al., 2012). To exclude bias from personal hypotheses, the entire gel lane can be cut into small slices and each slice is analyzed for protein content by mass spectrometry. Mass spectrometry gives a great depth of detection and estimates of the quantitative distribution of detected proteins across the gel lane. By identifying correlating distribution patterns, evidence for protein-protein interactions and the formation of protein complexes can be obtained. The method was described before for mitochondrial complexes in mammals (Wittig et al., 2006; Heide et al., 2012), plants (Kiirika et al., 2013; Senkler et al., 2017), and yeast (Eydt et al., 2017), and bacterial protein complexes of sulfate-reducing (Wöhlbrand et al., 2016), oxygen respiration in nitrate-reducing (Schimo et al., 2017) and anammox bacteria (de Almeida et al., 2016). A complication of complexome analyses is the fact that many of the protein complexes, especially those involved in respiration, are membrane bound and detergents must be applied to detach protein complexes from the membrane. The solubilization step with detergents, however, is crucial as solubilization needs to be strong enough to extract membrane-integrated proteins but weak enough to keep protein 3-D structures and protein-protein interactions intact.

The objective of this study is to obtain more and clearer evidence on the organization of the unique quinone-free respiratory complex in *D. mccartyi* strain CBDB1. Due to the low amount of biomass available we were restricted to methods applicable with low amounts of protein. Therefore, we performed a focused complexome analysis with the main aim to analyse protein components and modules of the OHR complex rather than measuring all protein-protein interactions in the proteome. This approach based on earlier data showed that the proteins in the OHR complex are all at high relative abundance compared to anabolic or structural proteins in the strain. The application of low protein amounts onto blue native gels therefore excluded the detection of low-abundance complexes and proteins but was expected to improve the resolution on the gel. To obtain information on the different strengths of protein-protein interactions we applied three different protocols for protein extraction from cells varying in their solubilization strength.

MATERIALS AND METHODS

Chemicals, Cultures, and Cell Harvest

Chemicals were purchased at the highest available purity. Hexachlorobenzene of technical purity was purchased from Campro Scientific and 1,2,4,5-tetrabromobenzene from Alfa Aesar at a purity of 94%. Titanium(III) citrate was prepared from technical grade 15% titanium(III) chloride solution (Merck-Schuchard) as described (Adrian et al., 2007a).

Dehalococcoides mccartyi strain CBDB1 was grown in defined mineral medium, pH-buffered to 7.2 with carbonate, reduced with 2 mM L-cysteine or 0.15% titanium(III)citrate, with 5 mM acetate as carbon source, 7.5 mM nominal concentration of hydrogen as electron donor and hexachlorobenzene or 1,2,4,5-tetrabromobenzene as electron acceptor under strictly anaerobic conditions as described previously (Adrian et al., 2000). Cultivation led to a final cell density of about 10^7-10^8 cells mL^{-1}. Cells were harvested from culture volumes of 400–700 mL by using a SandTrap as recently described (Frauenstein et al., 2017). Eluents from the SandTrap were subsequently concentrated by a multi-step centrifugation (2–6 steps) each at 6,000 $\times$ g and 16°C for 60 min, removing about 50% of the supernatant in each step to avoid the strong losses of cells by other procedures as described in detail previously (Frauenstein et al., 2017). Due to low cell numbers harvested and the small cell size of the bacteria no visible pellet was formed. Nevertheless, as calculated from monitoring the centrifugation steps by direct epifluorescence microscopic cell counting after SYBR-green staining on agarose-coated slides (Adrian et al., 2007a) this non-visible pellet containing about 10^9 cells was used for further steps. Assuming a protein content of 30 fg protein $cell^{-1}$ (Cooper et al., 2015) this represents about 30 μg protein as starting material for each of the described native electrophoresis/complexome analyses. The details for each of the three complexome analyses described in this study are summarized in **Table 1**.

TABLE 1 | Experimental details in complexome analyses with the three different extraction modes.

Experimental stage	Experimental parameter	Complexome analysis 1	Complexome analysis 2	Complexome analysis 3
Culture	Culture name	LB99c	LB104c	LB99b
	e^--Acceptor	HCB	1,2,4,5-TeBB	HCB
	Reducing agent	L-Cysteine	L-Cysteine	Titanium(III)citrate
	Culture volume (mL)	700	400	650
	Culture cell number (cells mL^{-1})	2.7E+07	7.0E+07	5.7E+07
SandTrap harvest	SandTrap size	SandTrap GL32	SandTrap GL25	SandTrap GL32
	Volume after SandTrap	25 mL	9 mL	30 mL
	Cell number after SandTrap (cells mL^{-1})	1.3E+08	7.0E+08	1.3E+08
Centrifugation steps	Centrifugation condition	6x centrifugation each 6,000 *g*, 1 h, 16°C; ∼50% of the SN removed	4x centrifugation each 6,000 *g*, 1 h, 16°C; ∼50% of the SN removed	2x centrifugation each 6,000 *g*, 1 h, 16°C; ∼50% of the SN removed
	Volume after concentration (mL)	0.1	0.25	0.85
	Cell number after concentration (cells mL^{-1})	1.4E+09	3.1E+10	3.0E+09
Solubilization	Extraction mode	1	2	3
		"whole-cell DDM extraction"	"membrane fraction DDM extraction"	"disrupted cell DDM extraction"
	Extraction procedure	solubilization	beat-beating then ultracentrifugation then solubilization	beat-beating and solubilization
		During solubilization an unknown amount of cells/protein is lost		
BN-PAGE	Total volume added to each lane (µL)	35	25	35
	Volume of cell extract added per lane (µL)	25	18.125	25
Calculated amounts if no loss occurred during extraction	Cells per lane	3.5E+07	5.6E+08	7.5E+07
	Protein per lane (µg)	1.1	16.9	2.3
Mass spectrometry	Measured total area counts of detected proteins[a]	3.9E+10	1.9E+10	1.8E+10

[a]*see also* ***Table 2***.

Extraction of Protein Complexes

Proteins were extracted from the non-visible pellet in three different ways with the aim to detach complexes from the membrane while preserving protein-protein interactions as much as possible.

(i) In the first extraction mode, previously used in our group (Kublik et al., 2016), the cell pellet was resuspended in 1× PBS buffer (10 mM disodium hydrogen phosphate, 2 mM potassium dihydrogen phosphate, 137 mM sodium chloride, 2.7 mM potassium chloride, pH 7.4) and amended with 1% (w/v) N-dodecyl-ß-D-maltoside (DDM). The suspension was incubated for 60 min on ice with gentle shaking. Insoluble material was then removed by centrifugation (45 min, 16,600 × g, 16°C) and the supernatant was used for blue native polyacrylamide gel electrophoresis (BN-PAGE). We refer to this extraction mode as "whole-cell DDM extraction."

(ii) In the second extraction mode, previously described for sulfate reducing bacteria (Wöhlbrand et al., 2016), the pellet was suspended in 250 µL culture medium and cells were lysed by bead beating (0.5 mm glass beads, Stretton Scientific; Fast Prep TM FP120, Thermo Savant) at a speed of 4 m s^{-1} for 20 s at room temperature. Beads were removed by centrifugation (3,000 × g, 1 min, room temperature) and the supernatant was processed by ultracentrifugation (100,000 × g, 60 min, 4°C) to spin down membrane fractions. The ultracentrifugation supernatant was removed and the pellet frozen overnight at −80°C under anoxic conditions. Afterwards the membrane pellet was gently thawed and resuspended in ACA750 buffer (Wöhlbrand et al., 2016) (750 mM amino capronic acid, 50 mM Bis-Tris, 0.5 mM EDTA, pH 7.0) containing 1% (w/v) DDM. Solubilization was performed by gently shaking for 60 min at 4°C. This extraction mode will be referred as "membrane fraction DDM extraction."

(iii) For the third extraction mode the cell pellet was resuspended in 850 µL 1 × PBS containing 1% (w/v) DDM (at room temperature) and the cells were then disrupted by bead beating applying 4 m s^{-1} for 30 s at room temperature.

This resulted in the formation of a minor amount of foam. The resulting crude extract was then centrifuged for 15 min at 14,000 × g and 4°C. The supernatant with solubilized proteins was transferred to a fresh tube and stored on ice for several minutes before the sample was loaded on blue native polyacrylamide gel. This extraction mode will be referred to as "disrupted cell DDM extraction."

BN-PAGE

BN-PAGE was performed in an anoxic glove box and cooled with cooling packs using the XCell SureLock Mini-Cell (Invitrogen) electrophoresis system with precast 4–16% gradient Bis-Tris gels (NativePAGE Novex, Invitrogen). The anode buffer and the light blue cathode buffer were prepared according to the manufacturer's manual. A protein marker (5 μL of 1:20 diluted NativeMark Unstained Protein Standard, Invitrogen) in 1× sample buffer (Invitrogen) was used in one lane of all gels. Samples were amended with 4× sample buffer and 0.125–0.178% (v/v) Coomassie G-250 according to the manufacturer's instructions before electrophoresis was run at 150 V for 1 h and then at 250 V until the marker reached the bottom of the gel. After electrophoresis proteins were visualized by a mass spectrometry-compatible silver staining procedure (Nesterenko et al., 1994). Then the stained gel lanes were cut into regular slices of 1–2 mm width using a razor blade that was cleaned with ethanol after each cut. In the three different complexome analyses the gels were cut into 26, 65 and 64 slices, respectively.

Mass Spectrometric Analysis

Silver stained proteins in gel slices were prepared for nano-liquid chromatography tandem mass spectrometry (nLC-MS/MS) analysis by destaining, cysteine derivatization and tryptic in-gel digest as described (Kublik et al., 2016). Peptide samples were desalted using ZipTip-μC18 material (Merck Millipore) prior to analysis with nLC-MS/MS using an Orbitrap Fusion Tribrid mass spectrometer (Thermo Scientific) equipped with a nanoLC system (Dionex Ultimate 3000RSLC; Thermo Scientific). Peptides were separated on a separation column (Acclaim PepMap100 C18, Thermo Scientific) at a flow rate of 0.3 μL min^{-1} by applying the following settings with eluent A (0.1% formic acid in water) and eluent B (80% (v/v) acetonitrile, 0.08% formic acid in water): column equilibration for 3 min at 4% B (corresponding to 3.2% (v/v) acetonitrile final concentration), then increasing within 40 min to 55% B (corresponding to 44% (v/v) acetonitrile), followed by increasing within 1 min to 90% B (corresponding to 72% (v/v) acetonitrile) and hold for 4 min at 90% B. Eluted peptides were ionized via an electrospray ion source (TriVersa NanoMate, Advion) operated in positive mode and scanned continuously between 350 and 2,000 *m/z* by the Orbitrap mass analyzer with a resolution of 120,000, an ion target value of 4×10^5 ions and maximum ion injection time of 50 ms. The two most intense ions with charge between 2+ and 7+ were picked for fragmentation with the quadrupole set to a window of 1.6 *m/z* and subjected either to higher energy collisional dissociation (HCD) mode with collision energy of 30% or collision induced dissociation (CID) mode with collision energy of 35% with an ion target value of 1×10^4 and maximum ion injection time of 120 ms. Fragment ions were analyzed in the ion trap mass analyzer. Dynamic exclusion was enabled for 45 s after fragmenting a peptide ion in order to prevent repeated fragment analysis of the same ion.

Protein identification was conducted by Proteome Discoverer (v2.2, Thermo Fisher Scientific) using the SequestHT search engine with the UniProt database of *D. mccartyi* strain CBDB1 with the following settings: cleavage enzyme trypsin, allowing up to two missed cleavages, precursor mass tolerance and fragment mass tolerance were set to 3 ppm and 0.6 Da, respectively. Oxidation of methionine residues was selected as dynamic modification and carbamidomethylation on cysteine residues as fixed modification. The false discovery rate of identified peptide sequences was kept to <1% using the Percolator node. Abundance of proteins and peptides was calculated by label-free quantification on the basis of area counts using the Minora node implemented in Proteome Discoverer. The relative protein abundance or relative peptide abundance as given in this study was defined as the abundance of a protein or peptide in one slice relative to the total abundance of this protein or peptide across all slices of the blue native gel lane. The hierarchical cluster analyses were performed with R.

RESULTS

Three different extraction modes were applied (denominated as complexome analysis 1, 2, and 3) to release protein subcomplexes from the membrane of *D. mccartyi* strain CBDB1. The three extraction modes were designed to exert different solubilization strengths and therefore to provide different snapshots of subcomplex states in different dissociation degrees allowing conclusions on the stability of membrane-bound subcomplexes. Solubilized protein complexes were separated under non-denaturing conditions by BN-PAGE. Instead of cutting single bands after staining, the entire gel lane was cut into regular 1–2 mm slices and proteins within each slice were trypsin digested, eluted and analyzed by mass spectrometry. The result was an in-depth and high-resolution picture of protein distribution across the gel lane at three different solubilization degrees.

Protein-Protein Interactions in the OHR Complex After Whole-Cell DDM Extraction (Extraction Mode 1)

Extraction mode 1, in which whole cells were incubated directly 60 min at 4°C with 1% (w/v) DDM, was the fastest and most direct protein extraction protocol tested in this study. This protocol was not designed to separate soluble cytoplasmic from membrane proteins but for having the fewest experimental steps avoiding protein loss. From the gel that was cut into 26 slices a total of 103 proteins were identified by mass spectrometry across all slices (**Supplemental Table 1**). All putative subunits of the OHR complex were identified: HupL, HupS, HupX, OmeA, OmeB, seven RdhA paralogs and one RdhB (**Table 2**). The distribution of the relative protein abundance of the OHR complex subunits across the gel lane showed that the OHR complex is organized in modules of several subunits under

TABLE 2 | Absolute abundance values for all suspected OHR complex subunits as a sum of the determined mass spectrometric area counts in all slices.

Protein	Extraction mode 1	Extraction mode 2	Extraction mode 3
Total detected proteins	**103**	**233**	**116**
Sum of all detected proteins	**3.9E+10**	**1.9E+10**	**1.8E+10**
HupL CbdbA129	2.8E+08	2.7E+07	8.9E+07
HupS CbdbA130	8.1E+07	2.5E+06	2.1E+07
HupX CbdbA131	6.9E+08	4.6E+08	2.9E+07
OmeA CbdbA195	5.2E+08	7.7E+07	3.2E+08
OmeB CbdbA193	4.6E+06	7.3E+07	4.2E+07
RdhB CbdbB3	2.6E+07	1.0E+08	1.5E+08
RdhA CbdbA80	8.6E+08	9.0E+07	1.9E+09
RdhA CbdbA84	7.4E+09	9.4E+06	4.5E+09
RdhA CbdbA88	3.6E+06		
RdhA CbdbA1453	7.0E+06		
RdhA CbdbA1455	3.5E+05		
RdhA CbdbA1588	5.4E+08		7.4E+08
RdhA CbdbA1618	2.4E+08	3.3E+07	6.9E+06
RdhA CbdbA1638	1.8E+06		2.5E+06

The color code for proteins is the same as elsewhere in this study. Protein abundance values are highlighted by gray shading corresponding to abundance values in each extraction mode (highly abundant, gray; lowly abundant, white).

extraction mode 1 (**Figure 2**). The subunits HupL and HupS showed identical migration patterns and shared their maximum of relative protein abundance in slice 20, indicating that they were tightly connected to each other and that they were forming a hydrogenase module. Although OmeA and OmeB shared their maximum in slice 18, their overall relative protein abundance distribution pattern was not identical, as OmeB formed a second slightly smaller maximum of relative protein abundance in slice 16, which was not present for OmeA. In contrast to HupL and HupS, HupX had its maximum of relative protein abundance in slice 18, identical to OmeA and OmeB indicating that these three subunits OmeA, OmeB, and HupX also formed a tightly bound module of the OHR complex and that HupX was not tightly bound to HupS/HupL. Overall, the HupL/HupS module had a completely different migration pattern than the OmeA/OmeB/HupX module indicating that no strong interactions between the two modules were present. Seven out of 32 different RdhA proteins encoded in the genome were found in the gel. From the seven identified RdhA proteins five showed a clear maximum of relative protein abundance in one of the slices (CbdbA1618 in slice 9; CbdbA88 and CbdbA1588 in slice 18; CbdbA1453 and CbdbA1638 in slice 20). Our data might indicate that CbdbA88 and CbdbA1588 are more strongly attached to the OmeA/OmeB/HupX module whereas CbdbA1453 and CbdbA1638 are more strongly attached to the HupL/HupS module. In contrast to the five RdhA proteins with clear relative maxima, CbdbA80 and CbdbA84 were more broadly distributed between the slices 16 to 21, therefore covering the whole range of the other OHR complex proteins and no separation was achieved. Indeed CbdbA80 and CbdbA84 were by far the most abundant among all RdhA proteins (**Table 2**), indicating that a better resolution could be achieved with lower amounts of protein. Only one RdhB protein was identified with a single peptide. This RdhB protein with the locus tag CbdbB3 is encoded in one operon together with the RdhA CbdbA80 and might be the specific membrane anchor for CbdbA80. In the blue native gel CbdbB3 had its maximum in slice 22, where none of the other OHR complex subunits had a maximum. Therefore, most of this RdhB protein appeared to have been detached from the overall protein complex by extraction mode 1. However, a second smaller maximum in relative protein abundance of CbdbB3 showed up in slice 18 where several RdhA proteins were also detected, including RdhA CbdbA80.

Protein-Protein Interactions in the OHR Complex After Membrane Protein DDM Extraction (Extraction Mode 2)

Extraction mode 2 was adapted from a previous complexome analysis of the sulfate reducing *Desulfobacula toluolica* (Wöhlbrand et al., 2016). The approach aimed at first isolating membrane fractions from which protein complexes were subsequently detached with DDM. The blue native gel lane was cut into 65 slices and 233 proteins were identified in total by mass spectrometry from all slices together (**Table 2**). Again all subunits of the complex were identified, but the distribution of the relative protein abundance across the gel lane appeared random instead of showing module formation (**Figure 3**). Overall only very few proteins had a relative abundance of more than 10% in one single slice and the total amount was often distributed across all 65 slices. One example was HupX which reached abundance of 1–3% in almost all 65 slices, but nowhere more than 5%. One exception was the RdhA CbdbA1618, which had clear maxima but was expressed at a very low absolute abundance (**Table 2**). More meaningful exceptions were the membrane integrated subunits HupS, OmeB and RdhB CbdbB3 which had local accumulations in the gel in the slices 1–9, 26–38, and 26–41 respectively. OmeB and RdhB CbdbB3 appeared to be co-localized suggesting strong interaction. HupS in contrast did clearly not interact with HupL as seen with extraction mode 1 and did not interact with the other two membrane subunits of the complex OmeB and RdhB but co-localized with RdhA CbdbA80. HupL had a high maximum of relative protein abundance in slice 41 at a size of ∼100 kDa, which is not fitting to the predicted monomeric molecular mass of 58 kDa. In the blue native gel after extraction mode 2 we obtained only about half the total area counts across all proteins and slices than those obtained after extraction mode 1 (**Table 2** and **Supplemental Table 1**). In contrast to this, more than twice as many proteins were detected in complexome analysis 2 compared to complexome analysis 1 (233 vs. 103). The extraction mode was aiming at enriching membrane proteins but also soluble proteins were present and enriched. Especially, many of the ribosomal proteins were detected with extraction mode 2 (33 identified ribosomal proteins in comparison to 2 ribosomal proteins detected under extraction modes 1 and 3) suggesting that ribosomes were

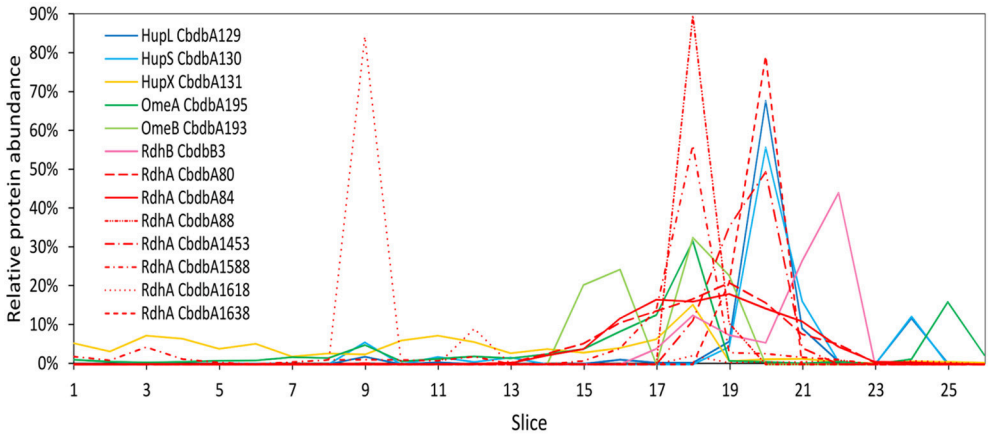

FIGURE 2 | Relative abundance of proteins associated with the OHR complex across the length of a blue native gel cut into 26 slices after whole-cell DDM solubilization (protein extraction mode 1). The color code is the same as shown in **Figure 1**. Different RdhA proteins are shown with different line types.

enriching in the ultracentrifugation step. A similar effect was seen with the ATPase subunits of which five were detected after extraction mode 2 but only one after extraction mode 1 and three after extraction mode 3.

Protein-Protein Interactions in the OHR Complex After Disrupted Cells DDM Extraction (Extraction Mode 3)

Extraction mode 3 was characterized by cell lysis via beat beating in the presence of detergent at room temperature (∼20°C) (Kublik et al., 2016). Although some foam formed and a part of the proteins was expected to be lost with it, it is a very fast and direct procedure and the BN-PAGE analysis could be started 20 min after addition of the detergent. After BN-PAGE the gel was cut into 64 gel slices that were analyzed for their protein content by mass spectrometry. In total 116 proteins were identified. Among these 116 proteins again all OHR complex subunits were identified (**Table 2**). Out of the 32 encoded RdhA paralogs five were identified, CbdbA80, CbdbA84, CbdbA1588, CbdbA1618, and CbdbA1638. As with the two other extraction modes, only one out of the 32 encoded RdhB, CbdbB3, was identified. The OHR complex disintegrated to an intermediate degree into modules but the modules were intact. The relative protein abundance of the OHR complex subunits across the blue native gel lane showed organization in at least three modules (**Figure 4**). One such module consisted of the subunits OmeA/OmeB/HupX and had its maximum relative protein abundance in slice 20, corresponding to a size of ∼540 kDa. Interestingly, a trace peak of HupL was also found in slice 20. A second smaller maximum for OmeA and HupX was found in slices 34 and 35, however, OmeB distribution was different in these slices. The second module formed by HupL and HupS showed very similar relative protein abundance distribution patterns over all slices for those two proteins. The maximum was found in slice 49 at a size of ∼60 kDa. A smaller part of this module was also found together with the maximum of RdhA CbdbA80 and RdhB CbdbB3 in slice 40 at ∼135 kDa. RdhA CbdbA80 and RdhB CbdbB3 showed the same maximum in slice 40 and also a similar overall distribution patterns thus forming a third module. As mentioned above, this module seemed to interact weakly with the HupL/HupS module. Although also other RdhA proteins were identified in slice 40 in minor amounts they had their maxima either at higher molecular mass (CbdbA1638 ∼250 kDa, CbdbA84 and CbdbA1588 ∼242 kDa) or for RdhA CbdbA1618 at a lower molecular mass of ∼75 kDa. This showed separation of different RdhA along the blue native gel lane. A remarkable observation is the occurrence of secondary maxima of OmeB and RdhB CbdbB3 in slice 32 independent of OmeA and HupX to which OmeB is normally tightly bound. No other RdhB proteins than CbdbB3 were identified in the gel. Therefore, it is not possible to judge if co-localization of these RdhB proteins with their respective RdhA occurred.

To test the reliability of our method we compared the distribution of OHR complex proteins across the gel lane with the distribution of each peptide detected of the specific protein because this distribution should be the same for each peptide. Indeed, this behavior was seen in all OHR complex proteins as exemplified in **Figure 5** for the RdhA CbdbA80. However, this calculation also showed that the distribution patterns became much more stable and better resolved when more peptides in a protein were detected. In this way, the distribution of proteins with less identified peptides (for example RdhB CbdbB3) are expected to be less reliable than proteins with many identified peptides. Analyzing the peptide distribution for all OHR complex subunits it was observed that besides of the expected situation that all peptides share the maximum of relative peptide abundance with the maximum of relative protein abundance of their respective protein, also a distribution was observed that the relative peptide abundance was split into two or more maxima in slices next to each other (**Supplemental Figures 1**, **2**). OHR subunits were peptides showed such a split of maxima for relative peptide abundance were OmeA, RdhA CbdbA84

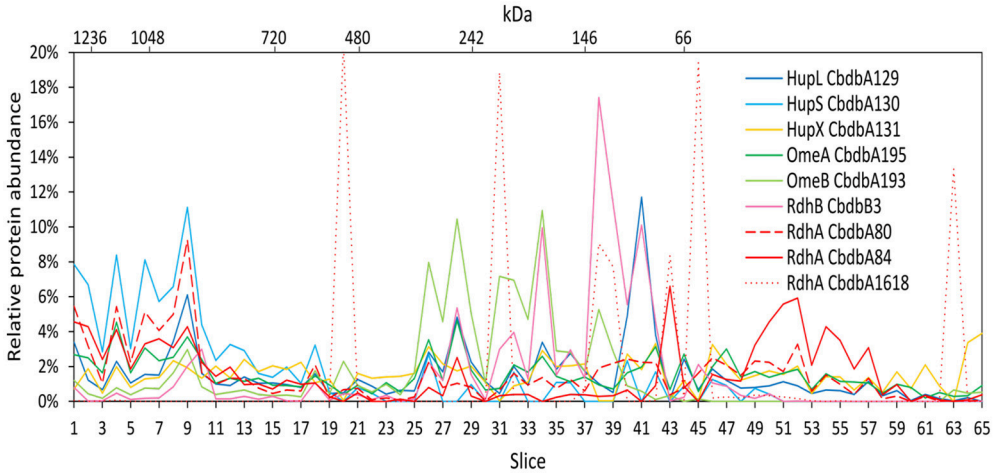

FIGURE 3 | Relative abundance of proteins associated with the OHR complex across the length of a blue native gel cut into 65 slices after membrane fraction DDM extraction (protein extraction mode 2). The color code is the same as used in **Figure 1**. Different RdhA proteins are shown with different line types.

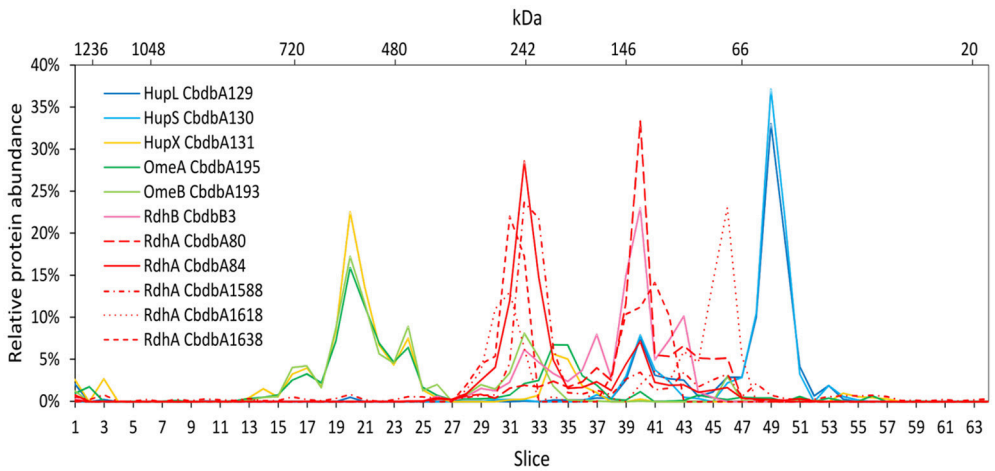

FIGURE 4 | Relative abundance of proteins associated with the OHR complex across the length of a blue native gel cut into 64 slices after disrupted cell DDM extraction (protein extraction mode 3). The color code is the same as used in **Figure 1**. Different RdhA proteins are shown with different line types.

(**Supplemental Figure 1C**), and RdhA CbdbA1588 (data not shown).

Hierarchical Cluster Analyses

Hierarchical cluster analyses comparing distribution patterns of the different proteins across gel slices were calculated for all three extraction modes to quantitatively describe interactions between subunits (**Figure 6** for proteins suspected to be within the OHR complex; **Supplemental Figure 3** for all detected proteins). As suggested by the distribution graphs (**Figures 2–4**), the trees confirm that extraction mode 3 preserved the integrity of the three modules HupL/HupS, OmeA/OmeB/HupX, and RdhA/RdhB CbdbB3 and at the same time separated them from each other and from other protein complexes such as the ATPase complex (**Figure 6C**). HupL and HupS were clustering closely together and clearly formed a cluster distinct from other OHR complex proteins and other proteins (**Supplemental Figure 3C**). Also OmeA/OmeB/HupX formed a cluster of proteins with very similar slice distribution. It is worth noticing, that HupX followed even closer the gel distribution of OmeA than the membrane protein OmeB. Two further proteins were identified to cluster with the OmeA/OmeB/HupX module, which are annotated as a hypothetical periplasmic protein (CbdbA1106) and a K^+-insensitive pyrophosphate energized proton pump HppA (CbdbA738) (**Figure 6C**). Similar to HupS and HupX, CbdbA1106 is predicted to be located on the outer side of the cytoplasmic membrane with the largest part of its 254 amino acid residues, anchored to the membrane by one single transmembrane helix at the N-terminus. In contrast, CbdbA738 is predicted to be a large 708 amino acids containing integral membrane protein with 15 transmembrane helices. Although the cluster analysis cannot differentiate between

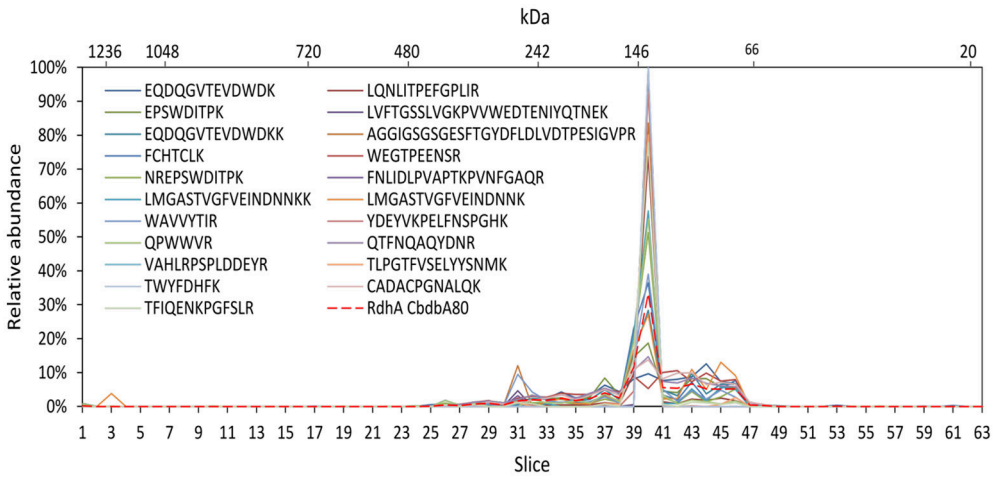

FIGURE 5 | Analysis of single peptide distributions across the blue native gel lane. Relative distribution of RdhA CbdbA80 across the gel lane (red dashed line) together with the distribution of all single detected peptides of RdhA CbdbA80 after protein extraction according to mode 3. The peptide maxima are all in slice 40.

specific and unspecific interactions it gives evidence for a very similar distribution across the native gel as seen for the OmeA/OmeB/HupX module. In the cluster analysis of the complexome analysis RdhA proteins were separated from the main peaks of the other suspected OHR complex proteins. RdhA CbdbA80 clustered directly with CbdbB3, the RdhB protein associated with it in the genome. Also RdhA CbdbA84 and RdhA CbdbA1588 were very similarly distributed in the gel slices and formed a distinct subcluster in the cluster analysis, however, in the phylogenetic tree of RdhA proteins they are not particularly closely related to each other (Hug et al., 2013).

Extraction mode 2 in contrast led to almost complete disruption of all modules into their subunits (**Figure 6B**). This can best be seen at the ATPase subunits distributed across the tree. Even the otherwise tightly bound HupL/HupS module was disrupted. Interactions that can still be observed under these strongly dissociating conditions were the association of OmeA with HupX and the association of OmeB with RdhB CbdbB3, as tentatively observed in **Figure 3**. These two interactions seem to be the strongest in the OHR complex of strain CBDB1.

Extraction mode 1 (**Figure 6A**) more strongly conserved the integrity of the OHR complex than extraction mode 2 (almost complete disruption of the complex and modules) and 3 (disruption of the complex but preservation of module integrity). Therefore, interactions of modules can be monitored under extraction mode 1. The strong interactions between OmeA and HupX and between OmeB and RdhB are conserved. Also the HupL/HupS interaction is maintained indicating that this interaction is also strong even if less than the previously mentioned interactions. Also weaker interaction were preserved: between the hydrogenase module (HupL/HupS) and the RdhA proteins CbdbA1455, CbdbA1638, and/or CbdbA1454; and between CbdbA80 and CbdbB3.

The cluster analysis reveals the presence of further complexes within the proteome of strain CBDB1 (**Supplemental Figure 3C**). For example, the three subunits of the ATP synthase complex detected in complexome analysis 3, AtpA, AtpC and AtpF, corresponding to the alpha (F_1 unit), epsilon (F_1 unit) and b subunit (F_0 unit), shared very similar distribution profiles of relative protein abundance across the gel slices. All three had their maximum relative abundance in slice14, corresponding to a molecular weight of about 780 kDa. In the cluster analysis AtpA and AtpF clustered closer together than each with AtpC. Another identified protein complex in the analysis of extraction mode 3 was the cytoplasmatic Vhu hydrogenase complex with its two subunits VhuA and VhuG closely clustering in their distribution profile. The same was found for CarA and CarB the small and large subunit of the carbamoyl-phosphate-synthase. From the riboflavin biosynthesis pathway RibE (riboflavin synthase)/RibH (6,7-dimethyl-8-ribityllumazine synthase) were identified which do not cluster together but share their maximum of relative protein abundance in slice 13. For PurQ/PurL the phosphoribosylformylglycinamide synthase I and II of the purine biosynthetic pathway (maximum in slice 36) of complexome analysis 3 the same observation was made. More proteins involved in the purine biosynthetic pathway were detected, PurA, PurD, PurE and PurH, but did not cluster together and also did not share the maximum in relative protein abundance indicating the absence of a larger protein complex. Furthermore, a module of the pyruvic-ferredoxin oxidoreductase was identified. The subunits PorA and PorB clustered together although they had their maxima in relative protein abundance in slice 32 and 33 of complexome analysis 3, respectively. The third subunit PorG had its maximum in relative protein abundance also in slice 32, but was in the cluster analysis slightly distant from the other two subunits. The last subunit PorD was not identified in this analysis. None of the 11 subunits of the predicted complex I (Nuo) was identified in the gel slices indicating it was at low abundance. Only two of the 53 encoded ribosomal subunits were identified in complexome analysis 3

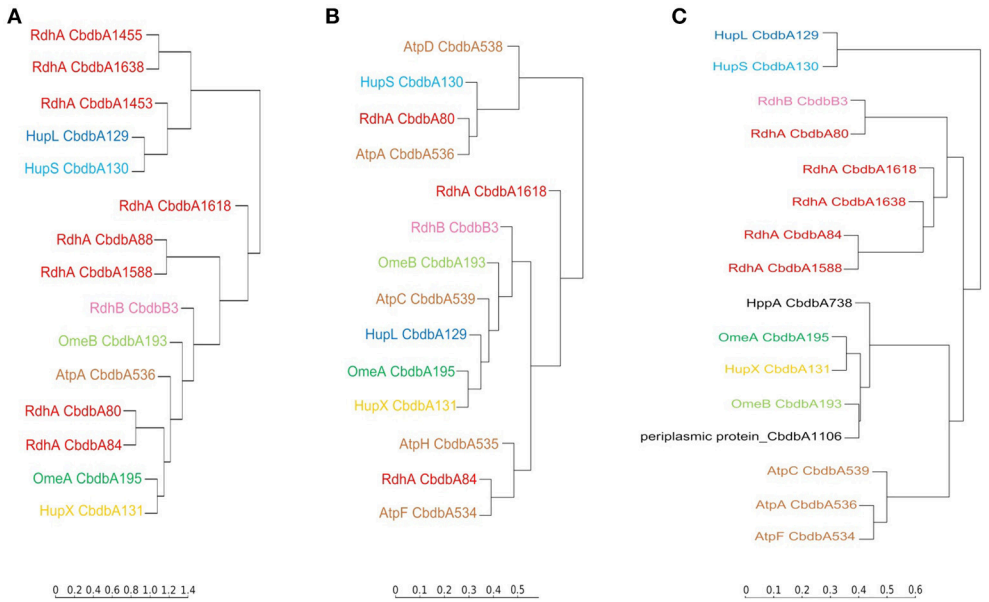

FIGURE 6 | Cluster analysis of the distribution profiles of proteins suspected to be part of the OHR complex across blue native gels after application of the three extraction modes. **(A)** Distribution on blue native gels after extraction mode 1; **(B)** after extraction mode 2; **(C)** after extraction mode 3. The cluster analysis places proteins with similar migration pattern together. Colors are used as elsewhere in this study. ATP synthase subunits (brown) are added as reference. Two other proteins having a similar distribution of relative protein abundance across the gel in extraction mode 3 as the OmeA/OmeB/HupX module are displayed in black. The full analyses are given in **Supplemental Figure 3**.

RplA (L1) and RplL (L7/L12), both 50S ribosomal proteins, and they also were present in one cluster.

DISCUSSION

In this study we provide detailed information on a large protein complex in *D. mccartyi* strain CBDB1 able to catalyze a "stand-alone" respiration, dependent only on one protein assembly, not on quinoid electron mediators. To our knowledge, this is the only known example yet of such an autonomous respiration directly with physiological electron donors and electron acceptors within one protein complex. Although few other bacteria (acetogens) and archaea (methanogens) have been described to lack quinones (Schoepp-Cothenet et al., 2013), they still generate a proton or sodium gradient across the membrane by oxidizing and reducing mediating cofactors, such as ferredoxin or NADH, not the substrates directly. Therefore, it is important to study this OHR complex in more detail even if the applicable methods are strongly confined to those with very good sensitivity, excluding the majority of standard biochemical characterization procedures. We here explored successfully the potential of complexome analyses for the characterization of the OHR complex. By using different protein extraction modes, representing different solubilization strengths, we also obtained information about the dynamics of the protein interactions. In addition we acquired evidence for the presence of at least three modules in the complex and evidence on specific protein-protein interactions within the complex.

Complexome analyses can give a detailed description of cellular complexes (Wittig et al., 2006; Wittig and Schägger, 2009). In combination with high-resolution mass spectrometry a high protein identification depth can be reached allowing to trace many proteins in one single experiment. In our study, we applied only low amounts of proteins onto the native gels and obtained good resolution of protein clusters but no strong detection depth, meaning that we only detected the most abundant proteins. Indeed, in comparison to previous work, describing the full proteome of *D. mccartyi* strain CBDB1 (Schiffmann et al., 2014) the total number of detected proteins in the present study is low. However, we aimed at good resolution of protein subcomplexes in the gel and less on the identification depth because we focused on the composition of the abundant OHR complex and protein-protein interactions within this complex. We also obtained experimental evidence for this argumentation when we got much better spatial focusing of RdhA proteins when they were at low concentration than when they were at high concentration (CbdbA88, CbdbA1453, CbdbA1588 and CbdbA1638 with narrow focus vs. CbdbA80 and CbdbA84 with broader distribution **Figure 2**). In all three complexome analyses done in this study, all seven suspected OHR complex subunits were detected and especially in the complexome analysis 3 OHR modules were well separated from each other but still intact. In addition to the information on the complex composition these results again confirm the dominant role of the OHR complex in the physiology, biochemistry and evolution of *Dehalococcoides* species. Another reason impacting the total number of detected proteins in our analyses was the

choice to optimize the instrument measurement time toward more precursor scans (MS1 scans) than done in previous studies (Schiffmann et al., 2014; Kublik et al., 2016) to obtain more precise label-free quantification results.

Complexome analysis data depend strongly on the protein extraction mode, as also exemplified by our data. With different detergent types, detergent concentrations, temperatures and incubation times different solubilization strengths can be applied resulting in different observable protein-protein interactions. Each of the three complexome analyses presented here is a snapshot of one particular solubilization degree. In our previous work we have evaluated different detergents (Kublik et al., 2016) but here we focused on DDM at a concentration of 1% and varied the incubation time and preparation sequence in the different extraction modes. Although we started with the largest amount of cells in complexome analysis 2 (using extraction mode 2 which included membrane preparation by ultracentrifugation) the resulting complexome data indicates that only a low amount of protein was applied to the gel, meaning that a large portion of protein was lost during the ultracentrifugation step. This is indicated by the total amount of area counts for all detected proteins together (1.9E + 10), which was only half of that found after extraction mode 1 (3.9E + 10) (**Table 2**) although 16 times more cells were used for the complexome analysis 2 (calculated to the applied volume onto the gel). Also the relative distribution of the proteins and modules on the gel showed that extraction mode 2 described for *Desulfobacula toluolica* (Wöhlbrand et al., 2016) was not conserving OHR complex integrity (**Figure 3**). All together this indicates that membrane isolation by ultracentrifugation is heavily biasing the results leading to massive loss of proteins. It is surprising that many ribosomal proteins were detected in the membrane preparations (extraction mode 2) indicating that ribosomes were enriched by this procedure. The extraction mode 2 however, was useful in observing tight interactions between integrated membrane proteins which seem also to be enriched with this mode. For the analysis of loosely attached peripheral membrane proteins the extraction modes 1 and 3 were better suited, especially because much less protein was lost. Still, in extraction mode 3 much more protein was lost than in mode 1 as seen by the total area counts after mass spectrometry (**Table 2**). This might be due to foam formation when cell lysis was done in the presence of detergent. However, complexome analysis 3 provided a precise separation of the OHR complex modules.

From the distribution of single peptide identifications all stemming from the same protein, confidence for the results could be drawn. Overall, the peptide distributions were very reliable and matched the protein distribution, indicating that false positive detections did not play a major role. Generally that also means that the obtained results were more stable for proteins with more peptide identifications than for those with few or only one peptide identification, most notably RdhB CbdbB3 and RdhA CbdbA1618. Exceptions, where not all peptides showed the exact same distributions were RdhA CbdbA84, RdhA CbdbA1588 and OmeA, where peptide relative abundance maxima split into two maxima in neighboring gel slices (**Supplemental Figure 1**). We cannot explain this observed behavior, but we speculate that interactions with other proteins partially prevented the tryptic digest in some slices and therefore changed the relative abundances.

One of the major challenges of this study was the solubilization and mass spectrometric detection of integral membrane proteins. The OHR complex is believed to contain two integral membrane proteins, OmeB (10 predicted transmembrane helices) and RdhB (three predicted transmembrane helices). Only three OmeB peptides and only one single peptide from the 32 RdhB proteins encoded in the genome were identified in all our mass spectrometric data together. The single peptide identified from RdhB CbdbB3 had the sequence FIQYLK and is located in the cytoplasmic loop of the protein, requiring two trypsin cuts on the cytoplasmic sides of two transmembrane helices. This is only possible if the loop is not interacting with other proteins. Accordingly, the detection of this peptide across the whole blue native lane supports that the RdhA is bound to the extracytoplasmic surface of RdhB as considered in our model (**Figure 1**). The peptide also allowed the tracing of interactions with its associated RdhA CbdbA80, but we were not able to monitor other RdhB proteins. These difficulties in detecting integral membrane proteins are often described and are due to problems in solubilization, trypsin cleavage and fragmentation. This is especially true for RdhB proteins which are very small proteins with only about 90 amino acids and have only few trypsin digestion sites of which some might be protected by protein-protein interactions. The detection of further RdhB proteins by mass spectrometry is a topic that needs to be addressed in the future.

With extraction mode 3 three different OHR complex modules were observed, mostly separated from each other. Each of the modules contained several single protein subunits which interacted more strongly with each other than the modules interacted with each other. The largest module consisted of OmeA, OmeB and HupX with a relative protein abundance maximum of about 540 kDa. HupX showed a much stronger interaction with OmeA than with the other two hydrogenase subunits HupL and HupS, although it is encoded in an operon with HupL/HupS. This result is in agreement with previous results showing co-localization of HupX with OmeA/OmeB in *Dehalococcoides* strains (Kublik et al., 2016; Hartwig et al., 2017) but we can here confirm this with better spatial resolution and also by a clustering calculation. However, this higher resolution also indicated that the calculated size of the module (181.6 kDa) is not fitting to the size where the relative protein abundance maximum was identified (∼540 kDa). Consequently this module is either interacting with other proteins or polymerizes to a homotrimer. Potential further interaction partners of the OmeA/OmeB/HupX module where identified by cluster analysis (**Figure 6C**) where we found identical migration patterns for the hypothetical periplasmic protein CbdbA1106 and a K^+ insensitive pyrophosphate energized proton pump CbdbA738/HppA. Interestingly CbdbA1106 and HppA were identified also in previous analyses on BN-PAGE and SDS-PAGE of surface cross-linked samples of strain CBDB1, but not on 2D BN/SDS-PAGE (Kublik et al., 2016). Due to the similar predicted topology of CbdbA1106, HupS and HupX observed interactions could

also be unspecific via interactions of the transmembrane helices. HppA is thought to utilize the energy from pyrophosphate hydrolysis to generate a proton motif force and it is predicted to have 15 transmembrane helices. Until now it is not known how protons are translocated across the membrane by the OHR complex. One hypothesis describes OmeB as potential proton pump with a glutamate residue in helix eight possibly involved in proton pumping (Zinder, 2016). Another possibility is that an additional protein such as HppA is interacting with the complex to generate the proton motif force needed for ATP synthesis.

The second module identified in extraction mode 3 consisted of the Hup subunits HupL and HupS with a maximum of relative protein abundance at a molecular weight of ∼60 kDa. The calculated size of HupL and HupS together is 95 kDa and is therefore higher than indicated by BN-PAGE. However, this seems to be a typical migration behavior of smaller protein assemblies in BN-PAGE analyses and is influenced by detergents and Coomassie G-250 additive (Crichton et al., 2013). The separation of HupL/HupS from the other complex subunits in BN-PAGE analyses after solubilization was found previously (Kublik et al., 2016).

In contrast to previous approaches we could separate clearly different RdhA module versions by BN-PAGE. Whereas, complexome analysis 1 did not separate the two most abundant RdhA proteins CbdbdA80 and CbdbA84, they were well separated in complexome analysis 3. The reason, why CbdbA84 was at a much higher molecular mass than CbdbA80 is not clear. However, we know that CbdbA84 is an active reductive dehalogenase (Adrian et al., 2007b). A similar separation between two RdhA proteins can be seen with CbdbA1588 (together with CbdbA84 at 240 kDa) and CbdbA1638 (together with CbdbA80 at 140 kDa). Interestingly, the two single separated peaks of CbdbA1588 and CbdbA1638 can also be seen in complexome analysis 1, suggesting that the separation was only efficient for RdhA proteins at low concentration. Never, RdhA proteins were found at the monomeric mass of ∼55 kDa. Taking the results from complexome analyses 1 and 3 together it appears that the Rdh module at 240 kDa was attached to the OmeA/OmeB/HupX module whereas the Rdh-module at 140 kDa was associated with the HupL/HupS module. A separation of RdhA proteins into bands between 130 and 300 kDa was seen before in 2D BN-PAGE/SDS-PAGE gels and was dependent on the detergent type concentration (Kublik et al., 2016). We here show that the complexes with different sizes contain a different complement of RdhA proteins. Only by observing this separation between RdhA proteins we could for the first time observe the co-migration of an RdhA protein with the RdhB protein located with it in the genome. This strongly suggests that indeed there is a specific interaction between an RdhA and an RdhB protein. It has to be investigated if this is transferrable to other RdhA/RdhB interactions.

Previously the main reductive dehalogenase activity in BN-PAGE gels was identified at a position of around 242 kDa with 1,2,3,4-tetrachlorobenzene as electron acceptor (Kublik et al., 2016). This correlates well with position of the RdhA CbdbA84 identified here in our complexome analysis 3. CbdbA84 has previously been described as chlorobenzene reductive dehalogenase (CbrA) (Adrian et al., 2007b).

Our results also clearly indicate module-module interactions that can be seen in the two module-conserving analyses 1 and 3. In analysis 3 the different modules were mostly separated from each other. However, minor peaks, where a small part of one module putatively interacted with another module, were located at different positions than the main peak. This can be observed in **Figure 4** where the main part of the HupL/HupS module was located in slices 47–51, whereas a minor part interacted with the RdhA/RdhB module in slices 39–41. This is the same peak that was observed in complexome analysis 1 (**Figure 2**) in slice 20 as shown by the indicative presence of the single peak of the RdhA CbdbA1453. In this slice 20, however, almost all of the HupL/HupS module was present whereas only a minor fraction of the HupL/HupS module was migrating together without RdhA subunits to slice 24. This shows that the solubilization strength in complexome analysis 3 was higher than in complexome analysis 1 and that therefore in complexome analysis 1 still a major part of the HupL/HupS module was associated with the RdhA protein(s). A tiny but significant portion of the HupL/HupS module was also co-migrating with the OmeA/OmeB/HupX module in slice 20 of complexome analysis 3 (**Figure 4**). Another module-module interactions can be seen in complexome analysis 1 (**Figure 2**) between the OmeA/OmeB/HupX module and the RdhA/RdhB module in slice 18.

Taking the results of our current study together we might need to revise the hypothesis of a linear model for the OHR complex in which HupL/HupS, OmeA/OmeB/HupX and RdhA/RdhB are linearly organized (Kublik et al., 2016). Especially, because we here found evidence for the direct interaction of HupL/HupS with RdhA/RdhB without mediation by OmeA/OmeB/HupX in slice 40 of complexome analysis 3 (**Figure 4**) an in slice 20 of complexome analysis 1 (**Figure 2**). Hence, we now prefer a triangular model in which all three modules are interacting with each other. However, we still do not have evidence for the stoichiometry between the different modules in the complex and also we do not have information about the number of subunits in each of the three modules. It could be expected that such a stoichiometry can be inferred from the size estimation of the blue native gels using the applied marker, but we have realized that this size estimation is not precise and complexes often migrate different from what is expected. For example the HupL/HupS module always migrates at about 60 kDa although the two proteins together should already have 95 kDa. Also the OmeA/OmeB/HupX module together with a theoretical mass of 180 kDa was located in gel slices corresponding to a molecular weight of around 540 kDa. The RdhA-containing modules are always distributed within the range between 130 and 260 kDa and it would be very speculative to predict the subunit composition of the submodules. A more precise size estimation is necessary and therefore, the elucidation of the exact stoichiometry and organization of the complex needs to await further work.

In addition to information on the OHR complex we also obtained evidence for several other protein-protein interactions in strain CBDB1. However, the absence of any further highly expressed protein complexes is more surprising than the

detection of expected interactions between subunits such as VhuA/VhuG or AtpA/AtpF/AtpC. Indeed most remarkable is the absence of indications for a complex I (Nuo) which is encoded in the genome with all necessary subunits with the exception of the NADH-input domain NuoEFG.

AUTHOR CONTRIBUTIONS

KS and LA conceived the study and designed the experiments. KS and JK did the lab experiments, KS, JK, and LA analyzed the data KS, JK, and LA wrote the manuscript.

FUNDING

The work was financed by the German Research Council (DFG) within the Research Group FOR1530. Protein mass spectrometry was done at the Centre for Chemical Microscopy (ProVIS) at the Helmholtz Centre for Environmental Research, which is supported by European regional development funds (EFRE–Europe Funds Saxony) and the Helmholtz Association.

ACKNOWLEDGMENTS

We thank Chang Ding for support in data analysis and Benjamin Scheer for technical support.

SUPPLEMENTARY MATERIAL

The Supplementary Material for this article can be found online at: https://www.frontiersin.org/articles/10.3389/fmicb.2018.01130/full#supplementary-material

Supplemental Figure 1 | Analysis of single peptide distributions across the native gel lane together with the respective proteins. **(A)** HupL, **(B)** OmeA, **(C)** RdhA CbdbA84. Splitting of peak maxima was observed in OmeA and CbdbA84.

Supplemental Figure 2 | Hierarchical cluster analysis of the distribution across a blue native gel for all peptides of the OHR complex after extraction mode 3. The analysis indicates that peptides originating from the same protein mostly cluster together confirming the stability of our analyses. The three peptides that are isolated on the top were detected only once in a single slice each, explaining their separation in the tree. The color code is the same as elsewhere in this study, with exception of RdhA proteins. RdhA proteins are colored as following: CbdbA80, red, CbdbA84, purple, CbdbA1588, black, CbdbA1618, dark red, and CbdbA1638, bright red.

Supplemental Figure 3 | Cluster analysis of all detected proteins in the three complexome analyses. **(A)** after extraction mode 1; **(B)** extraction mode 2; **(C)** extraction mode 3. OHR-complex proteins and ATPase subunits are colorized as elsewhere in this study.

Supplemental Table 1 | List of all detected proteins and their identified peptides. The list gives absolute numbers of area counts determined by label-free quantification. The numbers represent the sum of all area count values obtained from the gel slices. Also the number of peptides identified for each protein is listed.

Supplemental Table 2 | Color code for the suspected OHR complex proteins used in this manuscript.

REFERENCES

Adrian, L., Dudkova, V., Demnerova, K., and Bedard, D. L. (2009). "*Dehalococcoides*" sp. strain CBDB1 extensively dechlorinates the commercial polychlorinated biphenyl mixture aroclor 1260. *Appl. Environ. Microbiol.* 75, 4516–4524. doi: 10.1128/AEM.00102-09

Adrian, L., Hansen, S. K., Fung, J. M., Görisch, H., and Zinder, S. H. (2007a). Growth of *Dehalococcoides* strains with chlorophenols as electron acceptors. *Environ. Sci. Technol.* 41, 2318–2323. doi: 10.1021/es062076m

Adrian, L., Rahnenführer, J., Gobom, J., and Hölscher, T. (2007b). Identification of a chlorobenzene reductive dehalogenase in *Dehalococcoides* sp. strain CBDB1. *Appl. Environ. Microbiol.* 73, 7717–7724. doi: 10.1128/AEM.01649-07

Adrian, L., Szewzyk, U., Wecke, J., and Görisch, H. (2000). Bacterial dehalorespiration with chlorinated benzenes. *Nature* 408, 580–583. doi: 10.1038/35046063

Bunge, M., Adrian, L., Kraus, A., Opel, M., Lorenz, W. G., Andreesen, J. R., et al. (2003). Reductive dehalogenation of chlorinated dioxins by an anaerobic bacterium. *Nature* 421, 357–360. doi: 10.1038/nature01237

Cooper, M., Wagner, A., Wondrousch, D., Sonntag, F., Sonnabend, A., Brehm, M., et al. (2015). Anaerobic microbial transformation of halogenated aromatics and fate prediction using electron density modeling. *Environ. Sci. Technol.* 49, 6018–6028. doi: 10.1021/acs.est.5b00303

Crichton, P. G., Harding, M., Ruprecht, J. J., Lee, Y., and Kunji, E. R. (2013). Lipid, detergent, and Coomassie Blue G-250 affect the migration of small membrane proteins in blue native gels: mitochondrial carriers migrate as monomers not dimers. *J. Biol. Chem.* 288, 22163–22173. doi: 10.1074/jbc.M113.484329

de Almeida, N. M., Wessels, H. J., de Graaf, R. M., Ferousi, C., Jetten, M. S., Keltjens, J. T., et al. (2016). Membrane-bound electron transport systems of an anammox bacterium: a complexome analysis. *Biochim. Biophys. Acta* 1857, 1694–1704. doi: 10.1016/j.bbabio.2016.07.006

Eydt, K., Davies, K. M., Behrendt, C., Wittig, I., and Reichert, A. S. (2017). Cristae architecture is determined by an interplay of the MICOS complex and the F1FO ATP synthase via Mic27 and Mic10. *Microb Cell* 4, 259–272. doi: 10.15698/mic2017.08.585

Fincker, M., and Spormann, A. M. (2017). Biochemistry of catabolic reductive dehalogenation. *Annu. Rev. Biochem.* 86, 357–386. doi: 10.1146/annurev-biochem-061516-044829

Frauenstein, D., Seidel, K., and Adrian, L. (2017). SandTraps are efficient, scalable, and mild systems for harvesting, washing and concentrating cells. *J. Microbiol. Methods* 132, 106–111. doi: 10.1016/j.mimet.2016.11.018

Hartwig, S., Dragomirova, N., Kublik, A., Turkowsky, D., von Bergen, M., Lechner, U., et al. (2017). A H_2 -oxidizing, 1,2,3-trichlorobenzene-reducing multienzyme complex isolated from the obligately organohalide-respiring bacterium *Dehalococcoides mccartyi* strain CBDB1. *Environ. Microbiol. Rep.* 9, 618–625. doi: 10.1111/1758-2229.12560

Hartwig, S., Thomas, C., Krumova, N., Quitzke, V., Türkowsky, D., Jehmlich, N., et al. (2015). Heterologous complementation studies in *Escherichia coli* with the Hyp accessory protein machinery from Chloroflexi provide insight into [NiFe]-hydrogenase large subunit recognition by the HypC protein family. *Microbiology* 161, 2204–2219. doi: 10.1099/mic.0.000177

Heide, H., Bleier, L., Steger, M., Ackermann, J., Drose, S., Schwamb, B., et al. (2012). Complexome profiling identifies TMEM126B as a component of the mitochondrial complex I assembly complex. *Cell Metab.* 16, 538–549. doi: 10.1016/j.cmet.2012.08.009

Hess, V., Schuchmann, K., and Müller, V. (2013). The ferredoxin:NAD+ oxidoreductase (Rnf) from the acetogen *Acetobacterium woodii* requires Na+ and is reversibly coupled to the membrane potential. *J. Biol. Chem.* 288, 31496–31502. doi: 10.1074/jbc.M113.510255

Hug, L. A., Maphosa, F., Leys, D., Löffler, F. E., Smidt, H., Edwards, E. A., et al. (2013). Overview of organohalide-respiring bacteria and a proposal for a classification system for reductive dehalogenases. *Philos. Trans. R. Soc. Lond. B Biol. Sci.* 368:20120322. doi: 10.1098/rstb.2012.0322

Imkamp, F., Biegel, E., Jayamani, E., Buckel, W., and Müller, V. (2007). Dissection of the caffeate respiratory chain in the acetogen *Acetobacterium woodii*: identification of an Rnf-Type NADH dehydrogenase as a potential coupling site. *J. Bacteriol.* 189, 8145–8153. doi: 10.1128/JB.01017-07

Jones, K. C., and de Voogt, P. (1999). Persistent organic pollutants (POPs): state of the science. *Environ. Pollut.* 100, 209–221.

Jugder, B. E., Ertan, H., Bohl, S., Lee, M., Marquis, C. P., and Manefield, M. (2016). Organohalide respiring bacteria and reductive dehalogenases: key tools in organohalide bioremediation. *Front. Microbiol.* 7:249. doi: 10.3389/fmicb.2016.00249

Kiirika, L. M., Behrens, C., Braun, H. P., and Colditz, F. (2013). The mitochondrial complexome of *Medicago truncatula*. *Front. Plant Sci.* 4:84. doi: 10.3389/fpls.2013.00084

Kube, M., Beck, A., Zinder, S. H., Kuhl, H., Reinhardt, R., and Adrian, L. (2005). Genome sequence of the chlorinated compound-respiring bacterium *Dehalococcoides* species strain CBDB1. *Nat. Biotechnol.* 23, 1269–1273. doi: 10.1038/nbt1131

Kublik, A., Deobald, D., Hartwig, S., Schiffmann, C. L., Andrades, A., von Bergen, M., et al. (2016). Identification of a multi-protein reductive dehalogenase complex in *Dehalococcoides mccartyi* strain CBDB1 suggests a protein-dependent respiratory electron transport chain obviating quinone involvement. *Environ. Microbiol.* 18, 3044–3056. doi: 10.1111/1462-2920.13200

Nesterenko, M. V., Tilley, M., and Upton, S. J. (1994). A simple modification of Blum's silver stain method allows for 30 minute detection of proteins in polyacrylamide gels. *J. Biochem. Biophys. Methods* 28, 239–242. doi: 10.1016/0165-022X(94)90020-5

Schiffmann, C. L., Jehmlich, N., Otto, W., Hansen, R., Nielsen, P. H., Adrian, L., et al. (2014). Proteome profile and proteogenomics of the organohalide-respiring bacterium *Dehalococcoides mccartyi* strain CBDB1 grown on hexachlorobenzene as electron acceptor. *J. Proteomics* 98, 59–64. doi: 10.1016/j.jprot.2013.12.009

Schimo, S., Wittig, I., Pos, K. M., and Ludwig, B. (2017). Cytochrome c oxidase biogenesis and metallochaperone interactions: steps in the assembly pathway of a bacterial complex. *PLoS ONE* 12:e0170037. doi: 10.1371/journal.pone.0170037

Schoepp-Cothenet, B., van Lis, R., Atteia, A., Baymann, F., Capowiez, L., Ducluzeau, A.-L., et al. (2013). On the universal core of bioenergetics. *Biochim. Biophys. Acta* 1827, 79–93. doi: 10.1016/j.bbabio.2012.09.005

Schubert, T., Adrian, L., Sawers, R. G., and Diekert, G. (2018). Organohalide respiratory chains: composition, topology and key enzymes. *FEMS Microbiol. Ecol.* 94:fiy035. doi: 10.1093/femsec/fiy035

Senkler, J., Senkler, M., Eubel, H., Hildebrandt, T., Lengwenus, C., Schertl, P., et al. (2017). The mitochondrial complexome of *Arabidopsis thaliana*. *Plant J.* 89, 1079–1092. doi: 10.1111/tpj.13448

Steffan, R. J., and Schaefer, C. E. (2016). "Current and future bioremediation applications: bioremediation from a practical and regulatory perspective," in *Organohalide-Respiring Bacteria,* eds L. Adrian and F.E. Löffler (Berlin; Heidelberg: Springer Berlin Heidelberg), 517–540.

Wittig, I., Braun, H.-P., and Schägger, H. (2006). Blue native PAGE. *Nat. Protocols* 1, 418–428. doi: 10.1038/nprot.2006.62

Wittig, I., and Schägger, H. (2009). Native electrophoretic techniques to identify protein–protein interactions. *Proteomics* 9, 5214–5223. doi: 10.1002/pmic.200900151

Wöhlbrand, L., Ruppersberg, H. S., Feenders, C., Blasius, B., Braun, H. P., and Rabus, R. (2016). Analysis of membrane-protein complexes of the marine sulfate reducer *Desulfobacula toluolica* Tol2 by 1D blue native-PAGE complexome profiling and 2D blue native-/SDS-PAGE. *Proteomics* 16, 973–988. doi: 10.1002/pmic.201500360

Yang, C., Kublik, A., Weidauer, C., Seiwert, B., and Adrian, L. (2015). Reductive dehalogenation of oligocyclic phenolic bromoaromatics by *Dehalococcoides mccartyi* strain CBDB1. *Environ. Sci. Technol.* 49, 8497–8505. doi: 10.1021/acs.est.5b01401

Zinder, S. H. (2016). *Dehalococcoides* has a dehalogenation complex. *Environ. Microbiol.* 18, 2773–2775. doi: 10.1111/1462-2920.13204

Conflict of Interest Statement: The authors declare that the research was conducted in the absence of any commercial or financial relationships that could be construed as a potential conflict of interest.

frontiers in Microbiology

ORIGINAL RESEARCH
published: 24 April 2018
doi: 10.3389/fmicb.2018.00755

The Membrane-Bound C Subunit of Reductive Dehalogenases: Topology Analysis and Reconstitution of the FMN-Binding Domain of PceC

*Géraldine F. Buttet[1], Mathilde S. Willemin[1], Romain Hamelin[2], Aamani Rupakula[1] and Julien Maillard[1]**

[1] *Laboratory for Environmental Biotechnology, Institute for Environmental Engineering, Swiss Federal Institute of Technology in Lausanne, Lausanne, Switzerland,* [2] *Protein Core Facility, Faculty of Life Sciences, Swiss Federal Institute of Technology in Lausanne, Lausanne, Switzerland*

Organohalide respiration (OHR) is the energy metabolism of anaerobic bacteria able to use halogenated organic compounds as terminal electron acceptors. While the terminal enzymes in OHR, so-called reductive dehalogenases, are well-characterized, the identity of proteins potentially involved in electron transfer to the terminal enzymes remains elusive. Among the accessory genes identified in OHR gene clusters, the C subunit (*rdhC*) could well code for the missing redox protein between the quinol pool and the reductive dehalogenase, although it was initially proposed to act as transcriptional regulator. RdhC sequences are characterized by the presence of multiple transmembrane segments, a flavin mononucleotide (FMN) binding motif and two conserved CX_3CP motifs. Based on these features, we propose a curated selection of RdhC proteins identified in general sequence databases. Beside the Firmicutes from which RdhC sequences were initially identified, the identified sequences belong to three additional phyla, the Chloroflexi, the Proteobacteria, and the Bacteriodetes. The diversity of RdhC sequences mostly respects the phylogenetic distribution, suggesting that *rdhC* genes emerged relatively early in the evolution of the OHR metabolism. PceC, the C subunit of the tetrachloroethene (PCE) reductive dehalogenase is encoded by the conserved *pceABCT* gene cluster identified in *Dehalobacter restrictus* PER-K23 and in several strains of *Desulfitobacterium hafniense*. Surfaceome analysis of *D. restrictus* cells confirmed the predicted topology of the FMN-binding domain (FBD) of PceC that is the exocytoplasmic face of the membrane. Starting from inclusion bodies of a recombinant FBD protein, strategies for successful assembly of the FMN cofactor and refolding were achieved with the use of the flavin-trafficking protein from *D. hafniense* TCE1. Mass spectrometry analysis and site-directed mutagenesis of rFBD revealed that threonine-168 of PceC is binding FMN covalently. Our results suggest that PceC, and more generally RdhC proteins, may play a role in electron transfer in the metabolism of OHR.

Keywords: organohalide respiration, PceC, RdhC, flavoproteins, flavin mononucleotide (FMN), protein reconstitution, flavin-trafficking proteins (Ftp), flavin transferase

OPEN ACCESS

Edited by:
Shanquan Wang,
Sun Yat-sen University, China

Reviewed by:
Matthew Lee,
University of New South Wales, Australia
Yan Xu,
Southeast University, China

****Correspondence:***
Julien Maillard
julien.maillard@epfl.ch

Specialty section:
This article was submitted to Microbiotechnology, Ecotoxicology and Bioremediation, a section of the journal Frontiers in Microbiology

Received: *31 January 2018*
Accepted: *04 April 2018*
Published: *24 April 2018*

Citation:
Buttet GF, Willemin MS, Hamelin R, Rupakula A and Maillard J (2018) The Membrane-Bound C Subunit of Reductive Dehalogenases: Topology Analysis and Reconstitution of the FMN-Binding Domain of PceC. Front. Microbiol. 9:755. doi: 10.3389/fmicb.2018.00755

INTRODUCTION

Organohalide respiration (OHR) is a respiratory metabolism that uses halogenated compounds as terminal electron acceptors, and allows an increasing number of anaerobic bacteria to conserve energy (Adrian and Löffler, 2016). While there is an extensive body of information on the reductive dehalogenases (RdhA, RDases), the key enzymes involved in the catalytic reduction of organohalides (for a review, see Jugder et al., 2016a), relatively little is known about the electron transport in OHR, and specifically about the redox proteins involved in donating electrons to RDases. Nevertheless, models of electron transport have been recently proposed (Goris et al., 2015b; Kublik et al., 2016; Maillard and Holliger, 2016; Fincker and Spormann, 2017), indicating that, depending on their phylogeny, organohalide-respiring bacteria (OHRB) must have developed various strategies to deliver electrons to the corrinoid cofactor of RDases at sufficiently low redox potential. Indeed, the Co^{II}/Co^{I} midpoint reduction potential for the corrinoid in the tetrachloroethene RDase (PceA) of *Dehalobacter restrictus* and in the chlorophenol RDase (CprA) of *Desulfitobacterium dehalogenans* have been measured at −350 and −370 mV, respectively (Schumacher et al., 1997; van de Pas et al., 1999). While menaquinones are involved in electron transfer to RDases in *D. restrictus* (Schumacher and Holliger, 1996), *Desulfitobacterium dehalogenans* (Kruse et al., 2015) and *Sulfurospirillum multivorans* (Miller et al., 1996), OHRB belonging to the Chloroflexi (*Dehalococcoides* and *Dehalogenimonas*) do not use quinones, suggesting that different pathways are used for conserving energy via OHR (Fincker and Spormann, 2017). In the quinone-dependent electron transfer to RDases, one question remains largely unresolved, that is the generation of low redox potential electrons from the quinol/quinone redox couple (with a well-accepted $E^{0'}$ value of −74 mV, Thauer et al., 1977). Possible mechanisms to solve this have been proposed, such as reverse electron flow in the case of *S. multivorans* (Miller et al., 1996) or electron bifurcation (Buckel and Thauer, 2013). Redox proteins involved in the electron transfer between the quinol pool and the RDases remains largely unexplored and their identification will shed light on the possible mechanisms of electron transfer in OHR.

Besides *rdhA* and *rdhB* which code for the RDase enzyme and its predicted membrane anchor, respectively, one particular gene, *rdhC*, was found in *rdh* gene clusters of several OHRB belonging to diverse phylogenetic groups. The RdhC homologs CprC, VcrC, PceC, and TmrC have been successively identified in *D. dehalogenans* (Smidt et al., 2000), *Dehalococcoides mccartyi* (Müller et al., 2004), *D. restrictus* (Maillard et al., 2005), and *Dehalobacter* sp. UNSWDHB (Jugder et al., 2016b; Wong et al., 2016), respectively. Analysis of the sequence of CprC has revealed a significant homology to proteins belonging to the NosR/NirI transcriptional regulators (Cuypers et al., 1992), suggesting that it may play a role in the regulation of the *cpr* gene cluster. Transcription analysis have shown that under OHR conditions *cprC* was transcribed with *cprD* and occasionally also as a *cprBACD* polycistronic RNA (Smidt et al., 2000), indicative for a function in the OHR metabolism. PceC is encoded in the conserved *pceABCT* gene cluster responsible for the tetrachloroethene (PCE) reductive dehalogenase activity in *D. restrictus*, but also in the genomes of *Desulfitobacterium hafniense* strain TCE1 (Maillard et al., 2005), strain Y51 (Futagami et al., 2006) and strain PCE-S (Goris et al., 2015a), as well as of less characterized OHRB (Duret et al., 2012). After the initial annotation, the role of NosR in the nitrous oxide reduction pathway was reconsidered and studies have demonstrated that it is likely playing a role in the activation of the nitrous oxide reductase (NosZ), as well as in electron transfer toward NosZ (Wunsch and Zumft, 2005; Zumft, 2005; Borrero-de Acuna et al., 2017).

PceC, and more generally RdhC proteins, are predicted to be integral membrane proteins with six transmembrane α-helices, a peripheral domain and two conserved CX_3CP motifs. The peripheral domain harbors a conserved sequence motif for covalent binding of the flavin mononucleotide (FMN) cofactor that is also found in NosR and in two well-characterized flavoproteins, the C subunit of the Na^+-translocating NADH-quinone reductase (NqrC) (Casutt et al., 2012; Vohl et al., 2014; Borshchevskiy et al., 2015) and in the G subunit of the *Rhodobacter* nitrogen fixation (RnfG) complex (Backiel et al., 2008; Suharti et al., 2014). Both NqrC and RnfG flavoproteins are part of large membrane-bound protein complexes involved in electron transfer and energy metabolism.

The sequence homology of PceC with NosR and other flavoproteins involved in electron transfer invited us to reconsider its function in the OHR metabolism. In this study, we present a curated selection of RdhC homologous sequences found in protein databases based on conserved sequence features. Then, the predicted membrane topology of PceC was validated with a targeted surfaceome analysis of *D. restrictus* cells. Last, we present the results of an experimental strategy developed for the heterologous production and successful reconstitution of the recombinant FMN-binding domain (rFBD) of PceC.

MATERIALS AND METHODS

Bacterial Strains and Cultivation

Dehalobacter restrictus PER-K23 and *D. hafniense* TCE1 were purchased at DSMZ culture collection (Braunschweig, Germany), while *Escherichia coli* strains DH5α and BL21(λDE3) were obtained from Novagen (Merck Millipore, Schaffhausen, Switzerland). A list of main bacterial features is given in **Table 1**.

Dehalobacter restrictus PER-K23 and *D. hafniense* TCE1 were cultivated anaerobically with hydrogen and tetrachloroethene (PCE) as electron donor and acceptor, respectively, as previously described (Prat et al., 2011; Comensoli et al., 2017).

Escherichia coli strains were routinely cultivated in Luria-Bertani liquid and solid media. For large-scale production of rFBD protein, *E. coli* BL21(λDE3) harboring the pFBD plasmid was cultivated in ZYM-5052 medium following the protocol established by Studier (2014). Antibiotics were supplemented depending on the plasmid, as indicated in **Table 2**.

Plasmid Construction

Polymerase Chain Reaction (PCR)

Standard PCR reaction mixtures for cloning consisted of a 50-μL reaction containing 5 μL Pfu DNA polymerase 10× buffer (Promega, Dübendorf, Switzerland), 75 μM dNTPs, 0.5 μM each primer and 0.5 μL of Pfu DNA polymerase. The DNA was amplified in T3 Biometra thermocycler (LabGene, Châtel-Saint-Denis, Switzerland) with the following steps: 2 min initial denaturation at 95°C, 30 cycles of 1 min denaturation at 95°C, 1 min of primer annealing at 52°C, 1 min of elongation at 72°C, and 10 min of final extension at 72°C.

Polymerase chain reaction reactions for site-directed mutagenesis consisted of 5 μL Pfu Turbo polymerase 10× buffer (Agilent Technologies, Morges, Switzerland), 12.5 μM each primer, 75 μM dNTPs, 50 ng of plasmid, 1 μL Pfu Turbo polymerase. The program used was the following: 30 s initial denaturation at 95°C, 30 cycles of 30 s denaturation at 95°C, 60 s of primer annealing at 55°C, 10 min of elongation at 68°C, and a final 7 min extension step at 68°C.

Polymerase chain reaction products for cloning were cleaned using the QIAquick PCR Purification kit (Qiagen AG, Hombrechtikon, Switzerland), following manufacturer's instructions. PCR products and other DNA samples were quantified with the NanoDrop 1000 apparatus (Life Technologies Europe B.V., Zug, Switzerland).

Cloning

A list of the plasmids and oligonucleotides used in this study is given in **Tables 2**, **3**, respectively.

The coding sequence for the FMN-binding domain (FBD) of PceC was amplified by PCR using genomic DNA from *D. hafniense* TCE1 and the primers FBD-24-F/R. The PCR product and the vector pET24d were digested with *Nco*I and *Xho*I in a 40-μL reaction mixture containing 4 μL of buffer D, 0.4 μL of BSA, 1 μL of each enzyme (all components from Promega) which was incubated at 37°C for 2 h. The digested vector was then incubated 15 min after addition of 1 μL of thermosensitive alkaline phosphatase (Promega). Both digested

TABLE 1 | Bacterial strains used in this study.

Strain	Features	Source/reference
Dehalobacter restrictus PER-K23	DSM 9455	Holliger et al., 1998
Desulfitobacterium hafniense TCE1	DSM 12704	Gerritse et al., 1999
E. coli DH5α	F^- endA1 glnV44 thi-1 recA1 relA1 gyrA96 deoR nupG purB20 φ80dlacZΔM15 Δ(lacZYA-argF) U169, hsdR17(rK^-mK^+), λ^-	Novagen
E. coli BL21(λDE3)	F^- ompT gal dcm lon hsdSB (Rb^-mB^-) λ(DE3 [santi lacUV5-T7 gene 1 ind1 sam7 nin5])	Novagen

TABLE 2 | Plasmids used in this study.

Plasmid	Features	Source/reference
pET24-d	IPTG-inducible T7 promoter, kanamycine^R (50 μg/mL), C-terminal His_6-tag	Novagen
pFBD	pET24d expressing FMN-binding domain of PceC (aa 41–200)	This study
pFBD-T168V	pFBD with single mutation expressing a valine variant of Thr168	This study
pETDuet-1	IPTG-inducible T7 promoter, ampicilline^R, two multiple cloning sites, MCS1 with C-terminal His_6-tag, MCS2 with C-terminal S•tag^{TM}	Novagen
pFTP1	pETDuet-1 expressing Ftp1 from MCS2	This study
pFTP2	pETDuet-1 expressing Ftp2 from MCS2	This study

TABLE 3 | Oligonucleotides used in this study.

Primer name	5′–3′ sequence	Features
FBD-24-F	GCGCCCATGGGACAATCGGTTGATTACAAGGGAATC	*Nco*I site
FBD-24-R	GCGCCTCGAGTAAATCGTAAGGGTTGGCCCATTG	*Xho*I site
FBD-T168V-F	ACGGTAACAGGTTCAGTAGTGTCGTCACATGCT	Thr-Val
FBD-T168V-R	AGCATGTGACGACACTACTGAACCTGTTACCGT	Thr-Val
pET24-F2	GGTGATGTCGGCGATATAGG	Sequencing
pET24-R2	CGTTTAGAGGCCCCAAGG	Sequencing
FTP1-F	GCGCCATATGAATGGGAAACCTGTACAACAG	*Nde*I
FTP1-R	GCGCCTCGAGATCTTTGACGAATTCGTACTC	*Xho*I
FTP2-F	GCGCCATATGTTGTCTGCAGAGACCAAGG	*Nde*I
FTP2-R	GCGCCTCGAGTTTGCTTTCTGGGGAAGGTGTC	*Xho*I
Duet-MCS2-F	TTGTACACGGCCGCATAATC	Sequencing
Duet-MCS2-R	GCTAGTTATTGCTCAGCGG	Sequencing

PCR product and vector were purified with the QIAquick PCR Purification kit (Qiagen) and eluted in 30 μL of ddH_2O. After DNA quantification, the ligation reaction was set-up as follows: a 10-μL reaction consisted of 1 μL of T4 DNA ligase (Roche, Sigma-Aldrich, Buchs, Switzerland), 1 μL of 10 mM ATP, insert and vector DNA in 3:1 molar ratio and 1 μL of T4 DNA ligase (Roche). The reaction was incubated for 2 h at room temperature. Five μL of the ligation reaction was directly transformed by heat-shock into 50 μL of RbCl-competent *E. coli* DH5α cells, following standard protocol (Sambrook et al., 1989). Positive transformants were selected by colony PCR using primers pET24d-F2/R2. Plasmids were recovered from overnight 10-mL *E. coli* cultures using QIAprep Spin Miniprep kit (Qiagen) and sequenced for verification as described previously (Duret et al., 2012). The resulting plasmid was named pFBD and used for the production of the C-terminal His_6-tagged rFBD protein.

Cloning of the coding sequence for Ftp1 and Ftp2 was done with the same procedure by using primers FTP1-F/R and FTP2-F/R, respectively, the vector pETDuet-1 and the restriction enzymes *Nde*I and *Xho*I. Sequence verification of the plasmids was done by colony PCR with the primers Duet-MCS2-F/R. The resulting plasmids were named pFTP1 and pFTP2, respectively and used for the production of rFtp1 and rFtp2 proteins with C-terminal S●tag™.

Site-Directed Mutagenesis

The T168V variant of rFBD was obtained by applying the QuikChange site-directed mutagenesis protocol established by Stratagene with the plasmid pFBD and the primers FBD-T168V-F/R. The resulting PCR product was digested for 1 h at 37°C with 1 μL of *Dpn*I (Promega), prior to transformation into *E. coli* DH5α as described above. The mutation was verified by sequencing.

Sequence Analysis

The following software were used to analyze and compare the sequences of RdhC proteins: ClustalX2.0 for sequence alignment (Larkin et al., 2007); iTOL for drawing sequence likelihood trees (Letunic and Bork, 2016); Weblogo for sequence motifs (Crooks et al., 2004); CCTOP for topology prediction (Dobson et al., 2015) and TOPO2 for graphic representation of the topology (developed by S. J. Johns[1]).

The procedure for the identification and selection of RdhC homologous sequences from protein databases is presented in section "Sequence Analysis of RdhC Proteins" of the Supplementary Material.

Surfaceome Analysis

Biomass Collection and Sample Preparation

For surfaceome analysis, the biomass from a 200-mL culture of *D. restrictus* PER-K23 was harvested by centrifugation when approximately 70% of PCE was consumed. The biomass was collected by 30 min centrifugation at 1000 × *g* and 4°C. After carefully decanting the supernatant, the biomass pellet was resuspended in 10 mL ice-cold wash buffer (20 mM Tris-HCl, pH 7.5, 150 mM NaCl) by stirring gently the tube to avoid cell lysis. The biomass was collected by 15 min centrifugation as before and washed twice more. The pellet was then resuspended in 4 mL of digestion buffer (wash buffer supplemented with 0.1 M arabinose and 10 mM $CaCl_2$). Prior to adding the trypsin (10 μL of trypsin (Gold-Mass spec grade, Promega at 1 mg/mL in digestion buffer), the biomass suspension was split into two samples in 15-mL Falcon tubes. The trypsin was added to one of the samples ('shaved' sample), while the other one served as negative control. Both tubes were incubated for 15 min at 37°C by stirring at 120 rpm, then placed on ice for 5 min and centrifuged for 10 min at 1000 × *g* and 4°C. The supernatant was collected, filtered at 0.22 μm and flash-frozen in liquid nitrogen. In order to produce a membrane reference sample, the pellet from the control sample was resuspended in 2 mL of wash buffer and the biomass was lyzed by sonication with 10 cycles of 10× 1 s pulses at 60% amplitude on Sonic Dismembrator FB120 (Fisher Scientific, Reinach, Switzerland). After 5 min centrifugation as above, unbroken cells were discarded and the membranes were obtained from the supernatant by ultracentrifugation for 20 min at 100,000 × *g* and 4°C. The resulting pellet (membrane fraction) was resuspended in 2 mL of wash buffer, flash-frozen in liquid nitrogen. All samples were stored at −80°C until further analysis.

In-Solution Digestion

'Shaved' and 'control' samples were reconstituted in 4 M Urea, 10% acetonitrile and buffered with Tris-HCl pH 8.5 to a final concentration of 30 mM. Proteins were reduced, alkylated, and digested using trypsin as previously described (Dalla Vecchia et al., 2014). Total membrane lysate was heated 10 min at 80°C in Rapigest SF surfactant 0.2% and sonicated 5 min in order to increase the solubility of hydrophobic proteins. Proteins were buffered with Tris-HCl pH 8.5 to a final concentration of 30 mM and reduced using 10 mM dithioerythritol (DTE) at 37°C for 60 min. Proteins were incubated in 40 mM iodoacetamide at 37°C for 45 min in the dark and the reaction was further quenched by the addition of DTE to a final concentration of 10 mM. Protein lysate was first diluted threefold using ammonium bicarbonate at 50 mM and samples were digested overnight at 37°C using 1 μg of mass spectrometry grade trypsin gold and 10 mM $CaCl_2$. Rapigest was cleaved by the addition of trifluoroacetic acid 10% (final pH < 2) and incubated 45 min at 37°C. Peptides from the shaving experiment and the total membrane lysate were desalted in StageTips using 6 disks from an Empore C18 (3 M) filter based on the standard protocol (Rappsilber et al., 2007). Purified samples were dried down by vacuum centrifugation and stored at −20°C.

Mass Spectrometry and Data Analysis

Samples were resuspended in 2% acetonitrile containing 0.1% formic acid for LC–MS/MS injections. Reverse phase separation were performed on a Dionex Ultimate 3000 RSLC nano UPLC system connected online with an Orbitrap Lumos Fusion Mass-Spectrometer. To ensure a robust detection of Dehre_2396 peptides (PceC), an inclusion list corresponding to

[1]http://www.sacs.ucsf.edu/TOPO2/

the expected peptides was established using Skyline 3.1.0.7312 and was further included in the data acquisition method. Raw data was processed using MS-Amanda (Dorfer et al., 2014) and SEQUEST in Proteome Discoverer v.1.4 against the proteome of *D. restrictus* PER-K23. Spectra were searched with a fragment ion mass tolerance of 0.050 Da and a parent ion tolerance of 10.0 PPM. Carbamidomethylation of cysteine residues was specified as a fixed modification. Glutamine to pyro-glutamate of N-termini, oxidation of methionine residues, phosphorylation of serine, threonine, and tyrosine residues and FMN covalently bound to threonine residues were specified as variable modifications. Data was further processed by X!tandem, inspected in Scaffold 4 and spectra of interest were manually validated.

Heterologous Protein Production and Purification

Production and Purification of Recombinant FMN-Binding Domain of PceC (rFBD)

An overnight pre-culture (37°C and 180 rpm) of *E. coli* BL21(λDE3) harboring the pFBD plasmid was done in 50 mL LB medium. Starting from here, two different batches of rFBD production were performed as follows. For the first batch (P1), 2 L of LB medium were inoculated with 20 mL of pre-culture (1:100 dilution) and cultivated until the optical density ($OD_{600\ nm}$) reached approximately 1.0. IPTG was added at 0.1 mM (final concentration) to induce the protein production and the culture was further incubated for 2 h in the same conditions. $OD_{600\ nm}$ reached a value of 2.5 and 6 g of (wet weight) biomass was collected. For the second batch (P2), 2 L of ZYM-5052 (auto-induction) medium were inoculated with 2 mL of pre-culture (1:1000 dilution) and cultivated for 16 h at 20°C and 250 rpm. Cell density reached a value of 10 and 20 g of biomass was collected.

Purification of rFBD inclusion bodies from the collected biomass was applied as follows. The biomass pellet was resuspended in lysis buffer [50 mM Tris-HCl, pH 7.5, 100 mM NaCl, SigmaFast protease inhibitors (Sigma-Aldrich), a few DNase crystals (Roche)] at 10 mL per g of biomass. After three cycles of French press (1000 PSI), the lysate was centrifuged 5 min at 500 × *g* ant 4°C and unbroken cells were removed. The supernatant was centrifuged 15 min at 12,000 × *g* and 4°C. The resulting pellet was rinsed in wash buffer [50 mM Tris-HCl, pH 7.5, 100 mM NaCl, 1 mM EDTA, 1% (w/v) Triton X-100 and 1 M urea], and inclusion bodies were resuspended in solubilization buffer (50 mM Tris-HCl, pH 7.5, 100 mM NaCl, supplemented with 4–8 M urea, depending on the experiments) at 10 mL/g. After one freeze-thaw cycle at −20°C, the suspension was centrifuged at 12,000 × *g* as above and the supernatant containing solubilized rFBD protein was collected.

Production of Recombinant Flavin-Trafficking Proteins (rFtp)

Recombinant rFtp1 and rFtp2 proteins were produced in *E. coli* BL21(λDE3) similarly as rFBD with the following changes. Starting from an overnight pre-culture, 1 L of each culture was performed as above, but induction was achieved by 3 h incubation at 30°C. Each culture reached an $OD_{600\ nm}$ value of 2.9, corresponding to 3.4 and 3.6 g of biomass, respectively. After cell lysis and fractionation as presented above, soluble cell-free extracts were obtained and used for reconstitution experiments.

Protein concentration was estimated with the Pierce BCA assay (Thermo Fisher Scientific, Lausanne, Switzerland) following the manufacturer's instructions. Calibration curve was done with BSA in the same buffer conditions as the analyzed samples.

Reconstitution of rFBD Proteins

Reconstitution by Reverse Urea Gradient

One sample of urea-denatured rFBD protein (obtained from 1 g of biomass sample P1, see above) was loaded on a 1-mL His-Trap Ni-NTA affinity column connected to ÄKTAprime plus™ system (GE Healthcare, Glattbrugg, Switzerland) in buffer A (50 mM Tris-HCl, pH 7.5, 150 mM NaCl, 25 mM imidazole, 1 mM dithiothreitol) supplemented with 4 M urea (buffer A+). After extensive removal of unbound proteins with buffer A+, the column was disconnected from the system and a 10-step reverse urea gradient was manually applied by injecting one column volume (CV) of buffers with decreasing concentration of urea (see Supplementary Table 1 for details). Then, the column was further rinsed with 15 CV of buffer A before rFBD protein was eluted by injection of 10 successive CV of buffer B (buffer A supplemented with 0.6 M imidazole). Ten µL aliquots were run on SDS-PAGE following standard protocol (Sambrook et al., 1989), then FMN-containing proteins were detected under UV illumination. Last, the gel was stained with Coomassie Blue [0.1% (w/v) Coomassie Blue R250 in 10% (v/v) acetic acid and 40% (v/v) ethanol].

Reconstitution by Stepwise Dialysis

Inclusion bodies were purified from 5 g of *E. coli* producing rFBD (biomass sample P2, see above) and resuspended in solubilization buffer containing 8 M urea. After 15 min centrifugation at 4500 × *g* and 4°C, the solubilized and urea-denatured rFBD sample (20 mL) was filtered at 0.45 µm and transferred to a dialysis tube (Spectra/Por with 6-8000 MWCO, Spectrum Labs, Breda, Netherlands) in 2 L dialysis buffer (50 mM Tris-HCl, pH 7.5, 150 mM NaCl, 1 mM dithiothreitol) supplemented with 4 M urea. Dialysis was performed for 2 h at room temperature. The sample was collected from the tube, supplemented with 1.4 mg of rFtp1-containing protein extract, 5 mM $MgSO_4$ and 1 mM FAD, incubated for 20 min at room temperature, and transferred to a fresh dialysis tube. Dialysis was done as before in a buffer containing 2 M urea. The sample was collected, supplemented with rFtp1, then incubated for 20 min and dialysed as before in a buffer lacking urea. Last, the sample was dialysed overnight in fresh buffer to remove residual urea and excess of FAD. A volume of 25 mL of soluble rFBD protein was recovered in the supernatant after 20 min of centrifugation at 15,500 × *g* and 4°C and its concentration estimated at 1.9 mg/mL. Aliquots of each step were analyzed by SDS-PAGE as described above.

Mass Spectrometry Analyses of rFBD Proteins

The methods used for mass spectrometry analysis of rFBD protein are presented in Section "Mass Spectrometry Analyses of the Reconstituted rFBD Protein" of the Supplementary Material.

RESULTS

Sequence Analysis of PceC

The alignment of the four reported RdhC sequences reveals important conserved features (**Figure 1**). Topology and conserved domain predictions suggest the presence of six transmembrane α-helices and a peripheral FBD (FMN-bind, smart00900) located on the outside of the cytoplasmic membrane between helix 1 and 2. The FBD of RdhC sequences shows similarity to NqrC, a subunit of the NADH:quinone oxidoreductase. NqrC has been reported to bind FMN covalently (Nakayama et al., 2000; Borshchevskiy et al., 2015).

Additional sequence homology and protein domain architecture analysis revealed some similarity between PceC and the functionally characterized membrane-bound proteins NosR and NapH (Supplementary Figure 1). PceC displays most features of NosR (Wunsch and Zumft, 2005) but harbors a shorter extra-cytoplasmic loop and lacks Fe–S clusters at the C-terminal end. The C-terminal end of PceC also shows similarities to the domain architecture of the nitrate reductase membrane-bound subunit NapH, which together with NapG is playing a role in transferring electrons from menaquinones to NapA (Kern and Simon, 2008).

Diversity of RdhC Sequences and Definition of the RdhC Protein Family

Looking at the diversity of RdhC sequences in databases, a first selection of 433 sequences was obtained by sequence homology analysis (see section "Sequence Analysis of RdhC Proteins" of the Supplementary Material for a detail description of the selection procedure). Sequence alignment and clustering with 95% identity has reduced the number to 236 unique clusters. From this selection, only those coming from genomes harboring at least one *rdhA* gene were considered. This new selection delivered 117 RdhC clusters comprising a total of 199 unique sequences, each cluster displaying between 1 and 9 unique sequences (see Supplementary Table 2). Sequence likelihood analysis of RdhC clusters is displayed in **Figure 2**. A total of 71 RdhC clusters covering 135 unique sequences come from known OHRB. Among them, with the exception of PceC which is found in both *Dehalobacter* and *Desulfitobacterium*, each RdhC cluster is exclusively found in one specific genus. *Dehalobacter* displays the highest number of clusters (28 clusters with 42 unique sequences), while 20 clusters (30 sequences) are found in *Desulfitobacterium*. *Dehalococcoides,* and *Dehalogenimonas*, the *Chloroflexi* members of OHRB, display 12 and 9 clusters, respectively, comprising 45 and 10 unique sequences (Supplementary Table 2). Three additional RdhC clusters were found in newly identified OHRB: *Geobacter lovleyi*, *Shewanella sediminis,* and *Desulfoluna spongiiphila*. The remaining 43 clusters (88 unique sequences) belong to bacteria that have not been recognized as OHRB yet, suggesting that the reservoir for new OHRB remains largely unexplored. Among them, three bacterial genera harbor 25 clusters with 37 unique sequences (16 sequences for the genus *Vibrio*, 11 for *Photobacterium,* and 10 for *Ferrimonas*) making them interesting candidates to expend the phylogeny of OHRB. All three genera belong to marine Gammaproteobacteria, suggesting that, while OHRB were mostly isolated from sediments of contaminated sites, marine environments represent an important ecological niche for OHRB.

The alignment of the 117 unique sequences revealed three well-conserved sequence motifs, which are defining the RdhC family (**Figure 3**). In the FMN-binding motif (**Figure 3A**), the hydroxyl side chain of the fully conserved threonine is predicted to covalently bind the cofactor in a phosphoester-threonyl-FMN bond (Backiel et al., 2008). A consensus for the FMN-binding motif in RdhC sequences is proposed here as [S/T]G[A/S]TX[S/T], similarly to the motif proposed earlier (Deka et al., 2015). The two other conserved motifs are of the type CX_3CP, for which, however, no function has been yet assigned (**Figures 3B,C**).

Experimental Validation of PceC Topology and FMN-Binding

The FBD of PceC was predicted to face the outside of the cytoplasmic membrane. In order to validate the prediction, a peptide shaving experiment was done with whole cells of *D. restrictus* (**Figure 4**). Proteomic analysis of the cell surface (so-called surfaceome) clearly showed that six peptides of the FBD were detected, while none of the peptides predicted to be located in the cytoplasmic loops were identified. In contrast, three of the cytoplasmic-oriented peptides were detected in the control membrane sample. This unambiguously demonstrates that the FMN-binding peripheral domain of PceC is exposed to the exocytoplasmic side of the membrane.

The presence of a covalently-bound FMN in PceC was investigated using a crude membrane fraction from a culture of *D. restrictus* PER-K23. In-solution digested proteins were further analyzed by LC–MS/MS. Multiple detections of the peptide containing the expected modified threonine were achieved (**Figure 5**). The high quality of the spectra allowed a clear detection of FMN+H and its expected fragments as described previously (Guyon et al., 2008). All these evidences confirmed the presence of the FMN at position T168 of PceC.

Heterologous Production of the FMN-Binding Domain of PceC (rFBD)

The highly hydrophobic nature of PceC prevents its production in a soluble form. Therefore, it was decided to produce the peripheral FBD of PceC in *E. coli*. From sequence prediction analysis, the FBD of PceC from *D. hafniense* TCE1 was defined as the region between residues 41 and 200 (Supplementary Figure 2). The corresponding DNA sequence was cloned in fusion with a C-terminal His_6-tag giving the plasmid pFBD (see

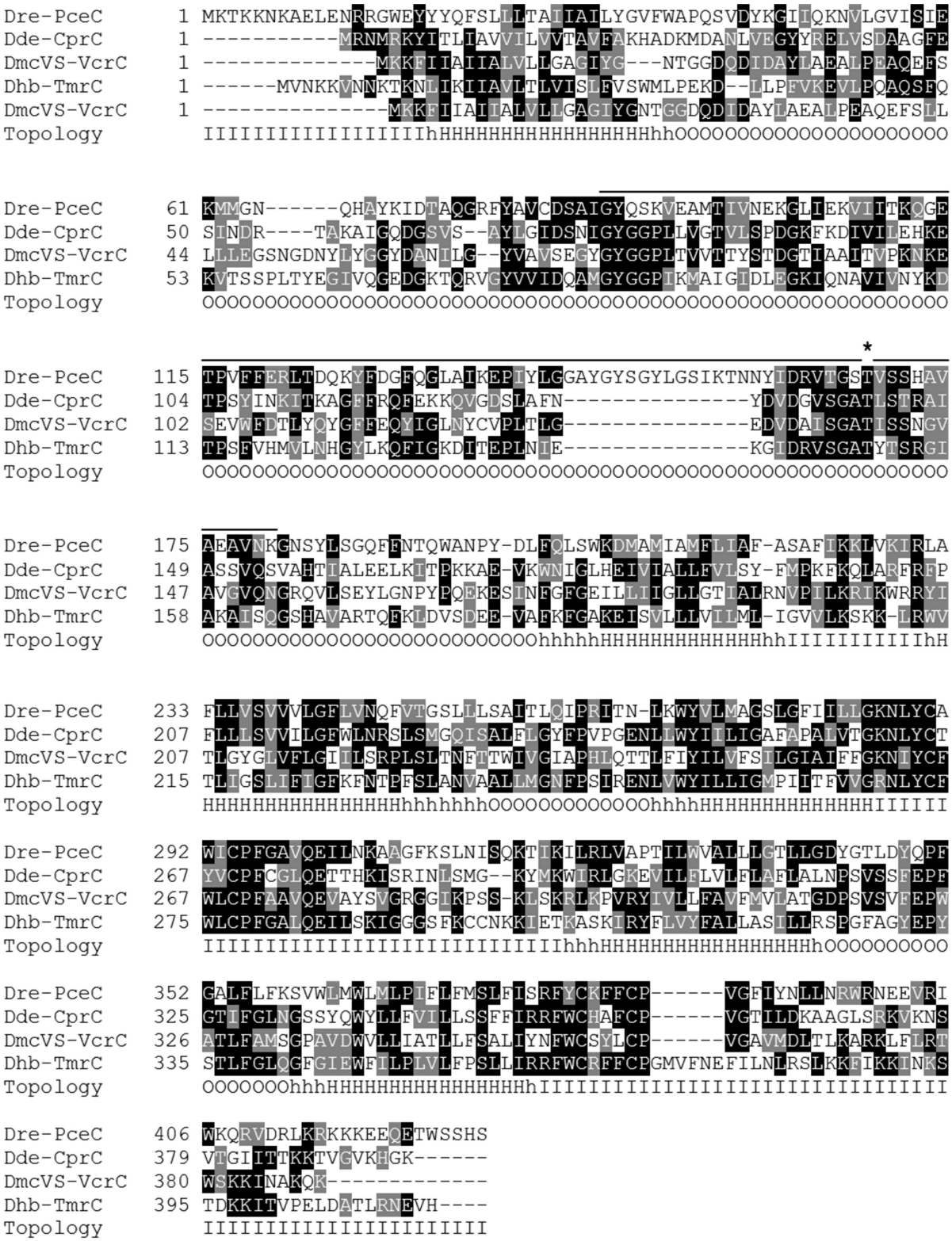

FIGURE 1 | Sequence alignment of four typical members of the RdhC enzyme family: PceC (CAG70347.1) of *Dehalobacter restrictus* (Dre); CprC (AAD44543.2) of *Desulfitobacterium dehalogenans* (Dde); VcrC (ACZ62389.1) of *Dehalococcoides mccartyi* strain VS (DmcVS); TmrC (WP_021315090.1) of *Dehalobacter* sp. strain UNSWDHB (Dhb). The predicted topology is indicated under the alignment: O, outside; I, inside; H, transmembrane α-helices. The bold line above the alignment indicates the predicted FMN-binding domain (FBD, smart00900) with the conserved threonine residue predicted to bind FMN covalently (indicated by the asterisk).

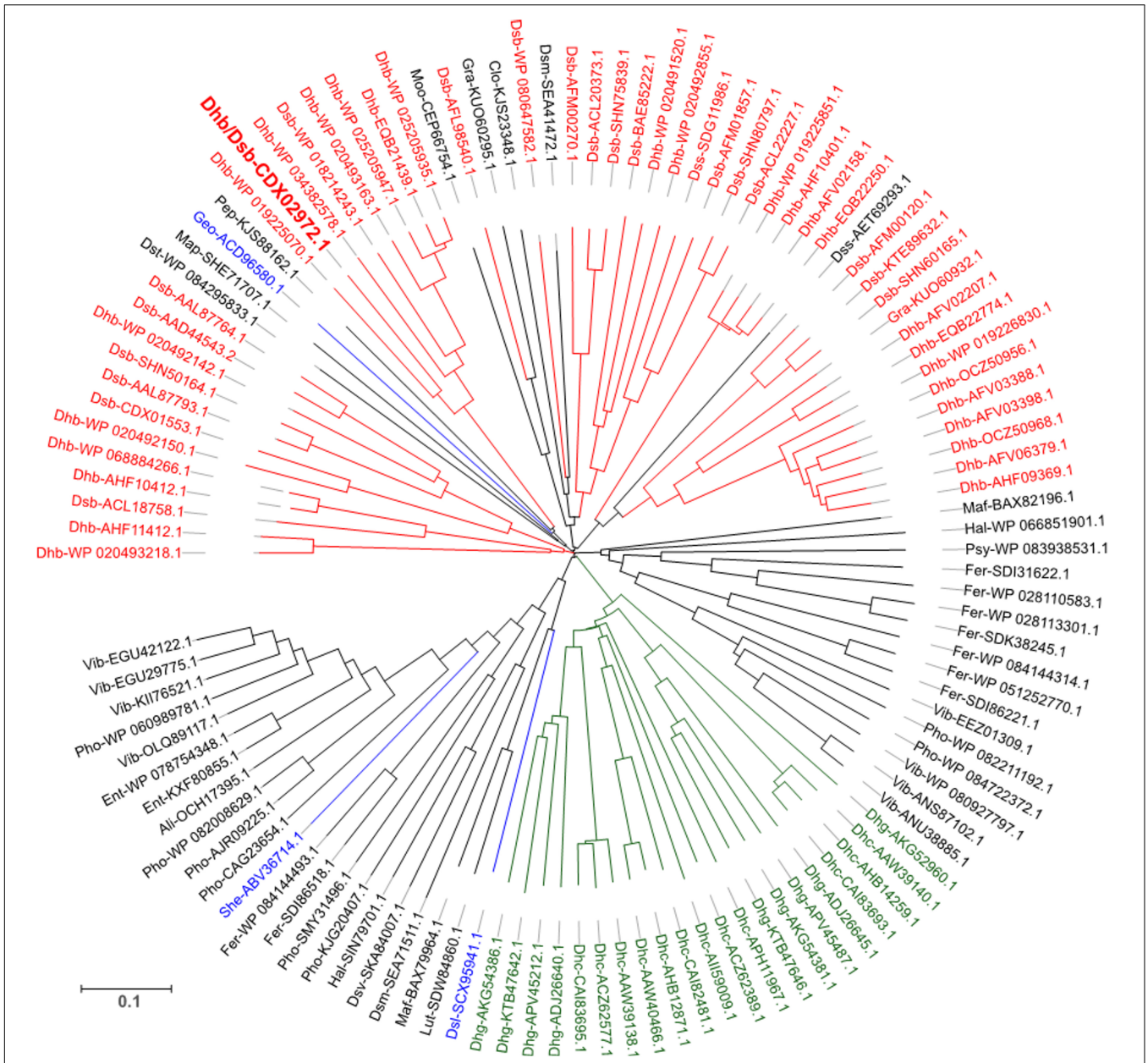

FIGURE 2 | Sequence likelihood analysis of 117 representative RdhC proteins. Sequences are annotated with an abbreviation of the corresponding species followed by the reference number. The sequence annotated in bold red is PceC from *Desulfitobacterium hafniense*, the representative sequence for the protein under investigation in this study. Colors indicate sequences belonging to well-described OHR bacterial genera: red, *Dehalobacter* and *Desulfitobacterium*; green, *Dehalococcoides* and *Dehalogenimonas*; blue, additional OHRB. Detailed information on the overall database used is available in Supplementary Material (Supplementary Table 2).

Table 2). Early attempts revealed that the rFBD was prone to strong protein aggregation in *E. coli* (Supplementary Figure 3A), suggesting that denaturation and refolding are necessary to produce rFBD in a soluble form. Addition of flavins during protein production did not produce any soluble rFBD either (Supplementary Figure 3B). Using a strategy of auto-induction (Studier, 2014), large amount of rFBD was produced in form of inclusion bodies in *E. coli* (Supplementary Figure 3C). Inclusion bodies were easily recovered by fractionation of the lysed *E. coli* biomass and efficiently solubilized in buffer containing 4–8 M urea. Refolding attempts using various strategies such as reverse urea gradient using affinity chromatography or dialysis with decreasing concentration of urea were unsuccessful (data not shown). Recent literature on flavoproteins which display covalently-bound FMN (Bertsova et al., 2013; Deka et al., 2016; Zhang et al., 2017) have suggested that these proteins required a helper protein for efficient assembly of the FMN cofactor and successful folding.

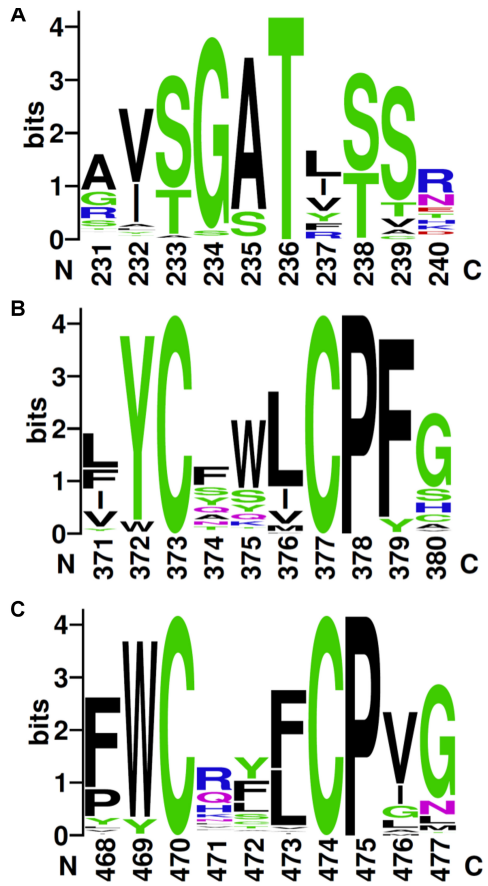

FIGURE 3 | Conserved sequence motifs in RdhC family. Based on the alignment of the 117 RdhC non-redundant representative sequences, motifs were drawn using Weblogo: **(A)** the FMN-binding motif, with the fully conserved threonine involved in binding FMN covalently; **(B,C)** the two CX_3P signatures. Residue numbering follows the alignment.

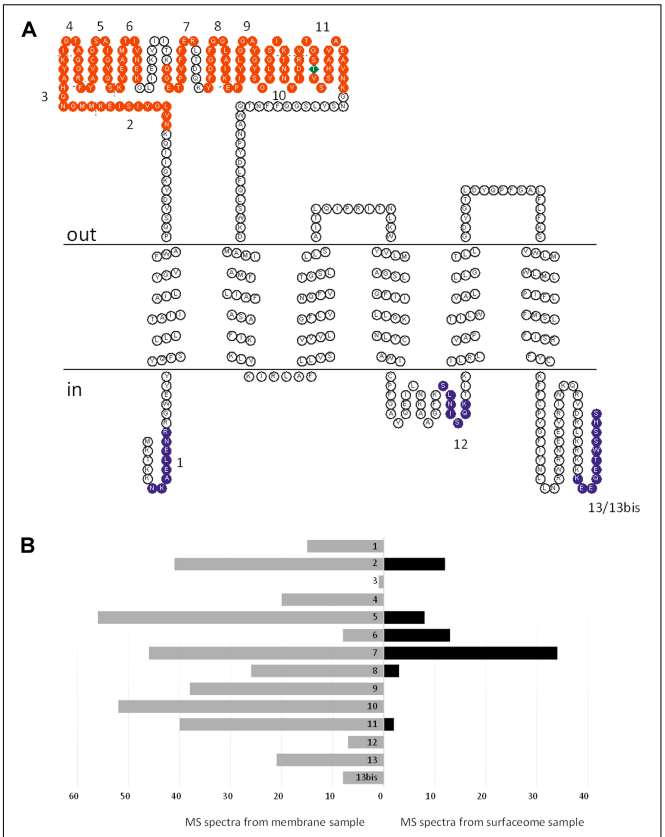

FIGURE 4 | Topology analysis of *D. restrictus* PceC from shaving experiment. **(A)** The predicted topology of PceC is shown. In red are indicated the peptides detected at the surface of *D. restrictus* cells, while in purple the ones exclusively detected in the membrane sample. **(B)** Graphical view of the number of detected peptides in the membrane sample (in gray) and in the surfaceome (in black).

Identification and Production of Flavin-Trafficking Proteins (Ftp) From *D. hafniense* TCE1

Flavin-trafficking proteins [Ftp, previously named ApbE (Deka et al., 2015)] are FAD-binding proteins, from which two classes have been defined. One of them shows FAD hydrolysing activity and is able to deliver FMN to flavoproteins (Deka et al., 2016). Two Ftp encoding genes were identified in the genome of *D. hafniense* TCE1 with locus number DeshaDRAFT_4346 and _4351[2]. Both genes are located in a multi-gene cluster with no clear function. One gene of this cluster is coding for a predicted FMN-binding lipoprotein (DeshaDRAFT_4350), suggesting that the Ftp proteins are primarily involved in the maturation of this protein (Supplementary Figure 4A). Sequence analysis of both Ftp proteins revealed the presence of a clear lipoprotein signal peptide similarly to Ftp of *Treponema pallidum* which was proposed to be anchored in the cytoplasmic membrane facing the periplasmic side of the cell (Deka et al., 2013). Conserved residues suggest that both Ftp of *D. hafniense* belong to the Mg^{2+}-dependent hydrolysing class (Supplementary Figure 4B) and are thus likely to be involved in the maturation of flavoproteins.

Initially, both *ftp* genes of *D. hafniense* TCE1 were cloned for heterologous expression in *E. coli*. In order to avoid protein aggregation, the coding sequence for the predicted lipid anchor of Ftp was omitted, as shown for Ftp1 (Supplementary Figure 5). Both recombinant Ftp (rFtp1, rFtp2) were successfully produced in a soluble form (Supplementary Figure 6). Soluble protein extracts of *E. coli* cells producing rFtp1 was further used to reconstitute rFBD protein.

Reconstitution of rFBD Proteins

The rFBD protein was obtained from purified inclusion bodies, denatured with urea as presented above, and subjected to different reconstitution strategies with the help of rFtp1. Initially, a simple dilution experiment was performed with both rFtp1 and rFtp2 extracts (see detail description of the method in Section "Reconstitution by Dilution" of the Supplementary

[2]https://genome.jgi.doe.gov/

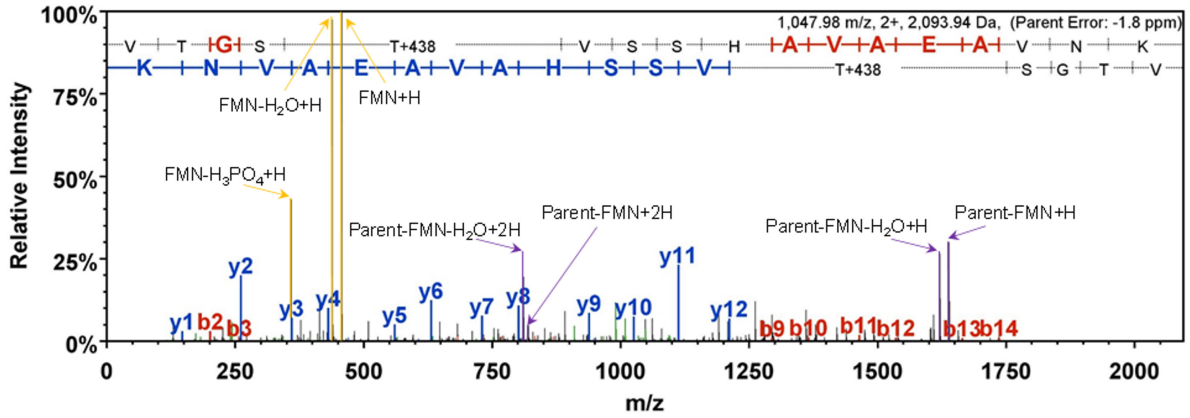

Protein Group	Peptide Sequence	SEQUEST XCorr	X! Tandem	MS-Amanda	Modifications	Observed	Charge	Delta PPM	Sequence Start	Sequence Stop
Dehre_2396	(R)VTGStVSSHAVAEAVNK(G)	3.10	5.68	298.36	FMN (+438)	1047.9763	2	-1.786	164	180

FIGURE 5 | Representative MS/MS spectrum confirming the FMN localization at position T168 of PceC. Diagnostic ions corresponding to the FMN+H and its fragments are highlighted in yellow allowing unambiguous identification of the post-translational modification.

Material). UV illuminated gels showed a fluorescent signal at the expected size of rFBD, however very weak (data not shown). Therefore, two other reconstitution strategies were applied using rFtp1 where care was taken to remove urea more extensively.

Reconstitution by Reverse Urea Gradient on Ni-NTA Column

Urea-denatured rFBD protein (corresponding to 1 g of P1 biomass) was reconstituted on column by gradually removing urea in presence of FAD and rFtp1 cell extract. Samples collected during this experiment were analyzed by SDS-PAGE, Coomassie blue staining and UV illumination (**Figure 6A**). While most of the denatured rFBD protein was bound to the column, the elution pattern after reconstitution suggested that only a relatively small portion of it could be recovered (mostly in sample E1 with 0.22 mg protein). However, the protein in this sample was fully soluble (data not shown) and emitted a strong fluorescent signal, indicative for a successful assembly of the FMN cofactor. Some residual protein remained attached to the column (sample U in **Figure 6A**), which also prevented the recovery of significant amount of soluble and reconstituted rFBD protein.

Reconstitution by Stepwise Dialysis

In order to improve the yield and scale up the reconstitution procedure, a strategy with stepwise dialysis was developed. Inclusion bodies from 5 g of P2 biomass were solubilized in 8 M urea and subjected to successive dialysis with decreasing concentrations of urea. FAD and rFtp1 were also added in the dialysis tube at each step. The level of fluorescence observed along the successive dialysis steps shows that flavin transfer occurs already in presence of 4 M of urea, suggesting a significant robustness of rFtp1. The fluorescent signal further increased with decreasing urea concentrations (**Figure 6B**). While a significant amount of protein remained insoluble, approximately 50 mg of reconstituted soluble rFBD protein could be produced with this strategy.

Characterization of the Reconstituted rFBD Protein

Reconstituted rFBD Protein Displays One Covalently-Bound FMN Cofactor

Mass spectrometry analysis of the mass of rFBD gave further evidence for the presence of covalently-bound FMN. A clearly dominating mass of 19,212.4 Da was detected for rFBD, which corresponds to the theoretical mass of rFBD (18,905.3 Da), from which the initial methionine was cleaved off (18,774.1 Da), and which contains one FMN (456.3 Da) attached to the threonine residue (H_2O was released upon flavinylation, −18 Da) (Supplementary Figure 7). This results in a theoretical mass of 19,212.4 Da, fully matching with the observed mass. It is also worth noting that, although the analysis was not quantitative, no mass corresponding to non-flavinylated rFBD protein was detected, suggesting that the yield of flavinylation was nearly 100% in rFBD present in the soluble fraction.

FMN Is Covalently Bound to the Predicted Threonine in rFBD

As suggested by sequence alignment and prediction (**Figure 3A**), threonine-168 of PceC is likely to be involved in binding FMN covalently. The reconstituted rFBD protein was subjected to top–down mass spectrometry analysis which could localize FMN on the string of four residues (GSTV) of rFBD (Supplementary Figure 8 and Supplementary Tables 3, 4), where the threonine (residue 129 in rFBD) corresponds to threonine-168 of the full-length PceC sequence.

Additional evidence for this was obtained after reconstitution was applied to a valine variant of the conserved threonine (**Figure 7**). In contrast to rFBD wild-type protein, the valine

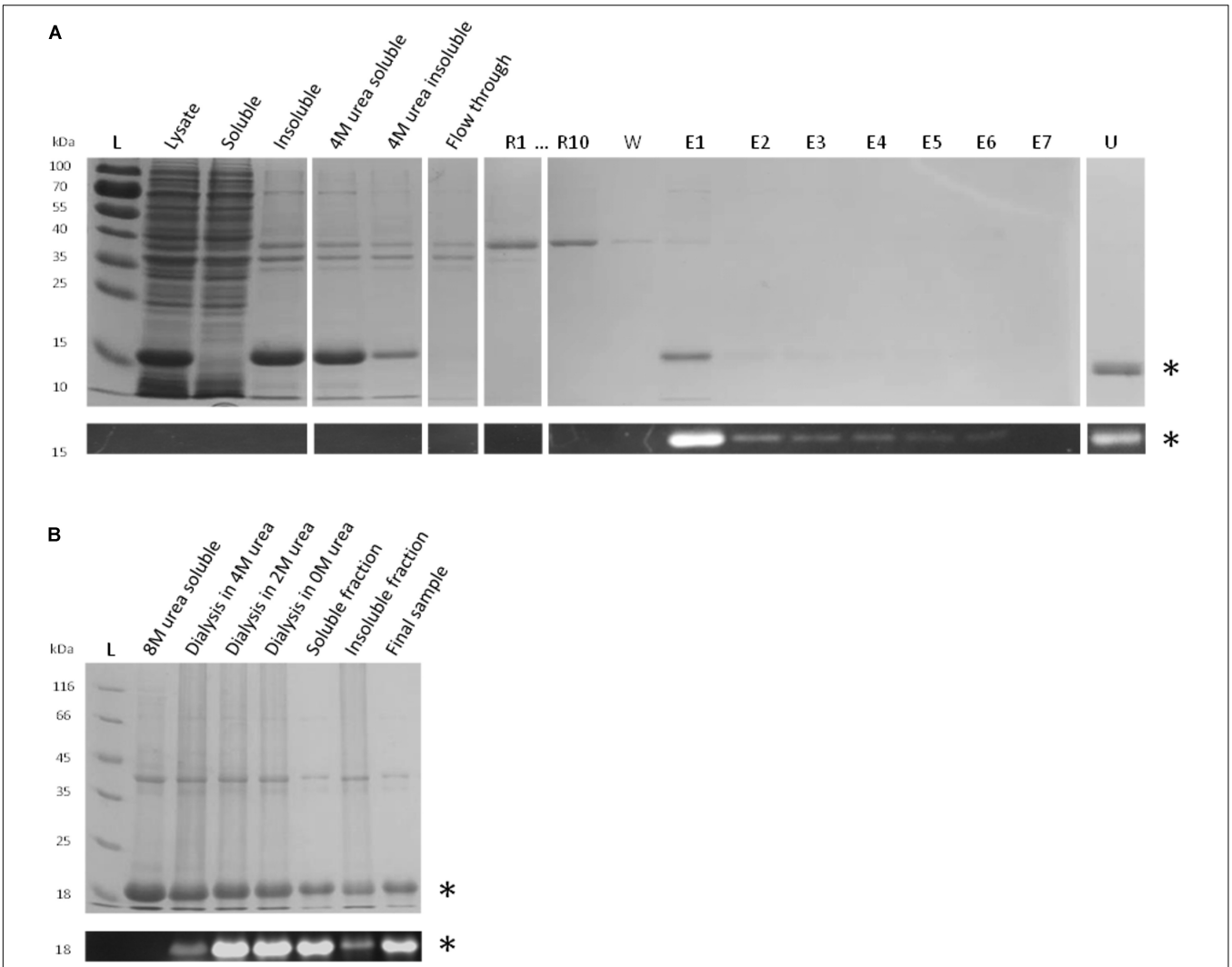

FIGURE 6 | Reconstitution strategies for rFBD. **(A)** Reconstitution of rFBD by reverse urea gradient on Ni-NTA column. For the reconstitution steps, only the first (R1) and the last sample (R10) are shown. Legend: L, protein ladder; R#, 10 successive gradient steps with decreasing urea concentration; W, wash step; E#, successive eluted samples; U, sample eluted with 4 M urea. **(B)** Reconstitution of rFBD by dialyzing out urea in a stepwise manner. For both **(A,B)**, the top panels show Coomassie blue stained gels, while the bottom panels display the same gels under UV illumination. Stars indicate rFBD proteins.

variant could not be loaded with FMN and was only found in the insoluble fraction after reconstitution. This unambiguously confirmed that threonine-168 of PceC (threonine-129 of rFBD) is involved in FMN-binding, and further highlights that FMN insertion is required for refolding rFBD protein into a soluble protein.

DISCUSSION

Among the variety of genes found in *rdh* gene clusters of OHRB (Kruse et al., 2016), the product of only few genes (RdhA, RdhK, and RdhT) have been functionally characterized. PceC, and more generally RdhC proteins are encoded in many *rdh* gene clusters identified in organohalide-respiring Firmicutes. Typically, genomes of *Desulfitobacterium* spp. harbor an *rdhC* homolog in most of *rdh* gene clusters (Kruse et al., 2017), while it is present in 10 out of 24 clusters in *D. restrictus* (Kruse et al., 2013; Rupakula et al., 2013). Our conservative survey for RdhC sequences present in protein databases highlights the presence of *rdhC* in *rdh* gene clusters belonging to other phyla than the Firmicutes, such as the Chloroflexi, the Proteobacteria, and the Bacteriodetes. This strongly suggests that, although RdhC appears to be dispensable for OHR metabolism in many bacteria, it must have emerged early in the evolution of *rdh* gene clusters.

Sequence analysis of RdhC and their corresponding RdhA in *rdh* gene clusters of *D. restrictus* also seems to indicate that the occurrence of specific *rdhA* and *rdhC* genes is not the result of random genetic rearrangements (Supplementary Figure 9). Rather, RdhC proteins have likely co-evolved together with their cognate reductive dehalogenases, suggesting a possible functional

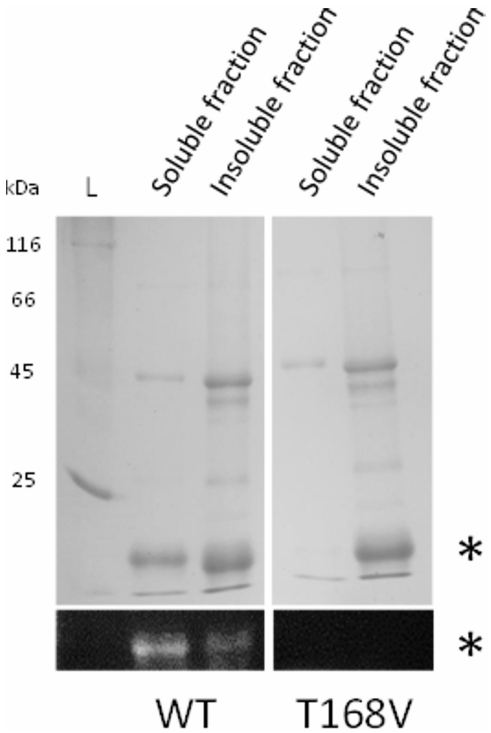

FIGURE 7 | Reconstitution of rFBD wild-type (WT) and threonine-168 variant (T168V). The top panels show Coomassie blue stained gels, while the bottom panels display the same gels under UV illumination. Stars indicate rFBD proteins. L, protein ladder.

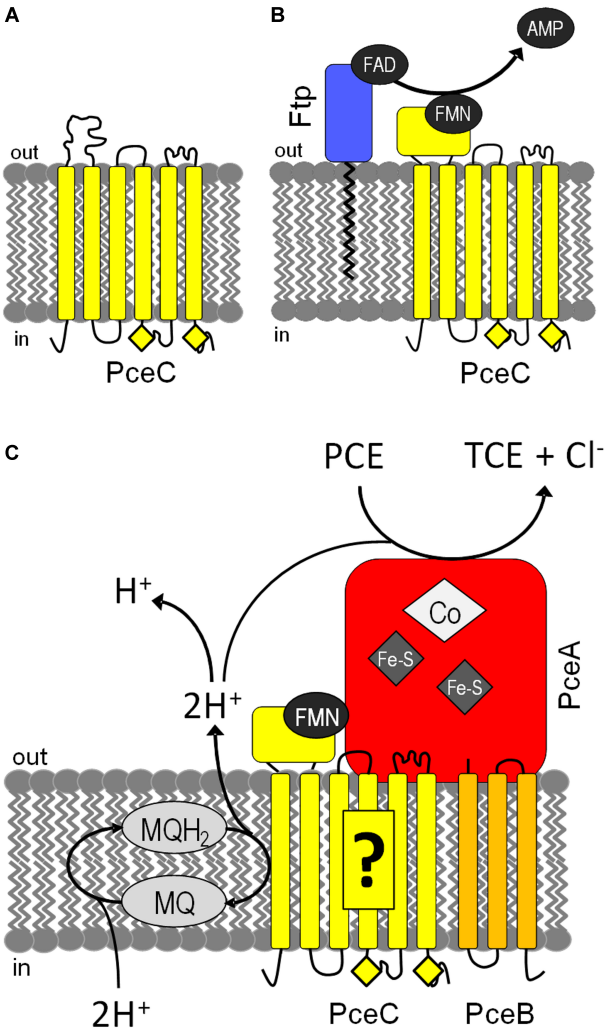

FIGURE 8 | Tentative models for the assembly and function of PceC in *D. hafniense*. **(A)** PceC (in yellow) is likely inserted in the cytoplasmic membrane while the FBD is in an unfolded state. **(B)** On the exocytoplasmic face of the membrane, Ftp (in blue) catalyzes the hydrolysis of FAD to FMN and AMP, and attaches FMN to the threonine-168 of PceC, resulting in the folding of the FBD. **(C)** PceC is hypothesized to build a protein complex with PceA (in red) and PceB (in orange), and to play the role of electron transfer from the menaquinol (MQ) pool to the redox centers of PceA via the FMN cofactor. Yellow diamonds represent the conserved CX_3CP sequence motifs.

relationship. Although the function of RdhC in OHR remains elusive, several sequence features, but also the topology of RdhC in the membrane point toward a possible role in electron transfer, disregarding the initial hypothesis that it is a transcriptional regulator (Smidt et al., 2000). While a transfer of electrons from reduced menaquinones to RdhA enzymes remains disputable in terms of thermodynamics, one could conceive that a flavoprotein like RdhC may render this reaction feasible by a mechanism of electron bifurcation.

In this study, we have unambiguously shown that, in its native state, PceC displays a covalently-bound FMN cofactor and that the FBD of PceC is oriented toward the exocytoplasmic face of the membrane, similarly to the topology of NosR from *Pseudomonas stutzeri* (Wunsch and Zumft, 2005). As for threonine-166 of RnfG from *Methanosarcina acetivorans* (Suharti et al., 2014), site-directed mutagenesis of rFBD clearly confirmed that threonine-168 of PceC is the covalent FMN-binding site. Moreover, reconstitution of the FMN-binding site had a significantly positive effect on folding and solubility of the rFBD protein *in vitro*. The topology of the FBD of PceC, and more generally RdhC, invites to consider the possibility that RdhC proteins may play a role in electron transfer toward the reductive dehalogenase. This hypothesis is in line with the abolition of the nitrous oxide reductase activity of NosZ in presence of a NosR variant, for which the FBD was deleted (Wunsch and Zumft, 2005). Moreover, the midpoint redox potential of flavoproteins ranges from +153 mV to as low as −495 mV (Fagan and Palfey, 2010), a value that is highly variable in comparison to free FMN (−205 mV, Draper and Ingraham, 1968). The redox activity of rFBD and full-length PceC needs to be characterized and will be the focus of further investigation.

In addition to the N-terminal FBD, RdhC sequences share a common membrane module (four membrane segments and two CX_3CP motifs) with NapH and NosR. The striking difference between RdhC and these proteins is the lack in RdhC of the two 4Fe–4S binding motifs in the C-terminal part. Nevertheless, NapH of *Wolinella succinogenes* was shown to participate with NapF and NapG in electron transfer to the periplasmic nitrate

reductase. The membrane segments of NapH were proposed to act as the quinol-oxidizing domain by receiving electrons from the quinol pool and donating them further to redox centers of NapG (Kern and Simon, 2009a). A similar role is conceivable for the membrane domain of RdhC proteins. The mutation of the CX_3CP motifs in NapH has further demonstrated that both motifs had a severe effect on the integrity of NapH as its partner protein NapG was not associated with the membrane (Kern and Simon, 2008). Moreover, the first cysteine motif of NapH is required for the interaction with NapF and for electron transfer during nitrate respiration (Kern and Simon, 2009b). Similarly, variants of the first cysteine motifs in NosR from *P. stutzeri* completely abolished the activity of NosZ (Wunsch and Zumft, 2005). Whether the CX_3CP motifs of RdhC build disulphide bridges, like in thioredoxins, or a 2Fe–2S center is not known. However, the former scenario seems to be more likely, since not more than eight atoms of Fe have been detected per molecule of NosR, corresponding to the two 4Fe–4S centers (Wunsch and Zumft, 2005). The high degree of sequence conservation of the CX_3CP motifs in RdhC proteins and the analogy to NapH and NosR suggest that these motifs are likely determinant for the function of RdhC and will require further investigation.

In vitro reconstitution of rFBD protein was made possible with the use of recombinant Ftp1. Our results with Ftp proteins of *D. hafniense* add up to the functional reassignment of ApbE proteins from the role in thiamine synthesis (Beck and Downs, 1998) to a flavin-binding protein (Boyd et al., 2011) and recently to flavin-trafficking proteins (Deka et al., 2015). In contrast to *D. hafniense* TCE1 where both *ftp* genes are encoded in an operon with unknown function, the *ftp* (*apbE*) gene in the genome of *D. restrictus* is located within the operon coding for the Twin-arginine translocation system in a region of the genome harboring 10 *rdh* gene clusters (Rupakula et al., 2013). This suggests a dedicated role of Ftp toward the assembly of RdhC proteins in *D. restrictus*. This is supported by the results of the identification of possible protein candidates with covalently-bound FMN in the theoretical proteomes of *D. hafniense* TCE1 and *D. restrictus* PER-K23. The FMN-binding motif $[DN]X_2[ST]G[AS]TX[ST]$, as defined previously (Deka et al., 2015), was identified in 13 and 11 proteins in *D. hafniense* and *D. restrictus*, respectively. While all proteins but one are RdhC homologs in the latter, the functional diversity of FMN-binding proteins is much higher in *D. hafniense* (data not shown).

CONCLUSION

A tentative model for the assembly and function of PceC in *D. hafniense* is presented (**Figure 8**). It is speculated that PceC is targeted to the cytoplasmic membrane in a partially unfolded state via either the signal recognition particle (SRP) or the secretion (Sec) pathway (Luirink et al., 2012) before the FMN cofactor is inserted. Then, the lipid-anchored Ftp catalyzes the hydrolysis of FAD and transfers FMN into the FBD of PceC (**Figure 8A**). The membrane-bound redox PceC protein is proposed to build a complex together with the reductive dehalogenase PceA and with PceB, the predicted membrane anchor of PceA. The membrane segments of PceC would receive electrons from the menaquinol pool and reduce the FMN cofactor, which in turn transfers the electrons to PceA (**Figure 8B**). The mechanism of electron transfer through the redox centers and the implication of the conserved cysteine motifs in the electron transfer remain unknown. These questions need to be addressed in order to challenge the hypothesis of the involvement of PceC in the thermodynamically unfavorable electron transfer from reduced menaquinones to the redox centers of PceA.

AUTHOR CONTRIBUTIONS

GB and RH: conducted the experiments and participated in writing the manuscript. MW and AR: conducted the experiments. JM: conceived and led the project, conducted the experiments, and wrote the manuscript.

FUNDING

The Swiss National Science Foundation (SNSF) is thanked for the financial support in frame of the SNF (Project Nos. 31003A_138114 and 31003A_156950).

ACKNOWLEDGMENTS

Laure Menin (Mass Spectrometry Facility, ISIC, EPFL) is thanked for the mass spectrometry analysis of rFBD proteins. Christof Holliger (LBE, EPFL) is also thanked for the fruitful discussions and for the laboratory infrastructure.

SUPPLEMENTARY MATERIAL

The Supplementary Material for this article can be found online at: https://www.frontiersin.org/articles/10.3389/fmicb.2018.00755/full#supplementary-material

REFERENCES

Adrian, L., and Löffler, F. (2016). *Organohalide-Respiring Bacteria*. Berlin: Springer-Verlag.

Backiel, J., Juarez, O., Zagorevski, D. V., Wang, Z., Nilges, M. J., and Barquera, B. (2008). Covalent binding of flavins to RnfG and RnfD in the Rnf complex from *Vibrio cholerae*. *Biochemistry* 47, 11273–11284. doi: 10.1021/bi800920j

Beck, B. J., and Downs, D. M. (1998). The *apbE* gene encodes a lipoprotein involved in thiamine synthesis in *Salmonella typhimurium*. *J. Bacteriol.* 180, 885–891.

Bertsova, Y. V., Fadeeva, M. S., Kostyrko, V. A., Serebryakova, M. V., Baykov, A. A., and Bogachev, A. V. (2013). Alternative pyrimidine biosynthesis protein ApbE is a flavin transferase catalyzing covalent attachment of FMN to a threonine residue in bacterial flavoproteins. *J. Biol. Chem.* 288, 14276–14286. doi: 10.1074/jbc.M113.455402

Borrero-de Acuna, J. M., Timmis, K. N., Jahn, M., and Jahn, D. (2017). Protein complex formation during denitrification by *Pseudomonas aeruginosa*. *Microb. Biotechnol.* 10, 1523–1534. doi: 10.1111/1751-7915.12851

Borshchevskiy, V., Round, E., Bertsova, Y., Polovinkin, V., Gushchin, I., Ishchenko, A., et al. (2015). Structural and functional investigation of flavin binding center of the NqrC subunit of sodium-translocating NADH:quinone oxidoreductase from *Vibrio harveyi*. *PLoS One* 10:e0118548. doi: 10.1371/journal.pone.0118548

Boyd, J. M., Endrizzi, J. A., Hamilton, T. L., Christopherson, M. R., Mulder, D. W., Downs, D. M., et al. (2011). FAD binding by ApbE protein from *Salmonella enterica*: a new class of FAD-binding proteins. *J. Bacteriol.* 193, 887–895. doi: 10.1128/jb.00730-10

Buckel, W., and Thauer, R. K. (2013). Energy conservation via electron bifurcating ferredoxin reduction and proton/Na+ translocating ferredoxin oxidation. *Biochim. Biophys. Acta* 1827, 94–113. doi: 10.1016/j.bbabio.2012.07.002

Casutt, M. S., Schlosser, A., Buckel, W., and Steuber, J. (2012). The single NqrB and NqrC subunits in the Na+-translocating NADH: quinone oxidoreductase (Na+-NQR) from *Vibrio cholerae* each carry one covalently attached FMN. *Biochim. Biophys. Acta* 1817, 1817–1822. doi: 10.1016/j.bbabio.2012.02.012

Comensoli, L., Maillard, J., Albini, M., Sandoz, F., Junier, P., and Joseph, E. (2017). Use of bacteria to stabilize archaeological iron. *Appl. Environ. Microbiol.* 83:e03478-16. doi: 10.1128/aem.03478-16

Crooks, G. E., Hon, G., Chandonia, J. M., and Brenner, S. E. (2004). WebLogo: a sequence logo generator. *Genome Res.* 14, 1188–1190. doi: 10.1101/gr.849004

Cuypers, H., Viebrock-Sambale, A., and Zumft, W. G. (1992). NosR, a membrane-bound regulatory component necessary for expression of nitrous oxide reductase in denitrifying *Pseudomonas stutzeri*. *J. Bacteriol.* 174, 5332–5339. doi: 10.1128/jb.174.16.5332-5339.1992

Dalla Vecchia, E., Shao, P. P., Suvorova, E., Chiappe, D., Hamelin, R., and Bernier-Latmani, R. (2014). Characterization of the surfaceome of the metal-reducing bacterium *Desulfotomaculum reducens*. *Front. Microbiol.* 5:432. doi: 10.3389/fmicb.2014.00432

Deka, R. K., Brautigam, C. A., Liu, W. Z., Tomchick, D. R., and Norgard, M. V. (2013). The TP0796 lipoprotein of *Treponema pallidum* is a bimetal-dependent FAD pyrophosphatase with a potential role in flavin homeostasis. *J. Biol. Chem.* 288, 11106–11121. doi: 10.1074/jbc.M113.449975

Deka, R. K., Brautigam, C. A., Liu, W. Z., Tomchick, D. R., and Norgard, M. V. (2015). Evidence for posttranslational protein flavinylation in the syphilis spirochete *Treponema pallidum*: structural and biochemical insights from the catalytic core of a periplasmic flavin-trafficking protein. *mBio* 6:e00519-15. doi: 10.1128/mBio.00519-15

Deka, R. K., Brautigam, C. A., Liu, W. Z., Tomchick, D. R., and Norgard, M. V. (2016). Molecular insights into the enzymatic diversity of flavin-trafficking protein (Ftp; formerly ApbE) in flavoprotein biogenesis in the bacterial periplasm. *MicrobiologyOpen* 5, 21–38. doi: 10.1002/mbo3.306

Dobson, L., Remenyi, I., and Tusnady, G. E. (2015). CCTOP: a consensus constrained TOPology prediction web server. *Nucleic Acids Res.* 43, W408–W412. doi: 10.1093/nar/gkv451

Dorfer, V., Pichler, P., Stranzl, T., Stadlmann, J., Taus, T., Winkler, S., et al. (2014). MS Amanda, a universal identification algorithm optimized for high accuracy tandem mass spectra. *J. Proteome Res.* 13, 3679–3684. doi: 10.1021/pr500202e

Draper, R. D., and Ingraham, L. L. (1968). A potentiometric study of the flavin semiquinone equilibrium. *Arch. Biochem. Biophys.* 125, 802–808. doi: 10.1016/0003-9861(68)90517-1

Duret, A., Holliger, C., and Maillard, J. (2012). The physiological opportunism of *Desulfitobacterium hafniense* strain TCE1 towards organohalide respiration with tetrachloroethene. *Appl. Environ. Microbiol.* 78, 6121–6127. doi: 10.1128/aem.01221-12

Fagan, R. L., and Palfey, B. A. (2010). "Flavin-dependent enzymes," in *Comprehensive Natural Products II: Chemistry and Biology*, eds M. Lewis and L. Hung-Wen (New York, NY: Elsevier Ltd), 37–113.

Fincker, M., and Spormann, A. M. (2017). Biochemistry of catabolic reductive dehalogenation. *Annu. Rev. Biochem.* 86, 357–386. doi: 10.1146/annurev-biochem-061516-044829

Futagami, T., Tsuboi, Y., Suyama, A., Goto, M., and Furukawa, K. (2006). Emergence of two types of nondechlorinating variants in the tetrachloroethene-halorespiring *Desulfitobacterium* sp. strain Y51. *Appl. Microbiol. Biotechnol.* 70, 720–728. doi: 10.1007/s00253-005-0112-9

Gerritse, J., Drzyzga, O., Kloetstra, G., Keijmel, M., Wiersum, L. P., Hutson, R., et al. (1999). Influence of different electron donors and acceptors on dehalorespiration of tetrachloroethene by *Desulfitobacterium frappieri* TCE1. *Appl. Environ. Microbiol.* 65, 5212–5221.

Goris, T., Hornung, B., Kruse, T., Reinhold, A., Westermann, M., Schaap, P. J., et al. (2015a). Draft genome sequence and characterization of *Desulfitobacterium hafniense* PCE-S. *Stand. Genomic Sci.* 10:15. doi: 10.1186/1944-3277-10-15

Goris, T., Schiffmann, C. L., Gadkari, J., Schubert, T., Seifert, J., Jehmlich, N., et al. (2015b). Proteomics of the organohalide-respiring Epsilonproteobacterium *Sulfurospirillum multivorans* adapted to tetrachloroethene and other energy substrates. *Sci. Rep.* 5:13794. doi: 10.1038/srep13794

Guyon, L., Tabarin, T., Thuillier, B., Antoine, R., Broyer, M., Boutou, V., et al. (2008). Femtosecond pump-probe experiments on trapped flavin: optical control of dissociation. *J. Chem. Phys.* 128:075103. doi: 10.1063/1.2828558

Holliger, C., Hahn, D., Harmsen, H., Ludwig, W., Schumacher, W., Tindall, B., et al. (1998). *Dehalobacter restrictus* gen. nov. and sp. nov., a strictly anaerobic bacterium that reductively dechlorinates tetra- and trichloroethene in an anaerobic respiration. *Arch. Microbiol.* 169, 313–321. doi: 10.1007/s002030050577

Jugder, B. E., Ertan, H., Bohl, S., Lee, M., Marquis, C. P., and Manefield, M. (2016a). Organohalide respiring bacteria and reductive dehalogenases: key tools in organohalide bioremediation. *Front. Microbiol.* 7:249. doi: 10.3389/fmicb.2016.00249

Jugder, B. E., Ertan, H., Wong, Y. K., Braidy, N., Manefield, M., Marquis, C. P., et al. (2016b). Genomic, transcriptomic and proteomic analyses of *Dehalobacter* UNSWDHB in response to chloroform. *Environ. Microbiol. Rep.* doi: 10.1111/1758-2229.12444 [Epub ahead of print],

Kern, M., and Simon, J. (2008). Characterization of the NapGH quinol dehydrogenase complex involved in *Wolinella* succinogenes nitrate respiration. *Mol. Microbiol.* 69, 1137–1152. doi: 10.1111/j.1365-2958.2008.06361.x

Kern, M., and Simon, J. (2009a). Electron transport chains and bioenergetics of respiratory nitrogen metabolism in *Wolinella* succinogenes and other Epsilonproteobacteria. *Biochim. Biophys. Acta* 1787, 646–656. doi: 10.1016/j.bbabio.2008.12.010

Kern, M., and Simon, J. (2009b). Periplasmic nitrate reduction in *Wolinella* succinogenes: cytoplasmic NapF facilitates NapA maturation and requires the menaquinol dehydrogenase NapH for membrane attachment. *Microbiology* 155(Pt 8), 2784–2794. doi: 10.1099/mic.0.029983-0

Kruse, T., Goris, T., Maillard, J., Woyke, T., Lechner, U., de Vos, W., et al. (2017). Comparative genomics of the genus *Desulfitobacterium*. *FEMS Microbiol. Ecol.* 93:fix135. doi: 10.1093/femsec/fix135

Kruse, T., Maillard, J., Goodwin, L., Woyke, T., Teshima, H., Bruce, D., et al. (2013). Complete genome sequence of *Dehalobacter restrictus* PER-K23(T.). *Stand. Genomic Sci.* 8, 375–388. doi: 10.4056/sigs.3787426

Kruse, T., Smidt, H., and Lechner, U. (2016). "Comparative genomics and transcriptomics of organohalide-respiring bacteria and regulation of *rdh* gene transcription," in *Organohalide-Respiring Bacteria*, eds L. Adrian and F. Löffler (Berlin: Springer-Verlag), 345–376.

Kruse, T., van de Pas, B. A., Atteia, A., Krab, K., Hagen, W. R., Goodwin, L., et al. (2015). Genomic, proteomic, and biochemical analysis of the organohalide respiratory pathway in *Desulfitobacterium dehalogenans*. *J. Bacteriol.* 197, 893–904. doi: 10.1128/JB.02370-14

Kublik, A., Deobald, D., Hartwig, S., Schiffmann, C. L., Andrades, A., von Bergen, M., et al. (2016). Identification of a multi-protein reductive dehalogenase complex in *Dehalococcoides mccartyi* strain CBDB1 suggests a protein-dependent respiratory electron transport chain obviating quinone involvement. *Environ. Microbiol.* 18, 3044–3056. doi: 10.1111/1462-2920.13200

Larkin, M. A., Blackshields, G., Brown, N. P., Chenna, R., McGettigan, P. A., McWilliam, H., et al. (2007). Clustal W and clustal X version 2.0. *Bioinformatics* 23, 2947–2948. doi: 10.1093/bioinformatics/btm404

Letunic, I., and Bork, P. (2016). Interactive tree of life (iTOL) v3: an online tool for the display and annotation of phylogenetic and other trees. *Nucleic Acids Res.* 44, W242–W245. doi: 10.1093/nar/gkw290

Luirink, J., Yu, Z., Wagner, S., and de Gier, J. W. (2012). Biogenesis of inner membrane proteins in *Escherichia coli*. *Biochim. Biophys. Acta* 1817, 965–976. doi: 10.1016/j.bbabio.2011.12.006

Maillard, J., and Holliger, C. (2016). "The genus *Dehalobacter*," in *Organohalide-Respiring Bacteria*, eds L. Adrian and F. Löffler (Berlin: Springer-Verlag), 153–171.

Maillard, J., Regeard, C., and Holliger, C. (2005). Isolation and characterization of Tn-Dha1, a transposon containing the tetrachloroethene reductive dehalogenase of *Desulfitobacterium hafniense* strain TCE1. *Environ. Microbiol.* 7, 107–117. doi: 10.1111/j.1462-2920.2004.00671.x

Miller, E., Wohlfarth, G., and Diekert, G. (1996). Studies on tetrachloroethene respiration in *Dehalospirillum multivorans*. *Arch. Microbiol.* 166, 379–387. doi: 10.1007/BF01682983

Müller, J. A., Rosner, B. M., Von Abendroth, G., Meshulam-Simon, G., McCarty, P. L., and Spormann, A. M. (2004). Molecular identification of the catabolic vinyl chloride reductase from *Dehalococcoides* sp. strain VS and its environmental distribution. *Appl. Environ. Microbiol.* 70, 4880–4888. doi: 10.1128/aem.70.8.4880-4888.2004

Nakayama, Y., Yasui, M., Sugahara, K., Hayashi, M., and Unemoto, T. (2000). Covalently bound flavin in the NqrB and NqrC subunits of Na+-translocating NADH-quinone reductase from *Vibrio alginolyticus*. *FEBS Lett.* 474, 165–168. doi: 10.1016/S0014-5793(00)01595-7

Prat, L., Maillard, J., Grimaud, R., and Holliger, C. (2011). Physiological adaptation of *Desulfitobacterium hafniense* strain TCE1 to tetrachloroethene respiration. *Appl. Environ. Microbiol.* 77, 3853–3859. doi: 10.1128/aem.02471-10

Rappsilber, J., Mann, M., and Ishihama, Y. (2007). Protocol for micro-purification, enrichment, pre-fractionation and storage of peptides for proteomics using StageTips. *Nat. Protoc.* 2, 1896–1906. doi: 10.1038/nprot.2007.261

Rupakula, A., Kruse, T., Boeren, S., Holliger, C., Smidt, H., and Maillard, J. (2013). The restricted metabolism of the obligate organohalide respiring bacterium *Dehalobacter restrictus*: lessons from tiered functional genomics. *Philos. Trans. R. Soc. Lond. B Biol. Sci.* 368, 20120325. doi: 10.1098/rstb.2012.0325

Sambrook, J., Fritsch, E. F., and Maniatis, T. (1989). *Molecular Cloning: A Laboratory Manual*. New York, NY: Cold Spring Harbor Laboratory.

Schumacher, W., and Holliger, C. (1996). The proton/electron ration of the menaquinone-dependent electron transport from dihydrogen to tetrachloroethene in "*Dehalobacter restrictus*". *J. Bacteriol.* 178, 2328–2333. doi: 10.1128/jb.178.8.2328-2333.1996

Schumacher, W., Holliger, C., Zehnder, A. J., and Hagen, W. R. (1997). Redox chemistry of cobalamin and iron-sulfur cofactors in the tetrachloroethene reductase of *Dehalobacter restrictus*. *FEBS Lett.* 409, 421–425. doi: 10.1016/S0014-5793(97)00520-6

Smidt, H., van Leest, M., van der Oost, J., and de Vos, W. M. (2000). Transcriptional regulation of the *cpr* gene cluster in ortho-chlorophenol-respiring *Desulfitobacterium dehalogenans*. *J. Bacteriol.* 182, 5683–5691.

Studier, F. W. (2014). Stable expression clones and auto-induction for protein production in *E. coli*. *Methods Mol. Biol.* 1091, 17–32. doi: 10.1007/978-1-62703-691-7_2

Suharti, S., Wang, M., de Vries, S., and Ferry, J. G. (2014). Characterization of the RnfB and RnfG subunits of the Rnf complex from the archaeon *Methanosarcina acetivorans*. *PLoS One* 9:e97966. doi: 10.1371/journal.pone.0097966

Thauer, R. K., Jungermann, K., and Decker, K. (1977). Energy conservation in chemotrophic anaerobic bacteria. *Bacteriol. Rev.* 41, 100–180.

van de Pas, B. A., Smidt, H., Hagen, W. R., van der Oost, J., Schraa, G., Stams, A. J., et al. (1999). Purification and molecular characterization of ortho-chlorophenol reductive dehalogenase, a key enzyme of halorespiration in *Desulfitobacterium dehalogenans*. *J. Biol. Chem.* 274, 20287–20292. doi: 10.1074/jbc.274.29.20287

Vohl, G., Nedielkov, R., Claussen, B., Casutt, M. S., Vorburger, T., Diederichs, K., et al. (2014). Crystallization and preliminary analysis of the NqrA and NqrC subunits of the Na+-translocating NADH:ubiquinone oxidoreductase from *Vibrio cholerae*. *Acta Crystallogr. F Struct. Biol. Commun.* 70(Pt 7), 987–992. doi: 10.1107/s2053230x14009881

Wong, Y. K., Holland, S. I., Ertan, H., Manefield, M., and Lee, M. (2016). Isolation and characterization of *Dehalobacter* sp. strain UNSWDHB capable of chloroform and chlorinated ethane respiration. *Environ. Microbiol.* 18, 3092–3105. doi: 10.1111/1462-2920.13287

Wunsch, P., and Zumft, W. G. (2005). Functional domains of NosR, a novel transmembrane iron-sulfur flavoprotein necessary for nitrous oxide respiration. *J. Bacteriol.* 187, 1992–2001. doi: 10.1128/jb.187.6.1992-2001.2005

Zhang, L., Trncik, C., Andrade, S. L., and Einsle, O. (2017). The flavinyl transferase ApbE of *Pseudomonas stutzeri* matures the NosR protein required for nitrous oxide reduction. *Biochim. Biophys. Acta* 1858, 95–102. doi: 10.1016/j.bbabio.2016.11.008

Zumft, W. G. (2005). Biogenesis of the bacterial respiratory CuA, Cu-S enzyme nitrous oxide reductase. *J. Mol. Microbiol. Biotechnol.* 10, 154–166. doi: 10.1159/000091562

Conflict of Interest Statement: The authors declare that the research was conducted in the absence of any commercial or financial relationships that could be construed as a potential conflict of interest.

frontiers in Microbiology

ORIGINAL RESEARCH
published: 22 August 2018
doi: 10.3389/fmicb.2018.01927

Syntrophic Partners Enhance Growth and Respiratory Dehalogenation of Hexachlorobenzene by *Dehalococcoides mccartyi* Strain CBDB1

Anh T. T. Chau[1,2], *Matthew Lee*[2], *Lorenz Adrian*[3] *and Michael J. Manefield*[2,4]*

[1] College of Agriculture and Applied Biology, Cantho University, Can Tho, Vietnam, [2] School of Civil and Environmental Engineering, University of New South Wales, Sydney, NSW, Australia, [3] Department Isotope Biogeochemistry, Helmholtz Centre for Environmental Research – UFZ, Leipzig, Germany, [4] School of Chemical Engineering, University of New South Wales, Sydney, NSW, Australia

This study investigated syntrophic interactions between chlorinated benzene respiring *Dehalococcoides mccartyi* strain CBDB1 and fermenting partners (*Desulfovibrio vulgaris*, *Syntrophobacter fumaroxidans,* and *Geobacter lovleyi*) during hexachlorobenzene respiration. Dechlorination rates in syntrophic co-cultures were enhanced 2-3 fold compared to H_2 fed CBDB1 pure cultures (0.23 ± 0.04 μmol Cl^- day^{-1}). Syntrophic partners were also able to supply cobalamins to CBDB1, albeit with 3–10 fold lower resultant dechlorination activity compared to cultures receiving exogenous cyanocobalamin. Strain CBDB1 pure cultures accumulated ∼1 μmol of carbon monoxide per 87.5 μmol Cl^- released during hexachlorobenzene respiration resulting in decreases in dechlorination activity. The syntrophic partners investigated were shown to consume carbon monoxide generated by CBDB1, thus relieving carbon monoxide autotoxicity. Accumulation of lesser chlorinated chlorobenzene congeners (1,3- and 1,4-dichlorobenzene and 1,3,5-trichlorobenzene) also inhibited dechlorination activity and their removal from the headspace through adsorption to granular activated carbon was shown to restore activity. Proteomic analysis revealed co-culturing strain CBDB1 with *Geobacter lovleyi* upregulated CBDB1 genes associated with reductive dehalogenases, hydrogenases, formate dehydrogenase, and ribosomal proteins. These data provide insight into CBDB1 ecology and inform strategies for application of CBDB1 in ex situ hexachlorobenzene destruction technologies.

Keywords: syntrophy, hexachlorobenzene, organohalide respiration, *Dehalococcoides mccartyi* strain CBDB1, carbon monoxide

OPEN ACCESS

Edited by:
Elisabet Aranda, Universidad de Granada, Spain

Reviewed by:
Elizabeth Anne Edwards, University of Toronto, Canada
Siavash Atashgahi, Wageningen University & Research, Netherlands

***Correspondence:**
Michael J. Manefield
manefield@unsw.edu.au

Specialty section:
This article was submitted to Microbiotechnology, Ecotoxicology and Bioremediation, a section of the journal Frontiers in Microbiology

Received: *06 April 2018*
Accepted: *30 July 2018*
Published: *22 August 2018*

Citation:
Chau ATT, Lee M, Adrian L and Manefield MJ (2018) Syntrophic Partners Enhance Growth and Respiratory Dehalogenation of Hexachlorobenzene by Dehalococcoides mccartyi Strain CBDB1. Front. Microbiol. 9:1927. doi: 10.3389/fmicb.2018.01927

INTRODUCTION

Chlorinated benzenes including hexachlorobenzene (HCB) are toxic and persistent compounds that have been studied extensively in the context of microbiological degradation (Field and Sierra-Alvarez, 2008). Whilst lesser chlorinated benzenes are susceptible to aerobic biodegradation in conventional activated sludge treatment processes (van Agteren et al., 1998) microbes can

only degrade hexachlorobenzene, pentachlorobenzene, 1,2,3,4-tetrachlorobenzene, and 1,3,5-trichlorobenzene through anaerobic or reductive reactions (Adrian and Görisch, 2002). Such reductive reactions have been linked to bacterial growth (Adrian and Görisch, 2002) and therefore have potential as a biotechnology for commercial chlorinated benzene disposal. The world's largest stockpile of HCB (8,000 tons) is maintained in Sydney, Australia.

To date, only two genera, *Dehalococoides* and *Dehalobacter* are known to contain species that use HCB as an electron acceptor in a respiratory process. *Dehalococcoides mccartyi* strains are obligate hydrogenotrophs and are restricted to organohalides as electron acceptors. *D. mccartyi* strain CBDB1 grows in mineral medium with H_2 as the electron donor, acetate as an organic carbon source, and chlorobenzenes as electron acceptors, in conjunction with cyanocobalamin as an essential cofactor (Adrian et al., 2000).

Syntrophic interactions between fermentative bacteria and organohalide respiring bacteria (ORB) are of interest because they underpin dechlorination reactions in organochlorine contaminated environments where H_2 is generated via fermentation of organic matter. The term syntrophy has been used to describe microbial cross-feeding as a cooperation where both partners are involved in metabolic activity and cannot be replaced by adding a co-substrate or any type of nutrient (Schink, 1997). The benefits that syntrophic growth in co-culture can offer over a pure culture include the generation of a metabolic resource by one microbe serving as a resource for another and enhancing the growth/metabolism of one microbe by preventing accumulation of inhibitory compounds consumed by another (McInerney et al., 2008; Morris et al., 2013; Worm et al., 2014). Specifically, in the context of this study, the principal mode of syntrophy involves H_2 produced by fermentation of reduced organic substrates serving as an electron donor for hydrogenotrophic ORB that in turn maintain low H_2 partial pressures enabling fermentation to proceed (Becker et al., 2005).

Despite the importance of syntrophy in ecology and engineering settings, data on syntrophic interactions involving ORB remain limited. Breakthrough studies in this area focused on syntrophic growth of a dechlorinating organism (DCB-1), a benzoate degrader (BZ-1), and a lithotrophic methanogen (*Methanospirillum* strain PM-1) in dechlorination of 3-chlorobenzoate (Dolfing and Tiedje, 1986) and methanogenic incubation with *Syntrophus* species degrading 3-chlorobenzoate and 2-chlorophenol (Becker et al., 2005). Research more closely related to the current study focused on syntrophic growth of chlorinated ethene respiring *D. mccartyi* strain 195 with fermenters *Desulfovibrio desulfuricans* and/or *Acetobacterium woodii* (He et al., 2007), interspecies corrinoid transfer between *Geobacter lovleyi* and *D. mccartyi* strains BAV1 and FL2 (Yan et al., 2012, 2013) and interspecies cobamide transfer from the methanogen *Methanobacterium congolense* to *D. mccartyi* (Men et al., 2012).

Carbon monoxide (CO) was recently discovered to inhibit chlorinated ethene dechlorination of *D. mccartyi* strain 195 but the presence of a syntrophic partner was shown to mitigate this toxicity and enhance the growth as well as dechlorination activity (Zhuang et al., 2014; Mao et al., 2015). Additionally, organochlorine dechlorination products can inhibit dechlorination activity (Wei et al., 2016). To date, the inhibitory impacts of lesser chlorinated ethenes alone have been investigated for such inhibition (Yu and Semprini, 2004; Yu et al., 2005; Popat and Deshusses, 2011; Wang et al., 2014; Jiang et al., 2015).

In this study syntrophic interactions of HCB respiring *D. mccartyi* strain CBDB1 and fermentative partners during reductive dechlorination of HCB were investigated, with a view to utilizing syntrophic co-cultures or enrichment cultures in *ex situ* remediation technologies for HCB destruction where full-scale deployment of gaseous hydrogen is considered a safety hazard. Three syntrophic partners were examined, namely *Desulfovibrio vulgaris*, *Geobacter lovleyi,* and *Syntrophobacter fumaroxidans* provided with lactate, acetate and propionate respectively as carbon and energy sources. *D. mccartyi* cannot derive energy from these organic substrates and none of the syntrophic partners can utilize HCB creating syntrophic dependencies.

This is the first study to reveal syntrophic interactions in HCB respiration between strain CBDB1 and fermenters. CO auto-toxicity to strain CBDB1 is described along with the impact of CO consumption by syntrophic partners. Daughter product inhibition is also described along with a demonstration of the impact of removing lesser chlorinated chlorobenzenes from culture headspace. The data generated broadens our understanding of syntrophic metabolism in organohalide respiration by *D. mccartyi* and provides information relevant to bioreactor applications for HCB destruction.

MATERIALS AND METHODS

Bacterial Cultures and Growth Conditions

D. mccartyi strain CBDB1 was grown in a basal medium with 5 mM acetate as described previously (Adrian et al., 1998). Briefly, mineral salts medium was amended with a vitamin solution, SL-9 minerals and Trace B mineral solution (Adrian et al., 1998). Final concentrations of 100 mM $NaHCO_3$ solution was used to buffer the media to pH 6.8–7.0. Aliquots (80 mL) were dispensed into 160 mL serum flasks and flushed with N_2 gas, sealed with Teflon septa and sterilized at 121°C for 20 min. After cooling Ti (III) citrate solution was amended to 1 mM and 0.2 bar of N_2:CO_2 (4:1, vol/vol) and 0.3 bar of H_2 were added to the headspace. Hexachlorobenzene (20 mg, Sigma-Aldrich) was added as electron acceptor and H_2 as electron donor with nominal concentration of 7.5 mM as described previously (Jayachandran et al., 2003).

Desulfovibro vulgaris (DSM 2119) and *Syntrophobacter fumaroxidans* (DSM 10017) were obtained from the German Collection of Microorganisms (DSMZ) and grown according to DSMZ recommendations. Briefly, *D. vulgaris* was grown in the medium described above with 10 mM lactate as carbon and energy source and 10 mM sulfate as electron acceptor. *S. fumaroxidans* was grown in MPOB medium with 20 mM sodium fumarate as described previously (Harmsen et al., 1998). *Geobacter lovleyi* was isolated by dilution to extinction from a

chlorinated ethene contaminated aquifer in Sydney, Australia using acetate and Fe (III) citrate as electron donor and acceptor respectively. Purity was confirmed through microscopy and molecular fingerprinting and the species was identified by sequencing the near full length 16S rRNA gene (98% similarity to *G. lovleyi* strain SZ).

Co-cultures containing *D. mccartyi* strain CBDB1 with *D. vulgaris* (DSV/CBDB1), with *S. fumaroxidans* (SFO/CBDB1), or with *G. lovleyi* (GBL/CBDB1) were grown in the media described above for strain CBDB1 with the substitutions of 10 mM lactate, 30 mM propionate or 30 mM acetate, respectively as electron donor with no exogenous H_2 added. Cyanocobalamin (1 μM VB_{12}) was added as indicated. All cultures were inoculated to an total initial density of ∼5 × 10^6 cells mL^{-1} and incubated in the dark at 30°C without agitation.

Application of Granular Activated Carbon (GAC) to Mitigate HCB Daughter Product Toxicity

GAC (0.5 g, G60 powder, 100 mesh, Sigma-Aldrich) was mounted in glass Pasteur pipettes sealed at one end and placed into CBDB1 co-cultures such that the sealed end was submerged and the open end exposed to the headspace enabling exposure of GAC to the headspace but avoiding direct contact between GAC and the culture medium (**Figure S3**). Thus volatile organic substances (lesser chlorinated benzenes) could be adsorbed from the headspace. To quantify trichlorobenzene (TCB) and dichlorobenzene (DCB) removal from the headspace, GAC was extracted five times using 3 mL of dichloromethane (DCM). DCM was reduced to a final volume of 1 mL via evaporation prior to analysis by gas chromatography with flame ionization detection (GC-FID). Extraction recovery was determined to be 90-95% (data not shown).

Quantification of Chlorinated Benzenes

Chlorinated benzenes were quantified by headspace analysis gas chromatography using a Shimadzu GC-2010 Plus gas chromatograph with flame ionization detection (GC-FID) fitted with a J&W DB-5 30 m × 0.32 mm (inner diameter) × 0.25 μm column and a Shimadzu headspace auto-sampler (Koutsogiannouli et al., 2009). Culture (1 mL) was transferred into a 10 mL headspace sample vial. Prior to injection, the samples were heated to 80°C and shaken for 2 min. The injector and detector temperature were set at 250°C. The oven temperature was held at 100°C for 1 min, followed by a 25°C min^{-1} increase, and then held at 250°C for 0.5 min. Aqueous chlorinated benzene standards were prepared with the same gas to liquid space ratio as the cultures flasks accounting for phase partitioning according to Henry's Law. The amount of chloride released was calculated by multiplying the concentration of daughter products (mmole l^{-1}) by the difference in Cl^- number between the parent and the daughter compounds.

Carbon Monoxide Quantification

Carbon monoxide (CO) was quantified with a Shimadzu GC-2010 Plus GC, equipped with a pulsed discharge detector (GC-PDD) and fitted with a J&W Molecular sieve (30 m × 0.32 mm (inner diameter) × 0.25 μm column (Wurm et al., 2003). Helium was used as the carrier gas with a split ratio of 1:10. The oven was held at 30°C for 1.5 min, ramped at 20°C min^{-1} to 50°C, then held for 7.5 min. The samples were analyzed with the PDD at 140°C. Aliquots (100 μL) of sample headspace were manually injected with a gas tight syringe. CO standards (0.5–12 μmol) were prepared in 80 mL of CBDB1 media in 160 mL flasks.

Quantitative Polymerase Chain Reaction (qPCR)

Liquid samples (2 ml) were harvested by centrifugation (8000 × g, 20 min at 4°C). Genomic DNA was extracted from cell pellets as described previously (Urakawa et al., 2010). qPCR was used to determine *Dehalococcoides* spp. and total Bacterial 16S rRNA gene copies in the cultures using *Dehalococcoides* specific primers Dco728F (5′-AAGGCGGTTTTCTAGGTTGTCAC-3′) and Dco994R (5′-CTTCATGCATGTCAAAT-3′) (Smits et al., 2004), and universal bacterial primers Eub1048F (5′-GTGSTGCAYGGYTGTCGTCA-3′) and Eub1194R (5′-ACGTCRTCCMCACCTTCCTC-3′) (Horz et al., 2005). Reaction mixtures (10 μL final volume) contained 5 μL SsoFast Eva Green Supermix (BioRad), 100 nM of each forward and reverse primer, 2 μL template, 0.1 mg bovine serum albumin (Thermo Fisher Scientific) and 2.7 μL nuclease free water (Thermo Fisher Scientific). For total bacteria quantification, cycling conditions on a CF96 Real Time System (BioRad) were as follows: 3 min at 98°C, 39 cycles of 0.2 min at 95°C and 0.5 min at 62°C, followed by melt curve analysis from 60 to 99°C. For *Dehalococcoides*, cycling conditions were as follows: 3 min at 98°C, 44 cycles of 0.3 min at 94°C and 0.45 min at 58°C, followed by melt curve analysis from 55 to 95°C. Quantification of total Bacteria and *Dehalococcoides* 16S rRNA gene copies was performed by analyzing serial dilution of known quantities of plasmids containing partial *Dehalococcoides* spp. genes.

Microbiological Cobalamin Assay

To quantify extracellular cobamides in pure cultures and co-cultures, a microbiological assay using the cobamide-auxotroph *Lactobacillus delbrueckii* (ATCC7830) was performed as described previously (Yan et al., 2012). Cells from 1.5 mL of culture were removed by centrifugation at 14,000 xg for 1 min, and the supernatants were passed through 0.22 μm membrane filters. Cell-free supernatant (150 μl) was diluted from 2- to 20-fold with water and distributed into 96 well plates filled with 150 μl of double-strength vitamin B_{12} assay medium (Difco). To prepare vitamin B_{12}-free inocula, cell pellets were washed with sterile, deionized water three times. The cells were suspended in double-strength vitamin B_{12} assay medium diluted with an equal amount of sterile, deionized water and then incubated at 37°C for 3 h to deplete carryover VB_{12} from the inoculum broth. The 96 well plate was sealed with an adhesive optical cover and incubated at 37°C in the dark. After 24 h of incubation, the optical density in each well was recorded at 630 nm using a

96 well plate reader (BioTek, Winooski, VT). A standard curve generated by adding known concentrations of vitamin B_{12} was included on each plate. The assay had a linear range from 5 to 50 ng/L of vitamin B_{12} with a detection limit of 2 ng/L. Cobamides measured using this microbiological approach were reported as vitamin B_{12} equivalents.

Estimation of the Limits of Interspecies Distance for H_2 Transfer

The maximum interspecies distances between strain CBDB1 and syntrophic partners that would enable the observed dechlorination rates for substrates fermentation were estimated using Fick's diffusion law according to the procedure described by Mao et al. (2015):

$$J_{H2} = A_{syn} \times D_{H2} \times \frac{C_{H2-syn-C_{H2}-CBDB1}}{d_{syn-CBDB1}}$$

J_{H2} is the flux of H_2 between syntrophic cells and CBDB1, A_{syn} is the surface area of a syntrophic cell, D_{H2} is the H_2 diffusion constant in water, at 35°C (6.31×10^5 cm^2 s^{-1}, Haynes, 2013). C_{H2-syn} is the H_2 concentration immediately outside syntroph cells (representing the maximum H_2 concentration enabling exergonic fermentation). $C_{H2-CBDB1}$ is the H_2 concentration immediately outside CBDB1 cells (representing the theoretical minimum H_2 concentration that strain CBDB1 can use for energy generation from HCB dechlorination). $d_{syn-CBDB1}$ is the distance between syntroph and CBDB1 cells that enables syntrophic oxidation.

Proteomics

D. mccartyi CBDB1 was grown with 5 mM acetate, 7.5 mM H_2 and excess HCB as described above. *Geobacter lovleyi* was grown with 10 mM acetate and 20 mM Fe (III) citrate. *D. mccartyi* CBDB1 and *G. lovleyi* co-culture (CBDB1/GL) was grown in the same medium as strain CBDB1 pure culture, with 30 mM acetate and no exogenous H_2. All cultures were grown in triplicate in 100 mL media. Cells were collected from pooled replicates (x3) during exponential growth when cell density reached ∼10^8 cell/mL (∼90 days of incubation). Cells were harvested using 0.2 μm filters (Millipore, Germany) as described previously (Schiffmann et al., 2016). Cells were washed from filters with 50 mM ammonium hydrogen carbonate. Three analytical replicates were analyzed for each sample.

Samples were prepared for in-solution digestion as described previously (Schiffmann et al., 2014). CBDB1 cells were lysed by three cycles of freeze (liquid nitrogen) and thaw (1 min at 40 °C). The protein lysates obtained were reduced with 50 mM dithiothreitol (Invitrogen, USA) for 1 h at 30°C and alkylated using 130 mM iodoacetamide (Sigma-Aldrich, Australia) for 1 h at 30°C. Proteolysis was performed overnight using trypsin at 37°C. The tryptic digestion was stopped with formic acid to a final concentration of 1% followed by desalting using ZipTip-μC18 tips and re-suspended in 1% formic acid, 2% acetonitrile (ACN), prior to LC–MS/MS analysis.

Digested peptides were separated by nano-LC using an Ultimate nano RSLC UPLC and auto-sampler system (Dionex, Amsterdam, Netherlands) as described previously (Jugder et al., 2016). Samples (2.5 mL) were concentrated and desalted onto a micro C18 pre-column (300 mm × 5 mm, Dionex) with 2% ACN in water with 0.1% triflouroacetic acid (TFA) at 15 ml/min. After a 4 min wash the pre-column was switched (Valco 10 port UPLC valve, Valco, Houston, Tx) into line with a fritless nano column (75 m × ∼15 cm) containing C18AQ media (1.9 μ, 120 Å Dr Maisch, Ammerbuch-Entringen Germany). Peptides were eluted using a linear gradient of 2%−36% ACN in water containing 0.1% (v/v) formic acid at 200 nl/min over 30 min. High voltage (2000 V) was applied to low volume Titanium union (Valco) with the column oven heated to 45°C (Sonation, Biberach, Germany) and the tip positioned ∼0.5 cm from the heated capillary (T = 300°C) of a QExactive Plus (Thermo Electron, Bremen, Germany) mass spectrometer. Positive ions were generated by electrospray and the QExactive operated in data dependent acquisition mode (Yang et al., 2010). A survey scan m/z 350-1750 was acquired (resolution = 70,000 at m/z 200, with an accumulation target value of 1,000,000 ions) and lockmass enabled (m/z 445.12003). Up to the 10 most abundant ions (> 80,000 counts, underfill ratio 10%) with charge states > +2 and < +7 were sequentially isolated (width m/z 2.5) and fragmented by HCD (NCE = 30) with an AGC target of 100,000 ions (resolution = 17,500 at m/z 200). M/z ratios selected for MS/MS were dynamically excluded for 30 s. Peak lists generated were submitted to the database search program MASCOT (version 2.5.1, Matrix Science). All MS/MS spectra were searched against a custom database consisting of all proteins in *D. mccartyi* strain CBDB1 and *G. lovleyi* genomes from Uniprot. Search parameters were: Precursor tolerance 4 ppm and product ion tolerances ±0.05 Da; Met(O) carboxyamidomethyl-Cys specified as variable modification, enzyme specificity was trypsin, 1 missed cleavage was possible and the non-redundant protein database from Uniprot (Jan 2015) searched. The results were exported to both XML and ROV file format prior to loading into Scaffold for further analysis.

Label free quantification was carried out in Scaffold Q1 software (version Scaffold 4.7.2, Proteome Software) according to the precursor intensity-based method, where differences in protein abundance (defined here as proteins differentially expressed relative to total cell protein) between pure culture and co-culture samples were found based on the average precursor intensity acquired. Protein identifications were accepted if they could be established at greater than 95.0% probability and contained at least 2 identified peptides. Protein probabilities were assigned by the Protein Prophet algorithm (Nesvizhskii et al., 2003). Proteins that contained similar peptides and could not be differentiated based on MS/MS analysis alone were grouped to satisfy the principles of parsimony. Proteins sharing significant peptide evidence were grouped into clusters.

Statistical Tests

The data was assumed to be normally distributed. One-way analysis of variance (ANOVA) tests and *T*-test were calculated to determine the significance of results using an alpha level of 0.05. Multiple comparisons were calculated with Dunnet's test, where

applicable. All statistical tests were performed using GraphPad Prism 6 software.

RESULTS

Syntrophic Growth of *D. mccartyi* Strain CBDB1 and Syntrophic Partners

Three bacterial strains were selected as hydrogen producing syntrophic partners for *D. mccartyi* strain CBDB1 based on the diversity of substrates used. The partner organisms included Deltaproteobacteria *Desulfovibrio vulgaris* (DSV) and *Geobacter lovleyi* (GBL) and Firmicute *Syntrophomonas fumaroxidans* (SFO). These organisms were supplied with lactate, acetate and propionate respectively as electron donors. Syntrophic growth of *D. mccartyi* strain CBDB1 and H_2 producing partners was established enabling reductive dechlorination of hexachlorobenzene (HCB) to 1,3,5-trichlorobenzene (1,3,5-TCB), 1,3-dichlorobenzene (1,3-DCB), and 1,4-dichlorobenzene (1,4-DCB) without exogenous H_2 provision.

Dechlorination rates were comparable with the different partners with the highest observed in the *D. vulgaris* and CBDB1 (DSV/CBDB1) co-culture (0.59 ± 0.05 μmol Cl^- day^{-1}) with the rates in the other co-cultures at 0.39 ± 0.15 and 0.45 ± 0.09 μmol Cl^- day^{-1} in the *S. fumaroxidans* and CBDB1 (SFO/CBDB1) and *G. lovleyi* and CBDB1 (GBL/CBDB1) co-cultures, respectively (**Table 1**). The dechlorination rates in all co-cultures were significantly higher (2-3 fold, *t*-test, $P < 0.05$) compared to pure H_2/acetate fed CBDB1 culture (0.23 ± 0.04 μmol Cl^- day^{-1}).

Acetate and H_2 accumulated to a maximum of 1.8 (±0.06) mM and 2.0 (±0.09) mM respectively in the DSV/CBDB1 co-culture, while in the SFO/CBDB1 co-culture accumulation was slightly lower with 1.1 (±0.02) mM of acetate and 1.2 (±0.03) mM of H_2 observed (**Figure 1**). Thereafter, acetate and H_2 concentrations decreased, presumably as a function of consumption by CBDB1. In the acetate fed GBL/CBDB1 co-culture, acetate consumption corresponded with H_2 concentration peaking at 0.5 (±0.01) mM followed by consumption and stabilization of H_2 concentration and ongoing acetate consumption (**Figure 1**). After two months incubation, 5.1 (±0.41), 9.4 (±0.98), and 13.7 (±0.94) mM lactate, propionate and acetate had been consumed respectively.

TABLE 1 | Maximum dechlorination rate and cell yield of *D. mccartyi* in syntrophic growth with syntrophic partners.

Co-culture	Dechlorination rate (μmol Cl^- day^{-1})	CBDB1 cell yield (cells μmol^{-1} Cl^- day^{-1})	*P*-value (*T*-test)
DSV/CBDB1	0.59 ± 0.05***	3.7 (±0.3) × 10^8	0.0005
SFO/CBDB1	0.39 ± 0.12*	2.7 (±0.1) × 10^8	0.048
GBL/CBDB1	0.45 ± 0.09**	3.8 (±0.8) × 10^8	0.003
CBDB1	0.23 ± 0.04	2.3 (±0.3) × 10^8	

*P-values for rates. Significantly higher than CBDB1 culture alone at *P < 0.05, **P < 0.01, ***P < 0.001. Values are given as means ± the standard deviation from triplicate cultures.*

Growth of *D. mccartyi* strain CBDB1 in co-culture was measured by quantitation of 16S rRNA genes using universal bacterial and *Dehalococcoides* specific primers. Cell numbers increased over 90 days. Initial 16S rRNA gene copy concentrations were 2.0 (±0.15) × 10^6 and 1.2 (±0.4) × 10^6 copies/mL for total bacteria and *Dehalococcoides* respectively. Deltaproteobacterial co-cultures DSV/CBDB1 and GBL/CBDB1 had the largest increase in both total bacterial gene copies and *Dehalococcoides* gene copies (110–125 fold) up to 2.2 (±1.2) × 10^8 and 1.5 (±1.8) × 10^8 copies /mL, respectively. The SFO/CBDB1 co-culture showed the lowest *Dehalococcoides* cell growth up to 8.4 (±0.3) × 10^7 copies/mL (70-fold increase) congruent with dechlorination activity data.

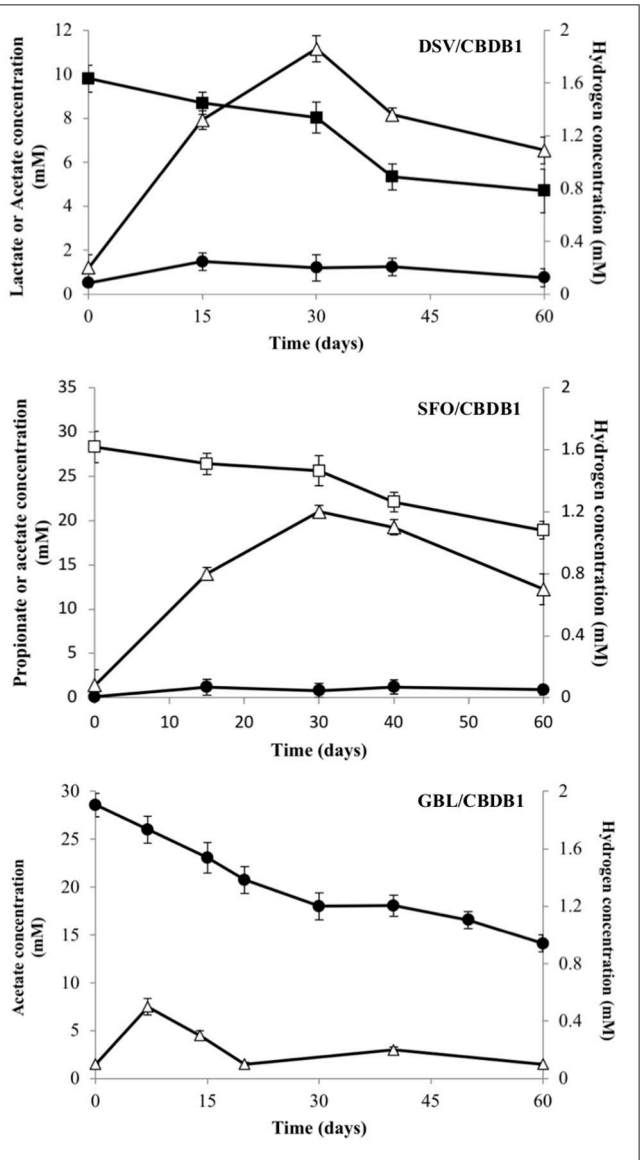

FIGURE 1 | Electron donor production and consumption in HCB reducing syntrophic co- cultmes DSV/CBDB1, SFO/CBDB1 and GBL/CBDB1. H2 (triangles), Acetate (circles), Lactate (closed squares), Propionate (open squares). Error bars represents standard deviation of the mean ($n = 3$).

Cell to Cell Distance and Thermodynamic Considerations in Syntrophic Co-cultures

The maximum interspecies distance for molecular hydrogen transfer between cells of strain CBDB1 and syntrophic partners can be calculated using Fick's diffusion law as previously described for other *D. mccartyi* strains (Mao et al., 2015). This distance was calculated for the syntrophic co-cultures of strain CBDB1 and partners with lactate, propionate and acetate as substrates. In the randomly dispersed cells of DSV/CBDB1, GBL/CBDB1 and SFO/CBDB1 co-cultures, the average distance enabling interspecies H_2 transfer was calculated to be 178, 10 and 19 μm, respectively (**Table 2**). The values for cell-cell distances in DSV/CBDB1, GBL/CBDB1 and SFO/CBDB1 co-cultures calculated using 16S qPCR data for bacteria as proxy were 16.8, 19.5, and 24.4 μm, respectively. The measured value for the DSV/CBDB1 co-culture was well below the theoretical maximum whilst the GBL/CBDB1 and SFO/CBDB1 co-cultures had measured values marginally above the theoretical maximum. This potentially explains the superior activity of the lactate fed DSV/CBDB1 co-culture across all quantified metrics (dechlorination activity, growth and acetate and H_2 production).

Effect of Syntrophic Partners on CO Concentrations in CBDB1 Co-cultures

Carbon monoxide (CO) has previously been shown to be inhibitory to *D. mccartyi* strain 195 (Zhuang et al., 2014). Consequently, CO toxicity, production and consumption was examined in strain CBDB1. **Figure 2** shows that CO concentrations above 1 μmol flask^{-1} reduce the dechlorination activity of strain CBDB1 and 6 μmol flask^{-1} is completely inhibitory. The half maximal inhibitory concentration (IC50) was 2.24 ± 0.09 μmol flask^{-1}. **Figure 2** also shows that after 60 days incubation, CO accumulation in strain CBDB1 pure culture reached the threshold whereby CO toxicity manifests (0.9 ± 0.1 μmol flask^{-1}). After 60 days, 17% of the initial HCB amendment (70 μmol) was degraded to release 11.2 ± 0.2 μmol Cl^-. Hence, complete dechlorination of 70 μmol HCB could accumulate ∼5.6 μmol CO in pure culture. In syntrophic co-culture, regardless of the fermentative partner, the CO concentration remained below those shown to confer toxicity at 0.4 μmol flask^{-1} in all co-cultures after 60 days (**Figure 2**).

TABLE 2 | Estimation of the cell-cell distance in syntrophic co-culture at day 60 of incubation.

	D. vulgaris with strain CBDB1 on lactate	*G. lovleyi* with strain CBDB1 on acetate	*S. fumaroxidans* with strain CBDB1 on propionate
Total number of cells/ml [(a)]	2.11×10^8	1.34×10^8	6.89×10^7
Mean cell-cell distance (μm) [(b)]	16.8	19.5	24.4
Maximum interspecies distance for H_2 transfer (μm) [(c)]	178	10.1	18.6

(a) Total cell number for strain CBDB1 and syntrophic partners in co-cultures using 16S copies as proxy; (b) Calculated using 16S copies as a proxy for cell number; (c) Calculated using Fick's diffusion law for H_2 transfer from syntrophic partners to strain CBDB1. Detailed calculations for these values can be found in the Supplementary Materials ***Table S1****.*

Growth of CBDB1 With Syntrophic Partners Excluding Exogenous Cobalamin Supply

To examine whether the syntrophic partners could supply cobalamin to CBDB1, microcosms were established without exogenous cyanocobalamin. Data was collected after four transfers (10% v/v inoculation) of the parent culture representing a dilution of cobalamin from 0.5 μg/L to 0.05 ng/L. The total concentration of HCB dechlorination products were on average 28.3 ± 1.8 μM in all three co-cultures, compared to 72.4 ± 3.5 μM in pure CBDB1 culture (supplied with cyanocobalamin) at day 60 (**Figure 3**). Dechlorination activity in co-cultures was ten-fold less than in co-cultures amended with cyanocobalamin and three-fold less than a pure CBDB1 culture. Dechlorination

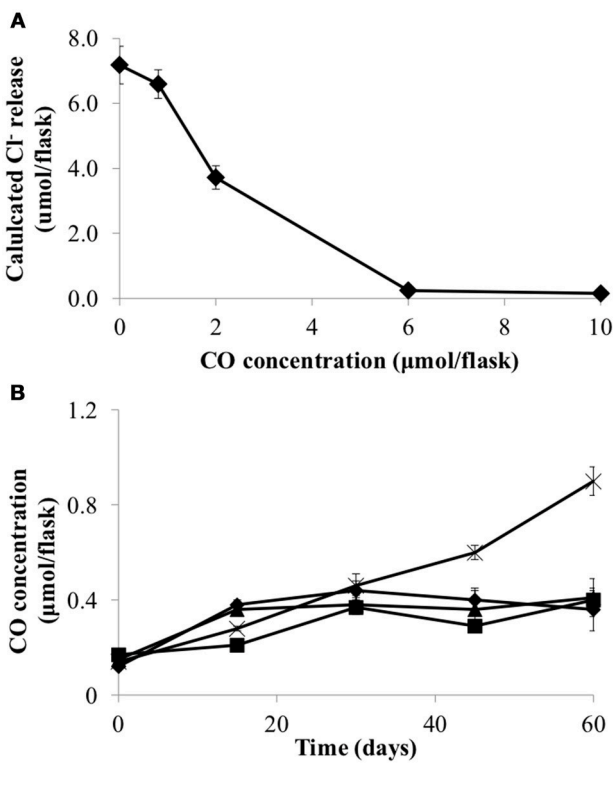

FIGURE 2 | (A) CO inhibits HCB dechlorination activity of *D. mccartyi* strain CBDB1 shown as Cl- ion release at the end of incubation (60 days) and **(B)** CO accumulation during HCB dechlorination by strain CBDB1 in pure culture (crosses) and in co-cultures with *D. vulgaris* (DSV/CBDB1, diamonds), *S. fumaroxidans* (SFO/CBDB1, squares) and *G. lovleyi* (GBL/CBDB1, triangles). After 60 days strain CBDB1 produced enough CO to confer autotoxicity. In co-cultures, CO concentration remained below that showing toxicity. Data points are averages of hiplicate cultures. Error bars represent the standard deviation ($n = 3$).

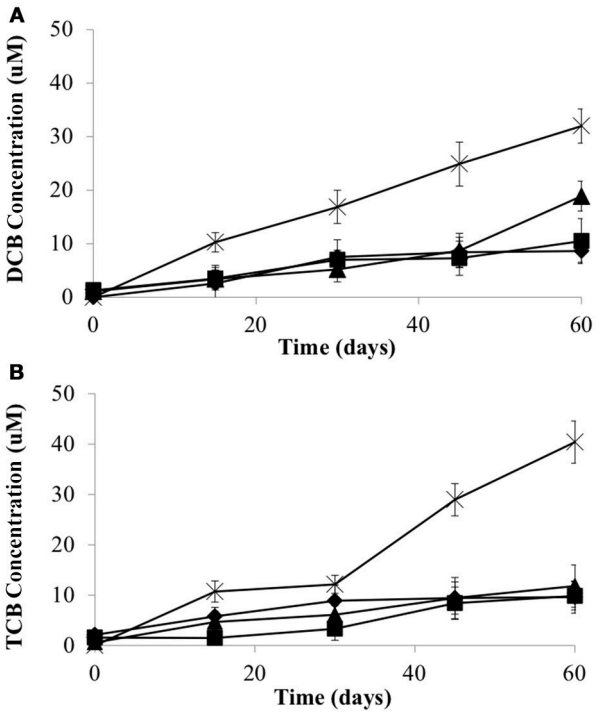

FIGURE 3 | Production of **(A)** 1,3-Dichlorobenzene and 1,4-Dichlorobenzene (sum total) and **(B)** 1,3,5-Trichlorobenzene from HCB by *Dehalococcoides mccartyi* strain CBDB1 in pure culture with exogenous provision of acetate, H_2 and Vitamin B_{12} (crosses), and in co-culture with *D. vulgaris* (diamonds), S. *fumaroxidans* (squares) or *G. lovleyi* (triangles) without exogenous provision of acetate, H_2 and Vitamin B_{12}. Data points are averages of triplicate cultures. Error bars represent standard deviation.

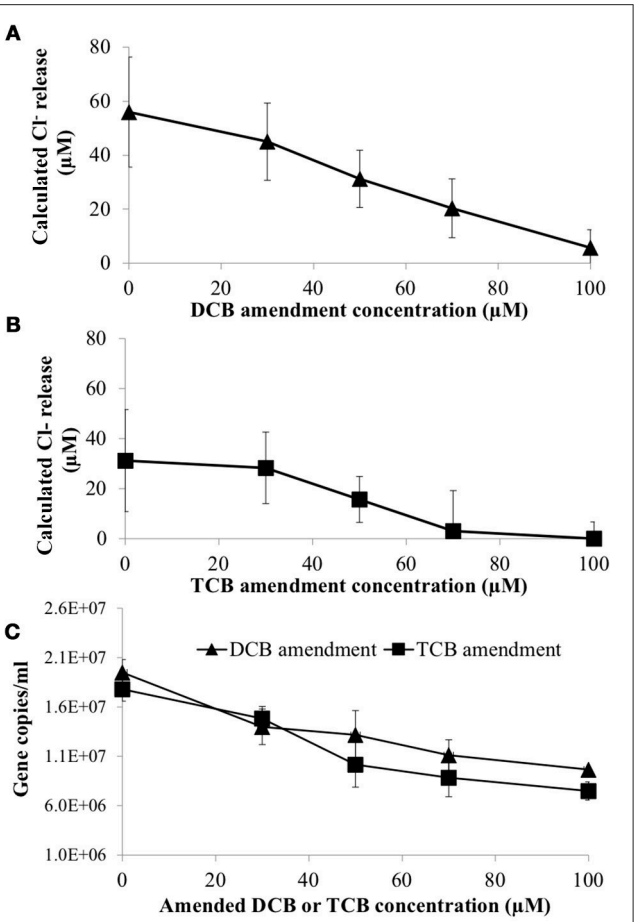

FIGURE 4 | Impact of daughter products from reductive dechlorination of HCB (Dichlorobenzene or Trichlorobenzene) on HCB reduction activity of *Dehalococcoides mccartyi* CBDB1 after 30 days incubation. **(A)** Chloride ion release calculated from concentrations of DCB and TCB produced from HCB in the presence of increasing amended DCB concentrations. **(B)** Chloride ion release calculated from concentrations of DCB and TCB produced from HCB in the presence of increasing TCB concentrations. **(C)** Impact of DCB and TCB on CBDB1 gene copy concentration after 30 days incubation. Error bars represent SD ($n = 3$).

was not observed in a control where CBDB1 pure cultures were not supplied exogenous cobalamin (data not shown).

Measurement of cobamides in co-culture supernatants was achieved using a biological assay involving the growth of the cobamide auxotroph *Lactobacillus delbrueckii*. Supernatants were analyzed at the end of the experiment (i.e., day 60). In GBL/CBDB1 cultures 6.0 ± 1.0 ng/L extracellular cobamide was detected. In the DSV/CBDB1 and SFO/CBDB1 co-cultures extracellular cobalamins were below the limits of detection. This suggests that none of the partners could produce sufficient cobalamin to support maximum HCB dechlorination activity by *D. mccartyi* strain CBDB1 (ie., activity observed with cyanocobalamin amendment).

HCB Respiration Products Inhibit *D. mccartyi* Strain CBDB1 Growth and Activity

To determine if 1,3- and 1,4-dichlorobenzene (DCB) and 1,3,5-trichlorobenzene (TCB) had an inhibitory impact on HCB respiration by *D. mccartyi* strain CBDB1, pure cultures were established with increasing concentrations of DCB or TCB. **Figure 4** shows that DCB and TCB have an inhibitory effect on HCB dechlorination activity and cell growth of CBDB1, with lower IC50 and LD50 values for TCB compared to DCB (45 μM and 70 μM, respectively).

DCB and TCB are volatile compounds so Granular Activated Carbon (GAC) was mounted in culture flask headspace (**Figure S3**) in an attempt to mitigate the inhibitory impacts of daughter product formation from HCB reduction. First order rate constants for DCB and TCB adsorption on GAC were −0.14 (±95% CI) day^{-1} and −0.16 (±90% CI) day^{-1}, respectively (**Figure S1**). In comparison, first order rate constants of DCB and TCB production in strain CBDB1 culture were 0.1 (±99% CI) day^{-1} and 0.07 (±97% CI) day^{-1}, respectively. Hence, trapping DCB and TCB on GAC could mitigate the inhibitory effect of DCB and TCB accumulation CBDB1 in co-cultures.

To test the mitigation strategy, DSV/CBDB1, SFO/CBDB1 and GBL/CBDB1 co-cultures were grown with and without 0.5 g GAC mounted in the culture headspace. At day 70, HCB

daughter products were analyzed both in the culture medium and adsorbed to GAC. The latter was analyzed by dichloromethane (DCM) extractions of the GAC. DCB and TCB production were significantly higher (2-fold, *t*-test, $P < 0.05$) in co-cultures amended with GAC for all three syntrophic partners (**Figure 5**). For example, treatments with GAC in DSV/CBDB1 co-cultures had a dechlorination rate of 1.1 ± 0.2 μmol Cl^- day^{-1}, compared to a rate of 0.6 ± 0.2 μmol Cl^- day^{-1} in the GAC-free treatments. Total bacterial growth in treatments with and without GAC was determined via 16S rRNA gene quantitative PCR using universal bacterial primers at day 0, 30 and 70 of incubation. After 70 days the gene copies in the presence of GAC were 2.1-2.7 fold higher (*t*-test, $P < 0.05$) than in the absence of GAC (**Figure 5**).

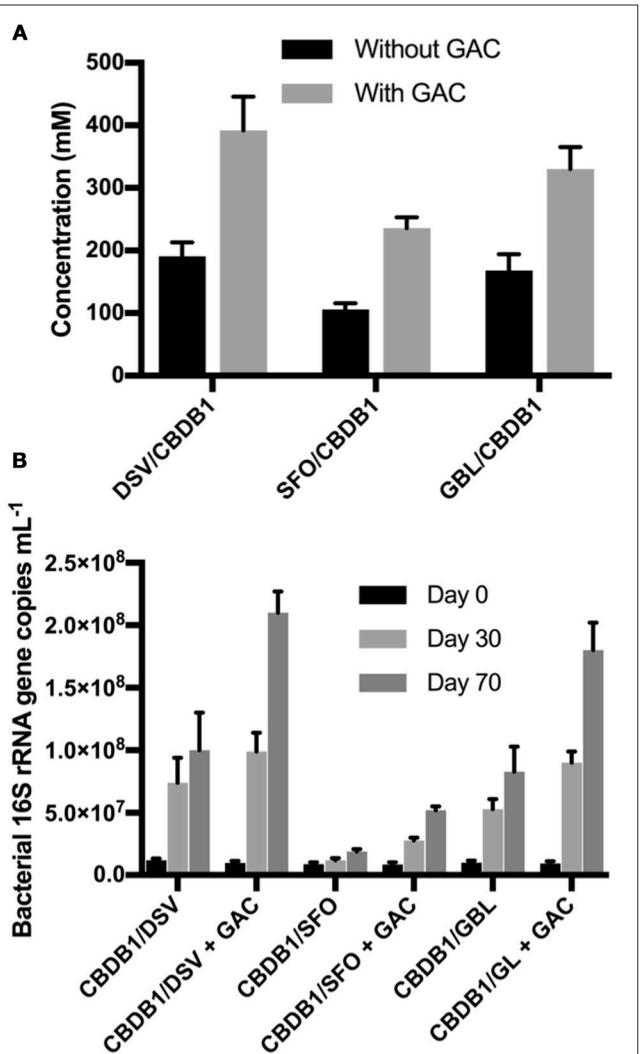

FIGURE 5 | (A) Total concentrations of HCB dechlorination products (1,3- and 1,4-DCB and 1,3,5-TCB) in different co-cultures of *D. mccartyi* strain CBDB1 with and without GAC after 70 days of incubation. Data points are averages of triplicate cultures. Error bars represent the standard deviation ($n = 3$). **(B)** Quantification of 16S rRNA gene copies in syntrophic co-cultures of *D. mccartyi* strain CBDB1 and partners with and without GAC after 70 days of incubation. All cultures were provided with cyanocobalamin, Ti (III) citrate, and without exogenous H_2. Data points are averages of triplicate cultures. Error bars represent the standard deviation.

Proteomic Analysis in GL/CBDB1 Co-culture

Whole cell proteomic analyses of CBDB1 grown alone and in co-culture with syntrophic partner *G. lovleyi* was undertaken to identify changes in gene expression in response to co-culture. In pure culture *G. lovleyi* was grown with Fe (III) citrate as electron acceptor. Equal amounts of total protein (∼30 μg) from late exponential phase samples (∼3 months incubation) were digested. Each sample was prepared via the filter aided sample preparation (FASP) method and subjected to LFQ by nano LC-MS/MS. A total of 363 *D. mccartyi* proteins and 404 *G. lovleyi* proteins were identified in pure and co-cultures (**Figure S2**). Of the *D. mccartyi* proteins, 119 were identified in co-culture with 62 of these exclusively observed in co-culture. Of the *G. lovleyi* proteins, 102 were observed in co-culture with 15 of these exclusive to the co-culture.

Table 3 reports *D. mccartyi* and *G. lovleyi* proteins for which expression was upregulated greater than five-fold (see **Table S2** for lesser fold upregulation and **Table S3** for the whole data set). Three reductive dehalogenases were identified from *D. mccartyi* including cbdbA84 (accession number CAI82345), cbdbA80 (accession number CAI82340) and cbdbA1453 (accession number CAI83480), which encode 1,2,3- and 1,2,4-TCB reductive dehalogenases. Among them, cbdbA84 and cbdbA80 were more abundant in the co-culture than in the pure CBDB1 culture suggestive of dependence of regulation on the presence of another organism (in this case a syntrophic partner).

Translation elongation factor Tu (locus cbdbA960), was among the high coverage proteins that were more abundant in the co-culture than in CBDB1 culture alone. Formate dehydrogenase (locus cbdbA195) was also shown to be more abundant during syntrophic growth than in the CBDB1 isolate. Several other conserved protein complexes involved in respiratory electron transfer were found in the CBDB1 isolate, including Rdh complexes, four hydrogenase complexes (Hup, Ech, Hyc, and Hym), NADH dehydrogenase complexes and two oxidoreductase complexes. Three hydrogenases, VhuA, HymB, and HymC, encoded by cbdbA597, cbdbA684, and cbdbA685, respectively, were found to be marginally more abundant in syntrophic growth than in the isolate (**Table S2**). The co-culture

TABLE 3 | Identified proteins with greater than five-fold increase in abundance in co-culture.

NCBI locus	Predicted functions	*D. mccartyi*	*G. lovleyi*
cbdbA84	Putative reductive dehalogenase	33	
cbdbA80	Putative reductive dehalogenase	14	
cbdbA195	Formate dehydrogenase, major subunit	8.2	
cbdbA960	Translation elongation factor Tu	5.6	
Glov_0477	Conserved hypothetical protein	_	8.6
Glov_1625	Malate dehydrogenase	_	6.6
Glov_0475	Alkyl hydroperoxide reductase	_	5.5

also possessed 16 ribosomal proteins that were detected with high expression compared to the CBDB1 isolate, congruent with the more robust growth of CBDB1 in co-culture. None of the cobalamin biosynthesis proteins were detected in either the co-culture or the CBDB1 isolate. Conversely, two types of cobalamin transporter, ABC-type cobalamin/Fe^{3+}-siderophores transport system ATPase component (locus cbdbA633) and periplasmic component (locus cbdbA636) were detected, with no difference in expression between the co-culture and CBDB1 isolate, both of which were amended with VB_{12}.

Among the 87 *G. lovleyi* proteins detected in both *G. lovleyi* culture alone and in co-culture (**Figure S2**), thiamine pyrophosphate protein (locus Glov_1628), succinate dehydrogenase or fumarate reductase (locus Glov_2213), as well as elongation factor and ribosomal proteins were among the proteins with the highest coverage. Proteins related to acetate oxidation, including malate dehydrogenase (locus Glov_1625), isocitrate dehydrogenase (locus Glov_1624) and citrate synthase (locus Glov_1379), were expressed more abundantly during syntrophic growth than in isolate cultures (**Table S2**). Two molybdopterinoxidoreductase proteins (loci Glov_3132 and Glov_0661) were detected less abundantly in the co-culture than in the *G. lovleyi* isolate, with fold change ratios of 0.7 and 0.1 respectively.

There were two proteins detected exclusively in the co-culture: peptidylprolylisomerase (locus Glov_2546) and histidinol dehydrogenase (encoded Glov_0822). Interestingly, there were two types of flagellin detected only during *G. lovleyi* growth with Fe (III) citrate, which were the flagellin domain protein (locus Glov_3371) and a flagellin basal associated-protein FilL (locus Glov_3294). In addition, three chemotaxis sensory transducers (encoded Glov_ 2776, Glov_ 1733 and Glov_1239) were found with less abundance during syntrophic growth than during pure culture growth on iron. Cobalamin-dependent proteins were identified in both *G. lovleyi* isolate and co-culture including ribonucleotide reductase, methionine synthase and methylmalonyl-CoA mutase. Among these proteins, only methylmalonyl-CoA mutase (encoded Glov_3260) was more abundant in co-culture than in the isolate, with a fold change of 2.0 (**Table S2**). Nicotinate-nucleotide/dimethylbenzimidazolephosphoribosyltransferase (CobT-Glov_3082) was the only cobalamin biosynthesis protein detected, which was from *G. lovleyi* in isolation.

TABLE 4 | Hydrogen-releasing and hydrogen-consuming reactions occurring in co-cultures.

HYDROGENOGENIC REACTIONS	
$C_3H_6O_3^- + 2\ H_2O \rightarrow\ CH_3COO^- + HCO_3^- + H^+ + 2H_2$	$\Delta G^{0'} = -\ 8.4$ kJ/reaction
$CH_3CH_2COO^- + 3\ H_2O \rightarrow\ CH_3COO^- + HCO_3^- + 3\ H_2$	$\Delta G^{0'} = +\ 76.1$ kJ/reaction
$CH_3COO^- + 2\ H_2O \rightarrow\ 2\ HCO_3^- + 4\ H_2 + H^+$	$\Delta G^{0'} = +\ 104.6$ kJ/reaction
HYDROGEN-CONSUMING REACTIONS	
$C_6Cl_6 + H_2 \rightarrow\ C_6HCl_5 + H^+ + Cl^-$	$\Delta G^{0'} = -\ 171.4$ kJ/reaction
$C_6Cl_6 + 4\ H_2 \rightarrow\ C_6H_4Cl_2 + 4\ H^+ + 4\ Cl^-$	$\Delta G^{0'} = -\ 447$ kJ/reaction

DISCUSSION

In this present study, lactate, propionate and acetate were supplied as organic carbon and energy sources for *D. mccartyi* strain CBDB1 in co-culture with *Desulfovibrio*, *Syntrophobacter* or *Geobacter*. Oxidation of these substrates by the syntrophic partners of CBDB1 was expected to provide H_2 for the reductive dechlorination of HCB. **Table 4** provides the $\Delta G^{0'}$ for the H_2 producing and H_2 consuming reactions revealing that H_2 production in the absence of the H_2 consuming reductive dechlorination reaction is marginally favorable or unfavorable thus representing the energetic dependency of the syntrophic interactions reported in this study. The enhanced dechlorination observed in this study between *D. mccartyi* strain CBDB1 and partners supports previous observations on the impact of syntrophic partners in organochlorine respiring cultures (He et al., 2007; Men et al., 2012; Yan et al., 2012). The fact that strain CBDB1 shows higher activity in syntrophic partnership with *Desulfovibrio*, *Syntrophobacter,* and *Geobacter* lineages in the presence of exogenous VB_{12} represents a proof of concept for a bioreactor in which HCB could be reduced to less persistent oxidisable compounds (DCB, TCB) using lactate, propionate or acetate as energy sources which are cost effective and safe compared to H_2.

From previous work, in addition to supplying electron donor (H_2), the robust growth of *D. mccartyi* strain 195 in syntrophic co-culture appears to stem from acetate supply by *D. vulgaris,* along with potential benefit from proton translocation, cobalamin-salvaging and amino acid biosynthesis as evidenced by gene expression analysis (Men et al., 2012). The impact of an incomplete Wood-Ljungdahl pathway i.e. the absence of CO dehydrogenase in the *D. mccartyi* genome, may also explain the more robust growth in co-culture and therefore further underpins the syntrophic interaction (Zhuang et al., 2014; Mao et al., 2015). *D. mccartyi* strain 195 was inhibited in pure culture by CO accumulating from acetyl-CoA cleavage due to the lack of CO dehydrogenase in *D. mccartyi* strain 195 (Zhuang et al., 2014).

In this study the inhibitory effect of CO on both dechlorination activity and cell growth of *D. mccartyi* strain CBDB1 was described. The adverse effect of CO toxicity on strain CBDB1 was mitigated by the presence of any of the tested syntrophic partners, (i.e. *Desulfovibro vulgaris, Syntrophobacter fumaroxidans,* or *Geobacter lovleyi*), which are capable of consuming CO (Davidova et al., 1994; Ragsdale, 2004; Diender et al., 2015). Other work using ^{13}C-labeling and bioinformatic analysis confirmed that Bacteria and Archaea exist in consortia as CO-oxidizing organisms capable of gaining additional energy via coexistence with *D. mccartyi* while simultaneously enhancing growth of *D. mccartyi* (Zhuang et al., 2014). The results from the present study support and broaden previous observations of metabolic exchange between *D. mccartyi* and syntrophic partners in dechlorinating microbial environments (Zhuang et al., 2014; Mao et al., 2015). In a pure culture bioreactor based on CBDB1

activity an alternative approach to removal of CO would need to be devised.

The theoretical maximum interspecies distances for strain CBDB1 and partners were calculated based on the observed substrate oxidation rate. These estimates showed that proximity is more essential for syntrophic acetate and propionate oxidation compared to lactate oxidation. In the present study, cell aggregation was not observed in co-culture. When strain CBDB1 grew with *D. vulgaris* in co-culture, the maximum interspecies distance (178 μm) allowed H_2 transfer between these bacteria without multi-lineage aggregate (flocculate) formation, whilst the other two co-cultures were close to the theoretical limit for H_2 transfer over distance suggesting a reduction in distance between cells would lead to higher dichlorination activity. This result is consistent with observations by Mao et al. (2015) that aggregation was not established in co-cultures of strain 195 and *Desulfovibrio vulgaris* while it did occur in *Syntrophomonas wolfei* and strain 195 co-culture. Previous studies reported that syntrophic co-cultures form cell aggregates during the growth for optimal H_2 transfer (Schink and Thauer, 1988; Stams et al., 2012; Felchner-Zwirello et al., 2013; Mao et al., 2015) or created biofilms in membrane bioreactors (Chung and Rittmann, 2008; Ziv-El et al., 2012). The cell aggregates reduce interspecies H_2 transfer distance. In a bioreactor context, these data suggest approaches to stimulate flocculation or suspended biofilm formation would be beneficial.

In co-culture with CBDB1, *G. lovleyi* was hypothesized to provide cobalamin to support dechlorination of HCB as in previous studies on co-cultures of *G. lovleyi* and *D. mccartyi* strain 195 (Yan et al., 2012). However, there was only 0.006 ± 0.01 μg/L of extracellular cobalamin detected in CBDB1/GBL co-culture, while in the other co-cultures cobalamins were under the limit detection of the assay used. The amount of cobalamin detected was much lower than the requirement of cobalamin (50 μg/L) for maximal reductive dechlorination rates in pure CBDB1 culture (Adrian et al., 2000). Hence, syntrophic growth of *D. mccartyi* strain CBDB1 still requires exogenous cyanocobalamin supply for maximum HCB respiration rates. This suggests cyanocobalamin would be required as an amendment for a bioreactor application with significant implications with respect to cost.

Proteomics plays a key role in exploring adaptive responses of microbes to environments or interactions among microorganisms (Wang et al., 2016). Previous proteomic studies have evaluated the effects of long-term syntrophic growth in oxidation of butyrate (Schmidt et al., 2013; Sieber et al., 2015) or methanogenic consortia in degradation of terephthalate (Wu et al., 2013). Additionally, Men et al. (2012) explored protein expression during syntrophic interactions between *D. mccartyi* strain 195 and *Desulfovibrio vulgaris* strain Hildenborough dechlorinating trichloroethene.

In the present study, almost all ribosomal proteins in strain CBDB1 were found to be more abundant in the co-culture than in the isolate. Ribosomal proteins are related to cell growth indicating a higher rate of protein synthesis, resulting in a faster growth rate in the co-culture compared with the pure culture. This was congruent with our growth data. Similar to the observations of Men et al. (2012), the higher abundance of three CBDB1 hydrogenase proteins (VhuA, HymB, and HymC) and lower abundance of proteins related to electron transport such as NADH, oxidoreductase complexes as well as HymS in co-culture compared to in isolation suggested that syntrophic growth involves different H_2 transfer systems than those used when H_2 is supplied exogenously.

Another CBDB1 protein found with high abundance in co-culture was formate dehydrogenase, encoded by the *cbdbA195* gene. This protein is expected to have another function other than formate utilization found in both *D. mccartyi* strains CBDB1 and 195 (Adrian et al., 2007; Morris et al., 2007). Recently, Kublik et al. (2016) revealed that this formate dehydrogenase-like enzyme highly expressed in *D. mccartyi* is a putative molybdopterin containing oxidoreductase that co-localizes with the active subunit of the reductive dehalogenase (RdhA). This may explain the high abundance of these two proteins detected in co-cultures where favorable growth conditions lead to more respiration. These results support the only previous proteomic analysis of ORB syntrophic growth with *D. mccartyi* strain 195 and *D. vulgaris* with TCE dechlorination (Men et al., 2012).

When comparing proteins detected in *G. lovleyi* in isolation and GBL/CBDB1 co-culture, there were two proteins detected exclusively in the latter: peptidylprolylisomerase and histidinol dehydrogenase. Histidinol dehydrogenase is responsible for catalyzing the reaction: L-histidinol + NAD^+ = L-histidine + NADH + H^+, while peptidylprolylisomerase plays the role of PceT, identified to be a trigger factor-like protein that functions as a dedicated chaperone for PceA (Maillard et al., 2011). The reason why these two proteins were only detected in co-culture and not expressed in *G. lovleyi* pure culture is unclear.

In the present study, no cobalamin biosynthesis proteins from *G. lovleyi* were detected and no differences in expression of cobalamin transport proteins were detected when comparing the co-culture with *G. lovleyi* in pure culture. These results might explain why cobalamin production by *G. lovleyi* was unable to support the GBL/CBDB1 co-culture. The observation that proteins related to acetate oxidation through the citric acid cycle (malate dehydrogenase, isocitratedehyrogenase and citrate synthase) were more abundant in co-culture than in the isolate is consistent with the stimulation of acetate oxidation by syntrophic growth. The lack of flagellin and lower expression of chemotaxis sensory transducer in co-culture supports the idea that syntrophic growth of CBDB1 and *G. lovleyi* occurs via interspecies H_2 transfer.

Cross-inhibition of co-contaminants and self-inhibition by biodegradation products in the environment has been widely reported (Chan et al., 2011; Schiffmacher et al., 2016). DCB and TCB amended in pure CBDB1 cultures were found to be inhibitory. The presence of GAC in CBDB1 co-culture headspace reduced the inhibitory effect of HCB daughter products on cell growth and dechlorination activity. Application of GAC to remove chlorinated compounds has been studied widely from water to soil in contaminated environments (Pavoni et al., 2006; Choi et al., 2009; Kjellerup et al., 2014; Dang et al., 2016). The data presented here suggests this approach could serve as an effective strategy in bioreactor applications with GAC mounted in a reactor headspace serving to continuously remove DCB and TCB to prevent daughter product inhibition.

CONCLUSIONS

Despite the ubiquity of syntrophic processes in anoxic environments, little is known about the mechanisms by which syntrophic consortia regulate their metabolism, such as the cross-supply of cobalamins or proteomic insights into syntrophic growth during organohalide respiration. Here we provide the first description of syntrophic growth of *D. mccartyi* strain CBDB1 and partners (*Desulfovibrio vulgaris, Syntrophobacter fumaroxidans* and *Geobacter lovleyi*) for exogenous provision of H_2, acetate and cobalamin for the reductive dechlorination of HCB. HCB dechlorination rates were enhanced two- to three-fold compared to pure cultures of *D. mccartyi* strain CBDB1. In co-cultures, acetate and H_2 were supplied from substrate oxidation by syntrophic partners, whilst amendment of exogenous cobalamin was necessary in all cultures to achieve maximal rates. Superior growth and dechlorination by strain CBDB1 in co-culture may be explained by the consumption of CO, preventing the adverse effect of CO toxicity by the presence of any of its syntrophic partners. Additionally, proteomic analysis in co-culture revealed an abundance of ribosomal proteins, reductive dehalogenase, hydrogenase proteins, and formate dehydrogenase, and down-regulation of proteins related to electron transport. The GAC application and results obtained from this study were the first investigation on GAC application in attempt to mitigate the inhibitory effect of HCB daughter products and thus enhance HCB dechlorination activity. This approach is relevant to bioreactor applications for HCB remediation with a potential low cost and easy application.

AUTHOR CONTRIBUTIONS

AC conceived, designed, analysed and executed the experimental work as well as drafted the manuscript. ML, LA, and MM conceived, designed, performed the data analysis, and the interpretation. ML, LA, and MM drafted the manuscript.

FUNDING

The authors acknowledge the Australian Research Council and Orica for funding (LP130100454) and the Australian Awards Scholarships (Department of Foreign Affairs and Trade) for supporting AC.

ACKNOWLEDGMENTS

AC is thankful to the Australian Awards Scholarships (Department of Foreign Affairs and Trade) for provision of PhD scholarship. The authors would like to acknowledge the valuable assistance from the Ramaciotti Centre for Genomics and the Bio-analytical Mass Spectrometry Facility at UNSW. We would like to thank Tammy Sihui Tang for provision of the *Geobacter lovleyi* culture.

SUPPLEMENTARY MATERIAL

The Supplementary Material for this article can be found online at: https://www.frontiersin.org/articles/10.3389/fmicb.2018.01927/full#supplementary-material

REFERENCES

Adrian, L., Görisch, H. (2002). Microbial transformation of chlorinated benzenes under anaerobic conditions. *Res. Microbiol.* 153, 131–137. doi: 10.1016/S0923-2508(02)01298-6

Adrian, L., Rahnenführer, J., Gobom, J., and Hölscher, T. (2007). Identification of a chlorobenzene reductive dehalogenase in *Dehalococcoides* sp. Strain CBDB1. *Appl. Environ. Microbiol.* 73, 7717–7724. doi: 10.1128/AEM.01649-07

Adrian, L., Szewzyk, U., and Gorisch, H. (1998). Physiological characterization of a bacterial consortium reductively dechlorinating 1,2,3- and 1,2,4-trichlorobenzene. *Appl. Environ. Microbiol.* 64, 496–503.

Adrian, L., Szewzyk, U., Wecke, J., and Gorisch, H. (2000). Bacterial dehalorespiration with chlorinated benzenes. *Nature* 408, 580–583. doi: 10.1038/35046063

Becker, J. G., Berardesco, G., Rittmann, B. E., and Stahl, D. A. (2005). The role of syntrophic associations in sustaining anaerobic mineralization of chlorinated organic compounds. *Environ. Health Perspect.* 113, 310–316. doi: 10.1289/ehp.6933

Chan, W. W. M., Grostern, A., Löffler, F. E., and Edwards, E. A. (2011). Quantifying the effects of 1,1,1-trichloroethane and 1,1-dichloroethane on chlorinated ethene reductive dehalogenases. *Environ. Sci. Technol.* 45, 9693–9702. doi: 10.1021/es201260n

Choi, H., Al-Abed, S. R., and Agarwal, S. (2009). Catalytic role of palladium and relative reactivity of substituted chlorines during adsorption and treatment of PCBs on reactive activated carbon. *Environ. Sci. Technol.* 43, 7510–7515. doi: 10.1021/es901298b

Chung, J., and Rittmann, B. E. (2008). Simultaneous bio-reduction of trichloroethene, trichloroethane, and chloroform using a hydrogen-based membrane biofilm reactor. *Water Sci. Technol.* 58, 495–536. doi: 10.2166/wst.2008.432

Dang, Y., Holmes, D. E., Zhao, Z., Woodard, T. L., Zhang, Y., Sun, D., et al. (2016). Enhancing anaerobic digestion of complex organic waste with carbon-based conductive materials. *Bioresour. Technol.* 220, 516–522, doi: 10.1016/j.biortech.2016.08.114

Davidova, M. N., Tarasova, N. B., Mukhitova, F. K., and Karpilova, I. U. (1994). Carbon monoxide in metabolism of anaerobic bacteria. *Can. J. Microbiol.* 40, 417–425, doi: 10.1139/m94-069

Diender, M., Stams, A. J. M., and Sousa, D. Z. (2015). Pathways and bioenergetics of anaerobic carbon monoxide fermentation. *Front. Microbiol.* 6:1275. doi: 10.3389/fmicb.2015.01275

Dolfing, J., and Tiedje, J. M. (1986). Hydrogen cycling in a three-tiered food web growing on the methanogenic conversion of 3-chlorobenzoate. *FEMS Microbiol. Lett.* 38, 293–298. doi: 10.1111/j.1574-6968.1986.tb01740.x

Felchner-Zwirello, M., Winter, J., and Gallert, C. (2013). Interspecies distances between propionic acid degraders and methanogens in syntrophic consortia for optimal hydrogen transfer. *Appl. Microbiol. Biotechnol.* 97, 9193–9205. doi: 10.1007/s00253-012-4616-9

Field, J. A. and Sierra-Alvarez, R. (2008). Microbial degradation of chlorinated benzenes. *Biodegradation* 19, 463–480. doi: 10.1007/s10532-007-9155-1

Harmsen, H., Van Kuijk, B., Plugge, C., Akkermans, A., De Vos, W., and Stams, A. (1998). *Syntrophobacter fumaroxidans* sp. nov., a syntrophic propionate-degrading sulfate-reducing bacterium. *Int. J. Syst. Bacteriol.* 48, 1383–1138. doi: 10.1099/00207713-48-4-1383

Haynes, W. M. (2013). *CRC Handbook of Physics and Chemistry, 95th Edn.* Boca Raton, FL: CRC Press, Inc.

He, J., Holmes, V. F., Lee, P. K. H., and Alvarez-Cohen, L. (2007). Influence of vitamin B12 and cocultures on the growth of *Dehalococcoides* isolates in defined medium. *Appl. Environ. Microbiol.* 73:2847. doi: 10.1128/AEM.02574-06

Horz, H. P., Vianna, M. E., Gomes, B. P. F. A., and Conrads, G. (2005). Evaluation of universal probes and primer sets for assessing total bacterial load in clinical samples: general implications and practical use in endodontic antimicrobial therapy. *J. Clin. Microbiol.* 43, 5332–5337. doi: 10.1128/JCM.43.10.5332-5337.2005

Jayachandran, G., Gorisch, H., and Adrian, L. (2003). Dehalorespiration with hexachlorobenzene and pentachlorobenzene by *Dehalococcoides* sp. strain CBDB1. *Arch Microbiol.* 180, 411–416. doi: 10.1007/s00203-003-0607-7

Jiang, L., Wang, Q., Liu, H., and Yao, J. (2015). Influence of degradation behavior of coexisting chlorobenzene congeners pentachlorobenzene, 1,2,4,5-tetrachlorobenzene, and 1,2,4-trichlorobenzene on the anaerobic reductive dechlorination of hexachlorobenzene in dye plant contaminated soil. *Water. Air. Soil Pollut.* 226, 1–9. doi:10.1007/s11270-015-2559-3

Jugder, B. E., Ertan, H., Wong, Y. K., Braidy, N., Manefield, M., Marquis, C. P., et al. (2016). Genomic, transcriptomic and proteomic analyses of Dehalobacter UNSWDHB in response to chloroform. *Environ. Microbiol. Rep.* 8, 814–824. doi: 10.1111/1758-2229.12444

Kjellerup, B. V., Naff, C., Edwards, S. J., Ghosh, U., Baker, J. E., and Sowers, K. R. (2014). Effects of activated carbon on reductive dechlorination of PCBs by ORB indigenous to sediments. *Water. Res.* 52, 1–10, doi: 10.1016/j.watres.2013.12.030

Koutsogiannouli, E. A., Moutou, K. A., Sarafidou, T., Stamatis, C., Spyrou, V., and Mamuris, Z. (2009). Major histocompatibility complex variation at class II DQA locus in the brown hare (*Lepus europaeus*). *Mol. Ecol.* 18, 4631–4649. doi: 10.1111/j.1365-294X.2009.04394.x

Kublik, A., Deobald, D., Hartwig, S., Schiffmann, C. L., Andrades, A., von Bergen, M., et al. (2016). Identification of a multi-protein reductive dehalogenase complex in *Dehalococcoides mccartyi* strain CBDB1 suggests a protein-dependent respiratory electron transport chain obviating quinone involvement. *Environ. Microbiol.* 18, 3044–3056. doi: 10.1111/1462-2920.13200

Maillard, J., Genevaux, P., and Holliger, C. (2011). Redundancy and specificity of multiple trigger factor chaperones in Desulfitobacteria. *Microbiology* 157, 2410–2421. doi: 10.1099/mic.0.050880-0

Mao, X., Stenuit, B., Polasko, A., and Alvarez-Cohen, L. (2015). Efficient metabolic exchange and electron transfer within a syntrophic trichloroethene-degrading coculture of *Dehalococcoides mccartyi* 195 and Syntrophomonas wolfei. *Appl. Environ. Microbiol.* 81, 2015–2024. doi: 10.1128/AEM.03464-14

McInerney, M. J., Struchtemeyer, C. G., Sieber, J., Mouttaki, H., Stams, A. J., Schink, B., et al. (2008). Physiology, ecology, phylogeny, and genomics of microorganisms capable of syntrophic metabolism. *Ann. N. Y. Acad. Sci*. 1125, 58–72. doi: 10.1196/annals.1419.005

Men, Y., Feil, H., Verberkmoes, N. C., Shah, M. B., Johnson, D. R., Lee, P. K., et al. (2012). Sustainable syntrophic growth of Dehalococcoides ethenogenes strain 195 with Desulfovibrio vulgaris Hildenborough and Methanobacterium congolense: global transcriptomic and proteomic analyses. *ISME J.* 6, 410–421. doi: 10.1038/ismej.2011.111

Morris, B. E. L., Henneberger, R., Huber, H., and Moissl-Eichinger, C. (2013). Microbial syntrophy: interaction for the common good. *FEMS Microbiol. Rev.* 37, 384–406. doi: 10.1111/1574-6976.12019

Morris, R. M., Fung, J. M., Rahm, B. G., Zhang, S., Freedman, D. L., Zinder, S. H., et al. (2007). Comparative proteomics of *Dehalococcoides* spp. reveals strain-specific peptides associated with activity. *Appl. Environ. Microbiol.* 73, 320–326. doi: 10.1128/AEM.02129-06

Nesvizhskii, A. I., Keller, A., Kolker, E., and Aebersold, R. (2003). A statistical model for identifying proteins by tandem mass spectrometry. *Anal. Chem.* 75, 4646–4658. doi: 10.1021/ac0341261

Pavoni, B., Drusian, D., Giacometti, A., and Zanette, M. (2006). Assessment of organic chlorinated compound removal from aqueous matrices by adsorption on activated carbon. *Water Res.* 40, 3571–3579. doi: 10.1016/j.watres.2006.05.027

Popat, S. C., and Deshusses, M. A. (2011). Kinetics and inhibition of reductive dechlorination of trichloroethene, cis-1,2-dichloroethene and vinyl chloride in a continuously fed anaerobic biofilm reactor. *Environ. Sci. Technol.* 45, 1569–1578. doi: 10.1021/es102858t

Ragsdale, S. W. (2004). Life with carbon monoxide. *Crit. Rev. Biochem. Mol. Biol.* 39, 165–195. doi: 10.1080/10409230490496577

Schiffmacher, E. N., Becker, J. G., Lorah, M. M., and Voytek, M. A. (2016). The effects of co-contaminants and native wetland sediments on the activity and dominant transformation mechanisms of a 1,1,2,2-tetrachloroethane (TeCA)-degrading enrichment culture. *Chemosphere* 147, 239–247. doi: 10.1016/j.chemosphere.2015.12.033

Schiffmann, C. L., Jehmlich, N., Otto, W., Hansen, R., Nielsen, P. H., Adrian, L., et al. (2014). Proteome profile and proteogenomics of the organohalide-respiring bacterium *Dehalococcoides mccartyi* strain CBDB1 grown on hexachlorobenzene as electron acceptor. *J. Proteomics* 98, 59–64. doi: 10.1016/j.jprot.2013.12.009

Schiffmann, C. L., Otto, W., Hansen, R., Nielsen, P. H., Adrian, L., Seifert, J., et al. (2016). Proteomic dataset of the organohalide-respiring bacterium Dehalococcoides mccartyi strain CBDB1 grown on hexachlorobenzene as electron acceptor. *Data Brief* 7, 253–256. doi: 10.1016/j.dib.2016.02.037

Schink, B. (1997). Energetics of syntrophic cooperation in methanogenic degradation. *Microbiol. Mol. Biol. Rev*. 61, 262–280.

Schink, B., and Thauer, R. K. (1988). "Energetics of syntrophic methane formation and the influence of aggregation," in *Granular Anaerobic Sludge: Microbiology and Technology*, ed G. Lettinga, A. J. B. Zehnder, J. T. C. Grotenhuis, and L. W. Hulshoff Pol (Wageningen: Pudoc), 5–17.

Schmidt, A., Müller, N., Schink, B., and Schleheck, D. (2013). A proteomic view at the biochemistry of Syntrophic Butyrate Oxidation in *Syntrophomonas wolfei*. *PLoS ONE* 8:e56905. doi: 10.1371/journal.pone.0056905

Sieber, J. R., Crable, B. R., Sheik, C. S., Hurst, G. B., Rohlin, L., Gunsalus, R. P., et al. (2015). Proteomic analysis reveals metabolic and regulatory systems involved in the syntrophic and axenic lifestyle of Syntrophomonas wolfei. *Front. Microbiol.* 6:115. doi: 10.3389/fmicb.2015.00115

Smits, T. H. M., Devenoges, C., Szynalski, K., Maillard, J., and Holliger, C. (2004). Development of a real-time PCR method for quantification of the three genera Dehalobacter, Dehalococcoides, and Desulfitobacterium in microbial communities. *J. Microbiol. Methods* 57, 369–378. doi: 10.1016/j.mimet.2004.02.003

Stams, A. J. M., Sousa, D. Z., Kleerebezem, R., and Plugge, C. M. (2012). Role of syntrophic microbial communities in high-rate methanogenic bioreactors. *Water Sci. Technol.* 66, 352–362. doi: 10.2166/wst.2012.192

Urakawa, H., Martens-Habbena, H. W., and stahl, D. A. (2010). High abundance of ammonia oxidizing Archaea in coastal waters, determined using a modified DNA extraction method. *Appl. Environ. Microbiol.* 76, 2129–2135. doi: 10.1128/AEM.02692-09

van Agteren, M. H., Keuning, S., and Oosterhaven, J. (1998). *Environmental Chemistry: Handbook on Biodegradation and Biological Treatment of Hazardous Organic Compounds*. Dordrecht: Springer.

Wang, D. Z., Kong, L. F., Li, Y. Y., and Xie, Z. (2016). Environmental microbial community proteomics: status, challenges and perspectives. *Int. J. Mole. Sci.* 17:1275. doi: 10.3390/ijms17081275

Wang, Q., Liu, H., Jiang, L., and Tang, J. (2014). Effect of the coexistence of chlorobenzene homologue on anaerobic degradation of hexachlorobenzene. *Huanjing Kexue/Environ. Sci.* 35, 1358–1365. doi: 10.13227/j.hjkx.2014.04.022

Wei, K., Grostern, A., Chan, W. W. M., Richardson, R. E., and Edwards, E. A. (2016). "Electron acceptor interactions between organohalide-respiring bacteria: cross-feeding, competition, and inhibition," *in Organohalide-Respiring Bacteria*, eds F. E. L. Lorenz (Berlin;Heidelberg: Springer), 283–308.

Worm, P., Koehorst, J. J., Visser, M., Sedano-Núñez, V. T., Schaap, P. J., Plugge, C. M., et al. (2014). A genomic view on syntrophic versus non-syntrophic lifestyle in anaerobic fatty acid degrading communities. *Biochim. Biophys. Acta* 1837, 2004–2016. doi: 10.1016/j.bbabio.2014.06.005

Wu, J. H., Wu, F. Y., Chuang, H. P., Chen, W. Y., Huang, H. J., Chen, S. H., et al. (2013). Community and proteomic analysis of methanogenic consortia degrading terephthalate. *Appl. Environ. Microbiol.* 79, 105–112. doi: 10.1128/AEM.02327-12

Wurm, D. B., Sun, K., and Winniford, W. L. (2003). Analysis of low levels of oxygen, carbon monoxide, and carbon dioxide in polyolefin feed streams using a pulsed discharge detector and two PLOT columns. *J. Chromatogr. Sci.* 41, 545–549. doi: 10.1093/chromsci/41.10.545

Yan, J., Im, J., Yang, Y., and Löffler, F. E. (2013). Guided cobalamin biosynthesis supports *Dehalococcoides mccartyi* reductive dechlorination activity. *Philo. Trans.* 368:20120320. doi: 10.1098/rstb.2012.0320

Yan, J., Ritalahti, K. M., Wagner, D. D., and Löffler, F. E., (2012). Unexpected specificity of interspecies cobamide transfer from *Geobacter* spp. *to*

Organohalide-Respiring *Dehalococcoides mccartyi* Strains. *Appl. Environ. Microbiol.* 78, 6630–6636. doi: 10.1128/AEM.01535-12

Yang, T. H., Coppi, M. V., Lovley, D. R., and Sun, J. (2010). Metabolic response of *Geobacter sulfurreducens* towards electron donor/acceptor variation. *Microbial Cell Factories* 9, 1–15. doi: 10.1186/1475-2859-9-90

Yu, S., Dolan, M. E., and Semprini, L. (2005). Kinetics and inhibition of reductive dechlorination of chlorinated ethylenes by two different mixed cultures. *Environ. Sci. Technol.* 39, 195–205. doi: 10.1021/es0496773

Yu, S., and Semprini, L. (2004). Kinetics and modeling of reductive dechlorination at high PCE and TCE concentrations. *Biotechnol. Bioeng.* 88, 451–464. doi: 10.1002/bit.20260

Zhuang, W. Q., Yi, S., Bill, M., Brisson, V. L., Feng, X., Men, Y., et al. (2014). Incomplete wood-ljungdahl pathway facilitates one-carbon metabolism in organohalide-respiring *Dehalococcoides mccartyi*. *Proc. Nat. Acad. Sci. U.S.A.* 111, 6419–6424. doi: 10.1073/pnas.1321542111

Ziv-El, M., Popat, S. C., and Cai, K. (2012). Managing methanogens and homoacetogens to promote reductive dechlorination of trichloroethene with direct delivery of H2 in a membrane biofilm reactor. *Biotechnol. Bioeng.* 109:2200–2210. doi: 10.1002/bit.24487

Conflict of Interest Statement: The authors declare that the research was conducted in the absence of any commercial or financial relationships that could be construed as a potential conflict of interest.

frontiers in Microbiology

ORIGINAL RESEARCH
published: 17 May 2018
doi: 10.3389/fmicb.2018.00812

Chlorinated Electron Acceptor Abundance Drives Selection of *Dehalococcoides mccartyi* (*D. mccartyi*) Strains in Dechlorinating Enrichment Cultures and Groundwater Environments

*Alfredo Pérez-de-Mora[1,2†], Anna Lacourt[1], Michaye L. McMaster[3], Xiaoming Liang[1], Sandra M. Dworatzek[4] and Elizabeth A. Edwards[1]**

[1] Department of Chemical Engineering & Applied Chemistry, University of Toronto, Toronto, ON, Canada, [2] Research Unit Analytical Biogeochemistry, Department of Environmental Sciences, Helmholtz Zentrum München, Neuherberg, Germany, [3] Geosyntec Consultants, Guelph, ON, Canada, [4] SiREM, Guelph, ON, Canada

OPEN ACCESS

Edited by:
Jianzhong He,
National University of Singapore,
Singapore

Reviewed by:
Siavash Atashgahi,
Wageningen University & Research,
Netherlands
Ernest Marco-Urrea,
Universitat Autònoma de Barcelona,
Spain
Mark Krzmarzick,
Oklahoma State University,
United States

***Correspondence:**
Elizabeth A. Edwards
elizabeth.edwards@utoronto.ca

†Present address:
Alfredo Pérez-de-Mora,
Business Unit Soil & Groundwater,
Tauw GmbH, Moers, Germany

Specialty section:
This article was submitted to Microbiotechnology, Ecotoxicology and Bioremediation, a section of the journal Frontiers in Microbiology

Received: 29 January 2018
Accepted: 10 April 2018
Published: 17 May 2018

Citation:
Pérez-de-Mora A, Lacourt A, McMaster ML, Liang X, Dworatzek SM and Edwards EA (2018) Chlorinated Electron Acceptor Abundance Drives Selection of Dehalococcoides mccartyi (D. mccartyi) Strains in Dechlorinating Enrichment Cultures and Groundwater Environments. Front. Microbiol. 9:812. doi: 10.3389/fmicb.2018.00812

Dehalococcoides mccartyi (*D. mccartyi*) strains differ primarily from one another by the number and identity of the reductive dehalogenase homologous catalytic subunit A (*rdhA*) genes within their respective genomes. While multiple *rdhA* genes have been sequenced, the activity of the corresponding proteins has been identified in only a few cases. Examples include the enzymes whose substrates are groundwater contaminants such as trichloroethene (TCE), *cis*-dichloroethene (cDCE) and vinyl chloride (VC). The associated *rdhA* genes, namely *tceA, bvcA,* and *vcrA*, along with the *D. mccartyi* 16S rRNA gene are often used as biomarkers of growth in field samples. In this study, we monitored an additional 12 uncharacterized *rdhA* sequences identified in the metagenome in the mixed *D. mccartyi*-containing culture KB-1 to monitor population shifts in more detail. Quantitative PCR (qPCR) assays were developed for 15 *D. mccartyi rdhA* genes and used to measure population diversity in 11 different sub-cultures of KB-1, each enriched on different chlorinated ethenes and ethanes. The proportion of *rdhA* gene copies relative to *D. mccartyi* 16S rRNA gene copies revealed the presence of multiple distinct *D. mccartyi* strains in each culture, many more than the two strains inferred from 16S rRNA analysis. The specific electron acceptor amended to each culture had a major influence on the distribution of *D. mccartyi* strains and their associated *rdhA* genes. We also surveyed the abundance of *rdhA* genes in samples from two bioaugmented field sites (Canada and United Kingdom). Growth of the dominant *D. mccartyi* strain in KB-1 was detected at the United Kingdom site. At both field sites, the measurement of relative *rdhA* abundances revealed *D. mccartyi* population shifts over time as dechlorination progressed from TCE through cDCE to VC and ethene. These shifts indicate a selective pressure of the most abundant chlorinated electron acceptor, as was also observed in lab cultures. These results also suggest that reductive

dechlorination at contaminated sites is brought about by multiple strains of *D. mccartyi* whether or not the site is bioaugmented. Understanding the driving forces behind *D. mccartyi* population selection and activity is improving predictability of remediation performance at chlorinated solvent contaminated sites.

Keywords: bioaugmentation, *rdhA* gene, *Dehalococcoides*, real-time PCR, chlorinated ethenes (CE), groundwater bioremediation, bioestimulation, reductive dechlorination

INTRODUCTION

There are thousands of public and private sites with chlorinated solvent groundwater contamination problems (McCarty, 2010). Chlorinated volatile organic compounds (cVOCs) such as tetrachloroethene (PCE) and trichloroethene (TCE) as well as their daughter products including the isomers of dichloroethene (DCE) and vinyl chloride (VC) are highly toxic compounds and TCE and VC are recognized human carcinogens by the National Toxicology Program. Clean-up of groundwater contaminated with these compounds takes time and is costly. Biostimulation (electron donor addition) and bioaugmentation (addition of inoculum) have gained significant acceptance as viable approaches for treatment of chlorinated ethenes in the subsurface (Stroo et al., 2010). The primary biotransformation mechanism for chlorinated ethenes in groundwater is reductive dechlorination under anaerobic conditions, which involves a stepwise replacement of Cl atoms with H atoms following the sequence: PCE, TCE, DCE (mainly cDCE), VC and finally non-toxic ethene (Maymó-Gatell et al., 2001; Duhamel et al., 2002, 2004; Cupples et al., 2003).

Diverse anaerobic microorganisms (e.g., *Dehalococcoides*, *Desulfitobacterium, Dehalobacter, Sulfurospirillum, Desulfuromonas, Geobacter, Dehalogenimonas*) can couple reductive dechlorination of chlorinated ethenes with growth in a process called organohalide respiration (Gerritse et al., 1996; Krumholz, 1997; Holliger et al., 1998; Luijten et al., 2003; Sung et al., 2006a; Moe et al., 2009). Nonetheless, dechlorination beyond DCE and VC has only been shown so far for members of the *Dehalococcoidales,* namely *Dehalococcoides* and *Dehalogenimonas* (Maymó-Gatell et al., 1997; Cupples et al., 2003; He et al., 2003; Duhamel et al., 2004; Sung et al., 2006b; Manchester et al., 2012; Yang et al., 2017). In practice, owing to subsurface heterogeneity, natural reductive dechlorination is incomplete in some locations, resulting in the accumulation of the daughter products cDCE and the carcinogen VC (Henry, 2010). This is generally attributed to poor mixing, lack of appropriate *Dehalococcoides mccartyi* organisms or electron donor, or inhibition of terminal dechlorination steps (Stroo et al., 2010).

Biostimulation and bioaugmentation with mixed cultures containing *D. mccartyi* can overcome stalling at cDCE or VC and reduce the time to clean up (Ellis et al., 2000; Major et al., 2002; Lendvay et al., 2003; Hood et al., 2008; Stroo et al., 2010; Dugat-Bony et al., 2012; Pérez-de-Mora et al., 2014; Kocur et al., 2016). The abundance of *D. mccartyi* in groundwater is most often assessed via quantitative PCR (qPCR) of the 16S rRNA gene (Rahm et al., 2006a; Lee et al., 2008; Hatt and Löffler, 2012; Hatt et al., 2013). While the abundance of *D. mccartyi* is general strongly correlated with dechlorination, sometimes dechlorination is still incomplete even at high abundance. The dechlorinating abilities of *D. mccartyi* strains is determined by the its complement of reductive dehalogenase genes and their activity. Thus, *D. mccartyi* strains with identical 16S rRNA may differ in the chlorinated compounds that they can respire and dehalogenate. Reductive dehalogenase enzymes (RDases) catalyze the cleavage of the carbon-halogen bond, and thus are an additional biomarker for tracking *D. mccartyi* strains. RDases are heterodimeric, membrane-bound enzymes, consisting of a catalytic active A unit of about 500 amino acids (aa) anchored outside of the cytoplasmic membrane by a small (100 aa) predicted integral membrane B subunit. These subunits are encoded by the so-called *rdhA* and *rdhB* genes, respectively (Smidt and de Vos, 2004). Due to their hydrophobic nature, oxygen sensitivity and complex association, only a few RDases have been biochemically characterized to date. Among these are the enzymes catalyzing the conversion of PCE to cDCE (coded by the *pceA* gene) and TCE to VC (coded by the *tceA* gene), as well as the RDases catalyzing the conversion of cDCE to ethene (coded by the *bvcA* and *vcrA* genes) (Magnuson et al., 1998, 2000; Krajmalnik-Brown et al., 2004; Müller et al., 2004; Fung et al., 2007; Tang et al., 2016). Quantitative PCR methods that target these specific genes have been developed and are being increasingly used as prognostic and diagnostic tools in the field to overcome the limitations of the 16S rRNA gene (Rahm et al., 2006b; Ritalahti et al., 2006, 2010; Lee et al., 2012; Lu et al., 2015).

The genomes of more than 10 *D. mccartyi* isolates have now been sequenced. These genomes are highly streamlined (∼1.4 Mb) and striking in their similarity, differing primarily in two regions termed High Plasticity Regions (HPR) on either side of the origin of replication (ORI). Each genome harbors many distinct full-length *rdh*AB homologous genes per genome (e.g., 17 in strain 195, 32 in strain CBDB1 and 36 in strain VS) (Kube et al., 2005; McMurdie et al., 2009; Seshadri et al., 2005). Hundreds if not thousands more putative *rdhAB* genes have been identified from metagenome sequencing efforts. Owing to the lack of functional characterization for most of this protein family, a sequence identity-based classification of orthologs into groups based on >90% aa identity was developed (Hug et al., 2013). This sequence-based classification was adopted prior to having a crystal structure to identify active site and other key residues. Fortunately, the two crystal structures recently solved (Bommer et al., 2014; Payne et al., 2015) support the original classification. The database of sequences and new ortholog groups continues to expand (Hug et al., 2013; Hug, 2016).

In this study, we aimed to distinguish different *D. mccartyi* strains from each other in mixed cultures and groundwater, where multiple *D. mccartyi* strains coexist. We define strains as genetic variants of *D. mccartyi* (e.g., differing in their *rdhA* complement) that have not necessarily been isolated as pure cultures. Our final aim was to better understand the contribution of native vs. introduced *D. mccartyi* to overall remediation at two contaminated sites where mixed dechlorinating culture KB-1 was used for bioaugmentation.

As it is very difficult to find unique regions within the genomes to distinguish strains, we decided to focus on quantifying a broader suite of *rdhA* genes, including both characterized and uncharacterized *rdhA* genes. We first compared the *rdh*A complement in the metagenome of the mixed culture KB-1 with those of eleven isolated *D. mccartyi* strains to identify *rdhA* sequences (and their corresponding Ortholog Groups) that are less commonly shared between strains. Methods for qPCR were developed for the selected *rdh*A genes and these assays were first tested in subcultures of KB-1 enriched on different chlorinated ethenes. Here, we hypothesized that a larger number of *D. mccartyi* strains should be present in the TCE-amended subcultures compared to those amended with cDCE, VC, or 1,2-DCA, because the latter have fewer dechlorination steps. Finally, we used the selected suite of *rdh*A genes to explore strain dynamics in groundwater samples from two sites that had been bioaugmented with KB-1.

MATERIALS AND METHODS

Cultures and Growth Conditions

The KB-1 consortium is a functionally-stable enrichment culture that originated from microcosms consisting of aquifer material from a TCE-contaminated site in southern Ontario (Duhamel et al., 2002). KB-1 is routinely maintained in batch mode with TCE as electron acceptor, and dechlorinates PCE through TCE, cDCE, and VC to ethene. A transfer from the original KB-1 culture has been grown and used commercially for more than a decade for bioaugmentation at cVOC-contaminated sites[1]. The main organisms in the KB-1 culture have been investigated over the years via clone libraries, qPCR and metagenome sequencing (Duhamel and Edwards, 2006, 2007; Chan et al., 2011; Hug, 2012; Hug et al., 2012; Waller et al., 2012). Two dechlorinating genera have been identified in the culture, namely *Dehalococcoides* and *Geobacter,* that are supported by many other organisms such as fermenters, acetogens, and methanogens (Hug et al., 2012; Waller, 2009). Many years ago, the original TCE-fed KB-1 enrichment culture was used to inoculate various sub-cultures maintained on different terminal electron acceptors (TCE, cDCE, VC and 1,2-dichloroethane [1,2-DCA]). These subcultures have been maintained with methanol (M), hydrogen (H_2), or a mixture of methanol and ethanol (ME) as electron donor. Supplementary Table S1 summarizes the main features and growth conditions of all the different cultures studied with the name format indicating electron acceptor amended/donor used and year created. The commercial KB-1 culture (KB-1®) is referred to as TCE/ME_2001_SiREM in Supplementary Table S1. All cultures were grown anaerobically in a defined minimum mineral medium (Duhamel et al., 2002). Cultures maintained at the University of Toronto are grown either in 0.25 L bottles sealed with screw caps with mininert valves or in 1 or 2 L glass bottles sealed with black butyl stoppers. Typically, bottles contained 10% by volume of headspace flushed with a N_2/CO_2 80%/20% as needed. These cultures are kept in the dark in an anaerobic glovebox at room temperature (22–25°C). At SiREM, KB-1 is grown in 100 L stainless steel vessels at 22–25°C. At the University of Toronto, dechlorinating cultures were typically re-amended every 2–3 weeks. Cultures maintained at SiREM are re-amended more frequently, typically every 3 to 4 days, as substrate is depleted.

KB-1 Metagenome Data and *rdh* Sequences

The parent KB-1 culture has been maintained at the University of Toronto since 1998 with TCE as the electron acceptor and methanol as the electron donor. This culture is referred to as "TCE/M_1998_Parent" in Supplementary Table S1 and all other KB-1 enrichments originated from this parent culture. The partially assembled metagenome sequence of TCE/M_1998_Parent is publically available at the Joint Genome Institute (JGI)[2]. Details on the extraction of genomic DNA for sequencing and the assembly of the KB-1 metagenome and of a draft chimeric genome *of D. mccartyi* strains are provided elsewhere (Hug et al., 2012; Islam et al., 2014). As the core genome of all *D. mccartyi* strains is almost identical, the search for unique non-coding regions in the metagenome yielded no positive results. The only differences found during comparative metagenomics were associated with the coding regions of the *rdhA* genes of the HPR regions. A total of 31 distinct *rdh*A gene sequences have been identified in the KB-1 cultures from multiple investigations (Hug, 2012; Hug and Edwards, 2013). Thirty sequences are associated with *D. mccartyi*, whereas one sequence is from the *Geobacter* population present in KB-1. Supplementary Table S2 compiles all previously identified KB-1 *rdhAB* sequences, which include the original 14 sequences found by Waller et al. (2005) as well as those identified more recently from metagenome sequencing (Hug et al., 2012) where an additional 13 *rdhAB* full sequences and two *rdhA* partial sequences were annotated (Hug and Edwards, 2013; Hug et al., 2013). For ease of reference and consistency, these additional *rdhAB* sequences have been renamed and are now deposited to Genbank under the accession numbers KP085015- KP085029 to replace the previous JGI gene locus tags (Supplementary Table S2).

Phylogenetic Analysis of *rdh*A Sequences

A total of 249 *D. mccartyi rdh*A sequences from sequenced and characterized isolated strains were retrieved from NCBI

[1]www.siremlab.com

[2]https://genome.jgi.doe.gov/portal/BioGr_2013843002/BioGr_2013843002.download.html

for phylogenic comparisons. These sequences include available sequences from eleven isolated and sequenced *D. mccartyi* strains, an incomplete set of 3 *rdhA* sequences from strain MB (available at the time of retrieval), and the *rdh*A sequences found in KB-1. The number of *rdhA* sequences contributed by each strain was as follows: 195 (17), Bav1 (10), BTF08 (20), CBDB1 (32), DCMB5 (23), FL2 (14), GT (20), GY50 (26), JNA (19), MB (3), VS (37), and KB-1 (28 [*Dhc*]+1 [*Geobacter*]). Two of the KB-1 *D. mccartyi rdhA* sequences and sequence VS_1308 are only partial sequences (less than 850 nucleotides) and were therefore not included in phylogenetic comparisons. Files containing all amino acid and nucleotide sequences as well as matching of tree nomenclature with protein names can be found in a folder labeled rdhA_Dhc_seq150420 at the following address: https://docs.google.com/folder/d/0BwCzK8wzlz8ON1o2Z3FTbHFPYXc/edit.

Phylogenetic analysis of *rdh*A nucleotide sequences, including bootstrapping, was performed with the ClustalX free software (version 2.0.12; University College Dublin[3]). All sequences were compared to each other by separate pairwise comparisons using the dynamic programming method with a gap opening of 10 (range of 0–100) and a gap extension of 0.1 (range 0–100). Results were then computed into a DNA weight matrix that determines the similarity of non-identical bases. Based on the DNA weight matrix, a dendrogram was constructed which in turn serves as guide for the final multiple alignment. Settings for the final multiple alignment were as follows: a gap opening penalty of 10 (range 0–100), a gap extension penalty of 0.2 (range 0–100), a delay divergent sequences switch set at 30% divergence and a DNA transition weight of 0.5 (range 0–1). The IUB weight matrix was used for computation. A phylogenetic tree was built using the Neighbor Joining (NJ) Algorithm with the same program. The NJ-tree was visualized and further edited with Figtree (version 1.4.0.1; Institute of Evolutionary Biology, University of Edinburgh[4]). The midpoint criterion was used for rooting.

A phylogenetic analysis based on *rdh*A amino acid sequences was also computed using the ClustalX v2.0.12. For computing the alignment, the following protein gap parameter options were considered: (i) the residue specific and hydrophilic residue penalties options were enabled, (ii) a gap separation distance of 4 (range 0–100) and (iii) no end gap separation, which treats end gaps the same way as internal gaps, was allowed. The phylogenetic tree was built using the Neighbor Joining (NJ) Algorithm and further visualized and edited with Figtree v1.4.0. As for the nucleotide-based phylogenetic tree the midpoint criterion was used for rooting. Ortholog groups were highlighted on the trees with Adobe Illustrator.

Groundwater Sampling and Site Description

Groundwater was collected from two TCE-contaminated sites prior to and after bioaugmentation with KB-1. The first site was located in Southern Ontario (ISSO site) and was characterized by contaminants in fractured bedrock. Supplementary Figure S1A shows details of relevant sampling dates and events related to this site. Samples corresponding to three different phases of the remediation were investigated: (i) predonor or pretreatment phase, (ii) biostimulation phase, consisting of the daily addition of ethanol as an electron donor and (iii) bioaugmentation phase, following the inoculation of KB-1 (Supplementary Figure S1A). At the ISSO site, a groundwater recirculation system consisting of two injection and three extraction wells was installed to improve the distribution of electron donor (ethanol) and microorganisms (Supplementary Figure S1B). During both the biostimulation and bioaugmentation phases, ethanol was added on a daily basis. Bioaugmentation with KB-1 consisted of one single addition of approximately 100 L of culture. Groundwater samples for molecular analysis were obtained from the composite pipeline, where groundwater from the three extraction wells was combined (Supplementary Figure S1B). Additional information on this site can be found in an earlier published study reporting on a microbial community survey at the site (Pérez-de-Mora et al., 2014).

The second site is located in the United Kingdom and consisted of a pilot test cell (30 m × 7 m × 4 m) for treatment of a DNAPL source area (∼1000 kg of DNAPL within the cell). The cell was conceived as an "in-Situ Laboratory" for investigating source area bioremediation (SaBRE project[5]). The relevant sampling dates and events related to this site and a sketch with sampling locations are shown in Supplementary Figures S2A,B. Samples for investigation were collected: (i) prior to any remediation action; and (ii) after donor addition of one single dose of donor SRS^{TM}, a commercially available emulsified vegetable oil (Terra Systems, Inc.) and bioaugmentation with KB-1 (Supplementary Figure S2A). Groundwater was collected from fully screened sampling wells (SW) at four locations within the test cell: (i) at the influent (INF); (ii) within the source zone (SW70); (iii) within the plume (SW75); and (iv) at the effluent (EFF), also within the plume. The test cell was operated initially for a 90-day baseline period to establish steady-state pre-treatment conditions. Groundwater was extracted at an average of 1.4 l per minute, corresponding to an average residence time within the cell of 45 days. A total of 2,400 kg of SRS^{TM} at a 5% concentration was used as the electron donor and injected along the test cell. Two weeks after donor injection approximately 65 L of KB-1 was added using the same injection ports that were used to add electron donor. Within the test cell, both TCE and cDCE were the main cVOCs. A dissolved phase plume emanating from the source and extending more than 400 m away was further characterized by the presence of VC and ethene.

The starting point (Day 0) was defined as the day following the end of the emulsified oil injection, which took approximately 1 week to complete. Further details on the SaBRE site can be found in technical bulletins freely available on the SaBRE-CL:Aire website (see above).

[3]http://www.clustal.org/clustal2/

[4]http://tree.bio.ed.ac.uk/software/figtree/

[5]http://www.claire.co.uk/index.php?option=com_content&view=article&id=53&Itemid=47

Nucleic Acid Extraction

Samples were collected from eleven different enrichment cultures at one or two times each during 2011 (Supplementary Table S1). Frozen DNA samples (−80°C) from the TCE/ME_2001_SiREM culture collected over 5 years were obtained from SiREM. DNA was also extracted from groundwater samples from the two field sites described above. For extraction and isolation of genomic DNA (gDNA), samples from cultures (10–50 mL) or groundwater (200–1000 mL) were filtered through Sterivex™ (Millipore, MA, United States) (0.22 μm pore size) filters using a centrifugal pump and dual-trap (two liquid traps in series) system. Filters were subsequently stored at −80°C until further processing. For gDNA extraction, the casing of the filter was opened and the filter cut in about 30 pieces of similar size. The latter were introduced into a 2 mL nucleic acid extraction tube containing buffers and beads (Mo Bio Laboratories UltraClean® Soil DNA Isolation Kit, CA, United States) and DNA extraction was completed following the manufacturer's instructions. Elution of nucleic acids from the silica membrane was performed using 50 μL of UltraPure™ DNase/RNase-Free distilled water (Invitrogen, CA) for samples from cultures as well as from the ISSO site in Canada, whereas 920 μL were used for elution of samples from the SaBRE site in the United Kingdom.

Quantitative PCR (qPCR) Amplification of Extracted DNA

Quantification of the 16S rRNA gene of *Dehalococcoides* and *Geobacter*-KB1 as well as a total of 15 *D. mccartyi rdhA* genes plus one *Geobacter rdh*A gene from the KB-1 culture was achieved via qPCR on an Opticon 2 thermocycler (MJ Research). Supplementary Table S3 provides details on the primer pairs used, their annealing temperatures and the length of the amplicon generated. With the exception of five genes (KB1-6/*bvcA*, KB1-14/*vcrA*, KB1-27/*tceA*, KB1-1 and KB1-5), new primers were designed for all other *rdhA* genes in this study. The specificity of the primers was tested *in silico* against the public NCBI NR nucleotide database and tested *in vitro* against DNA extracted from mixed dechlorinating and non-dechlorinating cultures. Supplementary Table S4 shows the number of mismatches for each primer pair with sequences belonging to the ortholog group of the targeted *rdhA* gene. The PCR reaction (20 μL) consisted of: 10 μL of SsoFast™ EvaGreen® Supermix (Bio-Rad, CA), 0.5 μL of each primer (10 mM), 7 μL of UltraPure™ DNase/RNase-Free distilled water (Invitrogen, CA) and 2 μL of template. The amplification program included an initial denaturation step at 98°C for 2 min followed by 40 cycles of 5 s at 98°C and 10 s at the corresponding annealing temperature. A final melting curve from 70 to 95°C degrees at increments of 0.5°C per second was performed. Since two concentrations were tested per template (undiluted and 10-fold diluted) for assessment of potential matrix-associated inhibitory effects, reactions for each dilution were performed in duplicate. The undiluted sample generally contained between 10–20 ng of DNA per μL as measured using a Nanodrop spectrophotometer (Thermo Scientific, DE). Generally, there was good agreement between the two measurements. Ten-fold serial dilutions of plasmid DNA containing one copy of the 16S *rRNA* gene or the *rdhA* gene (∼1000–1500 bases) were used as calibrators. Plasmids for calibration were prepared by PCR amplifying the desired *rdh*A from KB-1, inserting the gene into the pCR 2.1 PCR vector and subsequently transforming the construct into TOP10 *Escherichia coli* competent cells (Invitrogen, CA) as per the TOPO TA cloning® kit (Invitrogen, CA). Plasmid DNA was purified using the GenElute™ Plasmid Miniprep Kit following the manufacturer's instructions (Sigma-Aldrich, MO). DNA was eluted using 50 μL of Ultra Pure DNase/RNase-free distilled water (Invitrogen, CA). Standard curves exhibited linear behavior ($R^2 > 0.990$) when plotted on a logarithmic scale over seven orders of magnitude. Supplementary Table S5 provides the details on the standard curves for each primer pair, including slopes (efficiencies), *Y*-intercepts and calibration model fit. The specificity of the amplicons was checked by melt curve analysis as well as by agarose gel electrophoresis for selected samples. Non-template controls were included in each run. Absolute gene copy concentrations for all cultures and field samples are provided as Supplementary Tables S6–S8. The method detection limits (MDLs) were expressed in terms of gene copies per L of groundwater or per mL of culture and varied depending on the volume of sample filtered and the volume employed for elution of DNA from the purification column. The MDLs for each set of samples are provided in Supplementary Table S9.

Cluster Analysis of *rdh*A Sequences and Calculation of *rdh*A/16S rDNA *Dhc* Ratios

Phylogenetic analysis of *rdh*A nucleotide and amino acid sequences, including bootstrapping, was performed with the ClustalX free software (version 2.0.12; University College Dublin[6]). Protein sequences were clustered into ortholog groups as previously defined [90% pairwise identity in amino acid alignments as per (Hug et al., 2013)]. The similarity of the *Dehalococcoides* populations in the various KB-1 subcultures was investigated on the basis of their *rdhA* fingerprints (*rdhA*/16S rRNA gene *Dhc* ratios) by means of hierarchal cluster ordination analysis. The latter was performed with the free software Hierarchal Clustering Explorer (HCE) (version 3.5; Human-Computer Interaction Lab, University of Maryland[7]). The Unweighted Pair Group Method with Arithmetic Mean (UPGMA) was used as linkage clustering method, whilst Pearson's correlation coefficients were used to construct the similarity distance matrix. Heatmaps generated with the HCE v3 software were further edited manually for scale optimization in Excel 2010.

RESULTS AND DISCUSSION

Reductive Dehalogenase (*rdhA*) Genes in the KB-1 Consortium

As the core genome of all *D. mccartyi* strains is almost identical, the metagenome search for unique non-coding regions that could

[6]http://www.clustal.org/clustal2/

[7]www.cs.umd.edu/hcil/hce/

differentiate different strains yielded no positive results. As a consequence, efforts were turned to the complement of *rdhA* genes, which does vary significantly between strains. To visualize sequence similarities, we constructed phylogenetic trees using 249 amino acid (**Figure 1**) and nucleotide (Supplementary Figure S3) sequences that included all full RdhA sequences found in the KB-1 metagenome as well as those identified in 11 isolated and sequenced *D. mccartyi* strains. Amino acid sequences belonging to the same ortholog group (OG), defined as having >90% PID (Hug et al., 2013), are highlighted in different colors on the phylogenetic trees. These highlighted branches clearly support the classification and reveal how some RdhA sequences are common to all strains, while others only in a few (**Figure 1**). When the same sequences are compared at the nucleotide level (Supplementary Figure S3) identity within an ortholog group can be substantially lower than 90%. The terminology reductive dehalogenase *homologous* genes (*rdhA*) was adopted years ago, and perhaps implies more knowledge of common ancestry than is in fact known; still, it is not unreasonable to suspect that these genes arose from either speciation (orthologous) or duplication

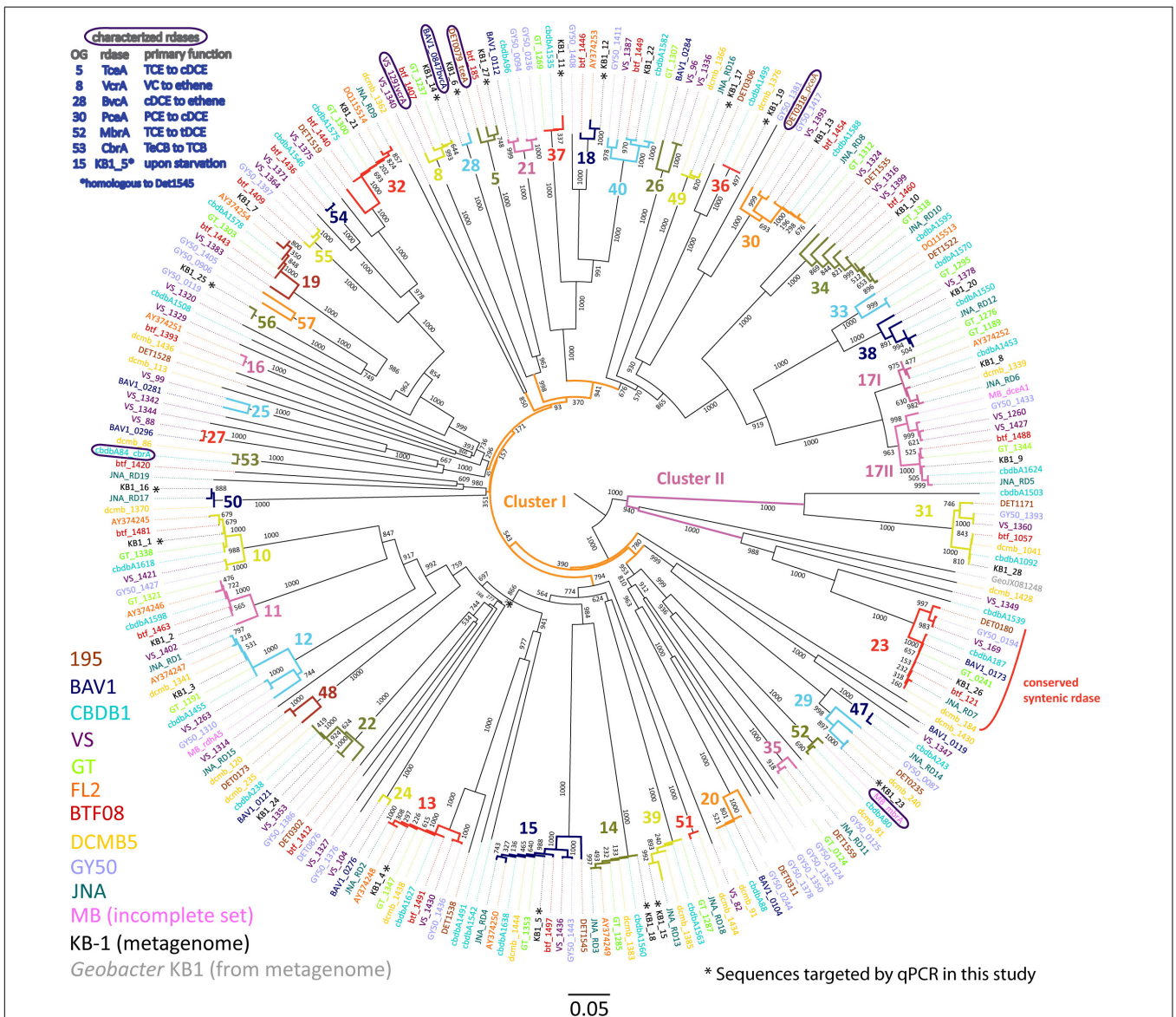

FIGURE 1 | Phylogenetic tree of *Dehalococcoides mccartyi* reductive dehalogenases based on amino acid sequences. Tree includes sequences predicted from 248 *rdhA* genes found in eleven isolated *D. mccartyi* strains as well as those found in the mixed dechlorinating culture KB-1, including the *rdhA* gene sequence found in *Geobacter* KB-1 as an outgroup. The scale is the number of substitutions per amino acid. Bootstraps are shown at tree nodes. Sequences names are colored corresponding to their source as shown in the legend at bottom left. The numbers and different branch colors highlight ortholog groups (OGs) where sequences have >90% PID. Sequences corresponding to characterized RDases are circled and their substrates shown in the top right legend (chlorinated substrate abbreviations as in text, plus TeCB, tetrachlorobenzene; TCB, trichlorobenzene).

(paralogous) events. Herein we use the term "ortholog" to refer to *rdhA* genes that group together according to the classification system cited above. The term "homologous" is used to refer to all *rdhA* genes regardless of which ortholog group they belong to.

The phylogenetic analysis of 249 *D. mccartyi* RdhA sequences generated a total of 43 ortholog groups (OG) including 6 previously un-described groups (OG 52 to 57). Of the 249 sequences analyzed in 2016, 37 sequences remained ungrouped, meaning without a single ortholog (**Figure 1**). At the amino acid level, none of the KB-1 *D. mccartyi* RdhA sequences is unique because each is more than 90% similar to a sequence in at least one other *D. mccartyi* strain. The existence of numerous shared *rdhA* genes among *D. mccartyi* is consistent with their co-localization with insertion sequences and other signatures for horizontal gene transfer, and within genomic islands in high plasticity regions (McMurdie et al., 2009).

Selection of Suite of Distinguishing KB-1 *rdh*A Genes

We selected a total of 15 characterized and uncharacterized *rdhA* sequences to track using qPCR. Ten uncharacterized *rdhA* sequences, KB1-25 (OG56), KB1-11 (OG37), KB1-12 (OG18), KB1-16 (OG50), KB1-17 (OG 49), KB1-19 (OG36), and KB1-23 (OG29), were selected as those with the fewest orthologs in other strains based on our trees (**Figure 1** and Supplementary Figure S3). KB1-15 (OG39) and KB1-18 (OG14) were selected because they were found on the same contig in the KB-1 metagenome and both share homology to genes in strains GT, CBDB1, DCMB5, and JNA, therefore they may be mobilized together (**Figure 1**). We included KB1-4 (OG13) because it appears to have orthologs in all other strains and could be useful for normalization, similar to the 16S rRNA gene. To this set of 10 uncharacterized genes, we added five more genes of interest: KB1-1 (OG10), KB1-5 (OG15), KB1_14/*vcrA* (OG8), KB1_6/*bvcA* (OG28) and KB1_27/*tceA* (OG5). KB1-1 and KB1-5 were selected because their corresponding proteins have previously been detected in KB-1 (Tang et al., 2013; Liang et al., 2015). Furthermore, KB1-5 (OG 15) which is expressed upon starvation, is orthologous to DET1545 from Strain 195 (Rahm and Richardson, 2008; Tang et al., 2013). KB1_14, KB1_6 and KB_27 correspond to the functionally-characterized vinyl chloride and trichloroethene reductases VcrA, BvcA, and TceA, respectively. We designed qPCR primers to these 10 uncharacterized genes, and used previously designed primers for the remaining 5 genes (Supplementary Table S4). Next we monitored the abundance of this suite of *rdhA* genes in DNA samples from 11 different KB-1 enrichment sub-cultures maintained over years on different chlorinated electron acceptors (Supplementary Table S1).

Quantification of *rdh*A Genes in KB-1 Enrichments With Different Chlorinated Electron Acceptors

To reflect shifts in *D. mccartyi* populations, qPCR results for each sample are presented as *rdhA* gene copies divided by 16S rRNA gene copies to provide an approximation of the relative proportion of each *rdhA* gene per *D. mccartyi* genome. *D. mccartyi* are known to harbor only one copy of the 16S rRNA gene per genome. *rdhA*/16S rRNA ratios were visualized using heatmaps with values ranging from above 0.6 (where more than 60% of all *D. mccartyi* genomes in the culture contains that gene) to less than 0.001 (where the gene is present in fewer than 0.1% of the *D. mccartyi* populations) (**Figure 2**). Although the primers were designed to target specific KB-1 *rdhA* sequences, most sequences within the same ortholog group would likely also be amplified. Supplementary Table S4 compiles all mismatches found between primers used and other sequences in the corresponding OG.

Dehalococcoides mccartyi rdhA/16S rDNA gene copy ratios measured in KB-1 enrichment cultures (**Figure 2**) revealed more variability of *D. mccartyi* strains than anticipated, considering the number of years of enrichment and the fact that they all originated from a common parent culture. Clustering analysis revealed *rdhA* genes common to all cultures and *rdhA* gene specific to a particular chlorinated electron acceptor. For instance, all subcultures were found to contain KB1-1 (OG10) (ratios all greater than 0.6), and to have consistently abundant *rdhA* sequences of KB1-4 (OG13) and KB1-5 (OG15), and KB1-14 (*vcrA*; OG8). The most striking finding (**Figure 2A**) is the clustering of specific patterns with terminal chlorinated electron acceptor. The VC enrichments show the lowest diversity of *rdhA* sequences and the most concordance between enrichments. These enrichments contain high abundances of 6 genes (KB1-1, KB1-14/*vcrA*, KB1-11, KB1-4, KB1-15, and KB1-18) with more variable but still abundant presence of KB1-5, KB1-23 and KB1-12. Other *rdhA* sequences are near or below detection. The cDCE enrichments form their own cluster, distinct from the VC enrichments, because they contain significant abundance of the KB1-6/*bvcA* gene, and much lower proportions of KB1-23 and KB1-12. These cDCE enrichments were the only ones consistently enriched in *bvcA*. The 1,2-DCA enrichments also formed a distinct cluster characterized by high ratios for KB1-16, KB1-17, KB1-19, KB1-25 as well as KB1-27/*tceA*. Finally, the TCE cultures reflect a blend of all the other enrichments, showing more variability, although favoring an *rdhA* ratio pattern most like the VC enrichments.

The clustering analysis also revealed co-variation among some of the *rdhA* genes regardless of the enrichment, suggesting co-location of these genes on the same genome as is the case of KB1-15 and -18, and possibly also KB1-16, -17, -19, and -25 (**Figure 2A**). The *Geobacter rdhA* gene was detected at similar abundance to the *Geobacter* 16S rRNA gene only in the TCE-amended cultures (at approximately 15–25% of *Dhc* abundance); in all other enrichments *Geobacter* 16S rDNA and *rdhA* genes were below the detection limits (Supplementary Tables S6, S7), as expected since *Geobacter* only dechlorinates PCE or TCE as far as cDCE. In control DNA samples from cultures without *D. mccartyi,* copies of *rdhA* genes were all below the MDL (data not shown).

The stability of the *rdhA* fingerprints over time was also assessed. For the VC, 1,2-DCA and cDCE enrichments, two samples from the same enrichment culture bottle were analyzed at 4 or 9 month's intervals (January and October or June and

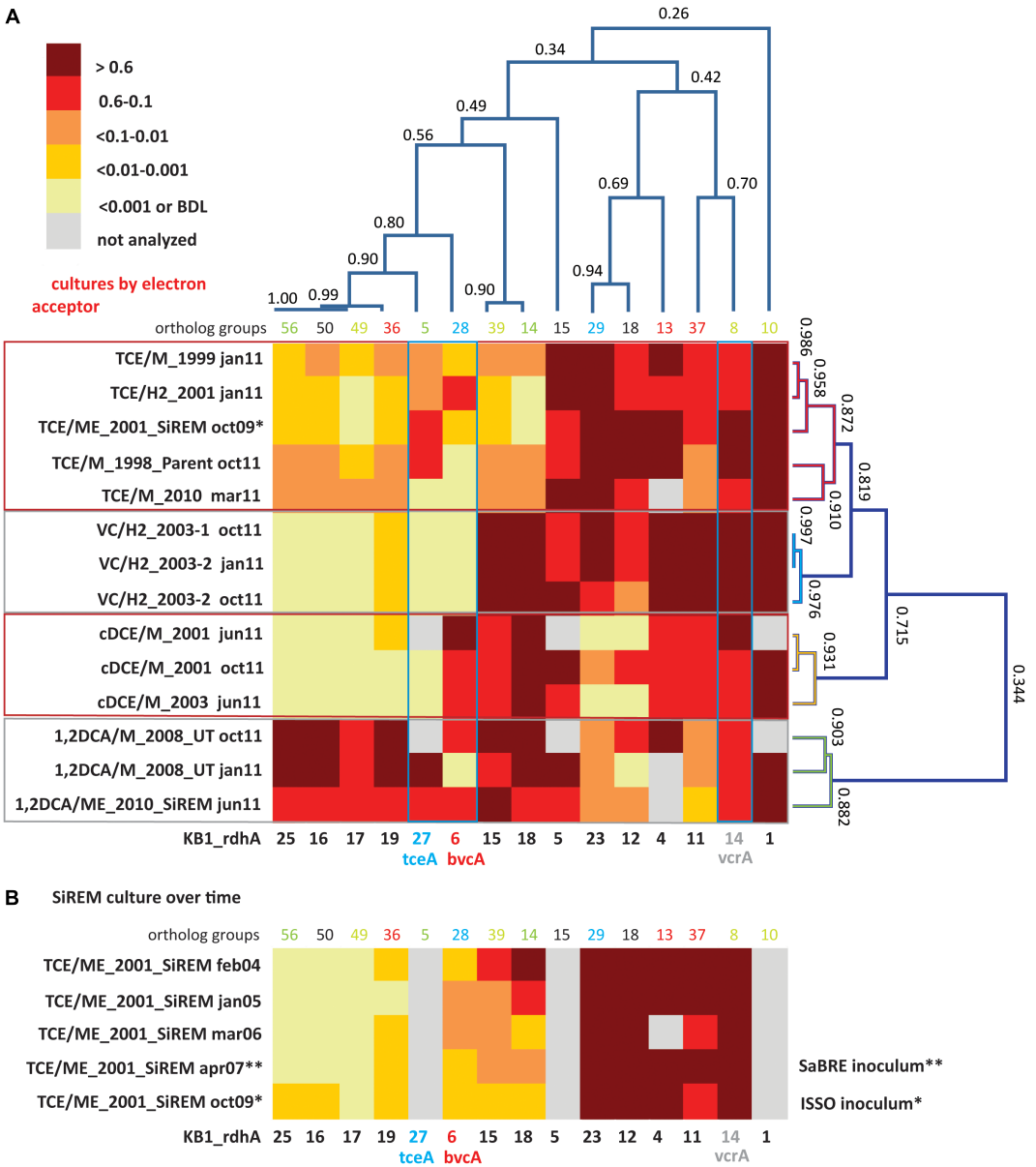

FIGURE 2 | Cluster analysis and heatmaps showing *D. mccartyi rdhA*/16S rRNA gene copy ratios measured in KB-1 enrichment cultures. **(A)** Shows how data clustered by the chlorinated electron acceptor amended to individual enrichment cultures as well as by *rdhA* sequence. The name format indicates electron acceptor amended/donor used_year created, followed by date sampled (e.g., TCE/M_1999 jan11 is a TCE and methanol enrichment culture first established in 1999 and sampled in January of 2011). The numbers on the cluster branches of both axes indicate the percentage similarity between samples based on the Pearson's correlation coefficient. **(B)** It is a heatmap of *rdhA*/16S rRNA gene copy ratios in the SiREM KB-1 culture over 5 years. Cultures indicated with * or ** are those used for bioaugmenting field sites in 2007 (SaBRE) and 2009 (ISSO).

October, 2011; **Figure 2A**). There was good agreement between the two time points, although small differences likely reflect changes in relative abundance of *D. mccartyi* strains in batch incubation conditions. For the TCE/ME_2001_SiREM culture, five DNA samples over a time span of 5 years (2004, 2005, 2006, 2007, and 2009) were available, and were investigated using a subset of *rdhA* genes (**Figure 2B**). The *rdhA* fingeprint was relatively stable over time except for three *rdhA* genes, namely KB1-18, KB1-15, and KB1-6/*bvcA*. Ratios for KB1-18 and KB1-15 gradually shifted from greater than 0.6 in 2004 to less than 0.01 and even less than 0.001 by 2009. KB1-6/*bvcA* ratios fluctuated over this time period between 0.01 and 0.1. As noted already, KB1-18 and KB1-15 appear to co-vary, supporting their co-localization in the same genome. These two genes are abundant in VC, cDCE, and 1,2-DCA enrichment cultures but not in the TCE enrichments and diminished over time in the TCE/ME_2001_SiREM. These data reveal that the dominant VC-dechlorinating, *vcrA*-containing *D. mccartyi* strains are not

the same in the TCE and VC enrichment cultures. It appears that the dominant *D. mccartyi* strain more recently present in the VC/H_2 sub-cultures is more similar to the one that was originally present in the parent culture, and that this population has been gradually surplanted in TCE/ME_2001_SiREM culture. This data indicates that a major shift can also happen in the *rdhA* fingerprint of a mixed culture even when maintained consistently on the same electron acceptor. This is different to the wholesale changes observed when the electron acceptor is changed, where a shift in the dominant *D. mccartyi* population may happen much faster, as demonstrated in studies by Mayer-Blackwell et al. (2014, 2016) where the dominant *D. mccartyi* population in a bioreactor shifted over a period of 50–100 days when the electron acceptor was switched for 1,2-DCA from TCE. In the field, significant changes in *Dhc* populations may also be expected within a few months due to changing conditions: for instance, in electron acceptor availability.

The clustered data for 15 *rdhA* genes across 14 DNA samples from 11 different cultures yielded four major groups corresponding to each of the four chlorinated electron acceptors (**Figure 2A**). To create a more visual representation of the distribution of these *rdhA* genes in the two High Plasticity Regions (HPRs) of *D. mccartyi* genomes, we mapped corresponding OG groups in the order and HPR they typically appear in published genomes (**Figure 3**). This map provides evidence not just of multiple strains but also of likely gene insertions and/or deletions (e.g., bvcA in the HPR1). As indicated previously, the considerable variability in the *rdhA* to 16S ratios within each culture and electron acceptor group was at first very surprising, because the cultures all derive from the same parent and have been enriched for so long on the same substrate. We expected to see only one clearly dominant population, especially in the VC to ethene and 1,2-DCA to ethene cultures that involve only a single dechlorination step. What the data show instead is a more complex pattern in each group, suggesting the presence of more than one *D. mccartyi* population even in the single-dechlorination step, highly enriched VC/H_2 cultures. We repeated many of the DNA extractions and qPCR reactions to verify results, with no appreciable changes. Recent analysis of these enrichments yielded similar results (data not shown). Early experiments by Duhamel et al. (2002, 2004) and Waller et al. (2005) had identified at least two distinct *D. mccartyi* populations (KB1-PCE and KB1-VC), the former containing KB1-6 (*bvcA*) and the latter not; these two strains could actually also be distinguished by a single nucleotide difference in their 16S rRNA sequences (Duhamel et al., 2004). Subsequently, Hug (Hug, 2012) was unable to close the assembly of a *D. mccartyi* genome from the KB-1 TCE/M_1998 parent culture metagenome, particularly in the high plasticity regions rich in *rdhA* genes, because of the presence of multiple, highly similar *D. mccartyi* populations. Considering the cluster diagram by enrichment culture (**Figure 2A**; right side), we can perhaps

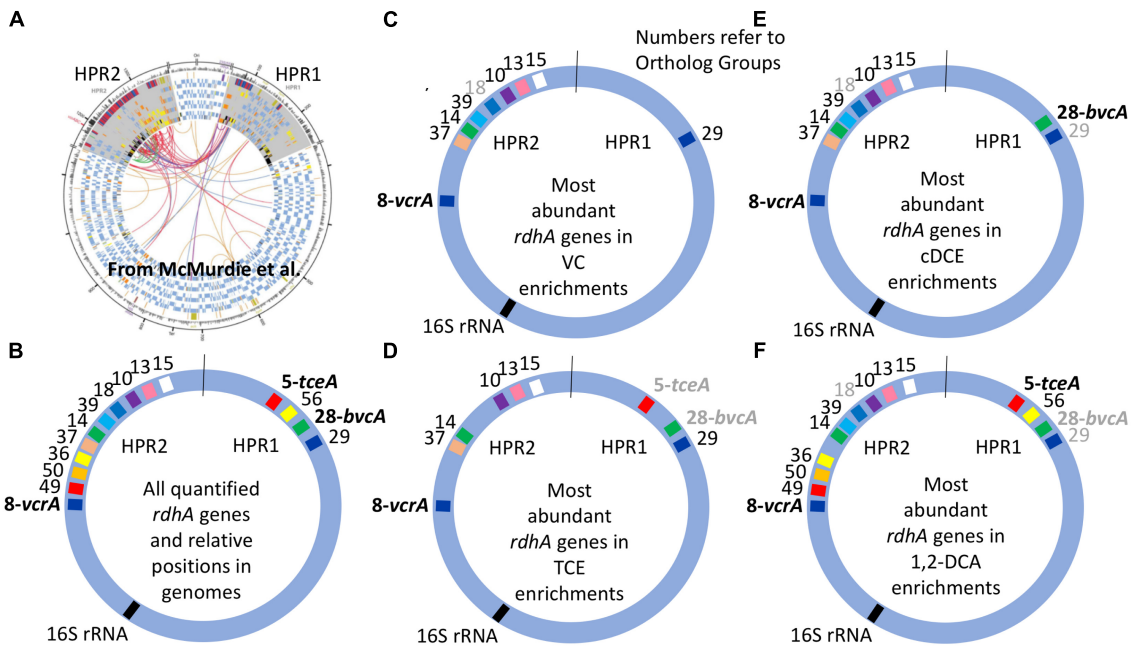

FIGURE 3 | Distribution of most abundant *D. Mccartyi* reductive dehalogenase homologous (*rdhA*) genes quantified in KB-1 enrichment cultures. RdhA sequences are represented by their corresponding ortholog group (OG) numbers and relative positions in High Plasticity Regions (HPR) 1 and 2, as defined by McMurdie et al. (2009).) **(A)** Circular map of four *Dehalococcoides* genomes reproduced from McMurdie et al. (2009), illustrating the two high plasticity regions where most *rdhA* genes are found; origin is at top. **(B)** Relative position of all of the rdhA sequences quantified by qPCR in this study. **(C–F)** Most abundant *rdhA* genes detected in the respective enrichment culture samples, with evidence for considerable strain variation within and between enrichment cultures. OG numbers that are gray correspond to genes that are abundant in only some of the samples from the respective enrichments. See Supplementary Table S3 or **Figure 1** for correspondence between OG and KB-1 *rdhA* numbers.

infer at least four distinct populations based on *rdhA* distribution in the TCE enrichments, at least two in the VC enrichments (one with and one without *rdhA* KB1-12 (OG18), at least two in the cDCE enrichments and three in the 1,2-DCA enrichments (**Figure 3**). In an attempt to verify these results, we sequenced metagenomes from representative VC, cDCE, and 1,2-DCA enrichments. Sequencing has confirmed the presence of multiple distinct *D. mccartyi* genomes in all enrichment cultures, even in the VC enrichments, upholding these results (data not shown; manuscript in preparation). The co-existence of multiple *D. mccartyi* strains at different cell densities within these enrichments likely arises from subtle substrate preferences of the expressed reductive dehalogenases and competition for available nutrients and vitamins. Functional characterization of some reductive dehalogenases reveals substrate overlap yet specific substrate preferences as observed for BvcA and VcrA (Yan et al., 2012). Moreover, availability and type of corrinoid can alter rates of dechlorination for certain enzymes (Yan et al., 2016). Low abundance populations may persist in these cultures because they are maintained in batch mode, with infrequent medium changes and thus long residence times from 30 to 100 days.

Quantification of *rdhA* Genes in Site Groundwater

A suite of 12 *rdhA* genes representative of both dominant and minor *D. mccartyi* strains was used to monitor population shifts before and after bioaugmentation with KB-1 (TCE/ME_2001_SiREM) at two TCE-contaminated sites: one in Canada (ISSO) and another site in the United Kingdom (SaBRE). At the United Kingdom site, the abundance of *Geobacter* 16S rRNA and *rdh* genes were also monitored.

The results from the Canadian ISSO site revealed that the two most abundant *rdhA* genes in native populations (monitored prior to any treatment) were orthologs to KB1-4 and KB1-6/*bvcA,* but that their titers were barely above detection limits, at approximately 3×10^5 copies per L (Supplementary Table S8). Although the *bvcA*-encoded dehalogenase is known to catalyze the dechlorination of cDCE all the way to ethene (Holmes et al., 2006), there was little dechlorination beyond cDCE before electron donor amendment (Pérez-de-Mora et al., 2014). During biostimulation with electron donor prior to bioaugmentation, *D. mccartyi* and *vcrA* copy numbers increased significantly, reaching a *vcrA*/16S rRNA gene ratio near one (**Figure 4A**), indicating growth of *vcrA*-bearing native populations. The abundance of *rdhA* genes orthologous to KB1-11, KB1-15, KB1-18 also increased during this period (**Figure 4A**). After bioaugmentation with KB-1, the *rdhA* profile did not change substantially, even though higher ethene concentrations and faster dechlorination were observed (**Figure 4A**). A reduction of the *bvcA*/16S rRNA gene ratio from ∼0.5 to 0.1 was the most notable change during this period (**Figure 4A**). The native populations that grew upon electron donor addition (prior to inoculation) harbored orthologs of 6 out of the 12 KB-1 *rdhA* genes monitored. From the data after bioaugmentation, it is clear that the dominant *D. mccartyi* populations from the KB-1 inoculum were not the ones responsible for the enhanced ethene production observed because KB1-12 and KB1-23 sequences that were dominant in the inoculum were not enriched in samples from the site. Instead a low-abundance *D. mccartyi* population in the inoculum grew at the site or, alternatively, bioaugmentation may have provided supporting organisms that enhance dechlorination of VC by the native *D. mccartyi.* This result is in agreement with previous analyses of data from this site (Pérez-de-Mora et al., 2014) that suggested that growth of a *Bacteroidetes* present in KB-1 capable of ethanol fermentation enhanced ethenogenesis after bioaugmentation. Other fermenters or acetogens capable of producing the lower base of vitamin B12, namely dimethylbenzimidazole (DMB), which is required by VcrA, may have grown at the site, although this could not be shown for the known strains in KB-1.

The *rdhA* survey also revealed *D. mccartyi* population shifts as dechlorination progressed in the field (**Figure 4A**). Specifically, prior to any active treatment and when cDCE was the dominant cVOC, *bvcA* and KB1-4 were the most abundant *rdhA* genes found, a feature only seen with the cDCE enrichments in the KB-1 subculture survey. During biostimulation with electron donor, there was a gradual decrease in cDCE concentration and an increase in the concentration of VC and ethene. After 15 months of biostimulation (Month 18), the relative abundance of several other *rdhA* genes increased to above 10%, including genes similar to KB1-11, KB1-15, KB1-18, and especially *vcrA* (**Figure 4A**). This parttern of *rdhA* genes was also seen in the KB-1 VC enrichments. Three months after bioaugmentation (Month 22), the proportion of ethene relative to VC and cDCE further increased. Here, the *bvcA* ratio decreased to less than 0.1 while the *vcrA* ratio remained at approximately 1. At Month 30, when there was almost no VC or cDCE left, the *vcrA* ratio returned to below 0.6. At this time, relative abundance of KB1-12 decreased substantially; these *rdhA* was also found to vary between enrichment cultures.

Ratios describe shifts in the underlying *D. mccartyi* strains, but the absolute abundance of *D. mccartyi* is also relevant to observed dechlorinating activity. Major changes in absolute abundance of *rdhA* genes KB1-11, KB1-15, KB1-18, and KB1-14/*vcrA* were observed as well, starting from below detection limit ($<\sim 10^5$ copies L^{-1}) up to 0.9–3 $\times$ 10^6 copies L^{-1} (Supplementary Table S8). The abundances of *vcrA* and *D. mccartyi* 16S rRNA genes increased up to the end of the monitoring period (Month 30) reaching concentrations of 1.6×10^6 and 6×10^6 copies L^{-1}, respectively. For the *rdhA* genes KB1-12 and KB1-23, characteristic of the dominant *D. mccartyi* populations in the inoculum (**Figure 4A**), there was no such significant change, further indicating that this population did not contribute to the enhanced dechlorination observed after bioaugmentation.

The *rdhA* gene suite also was used to investigate groundwater from the SaBRE bioaugmentation trial within a test cell at a TCE-contaminated site in the United Kingdom. Prior to any treatment, *D. mccartyi* gene copy numbers were below the detection limit ($<6 \times 10^4$ gene copies L^{-1}) in all wells studied except the effluent (EFF) location where *D. mccartyi* titers of about 10^5 gene copies L^{-1} were detected (data not shown).

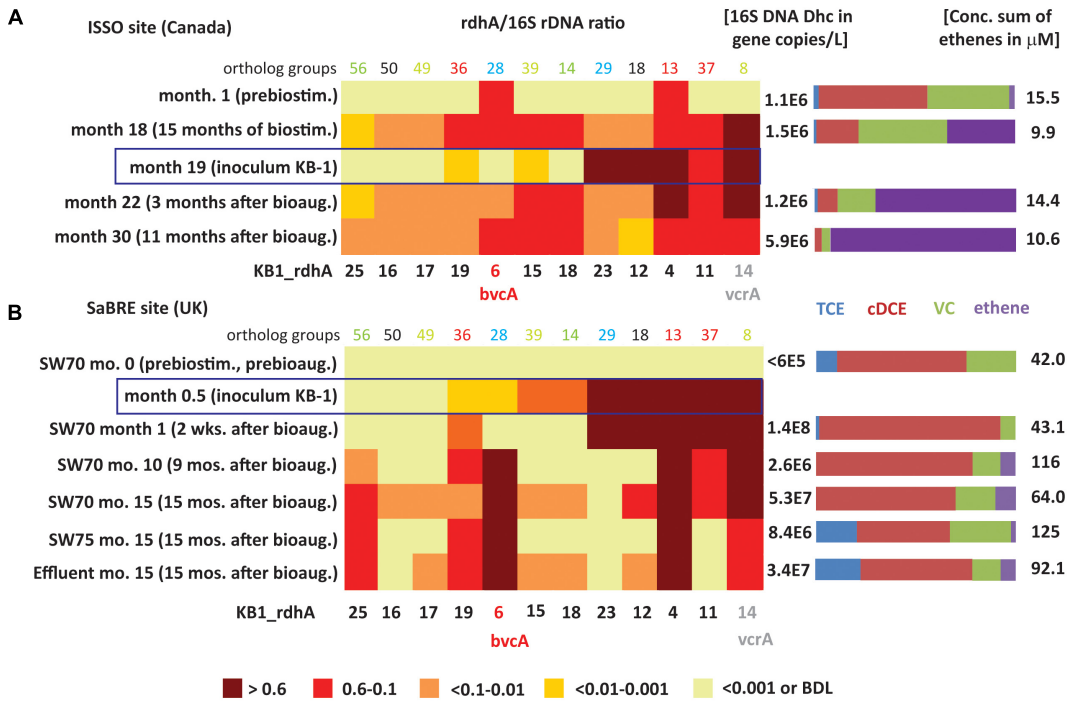

FIGURE 4 | Heatmaps showing *D. mccartyi rdhA*/16S rRNA gene copy ratios in field samples. **(A)** Canadian ISSO site. **(B)** United Kingdom SaBRE site. Corresponding absolute copies of *D. mccartyi* per L and concentrations of chlorinated ethenes are represented on the right side of each panel. Data from the ISSO site are from the composite pipeline (see Supplementary Figure S1). Data from the SaBRE site are from the influent (INF), sampling wells (SW70 and SW75) and effluent (EFF) of the test plot (see Supplementary Figure S2).

No significant VC and ethene concentrations were measured in these wells prior to treatment. Unfortunately, no samples were collected during biostimulation prior to inoculation of KB-1 (all data provided in Supplementary Table S8). Two weeks after bioaugmentation with KB-1 and about a month after a single donor addition event, *D. mccartyi* titers increased by three orders of magnitude in SW70, reaching 10^8 gene copies L^{-1} (Supplementary Table S8). In a sample from this well, all KB-1 biomarkers characteristic of the original inoculum, that is KB1-4, KB1-11, KB1-12, KB1-14/*vcrA*, and KB-23 were found to have *rdhA* ratios greater than 0.6 (**Figure 4B**). The KB-1 *Geobacter* 16S rRNA gene and the *Geobacter rdhA* gene were also detected at significant titers in the range 0.8–4.6 × 10^7 copies L^{-1} (Supplementary Table S8). These data indicate that the dominant KB-1 *D. mccartyi* strain in the inoculum grew within the test cell, at least in the vicinity of this particular well (SW70).

In samples from SW-70 taken 10 and 15 months after donor addition, the ratios of KB1-11, KB1-12, and KB1-23, abundant in the inoculum and at 1 month, gradually decreased from values greater than 0.6 down to 0.1 (**Figure 4B**). The decrease of the ratio for KB1-23 was even more pronounced with a conservative estimate of 0.001 at month 15. Over the same time, the *vcrA* ratio remained greater than 0.6, while the *bvcA* ratio increased from less than 0.01 to about one (**Figure 4B**), indicating a dramatic shift in the dominant *D. mccartyi* strains with time in this well. A feature of this site was the consistently high concentrations of cDCE that seems to have led to the growth of *bvcA*-containing strains. At month 15, downgradient sampling locations SW75 and EFF were dominated by KB1-6/*bvcA*, KB1-4 and KB1-14/*vcrA*, and were similar to well SW70. At the influent (INF) sample location, upgradient of where the inoculum was added, gene copy numbers of *D. mccartyi* and *rdhA* genes were all below their detection limits. Curiously, the *rdhA* and 16S rRNA genes from *Geobacter* were detected at levels just above the detection.

The Canadian ISSO and United Kingdom SaBRE sites differed in many ways. The former Ontario site had one order of magnitude lower cVOC concentrations, more complete dechlorination to ethene, a more-readily fermentable substrate (ethanol vs. emulsified oil) and a recirculation system that provided better mixing of substrates and microorganisms. The SaBRE site had higher concentrations of VOCs, giving rise to higher microbial and ethene concentrations than at the Canadian site, although the dominant compound at the site was cDCE. Particularly interesting at the SaBRE site was the co-presence of both *vcrA* (KB1-14) and *bvcA* (KB1-6) after month 10 at SW70 and after month 15 at both SW75 and Effluent. Co-presence of *bvcA* and *vcrA* at field sites has been reported in various studies, with greater abundance of *bvcA* over *vcrA* at some sites and vice versa at others (Lee et al., 2008; Carreon-Diazconti et al., 2009; van der Zaan et al., 2010; Atashgahi et al., 2017). Such differences have been attributed to redox potential, with *bvcA* perhaps more abundant under less reducing conditions

(van der Zaan et al., 2010). The redox potential at SaBRE was relatively low (−200 to −400 mV) and consistent over the length of the cell and the experimental time. Based on our laboratory cultures enriched with cDCE, it seems more likely that the high concentrations of cDCE and VC at a site exerted significant selective pressure on *D. mccartyi* strains harboring different *rdhA* genes, mimicking what we also observed in enrichment cultures.

Our results show that tracking specific *rdhA* fingerprints is challenging due to growth of minor populations of *D. mccartyi* either from native or inoculum-derived strains. Still, the approach employed in this study did reveal significant differences regarding the growth of the bioaugmented inoculum at the two sites. In future studies, it will be necessary to first identify site-specific *rdhA* genes that are not present at all in bioaugmentation cultures like KB-1, to track growth of indigenous populations. Perhaps a screening approach such as outlined in Hug and Edwards (2013) based on a set of 46 primer pairs to all known *rdhA* sequences, or the approach by Mayer-Blackwell et al. (2014) should be used to identify *rdh* genes in native strains prior to bioaugmentation. Then subsequent screens may be more discriminating.

More significantly, this study found clear selective pressure on *D. mccartyi* populations from the most abundant terminal chlorinated electron acceptor present. In both field samples and in well-established enrichment cultures, we found that *D. mccartyi* are not a homogeneous population but rather a complex and diverse mixture of strains harboring different complements of *rdhA* genes that respond and perhaps adapt selectively to external conditions – in particular electron acceptor – as revealed herein by monitoring *rdhA*/16S rRNA gene of *Dhc* ratios. The success of biostimulation and bioaugmentation approaches relies on the growth of populations with enzymes that actively convert chlorinated ethenes past VC to ethene. It seems that specific *rdhA* sequences confer populations and, by extent, mixed dechlorinating cultures, with fitness advantages depending on their local environment, and suggests that bioaugmenting with more refined cultures acclimated to intermediates like cDCE or VC that tend to accumulate at some sites may help to overcome stall and achieve complete dechlorination at some contaminated sites.

This study also underpins the need to further understand the role of horizontal gene transfer in these dechlorinating communities as suggested by the insertion/deletion of *rdhA* genes observed in the metagenomes of the KB-1 subcultures (**Figure 3**). These *rdhA* genes are often situated in regions of the genome that suggest potential for mobilization; yet we have no idea how quickly and under what conditions *rdhA* gene transfer occurs in organohalide-respiring bacteria such as *Dehalococcoides*. This may be particularly relevant for bioaugmented sites where native and non-native populations coexist.

AUTHOR CONTRIBUTIONS

AP-d-M conceived of the experiments, carried out the molecular experiments, performed the comparative analyses, and co-drafted the manuscript. AL and XL assisted with the molecular experiments, culture maintenance, and helped to draft the manuscript. SD and MM conceived and led both field bioaugmentation trials, coordinated field monitoring, and helped to draft the manuscript. EE participated in the design of the study and co-drafted the manuscript. All authors read and approved the final manuscript.

FUNDING

AP-d-M thanks the European Commission for financial support through an IOF Marie Curie Fellowship within the project AnDeMic (Contract 23974/7th Framework). The authors also wish to thank the Natural Sciences and Engineering Research Council of Canada (NSERC), the United States Department of Defense Strategic Environmental Research and Development Program (SERDP), Genome Canada and the Ontario Genomics Institute (2009-OGI-ABC-1405), the Government of Ontario through the ORF-GL2 program, and Sustainable Development Technology Canada (SDTC) for providing funding. The authors also acknowledge R&D in kind contributions by Geosyntec and SiREM to the project study.

ACKNOWLEDGMENTS

The authors wish to thank Adria Bells, Jeff Roberts, and Carey Austrins for the field assistance and Olivia Molenda for a thorough review of the manuscript.

SUPPLEMENTARY MATERIAL

The Supplementary Material for this article can be found online at: https://www.frontiersin.org/articles/10.3389/fmicb.2018.00812/full#supplementary-material

REFERENCES

Atashgahi, S., Lu, Y., Zheng, Y., Saccenti, E., Suarez-Diez, M., Ramiro-Garcia, J., et al. (2017). Geochemical and microbial community determinants of reductive dechlorination at a site biostimulated with glycerol. *Environ. Microbiol.* 19, 968–981. doi: 10.1111/1462-2920.13531

Bommer, M., Kunze, C., Fesseler, J., Schubert, T., Diekert, G., and Dobbek, H. (2014). Structural basis for organohalide respiration. *Science* 346, 455–458. doi: 10.1126/science.1258118

Carreon-Diazconti, C., Santamaria, J., Berkompas, J., Field, J. A., and Brusseau, M. L. (2009). Assessment of in situ reductive dechlorination using compound-specific stable isotopes, functional gene PCR, and geochemical data. *Environ. Sci. Technol.* 43, 4301–4307. doi: 10.1021/es803308q

Chan, W. W., Grostern, A., Löffler, F. E., and Edwards, E. A. (2011). Quantifying the effects of 1,1,1-trichloroethane and 1,1-dichloroethane on chlorinated ethene reductive dehalogenases. *Environ. Sci. Technol.* 45, 9693–9702. doi: 10.1021/es201260n

Cupples, A. M., Spormann, A. M., and McCarty, P. L. (2003). Growth of a *Dehalococcoides*-like microorganism on vinyl chloride and cis-dichloroethene as electron acceptors as determined by competitive PCR. *Appl. Environ. Microbiol.* 69, 953–959. doi: 10.1128/AEM.69.2.953-959.2003

Dugat-Bony, E., Biderre-Petit, C., Jaziri, F., David, M. M., Denonfoux, J., Lyon, D. Y., et al. (2012). In situ TCE degradation mediated by complex dehalorespiring communities during biostimulation processes. *Microb. Biotechnol.* 5, 642–653. doi: 10.1111/j.1751-7915.2012.00339.x

Duhamel, M., and Edwards, E. A. (2006). Microbial composition of chlorinated ethene-degrading cultures dominated by *Dehalococcoides*. *FEMS Microbiol. Ecol.* 58, 538–549. doi: 10.1111/j.1574-6941.2006.00191.x

Duhamel, M., and Edwards, E. A. (2007). Growth and yields of dechlorinators, acetogens, and methanogens during reductive dechlorination of chlorinated ethenes and dihaloelimination of 1,2-dichloroethane. *Environ. Sci. Technol.* 41, 2303–2310. doi: 10.1021/es062010r

Duhamel, M., Mo, K., and Edwards, E. A. (2004). Characterization of a highly enriched *Dehalococcoides*-containing culture that grows on vinyl chloride and trichloroethene. *Appl. Environ. Microbiol.* 70, 5538–5545. doi: 10.1128/AEM.70.9.5538-5545.2004

Duhamel, M., Wehr, S., Yu, L. Y., Rizvi, H., Seepersad, D., Dworatzek, S., et al. (2002). Comparison of anaerobic dechlorinating enrichment cultures maintained on tetrachloroethene, trichloroethene, cis- 1,2-dichloroethene and vinyl chloride. *Water Res.* 36, 4193–4202. doi: 10.1016/S0043-1354(02)00151-3

Ellis, D. E., Lutz, E. J., Odom, J. M., Buchanan, J. R. L., Bartlett, C. L., Lee, M. D., et al. (2000). Bioaugmentation for accelerated in situ anaerobic bioremediation. *Environ. Sci. Technol.* 34, 2254–2260. doi: 10.1021/es990638e

Fung, J. M., Morris, R. M., Adrian, L., and Zinder, S. H. (2007). Expression of reductive dehalogenase genes in *Dehalococcoides ethenogenes* strain 195 growing on tetrachloroethene, trichloroethene, or 2,3-dichlorophenol. *Appl. Environ. Microbiol.* 73, 4439–4445. doi: 10.1128/AEM.00215-07

Gerritse, J., Renard, V., Pedro-Gomes, T. M., Lawson, P. A., Collins, M. D., and Gottschal, J. C. (1996). *Desulfitobacterium* sp. Strain PCE1, an anaerobic bacterium that can grow by reductive dechlorination of tetrachloroethene or orotho-chlorinated phenols. *Arch. Microbiol.* 165, 132–140. doi: 10.1007/s002030050308

Hatt, J. K., and Löffler, F. E. (2012). Quantitative real-time PCR (qPCR) detection chemistries affect enumeration of the *Dehalococcoides* 16S rRNA gene in groundwater. *J. Microbiol. Methods* 88, 263–270. doi: 10.1016/j.mimet.2011.12.005

Hatt, J. K., Ritalahti, K. M., Ogles, D. M., Lebron, C. A., and Loffler, F. E. (2013). Design and application of an internal amplification control to improve *Dehalococcoides mccartyi* 16S rRNA gene enumeration by qPCR. *Environ. Sci. Technol.* 47, 11131–11138. doi: 10.1021/es4019817

He, J., Ritalahti, K. M., Aiello, M. R., and Löffler, F. E. (2003). Complete detoxification of vinyl chloride by an anaerobic enrichment culture and identification of the reductively dechlorinating population as a *Dehalococcoides* species. *Appl. Environ. Microbiol.* 69, 996–1003. doi: 10.1128/AEM.69.2.996-1003.2003

Henry, B. M. (2010). "Biostimulation for anaerobic bioremediation of chlorinated solvents," in *Situ Remediation of Chlorinated Solvent Plumes. SERDP and ESTCP Remediation Technology Monograph Series*, eds H. F. Stroo and C. H. Ward (New York, NY: Springer), 357–421.

Holliger, C., Hahn, D., Harmsen, H., Ludwig, W., Schumacher, W., Tindall, B., et al. (1998). *Dehalobacter restrictus* gen. nov. and sp. nov., a strictly anaerobic bacterium that reductively dechlorinates tetra- and trichloroethene in an anaerobic respiration. *Arch. Microbiol.* 169, 313–321. doi: 10.1007/s002030050577

Holmes, V., He, J., Lee, P., and Alvarez-Cohen, L. (2006). Discrimination of multiple *Dehalococcoides* strains in a trichloroethene enrichment by quantification of their reductive dehalogenase genes. *Appl. Environ. Microbiol.* 72, 5877–5883. doi: 10.1128/AEM.00516-06

Hood, E. D., Major, D. W., Quinn, J. W., Yoon, W.-S., Gavaskar, A., and Edwards, E. A. (2008). Demonstration of enhanced bioremediation in a tce source area at launch complex 34. Cape canaveral air force station. *Groundwater Monitor. Remediat.* 28, 98–107. doi: 10.1111/j.1745-6592.2008.00197.x

Hug, L. A. (2012). *A Metagenome-Based Examination of Dechlorinating Enrichment cultures: Dehalococcoides and the Role of the Non-Dechlorinating Microorganisms*. Ph.D. thesis, University of Toronto, Toronto.

Hug, L. A. (2016). "Chapter 16 in organohalide respiring bacteria," in *Diversity, Evolution, and Environmental Distribution of Reductive Dehalogenase Genes*, ed. L. Adrian (Berlin: Springer-Verlag).

Hug, L. A., Beiko, R. G., Rowe, A. R., Richardson, R. E., and Edwards, E. A. (2012). Comparative metagenomics of three *Dehalococcoides*-containing enrichment cultures: the role of the non-dechlorinating community. *BMC Genomics* 13:327. doi: 10.1186/1471-2164-13-327

Hug, L. A., and Edwards, E. A. (2013). Diversity of reductive dehalogenase genes from environmental samples and enrichment cultures identified with degenerate primer screens. *Fronti. Microbiol.* 4:341. doi: 10.3389/fmicb.2013.00341

Hug, L. A., Maphosa, F., Leys, D., Löffler, F. E., Smidt, H., Edwards, E. A., et al. (2013). Overview of organohalide-respiring bacteria and a proposal for a classification system for reductive dehalogenases. *Philos. Trans. R. Soc. Lond. B Biol. Sci.* 368:20120322. doi: 10.1098/rstb.2012.0322

Islam, M. A., Waller, A. S., Hug, L. A., Provart, N. J., Edwards, E. A., and Mahadevan, R. (2014). New insights into *Dehalococcoides mccartyi* metabolism from a reconstructed metabolic network-based systems-level analysis of *D. mccartyi* transcriptomes. *PLoS One* 9:e94808. doi: 10.1371/journal.pone.0094808

Kocur, C. M., Lomheim, L., Molenda, O., Weber, K. P., Austrins, L. M., Sleep, B. E., et al. (2016). Long term field study of microbial community and dechlorinating activity following carboxymethyl cellulose-stabilized nanoscale zero valent iron injection. *Environ. Sci. Technol.* 50, 7658–7670. doi: 10.1021/acs.est.6b01745

Krajmalnik-Brown, R., Hölscher, T., Thomson, I. N., Saunders, F. M., Ritalahti, K. M., and Löffler, F. E. (2004). Genetic identification of a putative vinyl chloride reductase in *Dehalococcoides* sp. strain BAV1. *Appl. Environ. Microbiol.* 70, 6347–6351. doi: 10.1128/AEM.70.10.6347-6351.2004

Krumholz, L. R. (1997). *Desulfuromonas chloroethenica* sp. nov. uses tetrachloroethylene and trichloroethylene as electron acceptors. *Int. J. Syst. Bacteriol.* 47, 1262–1263. doi: 10.1099/00207713-47-4-1262

Kube, M., Beck, A., Zinder, S. H., Kuhl, H., Reinhardt, R., and Adrian, L. (2005). Genome sequence of the chlorinated compound-respiring bacterium *Dehalococcoides* species strain CBDB1. *Nat. Biotechnol.* 23, 1269–1273. doi: 10.1038/nbt1131

Lee, P. K., MacBeth, T. W., Sorenson, K. S., Deeb, R. A., and Alvarez-Cohen, L. (2008). Quantifying gene and transcripts of to assess the in situ physiology of *Dehalococcoides* in a trichloroethene groundwater site. *Appl. Environ. Microbiol.* 74, 2728–2739. doi: 10.1128/AEM.02199-07

Lee, P. K., Warnecke, F., Brodie, E. L., MacBeth, T. W., Conrad, M. E., Andersen, G. L., et al. (2012). Phylogenetic microarray analysis of a microbial community performing reductive dechlorination at a TCE-contaminated site. *Environ. Sci. Technol.* 46, 1044–1054. doi: 10.1021/es203005k

Lendvay, J. M., Löffler, F. E., Dollhopf, M., Aiello, M. R., Daniels, G., Fathepure, B. Z., et al. (2003). Bioreactive barriers: a comparison of bioaugmentation and biostimulation for chlorinated solvent remediation. *Environ. Sci. Technol.* 37, 1422–1431. doi: 10.1021/es025985u

Liang, X., Molenda, O., Tang, S., and Edwards, E. A. (2015). Identity and substrate-specificity of reductive dehalogenases expressed in *Dehalococcoides*-containing enrichment cultures maintained on different chlorinated ethenes. *Appl. Environ. Microbiol.* 81, 4626–4633. doi: 10.1128/AEM.00536-15

Lu, Y., Atashgahi, S., Hug, L., and Smidt, H. (2015). "Primers that target functional genes of organohalide-respiring bacteria," in *Hydrocarbon and Lipid Microbiology Protocols. Springer Protocols Handbooks,* eds T. J. McGenity, K. N. Timmis, B. Nogales (Heidelberg: Springer).

Luijten, M. L., de Weert, J., Smidt, H., Boschker, H. T., de Vos, W. M., Schraa, G., et al. (2003). Description of *Sulfurospirillum halorespirans* sp nov., an anaerobic, tetrachloroethene-respiring bacterium, and transfer of *Dehalospirillum multivorans* to the genus *Sulfurospirillum* as *Sulfurospirillum multivorans* comb. nov. *Int. J. Syst. Evol. Microbiol.* 53, 787–793. doi: 10.1099/ijs.0.02417-0

Magnuson, J. K., Romine, M. F., Burris, D. R., and Kingsley, M. T. (2000). Trichloroethene reductive dehalogenase from *Dehalococcoides ethenogenes*: sequence of *tceA* and substrate range characterization. *Appl. Environ. Microbiol.* 66, 5141–5147. doi: 10.1128/AEM.66.12.5141-5147.2000

Magnuson, J. K., Stern, R. V., Gossett, J. M., Zinder, S. H., and Burriss, D. R. (1998). Reductive dechlorination of tetrachloroethene to ethene by a two-component enzyme pathway. *Appl. Environ. Microbiol.* 64, 1270–1275.

Major, D. W., McMaster, M. L., Cox, E. E., Edwards, E. A., Dworatzek, S. M., Hendrickson, E. R., et al. (2002). Field demonstration of successful bioaugmentation to achieve dechlorination of tetrachloroethene to ethene. *Environ. Sci. Technol.* 36, 5106–5116. doi: 10.1021/es0255711

Manchester, M. J., Hug, L. A., Zarek, M., Zila, A., and Edwards, E. A. (2012). Discovery of a *trans*-dichloroethene-respiring *Dehalogenimonas* species in the 1,1,2,2-tetrachloroethane-dechlorinating WBC-2 consortium. *Appl. Environ. Microbiol.* 78, 5280–5287. doi: 10.1128/AEM.00384-12

Mayer-Blackwell, K., Azizian, M. F., Machak, C., Vitale, E., Carpani, G., de Ferra, F., et al. (2014). Nanoliter qPCR platform for highly parallel, quantitative assessment of reductive dehalogenase genes and populations of dehalogenating microorganisms in complex environments. *Environ. Sci. Technol.* 48, 9659–9667. doi: 10.1021/es500918w

Mayer-Blackwell, K., Fincker, M., Molenda, O., Callahan, B., Sewell, H., Holmes, S., et al. (2016). 1,2-Dichloroethane exposure alters the population structure, metabolism, and kinetics of a trichloroethene-dechlorinating *Dehalococcoides mccartyi* consortium. *Environ. Sci. Technol.* 50, 12187–12196. doi: 10.1021/acs.est.6b02957

Maymó-Gatell, X., Chien, Y.-T., Gossett, J. M., and Zinder, S. H. (1997). Isolation of a bacterium that reductively dechlorinates tetrachloroethene to ethene. *Science* 276, 1568–1571. doi: 10.1126/science.276.5318.1568

Maymó-Gatell, X., Nijenhuis, I., and Zinder, S. H. (2001). Reductive dechlorination of cis-1,2-dichloroethene and vinyl chloride by *Dehalococcoides ethenogenes*. *Environ. Sci. Technol.* 35, 516–521. doi: 10.1021/es001285i

McCarty, P. L. (2010). "Groundwater contamination by chlorinated solvents: history, remediation technologies and strategies," in *Situ Remediation of Chlorinated Solvent Plumes*, eds H. F. Stroo, and C. H. Ward (New York, NY: Taylor & Francis), 1–24.

McMurdie, P. J., Behrens, S. F., Müller, J. A., Goke, J., Ritalahti, K. M., Wagner, R., et al. (2009). Localized plasticity in the streamlined genomes of vinyl chloride respiring *Dehalococcoides*. *PLoS Genet.* 5:e1000714. doi: 10.1371/journal.pgen.1000714

Moe, W. M., Yan, J. Y., Nobre, M. F., da Costa, M. S., and Rainey, F. A. (2009). *Dehalogenimonas lykanthroporepellens* gen. nov., sp. nov., a reductively dehalogenating bacterium isolated from chlorinated solvent-contaminated groundwater. *Int. J. Syst. Evol. Microbiol.* 59, 2692–2697. doi: 10.1099/ijs.0.011502-0

Müller, J. A., Rosner, B. M., von Abendroth, G., Meshulam-Simon, G., McCarty, P. L., and Spormann, A. M. (2004). Molecular identification of the catabolic vinyl chloride reductase from *Dehalococcoides* sp. strain VS and is environmental distribution. *Appl. Environ. Microbiol.* 70, 4880–4888. doi: 10.1128/AEM.70.8.4880-4888.2004

Payne, K. A., Quezada, C. P., Fisher, K., Dunstan, M. S., Collins, F. A., Sjuts, H., et al. (2015). Reductive dehalogenase structure suggests a mechanism for B12-dependent dehalogenation. *Nature* 517, 513–516. doi: 10.1038/nature13901

Pérez-de-Mora, A., Zila, A., McMaster, M. L., and Edwards, E. A. (2014). Bioremediation of chlorinated ethenes in fractured bedrock and associated changes in dechlorinating and non-dechlorinating microbial populations. *Environ. Sci. Technol.* 48, 5770–5779. doi: 10.1021/es404122y

Rahm, B. G., Chauhan, S., Holmes, V. F., Macbeth, T. W., Sorenson, K. S. J., and Alvarez-Cohen, L. (2006a). Molecular characterization of microbial populations at two sites with differing reductive dechlorination abilities. *Biodegradation* 17, 523–534.

Rahm, B. G., Morris, R. M., and Richardson, R. E. (2006b). Temporal expression of respiratory genes in an enrichment culture containing *Dehalococcoides ethenogenes*. *Appl. Environ. Microbiol.* 72, 5486–5491.

Rahm, B. G., and Richardson, R. E. (2008). Correlation of respiratory gene expression levels and pseudo-steady-state PCE respiration rates in *Dehalococcoides ethenogenes*. *Environ. Sci. Technol.* 42, 416–421. doi: 10.1021/es071455s

Ritalahti, K., Amos, B., Sung, Y., Wu, Q., Koenigsberg, S., and Loffler, F. (2006). Quantitative PCR targeting 16S rRNA and reductive dehalogenase genes simultaneously monitors multiple *Dehalococcoides* strains. *Appl. Environ. Microbiol.* 72, 2765–2774. doi: 10.1128/AEM.72.4.2765-2774.2006

Ritalahti, K. M., Hatt, J. K., Lugmayr, V., Henn, L., Petrovskis, E. A., Ogles, D. M., et al. (2010). Comparing on-site to off-site biomass collection for *Dehalococcoides* biomarker gene quantification to predict in situ chlorinated ethene detoxification potential. *Environ. Sci. Technol.* 44, 5127–5133. doi: 10.1021/es100408r

Seshadri, R., Adrian, L., Fouts, D. E., Eisen, J. A., Phillippy, A. M., Methe, B. A., et al. (2005). Genome sequence of the PCE-dechlorinating bacterium *Dehalococcoides ethenogenes*. *Science* 307, 105–108. doi: 10.1126/science.1102226

Smidt, H., and de Vos, W. M. (2004). Anaerobic microbial dehalogenation. *Annu. Rev. Microbiol.* 58, 43–73. doi: 10.1146/annurev.micro.58.030603.123600

Stroo, H. F., Major, D. W., and Gossett, J. M. (2010). "Bioaugmentation for anaerobic bioremediation of chlorinated solvents," in *Situ Remediation of Chlorinated Solvent Plumes*, eds H. F. Stroo, and C. H. Ward (New York, NY: Springer), 425–454. doi: 10.1007/978-1-4419-1401-9_13

Sung, Y., Fletcher, K. E., Ritalahti, K. M., Apkarian, R. P., Ramos-Hernández, N., Sanford, R. A., et al. (2006a). *Geobacter lovleyi* sp. nov. strain SZ, a novel metal-reducing and tetrachloroethene-dechlorinating bacterium. *Appl. Environ. Microbiol.* 69, 2775–2782.

Sung, Y., Ritalahti, K. M., Apkarian, R. P., and Löffler, F. E. (2006b). Quantitative PCR confirms purity of strain GT, a novel trichloroethene-to-etheneрespiring *Dehalococcoides* isolate. *Appl. Environ. Microbiol.* 72, 1980–1987.

Tang, S., Chan, W. W., Fletcher, K. E., Seifert, J., Liang, X., Löffler, F. E., et al. (2013). Functional characterization of reductive dehalogenases using blue native polyacrylamide gel electrophoresis. *Appl. Environ. Microbiol.* 79, 974–981. doi: 10.1128/AEM.01873-12

Tang, S., Wang, P. H., Higgins, S. A., Löffler, F. E., and Edwards, E. A. (2016). Sister dehalobacter genomes reveal specialization in organohalide respiration and recent strain differentiation likely driven by chlorinated substrates. *Front. Microbiol.* 7:119. doi: 10.3389/fmicb.2016.00100

van der Zaan, B., Hannes, F., Hoekstra, N., Rijnaarts, H., de Vos, W. M., Smidt, H., et al. (2010). Correlation of *Dehalococcoides* 16S rRNA and chloroethene-reductive dehalogenase genes with geochemical conditions in chloroethene-contaminated groundwater. *Appl. Environ. Microbiol.* 76, 843–850. doi: 10.1128/AEM.01482-09

Waller, A. S. (2009). *Molecular Investigation of Chloroethene Reductive Dehalogenation by the Mixed Microbial Community KB1*. Ph.D. thesis, University of Toronto, Toronto.

Waller, A. S., Hug, L. A., Mo, K., Radford, D. R., Maxwell, K. L., and Edwards, E. A. (2012). Transcriptional analysis of a *Dehalococcoides*-containing microbial consortium reveals prophage activation. *Appl. Environ. Microbiol.* 78, 1178–1186. doi: 10.1128/AEM.06416-11

Waller, A. S., Krajmalnik-Brown, R., Löffler, F. E., and Edwards, E. A. (2005). Multiple reductive-dehalogenase-homologous genes are simultaneously transcribed during dechlorination by *Dehalococcoides*-containing cultures. *Appl. Environ. Microbiol.* 71, 8257–8264. doi: 10.1128/AEM.71.12.8257-8264.2005

Yan, J., Ritahalati, K. M., Wagner, D., and Löffler, F. E. (2012). Unexpected specificity of interspecies cobamide transfer from *Geobacter* spp. to organohalide-respiring *Dehalococcoides mccartyi* strains. *Appl. Environ. Microbiol.* 78, 6630–6636. doi: 10.1128/AEM.01535-12

Yan, J., Şimşir, B., Farmer, A. T., Bi, M., Yang, Y., Campagna, S. R., et al. (2016). The corrinoid cofactor of reductive dehalogenases affects dechlorination rates and extents in organohalide-respiring *Dehalococcoides mccartyi*. *ISME J.* 10, 1092–1101. doi: 10.1038/ismej.2015.197

Yang, Y., Higgins, S. A., Yan, J., Şimşir, B., Chourey, K., Iyer, R., et al. (2017). Grape pomace compost harbors organohalide-respiring *Dehalogenimonas* species with novel reductive dehalogenase genes. *ISME J.* 11, 2767–2780. doi: 10.1038/ismej.2017.127

Conflict of Interest Statement: The authors declare that the research was conducted in the absence of any commercial or financial relationships that could be construed as a potential conflict of interest.

frontiers in Microbiology

ORIGINAL RESEARCH
published: 15 May 2018
doi: 10.3389/fmicb.2018.00952

Diversity and Dynamics of Microbial Community Structure in Different Mangrove, Marine and Freshwater Sediments During Anaerobic Debromination of PBDEs

Ya Fen Wang[1,2], Hao Wen Zhu[2], Ying Wang[2], Xiang Ling Zhang[3] and Nora Fung Yee Tam[2,4]*

[1] Laboratory of Basin Hydrology and Wetland Eco-restoration, School of Environmental Studies, China University of Geosciences, Wuhan, China, [2] Department of Biology and Chemistry, City University of Hong Kong, Kowloon Tong, Hong Kong, [3] School of Civil Engineering and Architecture, Wuhan University of Technology, Wuhan, China, [4] State Key Laboratory in Marine Pollution, City University of Hong Kong, Kowloon Tong, Hong Kong

OPEN ACCESS

Edited by:
Shanquan Wang,
Sun Yat-sen University, China

Reviewed by:
Meiying Xu,
Guangdong Institute of Microbiology (CAS), China
Yue Lu,
Hunan University, China

***Correspondence:**
Ya Fen Wang
wangyf@cug.edu.cn

Specialty section:
This article was submitted to Microbiotechnology, Ecotoxicology and Bioremediation, a section of the journal Frontiers in Microbiology

Received: *29 December 2017*
Accepted: *24 April 2018*
Published: *15 May 2018*

Citation:
Wang YF, Zhu HW, Wang Y, Zhang XL and Tam NFY (2018) Diversity and Dynamics of Microbial Community Structure in Different Mangrove, Marine and Freshwater Sediments During Anaerobic Debromination of PBDEs. Front. Microbiol. 9:952. doi: 10.3389/fmicb.2018.00952

Little is known about the diversity and succession of indigenous microbial community during debromination of polybrominated diphenyl ethers (PBDEs). This study examined the diversity and dynamics of microbial community structure in eight saline (mangrove and marine) and freshwater sediment microcosms exhibiting different debrominating capabilities for hexa-BDE 153, a common congener in sediments, using terminal restriction fragment length polymorphism (T-RFLP) and clone library analyses. The results showed that microbial community structure greatly differed between the saline and freshwater microcosms, likely leading to distinct variations in their debrominating capabilities and pathways. Higher relative abundances of Chloroflexi and Deltaproteobacteria succeed by Alphaproteobacteria and Betaproteobacteria were detected in the two mangrove microcosms with the fastest debrominating capabilities mainly via *para* pathway, respectively; the dominance of Alphaproteobacteria resulted in less accumulation of tetra-BDEs and more complete debromination of lower brominated congeners (from di- to tetra-BDEs). Meanwhile, the shifts in both microbial community structure and PBDE profiles were relatively small in the less efficient freshwater microcosms, with relatively more *ortho* and *meta* brominated products of BDE-153 resulted. Coincidently, one of the freshwater microcosms showed sudden increases of Chloroflexi and Deltaproteobacteria by the end of incubation, which synchronized with the increase in the removal rate of BDE-153. The significant relationship between microbial community structure and PBDEs was confirmed by redundancy analysis (18.7% of total variance explained, P = 0.002). However, the relative abundance of the well-known dechlorinator *Dehalococcoides* showed no clear correlation with the debrominating capability across different microcosms. These findings shed light in the significance of microbial community network in different saline environments on enhancement of PBDE intrinsic debromination.

Keywords: PBDEs, mangrove sediment, microbial community, reductive debromination, T-RFLP, salinity

INTRODUCTION

Polybrominated diphenyl ethers (PBDEs) are highly diverse, toxic and persistent organohalides, prevalent in sediments and soils around the world (Oros et al., 2005; Binelli et al., 2007; Li et al., 2012; Zhu et al., 2014a; McGrath et al., 2017). They share the structural similarity and environmental fate with other highly halogenated compounds like polychlorinated biphenyls (PCBs) and have been included in Stockholm Convention (2009) on the list of persistent organic pollutants (POPs). Concerns about their bioaccumulation and potential endocrine, reproductive and behavioral toxicity effects to human and wildlife have posed urgent needs for their remediation (Lam et al., 2010; Chakraborty and Das, 2016).

Microbial debromination of PBDEs played a major role in PBDE dissipation in soil, compared to plant uptake and other physiochemical processes (Huang et al., 2010). It has been well documented that PBDEs could be transformed to less-brominated congers under both aerobic and anaerobic conditions by bacterial isolates or consortia (Robrock et al., 2008; Lee et al., 2011; Ding et al., 2013; Zhang et al., 2013). The only key biodegradation mechanism for certain recalcitrant and highly brominated BDE congeners is reductive dehalogenation, during which the organohalides could serve as electron acceptors for bacteria to derive energy for their growth under anaerobic conditions (Mohn and Tiedje, 1992). This specific group of bacteria is known as organohalide-respiring bacteria (OHRB), which have been identified from limited bacterial phyla of Chloroflexi, Firmicutes, and Proteobacteria (Hug et al., 2013). Different OHRB exhibited highly specialized capabilities for the debromination of different BDE congeners (He et al., 2006; Robrock et al., 2009; Yang et al., 2015), suggesting that complete or effective remediation of PBDEs required the cooperation of different OHRB, and with other bacterial functional groups such as those capable of cleavage of aromatic rings. Moreover, *in situ* microbial remediation process would largely depend on the degradation network of the indigenous microbial community present (Lovley, 2003). However, our current knowledge of the diversity and dynamics of indigenous microbial community involved in the whole PBDE debrominating process is very limited.

Previous studies of PBDE remediation were mainly conducted in electronic wastes contaminated soils, sewage sludge and river sediments (Yen et al., 2009; Shih et al., 2012; Song et al., 2015; Stiborova et al., 2015). Microbial debromination could be enhanced by addition of co-substrates or electron donors, priming with other halogenated compounds, and stimulation with electrochemical technology (Gerecke et al., 2005; Qiu et al., 2012; Yang et al., 2013; Huang et al., 2014). More recent studies followed the application of new functional materials such as tourmaline, nanoscale zero-valent iron and carbonaceous materials during PBDE remediation (Zhang et al., 2014; Cai et al., 2015; Ma et al., 2016; Zhu et al., 2016). But exploration of PBDE debromination under natural environments were rather limited, especially in the marine/saline environments (Zanaroli et al., 2015). Nevertheless, our previous study showed that different types of sediments varying in salinity had great impacts on debromination of hexa-BDE153. More rapid and complete reductive debromination was observed in mangrove and marine sediments than in freshwater sediments (Zhu et al., 2014b). Although microbial reductive dechlorination potential and activities have been reported in marine coastal and subseafloor sediments (Futagami et al., 2013; Matturro et al., 2016a), studies focusing on the role of indigenous microbial community in reductive debromination in marine environments is scarce.

Additionally, most of the known OHRB were isolated from freshwater environments, with only seven (out of 74) from marine and estuarine sediments, and the phylogeny and functional diversity of certain genus like *Dehalococcoidia* were found more likely regional specific, e.g., greatly differing between marine and freshwater environments (Atashgahi et al., 2016; Zinder, 2016). Thus, the distribution of the extensively studied *Dehalococcoidia* in marine environments and their role in intrinsic debromination are also of particular interest to be explored.

In the present study, the structure and dynamics of indigenous microbial community were examined across eight different sediment microcosms varying in reductive debrominating capabilities for BDE-153 over a course of 90 days. We aimed to test the hypothesis if the debromination potential of different sediments was determined by their indigenous microbial community structure. Besides, the phylogeny of the microbial community involved in PBDE debromination was revealed to infer the role of the known OHRB during intrinsic debromination.

MATERIALS AND METHODS

Sample Description

Sediment slurry samples were taken from the batch microcosm experiment for evaluation of the intrinsic debromination potential of different sediments collected from Hong Kong, SAR. There were eight sediment microcosms, including five mangrove sediments from Mai Po Ramsar wetland (MP), Sha Tau Kok (STK), Ting Kok (TK), Ho Chung (HC), and Tai O (TO), two freshwater pond sediments from Mai Po (MPf) and Nam Sang Wai (NSW), and one marine sediment from Sai Kung (SK) (Supplementary Figure S1). The five intertidal mangrove sediments (MP, STK, HC, TK, and TO) were dominated by *Kandelia obovata*, with the salinity ranged from 29 to 35‰, pH from 7.55 to 7.92 and the total organic matter (TOM) from 2.07 to 8.98%, while the two freshwater sediments (MPf and NSW) were dominated by *Phragmites australis* with the salinity from 6 to 8‰, pH from 7.35 to 7.48 and the TOM from 6.59 to 7.22%. The marine sediment (SK) had a salinity of 34‰, pH of 8.08 and TOM of 3.54%.

The detailed set-up of the microcosms has been described by Zhu et al. (2014b). In brief, the minimal salt medium (MSM) containing (in g L^{-1}): K_2HPO_4, 0.27; KH_2PO_4, 0.35; NH_4Cl, 2.7; $MgCl_26H_2O$, 0.1; $CaCl_22H_2O$, 0.1; and the trace elements made up of $FeCl_24H_2O$, 0.009; $MnCl_24H_2O$, 0.004; $ZnCl_2$, 0.0014; $CoCl_46H_2O$, 0.001 and $(NH_4)_6\ Mo_7O_244H_2O$, 0.001 was prepared as described previously (Li et al., 2009). The salinity

was adjusted to be the same as that in the original sediment sample by adding appropriate amounts of NaCl into the MSM. The medium was autoclaved at 121°C for 30 min, then freshly prepared L-cysteine and sodium sulfide (Na_2S) (0.2 mM each) were added aseptically to eliminate residual oxygen. For each microcosm, 100 mL of the sterilized MSM were dispersed into a 250-mL Quickfit conical flask, 20 g of fresh sediment were then aseptically added in an anaerobic glove box under the flux of nitrogen gas and mixed thoroughly with the medium to form the sediment slurry. The anaerobic condition was maintained using N_2 refilling method, and all the microcosms were acclimated for 2 weeks. After acclimation, 200 μL stock solution of BDE-153 (Chem Service, AccuStandard, purity >99%) at 100 mg L^{-1} in acetone was spiked into each microcosm to obtain a nominal concentration of BDE-153 at 1.0 mg kg^{-1} (freeze-dried weight). The sediment slurry was shaken after spiking to let the slurry equilibrated with BDE-153 and let the small volume of acetone (0.2%) evaporated according to the previous study of Zhong et al. (2006). The actual spiked concentration of BDE-153 at day 0 was determined to be 1.08 ± 0.08 mg kg^{-1} (mean and standard deviation of three replicates). The solvent control with acetone was not included, as Fagervold et al. (2005) reported that the solvent control without the target pollutants, i.e., PCBs, showed little effects on the microbial dechlorinating activity and community profiles. All the microcosms in triplicates were incubated at 28°C on a horizontal shaker at 150 rpm for 90 days, to ensure the homogeneity of the sediment slurry. At regular time intervals, a 2 mL slurry was subsampled from each microcosm using sterile disposable syringes for PBDE analysis, in parallel, another 2 mL slurry was collected at days 1, 15, 30, 60, and 90, and stored at −70°C for later microbial community analysis.

DNA Extraction and PCR Amplification

Genomic DNA was extracted from 0.25 g of sediment using the FastDNA™ SPIN Kit for Soil (MP Biomedicals, Irvine, CA, United States). The bacterial 16S rDNA genes were amplified using the universal primers 8F: 5′-AGA GTT TGA TCC TGG CTC AG-3′ and 1492R: 5′-GGC TAC CTT GTT ACG ACT T-3′ (Lane, 1991). The 8F primer was labeled at the 5′ end with 6-carboxy-fluorescein phosphoramidite (FAM). The PCR cocktail composed of 10 μL 5× colorless GoTaq™ Flexi Buffer, 3 μL of $MgCl_2$ (25 mM), 1 μL of dNTP (10 mM), 0.5 μL of each primer (10 μM), 0.25 μL of GoTaq™ Hot Start Polymerase (5 U μL^{-1}) (Promega, Madison, WI, United States), 1 μL template DNA (3–10 ng), and the volume was made up to 50 μL using nuclease-free H_2O. The PCR condition was an initial denaturation at 94°C for 3 min; 30 cycles of 94°C, 45 s denaturation; 55°C, 45 s annealing; 72°C, 60 s extension; followed by a final extension at 72°C for 7 min. The PCR products (1.5 kb) were then verified by running a 1.2% (w/v) agarose gel electrophoresis in 1× Tris-acetate-EDTA (TAE) buffer (pH 7.4).

Terminal Restriction Fragment Length Polymorphism (T-RFLP) Analysis

The PCR products were concentrated and purified using the AxyPrep™ DNA Gel Extraction Kit (Axygen, United States), which resulted in sufficient abundance of T-RFs for detection after digestion with the restriction enzyme (the next step). Aliquots of the purified PCR products (500–800 ng) were digested with the restriction enzyme *Hae*III at 37°C according to the manufacture's protocol (New England Biolabs, Inc., United Kingdom). The total volume of the digestion system was 40 μL. Digested products were precipitated by two volumes of cold absolute ethanol at −20°C overnight, centrifuged at 14,000 rpm at 4°C for 20 min and washed with 100 μL of 70% cold ethanol. After centrifugation, the DNA pellets were dissolved in 20 μL of nuclease-free water. Purified products (10 μL) were mixed with 0.5 μL of the internal size standard (ET ROX-550, Amersham, United States). This mixture was denatured for 2 min at 95°C and immediately chilled on ice before electrophoresis on a MegaBASE genetic analyzer (Amersham, United States) operated in a Genotyping mode at the Coastal Marine Laboratory, Hong Kong University of Science and Technology.

The basic T-RF calling was performed using a Genetic Profiler in the MEGABACE software package (Amersham, United States). For each sample, peaks over a threshold of 50 fluorescence units were used, and T-RFs of <60 bp and >550 bp were excluded from the analysis to avoid detection of primers and uncertainties of size determination, respectively. The raw data file exported from MEGABACE was re-formatted and then processed by T-REX software developed by Culman et al. (2009), which helped to determine a baseline threshold for the identification of true peaks over noise, align T-RFs in all samples and construct data matrices based on the area of T-RF peaks.

A phylogenetic assignment tool, TRiFLe program for *in silico* T-RFLP analysis with user-defined sequence sets, was adopted (Junier et al., 2008). A total of 2,533 bacterial sequences tagged with "marine sediments" were selected from the RDP database and used as the reference data set for the simulation of the T-RF size distribution and identification of the candidate species in the sediment samples.

Cloning and Phylogenetic Analysis

16S rRNA gene fragments from the genomic DNA from microcosms were amplified with the universal bacterial primer pairs of 8F and 1492R as described above. The PCR amplicons were checked by agarose gel electrophoresis, purified and cloned to pGEM-T Easy Vector System I (Promega, Madison, WI, United States) according to the manufacturer's instructions. Positive colonies were selected randomly and sent to a company (Beijing Genomics Institute, Shenzhen, China) for sequencing. Near-complete 16S rRNA gene sequences were obtained and compared to other sequences via the Basic Local Alignment Search Tool (BLAST) of the National Centre for Biotechnology Information (NCBI[1]). The 16S rRNA gene sequences obtained from the clone libraries in this study have been deposited in NCBI GenBank database under the following accession numbers: MH091074- MH091326. The phylogenetic tree was constructed by the neighbor-joining method in MEGA 5.0 package as described by Tamura et al. (2011).

Quantification Analysis of *Dehalococcoides* sp. by qPCR

Real-time PCR was performed using an ABI 7300 real-time PCR instrument (Applied Biosystems, Carlsbad, CA, United States) with genus-specific primers for *Dehalococcoides* sp. (Deh467F and Deh564R) and universal primers for total bacteria (341F and 534R) (Muyzer et al., 1993; Freeborn et al., 2005). The amplification was performed in 25-μL reaction mixtures composed of 1×ABI SYBR® Green Master Mix (Applied Biosystems, Carlsbad, CA, United States), 0.2 μM of each primer and 2 μL of DNA template, containing 1–10 ng μL^{-1} of DNA. The amplification program and efficiency has been described in our previous study (Wang et al., 2015). The relative abundance of *Dehalococcoides* sp. was determined by normalizing the quantitative results of the specific genes to the total amount of bacterial 16S rRNA gene copies within the same sample (van der Zaan et al., 2010).

Statistical Analysis

The peak area data from T-RFLP analysis were analyzed by clustering and multidimensional scaling (MDS) analyses, as suggested by Culman et al. (2008), for the T-RFLP datasets with high beta diversities (≥2). Clustering and MDS analyses for the matrix of peak area were based on [Log(x+1)] transformation of percentage values and Bray–Curtis similarity. Significant differences between neighboring samples were evaluated by similarity profile (SIMPROF) tests with a significance level at 0.05 in cluster analysis. Exploratory tool similarity percentage analysis (SIMPER) was also used to study the similarity between complex T-RFLP profiles. The above analyses were performed using the PRIMER 6 software package (Clarke and Gorley, 2006). The PAST program (PAlaeontological STatistics ver.1.64) was used to calculate the Shannon and Simpson diversity indices. The relationship between the profiles of T-RFLP and different PBDE congeners were investigated using redundancy analysis (RDA), after checking the length of gradient of T-RFLP dataset (to be 3.360) by detrended correspondence analysis (DCA) in the CANOCO program for Windows v4.5 from Microcomputer Power (Ithaca, NY, United States). Monte Carlo permutation test was performed to test the significance of the first and all canonical axes in RDA.

RESULTS

Debrominating Pattern of BDE-153 in Different Sediments

Our previous study showed that reductive debromination of BDE-153 was detected more extensive in mangrove and marine sediments (the removal rate of BDE-153 up to approximately 98% after 90 days), than in the freshwater pond sediments. The half-lives of BDE-153 in the sediment microcosms varied from 7.6 days in STK to 165.0 days in MPf (Zhu et al., 2014b). The sequential debrominating products of hexa-BDE 153 ranging from penta- to di-BDEs were found in all the sediment microcosms after 90 days, however, the dominant BDE homolog groups varied greatly among sediments with different debrominating rates (**Figure 1**). Lower brominated congeners (di- and tri-) were detected within 15 days in STK and TO, the two most efficient sediment microcosms, and their proportions increased after 30 days of incubation, accounted for around 20% in STK and 14–34% in TO, while BDE-153 rapidly decreased during this period. In contrast, the proportions of these lower brominated congeners in the other sediment microcosms were very low (less than 3%). Penta- and tetra-BDEs were found as the main daughter BDE congeners in STK and TO, accounting for 53–62% of the total BDE congeners. However, tetra-BDEs were more dominant than penta-BDEs in TO after 30 days of incubation but the percentages of tetra- and penta-BDEs were more or less the same in STK, suggesting TO had a more rapid transformation of BDE-153 and penta-BDEs but slower transformation of tetra- to lower brominated products, which was quite different from that in STK. In the other mangrove and marine sediment microcosms, penta- and tetra-BDEs formed in a sequential manner, and their respective proportions ranged from 7 to 41% and from less than 3 to 24%. Only 4 to 21% of penta-BDEs were found in the freshwater microcosms (NSW and MPf) after 60 days onwards, and tetra-BDEs were even lower (less than 3%), suggesting much lower transformation abilities for hexa-BDE 153 in the freshwater microcosms.

T-RFLP Analysis of Total Microbial Communities

The 16S rRNA fragment genes were fingerprinted with T-RFLP to monitor the dynamics of microbial community structure across 40 different sediment samples during debromination of BDE-153. Totally, there were 270 T-RFs generated by *Hae*III digestion, with an average richness (number of T-RFs in each sample) of 36.1. The sample heterogeneity (also known as beta diversity) of T-RFLP dataset was very high (to be 6.5, greater than 5) as suggested by McCune and Grace (2002). The heterogeneity of the microbial community from replicated samples of the same treatment was small according to our previous study using fatty acid methyl ester (FAME) analysis and others with T-RFLP analysis (Sipilä et al., 2008; Wang Y.F. et al., 2014). Non-linear ordination method, MDS was thus employed to resolve the similarity of our T-RFLP data, which included 40 sediment samples at five sampling times from Days 1 to 90 (**Figure 2**).

All the sediment samples were firstly clustered along the salinity gradient, with mangrove and marine sediments on the left side and freshwater sediments on the right side of the MDS scatter plot. The mangrove sediments could be further separated with marine sediments from SK along the second axis, except for STK sediments collected after Days 60 and 90. The average similarity for each sediment site was calculated by SIMPER analysis, showing the temporal change was greatest in STK (21.94) and minimized in NSW (39.32). From the scatter plot, all the mangrove sites showed a clear temporal shift after Days 60 and 90 during the debrominating process, as well as for the freshwater sediment microcosm MPf after 90 days. By contrast, such temporal shifts were insignificant in marine microcosm

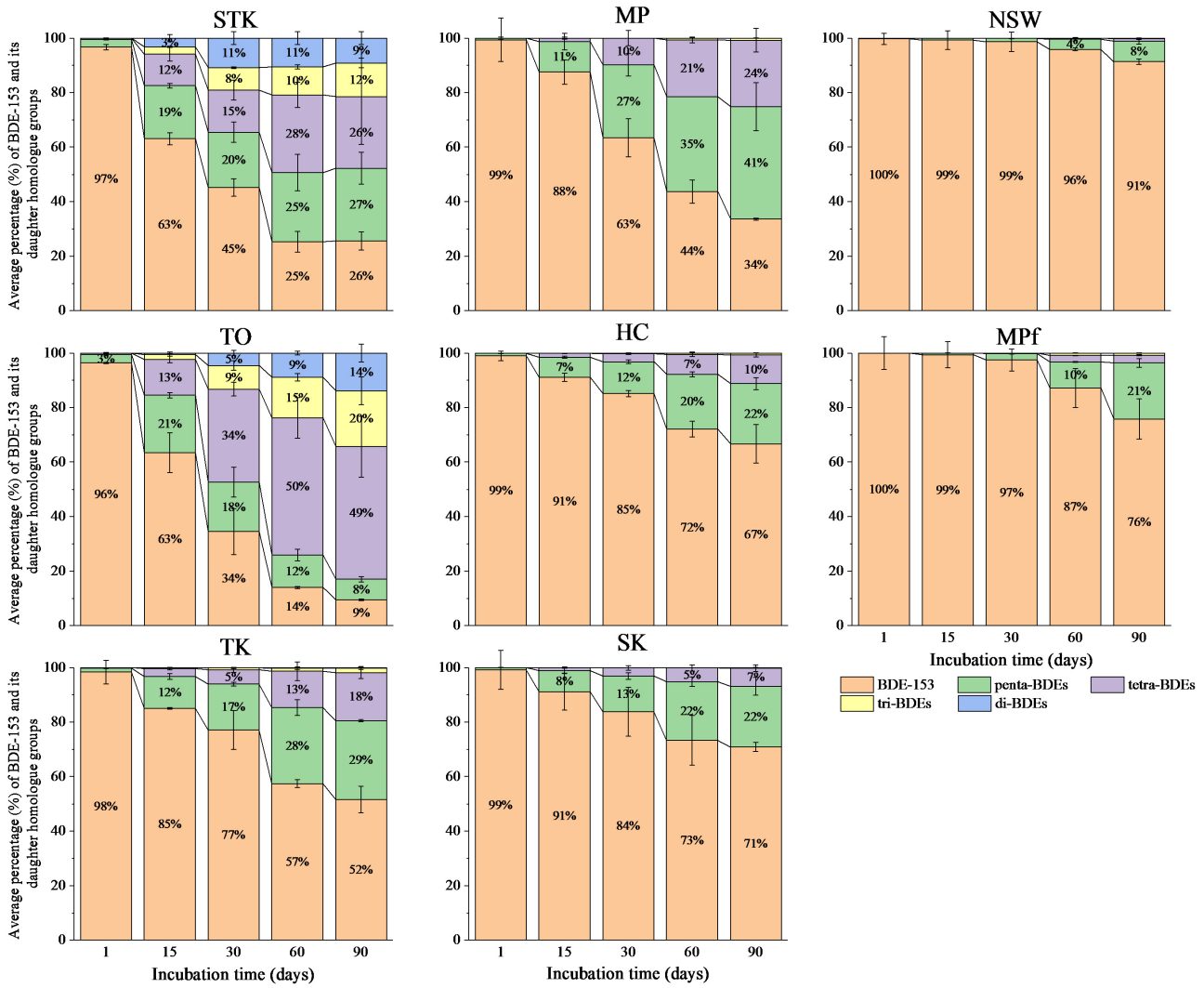

FIGURE 1 | Debromination pattern of BDE-153 to less-brominated congeners over time in the eight sediment microcosms. Data plotted are the mol percentage of the peak area of a BDE congener to the total peak areas of all BDE congeners identified in GC/MS chromatograms. Mean values of three replicates are shown. STK, TO, TK, HC, and MP are intertidal mangrove sediments collected from Sha Tau Kok, Tai O, Ting Kok, Ho Chung and Mai Po, respectively; SK is marine sediment collected from Sai Kung; MPf and NSW are fresh pond sediments collected from Mai Po nature reserve and Nam Sang Wai.

SK and another freshwater microcosm NSW at a similarity level of 30%.

Dynamics of the dominant terminal restriction fragments (T-RFs) were examined to identify the key bacterial species involved in PBDE debromination (**Figure 3**). For the two most active mangrove microcosms STK and TO, they shared T-RFs 206, 271 and 208 at Days 1 and 15, while the number of their shared T-RFs decreased from 23 to 9 after 90 days, with T-RFs 216, 231, and 194 dominated at STK and T-RFs 266 and 316 dominated at TO after Day 60, respectively. T-RFs 271 and 208 were also detected as dominant T-RFs in TK and HC at Day 1, but the dominant T-RFs shifted to 254, 314, and 192 bp in TK and HC after 60 days. Accordingly, the T-RFLP patterns in TK and HC were the most similar (average dissimilarity = 74.20, SIMPER) compared with other pairs of sediment microcosms. The dominant T-RFs in marine sediment SK resembled those detected in mangrove sediments, except for T-RFs 238 (at D1–D15), 261 (at D30–D90) and 411. The freshwater sediment NSW also held unique dominant T-RFs such as 230 (at D1–D15) and 337 (at D60–D90). However, it was interesting to find that both mangrove and freshwater sediments collected from MP shared certain dominant T-RFs, such as 193, 215, 221–225, and 306, but these T-RFs became dominant at different timing.

Molecular identification of the dominant T-RFs with cumulative contribution to the differences in T-RFLP profiles over time greater than 50% in each sediment microcosm were summarized (**Table 1**). The dominant T-RFs in mangrove and marine microcosms from Days 1 to 30 were identified to contain 16S rRNA gene sequences similar to uncultured deltaproteobacterium clones (T-RFs 206, 208, 238) and two

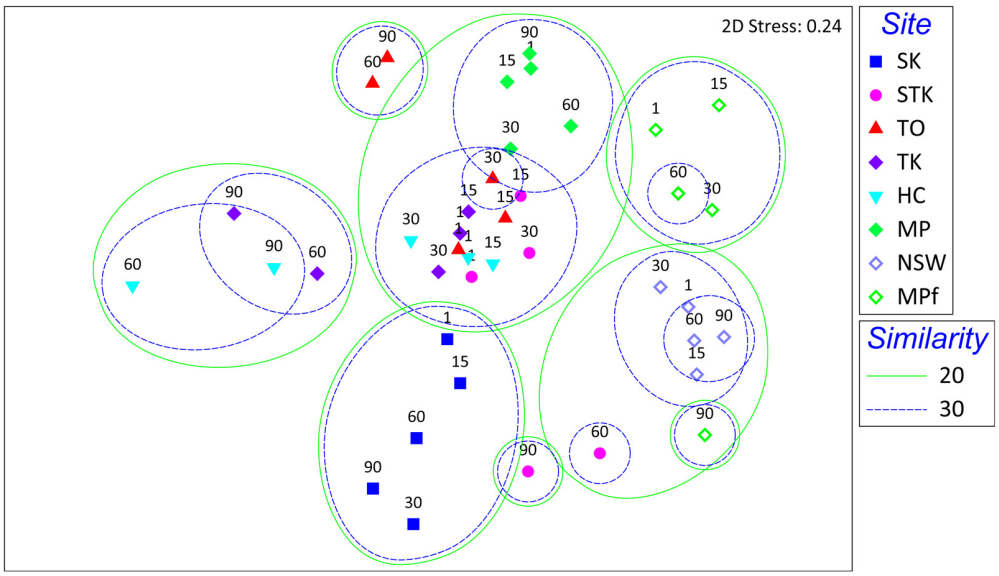

FIGURE 2 | Sample scatter plot of multidimensional scaling (MDS) analysis of T-RFLP profiles of total bacterial community from the eight sediment microcosms at Days 1, 15, 30, 60, and 90 after spiked with BDE-153. Neighboring samples clustered at a similarity level of 20 and 30% are indicated.

strains from the Firmicutes family of *Clostridiaceae* (T-RFs 257 and 271). The two T-RFs 225 and 220 were abundant in mangrove and freshwater microcosms from Mai Po at Day 1 and both belonged to the phylum of Chloroflexi. The partial 16S rRNA sequences of dominant T-RFs from Days 60 to 90 matched with more bacterial phyla, including Actinobacteria (T-RF 231, STK), Betaproteobacteria (T-RF 198, STK), Alphaproteobacteria (T-RFs 192, 253/254, mangrove microcosms), candidate division OP8 (T-RF 261, SK), and Bacteroidetes (T-RF 411, SK). T-RFs 266 and 316 enriched in TO after Day 60 were closely related to *Clostridium algidicarnis* and another uncultured Firmicutes, respectively. T-RF 215 shared by the two microcosms from Mai Po after Day 30 were 98% similar in the partial 16S rRNA sequence to one uncultured deltaproteobacterium clone, which was also detected from the anaerobic microbial community in oil-polluted subtidal sediments reported by Acosta-González et al. (2013).

Microbial Diversity and Phylogeny Involved in Debromination

Eight bacterial 16S rRNA clone libraries were constructed from four representative anaerobic microcosms of TO, STK, SK, and MPf at Days 1 and 90, respectively. Phylogenetic analysis revealed that 261 full-length 16S rRNA sequences were related to 20 bacterial phyla, including Gamma-, Alpha-, Delta-, and Beta-proteobacteria (n = 130, 50%), Bacteroidetes (n = 28, 11%), Firmicutes (n = 27, 10%), and Chloroflexi (n = 20, 8%). Other phyla with a few clones (less than 5% of the total), such as Verrucomicrobia, Actinobacteria, Planctomycetes, Acidobacteria, Gemmatimonadetes, and Chlorobi, as well as two candidate phyla WS3 and OP8, were also present (**Figure 4**). The phylum-level diversity distinctly decreased in the mangrove and marine microcosms (TO, STK, and SK) from 2.3 at Days 1 to 1.8 at Day 90 in average, while that in the freshwater microcosms (MPf) increased from 1.3 to 1.9. The distribution of dominant phyla also significantly differed between the saline and freshwater microcosms over time (**Figure 4**). The clones within Gamma-, Delta-proteobacteria, Bacteroidetes, Chloroflexi, and Firmicutes divisions from the saline microcosm libraries were more abundant than those from the freshwater ones, with distribution percentages accounting for 90, 90, 100, 55, and 74% of the total detected in the saline libraries, respectively. Furthermore, the percentages of the clones from the above first four phyla in the saline libraries detected at Days 1 and 90 dropped from 61 to 29%, 83 to 7%, 71 to 29%, and 50 to 5%, respectively. The respective values of the Alpha-, Beta-proteobacteria, and Firmicutes clones increased from 19 to 38%, 5 to 32%, and 22 to 52% in the saline libraries, but decreased from 24 to 19%, 50 to 14%, and 19 to 7% in the freshwater ones. The bloom of Chloroflexi (from 0 to 45%) was observed in MPf at Day 90, followed by that of Deltaproteobacteria (from 0 to 10%). Cluster analysis, in good accordance with the T-RFLP profiles, revealed a close clustering of the samples from MPf at Day 90 with those from STK and SK at Day 90, although the samples from STK, TO and SK microcosms differed greatly from MPf at Day 1 (Supplementary Figure S2).

A phylogenetic tree of all the 16S rRNA gene clones was constructed to clearly display the phylogenetic distribution of the whole microbial community across different microcosms and their phylogenetic association with 14 known dehalogenators (**Figure 5**). It was further explored on the major differences in the microbial community structure between STK and TO at Day 90, as these two most efficient microcosms also showed distinct PBDE profiles. *Chromatiales*, *Rhodocyclales*, and *Clostridia* were ranked as the three most abundant bacterial classes

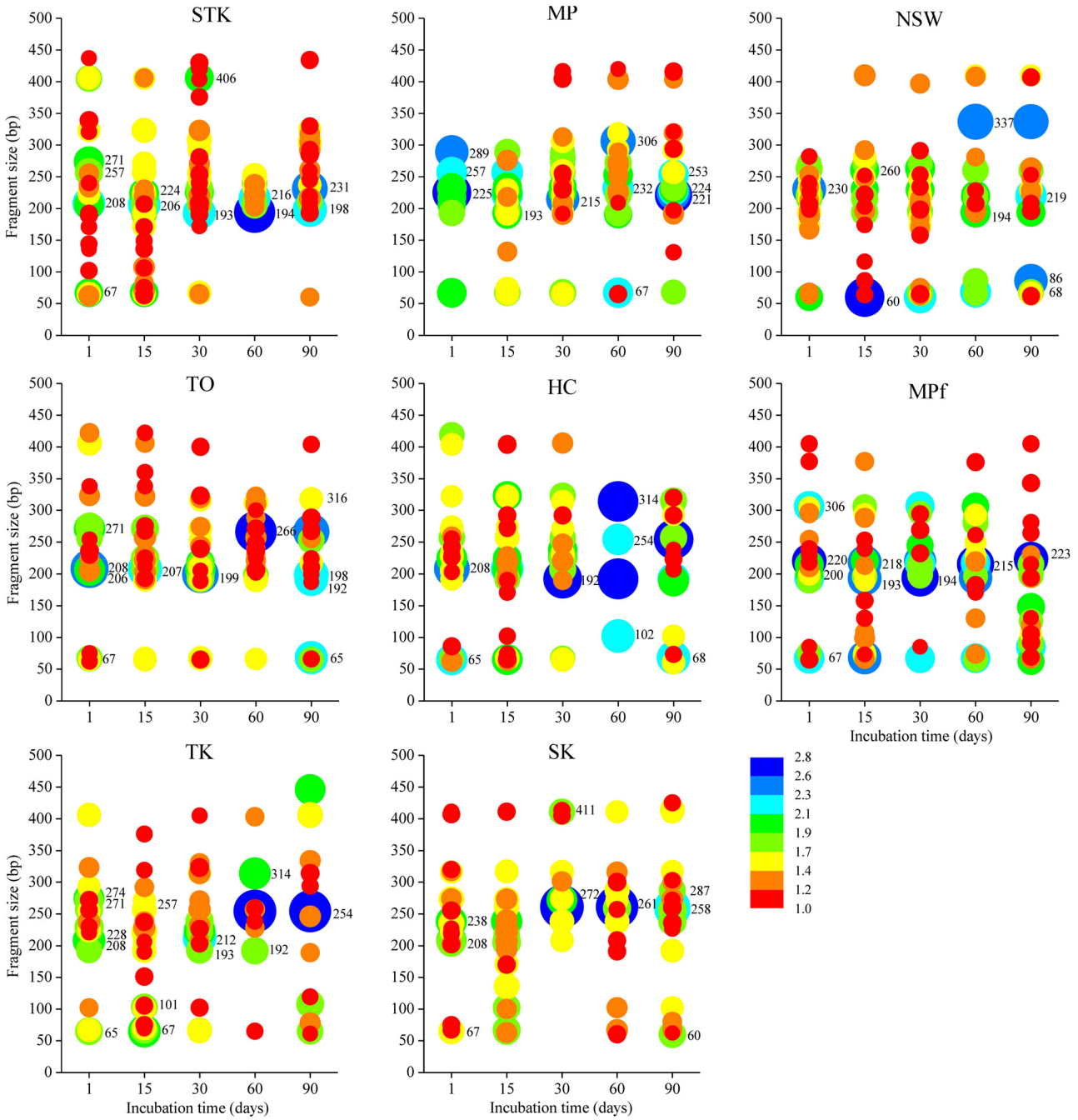

FIGURE 3 | Relative abundance of *Hae*III digested 16S rDNA T-RFs from total bacterial communities in the eight sediment microcosms from Days 1 to 90. The symbol color and size indicate the relative abundance of each T-RF as percentage of total peak area (log transformed).

in TO, while *Verrucomicrobia, Rhizobiales* and unclassified *Alphaproteobacteria* were the three most dominant classes in STK (**Table 2**).

Of the 20 OTUs of Chloroflexi, only one OTU (D90-MPf-22), identified as *Dehalogenimonas lykanthroporepellens* (95% similarity), fell into the class of *Dehalococcoidetes* and closely clustered with the most extensively studied *Dehalococcoides* spp. (Bootstrap value = 87). Another OTU of two Firmicutes clones (D90-TO-14 and D90-TO-22) were identified as *Desulfitobacterium* sp. and affiliated with *Dehalobacter restrictus* (U84497.2) (Bootstrap value = 100). One OTU (D90-STK-4) identified as *Ruegeria* sp. were also clustered with the Alphaproteobacterial OHRB *Ruegeria* sp. TM1040 (CP000377.1:144962-146416) (Bootstrap value = 64).

TABLE 1 | Molecular identification of the dominant terminal restriction fragments (T-RFs) with cumulative contribution to differences of T-RFLP profiles over time greater than 50% in each sediment microcosm by SIMER analysis.

Predicted T-RF length (bp)	Observed T-RF length (bp)	Phylogenetic group	Dominant in	Closest match from the clone libraries constructed in this study
Dominant at Day 1 ~ Day 30				
68	67	Gammaproteobacteria	All	Uncultured gamma proteobacterium (AM259852.1), 99%
208	208	Deltaproteobacteria	Saline[a]	Uncultured delta proteobacterium (EF061950.1), 98%
206	206	Deltaproteobacteria	STK, TO	Uncultured delta proteobacterium (DQ395025.1), 97%
237	238	Deltaproteobacteria	SK	Uncultured delta proteobacterium (EF655671.1), 96%
257	257	Firmicutes; Clostridia	Saline	Uncultured Clostridiaceae bacterium (FJ425601.1), 96%
270	271/272	Firmicutes; Clostridia	STK, TO, TK, SK	*Alkaliphilus peptidofermentans* Z-7036 (EF382660.1), 91%
224	225/224	Chloroflexi; Anaerolineae Anaerolineae	MP	Uncultured *Anaerolineaceae* bacterium (JF806903.1), 97%
221	220	Chloroflexi	MPf	Uncultured Chloroflexi bacterium (FM242343.1), 95%
Dominant at Day 60 ~ Day 90				
231	231	Actinobacteria	STK	Uncultured *Actinobacteridae* bacterium (FN582328.1), 98%
195	193	Gammaproteobacteria	STK	Uncultured gamma proteobacterium (JF344548.1), 96%
196	194	Deltaproteobacteria	MPf, NSW	*Desulfovibrio* sp. enrichment culture clone (HQ108123.1)[b]
266	266	Firmicutes; Clostridia	TO	*Clostridium algidicarnis* NCFB 2931 (X77676), 95%
199	198	Betaproteobacteria	STK, TO	Uncultured beta proteobacterium (AM713401.1), 100%
316	314/316	Firmicutes	TO, TK, HC	Uncultured Firmicutes bacterium (AM745203.1), 94%
192	192	Alphaproteobacteria	TO, TK, HC	*Pseudoruegeria aquimaris* (NR_043932.1), 92%
254	253/254	Alphaproteobacteria	TK, HC	Uncultured alpha proteobacterium (FJ666151.1), 90%
260	261	Candidate division OP8	SK	Uncultured candidate division OP8 (DQ811949.1), 97%
414	411	Bacteroidetes	SK	Uncultured Bacteroidetes bacterium (JF344262.1), 95%
310	306	Firmicutes; Bacilli	MP, MPf	*Bacillus* sp. G11001 (AB531397.1), 99%
215	215	Deltaproteobacteria	MP, MPf	Uncultured delta proteobacterium (JF344345.1), 98%

[a]*Saline sediments refer to all mangrove and marine sediments.* [b]*The underlined closest match is from the reference species rather than from the clone libraries in this study.*

Molecular Detection and Quantification of *Dehalococcoides* 16S rRNA Genes

All the sediment microcosms held 16S rRNA gene copies of the total bacteria and *Dehalococcoides* within the range of 10^6–10^9 and 10^2–10^6, respectively, suggesting the relative abundance of *Dehalococcoides* sp. within the whole microbial community was less than 1%. The relative abundances of *Dehalococcoides* sp. were above 10^{-4} at Day 1 in all the sediment microcosms, followed by "down-up" fluctuations from Days 1 to 30, and the fluctuations varied at different degrees among sediment microcosms in the later stage (Supplementary Figure S3). Notably, the relative abundances of *Dehalococcoides* sp. were found much higher in NSW at each sampling time (around $10^{-4} \sim 10^{-3}$) but became the lowest in the marine sediment SK after 60 days (as low as 10^{-6}).

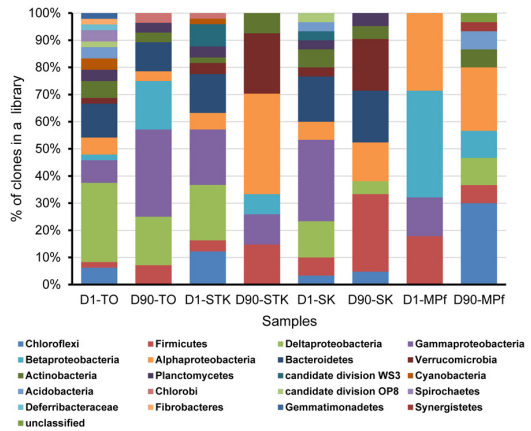

FIGURE 4 | Phylogenetic composition of the eight 16S rRNA gene clone libraries constructed from STK, TO, SK, and MPf sediment microcosms at Days 1 and 90, respectively.

DISCUSSION

Relationship Between Microbial Community Structure and Their Debrominating Capability

To our knowledge, this study presents the first attempt to compare the microbial community structure from different types of sediments with varying reductive debrominating capabilities. This is a crucial step to explore the key debrominating microorganisms responsible for the *in situ* bioremediation processes (Lovley, 2003). The distribution of the well-known OHRB, i.e., *Dehalococcoides*, *Dehalobacter,* and *Desulfitobacterium,* has previously been examined across debromination microcosms with 28 different soils and sediments, but their presence or absence was not necessarily related to the debrominating activity of samples (Lee and He, 2010). In the present study, the distinct different debrominating capabilities of sediment microcosms between saline and

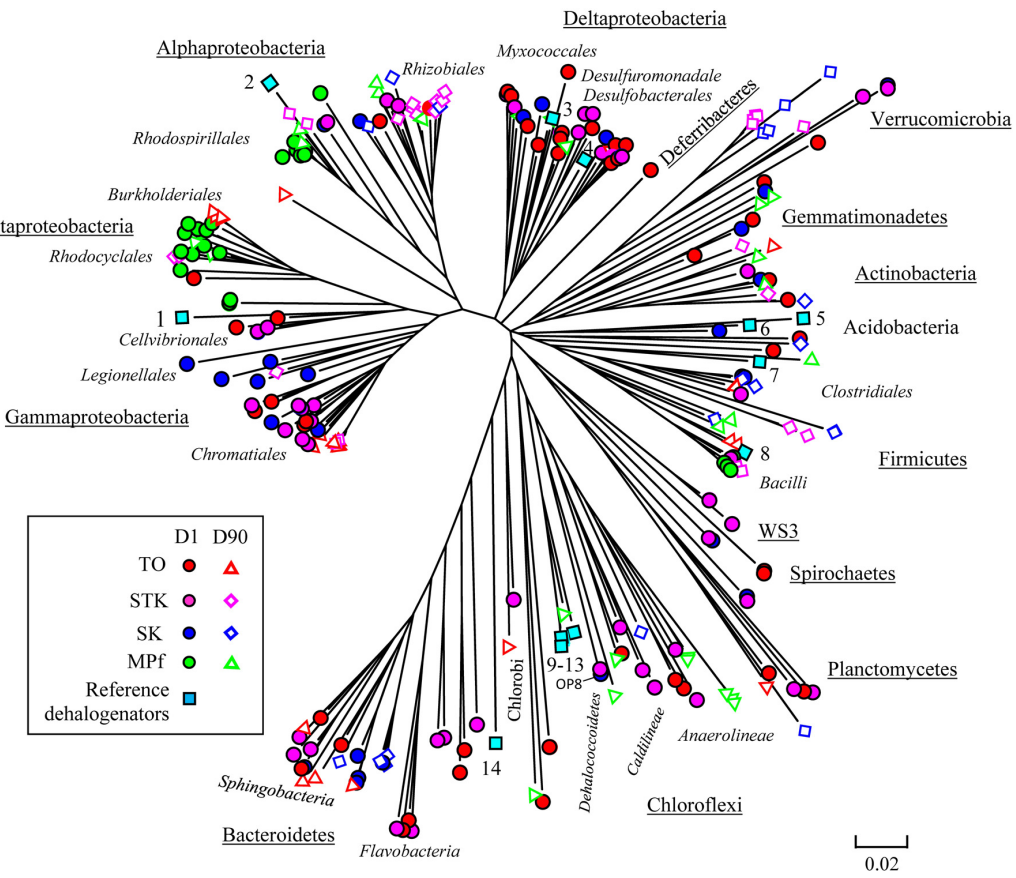

FIGURE 5 | Neighbor-joining phylogenetic tree of the 261 16S rRNA nucleotide sequences obtained from the STK, TO, SK, and MPf sediment microcosms at Days 1 and 90 with reference to members of 14 known dehalogenators (1) *Shewanella sediminis* strainHAW-EB3 (NR_074819.1); (2) *Ruegeria* sp. TM1040 (CP000377.1:144962-146416); (3) *Anaeromyxobacter dehalogenans* strain 2CP-1 (AF382396.1); (4) *Desulfomonile limimaris* (AF282177.1); 5. *Desulfovibrio* sp. TBP-1 (AF090830.1); (6) *Desulfovibrio dechloracetivorans* strain SF3 (NR_025078.1); (7) *Acetobacterium* sp. AG (JQ627627.1); (8) *Dehalobacter restrictus* (U84497.2); (9) *Dehalobium chlorocoercia* DF-1 (AF393781.1); (10) *Dehalococcoides* sp. BAV1 (AY165308.1); (11) *Dehalococcoides mccartyi* GY50 (NC_022964.1:c841590-840096); (12) *Dehalococcoides* sp. MB (EU073964.1); (13) *Dehalococcoides mccartyi* strain 195 (NR_114415.1); and (14) *Dehalospirillum multivorans* (X82931.1).

freshwater environments have been shown to rightly correspond to the differences in their microbial community structures (**Figure 2**). The significant relationship between microbial community structure determined by T-RFLP profiles and PBDE debrominating pattern was further confirmed using RDA, as previously demonstrated by Xu et al. (2012)). The first and all canonical axes contributed to explain 6.4 and 18.7% of the total variance in microbial species data, with *F*-values of 2.321 (P = 0.005) and 1. 563 (P = 0.002), respectively. The biplot with PBDEs and samples displayed clearly that the large variance of T-RFLP profiles among different samples was mainly attributed to the debromination degree in terms of total PBDE concentration and types of BDE congeners (**Figure 6**). This result complemented our previous study (Zhu et al., 2014b), and provided valuable evidence into the role of indigenous microbial community in the fate of PBDEs during natural attenuation. In addition, it extended our knowledge regarding PBDE debrominating capability mainly derived from studies with isolated dehalogenating bacteria or enriched cultures (He et al., 2006; Robrock et al., 2009; Zeng et al., 2010), which supported the differences in microbial community structure could lead to different debrominating capabilities, owing to the substrate specificity and specific debrominating pathways adopted by different OHRB species present.

The clone library analysis revealed that the mangrove and marine microcosms exhibiting more rapid and extensive debromination of PBDEs harbored a more diverse microbial community than that in the freshwater microcosm at Day 1. The positive correlation between bacterial diversity and their degradation efficiency has also been reported by Dell'Anno et al. (2012). More importantly, the distinct distribution patterns of the dominant bacterial phyla were observed between the saline and freshwater microcosms. Deltaproteobacteria and Chloroflexi were more abundant in the saline microcosms, while Alpha- and Beta-proteobacteria dominated the freshwater microcosm at the 1st day. According to the phylogenetic distribution of the known OHRB, Deltaproteobacteria and Chloroflexi are the two major phyla that harbor non-obligate and obligate OHRB, respectively (Atashgahi et al., 2016). The Chloroflexi strains, including *Dehalococcoides* and *o*-17/DF-1 like bacteria, have frequently been identified as the key dehalogenators in the chlorinated organics-contaminated sediments, but the complete removal of the substrates usually took a few months or years (Zanaroli et al., 2012; Wang and He, 2013). However, one study reported that the co-culture consisting of *Dehalococcoides* and *Desulfovibrio* (Deltaproteobacteria) strains exhibited a rapid and complete debromination of tetra- and penta-BDEs within 14 days (Lee et al., 2011). These findings could partially explain the rapid and extensive debrominating capabilities of microbial communities from STK and TO microcosms in the present study.

Meanwhile, Alpha- and Beta-proteobacteria that dominated in MPf at Day 1 became one of the dominant phyla in STK and TO microcosms, respectively, at Day 90, when they exhibited distinctly different PBDE profiles (**Figures 1**, **4**). The

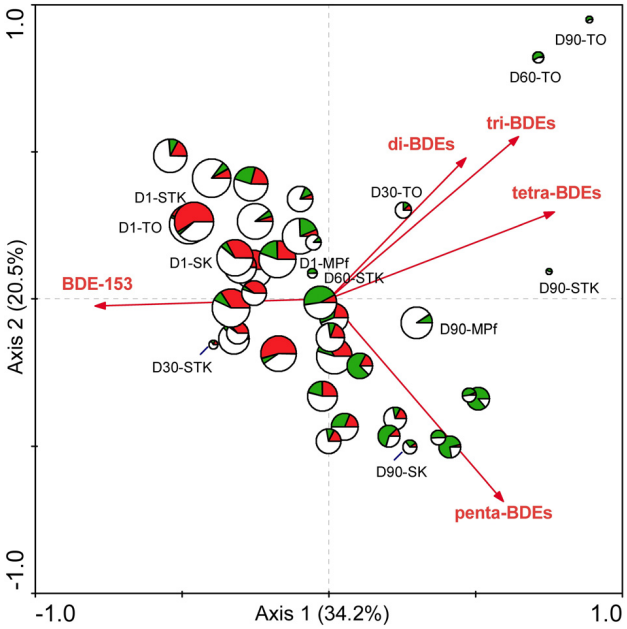

FIGURE 6 | The biplot diagram with PBDEs and samples based on RDA analysis of the T-RFLP and PBDE profiles from the eight sediment microcosms from Days 1 to 90, with the size of the sample symbols corresponding to total PBDE concentration, and the pies of the sample symbols corresponding to the distribution of different groups of T-RFs that were defined in **Table 1**. (red: dominant T-RFs at Days 1 ~ 30; green: dominant T-RFs at Days 60 ~ 90; blank: the remaining T-RFs detected).

dominance of Alphaproteobacteria has also been documented in PCB dechlorinating microcosms of marine sediments by the later stage of incubation (Matturro et al., 2016c). The cooperation between Alphaproteobacterial members with the potential PBDE debrominating strains from Deltaproteobacteria and Chloroflexi was inferred by their succeed dominance in different stages of PBDE debromination, and suggested to contribute to more rapid and complete debromination in STK microcosms compared to in TO microcosms that dominated by Beta- and Gamma-proteobacteria at the same time (**Table 2**). The Alpha- and Beta-proteobacterial members were reported to be capable of degrading less recalcitrant and lower brominated BDE congeners (from mono- to hexa-BDEs), such as *Sphingomonas* sp. PH-07, *Rhodococcus jostii* RHA1 and *Burkholderia xenovorans* LB400, owing to their aromatic ring-cleavage activity (Kim et al., 2007; Robrock et al., 2009). However, information on the reductive debromination of Alpha- and Beta-proteobacteria was rather limited. It is thus essential to gain deep insights in their metabolic interactions with the known OHRB for the complete debromination of PBDEs in contaminated sediments.

Unique distribution of *Planctomycetes*, *Gemmatimonadetes,* and *Verrucomicrobia* in the saline sediments were detected. These phyla have also been revealed to be actively involved in organic carbon utilization in the deep-sea environments

TABLE 2 | Relative abundance (%) of classes of Proteobacteria, Chloroflexi, and Firmicutes that known to contain organohalides-respiring bacteria (OHRB).

(Sub) Phylum	Class	TO		STK		SK		MPf		Representative species in the clone library
		D1	D90	D1	D90	D1	D90	D1	D90	
Alphaproteobacteria	Rhizobiales	2.1	0	2.1	18.5	0	10	0	6.7	Uncultured *Hyphomicrobium* sp.
	Rhodobacterales	0	0	4.3	7.4	3.0	0	31.0	10	*Thioclava* sp.
	Rhodospirillales	2.1	3.7	0	0	3.0	5.0	0	0	Uncultured *Rhodovibrio* sp.
	Sphingomonadales	0	0	0	0	0	0	0	6.7	Uncultured Sphingomonadales bacterium
	Unclassified-alpha	0	0	0	11.1	0	0	0	0	
Betaproteobacteria	Burkholderiales	0	0	0	7.4	0	0	17.2	10	*Ralstonia* sp.
	Rhodocyclales	2.1	18.5	0	0	0	0	17.2	0	*Denitromonas indolicum*
	Nitrosomonadales	0	0	0	0	0	0	3.4	0	*Thiobacillus thioparus*
Deltaproteobacteria	*Desulfobacterales	10.4	7.4	8.5	0	3.0	0	0	3.3	Uncultured Desulfobacteraceae bacterium
	*Desulfuromonadales	6.3	0	2.1	0	0	0	0	3.3	Uncultured *Desulfuromonas* sp.
	*Myxococcales	4.2	0	0	0	3.0	0	0	3.3	Uncultured Myxococcales bacterium
	Syntrophobacterales	2.1	0	2.1	0	3.0	0	0	0	Uncultured Syntrophaceae bacterium
	Unclassified-delta	2.1	0	4.3	0	3.0	0	0	0	
Gammaproteobacteria	Chromatiales	2.1	25.9	6.4	7.4	12.1	0	13.8	0	Ectothiorhodospiraceae bacterium
	Cellvibrionales	2.1	0	4.3	0	3.0	0	0	0	*Haliea* sp.
	Legionellales	0	0	2.1	3.7	3.0	0	0	0	*Legionella* sp.
	Thiohalophilus	0	3.7	0	0	3.0	0	0	0	*Thiohalophilus thiocyanatoxydans*
	Thiotrichales	0	0	0	0	3.0	0	0	0	Candidatus *Thiopilula aggregata*
	sulfur-oxidizing symbionts	0	3.7	0	0	0	0	0	0	
	Unclassified-gamma	8.3	0	6.4	0	6.1	0	0	0	
Chloroflexi	Anaerolineae	4.2	0	0	0	3.0	0	0	10	Uncultured Anaerolineaceae bacterium
	Caldilineae	0	0	0	0	0	0	0	6.7	Uncultured *Caldilinea* sp.
	*Dehalococcoidetes	0	0	0	0	0	0	0	3.3	*Dehalogenimonas lykanthroporepellens*
	Sphaerobacteridae	0	0	0	0	0	0	0	3.3	*Sphaerobacter thermophilus*
	Unclassified-Chloroflexi	2.1	0	12.8	0	0	5.0	0	6.7	
Firmicutes	Bacillales	0	0	2.1	7.4	3.0	0	17.2	0	*Bacillus* sp.
	*Clostridia	0	11.1	2.1	7.4	6.1	35.0	0	0	Clostridiaceae bacterium
	Unclassified-Firmicutes	2.1	0	0	0	0	0	0	6.7	
Overall relative abundance of the entire bacterial community		52.1	74.1	59.6	70.4	60.6	55.0	100	80	

**The class harboring the pure isolates of the known OHRB (Atashgahi et al., 2016).* [1]*http://www.ncbi.nlm.nih.gov*

(Li et al., 2016). Besides, most of the key T-RFs enriched were identified to belong to the known OHRB phyla, except for T-RF 261 being assigned to candidate division OP8. In our previous study on constructed mangrove microcosms for treatment of a mixture of wastewater-borne PAHs and PBDEs, a candidate division OP8 clone showing a high affinity with the *Dehalococcoides mccartyi* 195 was also detected (Wang et al., 2015). It was also once reported in a hydrocarbon- and chlorinated-solvent contaminated aquifer during intrinsic remediation (Dojka et al., 1998) and as representative members in mangrove sediments (Ikenaga et al., 2010). Further investigation on the role of these phyla in reductive debromination is needed and may help to discover new OHRB from marine/saline environments.

Dynamics of Microbial Community Structure and Their Debrominating Capability

It was found that the more rapid and divergent succession of microbial communities in the saline microcosms largely coincided with the changes in PBDE profiles. In contrast, the shifts in both microbial community structure and PBDE profiles were relatively small in the freshwater microcosms (**Figures 1**, **2**). Interestingly, a sudden change in the MPf microcosm till Day 90 was detected by T-RFLP analysis, with Chloroflexi and Deltaproteobacteria greatly enriched, and the removal rate of BDE-153 also greatly increased as observed in the mangrove and marine microcosms after Day 15. These results suggested that the microbial debrominating capability was not only determined by the microbial community structure, but greatly associated with the magnitude and dynamics of microbial community shifts over time. In fact, the succession of microbial community structure has been well documented in response to oil spill and could be used for prediction of the on-going remediation progress (Kimes et al., 2014). However, much less is known about microbial community shifts in response to PBDEs, further investigation is required to provide direct evidences, such as stable-isotope probing (SIP) and functional gene data, on the contribution of the enriched functional bacterial groups to PBDE debromination.

Relic DNA (referred to large amounts of extracellular DNA or in non-intact cells) has been demonstrated to significantly influence the structure of the microbial community, and its effects depended on the pH value of soil samples, which ranged from 3.5 to 8.0 as reported by Carini et al. (2016). Although the interference from relic DNA was not determined in the present study, the interference could be reflected by the dynamic analysis of the microbial community structure in each sediment microcosm, which just meant to resolve the succession of microbial communities. The pH values of the eight sediment samples in our study were all slight alkaline, from 7.4 to 8.0, so the effect of pH on relic DNA interference was considered insignificant as the pH gradient was relatively narrow. In addition, the presence of relic DNA did not obscure the detection of distinct shifts and sediment type-specific patterns in microbial communities from our sediment microcosms varying in the debromination capability.

The Role of Known OHRB During Intrinsic Debromination

So far only one isolate from the Chloroflexi, *Dehalococcoides mccartyi* GY50 could couple its growth with debromination of PBDEs and lead to more rapid and complete debromination compared to the co-metabolic pattern adopted by previously reported debrominating cultures (Ding et al., 2017). Detection and quantification of the well-known OHRB in dehalogenation microcosms have been widely applied to evaluate their role in intrinsic remediation processes (van der Zaan et al., 2010). Here, we only quantified 16S rRNA genes of *Dehalococcoides* because of the following reasons. Most of the known OHRB were isolated from the freshwater environments, with only seven originating from marine and estuarine sediments. Among the seven marine-originated OHRB isolates, two strains, i.e., *o*-17/DF-1 like bacteria, belong to the genus of *Dehalococcoides*, while the other five belonging to Delta- and Gamma-proteobacteria were all non-obligate OHRB, according to Atashgahi et al. (2016). We focused on monitoring the abundance of obligate OHRB, as many obligate degraders were identified as the key members responsible for the rapid bioremediation in marine environments, e.g., after oil spills (Yakimov et al., 2007). However, the obligate degraders were suggested as a minor seed population that would quickly withdraw after relief of the pollution stress (Yang et al., 2016). In the present study, *Dehalococcoides* were not dominant in the microbial community, and their relative abundances varied during the debromination process, with no clear pattern observed in relation to their debrominating efficiency across different microcosms (Supplementary Figure S1). For the role of OHRB in intrinsic debromination, Xu et al. (2012) found that that the known dechlorinating bacteria, such as *Dehalobacter*, showed low abundances in the enriched PBDE-degrading communities and some unclassified members could be involved in debromination by using barcoded pyrosequencing. In another recent study on tetrachloroethene (PCE) contaminated marine sediments, it has been found that the relative abundance of non-*Dehalococcoides* Chloroflexi retrieved from the original sediment took the predominance over *Dehalococcoides* sp. that added after 150 days, suggesting the important potential role of non-*Dehalococcoides* Chloroflexi during natural reductive dechlorination process (Matturro et al., 2016b). These results suggested that one or more unknown highly efficient debrominators rather than *Dehalococcoides*-like species would be present to perform extensive debromination in our microcosms.

Furthermore, different OHRB strains from even the same genus as *Dehalococcoides* showed quite different dehalogenation capabilities due to the different number and types of reductive dehalogenases (RDases) genes they possess (Hug et al., 2013). Recently, novel PCB dechlorinase genes *pcb*A1, *pcb*A4, and *pcb*A5 have been revealed in *D. mccartyi* strains by Wang S. et al. (2014), together with three PBDE RDases genes *pbr*A1, *pbr*A2, and *pbr*A3 in *D. mccartyi* strain GY50 by Ding et al. (2017). These

important discoveries would provide more specific biomarkers targeting reductive dehalogenase genes for evaluation the role of the known OHRB in debromination processes in more depth.

CONCLUSION

This is the first study comparing the microbial community structure and dynamics across different sediments during intrinsic debromination of PBDEs. Both the microbial community structure and their succession largely attributed to variations in the debrominating capabilities and pathways among sediment types. Mangrove and marine sediment microcosms with relatively higher abundance of Chloroflexi and Delta-proteobacteria showed faster debromination compared with freshwater microcosms. Moreover, nearly complete debromination of BDE-153 could be achieved with Alpha-proteobacteria being enriched in the later stage. Freshwater microcosms exhibited relatively slow debromination but the regeneration of those functional debrominating microorganisms were detected by the end of incubation. Further investigation is needed to compare the functional diversity of microbial communities involved in debromination in saline and freshwater sediments, or under different salinity gradient, combined with culture-dependent approaches and powerful deep sequencing and environmental microbiome technologies. These findings would improve our understanding on the role of indigenous microbial community in the debromination of PBDEs in natural sediments, and indicate the great potential to enrich and isolate debrominating microorganisms from mangrove sediments for further bioremediation purposes.

AUTHOR CONTRIBUTIONS

YW and NT designed the study. YW, HZ, and YW performed the microbial and PBDE analyses. All authors wrote the manuscript and the Supplementary Materials.

FUNDING

This present study was supported by the research funds from National Natural Science Foundation of China (Nos. 51509225 and 41630318), Laboratory of Basin Hydrology and Wetland Eco-restoration (No. BHWER201402), Hong Kong GRF Grant 9042542 and the State Key Laboratory in Marine Pollution, City University of Hong Kong.

ACKNOWLEDGMENTS

We thank Prof. Pei Yuan QIAN and Ms. Yin Ki TAM from the Coastal Marine Laboratory, the Hong Kong University of Science and Technology for assistance in T-RFLP sequencing work. We also express our great thanks for the reviewers for their thorough reviews and constructive comments, which greatly improved the manuscript.

SUPPLEMENTARY MATERIAL

The Supplementary Material for this article can be found online at: https://www.frontiersin.org/articles/10.3389/fmicb.2018.00952/full#supplementary-material

REFERENCES

Acosta-González, A., Rosselló-Móra, R., and Marqués, S. (2013). Characterization of the anaerobic microbial community in oil-polluted subtidal sediments: aromatic biodegradation potential after the Prestige oil spill. *Environ. Microbiol.* 15, 77–92. doi: 10.1111/j.1462-2920.2012.02782.x

Atashgahi, S., Lu, Y. and Smidt, H. (2016). "Overview of known organohalide-respiring bacteria—Phylogenetic diversity and environmental distribution," in *Organohalide-Respiring Bacteria*, eds L. Adrian, and F. E. Löffler (Berlin: Springer), 63–105.

Binelli, A., Sarkar, S. K., Chatterjee, M., Riva, C., Parolini, M., Bhattacharya, B. D., et al. (2007). Concentration of polybrominated diphenyl ethers (PBDEs) in sediment cores of Sundarban mangrove wetland, northeastern part of Bay of Bengal (India). *Mar. Pollut. Bull.* 54, 1220–1229. doi: 10.1016/j.marpolbul.2007.03.021

Cai, Y., Liang, B., Fang, Z., Xie, Y., and Tsang, E. P. (2015). Effect of humic acid and metal ions on the debromination of BDE209 by nZVM prepared from steel pickling waste liquor. *Front. Environ. Sci. Eng.* 9, 879–887. doi: 10.1007/s11783-014-0764-8

Carini, P., Marsden, P. J., Leff, J. W., Morgan, E. E., Strickland, M. S., and Fierer, N. (2016). Relic DNA is abundant in soil and obscures estimates of soil microbial diversity. *Nat. Microbol.* 2, 1–6. doi: 10.1038/nmicrobiol.2016.242

Chakraborty, J., and Das, S. (2016). Molecular perspectives and recent advances in microbial remediation of persistent organic pollutants. *Environ. Sci. Pollut. Res. Int.* 23, 16883–16903. doi: 10.1007/s11356-016-6887-7

Clarke, K. R., and Gorley, R. N. (eds). (2006). *PRIMER v6: User Manual/Tutorial*. Plymouth: PRIMER-E.

Culman, S. W., Bukowski, R., Gauch, H. G., Cadillo-Quiroz, H., and Buckley, D. H. (2009). T-REX: software for the processing and analysis of T-RFLP data. *BMC Bioinformatics* 10:171. doi: 10.1186/1471-2105-10-171

Culman, S. W., Gauch, H. G., Blackwood, C. B., and Thies, J. E. (2008). Analysis of T-RFLP data using analysis of variance and ordination methods: a comparative study. *J. Microbiol. Methods* 75, 55–63. doi: 10.1016/j.mimet.2008.04.011

Dell'Anno, A., Beolchini, F., Rocchetti, L., Luna, G. M., and Danovaro, R. (2012). High bacterial biodiversity increases degradation performance of hydrocarbons during bioremediation of contaminated harbor marine sediments. *Environ. Pollut.* 167, 85–92. doi: 10.1016/j.envpol.2012.03.043

Ding, C., Chow, W. L., and He, J. (2013). Isolation of *Acetobacterium* sp. Strain AG, which reductively debrominates octa- and pentabrominated diphenyl ether technical mixtures. *Appl. Environ. Microbiol.* 79, 1110–1117. doi: 10.1128/AEM.02919-12

Ding, C., Rogers, M. J., Yang, K. L., and He, J. (2017). Loss of the ssrA genome island led to partial debromination in the PBDE respiring *Dehalococcoides mccartyi* strain GY50. *Environ. Microbiol.* 19, 2906–2915. doi: 10.1111/1462-2920.13817

Dojka, M. A., Hugenholtz, P., Haack, S. K., and Pace, N. R. (1998). Microbial diversity in a hydrocarbon-and chlorinated-solvent-contaminated aquifer undergoing intrinsic bioremediation. *Appl. Environ. Microbiol.* 64, 3869–3877.

Fagervold, S. K., Watts, J. E., et al. (2005). Sequential reductive dechlorination of meta-chlorinated polychlorinated biphenyl congeners in sediment microcosms by two different *Chloroflexi* phylotypes. *Appl. Environ. Microbiol.* 71, 8085–8090. doi: 10.1128/AEM.71.12.8085

Freeborn, R., West, K., Bhupathiraju, V., Chauhan, S., Rahm, B., Richardson, R., et al. (2005). Phylogenetic analysis of TCE-dechlorinating consortia enriched on a variety of electron donors. *Environ. Sci. Technol.* 39, 8358–8368. doi: 10.1021/es048003p

Futagami, T., Morono, Y., Terada, T., Kaksonen, A. H., and Inagaki, F. (2013). Distribution of dehalogenation activity in subseafloor sediments of the Nankai Trough subduction zone. *Philos. Trans. R. Soc. B Biol. Sci.* 368:20120249. doi: 10.1098/rstb.2012.0249

Gerecke, A. C., Hartmann, P. C., Heeb, N. V., Kohler, H. P., Giger, W., Schmid, P., et al. (2005). Anaerobic degradation of decabromodiphenyl ether. *Environ. Sci. Technol.* 39, 1078–1083. doi: 10.1021/es048634j

He, J., Robrock, K. R., and Alvarez-Cohen, L. (2006). Microbial reductive debromination of polybrominated diphenyl ethers (PBDEs). *Environ. Sci. Technol.* 40, 4429–4434. doi: 10.1021/es052508d

Huang, H. L., Zhang, S. Z., Christie, P., Wang, S., and Xie, M. (2010). Behavior of decabromodiphenyl ether (BDE-209) in the soil-plant system: Uptake, translocation, and metabolism in plants and dissipation in soil. *Environ. Sci. Technol.* 44, 663–667. doi: 10.1021/es901860r

Huang, H. W., Chang, B. V., and Lee, C. C. (2014). Reductive debromination of decabromodiphenyl ether by anaerobic microbes from river sediment. *Int. Biodeter. Biodegr.* 87, 60–65. doi: 10.1016/j.ibiod.2013.10.011

Hug, L. A., Maphosa, F., Leys, D., Loffler, F. E., Smidt, H., Edwards, E. A., et al. (2013). Overview of organohalide-respiring bacteria and a proposal for a classification system for reductive dehalogenases. *Philos. Trans. R. Soc. B Biol. Sci.* 368:20120322. doi: 10.1098/rstb.2012.0322

Ikenaga, M., Guevara, R., Dean, A. L., Pisani, C., and Boyer, J. N. (2010). Changes in community structure of sediment bacteria along the florida coastal everglades marsh-mangrove-seagrass salinity gradient. *Microb. Ecol.* 59, 284–295. doi: 10.1007/s00248-009-9572-2

Junier, P., Junier, T., and Witzel, K. P. (2008). TRiFLe, a program for in silico terminal restriction fragment length polymorphism analysis with user-defined sequence sets. *Appl. Environ. Microbiol.* 74, 6452–6456. doi: 10.1128/aem.01394-08

Kim, Y. M., Nam, I. H., Murugesan, K., Schmidt, S., Crowley, D. E., and Chang, Y. S. (2007). Biodegradation of diphenyl ether and transformation of selected brominated congeners by *Sphingomonas* sp. ph-07. *Appl. Microbiol. Biotechnol.* 77, 187–194. doi: 10.1007/s00253-007-1129-z

Kimes, N. E., Callaghan, A. V., Suflita, J. M., and Morris, P. J. (2014). Microbial transformation of the deepwater horizon oil spill-past, present, and future perspectives. *Front. Microbiol.* 5:603. doi: 10.3389/fmicb.2014.00603

Lam, C., Neumann, R., Shin, P. K., Au, D. W., Qian, P. Y., and Wu, R. S. (2010). Polybrominated diphenylethers (PBDEs) alter larval settlement of marine benthic polychaetes. *Environ. Sci. Technol.* 44, 7130–7137. doi: 10.1021/es1012615

Lane, D. J. (1991). "16S/23S rRNA sequencing," in *Nucleic Acid Techniques in Bacterial Systematics*, eds E. Stackebrandt, and M. Goodfellow (New York, NY: John Wiley & Sons), 115–175.

Lee, L. K., Ding, C., Yang, K. L., and He, J. (2011). Complete debromination of tetra- and penta-brominated diphenyl ethers by a coculture consisting of *Dehalococcoides* and *Desulfovibrio* species. *Environ. Sci. Technol.* 45, 8475–8482. doi: 10.1021/es201559g

Lee, L. K., and He, J. (2010). Reductive debromination of polybrominated diphenyl ethers by anaerobic bacteria from soils and sediments. *Appl. Environ. Microbiol.* 76, 794–802. doi: 10.1128/AEM.01872-09

Li, C. H., Zhou, H. W., Wong, Y. S., and Tam, N. F.-Y. (2009). Vertical distribution and anaerobic biodegradation of polycyclic aromatic hydrocarbons in mangrove sediments in Hong Kong, South China. *Sci. Total Environ.* 407, 5772–5779. doi: 10.1016/j.scitotenv.2009.07.034

Li, M., Jain, S., and Dick, G. J. (2016). Genomic and transcriptomic resolution of organic matter utilization among deep-sea bacteria in guaymas basin hydrothermal plumes. *Front. Microbiol.* 7:1125. doi: 10.3389/fmicb.2016.01125

Li, Y., Lin, T., Chen, Y., Hu, L., Guo, Z., and Zhang, G. (2012). Polybrominated diphenyl ethers (PBDEs) in sediments of the coastal East China Sea: occurrence, distribution and mass inventory. *Environ. Pollut.* 171, 155–161. doi: 10.1016/j.envpol.2012.07.039

Lovley, D. R. (2003). Cleaning up with genomics: applying molecular biology to bioremediation. *Nat. Rev. Microbiol.* 1, 35–44. doi: 10.1038/nrmicro731

Ma, W., Yan, Y., Ma, M., Su, F., and Zhang, Y. (2016). Effect of black carbon on the migration and biodegradation of pentabromodiphenyl ether (BDE-99) during natural groundwater recharge with treated municipal wastewater. *Int. Biodeterior. Biodegrad.* 113, 177–186. doi: 10.1016/j.ibiod.2016.01.016

Matturro, B., Di Lenola, M., Ubaldi, C., and Rossetti, S. (2016a). First evidence on the occurrence and dynamics of *Dehalococcoides mccartyi* PCB-dechlorinase genes in marine sediment during Aroclor1254 reductive dechlorination. *Mar. Pollut. Bull.* 112, 189–194. doi: 10.1016/j.marpolbul.2016.08.021

Matturro, B., Presta, E., and Rossetti, S. (2016b). Reductive dechlorination of tetrachloroethene in marine sediments: Biodiversity and dehalorespiring capabilities of the indigenous microbes. *Sci. Total Environ.* 545–546, 445–452. doi: 10.1016/j.scitotenv.2015.12.098

Matturro, B., Ubaldi, C., Grenni, P., Caracciolo, A. B., and Rossetti, S. (2016c). Polychlorinated biphenyl (PCB) anaerobic degradation in marine sediments: microcosm study and role of autochthonous microbial communities. *Environ. Sci. Pollut. Res. Int.* 23, 12613–12623. doi: 10.1007/s11356-015-4960-2

McCune, B. and Grace, J. B. (eds). (2002). *Analysis of Ecological Communities*. Gleneden Beach, OR: MJM Software Design.

McGrath, T. J., Ball, A. S., and Clarke, B. O. (2017). Critical review of soil contamination by polybrominated diphenyl ethers (PBDEs) and novel brominated flame retardants (NBFRs); concentrations, sources and congener profiles. *Environ. Pollut.* 230, 741–757. doi: 10.1016/j.envpol.2017.07.009

Mohn, W. W., and Tiedje, J. M. (1992). Microbial reductive dehalogenation. *Microbiol. Rev.* 56, 482–507. doi: 10.1111/j.1574-6941.2000.tb00693.x

Muyzer, G., de Waal, E. C., and Uitterlinden, A. G. (1993). Profiling of complex microbial populations by denaturing gradient gel electrophoresis analysis of polymerase chain reaction-amplified genes coding for 16S rRNA. *Appl. Environ. Microbiol.* 59, 695–700.

Oros, D. R., Hoover, D., Rodigari, F., Crane, D., and Sericano, J. (2005). Levels and distribution of polybrominated diphenyl ethers in water, surface sediments, and bivalves from the San Francisco Estuary. *Environ. Sci. Technol.* 39, 33–41. doi: 10.1021/es048905q

Qiu, M., Chen, X., Deng, D., Guo, J., Sun, G., Mai, B., et al. (2012). Effects of electron donors on anaerobic microbial debromination of polybrominated diphenyl ethers (PBDEs). *Biodegradation* 23, 351–361. doi: 10.1007/s10532-011-9514-9

Robrock, K. R., Coelhan, M., Sedlak, D. L., and Alvarez-Cohen, L. (2009). Aerobic biotransformation of polybrominated diphenyl ethers (PBDEs) by bacterial isolates. *Environ. Sci. Technol.* 43, 5705–5711. doi: 10.1021/es900411k

Robrock, K. R., Korytár, P., and Alvarez-Cohen, L. (2008). Pathways for the anaerobic microbial debromination of polybrominated diphenyl ethers. *Environ. Sci. Technol.* 42, 2845–2852. doi: 10.1021/es0720917

Shih, Y. H., Chou, H. L., and Peng, Y. H. (2012). Microbial degradation of 4-monobrominated diphenyl ether with anaerobic sludge. *J. Hazard. Mater.* 213-214, 341–346. doi: 10.1016/j.jhazmat.2012.02.009

Sipilä, T. P., Keskinen, A. K., Akerman, M. L., Fortelius, C., Haahtela, K., and Yrjälä, K. (2008). High aromatic ring-cleavage diversity in birch rhizosphere: PAH treatment-specific changes of I.E.3 group extradiol dioxygenases and 16S rRNA bacterial communities in soil. *ISME J.* 2, 968–981. doi: 10.1038/ismej.2008.50

Song, M., Luo, C., Li, F., Jiang, L., Wang, Y., Zhang, D., et al. (2015). Anaerobic degradation of polychlorinated biphenyls (PCBs) and polychlorinated biphenyls ethers (PBDEs), and microbial community dynamics of electronic waste-contaminated soil. *Sci. Total Environ.* 502, 426–433. doi: 10.1016/j.scitotenv.2014.09.045

Stiborova, H., Vrkoslavova, J., Pulkrabova, J., Poustka, J., Hajslova, J., and Demnerova, K. (2015). Dynamics of brominated flame retardants removal in contaminated wastewater sewage sludge under anaerobic conditions. *Sci. Total Environ.* 533, 439–445. doi: 10.1016/j.scitotenv.2015.06.131

Stockholm Convention (2009). *Stockholm convention on persistent organic pollutants (POPs). Secretariat of the Stockholm Convention on Persistent Organic Pollutants: United Nations Environment Programme (UNEP)*. Available at: http://www.wipo.int/edocs/lexdocs/treaties/en/unep-pop/trt_unep_pop_2.pdf

Tamura, K., Peterson, D., Peterson, N., Stecher, G., Nei, M., and Kumar, S. (2011). MEGA5: molecular evolutionary genetics analysis using maximum likelihood, evolutionary distance, and maximum parsimony methods. *Mol. Biol. Evol.* 28, 2731–2739. doi: 10.1093/molbev/msr121

van der Zaan, B., Hannes, F., Hoekstra, N., Rijnaarts, H., de Vos, W. M., Smidt, H., et al. (2010). Correlation of Dehalococcoides 16S rRNA and chloroethene-reductive dehalogenase genes with geochemical conditions in chloroethene-contaminated groundwater. *Appl. Environ. Microbiol.* 76, 843–850. doi: 10.1128/AEM.01482-09

Wang, S., Chng, K. R., Wilm, A., Zhao, S., Yang, K. L., Nagarajan, N., et al. (2014). Genomic characterization of three unique *Dehalococcoides* that respire on persistent polychlorinated biphenyls. *Proc. Natl. Acad. Sci. U.S.A.* 111, 12103–12108. doi: 10.1073/pnas.1404845111

Wang, S., and He, J. (2013). Dechlorination of commercial PCBs and other multiple halogenated compounds by a sediment-free culture containing *Dehalococcoides* and *Dehalobacter*. *Environ. Sci. Technol.* 47, 10526–10534. doi: 10.1021/es4017624

Wang, Y. F., Wu, Y., Pi, N., and Tam, N. F. Y. (2014). Investigation of microbial community structure in constructed mangrove microcosms receiving wastewater-borne polycyclic aromatic hydrocarbons (PAHs) and polybrominated diphenyl ethers (PBDEs). *Environ. Pollut.* 187, 136–44. doi: 10.1016/j.envpol.2014.01.003

Wang, Y. F., Wu, Y., Wu, Z. B., and Tam, N. F. Y. (2015). Genotypic responses of bacterial community structure to a mixture of wastewater-borne PAHs and PBDEs in constructed mangrove microcosms. *J. Hazard. Mater.* 298, 91–102. doi: 10.1016/j.jhazmat.2015.05.003

Xu, M., Chen, X., Qiu, M., Zeng, X., Xu, J., Deng, D., et al. (2012). Barcoded pyrosequencing reveals the responses of PBDE-degrading microbial communities to electron donor amendments. *PLoS One* 7:e30439. doi: 10.1371/journal.pone.0030439

Yakimov, M. M., Timmis, K. N., and Golyshin, P. N. (2007). Obligate oil-degrading marine bacteria. *Curr. Opin. Biotechnol.* 18, 257–266. doi: 10.1016/j.copbio.2007.04.006

Yang, C., Kublik, A., Weidauer, C., Seiwert, B., and Adrian, L. (2015). Reductive dehalogenation of oligocyclic phenolic bromoaromatics by *Dehalococcoides mccartyi* Strain CBDB1. *Environ. Sci. Technol.* 49, 8497–8505. doi: 10.1021/acs.est.5b01401

Yang, T., Nigro, L. M., Gutierrez, T., D'Ambrosio, L., Joye, S. B., Highsmith, R., et al. (2016). Pulsed blooms and persistent oil-degrading bacterial populations in the water column during and after the Deepwater Horizon blowout. *Deep Sea Res. Part 2 Top. Stud. Oceanogr.* 129, 282–291. doi: 10.1016/j.dsr2.2014.01.014

Yang, Y., Xu, M., He, Z., Guo, J., Sun, G., and Zhou, J. (2013). Microbial electricity generation enhances decabromodiphenyl ether (BDE-209) degradation. *PLoS One* 8:e70686. doi: 10.1371/journal.pone.0070686

Yen, J. H., Liao, W. C., Chen, W. C., and Wang, Y. S. (2009). Interaction of polybrominated diphenyl ethers (PBDEs) with anaerobic mixed bacterial cultures isolated from river sediment. *J. Hazard. Mater.* 165, 518–524. doi: 10.1016/j.jhazmat.2008.10.007

Zanaroli, G., Balloi, A., Negroni, A., Borruso, L., Daffonchio, D., and Fava, F. (2012). A Chloroflexi bacterium dechlorinates polychlorinated biphenyls in marine sediments under in situ-like biogeochemical conditions. *J. Hazard. Mater.* 209-210, 449–457. doi: 10.1016/j.jhazmat.2012.01.042

Zanaroli, G., Negroni, A., Häggblom, M. M., and Fava, F. (2015). Microbial dehalogenation of organohalides in marine and estuarine environments. *Curr. Opin. Biotechnol.* 33, 287–295. doi: 10.1016/j.copbio.2015.03.013

Zeng, X., Massey Simonich, S. L., Robrock, K. R., Korytár, P., Alvarez-Cohen, L., and Barofsky, D. F. (2010). Application of a congener-specific debromination model to study photodebromination, anaerobic microbial debromination, and Fe0 reduction of polybrominated diphenyl ethers. *Environ. Toxicol. Chem.* 29, 770–778. doi: 10.1002/etc.119

Zhang, S., Xia, X., Xia, N., Wu, S., Gao, F., and Zhou, W. (2013). Identification and biodegradation efficiency of a newly isolated 2,2′,4,4′-tetrabromodiphenyl ether (BDE-47) aerobic degrading bacterial strain. *Int. Biodeterior. Biodegrad.* 76, 24–31. doi: 10.1016/j.ibiod.2012.06.020

Zhang, Z., Wang, C., Li, J., Wang, B., Wu, J., Jiang, Y., et al. (2014). Enhanced bioremediation of soil from Tianjin, China, contaminated with polybrominated diethyl ethers. *Environ. Sci. Pollut. Res. Int.* 21, 14037–14046. doi: 10.1007/s11356-014-3313-x

Zhong, Y., Luan, T., Zhou, H., Lan, C., and Tam, N. F. Y. (2006). Metabolite production in degradation of pyrene alone or in a mixture with another polycyclic aromatic hydrocarbon by *Mycobacterium* sp. *Environ. Toxicol. Chem.* 25, 2853–2859. doi: 10.1897/06-042R.1

Zhu, B., Wu, S., Xia, X., Lu, X., Zhang, X., Xia, N., et al. (2016). Effects of carbonaceous materials on microbial bioavailability of 2,2′,4,4′-tetrabromodiphenyl ether (BDE-47) in sediments. *J. Hazard. Mater.* 312, 216–223. doi: 10.1016/j.jhazmat.2016.03.065

Zhu, H. W., Wang, Y., Wang, X., Luan, T. G., and Tam, N. F. Y. (2014a). Distribution and accumulation of polybrominated diphenyl ethers (PBDEs) in Hong Kong mangrove sediments. *Sci. Total Environ.* 468-469, 130–139. doi: 10.1016/j.scitotenv.2013.08.021

Zhu, H. W., Wang, Y., Wang, X., Luan, T. G., and Tam, N. F. Y. (2014b). Intrinsic debromination potential of polybrominated diphenyl ethers in different sediment slurries. *Environ. Sci. Technol.* 48, 4724–4731. doi: 10.1021/es4053818

Zinder, S. H. (2016). "The genus *Dehalococcoides*," in *Organohalide-Respiring Bacteria*, eds L. Adrian, and F. E. Löffler (Berlin; Springer), 107–136. doi: 10.1007/978-3-662-49875-0_6

Conflict of Interest Statement: The authors declare that the research was conducted in the absence of any commercial or financial relationships that could be construed as a potential conflict of interest.

frontiers in Microbiology

ORIGINAL RESEARCH
published: 28 March 2018
doi: 10.3389/fmicb.2018.00567

Inhibitory Effects of Sulfate and Nitrate Reduction on Reductive Dechlorination of PCP in a Flooded Paddy Soil

*Yan Xu[1,2], Lili Xue[1,2], Qi Ye[1,2], Ashley E. Franks[3,4], Min Zhu[1,2], Xi Feng[1,2], Jianming Xu[1,2] and Yan He[1,2]**

[1] Institute of Soil and Water Resources and Environmental Science, College of Environmental and Resource Sciences, Zhejiang University, Hangzhou, China, [2] Zhejiang Provincial Key Laboratory of Agricultural Resources and Environment, Hangzhou, China, [3] Department of Physiology, Anatomy and Microbiology, School of Life Sciences, La Trobe University, Melbourne, VIC, Australia, [4] Centre for Future Landscapes, La Trobe University, Melbourne, VIC, Australia

Pentachlorophenol (PCP) is highly toxic and persistent in soils. Bioreduction of PCP often co-occurs with varying concentrations of sulfate and nitrate in flooded paddy soils where each can act as an electron acceptor. Anaerobic soil microcosms were constructed to evaluate the influence of sulfate and nitrate amendments and their redox processes. Microcosms with varying sulfate and nitrate concentrations demonstrated an inhibitory effect on reductive dechlorination of PCP compared to an untreated control. Compared to nitrate, sulfate exhibited a more significant impact on PCP dechlorination, as evidenced by a lower maximum reaction rate and a longer time to reach the maximum reaction rate. Dechlorination of PCP was initiated at the *ortho*-position, and then at the *para*- and *meta*-positions to form 3-CP as the final product in all microcosms. Deep sequencing of microbial communities in the microcosms revealed a strong variation in bacterial taxon among treatments. Specialized microbial groups, such as the genus of *Desulfovibrio* responding to the addition of sulfate, had a potential to mediate the competitive microbial dechlorination of PCP. Our results provide an insight into the competitive microbial-mediated reductive dechlorination of PCP in natural flooded soil or sediment environments.

Keywords: microbial community, nitrate, pentachlorophenol (PCP), reductive dechlorination, redox processes, sulfate

OPEN ACCESS

Edited by:
Shanquan Wang,
Sun Yat-sen University, China

Reviewed by:
Fang Wang,
Institute of Soil Sciences (CAS), China
Yi Yang,
The University of Tennessee, Knoxville, United States
Jiandong Jiang,
Nanjing Agricultural University, China

***Correspondence:**
Yan He
yhe2006@zju.edu.cn

Specialty section:
This article was submitted to Microbiotechnology, Ecotoxicology and Bioremediation, a section of the journal Frontiers in Microbiology

Received: *28 December 2017*
Accepted: *13 March 2018*
Published: *28 March 2018*

Citation:
Xu Y, Xue L, Ye Q, Franks AE, Zhu M, Feng X, Xu J and He Y (2018) Inhibitory Effects of Sulfate and Nitrate Reduction on Reductive Dechlorination of PCP in a Flooded Paddy Soil. Front. Microbiol. 9:567. doi: 10.3389/fmicb.2018.00567

INTRODUCTION

Pentachlorophenol (PCP) was widely used as a pesticide (e.g., herbicide and insecticide) and wood preservatives due to a broad-spectrum bactericidal activity (Olaniran and Igbinosa, 2011). Long-term exposure of humans and animals to low levels of PCP can cause damage to the liver, kidneys, blood plasma, and the nervous system (Rodenburg et al., 2010; Hiebl et al., 2011). While the use of PCP was banned in 2015 by 90 signatories to the Stockholm Convention (United Nations Environment Programme, 2015), PCP is a persistent organic pollutant and will remain a widespread problem in wetlands, aquatic environments, and soils for the immediate future (Vallecillo et al., 1999; Hong et al., 2005; Persson et al., 2007).

In the environment, PCP can be degraded through chemical, microbiological, and photochemical processes (Choudhury et al., 1986; Guemiza et al., 2017). Microbial anaerobic reductive dechlorination is considered as an environmentally friendly and low-cost method for bioremediation of soil under water logged conditions (Mcallister et al., 1996; Field and Sierra-Alvarez, 2008). Understanding the anaerobic degradation of PCP and environmental drivers which affect biodegradation is essential to improve the overall bioremediation process (Mcallister et al., 1996; Field and Sierra-Alvarez, 2008; Bosso and Cristinzio, 2014).

Under anaerobic environment, the global geochemical cycles of many elements are driven by redox processes that mediated by microorganisms in the soil environment (Dassonville et al., 2004; Kenwell et al., 2016). Oxidized compounds such as NO_3^-, Fe(III) minerals, and SO_4^{2-} often serve as terminal electron acceptors during microbial anaerobic respiration in soils (Adriaens et al., 1996; Lovley and Coates, 2000). In theory, electron acceptors utilized by anaerobes abided to a thermodynamically determined order, which is known as the microbial redox "tower" (Borch et al., 2010; Chen et al., 2017). Under the redox tower, NO_3^- is reduced by denitrifying bacteria first, followed by reduction of manganese and iron oxides. Then, sulfate reducers covert SO_4^{2-} to sulfide and finally methanogenesis occurs. The succession of reduction potentials gives rise to a functional and metabolic diversity which moderates the rate of key biogeochemical transformation processes under anaerobic condition.

Reductive dechlorination is one of the most important degradation processes for PCP removal under anaerobic conditions. Since PCP acts as an electron acceptor, dechlorination is expected to be a competitive process with the various electron acceptors that coexist simultaneously in natural soil systems. Many studies have demonstrated that Fe(III) reduction is able to promote reductive dechlorination (Li et al., 2008; Wu et al., 2010; Cao et al., 2012) including our previous studies (Xu et al., 2014, 2015; Xue et al., 2017). In mangrove sediments, dechlorination of PCP significantly suppressed the growth of SO_4^{2-} reducers, which, in turn, facilitated the production of CH_4 by diversion of electrons from SO_4^{2-} reduction to methanogenesis (Xu et al., 2015). The coupling of PCP, Fe(III), SO_4^{2-} reduction, and CH_4 production has important implications for microbial community function in contaminated soils.

The presence of both nitrate and sulfate can also influence the reductive dechlorination of PCP in anaerobic soils. Low concentrations of nitrate (<1 mM) can promote iron reduction and reductive dechlorination, due to nitrate acting as nutrients; while higher concentrations of nitrate (between 1 and 30 mM) inhibited the dechlorination of PCP (Yu et al., 2014). Inconsistent effects on dechlorination due to the presence of sulfate have also been reported previously. For example, sulfate reduction has been reported to inhibit the anaerobic degradation of chlorophenol due to competitive exclusion (Alder et al., 1993). In contrast, sulfate in the presence of lactate facilitated dechlorination of PCP (Yang et al., 2009).

To date, while several studies have examined the biodegradation of PCP under different redox conditions in anaerobic environments, inconsistent results have been reported due to incongruent conditions of different studies. Aside from dynamic processes (Yoshida et al., 2007; Bosso and Cristinzio, 2014), few studies have investigated the competitive reductive dechlorination of PCP co-occurring in the presence of different electron acceptors at a community level. The recent development of Nextgen sequencing provides the ability to investigate microbial community-mediated responses that underpin the competitive reductive dechlorination of PCP co-occurring with the reduction of different electron acceptors in natural complex soil environment.

In this study, NO_3^- and SO_4^{2-} were chose as two classical electron acceptors to investigate functional microbial-mediated competitive relationship between PCP dechlorination and soil redox processes. Anaerobic soil microcosms were constructed with the addition of sulfate and nitrate in varying concentrations and the microbial communities were studied in depth through 16S rRNA amplicon sequencing. We hypothesized that (1) addition of varying amounts of competitive electron acceptors, in our case sulfate and nitrate, would vary PCP dechlorination rates due to their relative different thermodynamic potential in regards to the redox tower and (2) under the increasing sulfate and nitrate reducing conditions, microbial community structures would be enriched with specific microbial functional groups underpinning the changed microbial-mediated competitive dechlorination of PCP.

MATERIALS AND METHODS

Soils

Paddy soil samples used in this study were collected from Jiaxing, Zhejiang province (30°50'8.74″ N, 120°43'3.68″ E), China. Soil was sampled from the surface (0–20 cm) and was free of detectable PCP or its dechlorinated products. In order to produce replicate homogenized samples, soils were air-dried and passed through a 2 mm mesh sieve and stored at 4°C prior to the batch experiments (Chen et al., 2014). The basic physicochemical properties of the soil were as follows: pH (6.6), NO_3^- (0.3 mg kg^{-1}), NH_4^+ (11.5 mg kg^{-1}), SO_4^{2-} (640.9 mg kg^{-1}), and free Fe (278.3 mg kg^{-1}).

Chemicals

Pentachlorophenol (≥98% purity), standard solution containing 2,3,4,5-tetrachlorophenol (TeCP), 3,4,5-trichlorophenol (TCP), 3,5-dichlorophenol (DCP) and 3-chlorophenol (3-CP) (≥99.9% HPLC purity), and Na_2MoO_4 (99.0%, AR) were all purchased from Sigma-Aldrich (St. Louis, MO, United States). $NaNO_3$ (99.0%, AR) and Na_2SO_4 (99.0%, AR) were purchased from Sinopharm Chemical Reagent Co., Ltd., China.

Soil Microcosms

Anaerobic incubation experiments were conducted in microcosms housed in 120 ml serum bottles with crimp sealed aters-coated butyl rubber stoppers (Chunbo, China). All serum bottles, butyl rubber stoppers, and water were sterilized by autoclave at 121°C for 20 min before use. Microcosms contained 15.0 g soil (dry weight), 20 mM lactate, and varying concentrations of sulfate and nitrate in a final 1:1 (w/v) soil/water

mixture in the serum bottles. Biological, sterile, and sulfate-reducing inhibited controls were created through the use of soil and lactate without addition of sulfate or nitrate, the use of gamma-radiated soil (50k Gy γ-ray sterilization) and the addition of 20 mM Na_2MoO_4, respectively. PCP that dissolved in methanol (1‰, v/v) solvent was added to each microcosm to a final concentration of 150 μM and dried for 24 h to remove methanol before incubation. Microcosms were uniformly mixed and purged under N_2 stream for 20 min to remove oxygen before being sealed with aters-coated butyl rubber stopper and crimp sealed, as previously described (Xu et al., 2015). The microcosms were then placed in an anaerobic chamber (Electrotex AW200SG, England) and incubated in the dark at 30°C. All treatments were conducted in triplicate and included: (1) the sterile control, (2) control without addition, (3) 20 mM Na_2MoO_4, (4) 5 mM Na_2SO_4, (5) 20 mM Na_2SO_4, (6) 5 mM $NaNO_3$, and (7) 10 mM $NaNO_3$. Treatments were sampled at days 0, 3 (only for NO_3^- detection), 7, 12, 17, 22, and 40.

Analyses of Microcosm Chemistry

Soil reduction processes, as represented by the dynamics in NO_3^-, SO_4^{2-}, Fe(II), and PCP concentrations, were measured at regular intervals. All treatments were sampled at each time point and analyzed for the concentrations of PCP and degradation products by ultrasonic extraction and subsequent derivatization as outlined in Xu et al. (2015). Briefly, 2 g of soil sample was freeze dried and adjusted to pH 4 using 9 mM H_2SO_4 before being extracted with a hexane/acetone mixture (v/v, 1:1) assisted by ultrasonics for 25 min. Supernatant was separated by centrifugation and soil residue extracted twice more. Pooled supernatants were concentrated to 1 ml, combined with 0.2 mM K_2CO_3 before derivatization by 0.5 ml acetic anhydride. Chlorinated phenols were separated with 2 ml hexane and dehydrated using anhydrous sodium sulfate before analysis. A gas chromatograph (Agilent 6890N, Agilent, Santa Clara, CA, United States) equipped with a ^{63}Ni electric capture detector (Hewlett-Packard 6890, Hewlett-Packard, Palo Alto, CA, United States) and a HP-5 MS capillary column (30 m × 0.25 mm i.d., ×0.25 μm film thickness) (J&W, Folsom, CA, United States) was used to quantify the different species of chlorophenols relative to standard controls. Temperature cycle was 80°C for 3 min, ramped at 10°C min^{-1} to 250°C, and held for 5 min. The analysis recoveries of the extraction procedures, namely the percentage of the detected PCP concentration to the initial added PCP concentration (based on 4, 8, 20, 40, and 80 μM spiked levels of PCP standard), were between 92.26 and 105.68%.

Soil pH was determined in a suspension of 1:2.5 soil/water ratio (w/v) with a pH meter (S975 SevenExcellence, Mettler-Toledo, Switzerland). Fe(II) concentration was measured using the 1,10-phenanthroline colorimetric method at 510 nm on a UV–vis spectrophotometer after extracting Fe(II) from the samples with dithionite-citrate (pH 3.0) and buffered with $NaHCO_3$, in the dark (Lin et al., 2012). The determination of HCl-extractable Fe(II) was similar to the free Fe(II), except using 0.5 M HCl as substituted extractant (Xu et al., 2014) and included a range of reduced Fe(II) species, such as dissolved Fe(II), FeS, and $FeCO_3$ (Heron et al., 1994). NH_4^+ was extracted at 1:10 (w/v) soil to KCl (1 mol l^{-1}) ratios for 1 h at 25°C before being quantified with a continuous flow analyzer (San^{++}, SKALAR, Netherlands). Nitrate and sulfate concentrations were determined by shaking 1.0 g of freeze dried soil or 2 ml soil slurry sample with 15 ml Milli-Q water for 30 min. The mixture was then centrifuged at 3000 × *g* for 10 min before being diluted 10-fold and analyzed by ion chromatography (Dionex ICS-2000, United States) equipped with an ASRS Ultra II self-regenerating suppressor as preciously described (Lin et al., 2012, 2014).

DNA Extraction, Amplicon Amplification, and Sequencing

The microbial community of the original soil collected at day 0 (called "Original") and soil samples collected at 40 were analyzed through amplification and sequencing of a 16S rRNA amplicon using Illumina Miseq high-throughput sequencing. The slurry sample was centrifuged for collection about 0.25 g soil and the total genomic DNA of each soil sample was extracted using FastDNA SPIN kit (Mpbio, United States) for soil according to the manufacturer's instructions. Each DNA extract was amplified with 520F (5-AYTGGGYDTAAAGNG-3) and 802R (5-TACNVGGGTATCTAATCC-3) to obtain an approximately 250-bp fragment on the V4 region of the 16S rRNA gene. Genome DNA would be normalized to 30 ng per PCR reaction. V4 dual-index Fusion PCR Prime Cocktail and PCR Master Mix (NEB Phusion High-Fidelity PCR Master Mix) were added to the PCR run. Amplification was conducted using the PCR conditions: 30 s at 98°C, 27 cycles of 30 s at 98°C, 30 s at 50°C, and 30 s at 72°C, and a final 5 min extension at 72°C. PCR products were purified with AmpureXP beads (Agencourt) to remove the unspecific products. The final library was qualified by PicoGreen (Invitrogen, Paisley, United Kingdom). Qualified libraries were sequenced pair end on the Illumina MiSeq platform with sequencing strategy PE250 (MiSeq Reagent Kit). Illumina (Highseq2000, Illumina, San Diego, CA, United States) sequencing services were provided by the Beijing Genomics Institute (BGI, Wuhan, China).

Sequence Analysis and Phylogenetic Classification

Fast Length Adjustment of Short Reads (FLASH) merged reads from original DNA amplicons were quality filtered following the published procedures (Caporaso et al., 2010; Magoč and Salzberg, 2011). A UPARSE pipeline (OTU clustering pipeline[1]) was used to pick operational taxonomic units (OTUs) and sequences were grouped into OTUs at 97% similarity (Edgar, 2013). A representative sequence for each OTU was selected and its identity was classified using the RDP Classifier (Wang et al., 2007). The gene sequences obtained from high-throughput analysis in this study were deposited in the NCBI sequence read archive under accession numbers SRP118766.

[1]http://drive5.com/uparse/

Statistical Analyses

The OTU lists of each sample were submitted to the LefSe pipeline (LDA Effect size[2]) to identify significant differential features of the OTUs among treatments (Segata et al., 2011). OTU-based community diversity indice (Shannon index) of each sample was generated based on three metrics calculated by UPARSE pipeline (Edgar, 2013). The taxonomic diversity of bacteria was calculated with the phyloseq package. Statistical analyses of the experimental data were performed using the SPSS 20.0 statistical software (IBM, Armonk, IL, United States). Differences were determined by one-way analysis of variance (ANOVA) on ranks followed by Fisher's least-significant difference. Logistic modeling was employed to examine the impacts of nitrate and sulfate on soil redox processes and PCP transformation through nonlinear curve fitting as follows (Aislabie et al., 2004; Liu et al., 2013):

$$C_t = \frac{a}{1 + be^{-kt}}$$

where t is the incubation time (d), C_t is the accumulated Fe(II) or decreased SO_4^{2-}/PCP concentrations at time t, respectively [mM for Fe(II) and SO_4^{2-}, μM for PCP], a is the maximum capacity of Fe(II) accumulation or SO_4^{2-}/PCP decrement, respectively, b is the regression coefficient, and k is the reaction rate constant (d^{-1}). The maximum reaction rate [V_{max}, mM d^{-1} for Fe(II) and SO_4^{2-}, μM d^{-1} for PCP] and the time to reach the V_{max} [$t_{V_{max}}$, d] can be calculated from 0.25 ak and $\ln b\, k^{-1}$ based on the equation.

Stoichiometric electron equivalent (eeq) analysis of the four reducing processes was carried out based on relevant half-reactions during anaerobic incubation time (Xu et al., 2015). Calculations were based on electron equivalents used for 1 mol electron acceptors of Fe(III), SO_4^{2-}, NO_3^-, and PCP, equating to 1, 8, 5, and 2 mol eeq, respectively.

[2]http://huttenhower.sph.harvard.edu/galaxy

RESULTS

Dynamics of Nitrate, Sulfate, Ferrous Iron, and PCP

Nitrate was depleted within 3 days in all treatments (**Figure 1A**). The sulfate reduction ratio (percentage of the decreased SO_4^{2-} concentration to the initial total SO_4^{2-} concentration) in the treatment with 20 mM sulfate (85.5%) was significantly lower than that in the control (89.8%) ($p < 0.05$) (**Figure 1B**), while treatment with 5 mM sulfate had no obvious difference in this ratio compared with the control. However, the V_{max} for sulfate reduction in treatments with sulfate was higher than that for the control, with the effect more pronounced in 20 mM than 5 mM sulfate addition (**Table 1**). The addition of nitrate exhibited no obvious effect on sulfate reduction, approaching a reduction

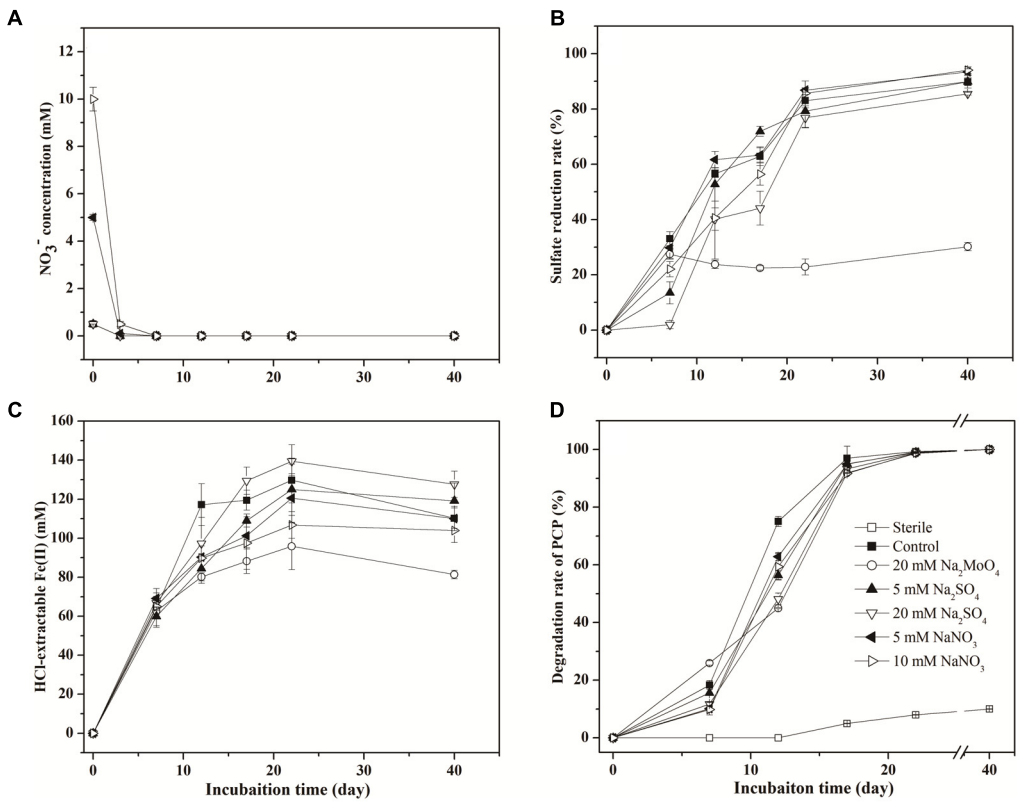

FIGURE 1 | Dynamics in the concentration of NO_3^- **(A)**, SO_4^{2-} **(B)**, HCl-extractable Fe(II) **(C)**, and PCP **(D)** in different treatments.

ratio of 93.4 and 94.3% in the treatments with 5 and 10 mM nitrate, respectively (**Figure 1B** and **Table 1**). When treated with molybdate, the sulfate reduction ratio on day 7 was 27.45%, and subsequently fluctuated around 25% during incubation.

Concentrations of HCl-extractable Fe(II) followed similar variation trends in all treatments, increasing markedly during the first 7 days (**Figure 1C**). Slight differences between treatments appeared after 7 days and proceeded to the end of incubation, with the concentration of HCl-extractable Fe(II) lower in treatments with nitrate than those with sulfate. However, the impacts of sulfate and nitrate on the Fe(III) reduction were more noticeable as shown by logistic modeling analysis (**Table 1**). The values of $V_{\max}$ were 8.76, 10.65, 10.94, and 12.41 mM d^{-1} in the treatments with 5 mM sulfate, 20 mM sulfate, 5 mM nitrate, and 10 mM nitrate, respectively, and that for the control was 22.75 mM d^{-1}. This suggested that addition of nitrate and sulfate both inhibited the Fe(III) reduction. And interestingly, addition of nitrate did not delay the $t_{V_{\max}}$ for Fe(III) reduction compared to those in the control, while sulfate did. Correspondingly, the lowest concentration of HCl-extractable Fe(II) was exhibited in the treatment with molybdate, recording the lowest Fe(II) production after 7 days' incubation (**Figure 1C**).

In the sterile treatment, PCP transformation was minimal (<10%) (**Figure 1D**), indicating that the decrease of PCP through abiotic process or sorption was negligible within the microcosms. As for the other non-sterile treatments, in the first 12 days, the PCP degradation was significantly inhibited following sulfate addition, compared to the control (75.1%). Degradation rates of 56.4% ($p < 0.05$) and 48.2% ($p < 0.05$) in 5 mM and 20 mM sulfate treatments were observed, respectively. PCP degradation also decreased to 62.9 and 59.4% with the addition of 5 and 10 mM nitrate, respectively ($p < 0.05$). The values of $V_{\max}$ and $t_{V_{\max}}$ during PCP degradation in **Table 1** showed similar inhibition influences of sulfate and nitrate on reductive dechlorination of PCP, with the effect more significant following sulfate addition by comparison with nitrate addition. However, on day 22, differences in the PCP degradation rates were no longer apparent between the control and treatments containing either nitrate or sulfate (**Figure 1D**). This suggested that both sulfate and nitrate addition inhibited the reductive dechlorination of PCP, but their inhibition effect lessened over time with no obvious difference at the end of incubation.

Anaerobic Transformation of PCP

The anaerobic transformation pathway of PCP was studied by detecting degradation metabolites in all treatments during the 40 days incubation (**Figure 2**). Dechlorinated metabolites, including TeCP, TCP, DCP, and 3-CP with one to four chlorines dechlorinated were detected in all treatments except sterilized control. No phenol and other isomeride dechlorinated metabolites were detected. The metabolites 2,3,4,5-TeCP and 3,4,5-TCP were detected in the first 7 days. On day 17, 3,4,5-TCP and 3-CP were detected as the major intermediate product, and little residual PCP was detected (varying from 4.49 to 12.39 μM). At the end of incubation, the 3-CP was the major end product of PCP degradation. As a result, PCP in our tested soil might be transformed through the pathway PCP → 2,3,4,5-TeCP → 3,4,5-TCP → 3,5-DCP → 3-CP during anaerobic incubation.

Microbial Community Composition

After quality control, 112022–155268 reads were retrieved after Illumina Miseq sequencing. The average OTU numbers ranged

TABLE 1 | The maximum reaction rate ($V_{\max}$) and the time to reach the $V_{\max}$ ($t_{V_{\max}}$) of SO_4^{2-} and Fe(III) reduction, as well as PCP degradation in different treatments.

Calculated parameters		Treatments					
		Control	20 mM Na_2MoO_4	5 mM Na_2SO_4	20 mM Na_2SO_4	5 mM $NaNO_3$	10 mM $NaNO_3$
SO_4^{2-} reduction	a[a]	5.91	–[b]	9.90	23.85	6.11	6.44
	b[a]	9.03	–	50.71	37.91	10.37	17.52
	k[a] (d^{-1})	0.21	–	0.35	0.24	0.23	0.21
	V_{max} (mM d^{-1})	0.31	–	0.87	1.43	0.35	0.34
	$t_{V_{\max}}$ (d)	10.48	–	11.22	15.15	10.17	13.63
	R^2	0.98	–	0.99	0.97	0.98	0.99
Fe(III) reduction	a	119.74	86.85	120.76	133.17	109.36	101.27
	b	179.09	37.79	10.09	12.14	11.78	19.21
	k (d^{-1})	0.76	0.65	0.29	0.32	0.40	0.49
	V_{max} (mM d^{-1})	22.75	14.11	8.76	10.65	10.94	12.41
	$t_{V_{\max}}$ (d)	6.83	5.59	7.97	7.80	6.17	6.03
	R^2	0.99	0.99	0.99	0.99	0.98	0.99
PCP degradation	a	149.61	146.70	151.48	151.42	149.36	148.63
	b	170.26	38.71	120.02	225.02	364.05	262.50
	k (d^{-1})	0.52	0.31	0.42	0.45	0.54	0.50
	V_{max} (μM d^{-1})	19.45	11.37	15.91	17.03	20.16	18.58
	$t_{V_{\max}}$ (d)	9.88	11.79	11.40	12.04	10.92	11.14
	R^2	1.00	0.99	1.00	1.00	1.00	1.00

[a] *The parameter values for model variables represent best-fit values.* [b] *Not suitable to be calculated with the tested modeling.*

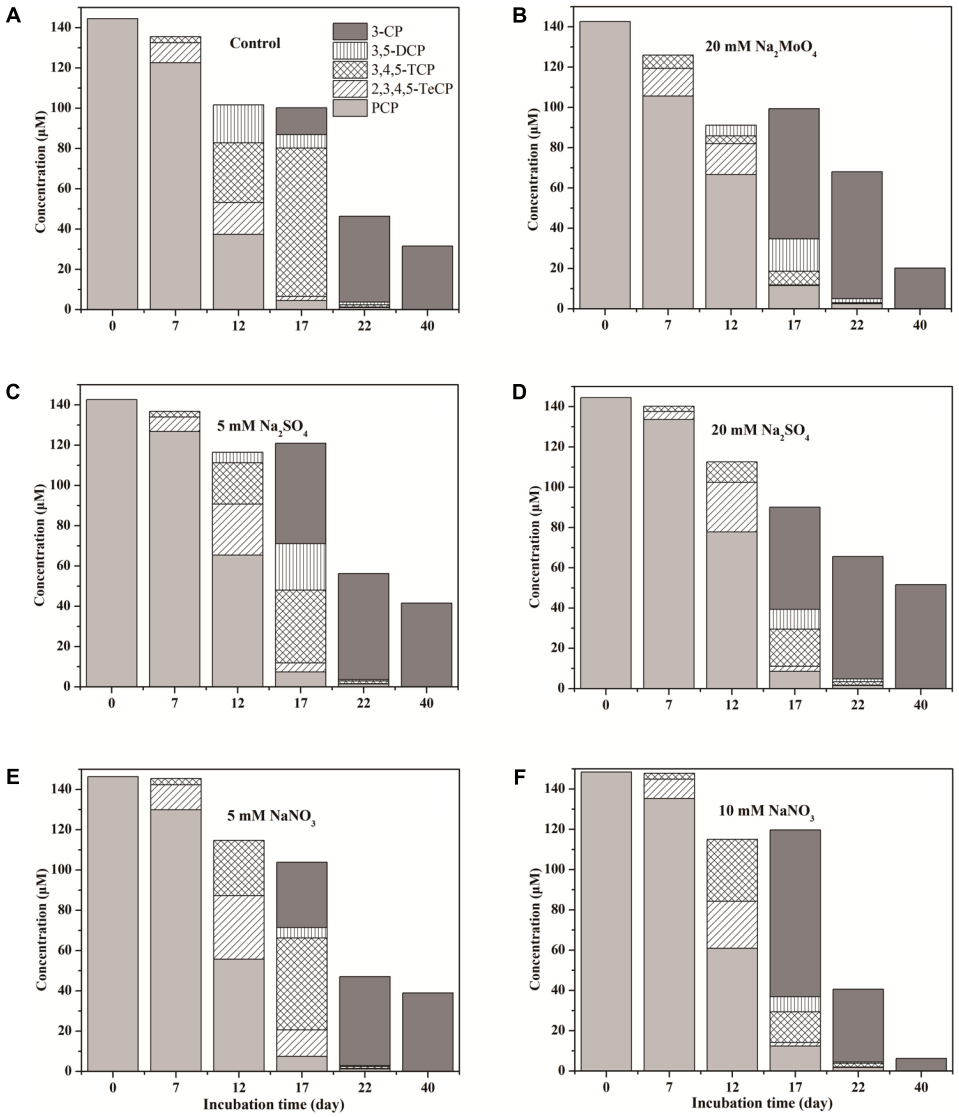

FIGURE 2 | Dynamics of PCP dechlorinated metabolites in treatments of Control **(A)**, 20 mM Na_2MoO_4 **(B)**, 5 mM Na_2SO_4 **(C)**, 20 mM Na_2SO_4 **(D)**, 5 mM $NaNO_3$ **(E)**, and 10 mM $NaNO_3$ **(F)**.

from 4349 to 4553 at 97% similarity across all treatments (**Table 2**). Shannon indexes in samples of 5 and 10 mM nitrate were 6.53 and 6.44, respectively. Moreover, the Shannon indexes were 6.51 and 6.24 with 5 and 20 mM sulfate, respectively. The Shannon indexes indicated a slight decrease in the bacterial diversity in high concentration of nitrate (10 mM) or sulfate (20 mM) when compared to the control (6.46).

Differences in bacterial community structures induced by different treatments were visualized by PCoA analysis (**Figure 3**). The separation was mainly explained by the PC1 with 51.3% of variance, and the PC2 with 18% of variance. After 40 days anaerobic incubation, the microbial community structure differentiated in the treatments compared to the original soil microbial community structure ($p < 0.001$). The bacterial communities in treatments with nitrate and 5 mM sulfate were clustered together, but differed in treatments with 20 mM sulfate and 20 mM molybdate, respectively, indicating that high sulfate concentration had a more significant influence on microbial community structures than nitrate.

The top 4 phyla in all treatments were Firmicutes, Proteobacteria, Actinobacteria, and Chloroflexi, accounting for more than 85% of the reads (**Figure 4**). In total, the relative abundance of Firmicutes increased while that of Chloroflexi decreased after incubation. At the class level, the microbial community was dominated by Clostridia in all treatments with a majority of other sequences being grouped into Alphaproteobacteria, Anaerolineae, Deltaproteobacteria, Thermoleophilia, Actinobacteria, and Gammaproteobacteria (**Figure 4**). Compared to the control, the relative abundance of Clostridia and Anaerolineae significantly decreased in

TABLE 2 | Community richness and diversity indices for the soil samples of different treatments.

Treatment[a]	OTU	Shannon index
Original soil	4362	6.32
Control	4407	6.46
20 mM Na_2MoO_4	4349	6.38
5 mM Na_2SO_4	4553	6.51
20 mM Na_2SO_4	4378	6.24
5 mM $NaNO_3$	4396	6.53
10 mM $NaNO_3$	4390	6.44

[a]*Original soil, sample was on day 0; other treatments, samples were on day 40.*

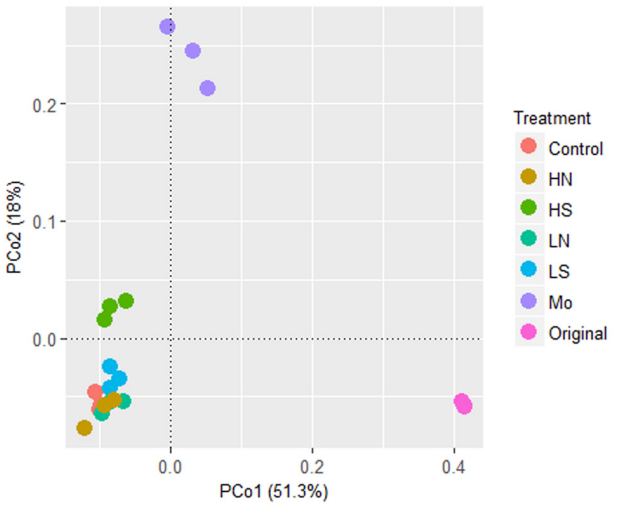

FIGURE 3 | PCoA analysis based on the relative abundances of bacterial pyrotag sequences. Symbols: Control, treatment without addition; HN, 10 mM $NaNO_3$; HS, 20 mM Na_2SO_4; LN, 5 mM $NaNO_3$; LS, 5 mM Na_2SO_4; Mo, 20 mM Na_2MoO_4; Original, the original soil at day 0. Three replicates were conducted among one treatment.

treatments with nitrate and sulfate addition (on an average, decreased from 33.4 to 27.1% and decreased from 9.9 to 8.8%, respectively, $p < 0.05$). Conversely, the relative abundance of Alphaproteobacteria, Deltaproteobacteria, Actinobacteria, Planctomycetia, and Bacilli increased in all the treatments ($p < 0.05$). Particularly, the relative abundance of group Acidobacteria increased in the treatments with nitrate addition but decreased with sulfate addition.

Dominant genera were mainly affiliated to Firmicutes and Proteobacteria, including the members of *Clostridium*, *Desulfosporosinus*, *Caloramator*, *Desulfobacca*, *Hyphomicrobium*, *Rhodoplanes*, *Pelotomaculum*, *Geobacter*, *Desulfitobacterium*, *Desulfovibrio*, and *Sedimentibacter* (**Figure 5**). Compared to the original day 0, the relative abundance of *Hyphomicrobium*, *Clostridium*, *Caloramator*, *Desulfosporosinus*, *Oxobacter*, and *Gracilibacter* in sulfate and nitrate treatments significantly increased after incubation. The relative abundances of most genera were lower in the treatment with molybdate than those with nitrate or sulfate, in particular for members of *Clostridium*, *Caloramator*, *Desulfovibrio*, *Pelotomaculum*, *Oxobacter*, and *Desulfosporosinus*. The relative abundance of *Desulfitobacterium* was below 1% in all treatments with sulfate and nitrate and was lower than that in the control but relatively higher than that in the day 0. The relative abundance of *Desulfovibrio* increased consistently following sulfate addition, with the difference reached significant in 20 mM sulfate treatment compared to that in 5 mM sulfate and control treatments ($p < 0.05$). The relative abundances of *Clostridium*, *Azospirillum*, and *Caloramator* increased with increased nitrate concentrations, while sulfate addition had no effect on the growth of these members as evidenced by their relative abundances.

DISCUSSION

The Effect of Sulfate and Nitrate on the Dechlorination of PCP

Our study conducted microcosm experiments to explore the effect of sulfate and nitrate on the degradation of PCP in the paddy soil using lactate as metabolic substrate. The anaerobic dechlorination ratios of PCP in all treatments in the first 7 days were slow. The lag time of 3–7 days was observed across all microcosms prior to dechlorination of PCP and likely due to limiting environmental conditions (e.g., soil nutrients, trace minerals, and electron donors) as reported in previous studies (Chen et al., 2012; Liu et al., 2013). Both NO_3^- and SO_4^{2-} have been reported to inhibit the reductive dechlorination of PCP in a paddy soil (Lin et al., 2014); however, other studies have also reported that PCP dechlorination was enhanced under sulfate reduction and inhibited during denitrification over 20-day incubation periods (Chang et al., 1996). In our study, dynamic processes combined with logistic model simulation indicated that both sulfate and nitrate were found to inhibit the reductive dechlorination of PCP and Fe(III) reduction (**Figure 1** and **Table 1**) even with different inhibition effect.

Although nitrate in most treatments was reduced within 3 days, it still had profound effects on the reduction of Fe(III) and PCP. Generally, nitrate is the first electron acceptor to be reduced once oxygen is depleted in paddy soils before Fe(III). In our study, the higher the concentration of nitrate, the lower the ratio of Fe(III) reduction (**Figure 1C**). This indicated the presence of nitrate inhibited Fe(III) reduction where nitrate and iron oxides coexisted and was similar to the previous studies (Cooper et al., 2003; Matocha and Coyne, 2007). Meanwhile, Fe(III) was reduced more quickly in the treatment with 20 mM sulfate than that with 5 mM sulfate (**Figure 1C**). Previous studies showed that the reduction of Fe(III) can be slowed and limited in the presence of a low sulfate concentration (0.2 mM), but increased >10 times with high sulfate amendment (10.2 mM) due to the increased biogenic-sulfide-driven-Fe(II) production (Kwon et al., 2014). Therefore, the Fe(III) reduction was significantly influenced mainly because that the nitrate and sulfate addition changed the availability of Fe(III) in our study.

Compared to nitrate, the addition of sulfate greatly inhibited PCP dechlorination since the value of V_{max} was relatively lower and $t_{V_{max}}$ was much higher when compared to these in

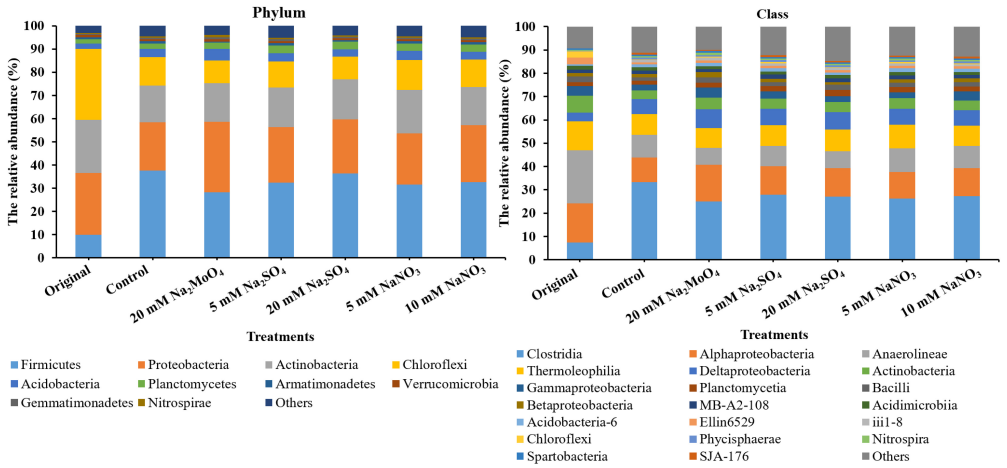

FIGURE 4 | The bacterial community structure at the phylum and class level. Original, soil sample was on day 0 and Other treatments, samples were on day 40.

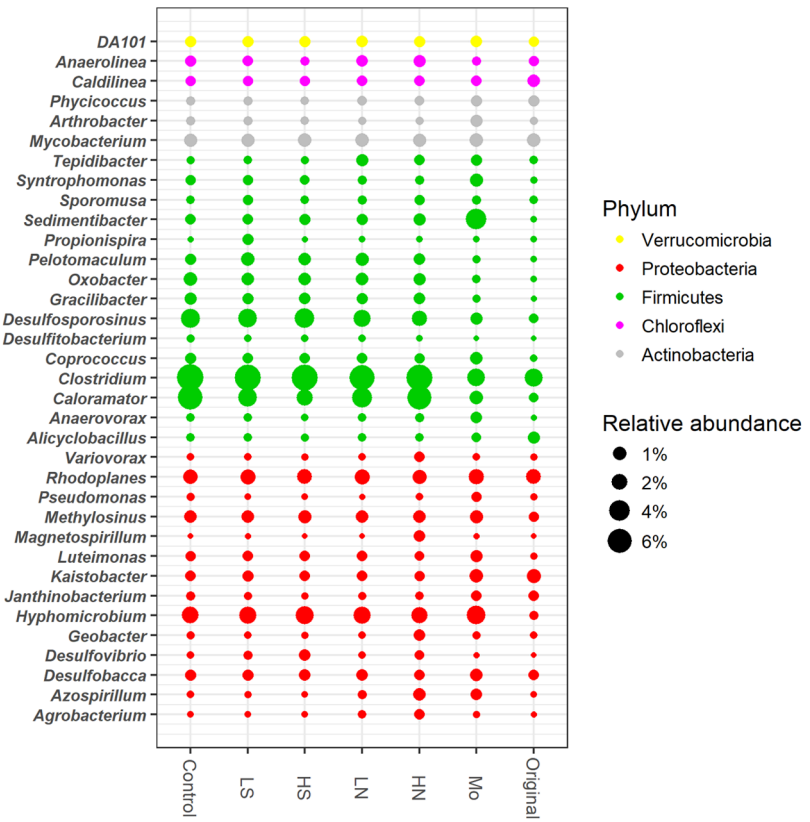

FIGURE 5 | Dominant bacterial genera in all treatments. Original, soil sample was on day 0. Other treatments, samples were on day 40. The meanings of the abbreviations in the graph are the same as in **Figure 3**.

the control (**Table 1**). Previous researches have proposed that electron acceptors (nitrate and sulfate) inhibited the degradation of organic pollutants due to competition for electron donors (Heimann et al., 2005; Aulenta et al., 2007; Chen et al., 2012). Lactate has been previously demonstrated to be an effective fermented electron donor for respiration by a wide range of microorganisms during the transformation of organic pollutants (Freeborn et al., 2005; Thomas and Gohil, 2011). From the balance of the electron equivalent (eeq) used in the incubation, most electrons transferred to the reduction of Fe(III) (1.22–1.91 mmol), sulfate (0.24–2.84 mmol), and nitrate (0.375–0.75 mmol), while PCP reductive dechlorination (0.02 mmol) was

TABLE 3 | Balance of the electron equivalents used for Fe(III)/SO_4^{2-}/NO_3^- reduction and PCP dechlorination at the end of incubation.

Treatment	Electron equivalents (eeq, mmol) used for					
	Eeq[a] added	Fe(III) reduction	NO_3^- reduction	SO_4^{2-} reduction	Dechlorination	Eeq consumed
Control	3.60	1.65	0	0.72	0.021	2.391
20 Mm Na_2MoO_4	3.60	1.22	0	0.24	0.021	1.481
5 Mm Na_2SO_4	3.60	1.78	0	1.26	0.020	3.060
20 Mm Na_2SO_4	3.60	1.91	0	2.84	0.020	4.770
5 Mm $NaNO_3$	3.60	1.65	0.375	0.75	0.021	2.796
10 Mm $NaNO_3$	3.60	1.56	0.75	0.76	0.022	3.092

[a]*Eeq, electron equivalents.*

a minor pathway for electron flow, accounting for only 5‰ of the total consumed electron equivalents (3.6 mmol) (**Table 3**). Our previous research found that supplying excess electron donors may not necessarily achieve substantial dechlorination (Xue et al., 2017). The rapid fermentation of lactate may also result in the transient build-up of H_2 to levels around two orders of magnitude higher compared to the steady-state conditions (Heimann et al., 2005). Hydrogen supplied by hollow-fiber membranes, maintaining adequate hydrogen above hydrogen thresholds for dechlorination, also inhibited dechlorination activity even when hydrogen was not limiting in the presence of nitrate and sulfate (Freeborn et al., 2005). Hence, competition for electron donor is not solely responsible for the inhibition of dechlorination in the presence of sulfate and nitrate, and the microbial interactions were thus predicted to have significant effects on these redox processes.

The Pathway of PCP Degradation

The vital step in the biodegradation of PCP is the removal of the chlorine atoms. Previous studies reported that PCP under anaerobic conditions first undergoes *ortho*-dechlorination (Susarla et al., 1997; Villemur et al., 2006; Zhang et al., 2012). Two pathways for PCP degradation have been proposed (Susarla et al., 1997). Under sulfate-reducing condition, PCP can be transformed through the pathway PCP → 2,3,5,6-TeCP → 2,3,5-TCP → 3,5-DCP → 3-CP. Under methanogenic condition, PCP may transform through the pathway PCP → 2,3,4,5-TeCP → 3,4,5-TCP → 3,4-DCP → 3-CP. In our study, PCP was transformed through the pathway PCP → 2,3,4,5-TeCP → 3,4,5-TCP → 3,5-DCP → 3-CP in all treatments. Bacteria such as *Desulfitobacterium dehalogenans*, *Desulfitobacterium chlororespirans*, *Desulfitobacterium hafniense*, and *Desulfitobacterium* sp. strain PCE1 preferentially remove the chlorine atom at the *ortho*-position of PCP rather than the *meta*- or *para*-positions (Dennie et al., 1998). Most *Desulfitobacterium* strains have been reported to play an important role in the degradation of halogenated organic compounds such as tetrachloroethene, trichloroethene, and carbon tetrachloride (Gerritse et al., 1996; Villemur et al., 2006; Bisaillon et al., 2010; Zhao et al., 2015), but very few have been studied for degradation of PCP, likely due to the toxicity of PCP to these bacteria. *D. hafniense* strain PCP-1 (formerly *frappieri* PCP-1) is the known strict anaerobic bacterium which has been proved capable of dechlorinating PCP at the *ortho*-, *para*-, and *meta*-position (Dennie et al., 1998; Bisaillon et al., 2010). The sequence of dechlorination was the same as our findings including no dechlorinated metabolites beyond 3-CP. *D. hafniense* strain PCP-1 was reported to have several reductive dehalogenase (RDase) genes that could carry out the sequential reductive dechlorination of PCP; and CprA3 reductive dehalogenase showed high *ortho*-dechlorination activity toward PCP (Bisaillon et al., 2010). In our study, members of *Desulfitobacterium* have been detected and the relative abundance was enriched during incubation with PCP stress. Therefore, the *Desulfitobacterium* is potentially an essential to PCP dechlorination in the tested soil.

Microbial Community Structure During Competitive Microbial Dechlorination of PCP in the Presence of Nitrate and Sulfate

The predominant genera *Desulfovibrio*, *Desulfosporosinus*, *Geobacter*, *Desulfobacca*, *Hyphomicrobium*, *Pelotomaculum*, *Sedimentibacter*, *Mycobacterium*, *Caloramator*, *Rhodoplanes*, and *Clostridium* were detected in the treatment with both nitrate and sulfate (**Figure 5**). The presence of such genera across all the microcosms and during dechlorination of PCP indicated that they were tolerant to PCP and the associated degradation products. The role, directly or indirectly, of this core group during PCP transformation in all treatments was of interest. The mentioned genera have been reported to have members capable of facilitating the dechlorination of chlorinated organic pollutants. For example, the genera *Desulfovibrio* and *Clostridium* were reported to have the ability of using lactate or acetate to generate H_2 serving as an electron donor in a dechlorinating consortium (Freeborn et al., 2005; Behrens et al., 2008). *Clostridium* has also been previously reported as one of the common microbial community members during PCP degradation (Tartakovsky et al., 2001). Thus, the potential interaction or competition between these above mentioned versatile or PCP tolerate groups and the known dechlorinators (e.g., *Desulfitobacterium*) would happen, which were considered as the cause of suppressed PCP dechlorination by sulfate or nitrate.

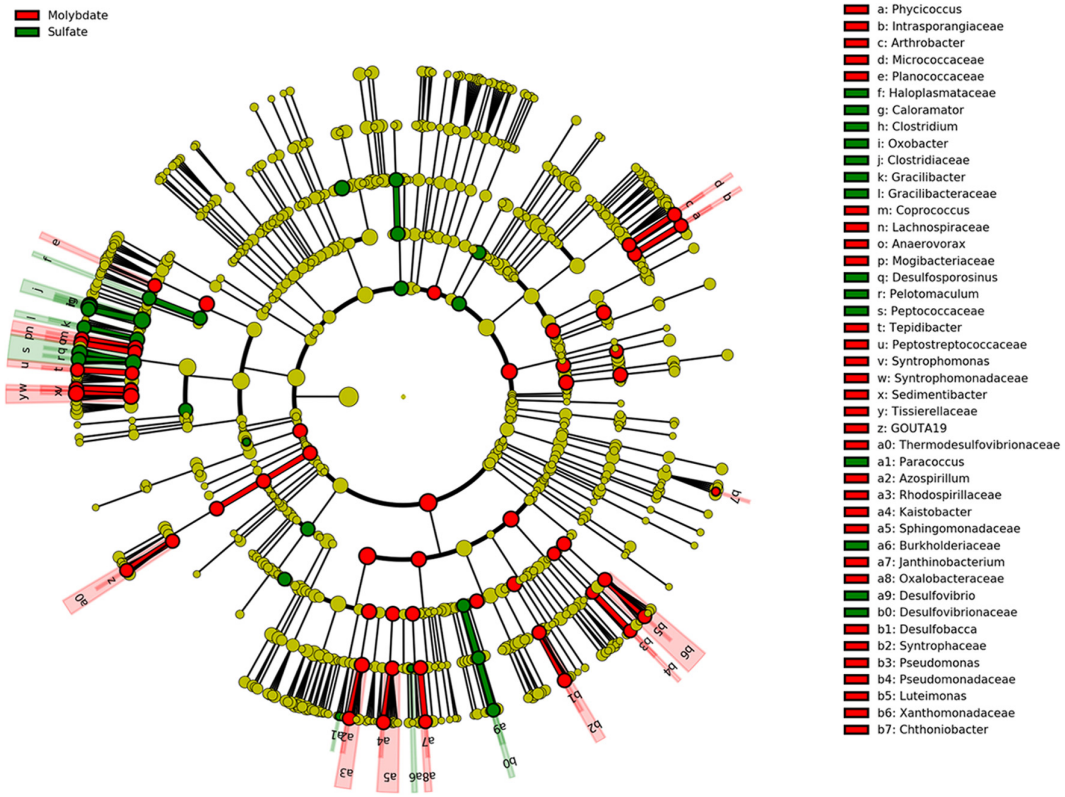

FIGURE 6 | Cladograms indicating the phylogenetic distribution of bacteria lineages associated with sulfate and molybdate addition. The phylum, class, order, family, and genus levels are listed in order from inside to outside of the cladogram and the labels for levels of family and genus are abbreviated by single letter. The green and red circles represent the bacteria with differences reached significant in the treatment with sulfate and molybdate addition, respectively; whereas the yellow circles represent the taxa with no significant differences between both treatments.

Compared with nitrate, sulfate addition imposed more severe inhibition effect on PCP dechlorination at the early stage of incubation (**Figure 1** and **Table 1**). Previous studies have shown that the reductive dechlorinating bacteria and sulfate-reducing bacteria often share biotopes in soils contaminated with chlorinated compounds (Drzyzga et al., 2001), which caused competition for available nutrients and other resources in the limited environment. This resulted in complicated interactions between and within the functional dechlorinators and sulfate-reducers inhabiting a common habitat. As mentioned before, indigenous carbon sources used in this study were adequate for the dechlorination of PCP and other redox processes (**Table 3**), therefore, the inhibition due to the limitation of resources is expected to be negligible in sulfate added treatments.

Molybdate was used as an inhibitor to estimate whether or not sulfate reducers could make a difference on PCP dechlorination, since it has the ability to inhibit the key enzyme of ATP sulfurylase in the pathway of sulfate reduction (Ranade et al., 1999). The sulfate reduction was greatly inhibited by molybdate addition, as well as PCP transformation (**Figures 1B,D**). A cladogram produced by LefSe highlighted the noticeable bacterial members that differed between sulfate and molybdate treatments (**Figure 6**). Results demonstrated that genera of *Caloramator*, *Clostridium*, *Oxobacter*, *Gracilibacter*, *Desulfosporosinus*, *Pelotomaculum*, *Paracoccus*, and *Desulfovibrio* exhibited significant variation following sulfate addition. Microbial analysis revealed a substantial decrease of most genera in molybdate treatments, especially for the known sulfate reducers, such as *Desulfovibrio* and *Desulfosporosinus* (**Figure 6**). Relatively, the *Desulfovibrio* was enriched in the treatments with sulfate but not abundant in the treatments with nitrate or the control (**Figure 5**). We can thus speculate that the addition of sulfate might stimulate the growth of *Desulfovibrio*.

Previous studies have shown that sulfate-reducing bacteria such as *Desulfovibrio vulgaris*, *Desulfovibrio gigas*, and *Desulfovibrio desulfuricans* are able to metabolize lactate or H_2 when grown in the absence of sulfate or in the media with low sulfate concentrations (Cabirol et al., 1998). Through syntrophic association with group of *Desulfovibrio*, dechlorinators such as *Desulfitobacteria* may acquire their electrons by interspecies hydrogen and acetate transfer (Cabirol et al., 1998). Syntrophy between the sulfate reducing bacteria *Desulfovibrio* and the dehalorespiring bacteria *Desulfitobacterium* via interspecies H_2 transfer occurred only at low concentrations or in the absence of sulfate, while in the high sulfate concentration environment (>2.5 mM), dechlorinating bacteria was outnumbered by sulfate reducer of *Desulfovibrio*, and dehalogenation was not

occurring (Drzyzga et al., 2001; Drzyzga and Gottschal, 2002; Maphosa et al., 2010). Thus, the inhibition effect of PCP dechlorination by sulfate should be ultimately ascribed to the sulfate reducers of *Desulfovibrio* to outcompete dechlorinators under high sulfate concentration, while deficient sulfate levels (e.g., the control) facilitated PCP transformation because of the syntrophic relationship between sulfate reducer of *Desulfovibrio* and dehalorespiring bacteria of *Desulfitobacterium*. In addition, the inhibition of sulfate and nitrate on reductive dechlorination of PCP in this study gradually lessened during the 40-day incubation, since the decrease in concentration of sulfate and nitrate would favor the growth of dechlorinating bacteria and thereby PCP transformation.

By coupling the typical soil redox processes with the response of the microbial community structure during PCP degradation in natural flooded paddy soils, this study improved the understanding regarding the microbial competitive dechlorination of PCP during nitrate and sulfate reduction. Increased sulfate and nitrate reduction inhibited the process of PCP dechlorination. PCP transformation started from *ortho*-position, then dechlorinate at *para*- and *meta*-position to form 3-CP as the final product. Analyses for the microbial community structures revealed that although soil bacterial community structure shared similar dominate species following addition of nitrate and sulfate, respectively, some specialized functional species were also responded contrastingly to the addition of sulfate and nitrate, with the genus of *Desulfovibrio* enriched in the treatments with sulfate individually, thereby mediated a different competitive microbial dechlorination of PCP. Overall, our results suggest that a shared existence of electron acceptors, such as sulfate and nitrate, could change the microbial diversity by allowing bacteria with special metabolic capabilities to grow in the soil and sediment polluted with PCP. This is crucial for understanding the self-purification function of paddy soils once they are polluted by PCP, under the condition of excessive use of nitrogen fertilizer as well as accumulation of iron sulfur minerals. Furthermore, besides nitrate and sulfate, iron plays a particularly important role in environmental biogeochemistry. Hence, the effect of Fe(III) reduction on the dechlorination of chlorinated compounds, through either biotic or abiotic way, will deserve to study in the future.

AUTHOR CONTRIBUTIONS

YX and LX were the main contributors to perform the experiments, analyze the data and write the manuscript. YH and JX designed the work. QY and XF participated in the experiments. MZ and QY participated in the data analysis. AF and YH carefully revised the manuscript.

FUNDING

This work was jointly supported by the National Key Research and Development Program of China (2016YFD0800207), the National Natural Science Foundation of China (41322006, 41771269, and 41601248), the China-Ontario Project (2016YFE0101900), and the National Program for Support of Top-notch Young Professionals.

REFERENCES

Adriaens, P., Chang, P., and Barkovskii, A. (1996). Dechlorination of PCDD/F by organic and inorganic electron transfer molecules in reduced environments. *Chemosphere* 32, 433–441. doi: 10.1016/0045-6535(95)00231-6

Aislabie, J., Hunter, D., Ryburn, J., Fraser, R., Northcott, G. L., and Di, H. J. (2004). Atrazine mineralisation rates in New Zealand soils are affected by time since atrazine exposure. *Soil Res.* 42, 783–792. doi: 10.1071/SR03096

Alder, A. C., Häggblom, M. M., Oppenheimer, S. R., and Young, L. Y. (1993). Reductive dechlorination of polychlorinated biphenyls in anaerobic sediments. *Environ. Sci. Technol.* 27, 530–538. doi: 10.1021/es00040a012

Aulenta, F., Pera, A., Rossetti, S., Papini, M. P., and Majone, M. (2007). Relevance of side reactions in anaerobic reductive dechlorination microcosms amended with different electron donors. *Water Res.* 41, 27–38. doi: 10.1016/j.watres.2006.09.019

Behrens, S., Azizian, M. F., McMurdie, P. J., Sabalowsky, A., Dolan, M. E., Semprini, L., et al. (2008). Monitoring abundance and expression of "*Dehalococcoides*" species chloroethene-reductive dehalogenases in a tetrachloroethene-dechlorinating flow column. *Appl. Environ. Microbiol.* 74, 5695–5703. doi: 10.1128/AEM.00926-08

Bisaillon, A., Beaudet, R., Lépine, F., Déziel, E., and Villemur, R. (2010). Identification and characterization of a novel CprA reductive dehalogenase specific to highly chlorinated phenols from *Desulfitobacterium hafniense* strain PCP-1. *Appl. Environ. Microbiol.* 76, 7536–7540. doi: 10.1128/AEM.01362-10

Borch, T., Kretzschmar, R., Kappler, A., Cappellen, P. V., Gindervogel, M., Voegelin, A., et al. (2010). Biogeochemical redox processes and their impact on contaminant dynamics. *Environ. Sci. Technol.* 44, 15–23. doi: 10.1021/es9026248

Bosso, L., and Cristinzio, G. (2014). A comprehensive overview of bacteria and fungi used for pentachlorophenol biodegradation. *Rev. Environ. Sci. Biotechnol.* 13, 387–427. doi: 10.1007/s11157-014-9342-6

Cabirol, N., Jacob, F., Perrier, J., Fouillet, B., and Chambon, P. (1998). Interactions between methanogenic and sulphate-reducing microorganisms during dechlorination of a high concentration of tetrachloroethylene. *J. Gen. Appl. Microbiol.* 44, 297–301. doi: 10.2323/jgam.44.297

Cao, F., Liu, T. X., Wu, C. Y., Li, F. B., Liu, X. M., Yu, H. Y., et al. (2012). Enhanced biotransformation of DDTs by an iron- and humic-reducing bacteria *Aeromonas hydrophila* HS01 upon addition of goethite and anthraquinone-2,6-disulphonic disodium salt (AQDS). *J. Agric. Food Chem.* 60, 11238–11244. doi: 10.1021/jf303610w

Caporaso, J. G., Kuczynski, J., Stombaugh, J., Bittinger, K., Bushman, F. D., Costello, E. K., et al. (2010). QIIME allows analysis of high-throughput community sequencing data. *Nat. Methods* 7, 335–336. doi: 10.1038/nmeth.f.303

Chang, B. V., Zheng, J. X., and Yuan, S. Y. (1996). Effects of alternative electron donors, acceptors and inhibitors on pentachlorophenol dechlorination in soil. *Chemosphere* 33, 313–320. doi: 10.1016/0045-6535(96)00174-9

Chen, J., Hanke, A., Tegetmeyer, H. E., Kattelmann, I., Sharma, R., Hamann, E., et al. (2017). Impacts of chemical gradients on microbial community structure. *ISME J.* 11, 920–931. doi: 10.1038/isme.2016.175

Chen, M., Shih, K., Hu, M., Li, F., Liu, C., Wu, W., et al. (2012). Biostimulation of indigenous microbial communities for anaerobic transformation of pentachlorophenol in paddy soils of southern China. *J. Agric. Food Chem.* 60, 2967–2975. doi: 10.1021/jf204134w

Chen, M., Tao, L., Li, F., and Lan, Q. (2014). Reductions of Fe(III) and pentachlorophenol linked with geochemical properties of soils from pearl river delta. *Geoderma* 21, 201–211. doi: 10.1016/j.geoderma.2013.12.003

Choudhury, H., Coleman, J., De Rosa, C. T., and Stara, J. F. (1986). Pentachlorophenol: health and environmental effects profile. *Toxicol. Ind. Health* 2, 483–571. doi: 10.1177/074823378600200409

Cooper, D. C., Picardal, F. W., Schimmelmann, A., and Coby, A. J. (2003). Chemical and biological interactions during nitrate and goethite reduction

by *Shewanella putrefaciens* 200. *Appl. Environ. Microbiol.* 69, 3517–3525. doi: 10.1128/AEM.69.6.3517-3525.2003

Dassonville, F., Godon, J. J., Renault, P., Richaume, A., and Cambier, P. (2004). Microbial dynamics in an anaerobic soil slurry amended with glucose, and their dependence on geochemical processes. *Soil Biol. Biochem.* 36, 1417–1430. doi: 10.1016/j.soilbio.2004.03.007

Dennie, D., Gladu, I., Lépine, F., Villemur, R., Bisaillon, J. G., and Beaudet, R. (1998). Spectrum of the reductive dehalogenation activity of *Desulfitobacterium frappieri* PCP-1. *Appl. Environ. Microbiol.* 64, 4603–4606.

Drzyzga, O., Gerritse, J., Dijk, J. A., Elissen, H., and Gottschal, J. C. (2001). Coexistence of a sulphate-reducing *Desulfovibrio* species and the dehalorespiring *Desulfitobacterium frappieri* TCE1 in defined chemostat cultures grown with various combinations of sulphate and tetrachloroethene. *Environ. Microbiol.* 3, 92–99. doi: 10.1046/j.1462-2920.2001.00157.x

Drzyzga, O., and Gottschal, J. C. (2002). Tetrachloroethene dehalorespiration and growth of *Desulfitobacterium frappieri* TCE1 in strict dependence on the activity of *Desulfovibrio fructosivorans*. *Appl. Environ. Microbiol.* 68, 642–649. doi: 10.1128/AEM.68.2.642-649.2002

Edgar, R. C. (2013). UPARSE: highly accurate OTU sequences from microbial amplicon reads. *Nat. Methods* 10, 996–998. doi: 10.1038/nmeth.2604

Field, J. A., and Sierra-Alvarez, R. (2008). Microbial degradation of chlorinated phenols. *Rev. Environ. Sci. Biotechnol.* 7, 211–241. doi: 10.1007/s11157-007-9124-5

Freeborn, R. A., West, K. A., and Alvarez-Cohen, L. (2005). Phylogenetic analysis of TCE-dechlorination consortia enriched on a variety of electron donors. *Environ. Sci. Technol.* 39, 8358–8368. doi: 10.1021/es048003p

Gerritse, J., Renard, V., Gomes, T. M. P., Lawson, P. A., Collins, M. D., and Gottschal, J. C. (1996). *Desulfitobacterium* sp. strain PCE1, an anaerobic bacterium that can grow by reductive dechlorination of tetrachloroethene or ortho-chlorinated phenols. *Arch. Microbiol.* 165, 132–140. doi: 10.1007/s002030050308

Guemiza, K., Coudert, L., Metahni, S., Mercier, G., Besner, S., and Blais, J. F. (2017). Treatment technologies used for the removal of As, Cr, Cu, PCP and/or PCDD/F from contaminated soil: a review. *J. Hazard. Mater.* 333, 194–214. doi: 10.1016/j.jhazmat.2017.03.021

Heimann, A. C., Friis, A. K., and Jakobsen, R. (2005). Effects of sulfate on anaerobic chloroethene degradation by an enriched culture under transient and steady-state hydrogen supply. *Water Res.* 39, 3579–3586. doi: 10.1016/j.watres.2005.06.029

Heron, G., Crouzet, C., Bourg, A. C., and Christensen, T. H. (1994). Speciation of FeII) and Fe(II) in contaminated aquifer sediments using chemical extraction techniques. *Environ. Sci. Technol.* 28, 1698–1705. doi: 10.1021/es00058a023

Hiebl, J., Lehnert, K., and Vetter, W. (2011). Identification of fungi-derived terrestrial halogenated natural product in wild boar (*Sus scrofa*). *J. Agric. Food Chem.* 59, 6188–6192. doi: 10.1021/jf201128r

Hong, H. C., Zhou, H. Y., Luan, T. G., and Lan, C. Y. (2005). Residue of pentachlorophenol in fresh water sediments and human breast milk collected from the Pearl River Delta. China. *Environ. Int.* 31, 643–649. doi: 10.1016/j.envint.2004.11.002

Kenwell, A., Navarre-Sitchler, A., Prugue, R., Spear, J. R., Hering, A. S., Maxwell, R. M., et al. (2016). Using geochemical indicators to distinguish high biogeochemical activity in floodplain soils and sediments. *Sci. Total Environ.* 563, 386–395. doi: 10.1016/j.scitotenv.2016.04.014

Kwon, M. J., Boyanov, M. I., Antonopoulos, D. A., Brulc, J. M., Johnston, E. R., Skinner, K. A., et al. (2014). Effects of dissimilatory sulfate reduction on FeIII (hydr)oxide reduction and microbial community development. *Geochim. Cosmochim. Acta* 129, 177–190. doi: 10.1016/j.gca.2013.09.037

Li, F., Wang, X., Li, Y., Liu, C., Zeng, F., Zhang, L., et al. (2008). Enhancement of the reductive transformation of pentachlorophenol by polycarboxylic acids at the iron oxide-water interface. *J. Colloid Interface Sci.* 321, 332–341. doi: 10.1016/j.jcis.2008.02.033

Lin, J., He, Y., and Xu, J. (2012). Changing redox potential by controlling soil moisture and addition of inorganic oxidants to dissipate pentachlorophenol in different soils. *Environ. Pollut.* 170, 260–267. doi: 10.1016/j.envpol.2012.07.013

Lin, J., He, Y., Xu, J., Chen, Z., and Brookes, P. C. (2014). Vertical profiles of pentachlorophenol and the microbial community in a paddy soil: influence of electron donors and acceptors. *J. Agric. Food Chem.* 62, 9974–9981. doi: 10.1021/jf502746n

Liu, Y., Li, F. B., Xia, W., Xu, J. M., and Yu, X. S. (2013). Association between ferrous iron accumulation and pentachlorophenol degradation at the paddy soil-water interface in the presence of exogenous low-molecular-weight dissolved organic carbon. *Chemosphere* 91, 1547–1555. doi: 10.1016/j.chemosphere.2012.12.040

Lovley, D. R., and Coates, J. D. (2000). Novel forms of anaerobic respiration of environmental relevance. *Curr. Opin. Microbiol.* 3, 252–256. doi: 10.1016/S1369-5274(00)00085-0

Magoč, T., and Salzberg, S. L. (2011). Flash: fast length adjustment of short reads to improve genome assemblies. *Bioinformatics* 27, 2957–2963. doi: 10.1093/bioinformatics/btr507

Maphosa, F., de Vos, W. M., and Smidt, H. (2010). Exploiting the ecogenomics toolbox for environmental diagnostics of organohalide-respiring bacteria. *Trends Biotechnol.* 28, 308–316. doi: 10.1016/j.tibtech.2010.03.005

Matocha, C. J., and Coyne, M. C. (2007). Short-term response of soil iron to nitrate addition. *Soil Sci. Soc. Am. J.* 71, 108–117. doi: 10.2136/sssaj2005.0170

Mcallister, K. A., Lee, H., and Trevors, J. T. (1996). Microbial degradation of pentachlorophenol. *Biodegradation* 7, 1–40. doi: 10.1007/BF00056556

Olaniran, A. O., and Igbinosa, E. O. (2011). Chlorophenols and other related derivatives of environmental concern: properties, distribution and microbial degradation processes. *Chemosphere* 83, 1297–1306. doi: 10.1016/j.chemosphere.2011.04.009

Persson, Y., Lundstedt, S., Öberg, L., and Thsklind, M. (2007). Levels of chlorinated compounds (PCPPs, PCDEs, PCDFs and PCDDs) in soils at contaminated sawmill sites in Sweden. *Chemosphere* 66, 234–242. doi: 10.1016/j.chemosphere.2006.05.052

Ranade, D. R., Dighe, A. S., Bhirangi, S. S., Panhalkar, V. S., and Yeole, T. Y. (1999). Evaluation of the use of sodium molybdate to inhibit sulphate reduction during anaerobic digestion of distillery waste. *Bioresour. Technol.* 68, 287–291. doi: 10.1016/S0960-8524(98)00149-7

Rodenburg, L. A., Du, S., Fennell, D. E., and Gavallo, G. J. (2010). Evidence for widespread dechlorination of polychlorinated biphenyls in groundwater, landfills and wastewater collection systems. *Environ. Sci. Technol.* 44, 7534–7540. doi: 10.1021/es1019564

Segata, N., Izard, J., Waldron, L., Gevers, D., Miropolsky, L., Garrett, W. S., et al. (2011). Metagenomic biomarker discovery and explanation. *Genome Biol.* 12:R60. doi: 10.1186/gb-2011-12-6-r60

Susarla, S., Yonezawa, Y., and Masunaga, S. (1997). Transformation kinetics and pathways of chlorophenols and hexachlorobenzene in fresh water lake sediment under anaerobic conditions. *Environ. Technol.* 18, 903–911. doi: 10.1080/09593331808616609

Tartakovsky, B., Manuel, M. F., Beaumier, D., Greer, C. W., and Guiot, S. R. (2001). Enhanced selection of an anaerobic pentachlorophenol-degrading consortium. *Biotechnol. Bioeng.* 73, 476–483. doi: 10.1002/bit.1082

Thomas, J. E., and Gohil, H. (2011). Microcosm studies on the degradation of o,p'- and p,p'-DDT, DDE, and DDD in a muck soil. *World J. Microbiol. Biotechnol.* 27, 619–625. doi: 10.1007/s11274-010-0497-1

United Nations Environment Programme (2015). *Report of the Conference of the Parties to the Stockholm Convention of Persistent Organic Pollutants on the Work at Its Seventh Meeting*, Geneva.

Vallecillo, A., Garcia-Encina, P. A., and Pena, M. (1999). Anaerobic biodegradability and toxicity of chlorophenols. *Water Sci. Technol.* 40, 161–168. doi: 10.1016/S0273-1223(99)00622-8

Villemur, R., Lanthier, M., Beaudet, R., and Lépine, F. (2006). The Desulfitobacterium genus. *FEMS Microbiol. Rev.* 30, 706–733. doi: 10.1111/j.1574-6976.2006.00029.x

Wang, Q., Garrity, G. M., Tiedje, J. M., and Cole, J. R. (2007). Naive Bayesian classifier for rapid assignment of rRNA sequences into the new bacterial taxonomy. *Appl. Environ. Microbiol.* 73, 5261–5267. doi: 10.1128/AEM.00062-07

Wu, C. Y., Zhuang, L., Zhang, S. G., Li, F. B., and Li, X. M. (2010). Fe(III)-enhanced anaerobic transformation of 2,4-dichlorophenoxyacetic acid by an iron-reducing bacterium *Comamonas Koreensis* CY01. *FEMS Microbiol. Ecol.* 71, 106–113. doi: 10.1111/j.1574-6941.2009.00796.x

Xu, Y., He, Y., Feng, X., Liang, L., Xu, J., Brookes, P. C., et al. (2014). Enhanced abiotic and biotic contributions to dechlorination of pentachlorophenol during Fe(III) reduction by an iron-reducing bacterium *Clostridium*

beijerinckii Z. *Sci. Total Environ.* 473, 215–223. doi: 10.1016/j.scitotenv.2013.12.022

Xu, Y., He, Y., Zhang, Q., Xu, J., and Crowley, D. (2015). Coupling between pentachlorophenol dechlorination and soil redox as revealed by stable carbon isotope, microbial community structure, and biogeochemical data. *Environ. Sci. Technol.* 49, 5425–5433. doi: 10.1021/es505040c

Xue, L., Feng, X., Xu, Y., Li, X., Zhu, M., Xu, J., et al. (2017). The dechlorination of pentachlorophenol under a sulfate and iron reduction co-occurring anaerobic environment. *Chemosphere* 182, 166–173. doi: 10.1016/j.chemosphere.2017.04.124

Yang, S., Shibata, A., Yoshida, N., and Katayama, A. (2009). Anaerobic mineralization of pentachlorophenol (PCP) by combining PCP-dechlorinating and phenol-degrading cultures. *Biotechnol. Bioeng.* 102, 81–90. doi: 10.1002/bit.22032

Yoshida, N., Yoshida, Y., Handa, Y., Kim, H. K., Ichihara, S., and Katayama, A. (2007). Polyphasic characterization of a PCP-to-phenol dechlorinating microbial community enriched from paddy soil. *Sci. Total Environ.* 381, 233–242. doi: 10.1016/j.scitotenv.2007.03.021

Yu, H. Y., Wang, Y. K., Chen, P. C., Li, F. B., Chen, M. J., Hu, M., et al. (2014). Effect of nitrate addition on reductive transformation of pentachlorophenol in paddy soil in relation to iron(III) reduction. *J. Environ. Manage.* 132, 42–48. doi: 10.1016/j.jenvman.2013.10.020

Zhang, C., Suzuki, D., Li, Z., Ye, L., and Katayama, A. (2012). Polyphasic characterization of two microbial consortia with wide dechlorination spectra for chlorophenols. *J. Biosci. Bioeng.* 114, 512–517. doi: 10.1016/j.jbiosc.2012.05.025

Zhao, S., Ding, C., and He, J. (2015). Detoxification of 1,1,2-trichloroethane to ethene by *Desulfitobacterium* and identification of its functional reductase gene. *PLoS One* 10:e0119507. doi: 10.1371/journal.pone.0119507

Conflict of Interest Statement: The authors declare that the research was conducted in the absence of any commercial or financial relationships that could be construed as a potential conflict of interest.

frontiers in Microbiology

ORIGINAL RESEARCH
published: 24 July 2018
doi: 10.3389/fmicb.2018.01664

Microbial Community Changes in a Chlorinated Solvents Polluted Aquifer Over the Field Scale Treatment With Poly-3-Hydroxybutyrate as Amendment

*Bruna Matturro[1], Lucia Pierro[2], Emanuela Frascadore[1], Marco Petrangeli Papini[2] and Simona Rossetti[1]**

[1] Water Research Institute, IRSA–CNR, Rome, Italy, [2] Department of Chemistry, Sapienza University of Rome, Rome, Italy

This study investigated the organohalide-respiring bacteria (OHRB) and the supporting microbial populations operating in a pilot scale plant employing poly-3-hydroxybutyrate (PHB), a biodegradable polymer produced by bacteria from waste streams, for the *in situ* bioremediation of groundwater contaminated by chlorinated solvents. The bioremediation was performed in ground treatment units, including PHB reactors as slow release source of electron donors, where groundwater extracted from the wells flows through before the re-infiltration to the low permeability zones of the aquifer. The coupling of the biological treatment with groundwater recirculation allowed to drastically reducing the contamination level and the remediation time by efficiently stimulating the growth of autochthonous OHRB and enhancing the mobilization of the pollutants. Quantitative PCR performed along the external treatment unit showed that the PHB reactor may efficiently act as an external incubator to growing *Dehalococcoides mccartyi*, known to be capable of fully converting chlorinated ethenes to innocuous end-products. The slow release source of electron donors for the bioremediation process allowed the establishment of a stable population of *D. mccartyi,* mainly carrying *bvcA* and *vcrA* genes which are implicated in the metabolic conversion of vinyl chloride to harmless ethene. Next generation sequencing was performed to analyze the phylogenetic diversity of the groundwater microbiome before and after the bioremediation treatment and allowed the identification of the microorganisms working closely with organohalide-respiring bacteria.

Keywords: reductive dehalogenation, *D. mccartyi*, PHB, reductive dehalogenase genes, groundwater circulation wells, bioremediation

OPEN ACCESS

Edited by:
Shanquan Wang,
Sun Yat-sen University, China

Reviewed by:
Maurizio Petruccioli,
Università degli Studi della Tuscia, Italy
Haitham Sghaier,
Centre National des Sciences et Technologies Nucléaires, Tunisia

****Correspondence:***
Simona Rossetti
rossetti@irsa.cnr.it

Specialty section:
This article was submitted to Microbiotechnology, Ecotoxicology and Bioremediation, a section of the journal Frontiers in Microbiology

Received: *30 March 2018*
Accepted: *04 July 2018*
Published: *24 July 2018*

Citation:
Matturro B, Pierro L, Frascadore E, Petrangeli Papini M and Rossetti S (2018) Microbial Community Changes in a Chlorinated Solvents Polluted Aquifer Over the Field Scale Treatment With Poly-3-Hydroxybutyrate as Amendment. Front. Microbiol. 9:1664. doi: 10.3389/fmicb.2018.01664

INTRODUCTION

Over the past 20 years, intense research efforts have been devoted to elucidate the overall mechanisms underlying the biological reductive dechlorination (RD) process and to develop effective technologies for the *in situ* remediation of contaminated sites (Lorenz and Löffler, 2016).

The RD process is performed by specialized organohalide-respiring bacteria (OHRB) which enable the complete and efficient detoxification of a variety of aliphatic and aromatic chlorinated

pollutants. Among the many bacterial species that are now known to reductively transform organohalides, *Dehalococcoides mccartyi* is considered as the biomarker of the process due to the unique ability of members of this genus to fully convert chlorinated solvents to harmless products through the activity of a class of enzymes called reductive dehalogenases (RDases) (Richardson, 2013). They are involved in the metabolic dechlorination of PCE or TCE to VC (TceA), of *cis*-DCE to VC and ethene (BvcA and VcrA) and are coded by the corresponding genes *tceA, bvcA,* and *vcrA* (Lee et al., 2006).

Recently, several site investigations showed the relevance of the geochemical monitoring integrated with the biomolecular analysis of both OHRB and flanking microbial communities (Kotik et al., 2013; Kao et al., 2016; Atashgahi et al., 2017). The use of an integrated monitoring approach may reduce uncertainties about the ongoing groundwater processes and allow an efficient long-term management of the remedial action (Majone et al., 2015).

In situ stimulation of native OHRB through the addition of fermentable substrates represents one of the main approaches used for remediating chlorinated solvents contaminated aquifers (Steffan and Schaefer, 2016). Recently, poly-β-hydroxy-butyrate (PHB) was shown to be effective as a slow-release electron donor for the RD process (Aulenta et al., 2008; Pierro et al., 2017). PHB is an inert, biocompatible and fully biodegradable material which has been proposed for several attractive biotechnological applications (Williams and Martin, 2005). It is a polyester synthesized as a carbon and energy reserve material by a wide number of prokaryotes. More than 300 species, mainly of bacteria, have been reported to produce these polymers (Olivera et al., 2001; Chanprateep, 2010; Centeno-Leija et al., 2014). PHB is industrially produced by microbial fermentation using bacterial strains, cultivated on inexpensive carbon sources such as beet and cane molasses, corn starch, alcohols, and vegetable oils (Lee, 1996; Chen, 2009, 2010; Chanprateep, 2010; Peña et al., 2011, 2014).

In order to act as slow-release electron donor, PHB is enzymatically hydrolyzed to 3-hydroxybutyrate (HB) which is then converted to acetate and H_2 through β-oxidation.

To date, only a few laboratory studies investigated the efficacy of PHB as electron donor in the RD process (Aulenta et al., 2008; Baric et al., 2012, 2014) and the first pilot scale PHB application was only recently documented (Pierro et al., 2017). A combination of a groundwater circulation wells (GCWs) with an external treatment unit, including a PHB reactor allowing continuous delivering of electron donor in the contaminated aquifer, was installed at a chlorinated solvent contaminated aquifer where partial biological RD quantitatively transformed higher chlorinated ethenes and ethanes (utilized at the site in industrial degreasing operation) in the less chlorinated *cis*-DCE and VC.

The effectiveness of PHB as a suitable electron donor source for enhancing the *in situ* RD of *cis*-DCE to non-toxic ethene in low permeability contaminated aquifer was clearly demonstrated during the plant operation and the RD process was found to be mirrored by the occurrence of both *D. mccartyi* and reductive dehalogenase genes (Pierro et al., 2017).

As an unexpected effect of the continuous recirculation of the contaminated groundwater through the external treatment unit, the occurrence of a biological dechlorination activity was revealed, after around 200 days of operation, both in the PHB and zero valent iron (ZVI) reactors with the almost quantitative removal of the extracted *cis*-DCE and VC. The stimulation of the biological reductive activity resulted from the *in situ* enhancement of the RD by the GCW operation. By this regard, extracted groundwater, enriched with OHRB as result of the electron donor continuous amendment, passes through the external reactors in the treatment unit where dechlorinating microorganisms find the optimal growth conditions (reductive redox conditions and electron donor concentration in the PHB and ZVI reactors).

In this paper, we report the throughout investigation on the microbial changes and the behavior of OHRB along the external operation unit of the pilot plant, focusing in particular on the PHB reactor and on the structure and role of the microbial community involved in the RD process driven by the fermentation of this slow release carbon source.

MATERIALS AND METHODS

Pilot Field Test

As described in Pierro et al. (2017), the process is carried out by extracting contaminated water through a multi-screened 30-m-deep IEG-GCW® and transferring it to an external treatment unit which comprises a sand tank (for suspended solid filtration), a reactor containing the fermentable PHB polymer and one with ZVI for the removal of the extracted contaminants before reinjection. Valves were installed along the plant for sample collection and analyses (**Figure 1**). IEG-GCW® plant was designed based on geological and hydrogeological conditions of the site and it consists in a single borehole screened at three different depths separated by packers (first permeable layer, low permeability intermediate layer, and deep permeable layer). Three centrifugal pumps were installed on the surface. Two pumps extracted groundwater from the deep permeable layer (from 22 to 26 m below the ground surface, bgs) and the low permeability intermediate layer, where a significant mass of chlorinated solvents was strongly retained by aging phenomena (from 15 to 19 m bgs). After passing through an external treatment unit, pumped groundwater is discharged back into the aquifer through the upper screened section (from 8 to 12 m bgs), thus creating two circulation groundwater cells (**Figure 1**). Groundwater recirculation by GCW coupled with electron donor continuous amendment (by the PHB reactor) effectively allowed chlorinated solvents mobilization and *in situ* RD stimulation in the low accessible heavily contaminated low permeable aquifer zones.

Chemical Analysis

Chlorinated solvents were determined by headspace gas chromatographic analysis. Groundwater samples were collected

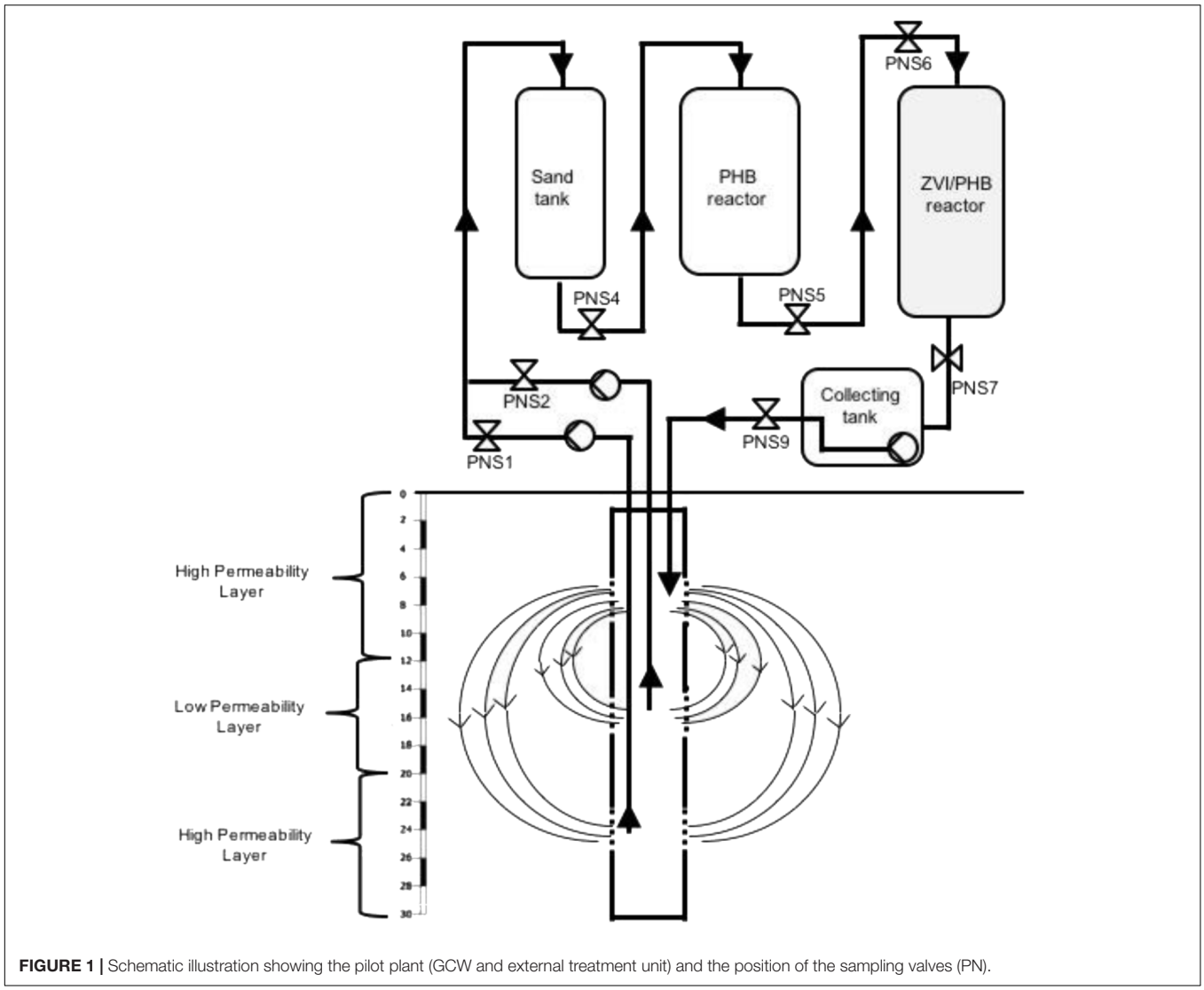

FIGURE 1 | Schematic illustration showing the pilot plant (GCW and external treatment unit) and the position of the sampling valves (PN).

directly from gate valves (PNS1-7) in 10 ml pyrex vials. Each vial was completely filled to leave almost no headspace, sealed with a Teflon-faced butyl septum and transported to the laboratory. In order to create headspace and to perform gas chromatographic analysis, 1 ml of each groundwater sample was transferred into a second 10 ml pyrex vial sealed with a Teflon-faced butyl septum. Headspace analysis of chlorinated compounds was performed using a gas chromatograph (Master DANI) equipped with a DANI 86.50 headspace autosampler. The chromatograph was fitted with a TRB 624 (75 m × 0.53 mm i.d) capillary column and a flame ionization detector (FID, 300°C). Sample injection was operated in splitless mode, where the injector temperature was set at 180°C. Helium was used as carrier gas at a constant flow of 10 mL min^{-1} and the GC oven was temperature programmed as follows: 50°C for 0.5 min increasing at 15°C min^{-1} to 180°C for 0 min then increasing at 40°C min^{-1} to 210°C for 0 min. The headspace autosampler conditions were: oven temperature 80°C, manifold temperature 120°C, transfer line temperature 180°C, shaking soft. The GC was previously calibrated with standard cis-DCE and VC concentrations over a linear response range.

Sampling for Biomolecular Analysis

Samples for biomolecular analysis (500 mL of groundwater) were collected before the bioremediation treatment (T = 0) from the groundwater wells PNS1 (groundwater from high permeable zone with low concentration of *cis*-DCE and VC) and PNS2 (groundwater from the low permeable zone with high concentration of *cis*-DCE and VC). Water samples were taken also after 570 days of plant operation from PNS1, PNS2 and from sampling points located in the external unit of the pilot plant PNS4 (out of the sand tank), PNS5, and PNS6 (out of the PHB reactor unit), PNS7 (out of the ZVI/PHB reactor unit).

Each groundwater sample was filtered on polycarbonate filters (pore size 0.22 μm, 47 mm diameter, Nuclepore) to harvest the biomass and DNA was extracted by Power Soil

DNA extraction kit (MoBio, Italy) following the manufacturer's instructions. Purified DNA from each sample was eluted in 100 μL sterile Milli-Q and stored at −20°C until further analysis.

Quantitative PCR

Quantitative PCR (qPCR) targeting *D. mccartyi* 16S rRNA genes and reductive dehalogenase genes *tceA, bvcA, vcrA* was conducted on DNA extracted from PNS1 and PNS2 before the bioremediation treatment and from the sampling points located in the external unit of the treatment plant (PNS1, PNS2, PNS4, PNS5, PNS7) after 570 days of operation. qPCR absolute quantification with TaqMan® chemistry was applied. Reactions were performed in 20 μL total volume of SsoAdvanced™ Universal Probes Supermix (Bio-Rad, Italy), including 3 μL of DNA as template, 300 nM of each primer and 300 nM of TaqMan® probe composed by 6-carboxyfluorescein (FAM) as the 5′ end reporter fluorophore and *N*,*N*,*N*,*N*,-tetramethyl-6-carboxyrhodamine (TAMRA) as the 3′ end quencher. Primers and probes used for each reaction are listed in Supplementary Table S1. Standard curves for the absolute quantification were constructed by using the long amplicons method previously reported in Matturro et al. (2013). Each reaction was performed in triplicate with CFX96 Touch™ Real-Time PCR Detection System (Bio-Rad, Italy). Quantitative data were expressed as gene copy numbers L^{-1} and error bars were calculated with Microsoft Excel® on triplicate reactions for each sample.

Next Generation Sequencing (NGS)

Next generation sequencing (NGS) was performed on groundwater samples collected at PNS1 and PNS2 before the PHB treatment ($T = 0$) and at the outlet of the PHB reactor (PNS5) after the bioremediation treatment (570 days of plant operation).

10 ng of DNA extracted from each groundwater sample (500 mL) was used for NGS analysis. 16S rRNA Amplicon Library Preparation (V1–3) was performed as detailed in Matturro et al. (2017). The procedure for bacterial 16S rRNA amplicon sequencing targeting the V1–3 variable regions is based on Caporaso et al. (2012), using primers adapted from the Human Gut Consortium (Ward et al., 2012). PCR reactions were performed in 25 μL reaction volume containing Phusion Master Mix High Fidelity (Thermo Fisher Scientific, United States) and 0.5 μM final concentration of the library adaptors with V1–3 primers (27F: 5′-AGAGTTTGATCCTGGCTCAG-3′; 534R: 5′-ATTACCGCGGCTGCTGG-3′). All PCR reactions were run in duplicate and pooled afterward. The amplicon libraries were purified using the Agencourt® AMpure XP bead protocol (Beckmann Coulter, United States). Library concentration was measured with Qubit 3.0 fluorometer (Thermo Fisher Scientific, United States). The purified libraries were pooled in equimolar concentrations and diluted to 4 nM. 10% Phix control library was spiked in to overcome low complexity issue often observed with amplicon samples. The samples were paired end sequenced (2 × 301 bp) on a MiSeq (Illumina) using a MiSeq Reagent kit v3, 600 cycles (Illumina, United States) following the standard guidelines for preparing and loading samples on the MiSeq.

Next generation sequencing secondary data were processed and analyzed using QIIME2 software tools 2018.2 release (Caporaso et al., 2010). The reads were demultiplexed using demux plugin[1], denoized, dereplicated and chimera-filtered using DADA2 algorithm (Callahan et al., 2016). The taxonomic analysis was based on a Naïve–Bayes classifier trained on 16S rRNA gene OTUs clustered at 99% similarities within the Silva 128 database (Quast et al., 2013). The alpha-diversity analysis was performed by PAST version 2.17 (Hammer et al., 2001) using total OTUs generated from each sample. Rarefaction curves were computed using the Vegan R package.

16S rRNA Gene Clone Library

A 16S rRNA gene clone library was obtained from DNA extracted at PNS5 sampling point after 570 days of plant operation. DNA was amplified using primers 27f (5′-AGAGTTTGATCMTGGCTCAG-3′) and 1492r (5′-TACGGYTACCTTGTTACGACTT-3′) using Hot Start Taq98 (Lucigen, Italy). PCR reactions were performed with the following cycles: 2 min at 98°C, 38 cycles for 30 s at 98°C, 30 s at 58°C, 1 min at 72°C and final 15 min at 72°C. PCR products were purified using the QIAquick® PCR purification kit (Qiagen, Milan, Italy). Cloning of PCR products was carried out using pGEM-T Easy Vector System (Promega, Italy) into *Escherichia coli* JM109 competent cells (Promega, Italy) according to the manufacturer's instructions. Positive inserts were amplified from recombinant plasmids obtained from white colonies by PCR using the sequencing primers T7f (5′-TAATACGACTCACTATAGGG-3′) and M13r (5′-TCACACAGGAAACAGCTATGAC-3′). PCR amplicons of 1,465 bp length were purified using the QIAquick PCR purification kit (Qiagen, Milan, Italy) and sequenced with primers 530F (5′-GTGCCAGCMGCCGCCG-3′) and 907R (5′-CCGTCAATTCMTTTRAGTTT-3′). A total of 100 clones were screened by PCR and multiple sequence alignments were performed with ClustalW2 to check the similarity among the sequences. The 16S rRNA gene sequences were deposited in the GenBank database under accession numbers from MG251533 to MG251561.

Phylogenetic Analysis

The 16S rRNA sequences were analyzed with the ARB software (Ludwig et al., 2004) using the SILVA 16S rRNA SSU Reference database release 102 (Pruesse et al., 2007). Sequences were screened for chimeras using DECIPHER (Wright et al., 2012). The phylogenetic tree was constructed using the maximum likelihood method implemented in the program RAxML (Stamatakis et al., 2008). Bootstrap analyses were conducted using 1,000 resampling replicates. *Planctomycetes* was chosen as outgroup.

[1]https://github.com/qiime2/q2-demux

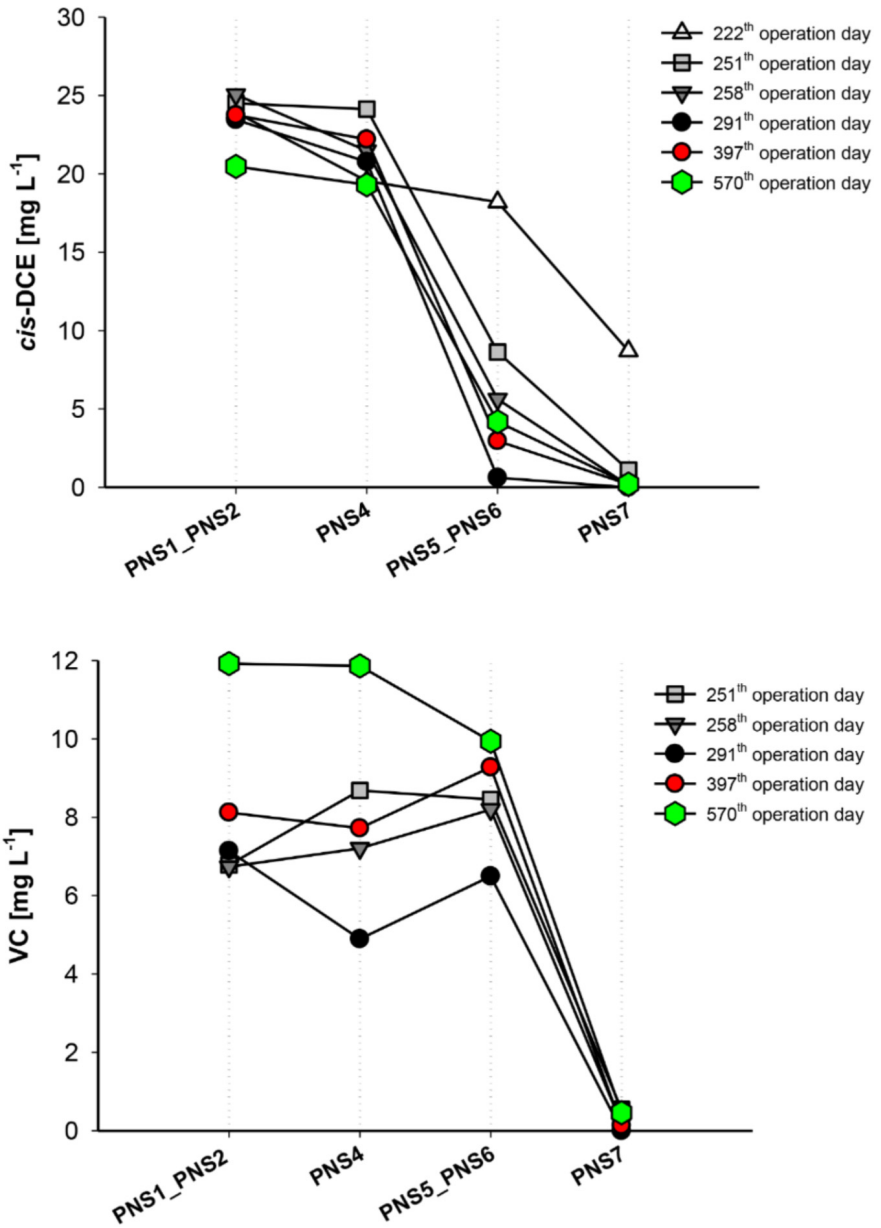

FIGURE 2 | *cis*-DCE and VC reductive dechlorination at different sampling times over long-term plant operation. PNS1 and PNS2 average concentrations are shown.

RESULTS

External Treatment Unit Performances After 200 Days of Operation

Profiles of *cis*-DCE and VC concentration along the external treatment unit at different operation days are shown in **Figure 2**. After about 200 days of continuous operations, *cis*-DCE concentration starts to decline in the PHB reactor and was almost quantitatively removed at the outlet of the ZVI/PHB reactor. VC concentration slightly increased in the PHB reactor and was then completely removed after passing through the ZVI/PHB reactor. Considering that no chemical reductants were present in the PHB reactor and that VC is not efficiently reduced by ZVI reactor, this behavior could be explained only by the occurrence of the biological RD of both *cis*-DCE and VC.

D. mccartyi and Reductive Dehalogenase Genes Quantification

The biomarkers of RD process, including *D. mccartyi* 16S rRNA and functional RDase genes *tceA, bvcA,* and *vcrA,* were quantified by qPCR in the groundwater samples collected before the treatment and after 19 months of plant operation (T = 570 days) at different sampling points along the external unit of the pilot plant (PNS1, PNS2, PNS4, PNS5, PNS6, PNS7). As shown in

Supplementary Figure S1, similar *D. mccartyi* abundances were found at PNS1 and PNS2 before treatment (2.24E + 06 and 4.02E + 06 16S rRNA gene copies L^{-1}, respectively). They were mainly composed by *D. mccartyi* strains carrying *tceA* and *vcrA* (PNS1: 2.02E + 06 *tceA* gene copies L^{-1}; 1.12E + 06 *vcrA* gene copies L^{-1}; PNS2: 3.06E + 06 *tceA* gene copies L^{-1}; 3.04E + 06 *vcrA* gene copies L^{-1}).

At the end of the treatment, *D. mccartyi* increased in both samples (3.12E + 07 and 7E + 07 gene copies L^{-1} in PNS1 and PNS2, respectively) and remained quite unvaried after the groundwater flew through the inert sand tank PNS4 (6.10E + 07 gene copies L^{-1}). Interestingly, *D. mccartyi* increased at the outlet of the PHB reactor (PNS5) where a total of 2.54E + 08 gene copies L^{-1} was found. At the sampling point located before the ZVI/PHB reactor (sampling point PNS6) *D. mccartyi* abundance was similar to PNS5 (2.49E + 08 gene copies L^{-1}) and slightly decreased to 6.72E + 07 gene copies L^{-1} before the re-inoculation of the groundwater into the aquifer (sampling point PNS7).

In line with chemical data, *D. mccartyi* strains carrying *bvcA* genes represented the main component with only a limited occurrence of *vcrA* and *tceA* genes along the all external treatment unit (**Figure 3**).

Microbial Community Composition of the PHB Reactor

The impact of the treatment on the structure and composition of the groundwater indigenous microbial communities was assessed by 16S rRNA gene high-throughput sequencing.

The analysis performed on groundwater samples collected from PNS1, PNS2, and PNS5 yielded between 63,546 and 108,169 sequence reads after bioinformatic processing (Supplementary Table S2). Rarefaction curves showed that the reads obtained were sufficient to capture sample diversity (Supplementary Figure S2).

As shown in Supplementary Figure S3, the contaminated groundwater before plant operation was mainly composed by *Proteobacteria* (∼50% of total OTUs in PNS1 and ∼67% of total OTUs in PNS2) whereas members of *Chloroflexi* phylum represented max ∼2% of total OTUs in both groundwater samples. Interestingly, sequences affiliated to *Parcubacteria* were found at high abundance (∼22%) in the groundwater from high permeable zone with low concentration of chlorinated contaminants (PNS1). Members of *Parcubacteria* were recently identified by phylogenetic analysis of 16S rRNA genes recovered from environmental samples and metabolic predictions indicate that they have very restricted metabolic potential, largely based on fermentation (Castelle et al., 2017).

After long-term operation (570 days), the microbiome composition of groundwater drastically changed with the marked increase of *Chloroflexi* (**Figure 4**). In detail, *Chloroflexi* represented up to 32% of total OTUs and included members of *Dehalococcoidaceae* (21% of total OTUs, mostly composed by sequences affiliated to *D. mccartyi* genus) and *Anaerolinaceae* (9% of total OTUs, mainly *Leptolinea* and *Pelolinea* genera) families (**Figure 4**). Other phyla found in PNS5 were affiliated to *Proteobacteria* (20% of total OTUs, including 9% of *Epsilonproteobacteria*, and 5% of *Deltaproteobacteria*), *Bacteroidetes* (15%), *Firmicutes* (7%), *Spirochaetes* (6%), *Cloacimonetes* (5%), and *Actinobacteria* (3%). Low-abundance OTUs were affiliated to *Microgenomates* (2.5%), *Alphaproteobacteria* (2.0%), *Caldithrix* (2%) and to a variety of taxa occurring at <1% of total OTUs (∼12%) including sequences affiliated to poorly characterized bacterial lineages such as *Aminicenantes*, *Caldiserica*, *Parcubacteria,* and *Peregrinibacteria*.

16S rDNA Clone Library

The characterization of the microbial communities selected in the PHB reactor was further performed by constructing 16S rDNA clone library to recover near-full-length 16S rRNA gene sequences. A total of 100 clones containing inserts with the expected size (about 1.5 kb) were selected from the total library, partially sequenced and sequence identities determined (**Table 1**). Partial sequences differing by ≤2% were considered a single relatedness group and representatives of most of these groups were fully sequenced on both strands. **Figure 5** shows the phylogenetic tree of representative full-length sequences in the contest of currently recognized bacterial phyla. The analysis of the sequences showed the occurrence of microorganisms mostly with low 16S rRNA gene similarity (<90%) to already previously identified and/or cultured neighbors (**Figure 5**). The highest number of the screened clones belonged to *Lentimicrobiaceae* (20%) and *Nitrospiraceae* (20%) families followed by *Dehalococcoidaceae* (15%), *Prolixibacteraceae* (14%), *Syntrophaceae* (8%), *Coriobacteriaceae* (6%), *Desulfovibrionaceae* (4%) and *Desulfuromonadaceae* (4%) families.

In addition, other bacterial taxa present in decreasing abundance were *Geobacter* species, *Dehalococcoides mccartyi,* and *Aeribacillus pallidus* (**Table 1**).

DISCUSSION

The reliable and robust application of bioremediation strategies requires the comprehension of the microorganisms responsible for the contaminant degradation as well as the role of the flanking microbial communities. The detailed description of the groundwater microbial community able to reduce chlorinated solvents by using PHB as a slow-release electron donor source is reported in this study. The pilot plant was installed in a site heavily contaminated by *cis*-DCE and was composed by a GCW system connected to an external treatment unit where a PHB tank was installed to deliver fermentation products directly through the low permeable zones and improve the distribution of soluble electron donors. This coupled system allowed to create an effective three-dimensional circulation cell in the aquifer reaching less permeable layers where significant masses of contaminants are potentially accumulated (Pierro et al., 2017).

Overall, the treatment changed the groundwater microbiome with the remarkable increase of specialized OHRB able to dechlorinate *cis*-DCE and VC to ethene. This finding is in

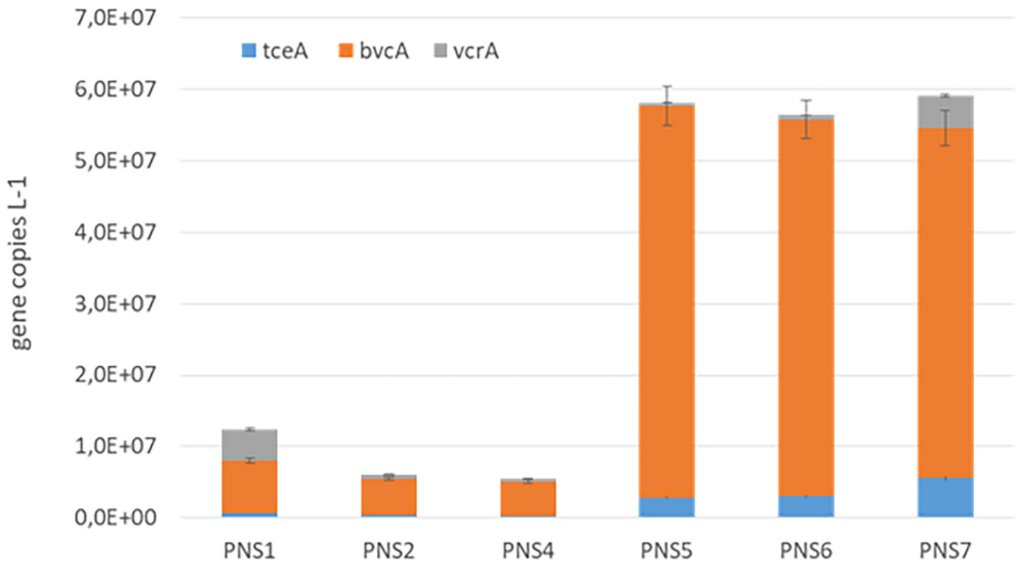

FIGURE 3 | Quantification of *D. mccartyi* strains carrying *tceA*, *bvcA*, and *vcrA* reductive dehalogenase genes along the external units of the pilot plant at 570 days of the plant operation.

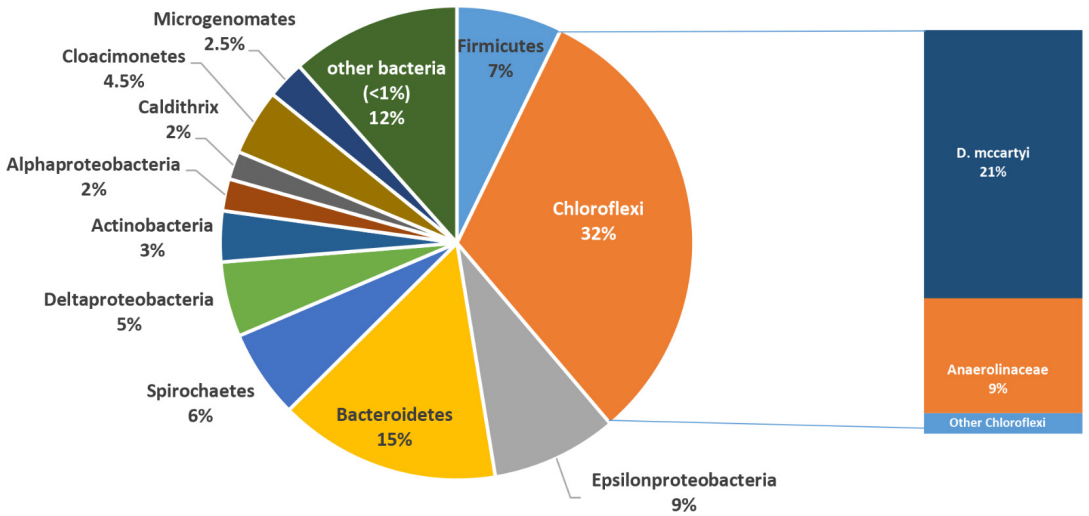

FIGURE 4 | Microbial community structure of the treated groundwater (PNS5 sampling point) after long-term plant operation.

line with the evidences obtained from a preliminary laboratory treatability study, performed on soil core and groundwater samples taken from the same site, which indicated PHB as an effective source of electron donor able to stimulate the RD until the formation of ethene via transient VC formation (Pierro et al., 2017).

The analysis conducted along the external unit of the pilot plant employing PHB for the biological RD has demonstrated that the PHB reactor may efficiently act as an external incubator to growing *D. mccartyi*. Indeed, a marked increase of *D. mccartyi* strains, able to dechlorinate VC metabolically and more efficiently produce ethene, was found in the outlet streams of the PHB and ZVI/PHB reactors.

Additionally, the treatment stimulated the growth of a wide range of putative fermentative bacteria. High throughput sequencing revealed the occurrence of sequences belonging to *Leptolinea* genus. *L. tardivitalis*, the sole isolate available so far, is an obligate anaerobe able to ferment sugars and proteinaceous carbon sources and produce as by-products a variety of volatile fatty acids and hydrogen (Yamada et al., 2006). Other *Chloroflexi* found after the PHB treatment were affiliated to *Pelolinea*, previously described to have several phenotypic traits in common with members of the class *Anaerolineae*, e.g., strictly anaerobic growth and chemo-organotrophic metabolism with sugars and polysaccharides (Imachi et al., 2014). Additionally, sequences belonging to *Bacteroidetes* phylum were found at high

TABLE 1 | Numbers of the screened clones and the corresponding taxonomic affiliation.

No. of clones (total clones: 100)	Fully sequenced clones	Taxonomic affiliation
20	Two clones (6PHB, 61PHB)	Bacteroidetes; *Lentimicrobiaceae*
20	Clone 76PHB	Nitrospirae; *Nitrospiraceae*
14	Three clones (14PHB, 66PHB, 3PHB)	Bacteroidetes; *Prolixibacteraceae*
13	Three clones (85PHB, 80PHB, 7PHB)	Deltaproteobacteria; *Geobacteraceae*
8	Two clones (12PHB, 81PHB)	Deltaproteobacteria; *Syntrophaceaea*
6	Clone: 74PHB	Actinobacteria; *Coriobacteriaceae*
5	Clone: 15PHB	Firmicutes; *Bacillaceae*
1	Clone: 4PHB	Firmicutes; *Peptococcaceae*
5	Clone: 72PHB	Chloroflexi; *Dehalococcoidaceae*
4	Clone: 59PHB	Deltaproteobacteria; *Desulfovibrionaceae*
4	Clones: 52PHB and 70PHB	Deltaproteobacteria; *Desulfuromonadaceae*

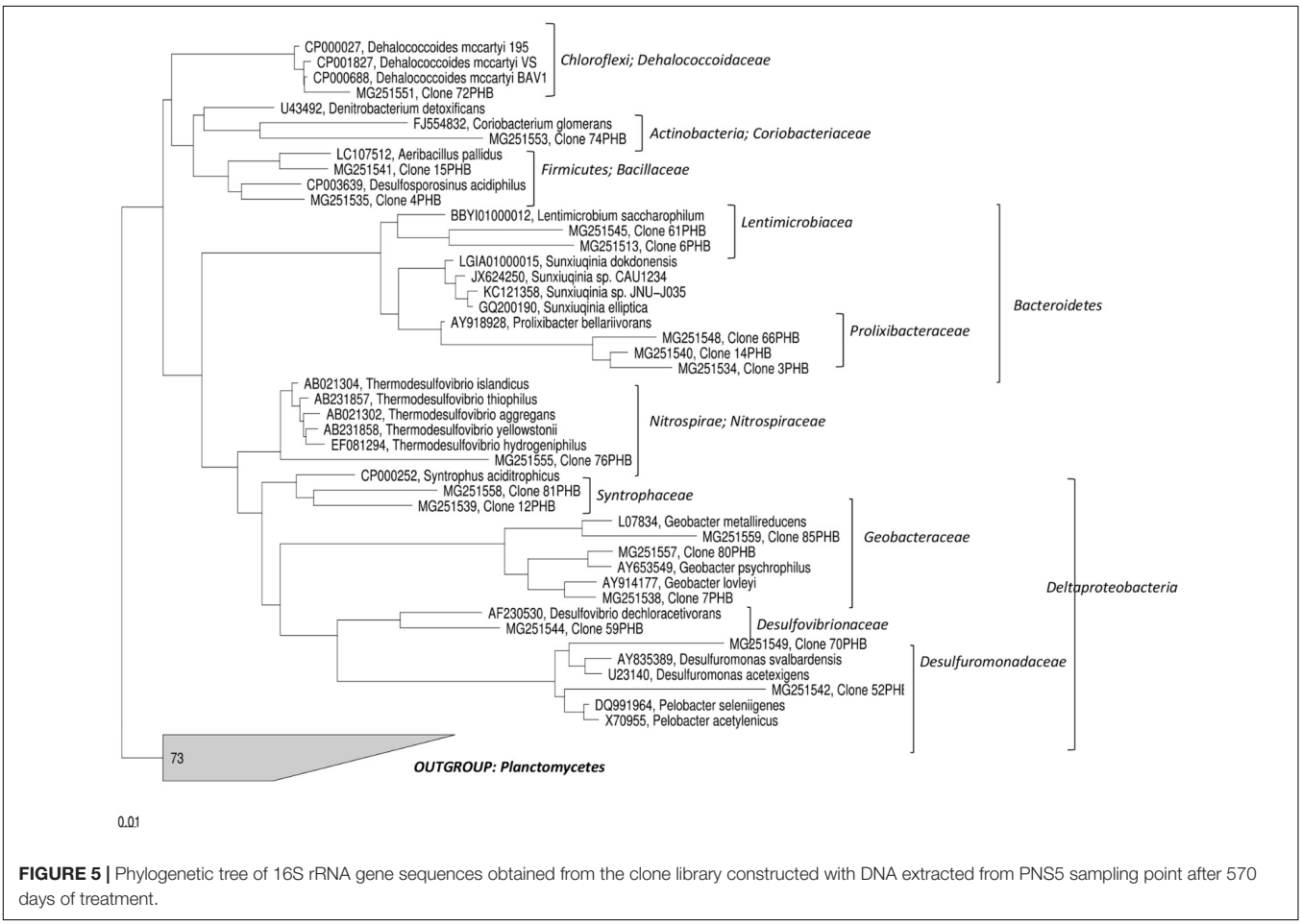

FIGURE 5 | Phylogenetic tree of 16S rRNA gene sequences obtained from the clone library constructed with DNA extracted from PNS5 sampling point after 570 days of treatment.

abundance by NGS (∼15% of total OTUs) mainly affiliated to *Lentimicrobiaceae*. The further analysis of the near-full-length 16S rRNA gene sequences, generated by the clonal analysis, showed that most of them have a low similarity to already previously identified and/or cultured neighbors (≤90% 16S rRNA gene similarity). Among others, the screened clones were indeed mostly affiliated to *Lentimicrobiaceae* and *Prolixibacteraceae* (*Bacteroidetes* phylum) (**Table 1**). *Lentimicrobiaceae* family contains strictly anaerobic and slow-growing bacteria able to ferment a wide range of compounds to acetate, malate, propionate, formate and hydrogen (Sun et al., 2016). Within this family, *Lentimicrobium saccharophilum,* an anaerobic bacterium isolated from a reactor treating high-strength starch-based organic wastewater (Sun et al., 2016), displayed the highest sequence similarity (89–90%) with clones 6PHB and 61PHB. The sequences belonging to *Prolixibacteraceae* shared low levels of 16S rDNA sequence similarity (<90%) to known members of this family such as *Sunxiuqinia*, retrieved in anaerobic deep-sea

environments (Qu et al., 2011) or *Prolixibacter*, fermentative bacterium isolated from a marine-sediment fuel cell (Holmes et al., 2007a), suggesting that they may belong to a novel taxonomic group at the genus level.

Additionally, a variety of sequences falling into taxonomic groups containing known sulfate- and Fe(III)- reducing bacteria was retrieved by the clonal analysis. They include members of *Nitrospiraceae,* mostly affiliated to the genus *Thermodesulfovibrio* (20% of the screened clones), and *Syntrophaceaea* family sharing 93–94% of sequence similarity with *Syntrophus aciditrophicus*, a fermenting bacterium able to grow on benzoate and certain fatty acids alone or in syntrophic association with hydrogen-consuming microorganisms (Elshahed and McInerney, 2001; Mouttaki et al., 2007). Furthermore, sequences related to *Denitrobacterium* genus (*Coriobacteriaceae* family) were found. This genus comprises a single species, *D. detoxificans,* able to grow via anaerobic respiration oxidizing hydrogen, formate or lactate for reduction of various oxidized nitrogen compounds (Anderson et al., 2000). Both NGS and clonal analysis revealed the occurrence of *Geobacteraceae* often found dominating in iron-reducing settings particularly in environments affected by anthropogenic influences (Holmes et al., 2007b). The *Geobacter* genus comprises anaerobic, non-fermenting chemoorganotrophic microorganisms able to reduce insoluble Fe(III) and Mn(IV) by employing several mechanisms including extracellular electron transfer via electric conductive nanowires. Being *Geobacter* species physiologically versatile, they are employed in environmental biotechnology, such as the natural attenuation of organic matter, bioremediation of aromatic hydrocarbons, heavy metals and organohalides, and generating bioenergy in microbial fuel cells and microbial electrolysis cells (Holmes et al., 2007b).

To lesser extent (4% of total clone library), sequences affiliated to *Desulfovibrionaceae* family were found sharing 97% of 16S rRNA sequence similarity with *Desulfovibrio dechloroacetivorans*, a microorganism able to coupling acetate oxidation to RD for growth (Sun et al., 2000). This group comprises strictly anaerobic members with a respiratory type or fermentative type of metabolism and most species are chemoorganoheterotrophs. Additionally, the analysis revealed the occurrence of sequences affiliated to *Desulfuromonadaceae* family, whose closest relatives were members of *Desulfuromonas* genus, such as *Desulfuromonas svalbardensis* able to reduce Fe(III) using common fermentation products such as acetate, lactate, propionate, formate or hydrogen as electron donors (Vandieken et al., 2006), and *Pelobacter* genus including microorganisms with the ability to grow fermentatively on short-chain organic acids such as lactate, citrate and pyruvate such as *Pelobacter seleniigenes* (Narasingarao and Häggblom, 2007).

It is worth noting the occurrence of low-abundance OTUs affiliated to poorly characterized bacterial lineages such as *Aminicenantes*, *Microgenomates,* and *Cloacimonetes* phyla previously found in a wide variety of anaerobic environments including oil reservoirs and hydrocarbon-impacted sites (Farag et al., 2014; Hu et al., 2016; Stolze et al., 2017).

CONCLUSION

The study confirmed the efficacy of the technology to remediate aquifers contaminated by chloroethenes and gave access the less represented species of the contaminated aquifer likely interacting with dechlorinators for the removal of chlorinated compounds through a wide range of metabolic reactions driven by the availability of PHB fermentation by-products. The results of this work clearly sustain the use of PHB as environmentally sustainable source of electron donor for bioremediation treatment of sites contaminated by chlorinated compounds and indicate the importance to further gain more insights into the metabolism networks of groundwater bacteria stimulated by the presence of PHB for the biological RD.

AUTHOR CONTRIBUTIONS

BM conducted qPCR, pyrosequencing, and analyzed the whole set of biological data. EF performed the bacterial 16S rRNA gene clonal analysis. LP performed the chemical analysis of the water samples and contributed to the interpretation of chemical data. SR and MPP conceived and coordinated the study. All authors contributed to the writing of the manuscript.

SUPPLEMENTARY MATERIAL

The Supplementary Material for this article can be found online at: https://www.frontiersin.org/articles/10.3389/fmicb.2018.01664/full#supplementary-material

REFERENCES

Anderson, R. C., Rasmussen, M. A., Jensen, N. S., and Allison, M. J. (2000). *Denitrobacterium detoxificans* gen. nov., sp. nov., a ruminal bacterium that respires on nitrocompounds. *Int. J. Syst. Evol. Microbiol.* 50, 633–638. doi: 10.1099/00207713-50-2-633

Atashgahi, S., Lu, Y., Zheng, Y., Saccenti, E., Suarez-Diez, M., Ramiro-Garcia, J., et al. (2017). Geochemical and microbial community determinants of reductive dechlorination at a site biostimulated with glycerol. *Environ. Microbiol.* 19, 968–981. doi: 10.1111/1462-2920.13531

Aulenta, F., Fuoco, M., Canosa, A., Petrangeli Papini, M., and Majone, M. (2008). Use of poly-beta-hydroxy-butyrate as a slow-release electron donor for the microbial reductive dechlorination of TCE. *Water Sci. Technol.* 57, 921–925. doi: 10.2166/wst.2008.073

Baric, M., Majone, M., Beccari, M., and Petrangeli Papini, M. (2012). Coupling of polyhydroxybutyrate (PHB) and zero valent iron (ZVI) for enhanced treatment of chlorinated ethanes in permeable reactive barriers (PRBs). *Chem. Eng. J.* 19, 22–30. doi: 10.1016/j.cej.2012.04.026

Baric, M., Pierro, L., Pietrangeli, B., and Papini, M. P. (2014). Polyhydroxyalkanoate (PHB) as a slow-release electron donor for advanced in situ bioremediation of chlorinated solvent-contaminated aquifers. *New Biotechnol.* 31, 377–382. doi: 10.1016/j.nbt.2013.10.008

Callahan, B. J., McMurdie, P. J., Rosen, M. J., Han, A. W., Johnson, A. J., and Holmes, S. P. (2016). DADA2: high-resolution sample inference from Illumina amplicon data. *Nat. Methods* 13, 581–583. doi: 10.1038/nmeth.3869

Caporaso, J. G., Kuczynski, J., Stombaugh, J., Bittinger, K., Bushman, F. D., Costello, E. K., et al. (2010). QIIME allows analysis of high-throughput community sequencing data. *Nat. Methods* 7, 335–336. doi: 10.1038/nmeth.f.303

Caporaso, J. G., Lauber, C. L., Walters, W. A., Berg-Lyons, D., Huntley, J., Fierer, N., et al. (2012). Ultra-high- throughput microbial community analysis on the Illumina HiSeq and MiSeq platforms. *ISME J.* 6, 1621–1624. doi: 10.1038/ismej.2012.8

Castelle, C. J., Brown, C. T., Thomas, B. C., Williams, K. H., and Banfield, J. F. (2017). Unusual respiratory capacity and nitrogen metabolism in a Parcubacterium (OD1) of the candidate phyla radiation. *Sci. Rep.* 7:40101. doi: 10.1038/srep40101

Centeno-Leija, S., Huerta-Beristain, G., Giles-Gómez, M., Bolivar, F., Gosset, G., and Martinez, A. (2014). Improving poly-3-hydroxybutyrate production in *Escherichia coli* by combining the increase in the NADPH pool and acetyl-CoA availability. *Antonie Van Leeuwenhoek* 105, 687–696. doi: 10.1007/s10482-014-0124-5

Chanprateep, S. (2010). Current trends in biodegradable polyhydroxyalkanoates. *J. Biosci. Bioeng.* 110, 621–632. doi: 10.1016/j.jbiosc.2010.07.014

Chen, G. (2009). A microbial polyhydroxyalkanoates (PHA) based bio-and materials industry. *Chem. Soc. Rev.* 38, 2434–2446. doi: 10.1039/b812677c

Chen, G. Q. (2010). "Plastics completely synthesized by bacteria: polyhydroxyalkanoates," in *Plastics from Bacteria: Natural Functions and Applications Microbiology Monographs*, ed. G.-Q. Chen (Berlin: Springer-Verlag), 17–37.

Elshahed, M. S., and McInerney, M. J. (2001). Benzoate fermentation by the anaerobic bacterium *Syntrophus aciditrophicus* in the absence of hydrogen-using microorganisms. *Appl. Environ Microbiol.* 67, 5520–5525. doi: 10.1128/AEM.67.12.5520-5525.2001

Farag, I. F., Davis, J. P., Youssef, N. H., and Elshahed, M. S. (2014). Global patterns of abundance, diversity and community structure of the Aminicenantes (Candidate Phylum OP8). *PLoS One* 9:e92139. doi: 10.1371/journal.pone.0092139

Hammer, Ø., David Harper, A. T., and Ryan, P. D. (2001). PAST: paleontological statistics software package for education and data analysis. *Palaeontol. Electron.* 4:9.

Holmes, D. E., Nevin, K. P., Woodard, T. L., Peacock, A. D., and Lovley, D. R. (2007a). *Prolixibacter bellariivorans* gen. nov., sp. nov., a sugar-fermenting, psychrotolerant anaerobe of the phylum *Bacteroidetes*, isolated from a marine-sediment fuel cell. *Int. J. Syst. Evol. Microbiol.* 57, 701–707. doi: 10.1099/ijs.0.64296-0

Holmes, D. E., O'Neil, R. A., Vrionis, H. A., N'Guessan, L. A., Ortiz-Bernad, I., Larrahondo, M. J., et al. (2007b). Subsurface clade of Geobacteraceae that predominates in a diversity of Fe(III)-reducing subsurface environments. *ISME J.* 1, 663–677. doi: 10.1038/ismej.2007.85

Hu, P., Tom, L., Singh, A., Thomas, B. C., Baker, B. J., Piceno, Y. M., et al. (2016). Genome-resolved metagenomic analysis reveals roles for candidate phyla and other microbial community members in biogeochemical transformations in oil reservoirs. *mBio* 7:e01669-15. doi: 10.1128/mBio.01669-15

Imachi, H., Sakai, S., Lipp, J. S., Miyazaki, M., Saito, Y., Yamanaka, Y., et al. (2014). *Pelolinea submarina* gen. nov., sp. nov., an anaerobic, filamentous bacterium of the phylum Chloroflexi isolated from subseafloor sediment. *Int. J. Syst. Evol. Microbiol.* 64, 812–818. doi: 10.1099/ijs.0.057547-0

Kao, C. M., Liao, H. Y., Chien, C. C., Tseng, Y. K., Tang, P., Lin, C. E., et al. (2016). The change of microbial community from chlorinated solvent-contaminated groundwater after biostimulation using the metagenome analysis. *J. Hazard. Mater.* 302, 144–150. doi: 10.1016/j.jhazmat.2015.09.047

Kotik, M., Davidova, A., Voriskova, J., and Baldrian, P. (2013). Bacterial communities in tetrachloroethene-polluted groundwaters: a case study. *Sci. Total Environ.* 45, 517–527. doi: 10.1016/j.scitotenv.2013.02.082

Lee, P. K. H., Johnson, D. R., Holmes, V. F., He, J. Z., and Alvarez-Cohen, L. (2006). Reductive dehalogenase gene expression as a biomarker for physiological activity of *Dehalococcoides* spp. *Appl. Environ. Microbiol.* 72, 6161–6168. doi: 10.1128/AEM.01070-06

Lee, S. Y. (1996). Bacterial polyhydroxyalkanoates. *Biotechnol. Bioeng.* 49, 1–14. doi: 10.1002/(SICI)1097-0290(19960105)49:1<1::AID-BIT1>3.0.CO;2-P

Lorenz, A., and Löffler, F. E. (2016). *Organohalide-Respiring Bacteria*. Berlin: Springer-Verlag.

Ludwig, W., Strunk, O., Westram, R., Richter, L., Meier, H., Yadhukumar, A., et al. (2004). ARB: a software environment for sequence data. *Nucleic Acids Res.* 32, 1363–1371. doi: 10.1093/nar/gkh293

Majone, M., Verdini, R., Aulenta, F., Rossetti, S., Tandoi, V., Kalogerakis, N., et al. (2015). *In situ* groundwater and sediment bioremediation: barriers and perspectives at European contaminated sites. *N. Biotechnol.* 32, 133–146. doi: 10.1016/j.nbt.2014.02.011

Matturro, B., Frascadore, E., and Rossetti, S. (2017). High-throughput sequencing revealed novel *Dehalococcoidia* in dechlorinating microbial enrichments from PCB-contaminated marine sediments. *FEMS Microbiol. Ecol.* 93:fix134. doi: 10.1093/femsec/fix134

Matturro, B., Heavner, G. L., Richardson, R. E., and Rossetti, S. (2013). Quantitative estimation of *Dehalococcoides mccartyi* at laboratory and field scale: comparative study between CARD-FISH and real time PCR. *J. Microbiol. Methods* 93, 127–133. doi: 10.1016/j.mimet.2013.02.011

Mouttaki, H., Nanny, M. A., and McInerney, M. J. (2007). Cyclohexane carboxylate and benzoate formation from crotonate in *Syntrophus aciditrophicus*. *Appl. Environ. Microbiol.* 73, 930–938. doi: 10.1128/AEM.02227-06

Narasingarao, P., and Häggblom, M. M. (2007). *Pelobacter seleniigenes* sp. nov., a selenate-respiring bacterium. *Int. J. Syst. Evol. Microbiol.* 57, 1937–1942. doi: 10.1099/ijs.0.64980-0

Olivera, E., Carnicero, D., Jodra, R., Miñambres, B., García, B., Abraham, G., et al. (2001). Genetically engineered *Pseudomonas*: a factory of new bioplastics with broad applications. *Environ. Microbiol.* 3, 612–618. doi: 10.1046/j.1462-2920.2001.00224.x

Peña, C., Castillo, T., García, A., Millán, M., and Segura, D. (2014). Biotechnological strategies to improve production of microbial poly-(3-hydroxybutyrate): a review of recent research work. *Microb. Biotechnol.* 7, 278–293. doi: 10.1111/1751-7915.12129

Peña, C., Castillo, T., Nuñez, C., and Segura, D. (2011). *Bioprocess Design: Fermentation Strategies for Improving the Production of Alginate and Poly-β-Hydroxyalkanoates (PHAs) by Azotobacter vinelandii*. Rijeka: INTECH, 217–242.

Pierro, L., Matturro, B., Rossetti, S., Sagliaschi, M., Sucato, S., Alesi, E., et al. (2017). Polyhydroxyalkanoate as a slow-release carbon source for in situ bioremediation of contaminated aquifers: from laboratory investigation to pilot-scale testing in the field. *N. Biotechnol.* 37, 60–68. doi: 10.1016/j.nbt.2016.11.004

Pruesse, E., Quast, C., Knittel, K., Fuchs, B. M., Ludwig, W., Peplies, J., et al. (2007). SILVA: a comprehensive online resource for quality checked and aligned ribosomal RNA sequence data compatible with ARB. *Nucleic Acids Res.* 35, 7188–7196. doi: 10.1093/nar/gkm864

Qu, L., Zhu, F., Hong, X., Gao, W., Chen, J., and Sun, X. (2011). *Sunxiuqinia elliptica* gen. nov., sp. nov., a member of the phylum *Bacteroidetes* isolated from sediment in a sea cucumber farm. *Int. J. Syst. Evol. Microbiol.* 61, 2885–2889. doi: 10.1099/ijs.0.026971-0

Quast, C., Pruesse, E., Yilmaz, P., Gerken, J., Schweer, T., Yarza, P., et al. (2013). The SILVA ribosomal RNA gene database project: improved data processing and web-based tools. *Nucleic Acids Res.* 41, 590–596. doi: 10.1093/nar/gks1219

Richardson, R. E. (2013). Genomic insights into organohalide respiration. *Curr. Opin. Biotechnol.* 24, 498–505. doi: 10.1016/j.copbio.2013.02.014

Stamatakis, A., Hoover, P., and Rougemont, J. (2008). A rapid bootstrap algorithm for the RAxML Web servers. *Syst. Biol.* 57, 758–771. doi: 10.1080/10635150802429642

Steffan, R. J., and Schaefer, C. E. (2016). "Current and future bioremediation applications: bioremediation from a practical and regulatory perspective," in *Organohalide-Respiring Bacteria*, eds L. Adrian and F. E. Löffler (Berlin: Springer-Verlag), 517–540.

Stolze, Y., Bremges, A., Maus, I., Puhler, A., Sczyrba, A., and Schluter, A. (2017). Targeted in situ metatranscriptomics for selected taxa from mesophilic and thermophilic biogas plants. *Microb. Biotechnol.* 11, 667–679. doi: 10.1111/1751-7915.12982

Sun, B., Cole, J. R., Sanford, R. A., and Tiedje, J. M. (2000). Isolation and characterization of *Desulfovibrio dechloracetivorans* sp. nov., a marine dechlorinating bacterium growing by coupling the oxidation of acetate to the reductive dechlorination of 2-chlorophenol. *Appl. Environ. Microbiol.* 66, 2408–2413. doi: 10.1128/AEM.66.6.2408-2413.2000

Sun, L., Toyonaga, M., Ohashi, A., Tourlousse, D. M., Matsuura, N., Meng, X. Y., et al. (2016). *Lentimicrobium saccharophilum* gen. nov., sp. nov., a strictly anaerobic bacterium representing a new family in the phylum *Bacteroidetes*, and proposal of *Lentimicrobiaceae* fam. nov. *Int. J. Syst. Evol. Microbiol.* 66, 2635–2642. doi: 10.1099/ijsem.0.001103

Vandieken, V., Mussmann, M., Niemann, H., and Jørgensen, B. B. (2006). *Desulfuromonas svalbardensis* sp. nov. and *Desulfuromusa ferrireducens* sp. nov., psychrophilic, Fe(III)-reducing bacteria isolated from Arctic sediments, Svalbard. *Int. J. Syst. Evol. Microbiol.* 56, 1133–1139. doi: 10.1099/ijs.0.63639-0

Ward, D. V., Gevers, D., Giannoukos, G., Earl, A. M., Methé, B. A., Sodergren, E., et al. (2012). Evaluation of 16S rDNA-based community profiling for human microbiome research. *PLoS One* 7:e39315. doi: 10.1371/journal.pone.0039315

Williams, S., and Martin, D. (2005). Applications of polyhydroxyalkanoates (PHA) in medicine and pharmacy. *Biolym. Online* 2005, 91–103. doi: 10.1002/3527600035.bpol4004

Wright, E. S., Yilmaz, L. S., and Noguera, D. R. (2012). DECIPHER, a search-based approach to chimera identification for 16S rRNA sequences. *Appl. Environ. Microbiol.* 78, 717–725. doi: 10.1128/AEM.06516-11

Yamada, T., Sekiguchi, Y., Hanada, S., Imachi, H., Ohashi, A., Harada, H., et al. (2006). *Anaerolinea thermolimosa* sp. nov., *Levilinea saccharolytica* gen. nov., sp. nov. and *Leptolinea tardivitalis* gen. nov., sp. nov., novel filamentous anaerobes, and description of the new classes *Anaerolineae classis* nov. and *Caldilineae classis* nov. in the bacterial phylum Chloroflexi. *Int. J. Syst. Evol. Microbiol.* 56, 1331–1340. doi: 10.1099/ijs.0.64169-0

Conflict of Interest Statement: The authors declare that the research was conducted in the absence of any commercial or financial relationships that could be construed as a potential conflict of interest.

frontiers in Microbiology

ORIGINAL RESEARCH
published: 27 March 2018
doi: 10.3389/fmicb.2018.00579

Typical Soil Redox Processes in Pentachlorophenol Polluted Soil Following Biochar Addition

*Min Zhu[1,2], Lujun Zhang[1,2], Liwei Zheng[1,2], Ying Zhuo[1,2], Jianming Xu[1,2] and Yan He[1,2]**

[1] Institute of Soil and Water Resources and Environmental Science, College of Environmental and Resource Sciences, Zhejiang University, Hangzhou, China, [2] Zhejiang Provincial Key Laboratory of Agricultural Resources and Environment, Hangzhou, China

Reductive dechlorination is the primary pathway for environmental removal of pentachlorophenol (PCP) in soil under anaerobic condition. This process has been verified to be coupled with other soil redox processes of typical biogenic elements such as carbon, iron and sulfur. Meanwhile, biochar has received increasing interest in its potential for remediation of contaminated soil, with the effect seldom investigated under anaerobic environment. In this study, a 120-day anaerobic incubation experiment was conducted to investigate the effects of biochar on soil redox processes and thereby the reductive dechlorination of PCP under anaerobic condition. Biochar addition (1%, w/w) enhanced the dissimilatory iron reduction and sulfate reduction while simultaneously decreased the PCP reduction significantly. Instead, the production of methane was not affected by biochar. Interestingly, however, PCP reduction was promoted by biochar when microbial sulfate reduction was suppressed by addition of typical inhibitor molybdate. Together with Illumina sequencing data regarding analysis of soil bacteria and archaea responses, our results suggest that under anaerobic condition, the main competition mechanisms of these typical soil redox processes on the reductive dechlorination of PCP may be different in the presence of biochar. In particularly, the effect of biochar on sulfate reduction process is mainly through promoting the growth of sulfate reducer (*Desulfobulbaceae* and *Desulfobacteraceae*) but not as an electron shuttle. With the supplementary addition of molybdate, biochar application is suggested as an improved strategy for a better remediation results by coordinating the interaction between dechlorination and its coupled soil redox processes, with minimum production of toxic sulfur reducing substances and relatively small emission of greenhouse gas (CH_4) while maximum removal of PCP.

Keywords: biochar, PCP dechlorination, dissimilatory iron reduction, sulfate reduction, AQDS, molybdate

OPEN ACCESS

Edited by:
Shanquan Wang,
Sun Yat-sen University, China

Reviewed by:
Lusheng Zhu,
Shandong Agricultural University, China
Siyan Zhao,
National University of Singapore, Singapore

***Correspondence:**
Yan He
yhe2006@zju.edu.cn

Specialty section:
This article was submitted to Microbiotechnology, Ecotoxicology and Bioremediation, a section of the journal Frontiers in Microbiology

Received: *03 January 2018*
Accepted: *13 March 2018*
Published: *27 March 2018*

Citation:
Zhu M, Zhang L, Zheng L, Zhuo Y, Xu J and He Y (2018) Typical Soil Redox Processes in Pentachlorophenol Polluted Soil Following Biochar Addition. Front. Microbiol. 9:579. doi: 10.3389/fmicb.2018.00579

INTRODUCTION

Pentachlorophenol (PCP, C6Cl5OH) was first produced in 1930s and extensively used in the following decades until it has been banned globally since late 20th century (Hong et al., 2005; Gao et al., 2008; Ruder and Yiin, 2011). As a representative compound with stable aromatic ring structure and high chlorine content, PCP has relative persistence, high toxicity and long half-life in

the natural environment (Zheng et al., 2011; Guyton et al., 2016; Piskorska-Pliszczynska et al., 2016; Louis et al., 2017). Therefore, soils and sediments became the major environmental sinks for PCP as well as its byproducts and were also potential sources of re-emission (Zheng et al., 2012; Chen et al., 2016; Diagboya et al., 2016; Cui et al., 2017). Under anaerobic conditions, reductive dechlorination process has proved to be of paramount importance for PCP degradation and in which PCP acts as an electron acceptor with electrons flow from electron donors. Our previous study had showed that the coexisting ionic species in the flooded soil, such as Fe(III), and SO_4^{2-}, can also be served as terminal electron acceptors during anaerobic redox reactions to compete with PCP (Lin et al., 2014, 2018; Xu et al., 2015; Xue et al., 2017). But as two sides of the same coin, the processes of dissimilation iron and/or sulfate reduction were also found to have positive effect on PCP reduction process mediating by the functional microorganisms and mediators (Ehlers and Rose, 2006; Yang et al., 2009; Xu et al., 2014). The presence of the right terminal electron acceptor is vital for the organohalide respiration process, but it is hard to know the practical effect in the natural environment (Adrian and Loffler, 2016). This makes a more complicated and confused processes for PCP anaerobic degradation in flooded soil. Hence, there is still a lack of understanding of how these natural soil redox process effect PCP dechlorination and the direct or indirect mechanisms involved under anaerobic environment.

Biochar, a carbonaceous material formed during pyrolysis of biomass, is considered as a strong and effective sorbent for contaminated soil remediation (Xiao and Pignatello, 2015; Moreira et al., 2017). It can potentially effect pollutant bioavailability, and modify soil microbial habitats and (or) directly influencing microbial metabolisms, which together induce changes in microbial activity and microbial community structures (García-Delgado et al., 2015; Dai et al., 2016; Yao et al., 2017; Zhu et al., 2017). In addition to their high sorption ability, it has been demonstrated recently that some of these effects on soil biogeochemistry are a direct consequence of its electrochemical properties. Biochars from various feedstock sources can either accept, donate or mediate substantial amounts of electrons in their environment, via abiotic or microbial processes (Prévoteau et al., 2016; Chacón et al., 2017; Yuan et al., 2017). Previous studies have shown that biochar can influence the Fe redox cycling not only indirectly by changing the soil structure and chemistry but also directly by mediating electron transfer processes, i.e., though functioning as an electron shuttle (Kappler et al., 2014; Xu et al., 2016). However, how biochar affects sulfate redox cycling through its modification for sulfate reducer and whether it can act as an electron shuttle during this process are currently unknown.

Moreover, the redox properties of biochar has also been studied and proposed as a possible cause for PCP transformation by enhancing the extracellular electron transfer in soils (Tong et al., 2014; Yu et al., 2015). But these studies were either conducted under relatively ideal circumstances (artificial buffer or optimal reaction conditions) or under the bacterium suspension system without soil, with adequate carbon sources. Further investigation with experimental condition closer to a real natural flooding environment is thus necessary.

In this study, in order to disclose the effects and mechanisms of biochar on soil microorganisms and transformation of PCP that coupled with soil biogeochemical processes under natural flooded soil, and the role of biochar involved in microbial mediated reduction processes, including dissimilatory iron and sulfate reduction, PCP dechlorination, and methanogenesis, were simultaneously investigated. Sterilized controls were set to deduct the changes of environmental physical-chemical processes. A typical electron shuttle, 2,6-sodium anthraquinone disulfonate (AQDS) was added for the comparison of differences in the redox properties of biochar. To determine the mechanisms of biochar effect on sulfate reduction process, molybdate was added as a microbial sulfate reduction inhibitor. We hypothesized that: (1) biochar will promote both ferric iron reduction process and sulfate reduction process, but mechanisms involved may be different; (2) with modification in natural soil redox processes and soil microbial diversity following biochar amendment, biochar's effect on PCP removal in flooded soil might be very different and complicate with previous found in dryland soil.

MATERIALS AND METHODS

Chemicals

Pentachlorophenol and its degradation intermediates (>98% purity), including 2,3,4,5-Tetrachlorophenol (2,3,4,5-TCP), 3,4,5-trichlorophenol (3,4,5-TCP) and 3,5-Dichlorophenol (3,5-DCP), were purchased from Sigma-Aldrich (St. Louis, MO, United States). The extractants (>99.9% purity), including methanol, n-hexane and acetone, were obtained from Merck KGaA (Darmstadt, Germany). The other analytical grade chemicals were obtained from Sinopharm Chemical Reagent Co., Ltd., Shanghai, China. Anhydrous sodium sulfate was muffle furnace-dried at 750°C for 4 h before use.

Soil Sampling

A deep layer (80–100 cm) of a coastal mangrove soil was collected near the Taishan city in Guangdong province, China (21°48.991'N, 112°27.848'E). The soil was air-dried, gently ground, and then partly passed through a 1 mm sieve for incubation. The soil had an average pH of 8.9, an organic matter content of 1.16%, and a composition of 17.49% clay, 62.62% silt, and 19.89% sand. The soil sulfate (SO_4^{2-}) and total Fe content were comparatively high and the values of which were 626.3 $\mu g\ g^{-1}$ and 33631.7 $\mu g\ g^{-1}$, respectively. The other basic physicochemical properties of the soil were analyzed and the results are described in Supplementary Table S1 in the supporting information (SI).

Biochar Preparation and Characterization

Maize straw biochar was produced from an oxygen-limited muffle furnace at 500°C for 2 h as previously described (Luo et al., 2011). After cooling down to room temperature, the

charred materials were milled to approximately 0.15 mm and sieved through a 100-mesh sifter. The elemental C, N, H, and S compositions of the biochar were determined using an elemental analyzer (Vario EL Cube, Elementar Co., Germany), and the O content was estimated by mass balance. The Brunauer–Emmett–Teller (BET) specific surface area of biochar was measured using Mastersizer 3000 (Malvern, United Kingdom). Nuclear magnetic resonance (NMR) analysis of biochar was conducted in the Center of Modern Analysis, Nanjing University (Bruker DRX 500, Germany). The essential properties of the biochar are given in Supplementary Table S2 in SI.

Anaerobic Incubation Experiment

Each serum bottles (150 mL) contained 15 g air-dry soil, amended with biochar at application levels of 0 and 1% (w/w), respectively. To obtain a PCP-spiked soil with a concentration of 20 $\mu g\ g^{-1}$ and maintain a 1:2 (w/v) soil/water mixture to guarantee the flooding condition, 30 mL sterilized Milli-Q water and 0.1 mL PCP stock solution (3000 mg PCP L^{-1}, dissolved in acetone) was added to each bottle. The abiotic controls that contained same soil and biochar were sterilized by γ-irradiation at 50 KGy to quantify the loss of PCP due to abiotic processes and systematic loss. For comparison, 100 μM anthraquinone-2,6- disulfonate (AQDS) was added as a known electron shuttle in the non-sterilized soil (Kappler and Haderlein, 2003). To investigate the effect of sulfate reduction process on the reductive transformation of PCP, additional vials also received 20 mM molybdate to inhibit the microbial activities of sulfate reducer (Patidar and Tare, 2005; Aguilar-Barajas et al., 2011). Briefly, three treatment groups were set as: sterilized abiotic group, unsterilized biotic group and unsterilized biotic molybdate group. Each group included three treatments, namely control, AQDS amendement, 1% biochar amendement. The bottles were then followed by vigorous shaking and purged with N_2 (99.99%) for 20 min (0.75 L min^{-1}) to eliminate the O_2 and the solvent acetone from the experimental systems according to a preliminary study. After then the bottles were sealed with Teflon-coated butyl rubber stoppers and crimp seals. All treatments were incubated at 25°C in an anaerobic chamber (Don Whitley Scientific, England) under a N_2 stream in the dark, for up to 120 days.

According to our previous study, triplicate samples from each treatment were destructively sampled for analysis at the end of the 120-day incubation for analysis. The sampling procedure was as follows: firstly, the gases (CO_2, CH_4) of each bottle was collected by the injection syringe and then injected in a 7 ml vacuum flask. Secondly, the redox potential (Eh) of the soil was measured *in situ* with a platinum electrode and a standard calomel electrode. The pH was also measured *in situ* with a complex electrode. The 0.5 ml slurry was then used for extraction to determine the HCl-extractable Fe(II) after vortexed 2 min. Finally, about two-thirds of the incubation mixtures were sampled and vacuum freezing-dried for other environmental variables (SO_4^{2-}, NO_3^-, dissolved organic carbon (DOC), dissolved organic nitrogen (DON), PCP and its intermediates products) analysis, and the remaining slurry was sampled and stored at −80°C immediately for DNA extraction, amplification and high throughput sequencing.

Analytical Methods

Soil Chemical Analysis

The major chemical molecules and ions in soil mentioned above were measured following previously described methods (Xu et al., 2015). Briefly, Fe(II) concentration was measured based on 1,10-phenanthroline spectrophotometer colorimetric method after 0.5 mol L^{-1} HCl extraction for 24 h. Concentrations of anions (SO_4^{2-} and NO_3^-) and DOC/DON concentrations were determined through Milli-Q water extraction at ratio of 1:10 (w/v) before analysis by ion chromatography and TOC analyzer, respectively. The concentrations of PCP and its intermediate products (2,3,4,5-TeCP, 3,4,5-TCP, and 3,5-DCP) in soils were extracted by ultrasonic extraction and subsequent derivatization by mixing with K_2CO_3 (10 mL, 0.2 M) and acetic anhydride (0.5 mL) (Lin et al., 2014). A gas chromatograph (Agilent 6890N, Agilent, Santa Clara, CA, United States) equipped with a ^{63}Ni electric capture detector (Hewlett-Packard 6890, Hewlett-Packard, Palo Alto, CA, United States) and a HP-5 MS capillary column (30 m by 0.32 mm diameter by 0.25 μm) (J&W Scientific, Inc., Folsom, CA, United States) was used to determine the quantity and the species of chlorophenols. The concentration of released CO_2 and CH_4 were monitored by gas chromatography (GC) equipped with a flame ionization detector (FID) combined with a methane converter (TECHCOMP, China).

Soil DNA Extraction and Illumina Sequencing

Total microbial genomic DNA was extracted from 0.5 g of soil sample using the MoBio PowerSoil DNA Isolation Kit (MoBio Laboratories, Carlsbad, CA, United States) according to the manufacturer's instructions. The quantity and quality of extracted DNA were checked photometrically using a NanoDrop® ND-1000 UVeVis spectrophotometer (NanoDrop Technologies, Wilmington, DE, United States). The V4 region of the bacterial 16S rRNA gene was amplified by the polymerase chain reaction (PCR) with the primer pair 520F (5′-AYTGGGYDTAAAGNG-3′) and 802R (5′-TAGNVGGGTATCTAATCC -3′). For archaeal genes, the V5-V6 region was amplified by the PCR. The forward and reverse primers were U789F: 5′-TAGATACCCSSGTAGTCC-3′ and U1068R: 5′-CTGACGRCGCCATGC-3′, respectively. The procedures for bacterial and archaeal DNA amplification were conducted by Personal Bio Co., Ltd., Shanghai, China. The sequences were submitted to the NCBI Sequence Read Archive (SRA) database (with accession number SRP127655 for the bacteria and SRP127707 for the archaea).

Statistical Analysis

Statistical analyses were performed using SPSS software version 18.0 (SPSS, Chicago, IL, United States). Treatment effects were tested by oneway ANOVA. Statistical significance was determined at the 5% level. To compare soil microbial communities, non-metric multidimensional scaling (NMDS) was given based on generalized UniFrac distance with "vegan" and "GUniFrac" packages on R platform[1]. UniFrac distance measured phylogenetic dissimilarities between communities

[1]http://www.r-project.org

(Lozupone and Knight, 2005) and NMDS visualized the distance in low dimensional space. Parameter α was set at 0.5 when calculating generalized UniFrac and 4 axes were remained for both archaea and bacteria to reduce stress less than 0.05. Dissimilarities between treatments were tested using permutation multivariate analysis of variance (PERMANOVA) (Anderson, 2001). Only the main effects of conditions (with or with molybdate) were tested. Associations between dominant species with abundance greater than 1% in archaea or bacteria and environmental factor were analyzed following Spearman's method and visualized using "ggplot2" package. The raw *p*-values were adjusted following Benjamini and Hochberg's (1995) procedure and the adjusted *p*-value less than 0.05 was considered significant.

RESULTS

Concentrations of PCP Residuals and Dechlorination Products

The residual concentrations of PCP in soils of all treatments are shown in **Figure 1A**. The PCP dissipation extents in biotic treatments were obviously greater than those in abiotic treatments. For the abiotic control treatment, PCP decreased from the initial value of 20 $\mu g\ g^{-1}$ to 15.8 $\mu g\ g^{-1}$ after 120 days. AQDS addition did not significantly affect the abiotic removal of PCP (14.7 $\mu g\ g^{-1}$); but biochar significantly decreased the residual concentration of PCP (13.9 $\mu g\ g^{-1}$) ($p < 0.05$, similarly hereinafter). For the biotic treatment groups, the degradation extent of PCP was significantly decreased by an average of 40% in the molybdate amended treatments. PCP degradation was significantly restrained with AQDS or biochar, especially with AQDS. Regardless of amendment molybdate, the PCP degradation extent decreased in the following order: soil + none (CK) > soil + 1% biochar (B) > soil + AQDS (A).

The major detectable intermediate products in the biotic treatment groups during PCP dechlorination were 2,3,4,5-TeCP and 3,4,5-TCP (Supplementary Figure S1), which were not detected in the abiotic treatment group. The variation of 2,3,4,5-TeCP concentration in different treatments was in accordance with PCP degradation extent, while 3,4,5-TCP stayed at very low concentrations (about 0.5 $\mu g\ g^{-1}$) in all treatments. Comparing with biochar-free controls, biochar did not change the 2,3,4,5-TeCP concentration significantly, with the final concentration of about 5 $\mu g\ g^{-1}$ and 10 $\mu g\ g^{-1}$ in the presence and absence of molybdate, respectively. Among all the biotic treatments, soils with AQDS accumulated the minimum amount of 2,3,4,5-TeCP both in the presence or absence of molybdate, which were 1.2 $\mu g\ g^{-1}$ and 4.5 $\mu g\ g^{-1}$, respectively.

Changes of Typical Redox Processes

The concentration of reduced iron [Fe(II)] (**Figure 1B**) was comparatively small in the abiotic group (ranging from 4.4 mg g^{-1} to 6.8 mg g^{-1}, close to the natural background levels of the soil samples (about 3 mg g^{-1}). In the biotic treatment

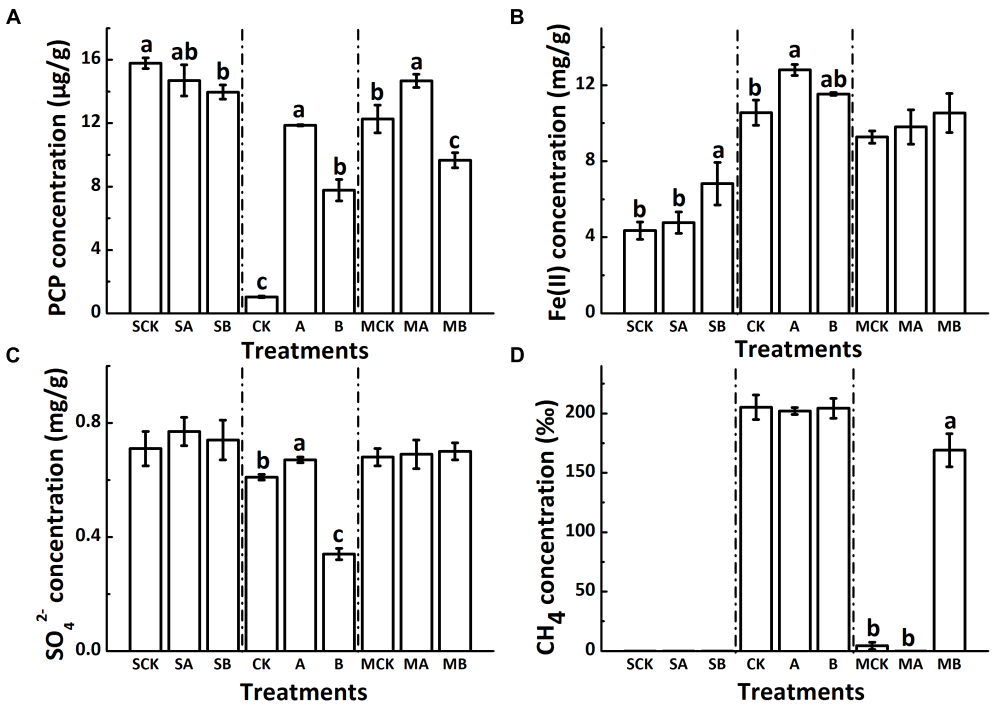

FIGURE 1 | Different soil redox processes at 120 days as shown by the concentration of PCP, Fe(II), SO_4^{2-} and CH_4 **(A–D)**. CK: Soil + none; A: Soil + AQDS; B: Soil + 1% biochar; the prefix "S": sterilized abiotic treatment group; the prefix "M": unsterilized biotic molybdate treatment group. Only significant differences ($p < 0.05$) were shown by the letter (a, ab, b, c) in lowercase on the top of data column.

groups, the increased concentration of Fe(II) multiplied and the average concentration of which was about 10 mg g^{-1}. Compared with biochar-free controls, biochar increased the accumulation of Fe(II), with changes not significant in all biotic treatments. In the absence of molybdate, the concentration of Fe(II) significantly increased by AQDS addition and reached a maximum values of 12.8 mg g^{-1} among the biotic treatments.

The sulfate concentration in soils decreased slightly in the biotic treatments with molybdate (on an average of 0.69 mg g^{-1}) as compared to that in the abiotic controls (on an average of 0.74 mg g^{-1}) (**Figure 1C**). Regardless of sterilization, neither AQDS nor biochar had significant effects on sulfate reduction in the treatments with molybdate. However, in the biotic treatments without molybdate, the sulfate reduction was significantly increased by biochar (from 0.74 to 0.34 mg g^{-1}) but decreased by AQDS (from 0.77 to 0.67 mg g^{-1}), as compared to that in the biochar-free control.

No methane was released from the soils of all abiotic treatments (**Figure 1D**). For the biotic treatments, the methanogenesis process was also inhibited with molybdate addition, with the concentration of methane only 4.34‰ in the control vials. Amendment of both molybdate and AQDS even further suppressed the release of methane to an undetectable level. However, the methanogenic activities could be increased with the coexistence of biochar, and the concentration of methane reached 169.1‰. For the biotic treatments without molybdate, the methanogenesis process was fully conducted and the concentration of methane reached a maximum of approximately 200‰, with no significant differences detected among this treatment group.

Changes of Bacteria and Archaea Communities

Taxonomic identity of each phylotype was determined using the Greengenes Classifier. A total of 777,455 and 818,579 trimmed sequences with the length of > 150 bp were obtained, and 1,600 and 389 operational taxonomic units (OTUs) with 97% similarity were identified for bacteria and archaea, respectively, from 18 soil samples of the biotic treatments. **Figures 2A,B** shows that the abundance-base diversity (α-diversity) indices of ACE, Chao 1, Simpson and Shannon of bacteria increased with biochar amendment but decreased with AQDS amendment in the presence or absence of molybdate. Comparing to the non-molybdate treatments, these indexes value slightly decreased with molybdate amendment. Besides, the changes of the α-diversity of archaea were exactly the opposite (**Figures 2C,D**). Molybdate addition increased α-diversity of archaea, these four indexes significantly increased in the AQDS treatments but decreased in the biochar treatments.

The non-metric multi-dimensional scaling (NMDS) analysis of OTUs relative abundance of bacteria (**Figure 3A**) showed an obvious separation of the six biotic treatments (stress = 0.04), indicating a significant effect of AQDS and biochar on bacteria communities along the MDS1, with the molybdate treatments obviously separated from the three control treatments along the MDS2. Additionally, the two treatments with AQDS, and the treatment with biochar only were also clearly separated from the other tree treatments in **Figure 3B** (stress = 0.03). This also

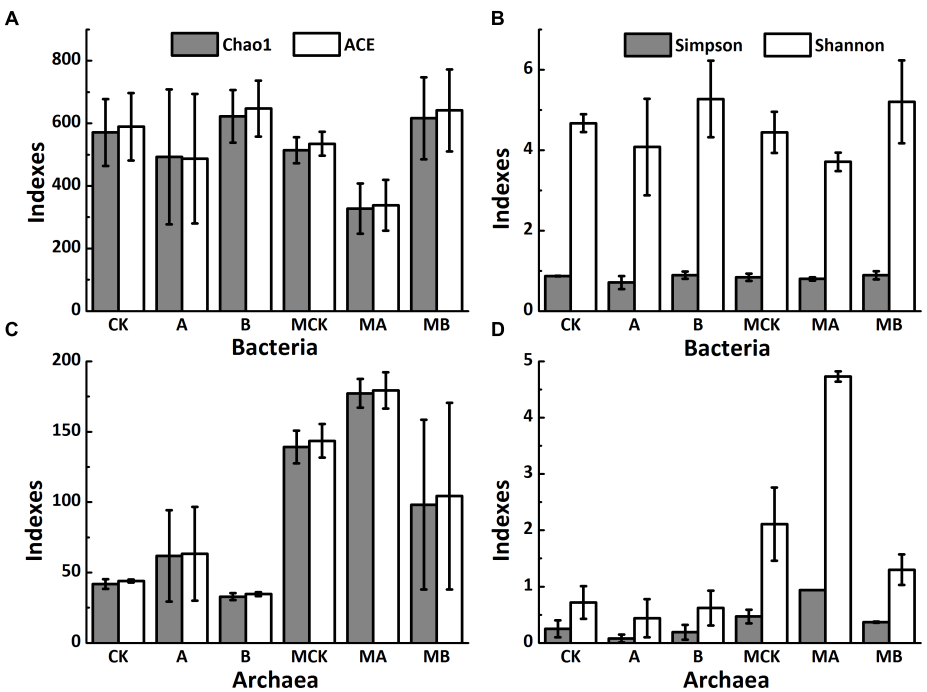

FIGURE 2 | Alpha diversity indexes of soil bacteria **(A,B)** and archaea **(C,D)** of different treatments. Abbreviations of the treatments are as **Figure 1**.

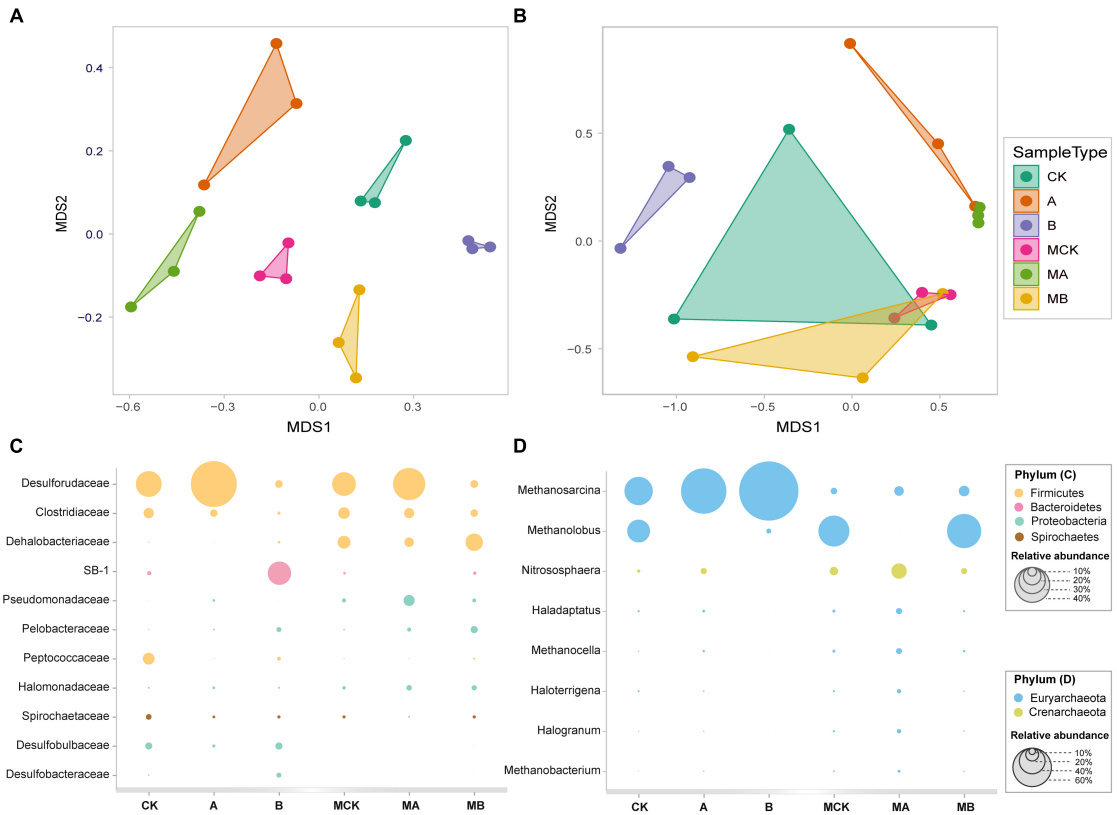

FIGURE 3 | The NMDS plots based on generalized UniFrac distance for bacterial **(A)** and archaeal **(B)** community structure, respectively, and the relative abundance of dominant bacterial community at family level **(C)** and archaeal community at genus level **(D)** in different treatments.

indicated significant differences of these treatments in archaeal communities. The other two dimension (MDS3 and MDS4) plot of bacteria and archaea were plotted in Supplementary Figure S2.

Bacterial relative abundance (>2%) of the six treatments was compared at family level (**Figure 3C**). Treatment groups with or without molybdate had the similar variation among the control, AQDS and biochar treatments. The most abundant phylum in the control was *Firmicutes* (>60%), followed by *Bacteroidetes* (>16%), *Proteobacteria* (>15%) and *Spirochaetes* (>3%). Compared with the control, the addition of biochar increased the relative abundances of *SB-1*, *Dehalobacteriaceae*, *Pelobacteraceae*, *Desulfobulbaceae,* and *Desulfobacteraceae* significantly (especially the *SB-1* that increased from 4.5 to 26.5%), but decreased the relative abundances of *Clostridiaceae* and *Peptococcaceae* significantly. With the amendment of AQDS, the relative abundance of *Desulforudaceae* increased significantly from 29.3 to 52.3%. The relative abundances of *Pseudomonadaceae* and *Halomonadaceae* also increased in the AQDS treatment. In the presence of molybdate, the relative abundance of *Desulforudaceae*, *Peptococcaceae*, *Spirochaetaceae*, *Desulfobulbaceae,* and *Desulfobacteraceae* decreased significantly, while that of *Clostridiaceae*, *Dehalobacteriaceae*, *Pseudomonadaceae,* and *Halomonadaceae* had a significant increase.

The archaea was mainly dominated by the phylum of *Euryarchaeota*, whose relative abundance accounted for > 90% of the control. Archaeal relative abundance (>1%) at genus level was plotted in **Figure 3D**. *Methanosarcina* and *Methanolobus* were the dominant genera, with their relative abundances accounted for 43.9 and 35.3% in the control, respectively. Biochar and AQDS amendment significantly increased the relative abundance of *Methanosarcina* to 92.1 and 70.5%, respectively. Besides, the relative abundance of *Methanolobus* significantly decreased to 7.4 and 0.01% in the biochar and AQDS treatments, respectively. In the presence of molybdate, the relative abundance of *Methanosarcina* of these treatments significantly decreased to no more than 20%, while the relative abundance of *Methanolobus* increased significantly except in the AQDS treatment. The other archaea genera were all increased in the coexistence of molybdate and AQDS, only with the exception of *Methanosarcina* and *Methanolobus*.

Correlations of Environmental Variables and Microbial Taxonomies

Heatmap based on the relative abundances of the dominant OTUs (>1%) in the data sets as gave detailed classification information between different treatments. As shown in **Figure 4**, all the dominant OTUs of archaea except OTU569, had exactly the same correlations with the environmental variables, which

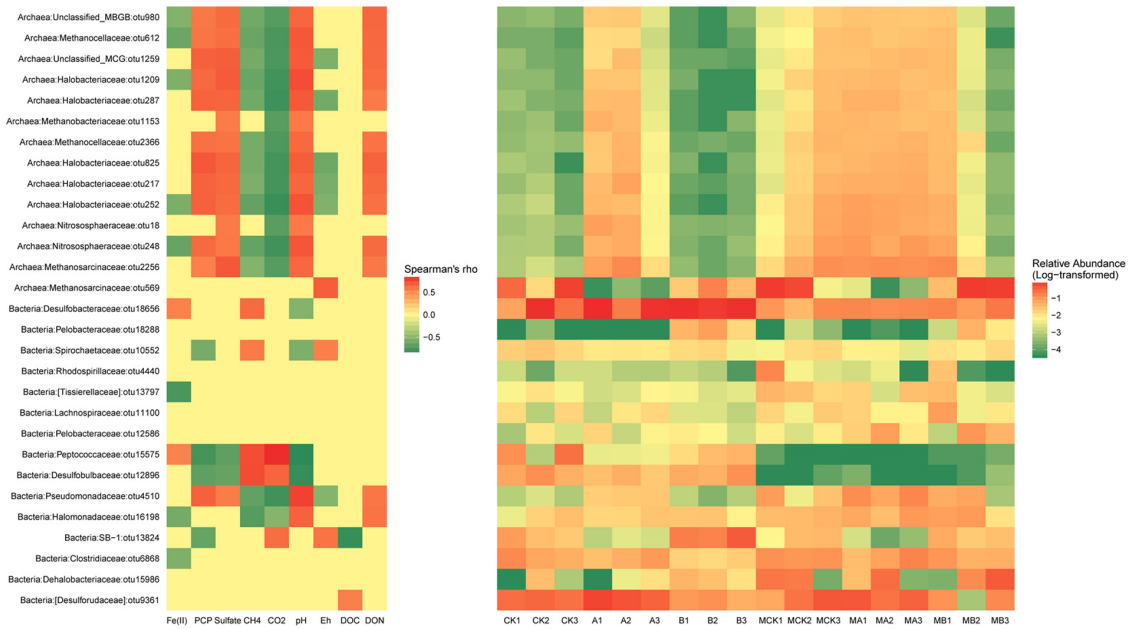

FIGURE 4 | The significant correlations (p-value < 0.05) between environmental factors and relative abundance of the dominant bacterial and archaeal OTUs (Left) and the relative abundance of these OTUs in different treatments (Right).

were positively correlated with the concentration of PCP, sulfate, DON and soil pH, but negatively correlated with the concentration of Fe(II), CH_4, CO_2, and soil Eh. The relative abundance of these OTUs increased in the presence of AQDS and/or molybdate. The outstanding OTU569 that belongs to family *Methnosarcinaceae* decreased significantly in the AQDS treatments. As to the dominant OTUs of bacteria, their relationship with environmental variables was more changeable. The OTU18656 (*Desulfobacteraceae*) and OTU15575 (*Peptococcaceae*) were positively correlated with the Fe(II) and CH_4. The relative abundance of these two OTUs increased in the treatments with AQDS or biochar. The OTU10552 (*Spirochaetaceae*), OTU15575 (*Peptococcaceae*), and OTU12896 (*Desulfobulbaceae*) had negative correlations with PCP residues and soil pH, but positively correlated with CH_4. The relative abundance of these three OTUs increased in the absence of molybdate. The OTU13824 (*SB-1*) also had a negative correlation with PCP residues, but its relative abundance increased in the presence of biochar.

DISCUSSION

Many studies have indicated that biochar amendment can directly and indirectly affect the fate of persistent organic pollutants and pesticides by acting as a geosorbent (Sun et al., 2012; Anyika et al., 2015), so the γ-irradiation sterilized abiotic treatment group was set in this study, in which the decreases in PCP concentration might be mainly due to sorption contribution of biochar. However, as no chlorophenols metabolites were detected in the sterilized abiotic soils, the sorption amount by biochar could not be deducted through comparison of differences between the abiotic control group and the biotic treatment group. Anyway, the results demonstrated that only a small proportion of PCP (less than 10%) was absorbed by amended biochar after 120-day incubation. Hence, the specific adsorption capacity and maximum adsorption capacity of biochar were not considered, and we speculated the differences in depletion of PCP and its metabolites among the treatments were mainly caused by the degradation ability of indigenous microorganisms in different treatments. The typical soil redox processes, sulfate reduction and methanogenesis, were also not significantly affected by biochar in the abiotic treatments (**Figure 1**).

The Role of Biochar in Enhanced Fe(III) Reduction Process

Usually, biochar is considered as a soil conditioner in many studies to improve soil fertility by increasing the pH and nutrient retention and shift soil biological community composition and abundance in soil and sediments (Tong et al., 2014; Yu et al., 2015, 2016). Biochar did not have a significant effect on the soil pH as the initial pH of the experimental soil is alkaline (Supplementary Figure S3A). The HCl-extractable Fe(II) is commonly accumulated as an end product of microbial Fe(III) reduction in natural environments. Therefore, a potential explanation for the enhanced generation of HCl-extractable Fe(II) in the presence of biochar is that biochar potentially stimulated the growth and activity of Fe(III) reducer. Our results showed that the addition of biochar and AQDS led to a significant increase in the abundance of *Pelobacteraceae*, especially in the presence of biochar (**Figure 3C**). This family has been discovered as the dominant iron reducer in many studies (Hori et al.,

2015), and reported as having a positive correlation with Fe(III) reduction in the ferrihydrite enrichment with the amendment of AQDS or biochar (Zhou et al., 2016).

Meanwhile, biochar has also been reported as an electron shuttle for microbial electron shuttling to transfer electrons onto a solid Fe(III) (ferrihydrite) electron acceptor from *Shewanella oneidensis* and significantly increased the rate of ferrihydrite reduction and extent of reduction (Kappler et al., 2014; Xu et al., 2016; Yuan et al., 2017). Hence, as biochar can donate, accept, or transfer electrons in their surrounding environments, either abiotically or via biological pathways, there is the possibility that biochar served as an electron mediator to enhance the generation of HCl-extractable Fe(II). As a commonly used quinone containing analog of humic substances in laboratory, AQDS is often used as a model electron shuttling compound in studies of dissimilatory microbial reduction of iron oxides and transformation of reductive organic compounds (Kappler and Haderlein, 2003; Liu et al., 2007; Kwon and Finneran, 2008; Costa et al., 2010). Though the above two pathways might thus work concurrently, given that the more prominent increase of HCl-extractable Fe(II) accumulated in the AQDS treatment, the electron shuttling pathway might play a more significant role in the Fe(III) reduction process with biochar amendment.

Effect of Biochar on Sulfate Reduction Process

Microbial dissimilatory sulfate reduction is also an important transformation that occurs under anaerobic environment (Muyzer and Stams, 2008). After 120 days incubation, the redox potential became downward into the range of SO_4^{2-} reduction (approximately-150 mV, Supplementary Figure S3B) (Connell and Patrick, 1968). But comparing with the abiotic group, the microbial reduction extend of sulfate was not strong in soils of the biotic treatments. Theoretically, competitive relationships are involved between different microbial metabolic pathways on account of their corresponding thermodynamic feasibility (Jin and Bethke, 2007; Burgin et al., 2011). As such, the microbial reduction of Fe(III) process is prior to the sulfate reduction process and always acts as a powerful competitor when both processes exist simultaneously. Hence, the results that why the concentration of HCl-extractable Fe(II) reached the maximum while the sulfate was reduced at the smallest extent in the presence of AQDS may be well explained (**Figures 1B,C**). This also provided a further proof that the electrons of this system might not be inadequate to the subsequent redox reactions after iron reduction. Put another way, electron shuttling might be not conducive to the microbial sulfate reduction if the iron reduction process is relatively active, especially under electron limited reducing environment.

The effect of biochar on microbial sulfate reduction process has been little investigated so far. The barely researches reported that biochar amendment did not increase the sorption capacity of soil for SO_4^{2-} (Zhao et al., 2017) and it could enhance the SO_4^{2-} reduction (to sulfide) by 85% compared to the initial concentration (Easton et al., 2015), but the mechanisms involved had not been well discussed. In our study, biochar amendment also significantly increased the microbiological reduction of SO_4^{2-}, which is highly consistent with increased abundance of sulfate reducer (*Desulfobulbaceae* and *Desulfobacteraceae*) with biochar amendment (**Figure 3C**). But the relative abundance of family *Desulforudaceae*, which has been observed likely involved in the biogeochemical cycling of sulfur in previous study (Rempfert et al., 2017), decreased significantly in the presence of biochar. We thus speculate that this family might not be the main active sulfate reducer in our study. Actually, the existing reports regarding the sulfate reducing function of this family in complex matrices such as soil is still limited. The molybdate ion is a functional analog sulfate during the process of cellular respiration that can be transported into the bacteria, resulting in the deprivation of sulfur reducing compounds (Patidar and Tare, 2005; Aguilar-Barajas et al., 2011). Thus, it acts as an ion specific metabolic inhibitor that limits sulfate reduction and is toxic to these microorganisms. Here, in the presence of molybdate, the relative abundances of the two families *Desulfobulbaceae* and *Desulfobacteraceae* decreased to almost zero with no significant difference among the three treatments, even in the presence of biochar (**Figure 3C**). Therefore, we deduced that the sulfate reduction process under anaerobic environment is predominantly controlled by the functional sulfate reducer but not the electron mediators like AQDS. The effect of biochar on sulfate reduction process is mainly through modifying the abundance and activities of functional microorganisms but not as an electron shuttle.

Coupling Effect of Biochar and Soil Redox Processes on PCP Reductive Dechlorination

Conventionally, organic contaminants sorbed onto biochar have been considered to be chemically and biologically inert (Lou et al., 2011; Xiao and Pignatello, 2015). The soil residual concentration of PCP in the biotic treatment with biochar was less than that without biochar (**Figure 1A**), which indicated that the reduced portions might be ascribed to the irreversible adsorption by biochar and this might decrease the microbial availability of PCP. Meanwhile, the experimental biochar in our study was produced at 500°C with comparatively high aromaticity and different surface functional groups (Supplementary Table S1), hence, the possibility that biochar acting as an electron shuttle in anaerobic environment should not be discounted. Additionally, similar to the role of biochar in soil redox processes, biochar also behaved multifunction in the biotransformation of organic contaminants in many studies (Zhu et al., 2017). Though a previous study has reported that biochar could positively enhance the extracellular electron transfer in soils to promote PCP transformation by stimulating the growth and metabolism of microorganisms in the soils, it is not close to the real soil environment by maintaining the pH at 7.0 with 30 mM PIPES buffer (Tong et al., 2014). The natural anaerobic soil environment is always more complicated with different electron donors, electron mediators, acceptors and microorganisms (Xu et al., 2015). In our study, the soil:water ratio was set at 1:2 to simulate the flooding environment and we found that AQDS and biochar

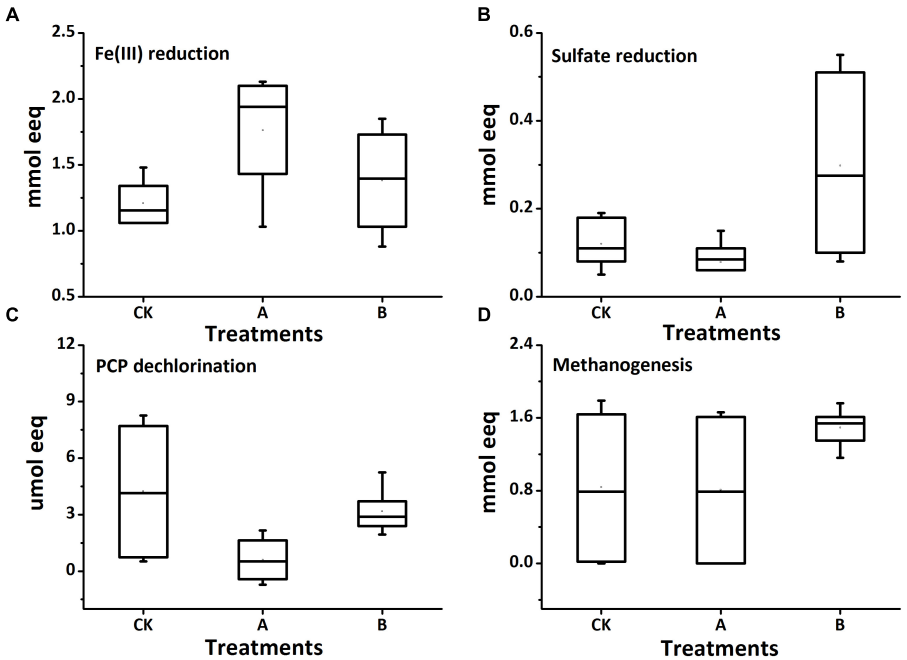

FIGURE 5 | Stoichiometric electron equivalent analysis of the receiving electrons during reduction of Fe(III) **(A)**, SO_4^{2-} **(B)**, PCP **(C)**, and methanogenesis **(D)** in the biotic treatments. Treatments with or without molybdate were grouped together for analysis.

TABLE 1 | Relevant half reactions of the electron acceptors during 120 days incubation.

Compound	Half Reaction	eeq/mol compound	Reference
Ferrous iron	$Fe^{3+} + e^- = Fe^{2+}$	1	Picardal et al., 1995
Sulfides	$SO_4^{2-} + 9H^+ + 8e^- = HS^- + 4H_2O$	8[a]	Flynn et al., 2014
Methane	$CH_3COOH = CH_4 + CO_2$	8[b]	Ferry, 1992;
	$CO_2 + 8H^+ + 8e^- = CH_4 + 2H_2O$		Liu and Whitman, 2008
TeCP[c]	$C_6Cl_5OH + H^+ + 2e^- = C_6HCl_4OH + Cl^-$	2	Kenneke and Weber, 2003
TCP[d]	$C_6Cl_5OH + 2H^+ + 4e^- = C_6H_2Cl_3OH + 2Cl^-$	4	

[a]Based on the assumption that the final reduction products during SO_4^{2-} reducing process are entirely existed in −2 valence; [b]Calculated with an average electron equivalents that required by one mole methane from acetate metabolism; [c,d]The electron equivalents from PCP transformation were calculated from the concentration changes of the main products of TeCP and TCP that generated from PCP dechlorination.

suppressed the PCP degradation, especially with the AQDS amendment. The original DOC and DON concentrations of the deep soil layer samples used in this study had been relatively low (about 150 mg kg^{-1} and 15 mg kg^{-1}, respectively, as shown in Supplementary Figures S3C,D), and we did not add any extra electron donors during the incubation. Therefore, the electron donors in the experimental soil were speculated to be very limited for guaranteeing a complete soil reduction processes. Under this circumstance, limited electrons might be transferred to the dominant more competitive one (in our case, Fe(III) reduction) by the amendments (AQDS or biochar) and thus inhibited the reductive dechlorination of PCP indirectly.

Though the relative abundance of the family *Dehalobacteriaceae* increased significantly in the presence of molybdate (**Figure 3C**), the PCP degradation extent reduced significantly comparing with the molybdate-free treatments (**Figure 1A**). It is inferred that the family *Dehalobacteriaceae* might be the main PCP dechlorinator in the molybdate-free treatments in this study. However, with the coexistence of molybdate and biochar, the relative abundance of this family is comparatively increased, which is coincidence with the enhanced PCP degradation. So biochar might have the ability to benefit the growth of dechlorinators by improving the environmental condition for the dechlorinators and easing the competition relation between dechlorinators and other microorganisms to affect the dechlorination process in the presence molybdate. Besides, the family *Peptococcaceae*, whose abundance decreased significantly in the presence of molybdate, includes many degrading genera like *Dehalobacter* and *Desulfitobacterium* (Dennie et al., 1998; Kranzioch-Seipel et al., 2016). Molybdate has been reported as capable of partially inhibit the dechlorination of polychlorinated biphenyls at a low concentration (1 mM) (Ye et al., 1999). Thus, it would not rule out the possibility that molybdate could inhibit other potential dechlorinators or microorganisms with other functions (e.g., sulfate reducer) to indirectly regulate the reductive dechlorination of PCP.

The electrons consumed for each microbial reduction process in biotic treatments were calculated and shown in **Figure 5** (Treatments with or without molybdate were grouped together for analysis; specific values of each treatment were plotted in Supplementary Table S3 in SI). The addition of molybdate decreased the total amount of electron equivalents needed by more than 50% (from an average of 3568 to 1759 μmol) (The calculation of each electron acceptor was based on assumption in **Table 1**). Total electrons consumed by microbial Fe(III) and sulfate reduction processes were significantly increased by the amendment of both AQDS and biochar, respectively, in the molybdate-free treatments [from 1217 to 2096 μmol and from 165 to 501 μmol for Fe(III) and sulfate reduction processes, respectively]; while the electrons subdivided to PCP reduction process were all decreased significantly. This suggested the presence of AQDS or biochar might shift part of electrons from dechlorination to Fe(III) and sulfate reduction. And interestingly, when the whole microbial reduction processes were inhibited to some extent by molybdate, the electrons consumed for dechlorination and methanogenesis significantly increased with biochar addition (from 0.15 to 0.40 μmol and from 34.56 and 1351.80 μmol for dechlorination and methanogenesis, respectively). Therefore, to make sure the exact biochar effect on reductive removal of PCP in flooded soil, more synthetic consideration is necessary to warrant a better result through balancing all the redox processes to avoid the production of both toxic reduced iron/sulfur substances and greenhouse gases while pollution remediation.

The Potential Functional Microbial Species Regulating Typical Soil Redox Processes in PCP Polluted Soil Following Biochar Addition

Based on the sequencing results, our studies clearly show that the addition of AQDS and biochar had significant influences on the archaea and bacteria structures (**Figures 3A,B**). The corresponding changes of the dominant OTUs (relative abundance $> 1\%$) were analyzed relating to the environmental variables and specific treatments (**Figure 4**). As the most abundant genus in the molybdate-free treatments, genus *Methanosarcina* apparently was the dominant methanogens in these treatments. However, the relative abundance of OTU569 (*Methanosarcina*, *Methanosarcinaceae*) was irrelevant to CH_4 but positively related with the DOC. There was no difference with CH_4 concentration among the treatments, evidently proved that this OTU was susceptible to the readily usable carbon source (electron donors). Another possible explanation is that OTU569 might be very stable in each treatment and had no relations with the major environmental variables.

Positive correlations of PCP with the notable OTU4510 that belongs to the family *Pseudomonadaceae* indicated that this group was resistant to PCP. The dominant OTUs included OTU10552 (*Spirochaeta*, *Spirochaetaceae*), OTU15575 (*Desulfosporosinus*, *Peptococcaceae*), OTU12896 (unclassified *Desulfobulbaceae*) and OTU13824 (unclassified *SB-1*) showed negative correlation with PCP residual, indicating these species might participate in the PCP dechlorination. The members of the *Desulfosporosinus* and *Desulfobulbaceae* have been previously suggested as popular sulfate reducer (Miletto et al., 2011; Engelbrektson et al., 2014). Since our results found that both OTU15575 and OTU12896 had a negative correlation with sulfate concentration, they would thus probably be the main functional sulfate reducers. In addition, these two OTUs were positively related to CH_4 and CO_2, which might also facilitate the methanogenesis process synergistically by accelerating the reduction of redox potential. Though these two species were found to be important for toluene and hexahydro-1,3,5-trinitro-1,3,5-triazine (RDX) degradation under various electron-accepting conditions (Sun et al., 2012; Cupples, 2016; Michalsen et al., 2016), they have not yet been reported in the chlorinated organic pollutants degradation researches. Their effects on PCP degradation might thus be in an indirect way.

The concentration of accumulated HCl-extractable Fe(II) was positively related to OTU18656 (unclassified *Desulfobacteraceae*) and OTU15575 *(Desulfosporosinus*, *Peptococcaceae*) whose relative abundances increased in the presence of biochar (**Figure 4**). This indicated that these two species played an important role in facilitating the Fe(III) reduction. It is reported that *Desulfobulbaceae* could partially share the electrons from the benzene as syntrophic partners in an iron-reducing enrichment culture (Kunapuli et al., 2007). Meanwhile, members of the family *Desulfobacteraceae* was also proved to be important for naphthalene degradation under sulfate-reducing conditions in freshwater environments (Kümmel et al., 2015). Therefore, members of this family might also be the muti-functional species that acted as both Fe(III) and SO_4^{2-} reducer under the stress of PCP pollution, especially in the presence of biochar.

AUTHOR CONTRIBUTIONS

MZ designed and carried out the research, data handling and analysis, and wrote the manuscript. LuZ contributed to the analysis of the Illumina sequencing data. LiZ and YZ gave assistance in lab work. JX provided the experimental materials and research platform. YH contributed to the design of the experiments, data mining, and revised the manuscript. All authors read and approved the final manuscript.

FUNDING

This research was financially supported by the National Natural Science Foundation of China (41721001, 41771269, and 41322006), and the National Key Research and Development Program of China (2016YFD0800207).

SUPPLEMENTARY MATERIAL

The Supplementary Material for this article can be found online at: https://www.frontiersin.org/articles/10.3389/fmicb.2018.00579/full#supplementary-material

REFERENCES

Adrian, L., and Loffler, F. E. (2016). *Organohalide Respiring Bacteria*, Vol. 85. Berlin: Springer, doi: 10.1007/978-3-662-49875-0_1

Aguilar-Barajas, E., Díaz-Pérez, C., Ramírez-Díaz, M. I., Riveros-Rosas, H., and Cervantes, C. (2011). Bacterial transport of sulfate, molybdate, and related oxyanions. *Biometals* 24, 687–707. doi: 10.1007/s10534-011-9421-x

Anderson, M. J. (2001). A new method for non-parametric multivariate analysis of variance. *Austral Ecol.* 26, 32–46. doi: 10.1111/j.1442-9993.2001.01070.pp.x

Anyika, C., Abdul Majid, Z., Ibrahim, Z., Zakaria, M. P., and Yahya, A. (2015). The impact of biochars on sorption and biodegradation of polycyclic aromatic hydrocarbons in soils–a review. *Environ. Sci. Pollut. Res. Int.* 22, 3314–3341. doi: 10.1007/s11356-014-3719-5

Benjamini, Y., and Hochberg, Y. (1995). Controlling the false discovery rate: a practical and powerful approach to multiple testing. *J. R. Stat. Soc. Series B* 57, 289–300.

Burgin, A. J., Yang, W. H., Hamilton, S. K., and Silver, W. L. (2011). Beyond carbon and nitrogen: how the microbial energy economy couples elemental cycles in diverse ecosystems. *Front. Ecol. Environ.* 9:44–52. doi: 10.1890/090227

Chacón, F. J., Cayuela, M. L., Roig, A., and Sánchez-Monedero, M. A. (2017). Understanding, measuring and tuning the electrochemical properties of biochar for environmental applications. *Rev. Environ. Sci. Bio.* 16, 695–715. doi: 10.1007/s11157-017-9450-1

Chen, Y., Yu, S., Tang, S., Li, Y., Liu, H., Zhang, X., et al. (2016). Site-specific water quality criteria for aquatic ecosystems: a case study of pentachlorophenol for Tai Lake. *China. Sci. Total Environ.* 541, 65–73. doi: 10.1016/j.scitotenv.2015.09.006

Connell, W. E., and Patrick, W. H. (1968). Sulfate reduction in soil: effects of redox potential and pH. *Science* 159, 86–87. doi: 10.1126/science.159.3810.86

Costa, M. C., Mota, S., Nascimento, R. F., and Dos Santos, A. B. (2010). Anthraquinone-2,6-disulfonate (AQDS) as a catalyst to enhance the reductive decolourisation of the azo dyes Reactive Red 2 and Congo Red under anaerobic conditions. *Bioresour. Technol.* 101, 105–110. doi: 10.1016/j.biortech.2009.08.015

Cui, Y., Liang, L., Zhong, Q., He, Q., Shan, X., Chen, K., et al. (2017). The association of cancer risks with pentachlorophenol exposure: focusing on community population in the areas along certain section of Yangtze River in China. *Environ. Pollut.* 224, 729–738. doi: 10.1016/j.envpol.2016.12.011

Cupples, A. M. (2016). Contaminant-degrading microorganisms identified using stable isotope probing. *Chem. Eng. Technol.* 39, 1593–1603. doi: 10.1002/ceat.201500479

Dai, Z., Hu, J., Xu, X., Zhang, L., Brookes, P. C., He, Y., et al. (2016). Sensitive responders among bacterial and fungal microbiome to pyrogenic organic matter (biochar) addition differed greatly between rhizosphere and bulk soils. *Sci. Rep.* 6:36101. doi: 10.1038/srep36101

Dennie, D., Gladu, I., Lépine, F., Villemur, R., Bisaillon, J. G., and Beaudet, R. (1998). Spectrum of the reductive dehalogenation activity of *Desulfitobacterium frappieri* PCP-1. *Appl. Environ. Microb.* 64, 4603–4606.

Diagboya, P. N., Olu-Owolabi, B. I., and Adebowale, K. O. (2016). Distribution and interactions of pentachlorophenol in soils: the roles of soil iron oxides and organic matter. *J. Contam. Hydrol.* 191, 99–106. doi: 10.1016/j.jconhyd.2016.04.005

Easton, Z. M., Rogers, M., Davis, M., Wade, J., Eick, M., and Bock, E. (2015). Mitigation of sulfate reduction and nitrous oxide emission in denitrifying environments with amorphous iron oxide and biochar. *Ecol. Eng.* 82, 605–613. doi: 10.1016/j.ecoleng.2015.05.008

Ehlers, G. A., and Rose, P. D. (2006). The potential for reductive dehalogenation of chlorinated phenol in a sulphidogenic environment in in situ enhanced biodegradation. *Water SA* 32, 243–248. doi: 10.4314/wsa.v32i2.5249

Engelbrektson, A., Hubbard, C. G., Tom, L. M., Boussina, A., Jin, Y. T., Wong, H., et al. (2014). Inhibition of microbial sulfate reduction in a flow-through column system by (per)chlorate treatment. *Front. Microbiol.* 5:315. doi: 10.3389/fmicb.2014.00315

Ferry, J. G. (1992). Methane from acetate. *J. Bacteriol.* 174, 5489–5495. doi: 10.1128/jb.174.17.5489-5495.1992

Flynn, T. M., O'Loughlin, E. J., Mishra, B., DiChristina, T. J., and Kemner, K. M. (2014). Sulfur-mediated electron shuttling during bacterial iron reduction. *Science* 344, 1039–1042. doi: 10.1126/science.1252066

Gao, J., Liu, L., Liu, X., Zhou, H., Huang, S., and Wang, Z. (2008). Levels and spatial distribution of chlorophenols – 2,4-Dichlorophenol, 2,4,6-trichlorophenol, and pentachlorophenol in surface water of China. *Chemosphere* 71, 1181–1187. doi: 10.1016/j.chemosphere.2007.10.018

García-Delgado, C., Alfaro-Barta, I., and Eymar, E. (2015). Combination of biochar amendment and mycoremediation for polycyclic aromatic hydrocarbons immobilization and biodegradation in creosote-contaminated soil. *J. Hazard. Mater.* 285, 259–266. doi: 10.1016/j.jhazmat.2014.12.002

Guyton, K. Z., Loomis, D., Grosse, Y., El Ghissassi, F., Bouvard, V., Benbrahim-Tallaa, L., et al. (2016). Carcinogenicity of pentachlorophenol and some related compounds. *Lancet Oncol.* 17, 1637–1638. doi: 10.1016/S1470-2045(16)30513-7

Hong, H., Zhou, H., Luan, T., and Lan, C. (2005). Residue of pentachlorophenol in freshwater sediments and human breast milk collected from the Pearl River Delta. *China. Environ. Int.* 31, 643–649. doi: 10.1016/j.envint.2004.11.002

Hori, T., Aoyagi, T., Itoh, H., Narihiro, T., Oikawa, A., Suzuki, K., et al. (2015). Isolation of microorganisms involved in reduction of crystalline Iron(III) oxides in natural environments. *Front. Microbiol.* 6:386. doi: 10.3389/fmicb.2015.00386

Jin, Q., and Bethke, C. M. (2007). The thermodynamics and kinetics of microbial metabolism. *Am. J. Sci.* 307, 643–677. doi: 10.2475/04.2007.01

Kappler, A., and Haderlein, S. B. (2003). Natural organic matter as reductant for chlorinated aliphatic pollutants. *Environ. Sci. Technol.* 37, 2714–2719. doi: 10.1021/es0201808

Kappler, A., Wuestner, M. L., Ruecker, A., Harter, J., Halama, M., and Behrens, S. (2014). Biochar as an electron shuttle between bacteria and Fe(III) minerals. *Environ. Sci. Technol. Lett.* 1, 339–344. doi: 10.1021/ez5002209

Kenneke, J. F., and Weber, E. J. (2003). Reductive dehalogenation of halomethanes in iron-and sulfate-reducing sediments. 1. Reactivity pattern analysis. *Environ. Sci. Technol.* 37, 713–720. doi: 10.1021/es0205941

Kranzioch-Seipel, I., Beckert, U., Shen, C., Yin, D., and Tiehm, A. (2016). Microbial dechlorination of HCB, PCP, PCB180, HCH and PCE in a Yangtze Three Gorges Reservoir enrichment culture, China. *Environ. Earth Sci.* 75:928. doi: 10.1007/s12665-016-5653-y

Kümmel, S., Herbst, F., Bahr, A., Duarte, M., Pieper, D. H., Jehmlich, N., et al. (2015). Anaerobic naphthalene degradation by sulfate-reducing Desulfobacteraceae from various anoxic aquifers. *FEMS Microbiol. Ecol.* 91:fiv006. doi: 10.1093/femsec/fiv006

Kunapuli, U., Lueders, T., and Meckenstock, R. U. (2007). The use of stable isotope probing to identify key iron-reducing microorganisms involved in anaerobic benzene degradation. *ISME J.* 1, 643–653. doi: 10.1038/ismej.2007.73

Kwon, M. J., and Finneran, K. T. (2008). Biotransformation products and mineralization potential for hexahydro-1,3,5-trinitro-1,3,5-triazine (RDX) in abiotic versus biological degradation pathways with anthraquinone-2,6-disulfonate (AQDS) and *Geobacter metallireducens*. *Biodegradation* 19, 705–715. doi: 10.1007/s10532-008-9175-5

Lin, J., He, Y., Xu, J., Chen, Z., and Brookes, P. C. (2014). Vertical profiles of pentachlorophenol and the microbial community in a paddy soil: influence of electron donors and acceptors. *J. Agric. Food Chem.* 62, 9974–9981. doi: 10.1021/jf502746n

Lin, J., Meng, J., He, Y., Xu, J., Chen, Z., and Brookes, P. C. (2018). The effects of different types of crop straw on the transformation of pentachlorophenol in flooded paddy soil. *Environ. Pollut.* 233, 745–754. doi: 10.1016/j.envpol.2017.10.114

Liu, C., Zachara, J. M., Foster, N. S., and Strickland, J. (2007). Kinetics of reductive dissolution of hematite by bioreduced anthraquinone-2,6-disulfonate. *Environ. Sci. Technol.* 41, 7730–7735. doi: 10.1021/es070768k

Liu, Y., and Whitman, W. B. (2008). Metabolic, phylogenetic, and ecological diversity of the methanogenic archaea. *Ann. N. Y. Acad. Sci.* 1125, 171–189. doi: 10.1196/annals.1419.019

Lou, L., Wu, B., Wang, L., Luo, L., Xu, X., Hou, J., et al. (2011). Sorption and ecotoxicity of pentachlorophenol polluted sediment amended with rice-straw derived biochar. *Bioresour. Technol.* 102, 4036–4041. doi: 10.1016/j.biortech.2010.12.010

Louis, L. M., Lerro, C. C., Friesen, M. C., Andreotti, G., Koutros, S., Sandler, D. P., et al. (2017). A prospective study of cancer risk among Agricultural Health Study farm spouses associated with personal use of organochlorine insecticides. *Environ. Health* 16:95. doi: 10.1186/s12940-017-0298-1

Lozupone, C., and Knight, R. (2005). UniFrac: a new phylogenetic method for comparing microbial communities. *Appl. Environ. Microb.* 71, 8228–8235. doi: 10.1128/AEM.71.12.8228-8235.2005

Luo, L., Lou, L., Cui, X., Wu, B., Hou, J., Xun, B., et al. (2011). Sorption and desorption of pentachlorophenol to black carbon of three different origins. *J. Hazard. Mater.* 185, 639–646. doi: 10.1016/j.jhazmat.2010.09.066

Michalsen, M. M., King, A. S., Rule, R. A., Fuller, M. E., Hatzinger, P. B., Condee, C. W., et al. (2016). Evaluation of biostimulation and bioaugmentation to stimulate hexahydro-1,3,5-trinitro-1,3,5,-triazine degradation in an aerobic groundwater aquifer. *Environ. Sci. Technol.* 50, 7625–7632. doi: 10.1021/acs.est.6b00630

Miletto, M., Williams, K. H., N'Guessan, A. L., and Lovley, D. R. (2011). Molecular analysis of the metabolic rates of discrete subsurface populations of sulfate reducers. *Appl. Environ. Microb.* 77, 6502–6509. doi: 10.1128/AEM.00576-11

Moreira, M. T., Noya, I., and Feijoo, G. (2017). The prospective use of biochar as adsorption matrix – A review from a lifecycle perspective. *Bioresour. Technol.* 246, 135–141. doi: 10.1016/j.biortech.2017.08.041

Muyzer, G., and Stams, A. J. M. (2008). The ecology and biotechnology of sulphate-reducing bacteria. *Nat. Rev. Microbiol.* 6, 441–454. doi: 10.1038/nrmicro1892

Patidar, S. K., and Tare, V. (2005). Effect of molybdate on methanogenic and sulfidogenic activity of biomass. *Bioresour. Technol.* 96, 1215–1222. doi: 10.1016/j.biortech.2004.11.001

Picardal, F., Arnold, R. G., and Huey, B. B. (1995). Effects of electron donor and acceptor conditions on reductive dehalogenation of tetrachloromethane by *Shewanella putrefaciens* 200. *Appl. Environ. Microb.* 61, 8–12.

Piskorska-Pliszczynska, J., Strucinski, P., Mikolajczyk, S., Maszewski, S., Rachubik, J., and Pajurek, M. (2016). Pentachlorophenol from an old henhouse as a dioxin source in eggs and related human exposure. *Environ. Pollut.* 208, 404–412. doi: 10.1016/j.envpol.2015.10.007

Prévoteau, A., Ronsse, F., Cid, I., Boeckx, P., and Rabaey, K. (2016). The electron donating capacity of biochar is dramatically underestimated. *Sci. Rep.* 6:32870. doi: 10.1038/srep32870

Rempfert, K. R., Miller, H. M., Bompard, N., Nothaft, D., Matter, J. M., Kelemen, P., et al. (2017). Geological and geochemical controls on subsurface microbial life in the Samail Ophiolite, Oman. *Front. Microbiol.* 8:56. doi: 10.3389/fmicb.2017.00056

Ruder, A. M., and Yiin, J. H. (2011). Mortality of US pentachlorophenol production workers through 2005. *Chemosphere* 83, 851–861. doi: 10.1016/j.chemosphere.2011.02.064

Sun, K., Gao, B., Ro, K. S., Novak, J. M., Wang, Z., Herbert, S., et al. (2012). Assessment of herbicide sorption by biochars and organic matter associated with soil and sediment. *Environ. Pollut.* 163, 167–173. doi: 10.1016/j.envpol.2011.12.015

Tong, H., Hu, M., Li, F. B., Liu, C. S., and Chen, M. J. (2014). Biochar enhances the microbial and chemical transformation of pentachlorophenol in paddy soil. *Soil Biol. Biochem.* 70, 142–150. doi: 10.1016/j.soilbio.2013.12.012

Xiao, F., and Pignatello, J. J. (2015). Interactions of triazine herbicides with biochar: steric and electronic effects. *Water Res.* 80, 179–188. doi: 10.1016/j.watres.2015.04.040

Xu, S., Adhikari, D., Huang, R., Zhang, H., Tang, Y., Roden, E., et al. (2016). Biochar-facilitated microbial reduction of hematite. *Environ. Sci. Technol.* 50, 2389–2395. doi: 10.1021/acs.est.5b05517

Xu, Y., He, Y., Feng, X., Liang, L., Xu, J., Brookes, P. C., et al. (2014). Enhanced abiotic and biotic contributions to dechlorination of pentachlorophenol during Fe(III) reduction by an iron-reducing bacterium *Clostridium beijerinckii* Z. *Sci. Total Environ.* 47, 215–223. doi: 10.1016/j.scitotenv.2013.12.022

Xu, Y., He, Y., Zhang, Q., Xu, J., and Crowley, D. (2015). Coupling between pentachlorophenol dechlorination and soil redox as revealed by stable carbon isotope, microbial community structure, and biogeochemical data. *Environ. Sci. Technol.* 49, 5425–5433. doi: 10.1021/es505040c

Xue, L., Feng, X., Xu, Y., Li, X., Zhu, M., Xu, J., et al. (2017). The dechlorination of pentachlorophenol under a sulfate and iron reduction co-occurring anaerobic environment. *Chemosphere* 182, 166–173. doi: 10.1016/j.chemosphere.2017.04.124

Yang, S., Shibata, A., Yoshida, N., and Katayama, A. (2009). Anaerobic mineralization of pentachlorophenol (PCP) by combining PCP-dechlorinating and phenol-degrading cultures. *Biotechnol. Bioeng.* 102, 81–90. doi: 10.1002/bit.22032

Yao, Q., Liu, J., Yu, Z., Li, Y., Jin, J., Liu, X., et al. (2017). Three years of biochar amendment alters soil physiochemical properties and fungal community composition in a black soil of northeast China. *Soil Biol. Biochem.* 110, 56–67. doi: 10.1016/j.soilbio.2017.03.005

Ye, D., Quensen, J. F., Tiedje, J. M., and Boyd, S. A. (1999). 2-Bromoethanesulfonate, sulfate, molybdate, and ethanesulfonate inhibit anaerobic dechlorination of polychlorobiphenyls by pasteurized microorganisms. *Appl. Environ. Microb.* 65, 327–329.

Yu, L., Wang, Y., Yuan, Y., Tang, J., and Zhou, S. (2016). Biochar as electron acceptor for microbial extracellular respiration. *Geomicrobiol. J.* 33, 530–536. doi: 10.1080/01490451.2015.1062060

Yu, L., Yuan, Y., Tang, J., Wang, Y., and Zhou, S. (2015). Biochar as an electron shuttle for reductive dechlorination of pentachlorophenol by *Geobacter sulfurreducens*. *Sci. Rep.* 5:16221. doi: 10.1038/srep16221

Yuan, Y., Bolan, N., Prévoteau, A., Vithanage, M., Biswas, J. K., Ok, Y. S., et al. (2017). Applications of biochar in redox-mediated reactions. *Bioresour. Technol.* 246, 271–281. doi: 10.1016/j.biortech.2017.06.154

Zhao, B., Nan, X., Xu, H., Zhang, T., and Ma, F. (2017). Sulfate sorption on rape (*Brassica campestris* L.) straw biochar, loess soil and a biochar-soil mixture. *J. Environ. Manage.* 201, 309–314. doi: 10.1016/j.jenvman.2017.06.064

Zheng, W., Wang, X., Yu, H., Tao, X., Zhou, Y., and Qu, W. (2011). Global trends and diversity in pentachlorophenol levels in the environment and in humans: a meta-analysis. *Environ. Sci. Technol.* 45, 4668–4675. doi: 10.1021/es1043563

Zheng, W., Yu, H., Wang, X., and Qu, W. (2012). Systematic review of pentachlorophenol occurrence in the environment and in humans in China: not a negligible health risk due to the re-emergence of schistosomiasis. *Environ. Int.* 42, 105–116. doi: 10.1016/j.envint.2011.04.014

Zhou, G., Yang, X., Li, H., Marshall, C. W., Zheng, B., Yan, Y., et al. (2016). Electron shuttles enhance anaerobic ammonium oxidation coupled to Iron(III) reduction. *Environ. Sci. Technol.* 50, 9298–9307. doi: 10.1021/acs.est.6b02077

Zhu, X., Chen, B., Zhu, L., and Xing, B. (2017). Effects and mechanisms of biochar-microbe interactions in soil improvement and pollution remediation: a review. *Environ. Pollut.* 227, 98–115. doi: 10.1016/j.envpol.2017.04.032

Conflict of Interest Statement: The authors declare that the research was conducted in the absence of any commercial or financial relationships that could be construed as a potential conflict of interest.

frontiers in Microbiology

ORIGINAL RESEARCH
published: 03 August 2017
doi: 10.3389/fmicb.2017.01439

Effects of 1,1,1-Trichloroethane and Triclocarban on Reductive Dechlorination of Trichloroethene in a TCE-Reducing Culture

*Li-Lian Wen[1,2], Jia-Xian Chen[1,2], Jia-Yi Fang[3], Ang Li[4] and He-Ping Zhao[1,2]**

[1] Department of Environmental Engineering, College of Environmental and Resource Sciences, Zhejiang University, Hangzhou, China, [2] Zhejiang Provincial Key Laboratory of Water Pollution Control and Environmental Safety, Zhejiang University, Hangzhou, China, [3] College of Agriculture and Biotechnology, Zhejiang University, Hangzhou, China, [4] School of Environment, Harbin Institute of Technology, Harbin, China

OPEN ACCESS

Edited by:
Shanquan Wang,
Sun Yat-sen University, China

Reviewed by:
Chen Zhou,
Arizona State University, United States
Wenhai Chu,
Tongji University, China
Songhu Yuan,
China University of Geosciences, China
Wen Zhang,
New Jersey Institute of Technology, United States

***Correspondence:**
He-Ping Zhao
zhaohp@zju.edu.cn;
hopechoil@hotmail.com

Specialty section:
This article was submitted to Microbiotechnology, Ecotoxicology and Bioremediation, a section of the journal Frontiers in Microbiology

Received: *21 June 2017*
Accepted: *17 July 2017*
Published: *03 August 2017*

Citation:
Wen L-L, Chen J-X, Fang J-Y, Li A and Zhao H-P (2017) Effects of 1,1,1-Trichloroethane and Triclocarban on Reductive Dechlorination of Trichloroethene in a TCE-Reducing Culture. Front. Microbiol. 8:1439. doi: 10.3389/fmicb.2017.01439

Chlorinated compounds were generally present in the environment due to widespread use in the industry. A short-term study was performed to evaluate the effects of 1,1,1- trichloroethane (TCA) and triclocarban (TCC) on trichloroethene (TCE) removal in a reactor fed with lactate as the sole electron donor. Both TCA and TCC inhibited TCE reduction, but the TCC had a more pronounced effect compared to TCA. The TCE-reducing culture, which had never been exposed to TCA before, reductively dechlorinated TCA to 1,1-dichloroethane (DCA). Below 15 μM, TCA had little effect on the transformation of TCE to *cis*-dichloroethene (DCE); however, the reduction of *cis*-DCE and vinyl chloride (VC) were more sensitive to TCA, and ethene production was completely inhibited when the concentration of TCA was above 15 μM. In cultures amended with TCC, the reduction of TCE was severely affected, even at concentrations as low as 0.3 μM; all the cultures stalled at VC, and no ethene was detected. The cultures that fully transformed TCE to ethene contained 5.2–8.1% *Dehalococcoides*. *Geobacter* and *Desulfovibrio*, the bacteria capable of partially reducing TCE to DCE, were detected in all cultures, but both represented a larger proportion of the community in TCC-amended cultures. All cultures were dominated by *Clostridium*_sensu_stricto_7, a genus that belongs to Firmicutes with proportions ranging from 40.9% (in a high TCC (15 μM) culture) to 88.2%. *Methanobacteria* was detected at levels of 1.1–12.7%, except in cultures added with 15 and 30 μM TCA, in which they only accounted for ∼0.4%. This study implies further environmental factors needed to be considered in the successful bioremediation of TCE in contaminated sites.

Keywords: trichloroethene, 1,1,1-trichloroethane, triclocarban, reductive dechlorination, electron distribution

INTRODUCTION

Three typical chlorinated compounds, trichloroethene (TCE), 1,1,1- trichloroethane (TCA) and triclocarban (TCC), are common environment contaminants as a result of widespread use in industrial processes and improper disposal (Grostern and Edwards, 2006; Brausch and Rand, 2011; USEPA, 2014). TCE is classified as a human carcinogen according to a Toxic Substances Control

Act (TSCA) Chemical Work Plan Chemical Risk Assessment for TCE (USEPA, 2014), and it has a maximum contaminant level (MCL) in drinking water of 5 μg/L (USEPA, 2017). TCA was banned from use and production for domestic use in United States since 2002 because it damages the ozone layer and may affect the liver, even cause death (ATDSR, 2006). The MCL of TCA in drinking water is less than 0.2 mg/L (USEPA, 2017). TCC has largely been added in detergents, soaps, cosmetics, and other personal care products at levels of 0.2–1.5% (w/w) since 1957 to inhibit microbes (Halden and Paull, 2005; Clarke and Smith, 2011; Carey et al., 2016; Souchier et al., 2016). TCC has detrimental impacts on wildlife and humans (Miller et al., 2008; Zhao J.L. et al., 2010), and the lowest effect concentration for aquatic biota is 0.101 μg/L (McClellan and Halden, 2010).

Microbially mediated anaerobic reductive dechlorination is a good strategy for the remediation of chlorinated compounds. For example, TCE can be converted to dichloroethene (DCE), vinyl chloride (VC), and finally non-toxic ethene in a stepwise manner (Lee et al., 2013; Wen et al., 2017) by various microorganisms. *Dehalococcoides* (which belong to Chloroflexi) are the only known bacteria that completely transform TCE all way down to ethene, although many other microorganisms have been found to partially reduce TCE to DCE or VC, including *Geobacter*, *Desulfovibrio*, *Desulfuromonas* (which belong to Proteobacteria), *Dehalobacter* and *Desulfitobacterium* (which belong to Firmicutes), and *Dehalobium*, and *Dehalogenimonas* (which belong to Chloroflexi) (Duhamel and Edwards, 2006; Maphosa et al., 2010).

Similarly, TCA can be transformed to 1,1-dichloroethane (DCA) and then to chloroethane (CA) via anaerobic reductive dechlorination by *Dehalobacter* or co-metabolism by *Desulfobacterium*, *Desulfovibrio*, *Clostridium,* and *Methanobacterium* (Egli et al., 1987; Gälli and McCarty, 1989). However, the degradation of TCC is quite different. Pycke et al. (2014) detected dichlorocarbanilide (DCC) and monochlorobanilide (MCC) in raw and treated sewage sludge and showed that anaerobic digestion only dechlorinated 0.4–2.1% of TCC. Souchier et al. (2016) performed field and laboratory experiments indicating that TCC reductive dechlorination occurred in anaerobic conditions to form 4,4-DCC and in aerobic circumstances to produce 3,4-DCC. Only a handful of microbial species are reportedly able to reductively reduce TCC, e.g., *Sphingomonas*, and *Ochrobactrum* (Mulla et al., 2016; Yun et al., 2017).

Trichloroethene and TCA frequently co-exist in contaminated sites due to their similar industrial uses. Data from the NPL database shows that approximately 20% of USEPA NPL sites are contaminated with both TCE and TCA. A northeastern American industrial area was polluted with 38 μM TCA and 8 μM TCE (Grostern and Edwards, 2006). Kaown et al. (2016) found that both chlorinated ethenes and ethanes were present in the industrial area of Asan, Korea, and the levels of monitored TCE and TCA ranged from 0.004 to 5.8 mg/L and from non-detected to 1.8 mg/L, respectively. Though initially was not suggested as an unidentified contamination (Halden and Paull, 2005), TCC was monitored at a value of 6750 ng/L with a frequency of 68% in United States water resources. Similarly, Zhao J.L. et al. (2010) measured 4.5–338 ng/L of TCC in the water of the Pearl River system in China and 58–2633 ng/L in its sediments. These sites were also possibly contaminated with TCE and TCA (Zhao J.L. et al., 2010; Kaown et al., 2016).

The presence of co-contaminants can greatly influence the efficiency and extent of chlorinated ethene dechlorination during *in situ* bioremediation of contaminated sites. Adamson and Parkin (2000) showed that TCA (below 20 μM) had an effect on tetrachloroethene (PCE) removal, while 10–15 μM of carbon tetrachloride (CT) inhibited the transformation of PCE and VC. Duhamel et al. (2002) found that the reduction of TCE always stalled at the step of VC conversion when the concentration of TCA was between 5.2 and 22 μM, and also stopped in the presence of 2.5 μM of chloroform (CF). Grostern and Edwards (2006) found that the presence of TCA inhibited the dechlorination of TCE and vice versa in way that was concentration independent and purely determined by the culture. Grostern et al. (2009) later suggested that chlorinated ethenes inhibited TCA dechlorination by directly affecting the reductive dehalogenase (RDase) enzymes. McDonnell and Russell (1999) reported that TCC poisoned gram-positive bacteria but had a less effect on gram-negative bacteria and fungi. Walsh et al. (2003) found that TCC was active against *Staphylococcus aureus*. Davis and Hidu (1969) reported that 0.1 μM (∼30 μg/L) of TCC caused abnormal growth of clams and reduced the survival of larvae. However, as they usually co-exist with TCE, the effects of TCA and TCC on TCE reduction remain unclear.

Dechlorinating microorganisms are always in a mixed culture, which contains many other syntrophic microbes, e.g., fermenters, methanogens and acetogens, that contribute to the rigorous nutrient requirements of the dechlorinators (He et al., 2003; Kittelmann and Friedrich, 2008; Men et al., 2013; Wen et al., 2017). Fermenters transform organic substrates, such as lactate, formate, and methanol, to acetate and hydrogen, which are used as a carbon source and electron donor, respectively, by dechlorinating microbes (Wei and Finneran, 2013; Wen et al., 2015). Homoacetogens are vital microbes that synthesize corrinoids, a significant cofactor for the growth of *Dehalococcoides* (Johnson et al., 2009; Ziv-El et al., 2012). Methanogens may also produce corrinoids for *Dehalococcoides* (Löffler et al., 1997; Wen et al., 2015). To date, TCA has been shown to inhibit methanogenesis and acetogenesis (Vargas and Ahlert, 1987; Adamson and Parkin, 2000), and TCC has been shown to inhibit methanogens and to alter microbial community structure in an anaerobic digester (Carey et al., 2016). Therefore, TCA and TCC might have negative effects on TCE reduction by affecting the microbial community structure, as they are largely consumed and always found in the environment.

The objective of this study is to explore the mechanisms behind the effects of TCC and TCA on TCE reduction. To achieve this goal, we will investigate the changes of reductive dechlorination, methane production and the electron donor distribution, along with the microbial community shifts under different conditions.

MATERIALS AND METHODS

Description of the TCE-Dechlorinating Culture

The TCE-dechlorinating culture YH had been maintained in the laboratory for 3 years with lactate as the sole electron donor (Kranzioch et al., 2013; Wen et al., 2016). This *Dehalococcoides*-dominated culture efficiently transformed TCE (0.3 mM) to non-toxic ethene in 10 days. The culture was incubated under anaerobic conditions in dark at 30°C.

The Effects of TCA and TCC on the TCE-Dechlorinating Culture

We prepared the anaerobic medium for TCE reduction according to Wen et al. (2015). The mineral salts medium contained the following reagents (per liter): 3.17 g KH_2PO_4, 14.33 g $Na_2HPO_4 \bullet 12H_2O$, 0.45 g $(NH_4)_2HPO_4$, 0.04 g $MgHPO_4 \bullet 3H_2O$, 1 mL of trace element solution A, and 1 mL of trace element solution B described by Kranzioch et al. (2013). We added 0.2 mM L-cysteine, 0.2 mM $Na_2S \bullet 9H_2O$ and 0.5 mM DL-dithiothreitol (DTT) as reducing agents, 10 mM $NaHCO_3$ and 10 mM *tris*-ethanesulfonic acid (TES) as buffering agents (He et al., 2007), and 0.025% (vol/vol) resazurin as a redox indicator (Amos et al., 2008). We transferred 75 mL of medium into 120-mL glass serum bottles under a stream of argon (Ar) and then sealed the bottles with butyl rubber stoppers and aluminum crimps. We injected 0.8 mL ATCC vitamin supplement (ATCC MD-VS, United States), 80 μL vitamin B_{12} (0.5 g/L in a stock solution, and final concentration was 0.5 mg/L), 200 μL lactate (1 M in a stock solution, and final concentration was 2.5 mM) and 2.4 μl TCE (99.9% in purity, and final concentration was 0.3 mM) into the bottles with micro-syringes in an anaerobic chamber (AW200SG).

We examined the effects of TCA and TCC on TCE dechlorination separately and in combination as follows. To explore the effect of TCA on the TCE-dechlorinating culture, we added TCA to final concentrations of 0.3, 3, 15, and 30 μM in four separate bottles. Each bottle was incubated with 5 mL bacterial solution from the YH culture. To test the effect of TCC, we similarly transferred 5 mL TCE-dechlorinating culture into bottles amended with 0.3, 3, or 15 μM of TCC. To evaluate the effects of both TCA and TCC together on TCE reduction, we added both to a final concentration of 0.3 μM in the same bottle and then incubated with 5 mL TCE-dechlorinating culture. We also maintained 5 mL YH culture in a bottle with only 0.3 mM of TCE as a positive control; a bottle containing 0.3 mM TCE, 0.3 μM 1,1,1-TCA and 0.3 μM TCC in 5 mL sterile medium instead of YH culture was used as a negative control.

Each bottle was sampled periodically for TCE analysis (every 12 h during TCE reduction; every 2 days after TCE was completely reduced). All experiments were performed with duplicate bottles. The results are presented as the average values from the duplicates.

Chemical Analysis

Chlorinated ethenes (TCE, *cis*-DCE, VC), ethene, chlorinated ethanes (TCA, DCA, CA) and methane were measured by injecting 100 μL of headspace samples with a gas-tight syringe into a gas chromatograph (Agilent Technologies GC system, model 6890N, Agilent Technologies, Inc., United States) equipped with a flame-ionization detector (FID), and a packed column (30 m long, 0.32 mm i.d., 0.5 μm thickness, cross-linked polydimethysiloxane film, J&W Scientific, United States) (Zhao H.P. et al., 2010; Ziv-El et al., 2011; Wen et al., 2017). N_2 was the carrier gas fed at a constant flow rate of 0.065 m^3/d, and the temperature conditions for injector and detector were 200 and 250°C, respectively. The program was as follows: holding at 60°C for 1 min, heating gradually to 200°C (20°C/min), and holding at 200°C for 2 min. Analytical grade chloroethenes, ethene, chloroethanes, and methane were added into 80 mL of water in 120 mL bottles to make standards for calibration curves, which were linear ($R^2 \geq 0.996$). We computed the concentrations of ethene and methane in the liquid according to their Henry's constants (K_H):

$$[\text{compound}]_{liq} = [\text{compound}]_{gas}/K_H$$

The calculated dimensionless Henry's constants (mM_{gas}/mM_{liq}, T = 25°C) used in this study were 8.35 for ethene and 28.99 for methane.

The volatile fatty acids (VFAs) lactate, acetate, and propionate were analyzed using liquid chromatography (LC, Waters) equipped with a 1525 Binary Pump, a 717 plus Autosampler, a 2487 Dual λ Absorbance Detector and an organic acid column (Acclaim^{TM} OA 5 μm, 4 mm × 250 mm). The monitored parameters were as follows: the mobile phase was 100 mM Na_2SO_4, the pH was adjusted to 2.65 with methylsulphonic acid (MSA), the flow rate was 0.6 mL/min, the column temperature was set at 30°C, the absorbance wavelength was 210 nm, and the injection volume was 10 μL. Liquid samples (1 mL) were filtered through a 0.22-μm polyvinylidene fluoride membrane syringe filter (Shanghai Xingya Purifying Materials Company, China) into 1 mL glass vials for subsequent analysis. Calibration curves were generated for all VFAs during every HPLC run. The detection limits for VFAs on the HPLC were 0.1 mg/L.

Electron Distribution Analysis

The electron distribution for each reaction was calculated as described previously (Delgado et al., 2012; Wen et al., 2015). The numbers of e^- equivalents (eq) required for dechlorination of TCE per mole are 2, 4, and 6 to DCE, VC, and ethene, respectively, and each mole of lactate can provide 12 e^- eq. The electron distributions were calculated as follows:

$$\%\text{Compound} = \frac{(\text{compound}) \times \frac{\text{electrons}}{\text{mole}}}{(H_2) \times \frac{2\text{electrons}}{\text{mole H}}} \times 100$$

The related reactions and equations are listed in Supplementary Table S1.

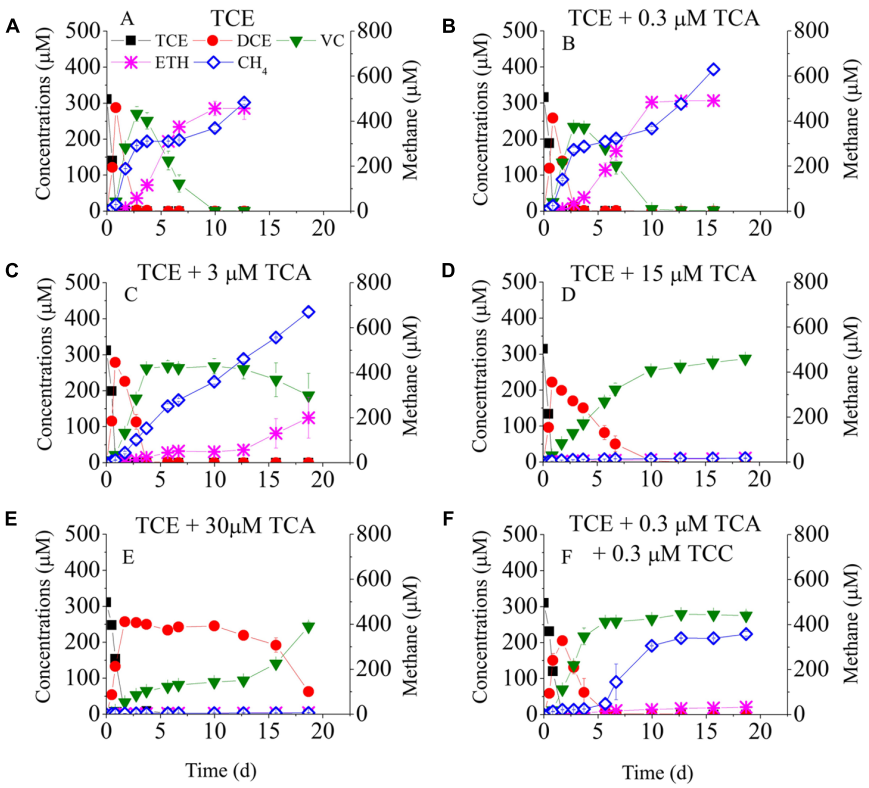

FIGURE 1 | Batch tests on the dechlorination of chlorinated ethenes in the cultures exposed to different concentrations of TCA. Left *Y*-axis is the concentrations of chlorinated ethenes and ethene. Batch test **(A)** TCE only; **(B)** TCE + 0.3 μM TCA; **(C)** TCE + 3 μM TCA; **(D)** TCE + 15 μM TCA; **(E)** TCE + 30 μM TCA; **(F)** TCE + 0.3 μM TCA + 0.3 μM TCC.

Molecular Biology Analysis

At the end of operation, we took 30 mL of liquid samples into 50-mL centrifuge tubes and then centrifuged for 1 h at 8000 rpm (5900 *g*) at 4°C (Eppendorf 5415R, Germany). We collected the pellets for DNA extraction as described by Zhong et al. (2017).

We used SYBR Premix Ex Taq Kits (Takara Bio, Inc., Japan) and performed qPCR amplification to target *Dhc* (for *Dehalococcoides*), *mcrA* (for methanogens), *FTHFS* (for acetogens) and the functional reductive dehalogenase genes *tceA* and *vcrA* (Wen et al., 2015). The slopes of the plasmid standard curves and efficiency values for quantification by qPCR are listed in Supplementary Table S2. We calculated gene copy numbers for biomass samples using the standard curves.

The DNA samples were sent to Novogene (Beijing, China) to perform Illumina MiSeq sequencing with standard protocols including amplicon generation, which used primers 341F (5′-CCTAYGGGRBGCASCAG-3′) and 806R (5′-GGACTACN NGGGTATCTAAT-3′) to target the conserved V3 to V4 regions of the bacterial 16S rRNA gene (Caporaso et al., 2010a), PCR products quantification, and library sequencing, which was generated using Illumina TruSeq DNA PCR-Free Library Preparation Kit (Illumina, United States) following manufacturer's recommendations. The library quality was assessed on the Qubit@ 2.0 Flurometer (Thermo Scientific) and Agilent Bioanalyzer 2100 system and finally the library was sequenced on an Illumina HiSe platform and generated 250 bp paired-end reads. The data were processed using the QIIME (version 1.7.0) pipeline (Caporaso et al., 2010b).

RESULTS

The Reductive Dechlorination of TCE in the Presence of TCC and TCA

Figure 1 shows TCE reduction at different concentrations of TCA. Approximately, 0.3 μM TCE was completely reduced to ethene in 10 days at a rate of 30 μmol Cl^-/(L-d) in the positive control batch and in the presence of 0.3 μM TCA. When the TCA concentration increased to 3 μM, same amount of TCE was mostly reduced to VC, but only 124.9 μM of ethene was detected at day 20. At concentrations of 15 and 30 μM, TCA significantly inhibited TCE reduction: *cis*-DCE was reduced to VC at day 10 and day 20, respectively, representing a delay of 6 and 16 days compared to 3 μM TCA.

Figure 2 shows TCE reduction at different concentrations of TCC. No TCE reduction was detected in the negative control. Unlike with TCA, all tested concentrations of TCC strongly inhibited TCE reduction. TCE was reduced to *cis*-DCE instantly, but the reductive rate of *cis*-DCE to VC decreased sharply, ranging from 127.9 to 20.2 μmol Cl^-/(L·d) with

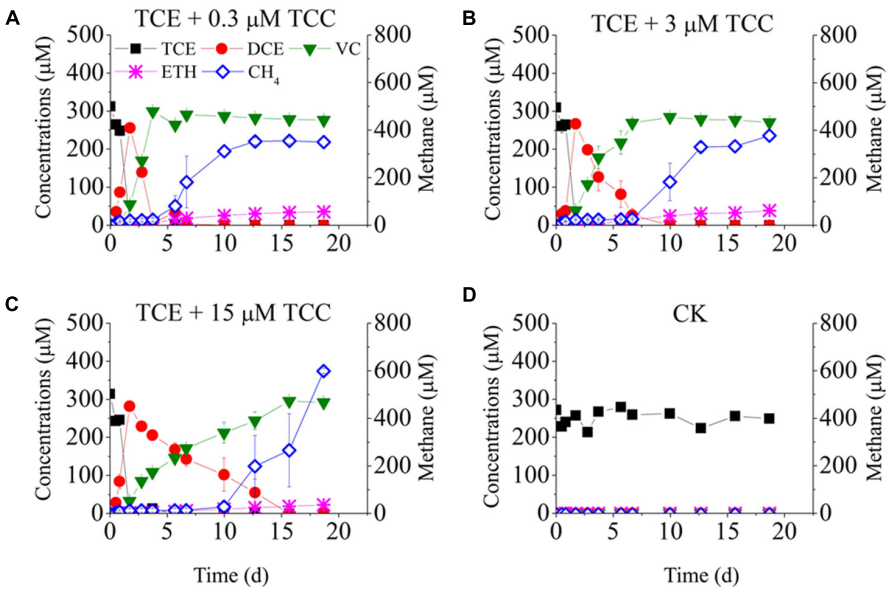

FIGURE 2 | Batch tests on the dechlorination of chlorinated ethenes in the cultures amended with different concentrations of TCC. Left *Y*-axis is the concentrations of chlorinated ethenes and ethene. Batch test **(A)** TCE + 0.3 μM TCC; **(B)** TCE + 3 μM TCC; **(C)** TCE + 15 μM TCC; **(D)** Negative Control.

increasing concentrations of TCC from 0.3 to 15 μM (*cis*-DCE was transformed to VC at days 4, 7, and 15 in the presence of 0.3, 3, and 15 μM TCC).

To evaluate the combined effects of TCA and TCC on TCE reduction, 0.3 μM TCA and 0.3 μM TCC were added to the cultures (**Figure 1F**). The pattern of TCE reduction was similar to that of the cultures amended with 0.3 μM TCC despite a lower dechlorinating rate, which indicated that the co-contaminants intensified the inhibition of TCE reduction.

Figures 1, **2** also plots the models of methane production. When only TCE was added to the cultures, methane was produced rapidly at the beginning, then maintained steady from day 3 to day 7, and then increased continually to 483 μM at the end of the experiment. Low concentrations of TCA (≤3 μM) did not affect the activity of methanogens, whereas high concentrations of TCA (≥15 μM) significantly inhibited methane generation. Methanogens underwent an acclimation phase in the cultures amended with different concentrations of TCC, with 4, 7, 10 days lag when exposed to 0.3, 3, and 15 μM TCC, respectively, compared with the positive control.

Before conducting this study, the TCE-reducing culture had never been exposed to TCA. Supplementary Figure S1 shows the dechlorination of the added TCA. Approximately 0.3 μM TCA was completely removed by day 4, and no DCA and CA were detected. When the TCA concentration was increased from 3 to 30 μM, the dechlorination of TCA lagged, allowing the accumulation of intermediates DCA.

Electron Donor Distribution in the Presence of TCC and TCA

In this study, 3 mM lactate was utilized as the electron donor for all tests, which theoretically corresponds to 36 mmol e^- equivalents/L. In the presence of TCA, lactate was fermented to acetate and propionate instantly despite the concentration of TCA (Supplementary Figure S2). However, it took 3 days for the lactate to be fermented to acetate and propionate when TCC was present at 15 μM (Supplementary Figure S3). Considering the fermentation of lactate, we calculated the electron distribution for all dechlorination activities and methanogenesis (**Figure 3**) by taking samples at day 13, when TCE was completely reduced to ethene in the positive control batch. Most of the electron donor was consumed in the process of acetogenesis, which synthesized H_2/HCO_3^- into acetate. In the presence of 0, 0.3, 3, and 15 μM TCA, 1.87, 1.84, 1.23, 1.11, and 0.83 mmol e^- equivalents, respectively were distributed to reductive dechlorination of TCE; the decrease was significant for exposures ≥ 3 μM TCA. Obviously, methanogenesis did not consume any electrons because no methane was generated at concentrations of TCA ≥ 15 μM. In the presence of 0.3, 3, and 15 μM TCC, 1.31, 1.30, and 1.18 mmol e^- equivalents, respectively, were distributed to the reductive dechlorination of TCE. In the batch containing only TCE and no added TCA or TCC, 1.87 mmol e^- equivalents were directed to TCE reduction. Clearly, the addition of TCC sharply decreased the electrons distributed to TCE reduction.

Functional Gene Abundance

We measured several functional genes (**Figure 4**), and dehalogenase genes (Supplementary Figure S4), in cultures amended with different electron acceptors using qPCR. In the presence of TCA, all the tested gene copies decreased with increasing concentrations of TCA. Consistent with the TCE reduction pattern, *Dhc* gene copies dropped an order of magnitude when the concentration of TCA increased to 3 μM; all

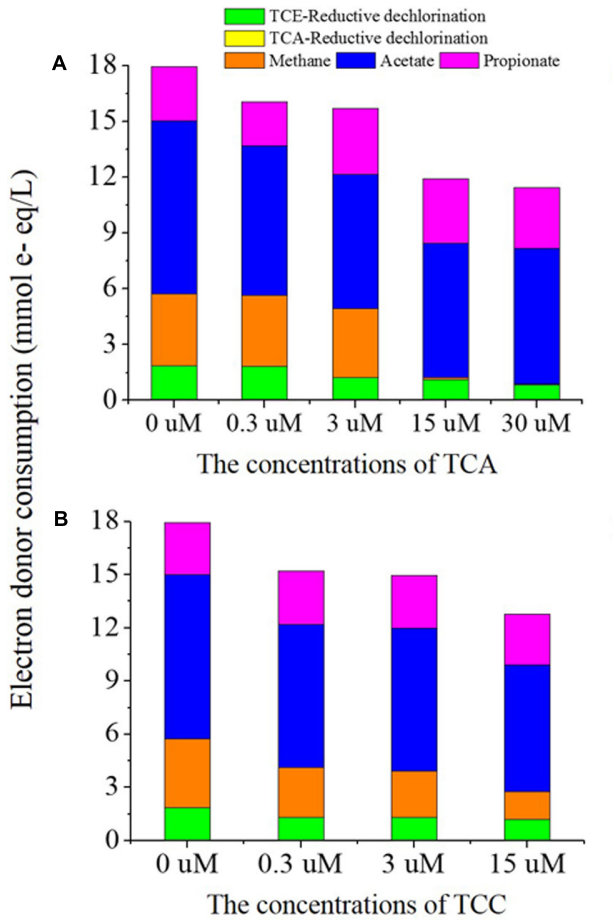

FIGURE 3 | The electron donor consumption of major chemical reactions including reductive dechlorination, methanogenesis, acetogenesis and fermentation in TCA added cultures **(A)** and TCC added cultures **(B)**.

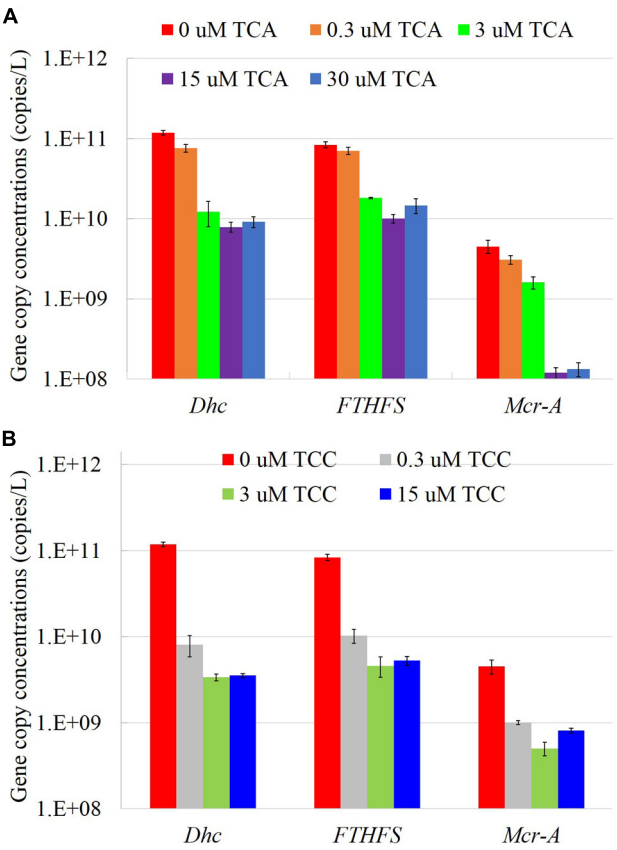

FIGURE 4 | The gene copy numbers in the TCA added cultures **(A)** and TCC added cultures **(B)**.

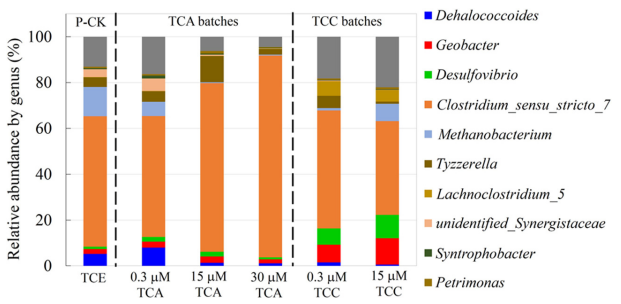

FIGURE 5 | The relative abundance of microbial structure composition at the genus level in different cultures. P-CK: positive control.

tested genes abundances showed a similar pattern, except *mcrA*. When the concentration of TCA increased to 15 μM, *mcrA* gene copies decreased sharply to 1.2×10^8, or 1.6 orders of magnitude lower than the positive control. In the presence of TCC, even at concentrations as low as 0.3 μM, copies of the *Dhc* and *FTHFS* genes decreased more than an order of magnitude compared to the batch containing TCE only. As shown in **Figures 1**, **2**, methanogenesis was not fully inhibited in the presence of TCC, the *mcrA* gene remained at a stable abundance regardless of the concentration of TCC.

Changes to Bacterial Community Structure

We examined constituents of the microbial community at the genus (**Figure 5**) and phylum (Supplementary Figure S5) levels by Illumina MiSeq sequencing at Novogene (Beijing, China). For practical reasons, we did not send DNA samples of cultures exposed to 3 μM TCA and 3 μM TCC. In the presence of 0.3 μM TCA, *Dehalococcoides* (8.1%) was slightly higher than the positive control (5.2%). This observation was not consistent with the qPCR results, which indicated a drop in the overall abundance of *Dhc* (see Discussion). At a TCA concentration of 15 μM, the *Dehalococcodies* abundance dramatically decreased to 1%. Similarly, *Methanobacteria* decreased from 12.8% to a negligible level as the concentration of TCA increased to 30 μM. *Geobacter* and *Desulfovibrio* were present in all the cultures at stable abundances ranging from 1.0 to 2.7% regardless of the concentrations of TCA added. *Clostridium* was enriched with the addition of increasing concentrations of TCA, reaching its

highest abundance of 88% in the presence of 30 μM TCA. In the presence of TCC, the proportion of *Dehalococcodies* in the community was remarkably low, dropping from 5.2% to 1.5 and 0.6% when TCC was present at 0, 0.3, and 15 μM, respectively. The abundances of *Geobacter* and *Desulfovibrio* were higher than the positive control: *Geobacter* accounted for 2.1, 7.7, and 11.5%; and *Desulfovibrio* accounted for 1.0, 7.1, and 10.2% when exposed to 0, 0.3, and 15 μM TCC, respectively. The proportion of *Methanobacteria* dramatically decreased from 12.8 to 1.1% when the culture was exposed to 0.3 μM TCC, but it increased to 7.6% in the culture exposed to 15 μM TCC, which was also reflected in the generation of methane. *Clostridium* also decreased with increasing TCC concentrations, dropping down to 48.7% in the 15 μM TCC cultures.

DISCUSSION

We investigated the effects of different concentrations of TCA and TCC on TCE reduction by examining the electron distribution, functional gene abundance, and bacterial community structure. This information is critical for the bioremediation of chlorinated compounds, which are generally present as co-contaminants in contaminated sites. TCA inhibited TCE reduction, previous studies demonstrated that the presence of <20 μM TCA slightly affected the removal of PCE (Adamson and Parkin, 2000). Duhamel et al. (2002) reported that VC transformation was always inhibited when the concentration of TCA ranged from 5.2 and 22 μM. We found that the complete reduction of TCE was inhibited at even lower concentrations of TCA (3 μM), and that the dechlorination of TCE stopped at the VC in the presence of ≥15 μM TCA. Grostern and Edwards (2006) suggested that the inhibition of TCA to TCE reduction was concentration independent; however, we found that 0.3 μM TCA had little effect on TCE removal. The inconsistent results may be due to the lower concentration tested in this study compared with 0.03 and 0.3 mM of TCA used in the experiment of Grostern and Edwards (2006).

Triclocarban was shown to have a more pronounced effect on TCE reduction compared with TCA that is possibly attributed to its structure with binuclear benzenes and NH_2 or NH group, which has a detrimental effect on biodegradation (Boethling et al., 1994). To our best knowledge, this is the first report on the influence of TCC on the reductive dechlorination of TCE. TCC is reported to actively inhibit gram-positive bacteria but not gram-negative bacteria and fungi (McDonnell and Russell, 1999). Davis and Hidu (1969) reported that 0.1 μM (∼30 μg/L) TCC caused abnormal growth of clams and reduced the survival of larvae. In the TCC-amended cultures, the inhibition of TCE reduction could possibly be attributed to the toxicity of TCC to *Dehalococcoides*. Triclosan, which has a similar structure to TCC, can poison a specific enzyme that is critical to many bacteria and fungi (McMurry et al., 1998; Levy et al., 1999; Ren et al., 2010), so TCC may work analogously.

As expected in the TCE-reducing cultures, we observed the reductive dechlorination of TCA to DCA, but no CA was detected, possibly due to the short incubation period. Adamson and Parkin (2000) demonstrated that a PCE dechlorinating culture was capable of reducing TCA to DCA even without exposure before enrichment. Grostern and Edwards (2006) enriched an anaerobic culture that dechlorinated TCA to CA from a TCA-contaminated site in the northeastern United States after 70 days incubation but found that no degradation occurred in the TCE-degrading culture KB-1.

The patterns of methane and acetate production were consistent with previous reports. Methanogenesis was inhibited in the presence of ≥15 μM TCA, which might be due to the effect of intermediates of TCA reduction. TCA (<20 μM) and its daughter product DCA have been reported to inhibit methanogenesis and acetogenesis (Vargas and Ahlert, 1987; Adamson and Parkin, 2000). Grostern et al. (2009) reported no occurrence of methanogenesis in the presence of TCA, but methanogenesis started during DCA reduction. Compared to TCA, TCC had little effect on methanogenesis, which is in contrast to the results of Carey et al. (2016), who claimed that TCC inhibited methanogens and altered the anaerobic digester microbial community structure (Carey et al., 2016).

The efficient diversion of donated electrons to the process of reductive dechlorination is key to the successful removal of TCE. Hence, we further investigated the electron distribution in the presence of different concentrations of TCA and TCC. Consistent with the TCE reduction pattern, the electrons distributed to TCE reduction decreased in the presence of ≥3 μM TCA and ≥0.3 μM TCC. Usually, the methanogens are major competitors with dechlorinators (Yang and McCarty, 2002) when electron donors are supplied in excess. However, that was not the case in this study: methanogenesis did not consume more electrons when the TCA and TCC concentration increased, so TCE reduction was more likely inhibited due to reasons other than electron competition. TCA has a similar structure with TCE, which would bound to the complex formed between VC and the RDase enzyme that catalyzes growth linked dichlorination of VC (Grostern et al., 2009). Chan et al. (2011) indicated that 30–270 μg/L of 1,1,1-TCA inhibited RDases involved in TCE, *cis*-DCE, and VC dechlorination.

In general, the culture with a highest dechlorinating rate contained the maximum level of *Dhc* and reductive dehalogenases genes. In this study, the *Dhc* gene abundance significantly dropped at concentrations of TCA ≥ 3 μM and TCC ≥ 0.3 μM. Grostern et al. (2009) suggested TCA would inhibit VC reduction by binding to the complex formed between VC and the dehalogenase enzyme. The relative abundance of *Dehalococcoides* was 5.2–8.1% in the completely ethene-producing cultures, which is relatively low compared with other reports (Ziv-El et al., 2011; Löffler et al., 2013), possibly due to the lack of sufficient time to reach a higher abundance. This illustrated a higher absolute abundance of *Dehalococcoides* was important for the TCE reductive dechlorination (Lee et al., 2013).

Based on the sequencing results, the relative abundance of *Geobacter* and *Desulfovibrio* increased in cultures with

higher concentrations of TCC, which indicated they were more tolerant to TCC. *Geobacter* and *Desulfovibrio*, belonging to ε-Proteobacteria, are capable of reducing chlorinated organic pollutants by dehalorespiration (Smidt and de Vos, 2004). Biological reductive dechlorination of chlorinated ethenes always occurs under methanogenic conditions (Freedman and Gossett, 1989; Wen et al., 2015). Ryzhkova (2003) suggested that methanogens produce precursor corrinoids to vitamin B_{12}. The abundance of *Methanobacterium* decreased when exposed to TCA and TCC, but it was less sensitive to TCC than TCA, as methanogenesis resumed after a lag phase in TCC-amended cultures. Acetogens such as Spirachaetes and *Clostridium* provide corrinoids for *Dehalococcoides* (Stupperich et al., 1988) and were present in the cultures. Zhao et al. (2008) reported that *Clostridium ganghwense* may ferment lactate to propionate. *Clostridium*_sensu_stricto_7 was highly enriched in TCA-amended cultures. Gälli and McCarty (1989) indicated that *Clostridium* sp. reduced 100 μg/L of TCA to DCA. The TCC-containing digesters had a lower fraction of *Clostridium* (Carey et al., 2016), which was consistent with the culture at a high concentration of TCC (15 μM). Many more research is needed to further understand the mechanism of the action of TCC in TCE-contaminated sites.

AUTHOR CONTRIBUTIONS

H-PZ designed the experiment, drafted and revised the manuscript; L-LW performed the experiment, analyzed the data, and drafted the manuscript; J-XC, J-YF, and AL helped collect the data and revise manuscript.

ACKNOWLEDGMENTS

Authors greatly thank the National Natural Science Foundation of China (Grant No. 21107091, 21377109, 21577123), the Natural Science Funds for Distinguished Young Scholar of Zhejiang Province (LR17B070001), and Fundamental Research Funds for the Central Universities (2017XZZX010-03) for their financial support.

SUPPLEMENTARY MATERIAL

The Supplementary Material for this article can be found online at: http://journal.frontiersin.org/article/10.3389/fmicb.2017.01439/full#supplementary-material

REFERENCES

Adamson, D. T., and Parkin, G. F. (2000). Impact of mixtures of chlorinated aliphatic hydrocarbons on a high-rate, tetrachloroethene-dechlorinating enrichment culture. *Environ. Sci. Technol.* 34, 1959–1965. doi: 10.1021/es990809f

Amos, B., Ritalahti, K. M., Cruz-Garcia, C., Padilia-Crespo, E., and Löffler, F. E. (2008). Oxygen effect on *Dehalococcoides* viability and biomarker quantification. *Environ. Sci. Technol.* 42, 5718–5726. doi: 10.1021/es703227g

ATDSR (2006). *Toxicological Profile for 1,1,1-Trichloroethane*. Available at: http://www.atsdr.cdc.gov/tfacts70.pdf.

Boethling, R. S., Howard, P. H., Meylan, W., Stiteler, W., Beauman, J., and Tirado, N. (1994). Group contribution method for predicting probability and rate of aerobic biodegradation. *Environ. Sci. Technol.* 28, 459–465. doi: 10.1021/es00052a018

Brausch, J. M., and Rand, G. M. (2011). A review of personal care products in the aquatic environment: environmental concentrations and toxicity. *Chemosphere* 82, 1518–1532. doi: 10.1016/j.chemosphere.2010.11.018

Caporaso, J. G., Bittinger, K., Bushman, F. D., DeSantis, T. Z., Andersen, G. L., and Knight, R. (2010a). PyNAST: a flexible tool for aligning sequences to a template alignment. *Bioinformatics* 26, 266–267. doi: 10.1093/bioinformatics/btp636

Caporaso, J. G., Kuczynski, J., Stombaugh, J., Bittinger, K., Bushman, F. D., Costello, E. K., et al. (2010b). QIIME allows analysis of high-throughput community sequencing data. *Nat. Methods* 7, 335–336. doi: 10.1038/nmeth.f.303

Carey, D. E., Zitomer, D. H., Hristova, K. R., Kappell, A. D., and McNamara, P. J. (2016). Triclocarban influences antibiotic resistance and alters anaerobic digester microbial community structure. *Environ. Sci. Technol.* 50, 126–134. doi: 10.1021/acs.est.5b03080

Chan, W. W. M., Grostern, A., Löffler, F. E., and Edwards, E. A. (2011). Quantifying the effects of 1,1,1-trichloroethane and 1,1-dichloroethane on chlorinated ethene reductive dehalogenases. *Environ. Sci. Technol.* 45, 9693–9702. doi: 10.1021/es201260n

Clarke, B. O., and Smith, S. R. (2011). Review of 'emerging' organic contaminants in biosolids and assessment of international research priorities for the agricultural use of biosolids. *Environ. Int.* 37, 226–247. doi: 10.1016/j.envint.2010.06.004

Davis, H. C., and Hidu, H. (1969). Effects of pesticides on embryonic development of clams and oysters and on survival and growth of the larvae. *Fish. Bull.* 67, 393–404.

Delgado, A. G., Parameswaran, P., Fajardo-Williams, D., Halden, R. U., and Krajmalnik-Brown, R. (2012). Role of bicarbonate as a pH buffer and electron sink in microbial dechlorination of chloroethenes. *Microb. Cell. Fact.* 11:128. doi: 10.1186/1475-2859-11-128

Duhamel, M., and Edwards, E. A. (2006). Microbial composition of chlorinated ethene-degrading cultures dominated by Dehalococcoides. *FEMS Microbiol. Ecol.* 58, 538–549. doi: 10.1111/j.1574-6941.2006.00191.x

Duhamel, M., Wehr, S. D., Yu, L., Rizvi, H., Seepersad, D., Dworatzek, S., et al. (2002). Comparison of anaerobic dechlorinating enrichment cultures maintained on tetrachloroethene, trichloroethene, *cis*-dichloroethene and vinyl chloride. *Water Res.* 36, 4193–4202. doi: 10.1016/S0043-1354(02)00151-3

Egli, C., Scholtz, R., Cook, A. M., and Leisinger, T. (1987). Anaerobic dechlorination of tetrachloromethane and 1,2-dichloroethane to degradable products by pure cultures of *Desulfobacterium* sp. and *Methanobacterium* sp. *FEMS. Microbiol. Lett.* 43, 257–261. doi: 10.1111/j.1574-6968.1987.tb02154.x

Freedman, D. L., and Gossett, J. M. (1989). Biological reductive dechlorination of tetrachloroethylene and trichloroethylene to ethylene under methanogenic conditions. *Appl. Environ. Microbiol.* 55, 2144–2151.

Gälli, R., and McCarty, P. L. (1989). Biotransformation of 1,1,1-trichloroethane, tichloromethane, and tetrachloromethane by a *Clostridium* sp. *Appl. Environ. Microbiol.* 55, 837–844.

Grostern, A., Chan, W. W. M., and Edwards, E. A. (2009). 1,1,1-Trichloroethane and 1,1-dichloroethane reductive dechlorination kinetics and co-contaminant effects in a dehalobacter-containing mixed culture. *Environ. Sci. Technol.* 43, 6799–6807. doi: 10.1021/es901038x

Grostern, A., and Edwards, E. A. (2006). A 1,1,1-trichloroethane-degrading anaerobic mixed microbial culture enhances biotransformation of mixtures of chlorinated ethenes and ethanes. *Appl. Environ. Microbiol.* 72, 7849–7856. doi: 10.1128/AEM.01269-06

Halden, R., and Paull, D. (2005). Co-occurrence of triclocarban and triclosan in U.S. water resources. *Environ. Sci. Technol.* 39, 1420–1426. doi: 10.1021/es049071e

He, J., Holmes, V. F., Lee, P. K. H., and Alvarez-Cohen, L. (2007). Influence of vitamin B12 and cocultures on the growth of *Dehalococcoides* isolates in defined medium. *Appl. Environ. Microbiol.* 73, 2847–2853. doi: 10.1128/AEM.02574-06

He, J. Z., Ritalahti, K. M., Aiello, M. R., and Löffler, F. E. (2003). Complete detoxification of vinyl chloride by an anaerobic enrichment culture and identification of the reductively dechlorinating population as a *Dehalococcoides* species. *Appl. Environ. Microbiol.* 69, 996–1003. doi: 10.1128/AEM.69.2.996-1003.2003

Johnson, D. R., Nemir, A., Andersen, G. L., Zinder, S. H., and Alvarez-Cohen, L. (2009). Transcriptomic microarray analysis of corrinoid responsive genes in *Dehalococcoides ethenogenes* strain 195. *FEMS Microbiol. Lett.* 294, 198–206. doi: 10.1111/j.1574-6968.2009.01569.x

Kaown, D., Jun, S. C., Kim, R. H., Woosik, S., and Lee, K. K. (2016). Characterization of a site contaminated by chlorinated ethenes and ethanes using multi-analysis. *Environ. Earth Sci.* 75, 745. doi: 10.1007/s12665-016-5536-2

Kittelmann, S., and Friedrich, M. W. (2008). Identification of novel perchloroethene-respiring microorganisms in anoxic river sediment by RNA-based stable isotope probing. *Environ. Microbiol.* 10, 31–46. doi: 10.1111/j.1462-2920.2007.01427.x

Kranzioch, I., Stoll, C., Holbach, A., Chen, H., Wang, L., Zheng, B., et al. (2013). Dechlorination and organohalide-respiring bacteria dynamics in sediment samples of the Yangtze Three Gorges Reservoir. *Environ. Sci. Pollut. Res.* 20, 7046–7056. doi: 10.1007/s11356-013-1545-9

Lee, P. K. H., Cheng, D., West, K. A., Alvarez-Cohen, L., and He, J. Z. (2013). Isolation of two new *Dehalococcoides mccartyi* strains with dissimilar dechlorination functions and their characterization by comparative genomics via microarray analysis. *Environ. Microbiol.* 15, 2293–2305. doi: 10.1111/1462-2920.12099

Levy, C. W., Roujeinikovai, A., Sedelnikova, S., Baker, P. J., Stuitje, A. R., Rice, D., et al. (1999). Molecular basis of triclosan activity. *Nature* 398, 383–384. doi: 10.1038/18803

Löffler, F. E., Ritalahti, K. M., and Tiedje, J. M. (1997). Dechlorination of chloroethenes is inhibited by 2-bromoethanesulfonate in the absence of methanogens. *Appl. Environ. Microbiol.* 63, 4982–4985.

Löffler, F. E., Yan, J., Ritalahti, K. M., Adrian, L., Edwards, E. A., Konstantinidis, K. T., et al. (2013). *Dehalococcoides mccartyi* gen. nov., sp. nov., obligately organohalide-respiring anaerobic bacteria relevant to halogen cycling and bioremediation, belong to a novel bacterial class, *Dehalococcoidia* classis nov., order *Dehalococcoidales* ord. nov. and family *Dehalococcoidaceae* fam. nov., within the phylum *Chloroflexi*. *Int. J. Syst. Evol. Microbiol.* 63, 625–635. doi: 10.1099/ijs.0.034926-0

Maphosa, F., Vos, W. M., and Smidt, H. (2010). Exploiting the ecogenomics toolbox for environmental diagnostics of organohalide-respiring bacteria. *Trends Biotechnol.* 28, 308–316. doi: 10.1016/j.tibtech.2010.03.005

McClellan, K., and Halden, R. U. (2010). Pharmaceuticals and personal care products in archived U.S. biosolids from the 2001 EPA national sewage sludge survey. *Water Res.* 44, 658–668. doi: 10.1016/j.watres.2009.12.032

McDonnell, G., and Russell, D. (1999). Antiseptics and disinfectants: activity, action, and resistance. *Clin. Microbiol. Rev.* 12, 147–179.

McMurry, L. M., Oethinger, M., and Levy, S. B. (1998). Triclosan targets lipid synthesis. *Nature* 394, 531–532. doi: 10.1038/28970

Men, Y., Lee, P. K. H., Harding, K. C., and Alvarez-Cohen, L. (2013). Characterization of four TCE-dechlorinating microbial enrichments grown with different cobalamin stress and methanogenic conditions. *Appl. Microb. Biotechnol.* 97, 6439–6450. doi: 10.1007/s00253-013-4896-8

Miller, T. R., Heidler, J., Chillrud, S. N., Delaquil, A., Ritchie, J. C., Mihalic, J. N., et al. (2008). Fate of triclosan and evidence for reductive dechlorination of triclocarban in estuarine sediments. *Environ. Sci. Technol.* 42, 4570–4576. doi: 10.1021/es702882g

Mulla, S. I., Hu, A., Wang, Y., Sun, Q., Huang, S. L., Wang, H., et al. (2016). Degradation of triclocarban by a triclosan-degrading *Sphingomonas* sp. strain YL-JM2C. *Chemosphere* 144, 292–296. doi: 10.1016/j.chemosphere.2015.08.034

Pycke, B. F. G., Roll, I. B., Brownawell, B. J., Kinney, C. A., Furlong, E. T., Kolpin, D. W., et al. (2014). Transformation products and human metabolites of triclocarban and triclosan in sewage sludge across the United States. *Environ. Sci. Technol.* 48, 7881–7890. doi: 10.1021/es5006362

Ren, J. R., Zhao, H. P., Song, C., Wang, S. L., Li, L., Xu, Y. T., et al. (2010). Comparative transmembrane transports of four typical lipophilic organic chemicals. *Bioresour. Technol.* 101, 8632–8638. doi: 10.1016/j.biortech.2010.06.121

Ryzhkova, E. P. (2003). Multiple functions of corrinoids in prokaryote biology. *Prikl. Biokhim. Mikrobiol.* 39, 139–159.

Smidt, H., and de Vos, W. M. (2004). Anaerobic microbial dehalogenation. *Annu. Rev. Microbiol.* 58, 43–73. doi: 10.1146/annurev.micro.58.030603.123600

Souchier, M., Casellas, C., Ingrand, V., and Chiron, S. (2016). Insights into reductive dechlorination of triclocarban in river sediments: field measurements and in vitro mechanism investigations. *Chemosphere* 144, 425–432. doi: 10.1016/j.chemosphere.2015.08.083

Stupperich, E., Eisinger, H. J., and Räutler, B. (1988). Diversity of corrinoids in acetogenic bacteria: *P*-Cresolylcobamide from *Sporomusa ovata*, 5-methoxy-6-methylbenzimidazolylcobamide from *Clostridium formicoaceticum* and vitamin B_{12} from *Acetobacterium woodii*. *Eur. J. Biochem.* 172, 459–464. doi: 10.1111/j.1432-1033.1988.tb13910.x

USEPA (2014). *Assessing and Managing Chemicals under TSCA*. Available at: https://www.epa.gov/assessing-and-managing-chemicals-under-tsca/tsca-work-plan-chemical-risk-assessment-0

USEPA (2017). *National Primary Drinking Water Regulations*. Available at: https://www.epa.gov/ground-water-and-drinking-water/national-primary-drinking-water-regulation-table

Vargas, C., and Ahlert, R. C. (1987). Anaerobic degradation of chlorinated solvents. *Res. J. Water Pollut. Control Fed.* 59, 964–968.

Walsh, S. E., Maillard, J. Y., Russell, A. D., Catrenich, C. E., Charbonneau, D. L., and Bartolo, R. G. (2003). Activity and mechanisms of action of selected biocidal agents on Gram-positive and -negative bacteria. *J. Appl. Microbiol.* 94, 240–247. doi: 10.1046/j.1365-2672.2003.01825.x

Wei, N., and Finneran, K. T. (2013). Low and high acetate amendments are equally as effective at promoting complete dechlorination of trichloroethylene (TCE). *Biodegradation* 24, 413–425. doi: 10.1007/s10532-012-9598-x

Wen, L. L., Yang, Q., Zhang, Z. X., Yi, Y. Y., Tang, Y., and Zhao, H. P. (2016). Interaction of perchlorate and trichloroethene bioreductions in mixed anaerobic culture. *Sci. Total Environ.* 571, 11–17. doi: 10.1016/j.scitotenv.2016.07.122

Wen, L. L., Zhang, Y., Chen, J. X., Zhang, Z. X., Yi, Y. Y., Tang, Y., et al. (2017). The dechlorination of TCE by a perchlorate reducing consortium. *Chem. Eng. J.* 313, 1215–1221. doi: 10.1016/j.cej.2016.11.021

Wen, L. L., Zhang, Y., Pan, Y. W., Wu, W. Q., Meng, S. H., Zhou, C., et al. (2015). The roles of methanogens and acetogens in dechlorination of trichloroethene using different electron donors. *Environ. Sci. Pollut. Res.* 22, 19039–19047. doi: 10.1007/s11356-015-5117-z

Yang, Y., and McCarty, P. L. (2002). Comparison between donor substrates for biologically enhanced tetrachloroethene DNAPL dissolution. *Environ. Sci. Technol.* 36, 3400–3404. doi: 10.1021/es011408e

Yun, H., Liang, B., Qiu, J., Zhang, L., Zhao, Y., Jiang, J., et al. (2017). Functional characterization of a novel amidase involved in biotransformation of triclocarban and its dehalogenated congeners in *Ochrobactrum* sp. TCC-2. *Environ. Sci. Technol.* 51, 291–300. doi: 10.1021/acs.est.6b04885

Zhao, H. P., Schmidt, K., and Tiehm, A. (2010). Inhibition of aerobic metabolic cis-1,2-di-chloroethene biodegradation by other chloroethenes. *Water Res.* 44, 2276–2282. doi: 10.1016/j.watres.2009.12.023

Zhao, J. L., Ying, G. G., Liu, Y. S., Chen, F., Yang, J. F., and Wang, L. (2010). Occurrence and risks of triclosan and triclocarban in the Pearl River system, South China: from source to the receiving environment. *J. Hazard. Mater.* 179, 215–222. doi: 10.1016/j.jhazmat.2010.02.082

Zhao, Y. G., Ren, N. Q., and Wang, A. J. (2008). Contributions of fermentative acidogenic bacteria and sulfate-reducing bacteria to lactate degradation and sulfate reduction. *Chemosphere* 72, 233–242. doi: 10.1016/j.chemosphere.2008.01.046

Zhong, L., Lai, C. Y., Shi, L. D., Wang, K. D., Dai, Y. J., Liu, Y. W., et al. (2017). The nitrate effect on chromate bio-reduction in a methane-based MBfR. *Water Res.* 115, 130–137. doi: 10.1016/j.watres.2017.03.003

Ziv-El, M., Delgado, A. G., Yao, Y., Kang, D. W., Nelson, K. G., Halden, R. U., et al. (2011). Development and characterization of DehaloR^2, a novel anaerobic microbial consortium performing rapid dechlorination of TCE to ethene. *Appl. Microbiol. Biotechnol.* 92, 1063–1071. doi: 10.1007/s00253-011-3388-y

Ziv-El, M., Popat, S. C., Parameswaran, P., Kang, D. W., Alexandra, P., Halden, R. U., et al. (2012). Using electron balances and molecular techniques to assess trichloroethene-induced shifts to a dechlorinating microbial community. *Biotechnol. Bioeng.* 109, 2230–2239. doi: 10.1002/bit.24504

Conflict of Interest Statement: The authors declare that the research was conducted in the absence of any commercial or financial relationships that could be construed as a potential conflict of interest.

frontiers in Microbiology

ORIGINAL RESEARCH
published: 20 July 2018
doi: 10.3389/fmicb.2018.01574

Effects of Ferric Oxyhydroxide on Anaerobic Microbial Dechlorination of Polychlorinated Biphenyls in Hudson and Grasse River Sediment Microcosms: Dechlorination Extent, Preferences, *Ortho* Removal, and Its Enhancement

Yan Xu[1,2]*, *Kelvin B. Gregory*[2] and *Jeanne M. VanBriesen*[2]*

[1] Department of Municipal Engineering, School of Civil Engineering, Southeast University, Nanjing, China, [2] Department of Civil and Environmental Engineering, Carnegie Mellon University, Pittsburgh, PA, United States

OPEN ACCESS

Edited by:
Shanquan Wang,
Sun Yat-sen University, China

Reviewed by:
Maoyong Song,
Research Center for Eco-Environmental Sciences (CAS), China
Na Liu,
Jilin University, China

***Correspondence:**
Yan Xu
xuxucalmm@seu.edu.cn
Jeanne M. VanBriesen
jeanne@cmu.edu

Specialty section:
This article was submitted to Microbiotechnology, Ecotoxicology and Bioremediation, a section of the journal Frontiers in Microbiology

Received: 30 March 2018
Accepted: 25 June 2018
Published: 20 July 2018

Citation:
Xu Y, Gregory KB and VanBriesen JM (2018) Effects of Ferric Oxyhydroxide on Anaerobic Microbial Dechlorination of Polychlorinated Biphenyls in Hudson and Grasse River Sediment Microcosms: Dechlorination Extent, Preferences, Ortho Removal, and Its Enhancement. Front. Microbiol. 9:1574. doi: 10.3389/fmicb.2018.01574

Microbial reductive dechlorination of polychlorinated biphenyls (PCBs) has been observed in many PCB-impacted sediments. However, this biodegradation is relatively site-specific and can be affected by PCB compositions and sediment geochemical conditions. To better understand the influence of a common competing electron acceptor, ferric oxyhydroxide (FeOOH), on dechlorination, two sediments (Hudson River and Grasse River sediments), and two PCB mixtures (PCB 5/12, 64/71, 105/114, and 149/153/170 in *Mixture 1* and PCB 5/12, 64/71, 82/97/99, 144/170 in *Mixture 2*) were used for this microcosm study. The addition of 40 mmole/kg FeOOH completely inhibited PCB dechlorination in the Hudson sediment, but only moderately inhibited PCB dechlorination in the Grasse sediment with a 3-week longer lag time. The inhibitory effect in the Grasse sediment was mainly due to the loss of unflanked *para* dechlorination activity. Fe(II) analysis showed that dechlorination started prior to the consumption of Fe(III), which indicates PCB reduction and Fe(III) reduction were able to take place concurrently. *Dehalococcoides* 16S rRNA genes increased with the commencement of dechlorination in the Grasse sediment, but not in the completely inhibited Hudson sediment. Rare *ortho* dechlorination pathways were identified in FeOOH-amended Grasse sediment microcosms, dominated by transformations of PCB 25(2̲4-3-CB) to PCB 13(3-4-CB) and PCB 28(2̲4-4-CB) to PCB 15(4-4-CB). The addition of carbon sources (acetate or a fatty acid mixture with acetate, propionate, and butyrate) after 27 weeks of incubation reinitiated dechlorination in FeOOH-amended Hudson sediment microcosms. Also, the addition of carbon sources greatly enhanced *ortho* dechlorination in FeOOH-amended Grasse microcosms, indicating the utilization of acetate and/or the fatty acid mixture for *ortho* dechlorination-related microorganisms. A dechlorination pathway analysis approach revealed that *para*-flanked *meta* dechlorination was primarily preferred followed by *ortho*-/double-flanked *meta* dechlorination and single-/double-flanked *para* dechlorination in the Grasse sediment.

Keywords: polychlorinated biphenyls, sediment, reductive dechlorination, electron acceptor, ferric oxyhydroxide, *Dehalococcoides*

INTRODUCTION

Polychlorinated biphenyls (PCBs), containing 209 individual congeners, are listed as persistent organic pollutants (POPs) by the Stockholm Convention (UNEP, 2001). They have 1–10 chlorine atoms substituted at 4 *ortho*, 4 *meta*, and 2 *para* sites on the biphenyl structure. Although the industrial production of PCBs was banned in late 1970s, the global occurrence of PCBs in the environment has raised concerns about potential negative effects on aquatic systems and human health (Brown et al., 1987; Safe, 1989; Quensen et al., 1998; IARC Monographs, 2016; Lyall et al., 2017). Hudson and Grasse Rivers are two historically PCB-impacted rivers in the United States. They received discharges from the capacitor manufacturing plants of the General Electric Company (GE) and an aluminum smelting and fabricating facility of the Aluminum Company of America (ˆAlcoa), respectively (EPA, 1997). Because PCBs are highly hydrophobic and persistent, they are predominantly adsorbed in sediment upon release into the aquatic environment and then enter the food chain via ingestion by benthic organisms (Kjellerup et al., 2008). As sediments are the sinks for PCBs in the environment, the remediation of PCB-contaminated sediments has been a regulatory priority for over three decades (EPA, 1997; Sowers and May, 2013).

Among the remediation methods, microbially mediated anaerobic reductive dechlorination of PCBs is particularly attractive due to its low cost and minimal disruption of the sediment (Bedard and Quensen, 1995; Sowers and May, 2013). Despite the prevalence of PCB dechlorination reported in a variety of natural sediment systems and laboratory microcosms, lack of knowledge of the interactions among sediment geochemical properties and dechlorinating microbial communities has hindered the progress of *in situ* treatment (Brown et al., 1987; Alder et al., 1993; Wiegel and Wu, 2000; Kjellerup et al., 2008; Xu et al., 2012; Sowers and May, 2013; Praveckova et al., 2016). In general, different sediments proceed to dechlorination following eight classified processes (Bedard and Quensen, 1995; Bedard et al., 2005; Hughes et al., 2010). However, the link among sediment properties, processes and dechlorinating microorganisms is not well understood. To date, only a few PCB dechlorinators within the *Chloroflexi* phylum have been identified. Bacterium *ortho*-17 (*o*-17), isolated from Baltimore Harbor sediment, is the only strain that is able to remove *ortho* chlorines (Cutter et al., 1998, 2001). *Dehalobium chlorocoercia* strain DF-1 growing with a *Desulfovibrio* sp. as co-species catalyzes PCBs with double-flanked chlorines (Wu et al., 2002), *Dehalococcoides mccartyi* strains 195, CBDB1, CG-1, CG-4, CG-5, and JNA were all found to preferentially target flanked (double-flanked or single-/double-flanked) *meta*/*para* chlorines (Fennell et al., 2004; Adrian et al., 2009; Wang and He, 2013; Laroe et al., 2014; Wang et al., 2014; Zhen et al., 2014). None of the identified PCB dechlorinators shows a dechlorination preference on unflanked chlorines. Additionally, among all these PCB dechlorinators, only *D. mccartyi* strains CBDB1 and JNA were found to match known dechlorination processes H and N, respectively (Adrian et al., 2009; Laroe et al., 2014). Therefore, the observed preferences (patterns) in most PCB dechlorination studies have not been attributed to the identified dechlorinators. Moreover, sediment geochemical conditions have been found to exhibit a significant impact on dechlorination preferences (Cho and Oh, 2005; Yan et al., 2006; Kjellerup et al., 2008). Among the geochemical properties, iron is crucial for sediment biogeochemistry. Fe (III) oxides can serve as alternative electron acceptors and inhibit reductive dechlorination (Morris et al., 1992; Paul et al., 2013), while surface-complexed Fe(II) can induce abiotic dechlorination (Jeong et al., 2011; Chen et al., 2016). Abiotic PCB dechlorination associated with biogenic absorbed Fe(II) was expected in PCB-spiked acetate-amended sediment reactors applied with low-voltage electric fields (Liu et al., 2017). Up to now, little is known about the impact of Fe(III) on PCB dechlorination extent and dechlorination pathway preferences in sediments. Organic carbon is also of great importance in PCB dechlorination. A previous review concluded that the impacts of exogenous organic carbon sources, such as acetate, formate, pyruvate, lactate, glucose, methanol, acetone, and a fatty acid mixture (acetate, propionate, and butyrate) on PCB dechlorination rate, extent, and process were equivocal (Wiegel and Wu, 2000). The addition of carbon sources can benefit PCB dechlorination by providing sufficient carbon and energy sources for PCB dechlorinating microorganisms, or by stimulating the growth of essential co-species of PCB dechlorinators (Wiegel and Wu, 2000). Yet, supplementary carbon can also result in the rapid growth of non-PCB dechlorinating microorganisms, which may ultimately inhibit PCB dechlorinators through competition (Wiegel and Wu, 2000; Zanaroli et al., 2012a). General conclusions are difficult to draw due to the variety of experimental conditions considered. In some cases, researchers add the carbon sources at the initiation of incubation (Pulliam Holoman et al., 1998; Fagervold et al., 2011; Ho and Liu, 2012; Kaya et al., 2017), while others add carbon periodically during incubation (Alder et al., 1993; Zhen et al., 2014; Matturro et al., 2016). No study has considered long-term incubation of PCB spiked sediment microcosms prior to carbon addition. Accordingly, the role of exogenous carbon sources when natural carbon may have been depleted (over long times) has not been evaluated. Also, carbon sources are expected to compensate the "electron donor demand" exhibited by amended Fe(III) (Wei and Finneran, 2011). In our previous study, by developing a data analysis approach focusing on chlorine neighboring conditions, we interpreted different PCB dechlorination extent and preferences in relatively low organic carbon content (1.26%) and low Fe (5310 mg/kg dry wt.) Hudson sediment compared with high organic carbon content (5.73%) and high Fe (18,000 mg/kg dry wt.) Grasse sediment. We reported on rare *ortho* dechlorination in the Grasse sediment (Xu et al., 2016). These lead to a hypothesis that Fe and carbon content may be the important factors for PCB dechlorination in these sediments.

In the present work, we investigate the effects of exogenous ferric oxyhydroxide (FeOOH) with a concentration relevant to background total Fe on PCB dechlorination in the two sediment systems, again with spiked PCB mixtures that allow us to focus on dechlorination preferences. The specific objectives

were to (1) understand changes in dechlorination extent and preferences as well as changes in the populations of putative dechlorinating microorganisms; (2) validate the chlorine per biphenyl (CPB) data analysis approach focusing on chlorine neighboring conditions; (3) further investigate the occurrence of *ortho* dechlorination under Fe(III)-reducing conditions. The findings of this study improve understanding of dechlorination inhibition caused by Fe(III). Moreover, this is the first attempt to enhance rare *ortho* dechlorination using simple carbon source amendments in sediment microcosms.

MATERIALS AND METHODS

Sediment Collection, Storage, and Characterization

Surficial sediments (the top 4 inches of sediments) were collected using a petite ponar dredge sampler from the Hudson River (N: 43°14′55.5506″; W: −073°35′37.4080″, Moreau, NY, United States) in October 2008, and the Grasse River (N:44°57′35.9577″; W: −074°48′59.8695″, Massena, NY, United States) in June 2009 as described elsewhere. The sediments were kept in filled 3-gallon plastic buckets in the dark at 4°C until used. The geochemical properties, including background PCBs, metals (e.g., Fe, Al), acid volatile sulfide, total phosphorous, total residue as percent solids, inorganic anions, and organic carbon content of the two sediments were determined previously (Xu et al., 2016).

Experimental Set-up

Thirteen PCB congeners were used in this study based on criteria previously described (Karcher et al., 2004; Xu et al., 2016). These 13 individual PCB congeners, related to 10 tracker pairs, were classified into two mixtures. PCB *Mixture 1* was composed of congeners PCB 5(23-CB)/12(34-CB), 64(236-4-CB)/71(26-34), 105(234-34-CB)/114(2345-4-CB), and 149(236-245-CB)/153(245-245-CB)/170(2345-234-CB). PCB *Mixture 2* contained congeners PCB 5/12, 64/71, 82(234-23-CB)/97(245-23-CB)/99(245-24-CB), 144(2346-25-CB)/170. The structures of selected PCB congeners, their theoretical first step dechlorination pathways and the possibly associated dechlorination processes were discussed previously (Xu et al., 2016).

The PCB-spiked dry sediment substrates containing 500 mg/kg of each PCB mixture were prepared as described previously (Xu et al., 2016). Modified reducing anaerobic media (RAMM) using 2 mM L-cysteine·HCl as the reducing agent was prepared and 1% (vol/vol) of Wolfe's vitamin solution was added (Shelton and Tiedje, 1984; Yan et al., 2006). The medium was adjusted to pH 7.0 and autoclaved for 20 min at 121°C under a nitrogen atmosphere. FeOOH stock solution (1.0 M) was synthesized following the method developed by Lovley and Phillips (1986).

Microcosms were established in an anaerobic glove box with a gas atmosphere of N_2-H_2 (99.1:0.9). Unless stated otherwise, 3 g PCB-spiked dry sediment substrate or dry sediment, 3 g fresh sediment inocula (dry weight basis), with or without 1.2 mmole FeOOH, and freshly prepared RAMM medium were added to a 50 ml serum bottle to achieve a total weight of 30 g. Four Fe(III)-amended PCB spiked experiments, four PCB-spiked experiments, two no PCB control experiments and sterile controls were set up (**Table 1**). Generally, a total PCB concentration of 50 mg/kg slurry was achieved in each PCB-spiked microcosm and an additional 40 mmole/kg slurry of FeOOH was added in each Fe(III)-amended PCB-spiked microcosm. Individual PCB concentrations of PCB *Mixture 1* and PCB *Mixture 2* in the sediment microcosms are tabulated in Supplementary Table S1. PCB *Mixture 1* had a CPB value of 4.36, with *ortho* CPB 1.56, *meta* CPB 1.58, and *para* CPB 1.23, while PCB *Mixture 2* had a CPB value of 4.27 with *ortho* CPB 1.64, *meta* CPB 1.48, and *para* CPB 1.16. The established microcosms were sealed with Teflon-lined gray butyl rubber septa (The West Pharmaceutical Co., PA) and crimped with aluminum crimp caps. After a 24-h rotation on a rotating mixer (40 rpm) in the dark, the first time point sampling was conducted and the rest of microcosms were stored statically at ambient temperature in the dark. Destructive sampling was conducted at 3-week intervals from Week 0 to Week 24, then at Week 30, Week 36, and Week 51 anaerobically. Unless stated otherwise, triplicate microcosms were sampled at each sampling point. The influences of carbon sources were investigated by adding acetate (pH = 7.0, sodium salt) or a fatty acid mixture (acetate/propionate/butyrate 1:1:1, pH = 7.0, sodium salts) after 27 weeks of incubation. The microcosms used for carbon source amendment were those that had been sampled and recapped at Week 21 and Week 24. At Week 27, 7.5 mM of acetate or a fatty acid mixture were added; at Week 30 and Week 36, 15 mM of acetate or a fatty acid mixture were added, respectively. To minimize the change of slurry volume, all the additions were conducted by injecting 200 times concentrated stock carbon source solutions. The sample collections for the triplicate acetate-amended microcosms and the triplicate fatty acid mixture-amended microcosm were non-destructive and performed at Week 30 and Week 36, right before the addition of extra carbon sources. The final sampling was conducted at Week 51. Sterile controls were sampled in duplicate at Week 0, Week 18, Week 36, and Week 51, and no dechlorination was observed.

Headspace Analysis

Prior to microcosm slurry withdrawal, 200 μl of headspace gas was analyzed to determine H_2, CH_4, and trace O_2 following an analytical method mentioned elsewhere (Xu et al., 2016). Considering biological gas production, the amount of each gas species was recalculated with the ideal gas law by simply assuming a constant 1.0 atm partial pressure of nitrogen in the headspace and a room temperature of 20°C.

Ferrous Iron Analysis

The reduction of Fe(III) to Fe(II) in the microcosms was tracked using a ferrozine method described elsewhere (Sorensen, 1982). Briefly, a subsample of 200 μl of sediment slurry was weighed and transferred into a 1.5-ml microcentrifuge tube containing 800 μl of 1.0 M HCl and reacted thoroughly. Thereafter, 10 μl of acid treated sample was added to 4.99 ml ferrozine

TABLE 1 | Sediment microcosms setup.

Experiments	Name	Sediment	Spiked PCBs	Ferric Iron
Fe(III)-amended PCB experiments	H-1-Fe	Hudson	PCB *Mixture 1*	FeOOH
	G-1-Fe	Grasse	PCB *Mixture 1*	FeOOH
	H-2-Fe	Hudson	PCB *Mixture 2*	FeOOH
	G-2-Fe	Grasse	PCB *Mixture 2*	FeOOH
PCB experiments	H-1	Hudson	PCB *Mixture 1*	–
	G-1	Grasse	PCB *Mixture 1*	–
	H-2	Hudson	PCB *Mixture 2*	–
	G-2	Grasse	PCB *Mixture 2*	–
No PCB controls	H	Hudson	–	–
	G	Grasse	–	–
Sterile controls (Killed controls)	H-1-Fe-K	Hudson	PCB *Mixture 1*	FeOOH
	G-1-Fe-K	Grasse	PCB *Mixture 1*	FeOOH
	H-2-Fe-K	Hudson	PCB *Mixture 2*	FeOOH
	G-2-Fe-K	Grasse	PCB *Mixture 2*	FeOOH

PCB, polychlorinated biphenyl.

solution and filtered. Dilutions with more ferrozine solution were performed when necessary. The absorption was measured at 562 nm by a UV-vis spectrophotometer (HACH, Macon, MO, United States).

PCB Extraction, Cleanup, and Analysis

The PCB extraction procedure was described elsewhere (Yan et al., 2006; Xu et al., 2016). Briefly, 2.0 g sediment slurry was collected anaerobically, and 1 μg of PCB 209 in 20 μl of hexane was added as surrogate. After the hexane fully evaporated, the slurry sample was extracted with 10 ml of acetone, followed by 10 ml of 1:1 acetone/hexane (v/v) twice, and 3 ml of hexane, respectively. The pooled extract was phase-separated with 8 ml of organic-free 2% NaCl solution. The obtained hexane layer was collected and concentrated to 2 ml. Tetrabutylammonium (TBA) sulfite was used to remove sulfur, following EPA Method 3660B. The TBA pretreated PCB extract was passed through a glass column (10 mm inner diameter) packed with 4 g Florisil and topped with 1.5 g anhydrous sodium sulfate. The column was pre-washed by 30 ml hexane. The eluate was loaded onto the column, followed by eluting with 30 ml n-hexane and 25 ml n-hexane/CH_2Cl_2 (4:1, v/v). The combined elutant was concentrated to exact 4.0 ml. The quantification of individual PCBs were performed by Hewlett Packard gas chromatograph (Model 6890) coupled with a micro-electron capture detector (μECD) and a 30-m DB-XLB capillary column (0.18 mm diameter and 0.18 μm film thickness; Agilent Technologies, Palo Alto, CA) (Xu et al., 2012, 2016). Complete dechlorination was confirmed by analyzing biphenyl in selected microcosms (duplicate bottles in each treatment at Week 36) at Energy & Environmental Research Center (EERC), University of North Dakota.

DNA Extraction and Quantitative PCR

The sediment pellet samples from 0.5 ml of slurries were harvested as described previously (Xu et al., 2016). Total genomic DNA was extracted from the sediment pellets using the MoBio PowerSoil DNA Isolation Kit (MoBio, Carlsbad, CA) following the manufacturer's protocols. Equal volumes of the triplicate DNA extracts at each sampling point were combined and mixed thoroughly for further microbial community analysis.

The 16S rRNA gene copies of total Bacteria, Fe(III)-reducing Family Geobacteraceae, *Dehalococcoides*, PCB degrading organism strains *ortho*-17 and *D. chlorocoercia* strain DF-1 (*o*-17/DF-1) were estimated using SYBR Green-based quantitative PCR (qPCR). Total Bacteria, Geobacteraceae, *Dehalococcoides*, and *o*-17/DF-1 were targeted with primer sets BAC338F/534R (Muyzer et al., 1993), Geo564F/840R(Cummings et al., 2003; Himmelheber et al., 2009), DHC1200F/1271R (He et al., 2003), and modified BAC908F/Dehal1265R (Edwards et al., 1989; Watts et al., 2005; Xu et al., 2012), respectively. qPCR reactions were performed in an ABI 7500 Real-Time PCR System (Applied Biosystems, Carlsbad, CA, United States) as described previously (Xu et al., 2016).

Identification of Dechlorination Preferences

The dechlorination preferences were identified using a modified CPB analysis approach (Xu et al., 2016). Based on the known *ortho*, *meta*, and *para* chlorine positions, the neighboring conditions of each chlorine are considered. Totally, nine chlorine categories are defined, including unflanked *ortho* (UF *ortho*), flanked *ortho* (so called *meta*-flanked *ortho*), unflanked *meta* (UF *meta*), *ortho*-flanked *meta* (OF *meta*), *para*-flanked *meta* (PF *meta*), double-flanked *meta* (DF *meta*) (neighbored with one *ortho* and one *meta* chlorine), unflanked *para* (UF *para*), single-flanked *para* (SF *para*) (so-called *meta* flanked *para*), and double-flanked *para* (DF *para*).

RESULTS

Headspace Gas

No O_2 was detected in any of the microcosms. In the Hudson sediment microcosms amended with FeOOH (H-1-Fe and H-2-Fe), only a trace amount of CH_4 (below 0.1% of the headspace gas) was detected in the time course of 51 weeks, indicating a complete inhibition of methanogenesis in these sediment microcosms. In the Grasse sediment microcosms, the addition of FeOOH significantly reduced but did not completely cease the generation of CH_4 (see Supplementary Figure S1). The trends of CH_4 production in different microcosm groups were generally G-2 > G-1 > G > G-2-Fe > G-1-Fe. The measured CH_4 concentrations in FeOOH-amended Grasse microcosms were 30–40% lower than those in microcosms without added FeOOH. This suggests that FeOOH can moderately inhibit methanogenesis in the Grasse sediment. H_2 was not detected in any Grasse sediment microcosms during the study period, while

in the Hudson sediment microcosms, trace H_2 (less than 0.2%) was only found at Week 0.

Fe(III) Reduction

The reduction of Fe(III) was directly confirmed by tracking the concentrations of Fe(II) in the slurries over time. Due to the presence of indigenous Fe, Fe(II) concentrations in FeOOH-amended (H-1-Fe, H-2-Fe, G-1-Fe, and G-2-Fe), non-FeOOH-amended (H-1, H-2, G-2, and G-2), and no PCB control (H, G) microcosms were all measured to better elucidate the influences of supplementary FeOOH and/or PCBs on Fe(III) reduction. The trends of increasing Fe(II) were distinct in the Hudson and the Grasse sediments, but very similar in the same sediment spiked with different PCB *Mixtures* (see Supplementary Figure S2). In the Grasse sediment microcosms, after approximately 15–18 weeks of incubation, the differences of Fe(II) levels between G-1-Fe (91.3 ± 4.0 mmole/kg slurry at Week 15) and G-1 (51.4 ± 1.2 mmole/kg slurry at Week 15) or between G-2-Fe (105.4 ± 5.1 mmole/kg slurry at Week 18) and G-2 (61.3 ± 1.2 mmole/kg slurry at Week 18) remained at around 40 mmole/kg slurry until the end of 51 weeks. This indicates the complete reduction of supplementary FeOOH was accomplished within a 15–18 weeks' incubation. Meanwhile, dissolved Fe(II) remained at 1.2–1.5 mmole/kg slurry, indicating the biogenic Fe(II) was mainly in the adsorbed form. In contrast, the Hudson sediment microcosms exhibited a much slower Fe(III) reduction. By the end of 51 weeks, Fe(II) concentrations in H-1-Fe, H-1, H-2-Fe, and H-2 were 47.3 ± 4.1 mmole/kg, 15.2 ± 0.9 mmole/kg, 47.1 ± 0.7 mmole/kg, and 13.2 ± 1.4 mmole/kg, respectively. The difference in corresponding microcosms in the presence and in the absence of supplementary FeOOH was smaller than 40 mmole/kg, suggesting FeOOH in H-1-Fe and H-2-Fe was not completely reduced to Fe(II) within the time course of 51 weeks. Dissolved Fe(II) ranged from 0.4 to 0.6 mmole/kg after 51 weeks of incubation. Additionally, the spiking of PCBs slightly favored Fe(III) reduction (G-1/G-2 with G, H-1/H-2 with H), especially in the first 21 weeks of incubation (Supplementary Figure S2), suggesting a complex microbial interaction in the presence of added alternative electron acceptors.

PCBs in Sediment Microcosms

No dechlorination products were observed in sterile controls (data not shown) or the FeOOH-amended Hudson sediment microcosms within the 51 weeks' incubation (Supplementary Tables S2, S3). This suggests that dechlorination was microbially catalyzed and the addition of FeOOH led to the complete inhibition of PCB dechlorination in the Hudson sediment. In addition, the negligible levels of generated CO_2 and CH_4 in H-1-Fe and H-2-Fe suggest low microbial activity in FeOOH-amended Hudson sediment microcosms. By contrast, supplementary FeOOH only moderately inhibited PCB dechlorination in the Grasse sediment microcosms. **Figure 1** depicts the total PCB mass over time for each experiment. Generally, the addition of FeOOH resulted in a longer lag time and lower dechlorination extent in the Grasse sediment microcosms. The lag time periods were as long as 6–9 weeks in G-1-Fe and approximately 6 weeks in G-2-Fe, which were around 3 weeks longer than lag times in G-1 and G-2. In addition, as mentioned earlier, it took 15–18 weeks to completely reduce the supplementary FeOOH in the Grasse sediment microcosms. PCB dechlorination occurred at least 9 weeks prior to the completion of FeOOH reduction, suggesting the concurrent Fe(III) reduction and PCB dechlorination. Comparing to the initially spiked PCBs of 50.0 mg/kg slurry, significantly higher residual PCBs (37.5 ± 0.7 and 36.8 ± 0.4 mg/kg slurry in G-1-Fe and G-2-Fe) were observed in FeOOH-amended sediment microcosms than those in non-FeOOH-amended sediment microcosms (32.6 ± 0.7 and 33.6 ± 0.2 mg/kg slurry in G-1 and G-2) after 51 weeks of incubation. Additionally, the reduction trends of total PCB mass were very similar in the Grasse sediment regardless of the PCB mixture spiked. The partial inhibition was also indicated by the changes of CPB values in the presence of supplementary FeOOH. By the end of 51 weeks, the CPB values for G-1-Fe and G-2-Fe declined by 33.8 and 40.2%, whereas the CPB values for the non-FeOOH-amended G-1 and G-2 declined by 52.2 and 49.9%. Seen in **Figure 1**, the declining trends of total PCB mass and CPB values in FeOOH-amended and non-FeOOH-amended Grasse sediment microcosms had not reached the plateau phase by the end of 51 weeks. This suggests the potential for further dechlorination in the Grasse sediment microcosms after even 1 year of incubation wasn't changed by supplementary FeOOH.

Dechlorination cannot change the number of PCB molecules unless monochlorinated biphenyls are completely dechlorinated to biphenyl molecules. Excluding any experimental loss of PCBs, the decrease of total PCB moles is attributed to complete dechlorination. Illustrated in **Figure 1**, the reduction of total PCB molar concentrations in G-1-Fe and G-2-Fe was significant ($p < 0.001$), but less than that in non-FeOOH-amended G-1 and G-2. This was confirmed by biphenyl analysis (data not shown). Analysis of biphenyl suggested that the source of identified biphenyls was not the residual PAHs in sediments, but the spiked PCBs. The decrease of total PCB moles in G-1-Fe and G-2-Fe was mainly attributed to complete dechlorination of the only non-*ortho* congener spiked in the microcosms-PCB 12 (34-CB) (see Supplementary Tables S4, S5).

Although FeOOH moderately inhibited overall PCB dechlorination in the Grasse sediment microcosms, the influence of FeOOH on the first step dechlorination of spiked PCB congeners was complex. Seen in **Figure 2**, by the end of 51 weeks, over 96% of parent PCBs had been transformed in all the Grasse sediment microcosms. The less extensive dechlorination observed in G-1-Fe and G-2-Fe was not due to the lack of capability to remove the first chlorine atom from spiked PCB congeners. The changes of typical congeners PCB 12 and PCB 170 in Grasse sediment microcosms are illustrated in **Figure 2**, and the changes of other congeners are provided in Supplementary Figures S3–S6. Based on the relative amount of parent PCB congeners under methanogenic (G-1 and G-2) and Fe(III)-reducing (G-1-Fe and G-2-Fe) conditions, the parent PCB congeners were classified into three groups (**Table 2**). The

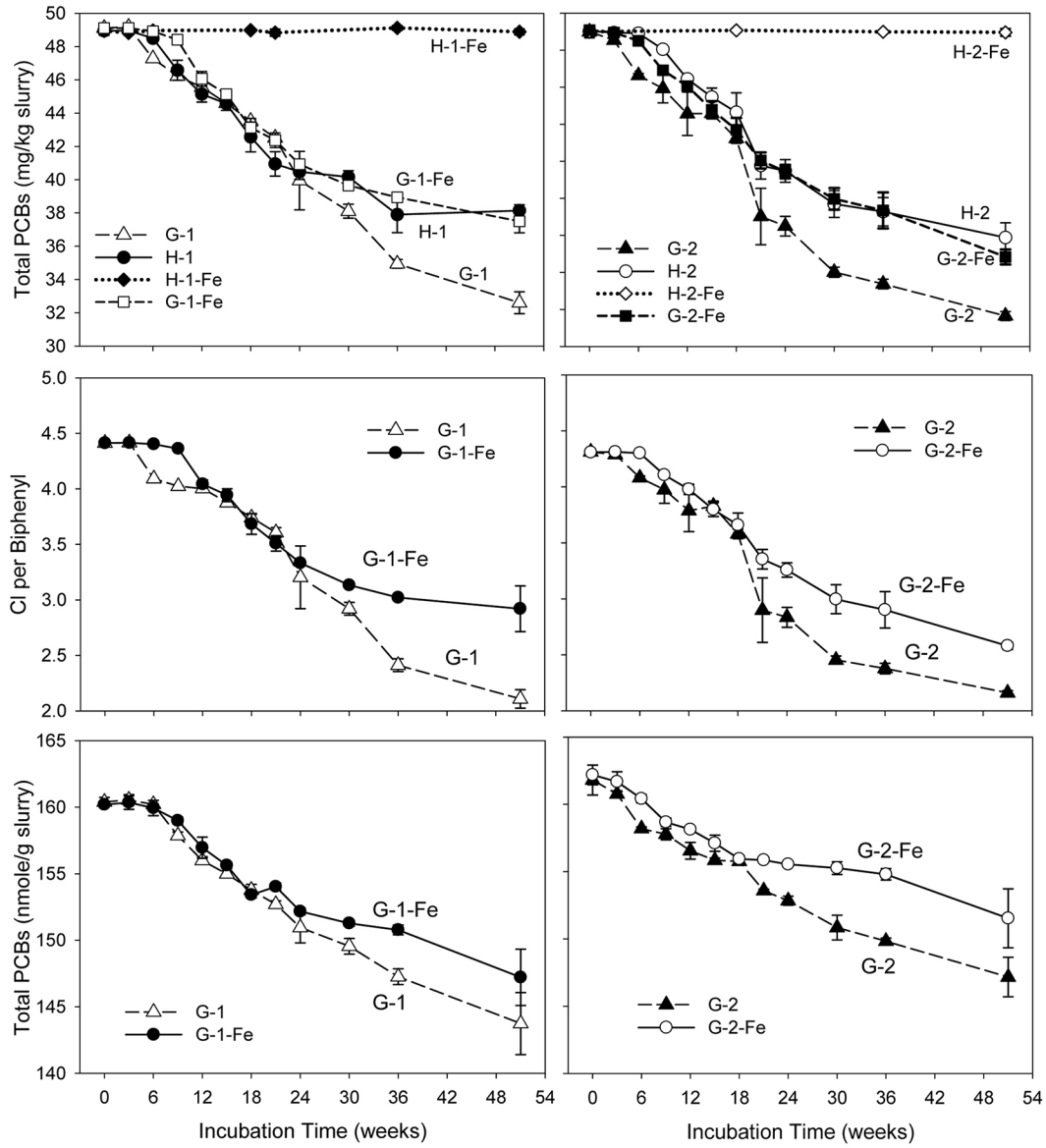

FIGURE 1 | Total PCB mass concentrations, CPB values, and molar concentrations over time in sediment microcosms. H-1, Hudson sediment spiked with PCB *Mixture 1*; H-1-Fe, Hudson sediment spiked with PCB *Mixture 1* and FeOOH; G-1, Grasse sediment spiked with PCB *Mixture 1*; G-1-Fe, Grasse sediment spiked with PCB *Mixture 1* and FeOOH; H-2, Hudson sediment spiked PCB *Mixture 2*; H-2-Fe, Hudson sediment spiked PCB *Mixture 2* and FeOOH; G-2, Grasse sediment spiked with PCB *Mixture 2*; G-2-Fe, Grasse sediment spiked with PCB *Mixture 2* and FeOOH. Data plotted are averages of triplicates. Error bars represent standard deviation. Error bars not visible are smaller than the symbol size.

first step of dechlorination for 10 out of 13 parent congeners in this study were either enhanced or not affected with FeOOH addition. Looking into the identical PCB congeners (PCB 5, 12, 64, and 71) spiked in the two PCB *Mixtures*, PCB *Mixture 2* tended to favor more rapid dechlorination of these congeners, as well as the concentration normalized PCB 170 (concentrations were normalized based on PCB 170 concentrations at Week 0) (**Figure 2** and Supplementary Figures S3, S4).

Notably, congener specific analysis of FeOOH-amended Grasse sediment microcosms revealed that *ortho* dechlorination occurred in G-1-Fe (Supplementary Table S4). The two identified pathways were PCB 25(24-3-CB) to PCB 13(3-4-CB) and PCB 28(24-4-CB) to PCB 15(4-4-CB). After 51 weeks of incubation, PCB 13 concentrations were found to be 1.2, 1.9, and 0.7 nmole/g slurry in triplicates, while the concentrations of PCB 15 were 2.3, 1.4, and 0.9 nmole/g slurry in triplicates. The above two *ortho* dechlorination pathways were also observed in non-FeOOH-amended G-1, suggesting the addition of FeOOH did not inhibit *ortho* dechlorination activity. Considering the changes of PCB 3(4-CB) in G-1-Fe, the concentrations were 10.8 ± 0.1 (10.8, 10.8, 10.9), 9.0 ± 0.6 (9.5, 8.2, 9.2), and 8.5 ± 4.6 (13.9, 5.4, 6.3) nmole/g at Week 18, Week 36, and Week 51, respectively.

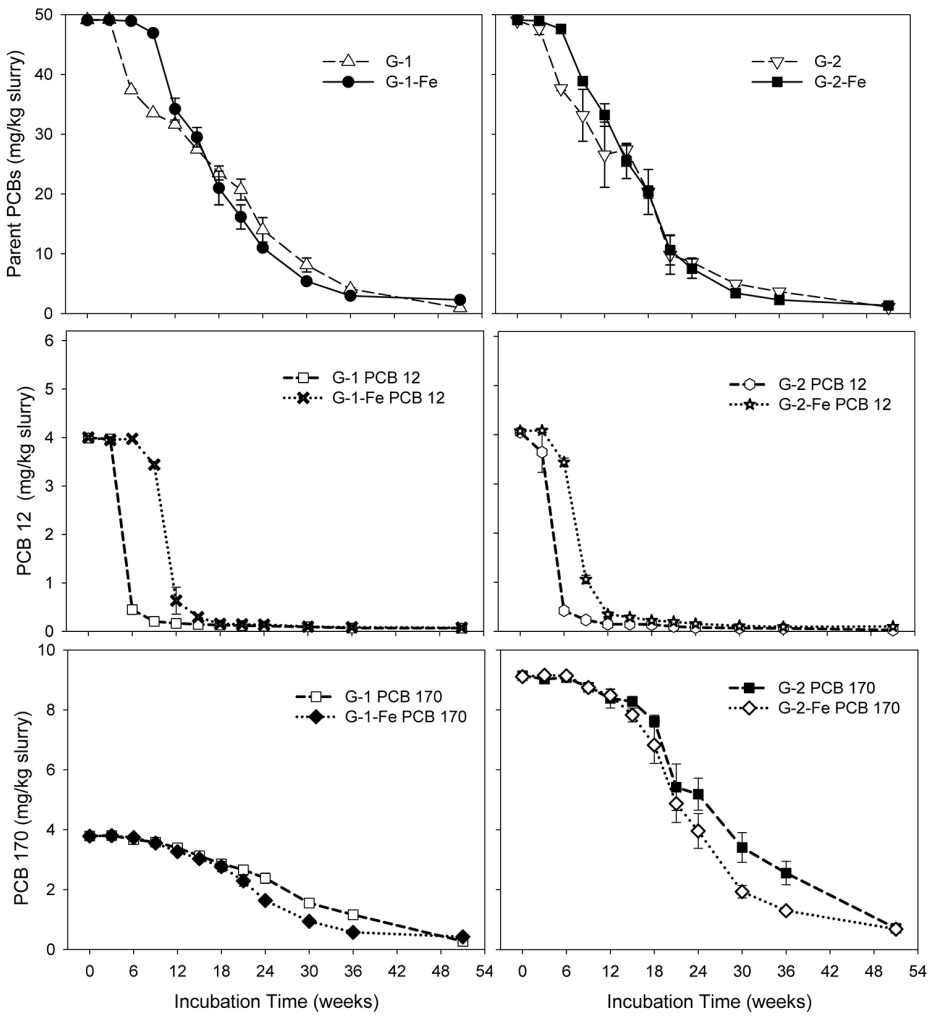

FIGURE 2 | Mass concentrations of parent PCBs, PCB 12, and PCB 170 over time in sediment microcosms. Data plotted are averages of triplicates. Error bars represent standard deviation. Error bars not visible are smaller than the symbol size.

TABLE 2 | Comparison of relative amounts of parent PCBs in the Grasse sediment microcosms.

Relative amount in treatments			PCB congeners	Duration
G-1/G-2	<	G-1-Fe/G-2-Fe	PCB 5(23-CB), PCB 12 (34-CB), PCB 71(26-34-CB)	3–51 weeks
G-1/G-2	=	G-1-Fe/G-2-Fe	PCB 64(236-4-CB), PCB 82(234-23-CB), PCB 97(245-23-CB), and PCB 99(245-24-CB)	15–51 weeks
G-1/G-2	>	G-1-Fe/G-2-Fe	PCB 105(234-34-CB), PCB 114(2345-4-CB), PCB 144(2346-25-CB), PCB 149(236-245-CB), PCB 153(245-245-CB), PCB 170(2345-234-CB)	18–36 weeks

PCB, polychlorinated biphenyl.

In other words, PCB 3 was reduced in two of the triplicates at Week 51, but increased sharply in the third. Moreover, the only spiked non-*ortho* PCB congener PCB 12(34-CB) was found to be at 0.7 ± 0.0, 0.4 ± 0.0, and 0.3 ± 0.0 nmole/g at Week 18, Week 36, and Week 51, respectively and could not contribute to the apparent increase of PCB 3 observed at Week 51. These results suggest that (1) dechlorination of unflanked *para* chlorines resumed after a long incubation; (2) the observed leveled PCB 3 in one of the microcosms at Week 51 was not directly linked to the dechlorination of PCB 12. The possible pathways included *meta*/*para* dechlorination of PCB 13(3-4-CB) or PCB 15(4-4-CB) and *ortho* dechlorination of PCB 7(24-CB) and PCB 8(2-4-CB). Regardless of the intermediates, the original parent PCB congeners were the dioxin-like mono-*ortho* PCB 105(234-34-CB) and PCB 114(2345-4-CB).

Identification of Attacked Chlorines

The changes of *ortho* CPB (OCPB), *meta* CPB (MCPB), and *para* CPB (PCPB) for FeOOH-amended Grasse sediment microcosms are plotted in **Figure 3**. Illustrated in **Figures 3A,B**, OCPB values

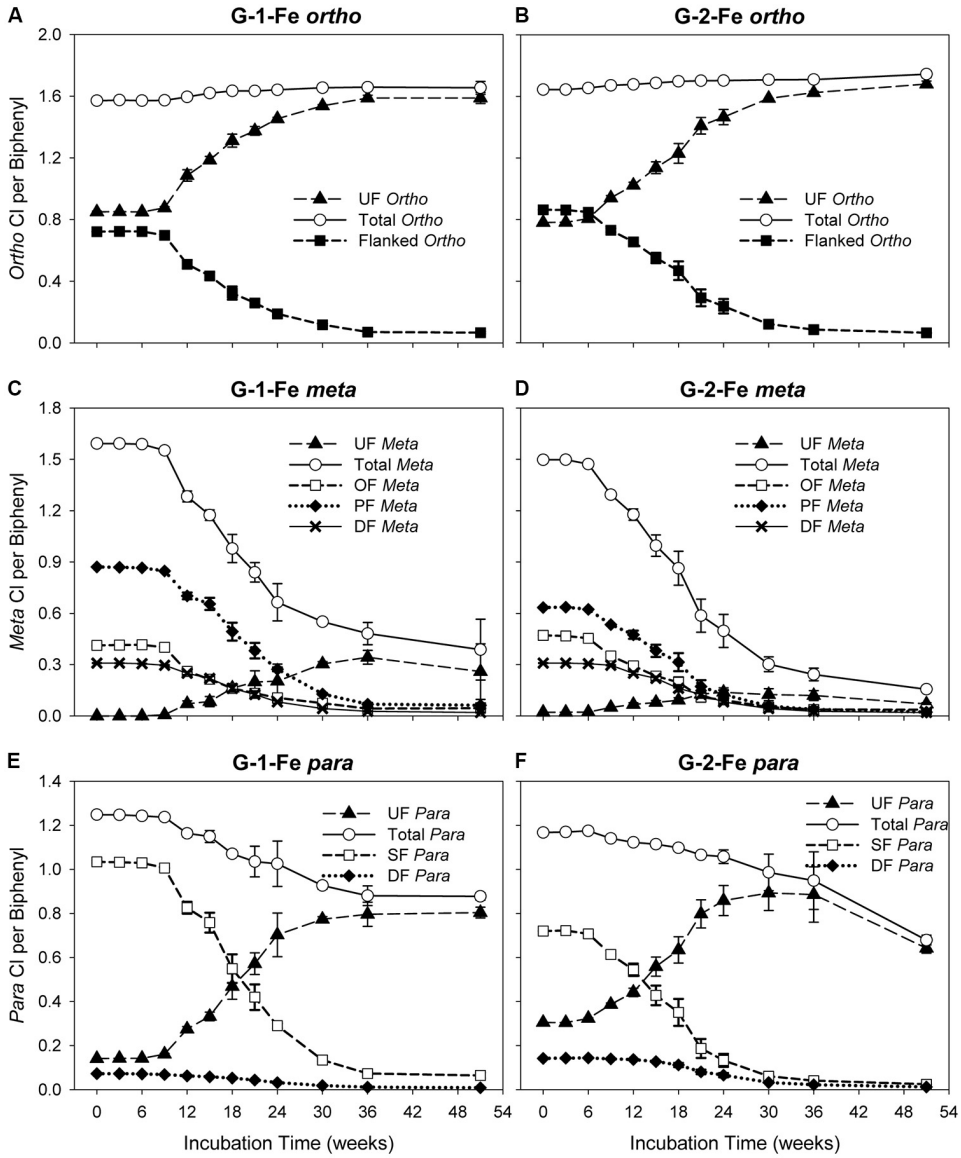

FIGURE 3 | Changes of *ortho*, *meta*, *para* chlorines over time in G-1-Fe and G-2-Fe. **(A)** *ortho* in G-1-Fe; **(B)** *ortho* in G-2-Fe; **(C)** *meta* in G-1-Fe; **(D)** *meta* in G-2-Fe; **(E)** *para* in G-1-Fe; **(F)** *para* in G-2-Fe. UF, unflanked; SF, single-flanked; DF, double-flanked; OF, *ortho*-flanked; PF, *para*-flanked. All data points averaged triplicate microcosms. Error bars represent standard deviation. Error bars not visible are smaller than the symbol size.

remained high in both G-1-Fe and G-2-Fe. In G-1-Fe, OCPB values slightly increased from 1.57 ± 0.00 to 1.66 ± 0.00 from Week 0 to Week 30. Thereafter, CPB values of 1.66 ± 0.01 and 1.65 ± 0.04 appeared at Week 36 and Week 51, respectively. In G-2-Fe, OCPB values kept increasing from 1.64 ± 0.00 to 1.74 ± 0.02 in the 51 weeks of incubation. The increase of OCPB was caused by the reduction of total molar concentration due to complete dechlorination of non-*ortho* PCB congener (PCB12, 34-CB) as decreasing the denominator in the OCPB calculation. A stable or reduced number of *ortho* chlorines was observed at Week 51 in G-1-Fe (**Figure 3A**), where *ortho* dechlorination occurred and was comparable with the reduction of total PCB molar concentration, resulting in similar decreases in the numerator and denominator in OCPB. In both G-1-Fe and G-2-Fe, unflanked *ortho* chlorines increased, whereas flanked *ortho* chlorines decreased over time. Considering the limited *ortho* dechlorination in G-1-Fe but not in G-2-Fe, the increase of unflanked *ortho* chlorines was due to the removal of *ortho*- or double-flanked *meta* chlorines, which resulted in fewer flanked chlorines on the *ortho* positioned chlorines but no overall change in the total number of *ortho* chlorines. By the end of 51 weeks, the remaining flanked *ortho* chlorines were as low as 0.07 ± 0.01 and 0.06 ± 0.00 in G-1-Fe and G-2-Fe, respectively, suggesting almost all *ortho* chlorines were unflanked at the end of the study. These findings were consistent with those observed in G-1 and G-2 (Xu et al., 2016),

indicating the effect of FeOOH on the shifts of OCPBs was very limited.

Meta dechlorination was preferred but PCB composition dependent. The initial MCPB values for both mixtures were similar (see in **Figures 3C,D**). After 51 weeks of incubation, MCPB values declined from 1.59 ± 0.00 to 0.39 ± 0.18 in G-1-Fe and from 1.50 ± 0.00 to 0.16 ± 0.01 in G-2-Fe. Approximately 80–90% of *meta* chlorines were removed and the declining trends suggest a further *meta* chlorination potential. Compared with G-1 (0.16 ± 0.05 at Week 51) and G-2 (0.17 ± 0.01 at Week 51), the inhibitory effect of supplementary FeOOH was relatively limited. The *meta* dechlorination rates in the rapid phase of G-1-Fe (9–24 weeks) and G-2-Fe (6–30 weeks) were 0.056 ± 0.002 Cl/week and 0.051 ± 0.002 Cl/week, respectively, which exceeded the corresponding rapid phase *meta* dechlorination rates in G-1 (0.043 ± 0.004 Cl/week) and G-2 (0.043 ± 0.002 Cl/week). Seen in **Figures 3C,D**, unflanked *meta* chlorines increased in the first 30–36 weeks, then decreased slightly (solid triangle). Due to the lack of *ortho* removal before 36 weeks, the accumulated unflanked *meta* chlorines could be attributed to the dechlorination of single-/double-flanked *para* chlorines, where *ortho* chlorine was absent for the target phenyl ring. The maximum unflanked *meta* chlorines per biphenyl for G-1-Fe (0.34 ± 0.04 at Week 36) were much higher than those for G-1 (0.18 ± 0.01 at Week 30), indicating a partially inhibitory effect for the unflanked *meta* dechlorination. But in G-2-Fe and G-2, the maximum unflanked *meta* chlorines per biphenyl were similar (0.14 ± 0.03 for G-2-Fe; 0.13 ± 0.01 for G-2). Thereafter, the slightly decreased unflanked *meta* chlorines were the result of dechlorination of unflanked *meta* chlorines. Similarly, the declining of *ortho*-flanked *meta* chlorines (open square) was caused by removal of *meta* chlorines. By comparing the reduction rates of *ortho*-flanked *meta* chlorines and *meta*-flanked *ortho* chlorines in the rapid phase (9–24 weeks in G-1-Fe and 6–24 weeks in G-2-Fe), *meta*-flanked *ortho* chlorines (0.035 ± 0.002 Cl/week for G-1-Fe, 0.035 ± 0.001 Cl/week for G-2-Fe) decreased faster than *ortho*-flanked *meta* chlorines (0.021 ± 0.003 Cl/week for G-1-Fe; 0.021 ± 0.001 Cl/week for G-2-Fe), suggesting *meta* dechlorination attacked both *ortho*-flanked and double-flanked *meta* chlorines. Moreover, the shifts of the sub *meta* chlorine groups illustrated that overall *meta* dechlorination was mainly due to the reduction of *para*-flanked *meta* chlorines (solid diamond) rather than *ortho*-flanked *meta* or double-flanked *meta*. Also, this confirmed the *meta* dechlorination preference when *meta* chlorines were *para*-flanked. In general, *meta* dechlorination was prevalent in FeOOH-amended Grasse sediment microcosms, and *para*-flanked, *ortho*-flanked, and double-flanked *meta*, as well as relatively limited unflanked *meta*, were all targeted.

Compared to *meta* chlorination, *para* dechlorination was less extensive in FeOOH-amended Grasse sediment microcosms; approximately 30–40% of *para* chlorines were removed (**Figures 3C–F**). In G-1-Fe, from Week 9 to Week 36, averaged *para* dechlorination rate was 0.013 ± 0.001 Cl/week, while in G-2-Fe, from Week 6 to Week 36, the rate was 0.007 ± 0.000 Cl/week. From Week 36 to Week 51, PCBP values for G-1-Fe remained at approximately 0.88, whereas the values for G-2-Fe decreased from 0.88 ± 0.13 to 0.68 ± 0.02. Meanwhile, the unflanked *para* per biphenyl values remained at around 0.80 for G-1-Fe, and declined from 0.80 ± 0.02 to 0.64 ± 0.02 for G-2-Fe. Compared with non-FeOOH-amended G-1 and G-2, 75 and 80% of *para* chlorines were removed and the remaining unflanked *para* chlorines per biphenyl were only 0.32 ± 0.04 and 0.18 ± 0.01 after 51 weeks of incubation. These results suggest that (1) the remaining *para* chlorines were predominantly unflanked after a long time of incubation in G-1-Fe and G-2-Fe; (2) the inhibitory effect of FeOOH on PCB dechlorination was solely due to the loss of *para* dechlorinating activities targeting unflanked *para*. The unflanked *para* dechlorination resumed in G-2-Fe after 36 weeks of incubation but not in G-1-Fe, suggesting that PCB composition affected dechlorination preferences. Seen in **Figures 3E,F**, the reduction rates of single-flanked *para* chlorines (open square) (0.047 ± 0.001 Cl/week from Week 9 to Week 24 for G-1-Fe, 0.033 ± 0.001 Cl/week from Week 6 to Week 24 for G-2-Fe) were three to four times faster than the overall *para* removal rates shown above. Along with the reduction of single-flanked *para* chlorines, unflanked *para* (solid triangle) increased rapidly at rates 0.035 ± 0.001 Cl/week, 0.031 ± 0.002 Cl/week in the same time periods for G-1-Fe and G-2-Fe, respectively. This suggests *para* dechlorination preferred flanked *para* chlorines, but *meta* removal was more prevalent for PCBs with a single *meta* and *para* chlorine on the same phenyl ring. In addition, double-flanked *para* chlorines, although not dominant in either mixture decreased over time, where *para* and *meta* dechlorination both occurred.

Quantification of Putative PCB Dechlorinating Bacteria and Fe(III)-Reducing Bacteria

The copy numbers of 16S rRNA genes of putative PCB dechlorinating bacteria *Dehalococcoides* over time are plotted in **Figure 4**. Initially, *Dehalococcoides* 16S rRNA genes in the Grasse sediment were one order of magnitude higher than those in the Hudson sediment. In H-1-Fe and H-2-Fe, no increase of *Dehalococcoides* 16S rRNA genes was observed over the course of incubation and the concentrations remained below 1.5×10^5 copies/ml, which was the minimum *Dehalococcoides* 16S rRNA gene number found in H-1 and H-2 showing dechlorination activities. This suggests that the complete inhibition of PCB dechlorination in the FeOOH-amended Hudson sediment microcosms was very likely due to the lack of active *Dehalococcoides*. By contrast, G-1-Fe and G-2-Fe showed clear increasing trends of *Dehalococcoides* 16S rRNA genes over time. The *Dehalococcoides* 16S rRNA genes increased from $2.4 \times 10^6 \pm 1.2 \times 10^5$ to $9.2 \times 10^7 \pm 3.1 \times 10^6$ copies/ml in G-1-Fe and from $1.8 \times 10^6 \pm 2.5 \times 10^5$ to $1.1 \times 10^8 \pm 3.1 \times 10^6$ copies/ml in G-2-Fe. The supplementary FeOOH led to 5–10 times more *Dehalococcoides* 16S rRNA genes than observed in G-1 and G-2. The high *Dehalococcoides* 16S rRNA genes found at Week 51 indicate a potential of continuing dechlorination in G-1-Fe and G-2-Fe. The relative abundance of *Dehalococcoides* in G-1-Fe and G-2-Fe expressed as the averaged percentage

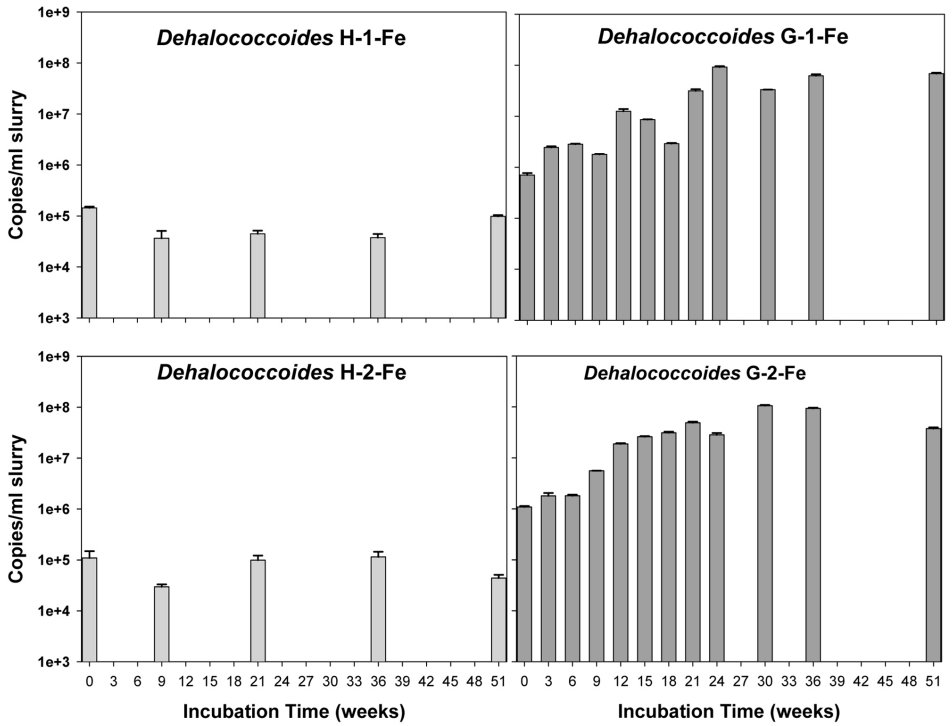

FIGURE 4 | Quantitative assessment of *Dehalococcoides* 16S rRNA genes in H-1-Fe, G-1-Fe, and H-2-Fe, G-2-Fe. All data points averaged duplicate tests. Error bars represent standard deviation.

of *Dehalococcoides* 16S rRNA genes in total *Bacteria* 16S rRNA genes is shown in **Figure 5**. The relative percentage of *Dehalococcoides* 16S rRNA genes increased from 0.2 to 2.5% in G-1-Fe and from 0.2 to 2.6% in G-2-Fe, while in G-1 and G-2, the percentage increased to around 1.0%. The addition of FeOOH enhanced not only the *Dehalococcoides* 16S rRNA gene numbers but also the relative abundance of *Dehalococcoides* in the microbial community. The *o*-17/DF-1 16S rRNA genes were much lower than those of *Dehalococcoides* and the relative abundance of *o*-17/DF-1 did not show any increase in G-1-Fe and G-2-Fe (data not shown). Thus, the *ortho* dechlorination activity observed in the Grasse sediment microcosms was likely associated with other unknown *ortho* dechlorinating organisms. Geobacteraceae 16S rRNA genes were from $2.5 \times 10^5 \pm 4.8 \times 10^4$ to $2.0 \times 10^6 \pm 5.3 \times 10^3$ copies/ml in H-1-Fe and H-2-Fe, while significantly higher Geobacteraceae 16S rRNA genes ($5.5 \times 10^5 \pm 1.3 \times 10^4$ to $1.1 \times 10^7 \pm 4.3 \times 10^5$ copies/ml) were found in control group H ($p < 0.01$). Additionally, Geobacteraceae 16S rRNA genes in H-1-Fe/H-2-Fe had no significant differences with those in H-1/H-2 ($p > 0.05$). These indicate that there was no Geobacteraceae enrichment by the addition of FeOOH. The low Geobacteraceae level could explain the weak Fe(III) reduction observed in H-1-Fe and H-2-Fe. Meanwhile, Geobacteraceae 16S rRNA genes detected in the Grasse sediment microcosms remained one to three orders of magnitude higher than those in the Hudson sediment microcosms (data not shown). Notably, the addition of FeOOH did not further stimulate the growth of Geobacteraceae.

Supplementary Carbon Sources and *Ortho* Dechlorination Enhancement

In the Hudson sediment microcosms amended with FeOOH, supplementary acetate or the fatty acid mixture led to extensive methanogenesis after the second addition at Week 36 (Supplementary Table S6). Along with the generation of CH_4, enhanced reduction of Fe(III) was observed in carbon-amended microcosms at Week 36 and Week 51 for H-1-Fe and at Week 51 only for the fatty acid mixture amended H-2-Fe (Supplementary Figure S7). Notably, PCB dechlorination was observed after the addition of carbon sources. **Table 3** shows the mass concentrations of total parent PCB concentrations at Week 36 and Week 51. By the end of 51 weeks, total parent PCBs were reduced by 3–20% on the average of triplicate microcosms with two carbon sources additions (incubating with carbon sources from Week 27 to Week 51). The fatty acid mixture and sole acetate additions both reinitiated PCB dechlorination in H-1-Fe and H-2-Fe. The dominant pathways included PCB 5(23-CB) to PCB 1(2-CB), PCB 12(34-CB) to PCB 2(3-CB) and PCB 3(4-CB), and PCB 64(236-4-CB) to PCB 32(26-4-CB). Flanked *meta* and flanked *para* dechlorination took place first. However, 16S rRNA genes of *Dehalococcoides* and *o*-17/DF-1 did not increase apparently in H-1-Fe and H-2-Fe when PCB dechlorination occurred after the supplementation of carbon sources, indicating the existence of other PCB dechlorinating organisms not closely related to *Dehalococcoides* or *o*-17/DF-1 (data not shown). Additionally, it was possible that biogenic Fe(II) also induced

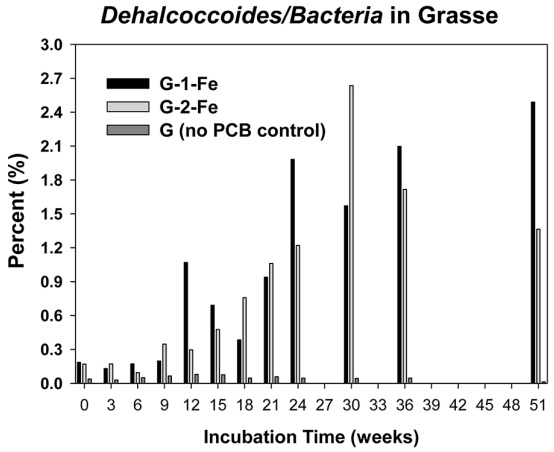

FIGURE 5 | Relative abundance of *Dehalococcoides* 16S rRNA genes in total *Bacteria* 16S rRNA genes of G-1-Fe, G-2-Fe, and G.

abiotic dechlorination. In contrast, the additions of carbon sources did not facilitate further dechlorination in H-1 or H-2 (Supplementary Table S7).

The supplementation of carbon sources into FeOOH-amended Grasse sediment microcosms did not significantly enhance overall dechlorination by re-initiating unflanked *para* dechlorination activity. However, it did favor the reduction of parent PCBs (**Table 3**). The reduction was more apparent for the highly chlorinated parent PCB congeners, indicating a relatively high carbon source-dependence for these congeners. Surprisingly, rare *ortho* dechlorination, targeting PCB congeners with exclusive unflanked *ortho* chlorines, was apparently enhanced by the addition of acetate or the fatty acid mixture in both G-1 and G-1-Fe (congener-specific concentrations provided in Supplementary Tables S8, S9). *Ortho* dechlorination products, which were only detected at Week 51 in G-1 and G-1-Fe without additional carbon sources, appeared 15 weeks ahead with carbon source addition. The enhancement was relatively weak in G-1 (see Supplementary Material). By contrast, in the triplicate acetate/fatty acid mixture amended G-1-Fe microcosms, PCB 13 and PCB 15 concentrations increased sharply from Week 36 to Week 51 (PCB 13 and PCB 15 were 15.0 $\pm$ 1.2, 7.0 $\pm$ 1.2 for acetate-amended G-1-Fe, 12.7 $\pm$ 5.0, 10.1 $\pm$ 5.0 for fatty acid mixture-amended G-1-Fe at Week 51) and no significant difference of the concentrations of *ortho* dechlorination products was observed by adding two carbon sources (Supplementary Table S9). Moreover, a rough mass balance could be obtained by the transformation of PCB 25 to PCB 13 and PCB 28 to PCB 15 between Week 36 and Week 51, where PCB 105, PCB 114, and their first and second generation dechlorination products were very low (see text in Supplementary Material and Supplementary Table S9). By the end of the incubation, in the G-1-Fe microcosms with carbon sources, *ortho* dechlorination products PCB 13 and PCB 15 accounted for 10–15% of the total PCB molar, which were over five times higher than those in the regular G-1-Fe microcosms without extra carbon sources. These findings suggest the similar enhancement ability of acetate or the fatty acid mixture and further confirmed the existence of *ortho* dechlorination pathways in Grasse River sediment. However, the 16S rRNA gene numbers of *Dehalococcoides* and *o*-17/DF-1 in the microcosms with carbon sources did not change significantly comparing with the microcosms without carbon source addition (data not shown). In addition, Fe(II) analysis in the FeOOH-amended Grasse sediment microcosms with supplementary carbon sources showed that no further Fe(III) reduction was induced. This further confirmed that Fe(III) reduction had completed prior to the addition of carbon sources. The supplementation of carbon sources stimulated prevalent methane production. The fatty acid mixture induced more methane production than did the addition of acetate alone (Supplementary Figure S1 and Supplementary Table S6).

DISCUSSION

Impact of Indigenous Sediment Properties and PCB Composition Under Fe(III)-Reducing Condition

Many studies suggested that the dechlorination of PCBs was controlled by their sediment geochemical properties and/or microbial species (Wiegel and Wu, 2000; Yan et al., 2006; Park et al., 2011; Payne et al., 2012). This is the first observation of complete dechlorination inhibition in Fe(III)-amended Hudson sediment. A previous study had reported that 50 mM FeOOH reduced dechlorination by 12% in enriched cultures of sediment collected from a different location in the Hudson River (Morris et al., 1992). Due to the lack of sediment property characterization in that study, the difference is difficult to explain. The relatively low background Fe concentration (approximately 19 mmole/kg slurry), low Geobacteraceae and slow Fe(III) reduction observed in our Hudson sediment suggest poor acclimation to high Fe concentration, resulting in complete inhibition of PCB dechlorination and methanogenesis in FeOOH-amended Hudson sediment microcosms. In the Fe(III)-amended Grasse sediment microcosms, there was a 20–30% reduction of overall dechlorination in a time course of 51 weeks compared to the non-FeOOH-amended Grasse sediment microcosms, mainly due to less *para* dechlorination. The high background Fe content (approximately 64 mmole/kg slurry), abundant Geobacteraceae and fast Fe(III) reduction suggest good capability for reducing competing electron acceptor and easy resumption of PCB dechlorination. Additionally, our previous study showed that *para* dechlorination in the high Fe content Grasse sediment (G-1, G-2) was slower than that in the low Fe content Hudson sediment (H-1, H-2) in the rapid phase (Xu et al., 2016). These results suggest that indigenous Fe content could profoundly influence dechlorination preferences. Also, FeOOH further slowed down *para* dechlorination, but facilitated *meta* dechlorination in the rapid phase of G-1-Fe and G-2-Fe, indicating that *meta*/*para* dechlorination activities might be competing with each other and Fe(III) was likely a controlling factor. Moreover, PCB composition, even with four identical PCB

TABLE 3 | Total parent PCB concentrations (mg/kg slurry) of the FeOOH-amended sediment microcosms with/without additional carbon sources.

Sediment	Incubation Time	PCB *Mixture 1*			PCB *Mixture 2*		
		No Carbon	Acetate	Fatty Acid Mix	No Carbon	Acetate	Fatty Acid Mix
Hudson	36 weeks	49.1 ± 0.1[a]	49.1 ± 0.3	48.9 ± 0.2	49.0 ± 0.1	49.1 ± 0.1	45.9 ± 5.3[b]
	51 weeks	48.9 ± 0.2	42.3 ± 4.3	46.8 ± 0.1	49.0 ± 0.2	47.6 ± 0.3	40.2 ± 11.1[b]
Grasse	36 weeks	2.97 ± 0.41	2.10 ± 0.13	2.10 ± 0.04	2.27 ± 0.19	2.00 ± 0.22	2.08 ± 0.15
	51 weeks	2.28 ± 0.41	0.98 ± 0.03	1.00 ± 0.07	1.34 ± 0.05	1.08 ± 0.07	1.12 ± 0.06

[a]*Data were present by mean ± standard deviation.* [b]*Dechlorination was very prevalent in one of the triplicate microcosms. PCB, polychlorinated biphenyl.*

congeners, the same total concentrations, and similar chlorine contents, was found to significantly affect PCB dechlorination in FeOOH-amended Grasse sediment microcosms. PCB *Mixture 2* favored the dechlorination of PCB 5, 12, 64, 71, and 170. This trend was found in non-FeOOH-amended G-1 and G-2, suggesting the addition of FeOOH did not alter the composition related dechlorination preferences. These findings might be explained by co-metabolism or halopriming effect in a mixture (Krumins et al., 2009; Fagervold et al., 2011; Xu et al., 2016). FeOOH, especially freshly precipitated FeOOH, has high specific surface area and thus can absorb significant amount of pollutants in sediment and soil (Herbich, 2000; Okkenhaug et al., 2013). In this study, freshly prepared FeOOH was introduced directly into the sediment microcosms and the microcosms were incubated statically. Therefore, it was likely that PCBs adsorbed on the sediment particles aggregated on FeOOH. Along with the reduction of Fe(III), there may have been more bioavailable PCBs in the niches, where prevalent Fe(III)-reducing bacteria as well as related PCB dechlorinators were expected. In addition, biogenic Fe(II), mostly as adsorbed Fe(II), was likely to contribute to PCB dechlorination (Watson et al., 2002; Gong et al., 2016; Liu et al., 2017). This hypothesis was partially supported by the observation that more hydrophobic PCB congeners (highly chlorinated PCB 144, 149, 153, 170, and coplanar PCB 105, 114) exhibited more rapid dechlorination when FeOOH was added. A previous study demonstrated enhanced PCB dechlorination following Processes M and Q with the addition of $FeSO_4$ in Hudson River sediment and proposed the beneficial effect caused by precipitation of toxic sulfide by Fe^{2+} (Zwiernik et al., 1998). However, the dechlorination induced by FeS could not be excluded (Watson et al., 2002). $FeCl_2$ without sulfate was also found to favor PCB dechlorination (Zwiernik et al., 1998). This further suggested that Fe(II) might be a reductant for chemical dechlorination. Generally, the mineral reactivity of dechlorination of chlorinated solvents was disorder FeS > FeS > FeS_2 > sorbed Fe^{2+} (He et al., 2015). This indicates that the influences of Fe(II)-containing minerals on PCB dechlorination might be complicated.

Putative PCB Dechlorinators and Fe(III) Reducers

Although exhibiting less extensive dechlorination, FeOOH-amended Grasse sediment microcosms showed an increase of *Dehalococcoides* 16S rRNA genes when compared with non-FeOOH-amended Grasse sediment microcosms. This indicates complex interactions between Fe(III)-reduction and *Dehalococcoides* growth. The possible mechanistic explanation is that some Fe(III) reducers within the Genus *Geobacter* of the Family Geobacteraceae, like *Geobacter sulfurreducens*, are involved in H_2 generation in cooperation with hydrogen-oxidizing microorganisms or produce H_2 via fermentation. H_2 is believed to be the preferred electron donor for *Dehalococcoides* (Cord-Ruwisch et al., 1998; He et al., 2003, 2005; Wei and Finneran, 2011; Zanaroli et al., 2012b; Karatas et al., 2014). Enrichment of *Dehalococcoides* has been reported during dechlorination of chlorinated solvents under Fe(III)-reducing conditions (Wei and Finneran, 2011). Moreover, two known Fe(III)-reducing bacteria, *Geobacter thiogenes* strain K and *Geobacter lovleyi* strain SZ were capable of utilizing organohalides as their terminal electron acceptors for energy conservation and growth (Sung et al., 2006), and more recently, indirect evidence linking PCB dechlorination with Geobacteraceae was reported, although *D. mccartyi* was still considered as the main dechlorinators (Praveckova et al., 2016). These reports suggest complex dechlorination mechanisms in the presence of Fe(III) in addition to the potential for competition for electron donors. Geobacteraceae were not stimulated in Fe(III)-amended Grasse sediments, suggesting that electron acceptor Fe(III) was no longer the limiting factor in the Fe rich sediment. Similar findings were reported in Fe rich sediment from South China (Liu et al., 2017).

Carbon Source and *Ortho* Dechlorination Enhancement

A previous study demonstrated that repeated addition of fatty acids (acetate, propionate, butyrate, and hexanoic acid) stimulated PCB dechlorination in carbon-limiting Hudson sediment, but not in high carbon content New Bedford Harbor and Silver Lake sediments.(Alder et al., 1993) In the present study, the influences of auxiliary carbon sources on PCB dechlorination were also sediment dependent. For the relatively low carbon and low Fe Hudson sediment, the addition of acetate or the fatty acid mixture did not enhance the overall dechlorination in H-1 and H-2 (under methanogenic conditions). This might be due to the experimental dechlorination limit observed as a flat plateau phase after 30 weeks. On the other hand, the addition of carbon sources led to the resumption of PCB dechlorination in FeOOH-amended microcosms (H-1-Fe and H-2-Fe, no methanogenesis activity before carbon sources addition),

suggesting the effective compensation of the extra "electron donor demand" derived from Fe(III) (Wei and Finneran, 2011). For the relatively higher carbon content and high Fe Grasse sediment, the addition of acetate or the fatty acid mixture did not enhance the overall dechlorination rate and extent in all the sediment microcosms (G-1, G-2, G-1-Fe, and G-2-Fe), where methanogenesis was remained. However, auxiliary carbon sources apparently shortened the lag time for *ortho* dechlorination and greatly favored *ortho* removal in G-1-Fe. These results indicate that the impact of carbon source was not only controlled by the sediment background carbon content, but also by the other geochemical properties, such as Fe(III).

This work provides the first observation of *ortho* dechlorination enhancement by auxiliary carbon sources (acetate or a fatty acid mixture). The isolated *ortho* dechlorinators *o*-17 is known as an acetate-utilizing bacterium (Cutter et al., 2001; May et al., 2006; Fagervold et al., 2011). It is expected that the *ortho* dechlorinating bacteria in this study are also utilizing acetate as their electron donor and carbon source. As there was no significant difference for the enhancement of *ortho* removal in acetate-amended and the fatty acid mixture-amended microcosms, acetate was not likely the obligate carbon source in this Grasse sediment. Most previous studies observed *ortho* dechlorination capable of dechlorinating PCBs with two or more *ortho* chlorines (Vandort and Bedard, 1991; Pulliam Holoman et al., 1998; Cutter et al., 2001; May et al., 2006; Fagervold et al., 2011; Kjellerup et al., 2014). *O*-17, isolated from Baltimore Harbor marine sediment preferentially dechlorinates *meta*-flanked *ortho* chlorine when the *meta* chlorine is only *ortho*-flanked and the target PCB congener contains two to three *ortho* chlorines, such as PCB 65(2356-CB) and PCB 90(235-24-CB) (May et al., 2006; Fagervold et al., 2007, 2011). Although PCB 65 was ultimately dechlorinated to PCB 14(35-CB) with PCB 23(235-CB) as an intermediate, the *ortho* dechlorination activity was not sustained when only PCB 23 was spiked, indicating *o*-17 lacks *ortho* dechlorination activity for mono-*ortho* substituted PCBs (May et al., 2006). Another marine sediment from Hunters Point California, in which a fatty acid mixture of acetate, propionate and butyrate was added, exhibited *ortho* removal targeting PCB 116(23456-CB) (*meta* chlorines are double-flanked) and the only dechlorination product was PCB 14(35-CB), indicating a stepwise reduction of two *ortho* chlorines.(Kjellerup et al., 2014) *Ortho* dechlorination observed in two freshwater sediments (Silver Lake and Woods Pond) without auxiliary carbon source, attacked unflanked *ortho* chlorine on PCB 30(246-CB) (Williams, 1994). Our previous study also revealed unflanked *ortho* dechlorination activity on PCB 28(24-4-CB) and PCB 25(24-3-CB) in Grasse River sediment without auxiliary carbon source (Xu et al., 2016). In the present study, the single unflanked *ortho* chlorine removal activity was maintained under Fe(III)-reducing conditions despite no change in known *ortho* dechlorinating organism populations. This further supports the existence of distinct *ortho* dechlorinating organisms in Grasse River sediment. Also, an easy approach to selectively enhance *ortho* dechlorination was provided. Most recently, a study in Grasse River sediment microcosms focusing on Aroclor 1254 detoxification used dioxin-like PCB 105 as a test congener, in which PCB 28 and PCB 25 were also the dominant dechlorination products after 180 days (Kaya et al., 2017). Therefore, the *ortho* dechlorination preference with the potential for complete dechlorination of mono-*ortho* PCB congeners, including some dioxin-like congeners, might be crucial for further potential risk reduction in Grasse sediment.

CONCLUSION

The amendment with FeOOH greatly affected PCB dechlorination and the influences were largely controlled by the indigenous differences in sediment. Generally, the low carbon content and low Fe Hudson sediment showed complete inhibition for PCB dechlorination after adding FeOOH, while the relatively high carbon content and high Fe Grasse sediment showed moderate inhibition in the presence of FeOOH. The dechlorination preferences analysis revealed that *para*-flanked *meta* dechlorination was primarily preferred followed by *ortho*-/double-flanked *meta* dechlorination and single-/double-flanked *para* dechlorination in Grasse sediment and the partially inhibitory effect was caused by the loss of unflanked *para* removal activity. Despite the longer lag time observed in the FeOOH-amended Grasse sediment microcosms, Fe(III) reduction and PCB reduction were found to take place concurrently. Rare *ortho* dechlorination pathways were confirmed in FeOOH-amended Grasse sediment microcosms. Auxiliary carbon sources (acetate, or a fatty acid mixture with acetate, propionate and butyrate) could reinitiate dechlorination in FeOOH-amended Hudson sediment microcosms, as well as support the favored *ortho* dechlorination in FeOOH-amended Grasse microcosms, indicating the utilization of acetate and/or fatty acids for *ortho* dechlorination related microorganisms in Grasse sediment.

AUTHOR CONTRIBUTIONS

YX has conducted the experiments, analyzed data, and prepared the manuscript. KG has written the manuscript. JV has conceived and led the project and finalized the manuscript. All authors approved the current version of the manuscript.

FUNDING

The work was funded by U.S. Department of Defense, Strategic Environmental Research and Development Program (SERDP) through the Environmental Restoration Program (Grant No. ER-1495), the National Natural Science Foundation of China (Grant Nos. 41671468 and 41301546), the Natural Science Foundation of Jiangsu Province (Grant No. BK20171356), State Key Laboratory of Pollution Control and Resource Reuse (Grant No. PCRRF16018), the Priority Academic Program Development of Jiangsu Higher Education Institutions and the Fundamental Research Funds for the Central Universities.

ACKNOWLEDGMENTS

The authors are grateful to collaborators at The Aluminum Company of America (ALCOA) for their kind support in provision of sediments.

SUPPLEMENTARY MATERIAL

The Supplementary Material for this article can be found online at: https://www.frontiersin.org/articles/10.3389/fmicb.2018.01574/full#supplementary-material

REFERENCES

Adrian, L., Dudkova, V., Demnerova, K., and Bedard, D. L. (2009). *Dehalococcoides* sp strain CBDB1 extensively dechlorinates the commercial polychlorinated biphenyl mixture Aroclor 1260. *Appl. Environ. Microbiol.* 75, 4516–4524. doi: 10.1128/aem.00102-09

Alder, A. C., Haggblom, M. M., Oppenhelmer, S. R., and Young, L. Y. (1993). Reductive dechlorination of polychlorinated-biphenyls in anaerobic sediments. *Environ. Sci. Technol.* 27, 530–538. doi: 10.1021/es00040a012

Bedard, D. L., and Quensen, J. F. (1995). "Microbial reductive dechlorination of polychlorinated biphenyls," in *Microbial Transformation and Degradation of Toxic Organic Chemicals*, eds L. Y. Young and G. E. Cerniglia (New York, NY: Wiley-Liss, Inc.), 127–216.

Bedard, D. L., Pohl, E. A., Bailey, J. J., and Murphy, A. (2005). Characterization of the PCB substrate range of microbial dechlorination process LP. *Environ. Sci. Technol.* 39, 6831–6838. doi: 10.1021/es050255i

Brown, J. F., Bedard, D. L., Brennan, M. J., Carnahan, J. C., Feng, H., and Wagner, R. E. (1987). Polychlorinated biphenyl dechlorination in aquatic sediments. *Science* 236, 709–712. doi: 10.1126/science.236.4802.709

Chen, M. J., Tong, H., Liu, C. S., Chen, D. D., Li, F. B., and Qiao, J. T. (2016). A humic substance analogue AQDS stimulates *Geobacter* sp abundance and enhances pentachlorophenol transformation in a paddy soil. *Chemosphere* 160, 141–148. doi: 10.1016/j.chemosphere.2016.06.061

Cho, Y. C., and Oh, K. H. (2005). Effects of sulfate concentration on the anaerobic dechlorination of polychlorinated biphenyls in estuarine sediments. *J. Microbiol.* 43, 166–171.

Cord-Ruwisch, R., Lovley, D. R., and Schink, B. (1998). Growth of *Geobacter sulfurreducens* with acetate in syntrophic cooperation with hydrogen-oxidizing anaerobic partners. *Appl. Environ. Microbiol.* 64, 2232–2236.

Cummings, D. E., Snoeyenbos-West, O. L., Newby, D. T., Niggemyer, A. M., Lovley, D. R., Achenbach, L. A., et al. (2003). Diversity of geobacteraceae species inhabiting metal-polluted freshwater lake sediments ascertained by 16S rDNA analyses. *Microb. Ecol.* 46, 257–269. doi: 10.1007/s00248-002-0005-8

Cutter, L., Sowers, K. R., and May, H. D. (1998). Microbial dechlorination of 2,3,5,6-tetrachlorobiphenyl under anaerobic conditions in the absence of soil or sediment. *Appl. Environ. Microbiol.* 64, 2966–2969.

Cutter, L. A., Watts, J. E. M., Sowers, K. R., and May, H. D. (2001). Identification of a microorganism that links its growth to the reductive dechlorination of 2,3,5,6-chlorobiphenyl. *Envrion. Microbiol.* 3, 699–709. doi: 10.1046/j.1462-2920.2001.00246.x

Edwards, U., Rogall, T., Blocker, H., Emde, M., and Bottger, E. C. (1989). Isolation and direct complete nucleotide determination of entire genes. Characterization of a gene coding for 16S ribosomal RNA. *Nucleic Acids Res.* 17, 7843–7853. doi: 10.1093/nar/17.19.7843

EPA (1997). *Phase II Reassessment: Data Evaluation and Interpretation Report for the Hudson River PCB Superfund Site*. Washington, DC: EPA.

Fagervold, S. K., May, H. D., and Sowers, K. R. (2007). Microbial reductive dechlorination of Aroclor 1260 in Baltimore Harbor sediment microcosms is catalyzed by three phylotypes within the phylum Chloroflexi. *Appl. Environ. Microbiol.* 73, 3009–3018. doi: 10.1128/aem.02958-06

Fagervold, S. K., Watts, J. E. M., May, H. D., and Sowers, K. R. (2011). Effects of bioaugmentation on indigenous PCB dechlorinating activity in sediment microcosms. *Water Res.* 45, 3899–3907. doi: 10.1016/j.watres.2011.04.048

Fennell, D. E., Nijenhuis, I., Wilson, S. F., Zinder, S. H., and Haggblom, M. M. (2004). *Dehalococcoides ethenogenes* strain 195 reductively dechlorinates diverse chlorinated aromatic pollutants. *Environ. Sci. Technol.* 38, 2075–2081. doi: 10.1021/es034989b

Gong, Y. Y., Tang, J. C., and Zhao, D. Y. (2016). Application of iron sulfide particles for groundwater and soil remediation: a review. *Water Res.* 89, 309–320. doi: 10.1016/j.watres.2015.11.063

He, J., Sung, Y., Krajmalnik-Brown, R., Ritalahti, K. M., and Loffler, F. E. (2005). Isolation and characterization of *Dehalococcoides* sp strain FL2, a trichloroethene (TCE)- and 1,2-dichloroethene-respiring anaerobe. *Environ. Microbiol.* 7, 1442–1450. doi: 10.1111/j.1462-2920.2005.00830.x

He, J. Z., Ritalahti, K. M., Aiello, M. R., and Loffler, F. E. (2003). Complete detoxification of vinyl chloride by an anaerobic enrichment culture and identification of the reductively dechlorinating population as a *Dehalococcoides* species. *Appl. Environ. Microbiol.* 69, 996–1003. doi: 10.1128/aem.69.2.996-1003.2003

He, Y. T., Wilson, J. T., Su, C., and Wilkin, R. T. (2015). Review of abiotic degradation of chlorinated solvents by reactive iron minerals in aquifers. *Ground Water Monit. Remediat.* 35, 57–75. doi: 10.1111/gwmr.12111

Herbich, J. B. (2000). *Handbook of Dredging Engineering*, 2nd Edn. New York City, NY: McGraw-Hill Professional.

Himmelheber, D. W., Thomas, S. H., Loffler, F. E., Taillefert, M., and Hughes, J. B. (2009). Microbial colonization of an in situ sediment cap and correlation to stratified redox zones. *Environ. Sci. Technol.* 43, 66–74. doi: 10.1021/es801834e

Ho, C. H., and Liu, S. M. (2012). Impact of coplanar PCBs on microbial communities in anaerobic estuarine sediments. *J. Environ. Sci. Health B* 45, 437–448. doi: 10.1080/03601231003800172

Hughes, A. S., Vanbriesen, J. M., and Small, M. J. (2010). Identification of structural properties associated with polychlorinated biphenyl dechlorination processes. *Environ. Sci. Technol.* 44, 2842–2848. doi: 10.1021/es902109w

IARC Monographs (2016). "Polychlorinated biphenyls and polybrominated biphenyls," in *IARC Monographs on the Evaluation of Carcinogenic Risks to Humans* (Lyon: International Agency for Research on Cancer).

Jeong, H. Y., Anantharaman, K., Han, Y. S., and Hayes, K. F. (2011). Abiotic reductive dechlorination of cis-dichloroethylene by Fe species formed during iron- or sulfate-reduction. *Environ. Sci. Technol.* 45, 5186–5194. doi: 10.1021/es104387w

Karatas, S., Hasar, H., Taskan, E., Ozkaya, B., and Sahinkaya, E. (2014). Bio-reduction of tetrachloroethen using a H-2-based membrane biofilm reactor and community fingerprinting. *Water Res.* 58, 21–28. doi: 10.1016/j.watres.2014.03.053

Karcher, S. C., Small, M. J., and Vanbriesen, J. M. (2004). Statistical method to evaluate the occurrence of PCB transformations in river sediments with application to Hudson River data. *Environ. Sci. Technol.* 38, 6760–6766. doi: 10.1021/es0494149

Kaya, D., Imamoglu, I., Sanin, F. D., Payne, R. B., and Sowers, K. R. (2017). Potential risk reduction of Aroclor 1254 by microbial dechlorination in anaerobic Grasse River sediment microcosms. *J. Hazard. Mater.* 321, 879–887. doi: 10.1016/j.jhazmat.2016.10.009

Kjellerup, B. V., Naff, C., Edwards, S. J., Ghosh, U., Baker, J. E., and Sowers, K. R. (2014). Effects of activated carbon on reductive dechlorination of PCBs by organohalide respiring bacteria indigenous to sediments. *Water Res.* 52, 1–10. doi: 10.1016/j.watres.2013.12.030

Kjellerup, B. V., Sun, X. L., Ghosh, U., May, H. D., and Sowers, K. R. (2008). Site-specific microbial communities in three PCB-impacted sediments are associated with different in situ dechlorinating activities. *Envrion. Microbiol.* 10, 1296–1309. doi: 10.1111/j.1462-2920.2007.01543.x

Krumins, V., Park, J. W., Son, E. K., Rodenburg, L. A., Kerkhof, L. J., Haggblom, M. M., et al. (2009). PCB dechlorination enhancement in Anacostia River

sediment microcosms. *Water Res.* 43, 4549–4558. doi: 10.1016/j.watres.2009.08.003

Laroe, S. L., Fricker, A. D., and Bedard, D. L. (2014). *Dehalococcoides mccartyi* strain JNA in pure culture extensively dechlorinates Aroclor 1260 according to polychlorinated biphenyl (PCB) dechlorination Process N. *Environ. Sci. Technol.* 48, 9187–9196. doi: 10.1021/es500872t

Liu, X. P., Wan, H., Xue, Y. Z., Feng, C. H., and Wei, C. H. (2017). Addition of iron oxides in sediments enhances 2,3,4,5-tetrachlorobiphenyl (PCB 61) dechlorination by low-voltage electric fields. *RSC Adv.* 7, 26019–26027. doi: 10.1039/c7ra02849k

Lovley, D. R., and Phillips, E. J. P. (1986). Organic-matter mineralization with reduction of ferric iron in anaerobic sediments. *Appl. Environ. Microbiol.* 51, 683–689.

Lyall, K., Croen, L. A., Sjodin, A., Yoshida, C. K., Zerbo, O., Kharrazi, M., et al. (2017). Polychlorinated biphenyl and organochlorine pesticide concentrations in maternal mid-pregnancy serum samples: association with autism spectrum disorder and intellectual disability. *Environ. Health Perspect.* 125, 474–480. doi: 10.1289/ehp277

Matturro, B., Ubaldi, C., and Rossetti, S. (2016). Microbiome dynamics of a polychlorobiphenyl (PCB) historically contaminated marine sediment under conditions promoting reductive dechlorination. *Front. Microbiol.* 7:1502. doi: 10.3389/fmicb.2016.01502

May, H. D., Cutter, L. A., Miller, G. S., Milliken, C. E., Watts, J. E. M., and Sowers, K. R. (2006). Stimulatory and inhibitory effects of organohalides on the dehalogenating activities of PCB-dechlorinating bacterium o-17. *Environ. Sci. Technol.* 40, 5704–5709. doi: 10.1021/es052521y

Morris, P. J., Mohn, W. W., Quensen, J. F., Tiedje, J. M., and Boyd, S. A. (1992). Establishment of a polychlorinated biphenyl-degrading enrichment culture with predominantly meta dechlorination. *Appl. Environ. Microbiol.* 58, 3088–3094.

Muyzer, G., Dewaal, E. C., and Uitterlinden, A. G. (1993). Profiling of complex microbial populations by denaturing gradient gel electrophoresis analysis of polymerase chain reaction-amplified genes coding for 16S rRNA. *Appl. Environ. Microbiol.* 59, 695–700.

Okkenhaug, G., Amstatter, K., Bue, H. L., Cornelissen, G., Breedveld, G. D., Henriksen, T., et al. (2013). Antimony (Sb) contaminated shooting range soil: sb mobility and immobilization by soil amendments. *Environ. Sci. Technol.* 47, 6431–6439. doi: 10.1021/es302448k

Park, J. W., Krumins, V., Kjellerup, B. V., Fennell, D. E., Rodenburg, L. A., Sowers, K. R., et al. (2011). The effect of co-substrate activation on indigenous and bioaugmented PCB dechlorinating bacterial communities in sediment microcosms. *Appl. Microbiol. Biotechnol.* 89, 2005–2017. doi: 10.1007/s00253-010-2958-8

Paul, L., Herrmann, S., Koch, C. B., Philips, J., and Smolders, E. (2013). Inhibition of microbial trichloroethylene dechorination by Fe (III) reduction depends on Fe mineralogy: a batch study using the bioaugmentation culture KB-1. *Water Res.* 47, 2543–2554. doi: 10.1016/j.watres.2013.02.029

Payne, R. B., May, H. D., and Sowers, K. R. (2012). Enhanced reductive dechlorination of polychlorinated biphenyl impacted sediment by bioaugmentation with a dehalorespiring bacterium. *Environ. Sci. Technol.* 45, 8772–8779. doi: 10.1021/es201553c

Praveckova, M., Brennerova, M. V., Holliger, C., De Alencastro, F., and Rossi, P. (2016). Indirect evidence link PCB dehalogenation with Geobacteraceae in anaerobic sediment-free microcosms. *Front. Microbiol.* 7:933. doi: 10.3389/fmicb.2016.00933

Pulliam Holoman, T. R., Elberson, M. A., Cutter, L. A., May, H. D., and Sowers, K. R. (1998). Characterization of a defined 2,3,5,6-tetrachlorobiphenyl-ortho-dechlorinating microbial community by comparative sequence analysis of genes coding for 16S rRNA. *Appl. Environ. Microbiol.* 64, 3359–3367.

Quensen, J. F., Mousa, M. A., Boyd, S. A., Sanderson, J. T., Froese, K. L., and Giesy, J. P. (1998). Reduction of aryl hydrocarbon receptor-mediated activity of polychlorinated biphenyl mixtures due to anaerobic microbial dechlorination. *Environ. Toxicol. Chem.* 17, 806–813. doi: 10.1002/etc.5620170507

Safe, S. (1989). Polychlorinated-biphenyls (PCBs) - mutagenicity and carcinogenicity. *Mutat. Res.* 220, 31–47. doi: 10.1016/0165-1110(89)90007-9

Shelton, D. R., and Tiedje, J. M. (1984). General-method for determining anaerobic biodegradation potential. *Appl. Environ. Microbiol.* 47, 850–857.

Sorensen, J. (1982). Reduction of ferric iron in anaerobic, marine sediment and interaction with reduction of nitrate and sulfate. *Appl. Environ. Microbiol.* 43, 319–324.

Sowers, K. R., and May, H. D. (2013). In situ treatment of PCBs by anaerobic microbial dechlorination in aquatic sediment: are we there yet? *Curr. Opin. Biotechnol.* 24, 482–488. doi: 10.1016/j.copbio.2012.10.004

Sung, Y., Fletcher, K. F., Ritalaliti, K. M., Apkarian, R. P., Ramos-Hernandez, N., Sanford, R. A., et al. (2006). *Geobacter lovleyi* sp nov strain SZ, a novel metal-reducing and tetrachloroethene-dechlorinating bacterium. *Appl. Environ. Microbiol.* 72, 2775–2782. doi: 10.1128/aem.72.4.2775-2782.2006

UNEP (2001). *Stockholm Convention on Persistent Organic Pollutants (POPs)*. Nairobi: UNEP.

Vandort, H. M., and Bedard, D. L. (1991). Reductive ortho-dechlorination and meta-dechlorination of a polychlorinated biphenyl congener by anaerobic microorganisms. *Appl. Environ. Microbiol.* 57, 1576–1578.

Wang, S. Q., Chng, K. R., Wilm, A., Zhao, S. Y., Yang, K. L., Nagarajan, N., et al. (2014). Genomic characterization of three unique *Dehalococcoides* that respire on persistent polychlorinated biphenyls. *Proc. Natl. Acad. Sci. U.S.A.* 111, 12103–12108. doi: 10.1073/pnas.1404845111

Wang, S. Q., and He, J. Z. (2013). Phylogenetically distinct bacteria involve extensive dechlorination of Aroclor 1260 in sediment-free cultures. *PLoS One* 8:e59178. doi: 10.1371/journal.pone.0059178

Watson, J. H. P., Ellwood, D. C., Pavoni, B., Lazzari, L., and Sperni, L. (2002). *Degradation and Removal of Sediment PCBs Using Microbially Generated Iron Sulfide*. Columbus, OH: Battelle Press.

Watts, J. E. M., Fagervold, S. K., May, H. D., and Sowers, K. R. (2005). A PCR-based specific assay reveals a population of bacteria within the *Chloroflexi* associated with the reductive dehalogenation of polychlorinated biphenyls. *Microbiology* 151(Pt 6), 2039–2046. doi: 10.1099/mic.0.27819-0

Wei, N., and Finneran, K. T. (2011). Influence of ferric iron on complete dechlorination of trichloroethylene (TCE) to ethene: Fe(III) reduction does not always inhibit complete dechlorination. *Environ. Sci. Technol.* 45, 7422–7430. doi: 10.1021/es201501a

Wiegel, J., and Wu, Q. Z. (2000). Microbial reductive dehalogenation of polychlorinated biphenyls. *FEMS Microbiol. Ecol.* 32, 1–15. doi: 10.1111/j.1574-6941.2000.tb00693.x

Williams, W. A. (1994). Microbial reductive dechlorination of trichlorobiphenyls in anaerobic sediment slurries. *Environ. Sci. Technol.* 28, 630–635. doi: 10.1021/es00053a015

Wu, Q. Z., Watts, J. E. M., Sowers, K. R., and May, H. D. (2002). Identification of a bacterium that specifically catalyzes the reductive dechlorination of polychlorinated biphenyls with doubly flanked chlorines. *Appl. Environ. Microbiol.* 68, 807–812. doi: 10.1128/AEM.68.2.807-812.2002

Xu, Y., Gregory, K. B., and VanBriesen, J. M. (2016). Microbial-catalyzed reductive dechlorination of polychlorinated biphenyls in Hudson and Grasse River sediment microcosms: determination of dechlorination preferences and identification of rare ortho removal pathways. *Environ. Sci. Technol.* 50, 12767–12778. doi: 10.1021/acs.est.6b03892

Xu, Y., Yu, Y., Gregory, K. B., and VanBriesen, J. M. (2012). Comprehensive assessment of bacterial communities and analysis of PCB congeners in PCB-contaminated sediment with depth. *J. Environ. Eng.* 138, 1167–1178. doi: 10.1061/(asce)ee.1943-7870.0000595

Yan, T., LaPara, T. M., and Novak, P. J. (2006). The impact of sediment characteristics on polychlorinated biphenyl- dechlorinating cultures: implications for bioaugmentation. *Bioremediat. J.* 10, 143–151. doi: 10.1080/10889860601021381

Zanaroli, G., Balloi, A., Negroni, A., Borruso, L., Daffonchio, D., and Fava, F. (2012a). A Chloroflexi bacterium dechlorinates polychlorinated biphenyls in marine sediments under in situ-like biogeochemical conditions. *J. Hazard. Mater.* 209, 449–457. doi: 10.1016/j.jhazmat.2012.01.042

Zanaroli, G., Negroni, A., Vignola, M., Nuzzo, A., Shu, H. Y., and Fava, F. (2012b). Enhancement of microbial reductive dechlorination of polychlorinated

biphenyls (PCBs) in a marine sediment by nanoscale zerovalent iron (NZVI) particles. *J. Chem. Technol. Biotechnol.* 87, 1246–1253. doi: 10.1002/jctb.3835

Zhen, H. J., Du, S. Y., Rodenburg, L. A., Mainelis, G., and Fennell, D. E. (2014). Reductive dechlorination of 1,2,3,7,8-pentachlorodibenzo-p-dioxin and Aroclor 1260, 1254 and 1242 by a mixed culture containing *Dehalococcoides mccartyi* strain 195. *Water Res.* 52, 51–62. doi: 10.1016/j.watres.2013.12.038

Zwiernik, M. J., Quensen, J. F., and Boyd, S. A. (1998). $FeSO_4$ amendments stimulate extensive anaerobic PCB dechlorination. *Environ. Sci. Technol.* 32, 3360–3365. doi: 10.1021/es9801689

Conflict of Interest Statement: The authors declare that the research was conducted in the absence of any commercial or financial relationships that could be construed as a potential conflict of interest.

frontiers in Microbiology

ORIGINAL RESEARCH
published: 01 September 2017
doi: 10.3389/fmicb.2017.01677

Dehalococcoides as a Potential Biomarker Evidence for Uncharacterized Organohalides in Environmental Samples

Qihong Lu[1†], Ling Yu[1†], Zhiwei Liang[1], Qingyun Yan[1], Zhili He[1], Tiangang Luan[2], Dawei Liang[3] and Shanquan Wang[1,4]**

[1] Environmental Microbiome Research Center and the School of Environmental Science and Engineering, Sun Yat-sen University, Guangzhou, China, [2] State Key Laboratory of Pest Control and Resource Utilization, School of Life Sciences, Sun Yat-sen University, Guangzhou, China, [3] Beijing Key Laboratory of Bio-inspired Energy Materials and Devices, School of Chemistry and Environment, Beihang University, Beijing, China, [4] Guangdong Provincial Key Laboratory of Environmental Pollution Control and Remediation Technology, Guangzhou, China

OPEN ACCESS

Edited by:
Qiang Wang,
Institute of Hydrobiology (CAS), China

Reviewed by:
Yan Hong Zeng,
Guangzhou Institute of Geochemistry (CAS), China
Junhui Li,
Northern Arizona University, United States

***Correspondence:**
Shanquan Wang
wangshanquan@mail.sysu.edu.cn
Dawei Liang
liangdw@buaa.edu.cn

[†] These authors have contributed equally to this work.

Specialty section:
This article was submitted to Microbiotechnology, Ecotoxicology and Bioremediation, a section of the journal Frontiers in Microbiology

Received: 20 July 2017
Accepted: 18 August 2017
Published: 01 September 2017

Citation:
Lu Q, Yu L, Liang Z, Yan Q, He Z, Luan T, Liang D and Wang S (2017) Dehalococcoides as a Potential Biomarker Evidence for Uncharacterized Organohalides in Environmental Samples. Front. Microbiol. 8:1677. doi: 10.3389/fmicb.2017.01677

The massive production and improper disposal of organohalides resulted in worldwide contamination in soil and water. However, their environmental survey based on chromatographic methods was hindered by challenges in testing the extremely wide variety of organohalides. *Dehalococcoides* as obligate organohalide-respiring bacteria exclusively use organohalides as electron acceptors to support their growth, of which the presence could be coupled with organohalides and, therefore, could be employed as a biomarker of the organohalide pollution. In this study, *Dehalococcoides* was screened in various samples of bioreactors and subsurface environments, showing the wide distribution of *Dehalococcoides* in sludge and sediment. Further laboratory cultivation confirmed the dechlorination activities of those *Dehalococcoides*. Among those samples, *Dehalococcoides* accounting for 1.8% of the total microbial community was found in an anaerobic granular sludge sample collected from a full-scale bioreactor treating petroleum wastewater. Experimental evidence suggested that the influent wastewater in the bioreactor contained bromomethane which support the growth of *Dehalococcoides*. This study demonstrated that *Dehalococcoides* could be employed as a promising biomarker to test the present of organohalides in wastestreams or other environmental samples.

Keywords: *Dehalococcoides*, biomarker, environmental samples, organohalide compounds, reductive dehalogenation

INTRODUCTION

Organohalide compounds are a giant group of halogen-substituted hydrocarbons produced in large quantities as solvents, plastics, pesticides, and chemical intermediates for industrial and agricultural uses (Stringer and Johnston, 2001; Jugder et al., 2016). The improper handling and disposal of harmful halogenated compounds resulted in their worldwide contamination in soil and water as well as bioaccumulation through food webs, posing threat to both human health and the environment (Stringer and Johnston, 2001; Zhou et al., 2004; Lu et al., 2017). Due to

the side effects on biota, 69 out of the 126 EPA Priority Pollutants are organohalide compounds (United States Environmental Protection Agency, 2013). However, detection and monitoring of their environmental transport and fate using chromatography-based methods were limited due to the extremely wide variety of organohalide compounds (Stringer and Johnston, 2001).

Anoxic aquatic sediments became the major environmental sink for hydrophobic organohalide compounds, facilitating the growth of dehalogenating bacteria through organohalide-respiration (Smidt and de Vos, 2004; Zhou and Song, 2004; Rossi et al., 2012). In the organohalide-respiration process, anaerobic bacteria couple their growth with halogen-removal using acetate as a carbon source, H_2 as an electron donor, and various organohalides as electron acceptors (Mohn and Tiedje, 1992; Holliger and Schumacher, 1994). Thus far, phylogenetically diverse bacterial groups have been identified to be able to remove halogens from organohalide compounds, including *Dehalococcoides*, *Dehalogenimonas*, *Dehalobium*, *Dehalobacter* and *Desulfitobacterium* (Smidt and de Vos, 2004; Zanaroli et al., 2015; Wang et al., 2016), which were normally originated from contaminated sites (Hendrickson et al., 2002; Taş et al., 2009; van der Zaan et al., 2010). Among them, *Dehalococcoides* are obligate organohalide-respiring bacteria that exclusively employ acetate as a carbon source, H_2 as an electron donor and organohalides as electron acceptors to conserve energy for growth (Löffler et al., 2013). *Dehalococcoides* were identified to have the most diverse and extensive dehalogenation activities on organohalide compounds, including chloroethenes (Maymó-Gatell et al., 1997; He et al., 2003; Müller et al., 2004), chlorobenzenes (Adrian et al., 2000), polychlorinated biphenyls (PCBs) (Bedard et al., 2007; Wang et al., 2014), polybrominated diphenyl ethers (PBDEs) (He et al., 2006), chloroethanes and chlorophenols (Fennell et al., 2004; Lookman et al., 2004; Adrian et al., 2007; Wang and He, 2013a,b). Therefore, *Dehalococcoides* might be employed as a potential biomarker, complementing current chromatography-based methods, to test the presence of organohalide compounds.

In this study, we first screened *Dehalococcoides* in sludge and sediment samples collected from various anaerobic bioreactors for industrial wastewater treatment and contaminated black-odorous urban rivers. Further source-tracking together with laboratory cultivation confirmed which organohalide compounds supported the growth of *Dehalococcoides*. These results opened up opportunities employing *Dehalococcoides* as a biomarker to track unknown sources of organohalide compounds in wastewater and environmental samples.

MATERIALS AND METHODS

Microbial Cultures Setup and Transfer

Sludge and sediment samples collected from bioreactors and black-odorous urban rivers were employed as inoculum for culture setup (**Table 1**). These samples were acquired directly by filling sterile 50 ml plastic Falcon tubes that were capped and transported to the laboratory at an ambient temperature. To control exposure of the samples to oxygen, Falcon tubes were sealed with Parafilm, and microcosm setup was performed in anaerobic chamber soon after their arrivals. For granular sludge, it was smashed into floc-form sludge before inoculation. Defined anaerobic mineral medium in 160 ml serum bottles for microbial cultivation was prepared as described (He et al., 2003; Wang and He, 2013a), which contains salts, trace elements and vitamins. L-cysteine and $Na_2S{\cdot}9H_2O$ (0.2 mM each) were added to the medium to achieved reduced conditions. The bottles were sealed with black butyl rubber septa and secured with aluminum crimp caps. The organohalide-fed cultures were transferred in 100 ml medium supplemented with 10 mM lactate, 10 mM 2-bromoethanesulphonate (BES, to inhibit methanogen growth), and 1 mM PCE or 10 ppm chloromethane. The control cultures without organohalide-amendment were transferred in the same mineral medium. Unless stated otherwise, cultures were incubated at 30°C in the dark without shaking. All the experiments were set up in duplicates.

Analytical Techniques

Headspace samples of chloroethenes (i.e., PCE, TCE, *cis*-DCE, *trans*-DCE, VC and ethane)and chloromethane were injected manually with a glass, gastight, luer lock syringe (Hamilton, Reno, NV, United States) into a gas chromatography (GC) 7890N equipped with a flame ionization detector (Agilent, Wilmington, DE, United States) and a GS-GasPro column (30 m × 0.32 mm; Agilent, Wilmington, DE, United States) as described (Wang and He, 2013b). The standards compounds (with analytical pure or above) were purchased from Sigma–Aldrich.

Fluorescence *In Situ* Hybridization (FISH)

The FISH experiment was performed according to protocols described previously (Amann et al., 1995). Granular sludge samples were fixed in a 4% paraformaldehyde solution for 8 h at 4°C, and embedded in Optimal Cutting Temperature (O.C.T.) compound (Fisher Healthcare, Houston, TX, United States). Then the freezing granules were cut into 15 μm-thick sections with CM3050S cryostat (Leica, Germany). Hybridization was performed at 46°C for 4 h with oligonucleotide probes Dhe1259 (Yang and Zeyer, 2003), EUBmix and ARCH915 (Amann et al., 1995) targeting *Dehalococcoides*, bacteria and archaea, respectively. Dhe1259 and EUBmix/ARCH915 for dual-staining FISH were labeled with Cyanine 3 (Cy3) and Cy5, respectively. FISH-stained images were captured CLSM (Leica TCS-SP2, Germany).

DNA Extraction, PCR, and Illumina Miseq Sequencing

Community gDNA was extracted using the FastDNA Spin Kit for Soil (MP Biomedicals, Carlsbad, CA, United States) according to the manufacturer's instructions. The 16S rRNA gene was amplified with the U515F forward primer and U909R reverse primer as described (Narihiro et al., 2015). Illumina Miseq sequencing (Illumina, San Diego, CA, United States) service was provided by BGI (Shenzhen, China). The provided pair-end (2 × 300 nd) demultiplexed sequences were assembled and filtered using Mothur v.1.33 (Schloss et al., 2009).

TABLE 1 | Sludge samples information which collected from anaerobic industrial wastewater treating bioreactors and environmental samples.

Sample No.	Sludge/sediments source	Sludge/sediments Form	Bioreactor type	*Dehalococcoides* occurrence	Dechlorination activity
1	Vitamin-C Industry	Granules	UASB	−	−
2	Petrochemical Industry	Granules	UASB	+	+
3	Brewery Industry	Granules	UASB	−	−
4	Paper mill Industry	Granules	UASB	−	−
5	Coke Industry	Flocs	Anaerobic digester	−	−
6	Acrylic textile Industry	Flocs	Anaerobic digester	−	−
7	Textile-dyeing Industry	Flocs	Anaerobic digester	−	−
8	WAS Anaerobic digestion Industry	Flocs	Anaerobic digester	−	−
9	Black-odorous River A	Flocs	N.A.	+	+
10	Black-odorous River B	Flocs	N.A.	+	+
11	Black-odorous River C	Flocs	N.A.	+	+

Quantitative Insights Into Microbial Ecology (QIIME, v1.8.0) was employed for the subsequent processing and downstream analysis (Caporaso et al., 2010).

Data Deposition

Raw Illumina Miseq sequencing reads were deposited into NCBI Sequence Read Archive (SRA) with accession no. SRP112682.

RESULTS

Screening of Obligate Organohalide-Respiring *Dehalococcoides* in Anaerobic Sludge and Sediment Samples

Dehalococcoides as an obligate dehalogenating bacterial group can only utilize organohalides as electron acceptors to support their growth (Löffler et al., 2013). In this study, sediment and sludge samples from black-odorous urban rivers and anaerobic bioreactors, respectively, were selected to screen the presence of *Dehalococcoides* (**Table 1**). PCR amplification with *Dehalococcoides* genus-specific primers, FpDHC1/RpDHC1377 (Hendrickson et al., 2002), showed the positive detection of *Dehalococcoides* in all urban river sediment samples, as well as in a granular sludge sample collected from a full-scale mesophilic UASB reactor treating petrochemical wastewater (**Table 1**). And the petrochemical wastewater contains organic compounds generated from terephthalic-acid industry, e.g., terephthalic-acid, benzoic acid, toluic acid, acetic acid and other intermediate compounds and byproducts (Lykidis et al., 2011).

To profile microbial communities of those *Dehalococcoides*-containing environmental samples, Miseq 16S rRNA gene sequencing was performed, showed the very different microbial community structure in samples between *Dehalococcoides*-containing granular sludge and urban river sediments (**Figure 1**). In granular sludge collected from the UASB reactor, acidogenic populations, *Syntrophorhabdus* (of *Syntrophorhabdaceae*) and *Syntrophus*, formed syntrophic interactions with methanogenic *Methanosaeta* and *Methanosarcinaceae* (**Figure 1**). Surprisingly, the obligate organohalide-respiring *Dehalococcoides* presented abundant in the full-scale UASB reactor, accounting for 1.83% of the total microbial community, comparable with the relative abundance of *Dehalococcoides* in enrichment cultures dechlorinating PCBs (Wang and He, 2013a) and PCE (Lee et al., 2015). The presence of abundant obligate organohalide-respiring *Dehalococcoides* implied that the TA-wastewater contained uncharacterized organohalide compound(s). In the UASB reactor, acetate and H_2 generated from degradation of aromatic compounds in petrochemical wastewater by *Syntrophorhabdus*, *Syntrophus* and other syntrophs, together with low redox potential and the uncharacterized organohalide compounds, provide ideal growth niches for the fastidious *Dehalococcoides*. No other obligate dechlorinating bacteria, e.g., *Dehalogenimonas* and *Dehalobacter*, were found in the granular sludge sample. In a control sample collected from a lab-scale anaerobic sludge digester without organohalide amendment, no known dechlorinating bacteria can be detected (**Figure 1**). The highly similar microbial community structures of the three black-odorous river sediments, distinguish themselves from the community compositions of the granular sludge, especially the predominant lineages of *Chloroflexi* (i.e., *Longilinea*, *GCA004*, *WCHB1-05* and *Anaerolinaceae*) and *Proteobacteria* (i.e., *Syntrophobacter* and *Dechloromonas*) (Şimsir et al., 2017) (**Figure 1**). *Dehalococcoides* were shown the appearance in the microbial community, on which indicate the potential of organohalides' contamination.

Dechlorination Activities in *Dehalococcoides*-Containing Cultures

To further evaluate the dechlorination activities, perchloroethene (PCE) was spiked into microcosms established with those *Dehalococcoides*-containing sediment and sludge samples. After around 2 months' incubation, PCE dechlorination activities were observed in all three microcosms with the river sediment inocula (data not shown). Subsequent consecutive culture transfers of the three microcosms generated three active cultures which reductively dechlorinate PCE into vinyl chloride (VC) or ethene (**Figure 2**). No dechlorination activity was observed in the control microcosm established with digester sludge (**Figure 2D**).

In contrast to PCE dechlorination in sediments of the three black-odorous urban rivers, microcosms inoculated with the

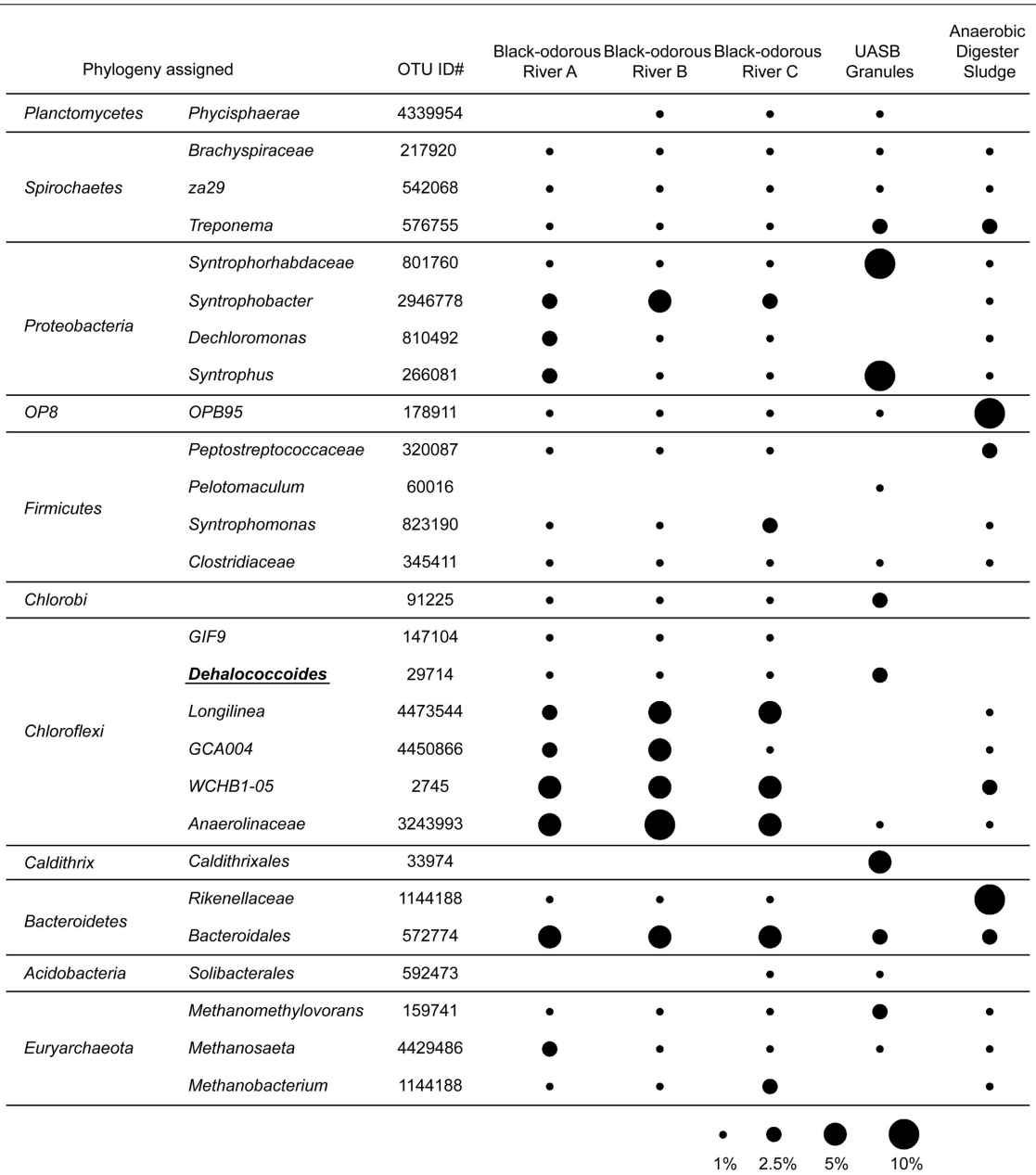

FIGURE 1 | The relative abundance (RA) of dominant microbial populations in environmental samples. Only populations with RA > 0.5% in at least one samples were shown here.

Dehalococcoides-containing granular sludge showed negative PCE-dechlorination activity. To identify potential organohalides to support the growth of *Dehalococcoides* in the granular sludge, organohalide pollution in the petrochemical wastewater as influent of the UASB reactor was evaluated. The petrochemical wastewater was generated from a AMOCO process that oxidize *para*-xylene to terephthalic-acid, using a homogeneous catalyst of cobalt and manganese together with bromide as a promoter, in which bromomethane was generated as a byproduct (Tomás et al., 2013). Due to difficulties in obtaining bromomethane, dehalogenation activity test was performed with chloromethane as a homolog alternative to bromomethane. In chloromethane-fed culture, over 70% chloromethane was dechlorinated within 8 days (**Figure 3**). No obvious dechlorination activity was observed in abiotic control.

Dehalococcoides in the Granular Sludge

The partial 16S rRNA gene sequences (∼400 bp) generated from Miseq sequencing of V4–V5 hypervariable regions were unable to differentiate *Dehalococcoides* between Cornell and Victoria subgroups. Therefore, *Dehalococcoides* genus-specific primers (i.e., FpDHC1/RpDHC1377) were utilized to generate longer 16S

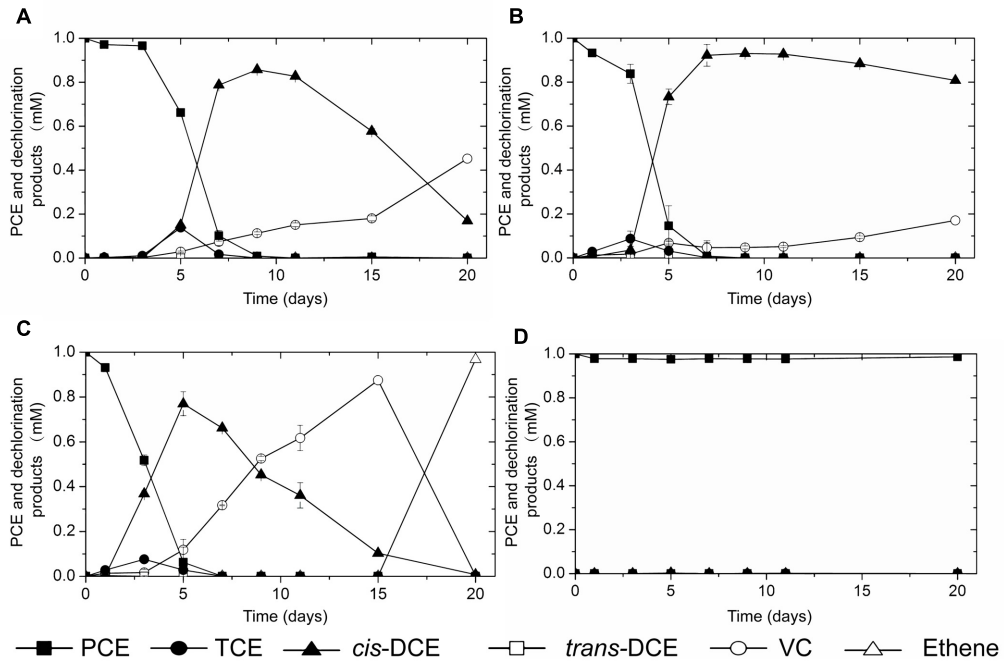

FIGURE 2 | PCE-dechlorination activity observed in cultures inoculated with **(A)** sediment of black-odorous river A, **(B)** sediment of black-odorous river B, **(C)** sediment of black-odorous river C, **(D)** anaerobic digester sludge.

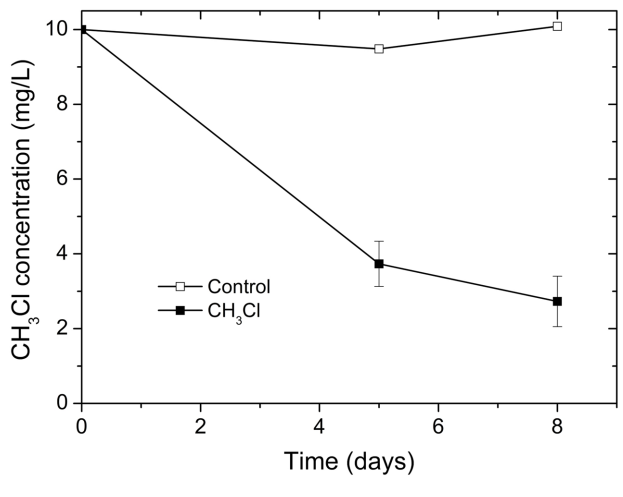

FIGURE 3 | Dechlorination of chloromethane by UASB granules.

rRNA gene sequences (∼1300 bp) to identify the *Dehalococcoides* in the anaerobic granular sludge. Phylogenetic analysis showed the close clustering of *Dehalococcoides* in TA-degrading granules with *D. mccartyi* 195 in Cornell subgroup (**Figure 4A**), sharing 99% 16S rRNA gene sequence similarity (2 bp difference over 1311 bp) with that of strain 195.

To provide insight into the spatial distribution of *Dehalococcoides* in the granular sludge, FISH was conducted with *Dehalococcoides*-specific, bacterial and archaeal oligonucleotide probes (Amann et al., 1995; Yang and Zeyer, 2003). FISH analysis showed the scattered distribution of *Dehalococcoides* inside granules, closely colonized with other bacteria (**Figure 4B**) but separated from archaea (**Figure 4C**). Degradation of aromatic compounds by fermentative bacteria is thermodynamically restricted and will become endergonic ($\Delta G > 0$) as metabolic byproducts (e.g., acetate and H_2) accumulate in the biosystem. Similar with methanogenic archaea, *Dehalococcoides* might form syntrophic interactions with aromatic compound degrading acidogens in the granular sludge: the degradation of aromatic compounds by *Syntrophorhabdus* and other syntrophs provide acetate as carbon source and H_2 as electron donor for the halorespiration of *Dehalococcoides*; correspondingly, *Dehalococcoides* help maintain acetate and H_2 at low concentration in the biosystem and 'pull' degradation of aromatic compounds toward completion through consuming metabolic byproducts generated by acidogenic bacteria. The close colonization of *Dehalococcoides* with syntrophic bacteria could facilitate the interspecies transfer of H_2 (Mao et al., 2015).

DISCUSSION

Thus far, it remains challenging to detect organohalide compounds in wastewater and environmental samples based on chromatography methods due to their extremely wide variety, e.g., PCBs are a family of 209 structurally similar congeners (Chu and Hong, 2004; Elder et al., 2008). Bromomethane, similar with many other organohalide compounds produced as intermediate or byproducts in chemical synthesis processes, was

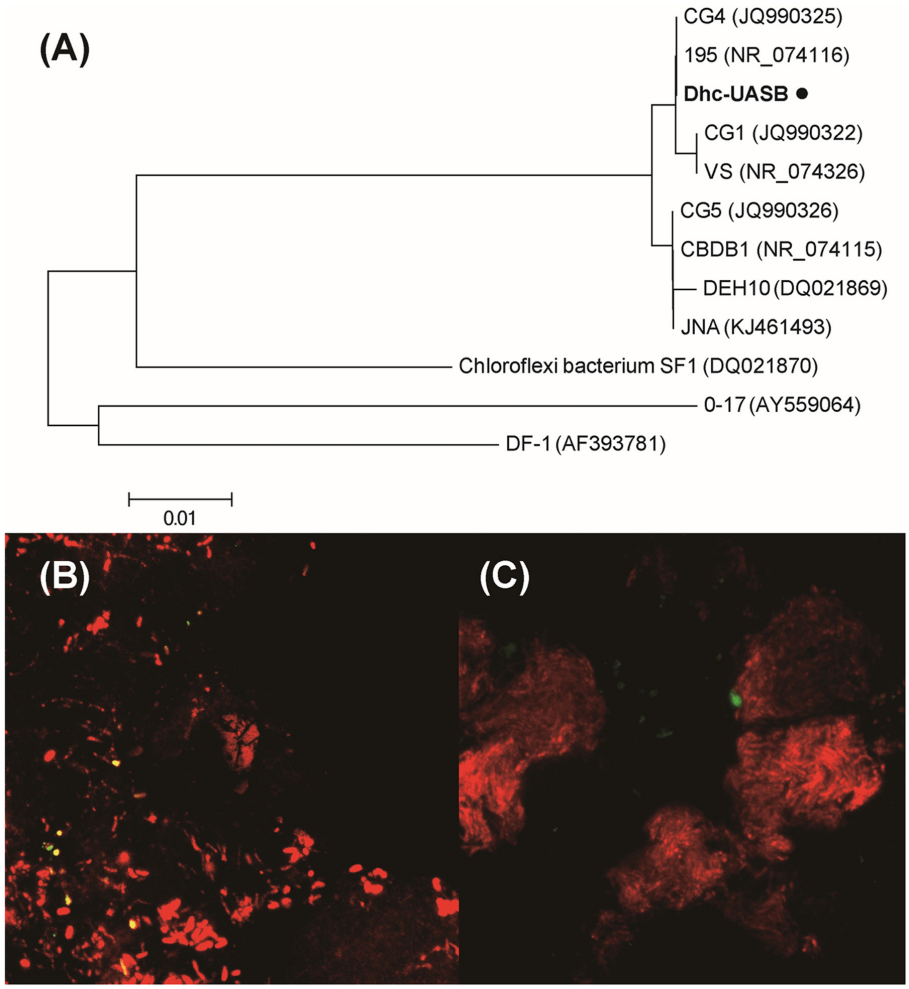

FIGURE 4 | (A) Phylogenetic tree of *Dehalococcoides* identified in TA-degrading anaerobic granular sludge. Phylogenetic tree was calculated by neighbor-joining method using MEGA4 (Tamura et al., 2007). FISH analysis revealed the space distribution of **(B)** bacteria (red) and *Dehalococcoides* (yellow), and **(C)** archaea (red) and *Dehalococcoides* (green).

a noteless synthesis byproduct in the petrochemical wastewater generated from terephthalic acid industry (Tomás et al., 2013). In this study, we reported the abundant presence of obligate organohalide-respiring *Dehalococcoides* in a full-scale UASB reactor for petrochemical wastewater treatment, and further cultivation experiments suggested the possible contamination of bromomethane in the petrochemical wastewater. Recent studies showed experimental evidences of biosynthesis of aromatic organohalides in nature, which might explain the detection of *Dehalococcoides* in the three black-odorous urban rivers (Agarwal et al., 2014; El Gamal et al., 2016; Şimsir et al., 2017). Also, *Dehalococcoides* was detected in various environmental samples contaminated with organohalides, including sludge/sediment collected from anaerobic digesters (Smith et al., 2015) and hyporheic zone of a wastewater treatment plant (WWTP)-impacted eutrophic river (Atashgahi et al., 2015). Therefore, *Dehalococcoides* might be a promising biomarker, complementing current chromatography-based methods, to test organohalide compounds in wastewater and environmental samples.

The UASB reactors provided ideal ecological niches for the growth of *Dehalococcoides* which further formed syntrophic interactions, as methanogens in syntrophic methanogenic communities (Stams and Plugge, 2009), with aromatic-compound degrading bacteria to overcome the thermodynamic limit through consuming acetate and H_2. To our knowledge, this is the first report of the strictly organohalide-respiring *Dehalococcoides* present abundantly in a full-scale bioreactor for industrial wastewater treatment. In previous studies, *Dehalococcoides* was documented in various lab-scale bioreactors, including membrane biofilm reactors (Chung et al., 2008), UASB reactor (Hwu and Lu, 2008) and anaerobic biotrickling filter (Popat and Deshusses, 2009). The presence of *Dehalococcoides* in high abundance in both full- and lab-scale bioreactors showed the feasibility of removing toxic and persistent organohalides from various industrial wastewaters in anaerobic bioreactors

through employing the microbial reductive dehalogenation process.

AUTHOR CONTRIBUTIONS

SW and DL conceived the idea. QL and LY performed the experiments and data analysis. SW, QY, TL, and ZH provided materials. QL, LY, and SW wrote the manuscript with inputs from all authors. All authors read and approved the final manuscript.

FUNDING

This study was supported by the National Natural Science Foundation of China (41671310) and the Key Program of National Natural Science Foundation of China (51638005).

ACKNOWLEDGMENT

We are very grateful to Feng Yan for providing sludge samples.

REFERENCES

Adrian, L., Hansen, S. K., Fung, J. M., Görisch, H., and Zinder, S. H. (2007). Growth of *Dehalococcoides* strains with chlorophenols as electron acceptors. *Environ. Sci. Technol.* 41, 2318–2323. doi: 10.1021/es062076m

Adrian, L., Szewzyk, U., Wecke, J., and Görisch, H. (2000). Bacterial dehalorespiration with chlorinated benzenes. *Nature* 408, 580–583. doi: 10.1038/35046063

Agarwal, V., El Gamal, A. A., Yamanaka, K., Poth, D., Kersten, R. D., Schorn, M., et al. (2014). Biosynthesis of polybrominated aromatic organic compounds by marine bacteria. *Nat. Chem. Biol.* 10, 640–647. doi: 10.1038/nchembio.1564

Amann, R. I., Ludwig, W., and Schleifer, K. H. (1995). Phylogenetic identification and in situ detection of individual microbial cells without cultivation. *Microbiol. Rev.* 59, 143–169.

Atashgahi, S., Aydin, R., Dimitrov, M. R., Sipkema, D., Hamonts, K., Lahti, L., et al. (2015). Impact of a wastewater treatment plant on microbial community composition and function in a hyporheic zone of a eutrophic river. *Sci. Rep.* 5:17284. doi: 10.1038/srep17284

Bedard, D. L., Ritalahti, K. M., and Löffler, F. E. (2007). The *Dehalococcoides* population in sediment-free mixed cultures metabolically dechlorinates the commercial polychlorinated biphenyl mixture aroclor 1260. *Appl. Environ. Microbiol.* 73, 2513–2521. doi: 10.1128/AEM.02909-06

Caporaso, J. G., Kuczynski, J., Stombaugh, J., Bittinger, K., Bushman, F. D., Costello, E. K., et al. (2010). QIIME allows analysis of high-throughput community sequencing data. *Nat. Methods* 7, 335–336. doi: 10.1038/nmeth.f.303

Chu, S., and Hong, C. S. (2004). Retention indexes for temperature-programmed gas chromatography of polychlorinated biphenyls. *Anal. Chem.* 76, 5486–5497. doi: 10.1021/ac049526i

Chung, J., Krajmalnik-Brown, R., and Rittmann, B. E. (2008). Bioreduction of trichloroethene using a hydrogen-based membrane biofilm reactor. *Environ. Sci. Technol.* 42, 477–483. doi: 10.1021/es702422d

El Gamal, A., Agarwal, V., Rahman, I., and Moore, B. S. (2016). Enzymatic reductive dehalogenation controls the biosynthesis of marine bacterial pyrroles. *J. Am. Chem. Soc.* 138, 13167–13170. doi: 10.1021/jacs.6b08512

Elder, D. P., Lipczynski, A. M., and Teasdale, A. (2008). Control and analysis of alkyl and benzyl halides and other related reactive organohalides as potential genotoxic impurities in active pharmaceutical ingredients (APIs). *J. Pharm. Biomed. Anal.* 48, 497–507. doi: 10.1016/j.jpba.2008.06.009

Fennell, D. E., Nijenhuis, I., Wilson, S. F., Zinder, S. H., and Häggblom, M. M. (2004). *Dehalococcoides* ethenogenes strain 195 reductively dechlorinates diverse chlorinated aromatic pollutants. *Environ. Sci. Technol.* 38, 2075–2081. doi: 10.1021/es034989b

He, J., Ritalahti, K. M., Yang, K. L., Koenigsberg, S. S., and Löffler, F. E. (2003). Detoxification of vinyl chloride to ethene coupled to growth of an anaerobic bacterium. *Nature* 424, 62–65. doi: 10.1038/nature01717

He, J., Robrock, K. R., and Alvarez-Cohen, L. (2006). Microbial reductive debromination of polybrominated diphenyl ethers (PBDEs). *Environ. Sci. Technol.* 40, 4429–4434. doi: 10.1021/es052508d

Hendrickson, E. R., Payne, J. A., Young, R. M., Starr, M. G., Perry, M. P., and Fahnestock, S. (2002). Molecular analysis of *Dehalococcoides* 16S ribosomal DNA from chloroethene contaminated sites throughout North America and Europe. *Appl. Environ. Microbiol.* 68, 485–495. doi: 10.1128/AEM.68.2.485-495.2002

Holliger, C., and Schumacher, W. (1994). Reductive dehalogenation as a respiratory process. *Antonie Van Leeuwenhoek* 66, 239–246. doi: 10.1007/BF00871642

Hwu, C. S., and Lu, C. J. (2008). Continuous dechlorination of tetrachloroethene in an upflow anaerobic sludge blanket reactor. *Biotechnol. Lett.* 30, 1589–1593. doi: 10.1007/s10529-008-9738-x

Jugder, B., Ertan, H., Bohl, S., Lee, M., Marquis, C. P., and Manefield, M. (2016). Organohalide respiring bacteria and reductive dehalogenases: key tools in organohalide bioremediation. *Front. Microbiol.* 7:249. doi: 10.3389/fmicb.2016.00249

Lee, P. K., Men, Y., Wang, S., He, J., and Alvarez-Cohen, L. (2015). Development of a fluorescence-activated cell sorting method coupled with whole genome amplification to analyze minority and trace *Dehalococcoides* genomes in microbial communities. *Environ. Sci. Technol.* 49, 1585–1593. doi: 10.1021/es503888y

Löffler, F. E., Yan, J., Ritalahti, K. M., Adrian, L., Edwards, E. A., Konstantinidis, K. T., et al. (2013). *Dehalococcoides mccartyi* gen. nov., sp. nov., obligate organohalide-respiring, anaerobic bacteria, relevant to halogen cycling and bioremediation, belong to a novel bacterial class, *Dehalococcoidetes* classis nov., within the phylum *Chloroflexi*. *Int. J. Syst. Evol. Microbiol.* 63, 625–635. doi: 10.1099/ijs.0.034926-0

Lookman, R., Bastiaens, L., Borremans, B., Maesen, M., Gemoets, J., and Diels, L. (2004). Batch-test study on the dechlorination of 1,1,1-trichloroethane in contaminated aquifer material by zero-vaalent iron. *J. Contam. Hydrol.* 74, 133–144. doi: 10.1016/j.jconhyd.2004.02.007

Lu, Q., Toledo, R. A., Xie, F., Li, J., and Shim, H. (2017). Reutilization of waste scrap tyre as the immobilization matrix for the enhanced bioremoval of a monoaromatic hydrocarbons, methyl tert-butyl ether, and chlorinated ethenes mixture from water. *Sci. Total Environ.* 583, 88–96. doi: 10.1016/j.scitotenv.2017.01.025

Lykidis, A., Chen, C. L., Tringe, S. G., McHardy, A. C., Copeland, A., Kyrpides, N. C., et al. (2011). Multiple syntrophic interactions in a terephthalate-degrading methanogenic consortium. *ISME J.* 5, 122–130. doi: 10.1038/ismej.2010.125

Mao, X., Stenuit, B., Polasko, A., and Alvarez-Cohen, L. (2015). Efficient metabolic exchange and electron transfer within a syntrophic trichloroethene-degrading coculture of *Dehalococcoides mccartyi* 195 and *Syntrophomonas wolfei*. *Appl. Environ. Microbiol.* 81, 2015–2024. doi: 10.1128/AEM.03464-14

Maymó-Gatell, X., Chien, Y.-T., Gossett, J. M., and Zinder, S. H. (1997). Isolation of a bacterium that reductively dechlorinates tetrachloroethene to ethene. *Science* 276, 1568–1571. doi: 10.1126/science.276.5318.1568

Mohn, W. W., and Tiedje, J. M. (1992). Microbial reductive dehalogenation. *Microbiol. Rev.* 56, 482–507.

Müller, J. A., Rosner, B. M., Von Abendroth, G., Meshulam-Simon, G., McCarty, P. L., and Spormann, A. M. (2004). Molecular identification of the catabolic vinyl chloride reductase from *Dehalococcoides* sp. strain VS and its environmental distribution. *Appl. Environ. Microbiol.* 70, 4880–4888. doi: 10.1128/AEM.70.8.4880-4888.2004

Narihiro, T., Nobu, M. K., Kim, N. K., Kamagata, Y., and Liu, W. T. (2015). The nexus of syntrophy-associated microbiota in anaerobic digestion revealed by long-term enrichment and community survey. *Environ. Microbiol.* 17, 1707–1720. doi: 10.1111/1462-2920.12616

Popat, S. C., and Deshusses, M. A. (2009). Reductive dehalogenation of trichloroethene vapors in an anaerobic biotrickling filter. *Environ. Sci. Technol.* 43, 7856–7861. doi: 10.1021/es901305x

Rossi, P., Shani, N., Kohler, F., Imfeld, G., and Holliger, C. (2012). Ecology and biogeography of bacterial communities associated with chloroethene-contaminated aquifers. *Front. Microbiol.* 3:260. doi: 10.3389/fmicb.2012.00260

Schloss, P. D., Westcott, S. L., Ryabin, T., Hall, J. R., Hartmann, M., Hollister, E. B., et al. (2009). Introducing mothur: open-source, platform-independent, community-supported software for describing and comparing microbial communities. *Appl. Environ. Microbiol.* 75, 7537–7541. doi: 10.1128/AEM.01541-09

Smidt, H., and de Vos, W. M. (2004). Anaerobic microbial dehalogenation. *Annu. Rev. Microbiol.* 58, 43–73. doi: 10.1146/annurev.micro.58.030603.123600

Smith, B. J., Boothe, M. A., Fiddler, B. A., Lozano, T. M., Rahi, R. K., and Krzmarzick, M. J. (2015). Enumeration of organohalide respirers in municipal wastewater anaerobic digesters. *Microbiol. Insights* 8, 9–14. doi: 10.4137/MBI.S31445

Stams, A. J., and Plugge, C. M. (2009). Electron transfer in syntrophic communities of anaerobic bacteria and archaea. *Nat. Rev. Microbiol.* 7, 568–577. doi: 10.1038/nrmicro2166

Stringer, R., and Johnston, P. (2001). Chlorine and the environment: an overview of the chlorine industry. *Environ. Sci. Pollut. Res.* 8, 146–159. doi: 10.1007/BF02987309

Şimsir, B., Yan, J., Im, J., Graves, D., and Löffler, F. E. (2017). Natural attenuation in streambed sediment receiving chlorinated solvents from underlying fracture networks. *Environ. Sci. Technol.* 51, 4821–4830. doi: 10.1021/acs.est.6b05554

Tamura, K., Dudley, J., Nei, M., and Kumar, S. (2007). MEGA4: molecular evolutionary genetics analysis (MEGA) software version 4.0. *Mol. Biol. Evol.* 24, 1596–1599. doi: 10.1093/molbev/msm092

Taş, N., Van Eekert, M. H., Schraa, G., Zhou, J., De Vos, W. M., and Smidt, H. (2009). Tracking functional guilds: "*Dehalococcoides*" spp. in European river basins contaminated with hexachlorobenzene. *Appl. Environ. Microbiol.* 75, 4696–4704. doi: 10.1128/AEM.02829-08

Tomás, R. A., Bordado, J. C., and Gomes, J. F. (2013). p-Xylene oxidation to terephthalic acid: a literature review oriented toward process optimization and development. *Chem. Rev.* 113, 7421–7469. doi: 10.1021/cr300298j

United States Environmental Protection Agency (2013). *List of Priority Pollutants*. Available at: http://water.epa.gov/scitech/methods/cwa/pollutants.cfm

van der Zaan, B., Hannes, F., Hoekstra, N., Rijnaarts, H., de Vos, W. M., Smidt, H., et al. (2010). Correlation of *Dehalococcoides* 16S rRNA and chloroethene-reductive dehalogenase genes with geochemical conditions in chloroethene-contaminated groundwater. *Appl. Environ. Microbiol.* 76, 843–850. doi: 10.1128/AEM.01482-09

Wang, S., Chen, S., Wang, Y., Low, A., Lu, Q., and Qiu, R. (2016). Integration of organohalide-respiring bacteria and nanoscale zero-valent iron (Bio-nZVI-RD): a perfect marriage for the remediation of organohalide pollutants? *Biotechnol. Adv.* 34, 1384–1395. doi: 10.1016/j.biotechadv.2016.10.004

Wang, S., Chng, K. R., Wilm, A., Zhao, S., Yang, K. L., Nagarajan, N., et al. (2014). Genomic characterization of three unique *Dehalococcoides* that respire on persistent polychlorinated biphenyls. *Proc. Natl. Acad. Sci. U.S.A.* 111, 12103–12108. doi: 10.1073/pnas.1404845111

Wang, S., and He, J. (2013a). Dechlorination of commercial PCBs and other multiple halogenated compounds by a sediment-free culture containing *Dehalococcoides* and *Dehalobacter*. *Environ. Sci. Technol.* 47, 10526–10534. doi: 10.1021/es4017624

Wang, S., and He, J. (2013b). Phylogenetically distinct bacteria involve extensive dechlorination of aroclor 1260 in sediment-free cultures. *PLoS ONE* 8:e59178. doi: 10.1371/journal.pone.0059178

Yang, Y., and Zeyer, J. (2003). Specific detection of *Dehalococcoides* species by fluorescence in situ hybridization with 16S rRNA-targeted oligonucleotide probes. *Appl. Environ. Microbiol.* 69, 2879–2883. doi: 10.1128/AEM.69.5.2879-2883.2003

Zanaroli, G., Negroni, A., Häggblom, M. M., and Fava, F. (2015). Microbial dehalogenation of organohalides in marine and estuarine environments. *Curr. Opin. Biotechnol.* 33, 287–295. doi: 10.1016/j.copbio.2015.03.013

Zhou, Q. X., Cheng, Y., Zhang, Q. R., and Liang, J. D. (2004). Quantitative analyses of relationships between ecotoxicological effects and combined pollution. *Sci. China Ser. C* 47, 332–339. doi: 10.1360/03yc0042

Zhou, Q. X., and Song, Y. F. (2004). *Principles and Methods of Contaminated Soil Remediation (in Chinese)*. Beijing: Science Press.

Conflict of Interest Statement: The authors declare that the research was conducted in the absence of any commercial or financial relationships that could be construed as a potential conflict of interest.

The reviewer JL declared a past co-authorship with one of the authors QL to the handling Editor.

Advantages of publishing in Frontiers

OPEN ACCESS
Articles are free to read for greatest visibility and readership

FAST PUBLICATION
Around 90 days from submission to decision

HIGH QUALITY PEER-REVIEW
Rigorous, collaborative, and constructive peer-review

TRANSPARENT PEER-REVIEW
Editors and reviewers acknowledged by name on published articles

Frontiers
Avenue du Tribunal-Fédéral 34
1005 Lausanne | Switzerland

Visit us: www.frontiersin.org
Contact us: info@frontiersin.org | +41 21 510 17 00

REPRODUCIBILITY OF RESEARCH
Support open data and methods to enhance research reproducibility

DIGITAL PUBLISHING
Articles designed for optimal readership across devices

FOLLOW US
@frontiersin

IMPACT METRICS
Advanced article metrics track visibility across digital media

EXTENSIVE PROMOTION
Marketing and promotion of impactful research

LOOP RESEARCH NETWORK
Our network increases your article's readership